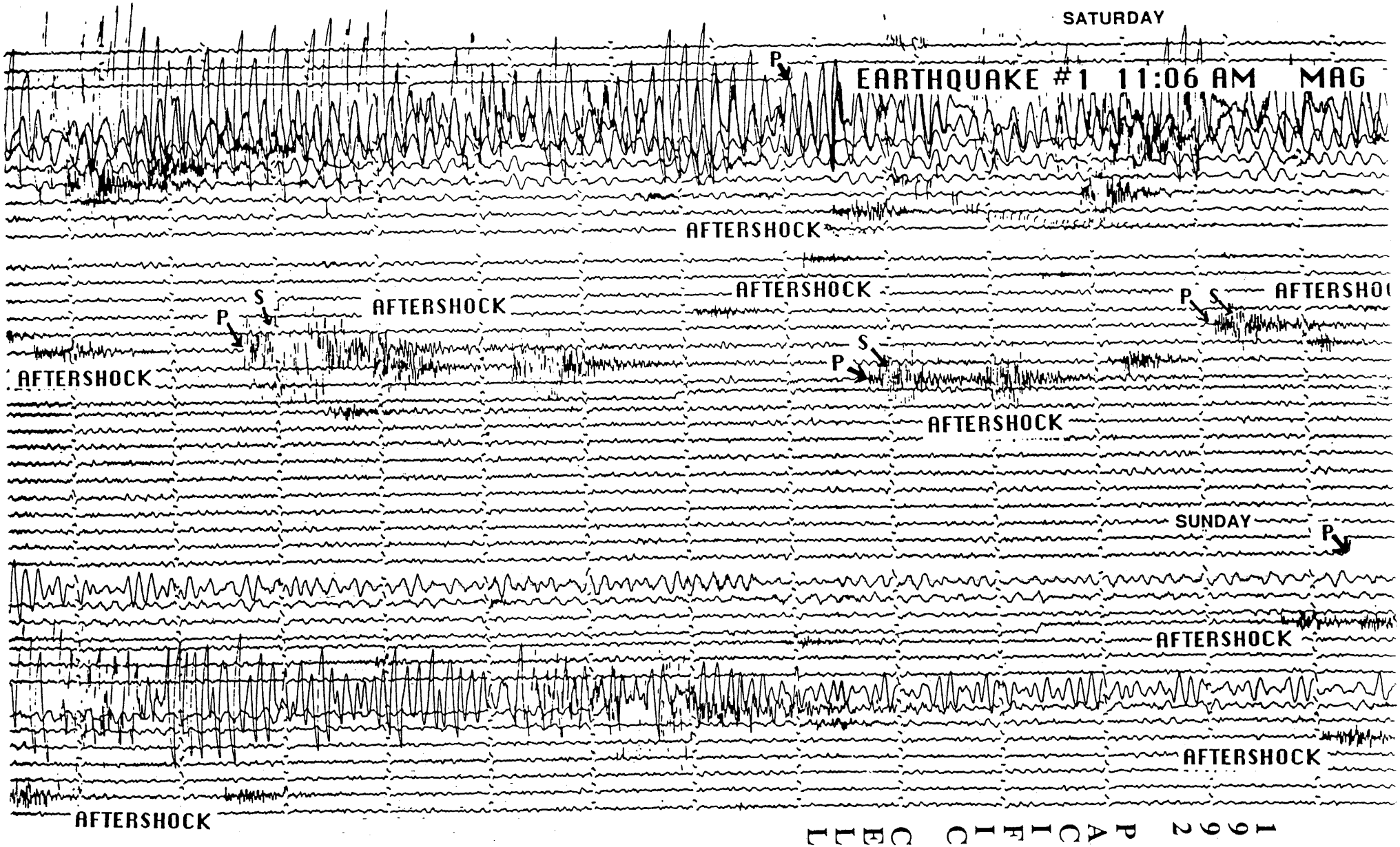

1992 PACIFIC CELL

FRIENDS OF THE PLEISTOCENE

NORTH COASTAL CALIFORNIA

PACIFIC CELL, FRIENDS OF THE PLEISTOCENE

GUIDEBOOK FOR THE FIELD TRIP TO

NORTHERN COASTAL CALIFORNIA

A look at the southern end of the Cascadia Subduction Zone
and
The Mendocino Triple Junction

June 5 - June 7, 1992

Guidebook coordinators* (i.e. non-editors!): R.M. Burke
G.A. Carver

Primary Field Trip Leaders:** G. A. Carver
D. J. Merritts
O. A. Chadwick
R. M. Burke
K. R. Aalto

Guidebook Contributors and Part-Time* Field Trip Leaders:**

Aalto, K. R.
Berger, G. W.
Bevis, K. A.
Bickner, F.
Bull, W. B.
Burke, R. M.
Carver, G. A.
Chadwick, O. A.
Clarke, Jr., S. H.
Dengler, L. A.
Dunklin, T.B.
Harvey, E. W.
Hendricks, D.M.
Johnson, R.
Knudsen, K.
Li, Wenhao
Manhart, C. S.
McLaughlin, R. J.
McPherson, R. C.
Merritts, D. J.
O'Dea, K. M.
Stein, A.
Stone, L.
Valentine, D.
Verhey, M.
Vick, G.
Vincent, K.
Weppner, E. M.
Wohl, E

SONG LEADER AND
HONORARY FOP LEADER: M. Reheis

* Means these guys are responsible for most errors in the guidebook and trip structure.
** Means these folks will be eating Rolaids, most concerned with logistics and crowd control.
***These people have done most of the science you came to see, talk to them if you have a question.

PREAMBLE TO THE 1992 PACIFIC CELL FRIENDS OF THE PLEISTOCENE FIELD TRIP

Welcome to the rugged, remote coast of northern California, Humboldt County. On Day 1 we will be visiting sites in and around the towns of Trinidad and Arcata. On Days 2 and 3, we will be working in a very remote, rural part of the north coast, where the local people are often third- and fourth-generation descendants of original European settlers. Most people are ranchers, and have strong feelings about, and ties to their land, roads, and streams. In general, they prefer not to have to deal with the tourists that flock to other parts of the region, such as Ferndale. They are very honest and strong people, they are reserved and cautious of outsiders, mostly in order to try to protect their special land from the development that has occurred along the rest of the coast of California.

We mention these attitudes because we have spent years getting to know the local families and developing their trust. They enjoy the attention the geology of their region is receiving (although certainly not the geologic activity itself!) and are themselves astute observers of tectonic and geomorphic processes. They are somewhat positive about the prospect of several hundred friends of the Pleistocene coming through to see the area firsthand. However, in order to avoid disrupting their lives and daily work, and negatively impacting either their property or some of the very fragile geologic exposures, we ask you to please abide by the following standards:

Please drive slowly and carefully on all roads, especially the Wildcat Road crossing from Ferndale to Petrolia, and the Mattole Road from Petrolia to our campsite on Day 2. The locals stay as far to the right as possible on roads that are one and one-half lanes at best. You might be tempted to ride the middle of the road, but please don't! This infuriates many local ranchers.

Please pull over if you are driving slowly and sight-seeing and a rancher or logging truck is behind you. There are numerous small pull-off sites on the local roads, and they are used extensively.

Because of the intensity of coastal erosion, mass movement, and channel incision, many of the Holocene and Pleistocene marine and fluvial terraces are mere remnants of once much larger surfaces. Please avoid disturbing the slopes along the outer edges of these features, and please do not remove any samples of shells or charcoal. If you see datable material, please notify one of the trip leaders. Many of the marine terrace sites that we have sampled in the past three years, for example, are now completely gone. We are working against the affects of time here to understand the Quaternary geologic history of the area before most evidence of it in the landscape is gone. Human impact has accelerated the rate of destruction of evidence, and the cars, footsteps, and hammering or clamoring of 300 geologists could wreak havoc. Walk gingerly!

DO NOT TRESPASS! Do not climb any fences, or open any closed gates, unless the trip leaders have clearly indicated that we have been given permission to do so.

If you ever wish to return to this area, you must obtain permission from local landowners to visit any of the sites included in Days 2 and 3. These are not public-access sites. In general, most of the sites we will visit are not suitable for multiple visits with classes or students, as the landowners simply are not up to it, and they don't want this field trip to result in a massive influx of future visitors.

Thank you for your courtesy. We think that some of the most spectacular examples of rapid uplift in North America can be seen in this area, and are grateful to the landowners who have given us permission to study this evidence over the years and during this trip. We don't want to offend them at all after so many years of graciousness and generosity.

UPDATE: The above verbiage written prior to the April 25, 1992 earthquake - the uplift is rapid!

THE GUIDEBOOK "ORGANIZATION" - or, HOW DID WE GET TO THIS POINT ?

When we were ask last June by Rob Negrini (a name we've talked about often over the past few weeks!) to consider running a trip to look at all of the geology being done in "That Humboldt Region" , we foolishly envisioned a fairly orderly review of many people's work and happily agreed to bring the Friends to northern California. Without effort, we talked Merritts, Chadwick, and others working near Cape Mendocino into joining those of us working a bit further north along the Cascadia Subduction Zone to provide the Friends with the best possible geologic overview of northern Coastal California. An invitation for guidebook contributions brought in some 20 articles, we became a bit nervous with the size of the guidebook. A trip announcement stating the following theme brought in about 150 participants, we became a bit nervous with the complexities of the logistics.

> The theme of the three day field trip will be the Quaternary geology of the southern end of the Cascadia subduction zone - Mendocino triple junction region. The trip will start at Patricks Point, situated in the fold and thrust belt of the subduction zone, and end in the vicinity off the triple junction near Petrolia. The field trip stops will focus of raised and deformed Pleistocene and Holocene marine and fluvial terraces, terrace soils and stratigraphy, subduction zone fold and thrust belt structures and tectonics, paleoseismic evidence for subduction zone earthquakes, late Pleistocene and Holocene uplift at the triple junction, and late to mid Pleistocene Eel River basin stratigraphy.

By mid-April , 1992 we had identified the tasks to be completed prior to your arrival at Patricks Point. With the occurrence of the April 25th/26th earthquakes, the trip changed scope - another 150 folks decided to come, logistics became as you see them today - Yikes!, and stops became dictated by parking and the desire of many to view (not walk on!) the uplifted reef near Petrolia. So, in keeping with the stated theme but with the sudden interest of half of you in mind, we will cut the northern end of the trip a bit short and spend a bit more time in the south. This will mean the road logs are only somewhat correct, and some of the contributors will not show you their field sites. The articles have been arranged in three general categories: (1) regional overview papers (good Thursday night reading); (2) field trip stop specific contributions (we'll have authors review these at the appropriate stop); and (3) site or regional discussions which have lend a great deal to our understanding of the regional geology, but which may be somewhat tangential to the stops we are now planning to make. In addition, each category of articles is approximately arranged in a north to south order, the direction of the 3 day trip.

ACKNOWLEDGEMENTS: To get this far in what we do know about the local geology, and to get this far in showing the Friends what we are able to see with limited exposures and large crowds, our acknowledgement list is huge! To single out individuals, with two exceptions, is an impossible task without producing a number of glaring oversights, which we do not wish to make. Therefore, we as your guidebook coordinators and local hosts would like to express our warmest and most sincere thanks to our families, our students, our colleagues, and the many landowners who have graciously cooperated over the years. The exception to individual recognition is to the HSU Geology Department staff under the direction of Camellia Armstrong and Scott North - they have been intimately involved in the support of all of our research and their recognition (and pay!) is far too small for their efforts. Finally, we wish to thank you, the Friends of the Pleistocene for your interest and input, your thoughts will help guide our future efforts. THANK YOU ALL. RMB and GAC

TABLE OF CONTENTS

	PAGE
Preamble to the 1992 Pacific Cell FOP Field trip	iii
Overview geology maps of the area to be traversed	1
Road logs: Day 1: Carver, Aalto, and Burke	3
Day 2 Aalto and Carver	15
Day 2 and 3: Merritts and Dunklin	22
CONTRIBUTED ARTICLES: REGIONAL OVERVIEW PAPERS	31
Late Cenozoic Deformation on the Cascadia Subduction Zone in the Region of the Mendocino Triple Junction: Carver, G.A., and Burke, R.M.	31
Neotectonic Framework of the Southern Cascadia Subduction Zone - Mendocino Triple Junction Region: Clarke, S. H., Jr. and McLaughlin, R. J.	64
Late Cenozoic Sediment Provenance and Tectonic Evolution of the Northernmost Coast Ranges, California: Aalto, K. R.	73
Depositional/Tectonic History of the Plio-Pleistocene Crescent City/Smith River, Del Norte County, California: Stone, L.	90
Style of Faulting at the Southern End of the Cascadia Subduction Zone: McPherson, R. C.	97
Historic Seismicity and Potential Source Areas of Large Earthquakes in North Coast California: Dengler, L. A., McPherson, R. C., and Carver, G. A.	112
Quaternary Tectonics and Topography, Mendocino Triple Junction: Merritts, D.J., Dunklin, T. B. , Vincent, K., Wohl, E., and Bull, W. B.	119
CONTRIBUTED ARTICLES: SPECIFIC FIELD TRIP STOP PAPERS	170
Thermoluminescence Dating of Coastal Sediments Near Eureka: Berger, G. W.	170
Sedimentology and Stratigraphy of the Mouth of Mad Unit, Humboldt County, California: Harvey, E. W. and Weppner, E. M.	176

Late Holocene Stratigraphy and Paleoseismicity, Humboldt Bay, California: Valentine, D., Vick, G., Carver, G. A., and Manhart, C. S. 182

High-Resolution Foraminiferid Stratigraphy as Evidence for Rapid, Coseismic Subsidence: Preliminary Results: Manhart, C. S. 188

Mattole River North Area Geology: Aalto, K.A. 195

Local Effects of 1991-1992 Earthquake Sequence: Dunklin, T. B. 197

Weathering and Soil Development on Marine Terraces Along the Lost Coast of California: Chadwick, O. A., Merritts, D. J., and Hendricks, D. M. 199

CONTRIBUTED ARTICLES: NON-SITE SPECIFIC DISCUSSION PAPERS 211

Hornblende Grain Etching as a Relative Dating Technique on Marine Terraces of Northern California: Bevis, K. A. 211

Geology and Stratigraphy of the Freshwater Creek Watershed, Humboldt County, California: Knudsen, K. 219

Analysis of Profiles of Streams that Cross a Portion of the Little Salmon Fault, Humboldt County, California: Stein, A. 224

Terrace Formation and Deformation on Yager Creek - Humboldt County, California: O'Dea, K. M. 229

The Late Holocene Subsidence Stratigraphy in the Eel River Syncline, Northern California: Li, Wenhao 235

An Investigation of Active Tectonics Along the Southern Limb of the Eel River Syncline: Verhey, M. 240

Soil Chronosequence and Tectonic Uplift Rates of Fluvial Terraces Near Garberville, California: Bickner, F. 247

Interpretation and Correlation of Holocene Coastal Debris Flow Fans Near the Mendocino Triple Junction: Johnson, R. 252

The Honeydew Earthquake of August 17, 1991: Evidence of Compressional Tectonics at the Mendocino Triple Junction: McPherson, R. C., and Dengler, L. A. 257

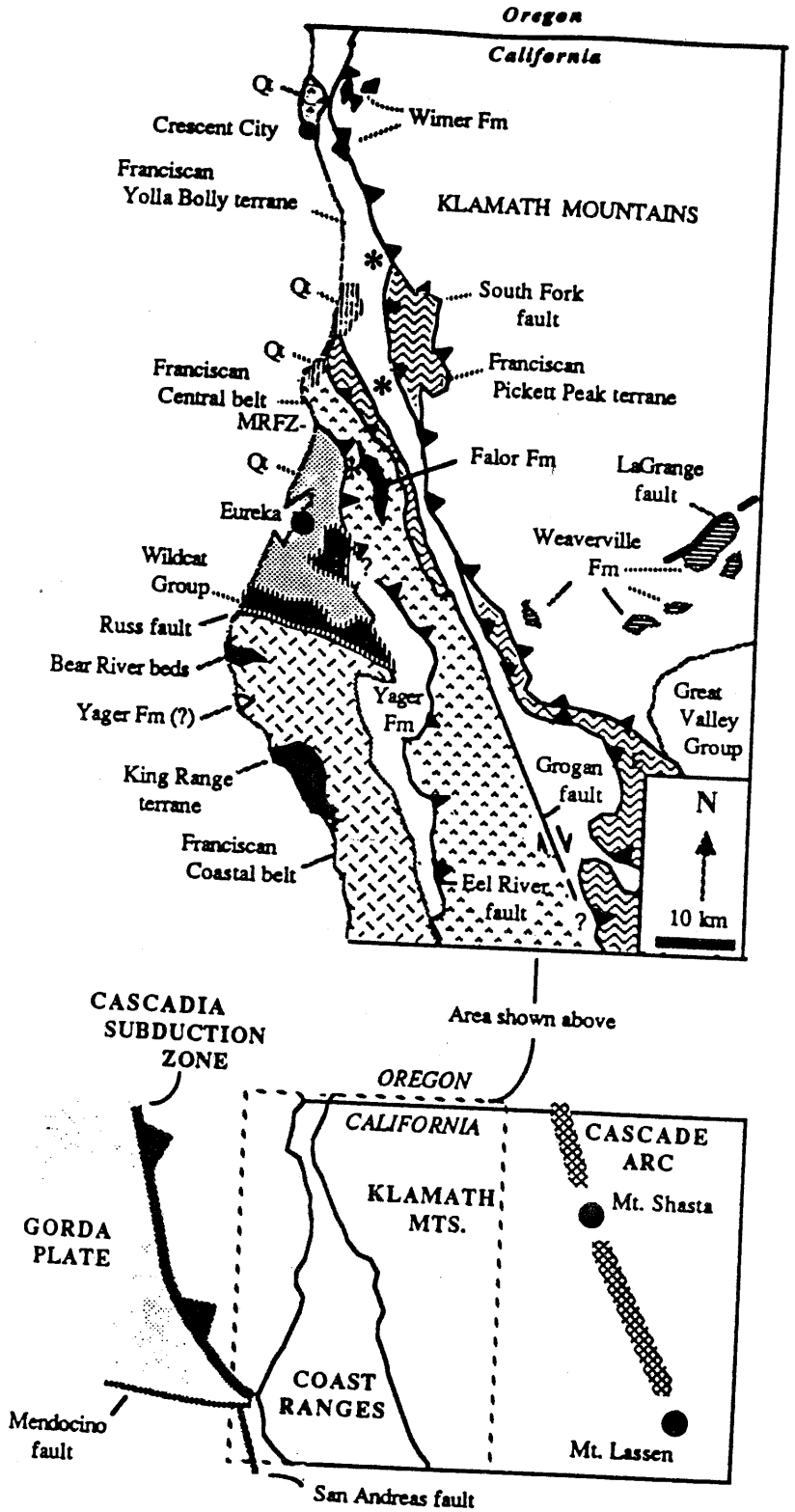

Generalized geologic map of northwestern California. Terrane nomenclature and distribution is from Blake et al. (1982, 1985a, 1985b), Miller and Aalto (1983) and Aalto (1989a). Qt depicts late Pleistocene and Holocene terrace deposits.

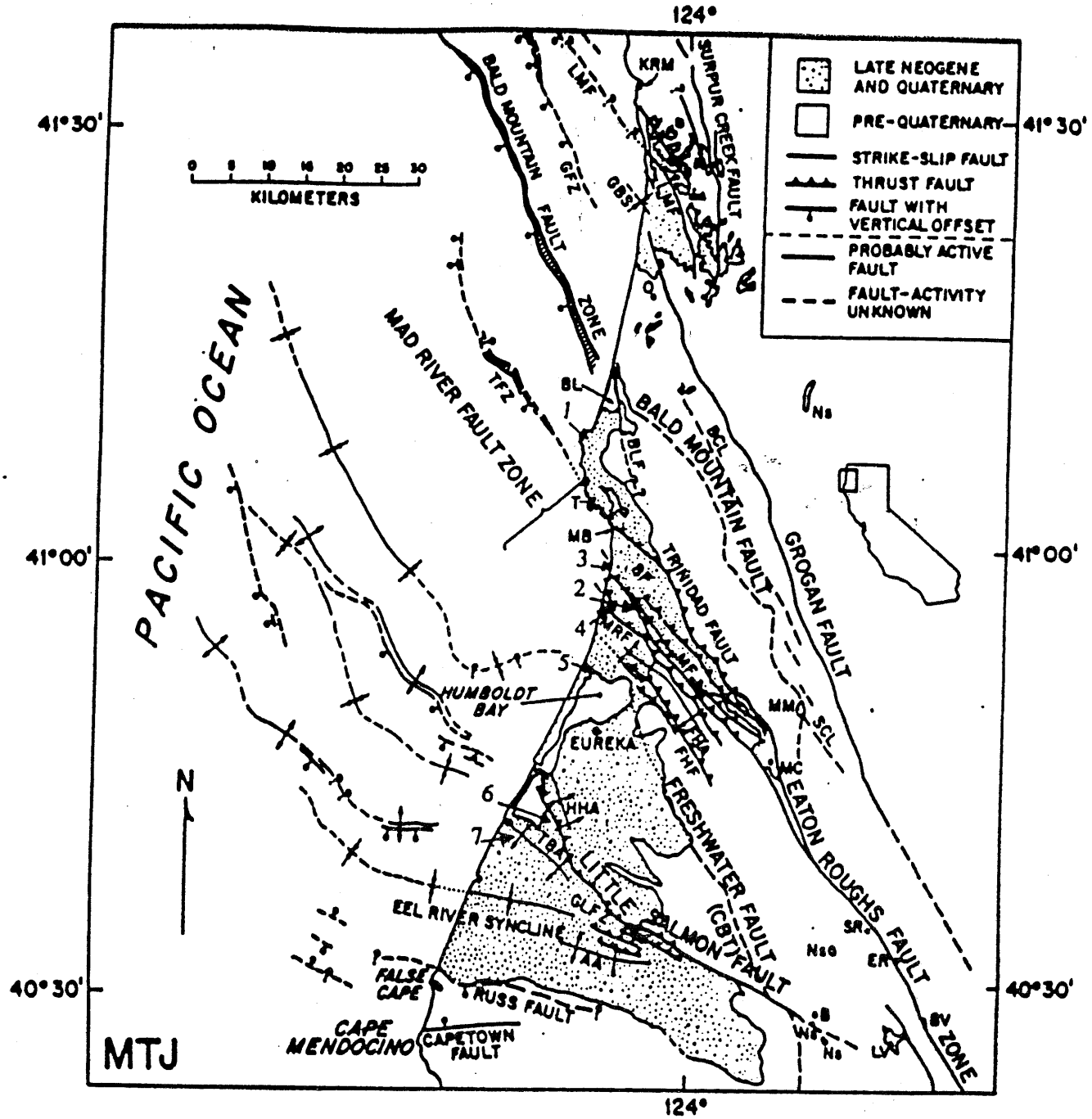

Map of the Humboldt Bay region showing some of the principal faults and folds at the southern end of the Cascadia subduction zone and the location of filed trip stops for Days 1 and 2.

ROAD LOG FROM PATRICKS POINT STATE PARK TO BEAR RIVER - DAY 1 AND 2

G.A. Carver, K.R. Aalto, and R.M. Burke

STOP 1 (and STOP 7 on your own tonight), Day 1

Agate Beach Pleistocene Section

Introduction

Quaternary units that unconformably overlie the Franciscan Complex within Patricks Point Park include a variably-tilted, unconformity-bound sequence of nearshore marine and non-marine sediments exposed in seacliffs at Agate Beach in the northeastern region of the park, and flat-lying to gently tilted marine terraces in most other areas. The total thickness of the Agate Beach section, extending north to Big Lagoon, is approximately 350 m. The section records marine transgression followed by oscillating nearshore marine, beach and lagoonal deposition (Nilsen and Clarke, 1987). The transgressive-regressive cycles most likely reflect glacially controlled Pleistocene sea level fluctuations. Page *et al.* (1982) provides information concerning dating and regional correlation of terraces. The following interpretations are from Aalto (1989).

Lower Agate Beach terrace

The lower Agate Beach terrace (Page, *et al.*, 1982) has been dated as being older than 0.73 Ma based on the paleomagnetic signature. At the south end of Agate Beach, this unit is approximately 15.5 m thick and consists of what are interpreted to be beach and lagoonal deposits that rest unconformably upon Franciscan unit KJFpp and tilt to the northeast at 12-14°.

To the west, the beach facies consists of tan conglomerate with chiefly subrounded clasts, tan sandstone, and intertonguing gray mudstone and tan sandstone, all arranged in a fining-upwards sequence. Crudely stratified boulder conglomerate forms a locally-derived, meter-thick basal lag deposit of metagraywacke and argillite that rests upon Franciscan rock. Above this 2.4 m of granule to pebble, parallel-laminated, crudely stratified conglomerate grades upwards into 4.1 m of medium to coarse-grained, laminated sandstone with occasional gravel-boulder lenses and trough crossbeds.

The top 8 m of the unit consists of intertonguing mudstone and massive to laminated, fine to medium sandstone with pebble lenses. Mudstone becomes more abundant to the east and is interpreted to be a lagoonal accumulation behind a barrier beach. In the very easternmost exposures, crudely stratified, inverse to normally graded, 1/2-1 meter-thick, clayey breccias intertongue with clayey mudstones and muddy sandstones. Breccia clasts consist chiefly of locally-derived Franciscan metagraywacke and argillite. These breccias are thought to have originated as debris flows that periodically swept into a narrow coastal lagoon.

Upper Agate Beach terrace

The poorly dated, late Pleistocene upper Agate Beach terrace (Page, *et al.*, 1982) consists of a thin basal lag deposit of Franciscan-derived, subrounded cobbles and boulders that rest upon an irregular buried erosion surface. Overlying this are crudely stratified, tan conglomerates and sandstones. These are arranged in repeating couplets that range in thickness from approximately 1/2-1 m. The couplets generally thicken upwards within the unit and consist of a basal one third pebbly sandstone or conglomerate and upper two thirds sandstone. The conglomerates typically contain poorly sorted, subangular to subrounded pebbles and grade upwards into pebbly sandstone or sandstone. The sandstones are typically medium- to coarse-grained, moderately to poorly

sorted, cross-stratified and may contain vertical burrows. Each couplet is interpreted as a major storm accumulation, with an upper portion later reworked by nearshore currents.

At the southern end of Agate Beach, the upper Agate Beach terrace is beveled by erosion and approximately 30 m thick. The unit rests in apparent disconformity upon the lower Agate Beach terrace. To the north its dip lessens and its thickness increases considerably, to approximately 300 m.

Patricks Point terrace

The Patricks Point terrace (Page, *et al.*, 1982) dips gently to the north in the northern region of the park where it rests in angular unconformity upon the upper Agate Beach terrace. Elsewhere it rests subhorizontally upon Franciscan rocks. It is approximately 15 m thick, interpreted to be a beach-backshore eolian dune deposit. The abrasion platform upon which this terrace accumulated is estimated to have been cut at 83 ka (Carver, 1985; Carver and Burke, this volume).

The base of the unit is marked by a thin pebble to cobble lag deposit. Clasts are generally subrounded and consist of chert, metagraywacke, argillite and a wide variety of volcanic and plutonic rock fragments, some of which may have been derived from a Klamath Mountains source. Overlying this are several meters of conglomerate-sandstone couplets similar to those described in the upper Agate Beach terrace. However, conglomerate is less abundant in these couplets. They grade upwards into large scale, trough cross-stratified, fine to medium-grained sandstones interpreted to be backshore dune deposits. Crossbed sets are as much as a meter thick. The upper part of the unit is poorly exposed.

Quaternary Tectonic Setting

Carver (1987) and Kelsey and Carver (1988) provide excellent summaries of the Quaternary tectonics of northernmost coastal California. Crustal strain within the North American plate results from the northward propagation of the Mendocino triple junction and subduction of the Gorda oceanic plate. It is accommodated by formation of numerous northwest-striking low angle reverse faults and associated folds. The progressive uplift and tilting of terraces in Patricks Point Park has resulted from intermittent displacement along active compressional faults located several kilometers both to the north and south of the park (the "Trinidad" and "Big Lagoon" faults of Carver, 1987). This ongoing deformation, combined with Quaternary eustatic fluctuations, accounts for the complexity of the Agate Beach stratigraphic section.

Mileage	Features of Geologic Interest
0.0	Parking lot - Agate Beach overlook
0.1	Octopus Grove - Old Sitka Spruce on N. side of camp site # 106-112 - subject to dendrochronological experiment with Jacoby.
0.7	Junction with Wedding Rock Loop Rd. - sea stacks on terrace - 2 levels may be different terraces (3D,4A??), or relief on platform, warping, or erosion.
1.3	State park entrance gate - large sea stack in trees on N. side of road is at terrace back edge.
1.4	Intersection with Scenic Dr. is on a terrace riser. Turn right and proceed on Scenic Dr. to Trinidad.

2.0	Driftwood Motel - the motel is on the top of the riser between the Patricks Point terrace and the Savage Creek (~105ka) terrace. The Savage Creek terrace is on the east side of the road.
2.2 - 2.4	Road is on riser.
2.55	Small piece of Savage Creek terrace at Oceanside Lodge.
3.2	Scotty's Point - Here one sees coastal landslides and melange slump earthflows.
3.8	Near the southern end of landslides and Savage Creek terrace remnants.
3.9	Road is on riser.
4.0	Intersection with Seawood Dr. - Note terrace riser.
4.3	Seacliff Motel - Patricks Point terrace is west of the road.
4.6	Intersection with Stage Coach Road - Larrupin Restaurant is on riser.
4.9	Bishop Pines - Savage Creek terrace.
5.9 - 6.0	Warped (?) edge of Savage Creek terrace.
6.0 - 6.2	Riser between Savage Creek terrace and Patricks Point terrace.
6.2	Ocean Grove - Patricks Point terrace on up side of Trinidad fault.
6.6	Trinidad - The town of Trinidad is located on the Patricks Point terrace. One branch of the Trinidad fault forms the scarp offseting the terrace behind the gas station.

Continue south on **SCENIC DRIVE (NOT ON HIGHWAY 101)**

7.1	View of the coastline cut into Franciscan melange. Sea stacks are blocks of greywhake sandstone, greenstone, and chert tectonically emplaced in highly sheared shaley matrix which erodes easily.
7.4	View of coast back to Trinidad Head.
7.5	Bingo
7.6	Offshore rocks at base of melange. One lane road!
7.8	Earth flow on left exposes shallow water marine sand beneath terrace above.
8.5	Luffenholtz Creek - active melange earthflows and road damage. Caution!
8.7-8.8	Luffenholtz parking area, raised terraces at mouth of creek above road to the east (inland). This is probably the 3c terrace.

9.0	Honda Point - roadcuts for the next several hundred meters expose the "Moonstone" sediments, probably of mid Pleistocene age. The late Pleistocene terrace is cut into these shallow marine sands at the top of the steep slope above the road.
9.5	Intersection with Westhaven Drive.
9.7	Moonstone Beach, mouth of the Little River. The Trinidad fault intersects the coast at this point. South of the fault a thick section of mid Pleistocene "Moonstone" and Falor formation sediments provides a uniform easily erodible material for coastal processes to cut a smooth straight coast, in contrast to the irregular shoreline cut into Franciscan rocks north of the fault.
9.8	Intersection with U. S. 101
10.3	Little River
10.9	Clam Beach terrace - for the next several miles U. S. 101 traverses this late Holocene raised terrace. The Paleo-sea cliff on the left side of the freeway was cut about 1100 years ago.
12.1	**CLAM BEACH EXIT** - Exit freeway, turn right at stop sign, and park in parking areas in Clam Beach Co. Park. Walk south on beach ~ i mile to the mouth of the Mad River. (Note, we may shuttle with busses to the river mouth, be alert for an announcement during trip).

STOP 2, Day 1, Mouth of the Mad River, Clam Beach.

This stop provides the opportunity to see a part of the McKinleyville fault in cross section where it is exposed in the recently eroded cliffs adjacent to the mouth of the Mad River. Also exposed at this location are the cover sediments on the Clam Beach terrace, a raised late Holocene marine terrace.

McKinleyville Fault.

The fault in the shallow subsurface is composed of many closely spaced small-displacement fault strands and fractures extending across a several hundred meter wide zone. The faults are arranged into two sets, a primary (synthetic) northeast dipping set and an secondary (antithetic) southwest dipping set. The dips range between 25 and 50 degrees, and the two sets of faults define a conjugate pattern indicating northeast-southwest directed nearly horizontal compression and columb fracture failure. The faults cut late Pleistocene shore facies sediments. Bedding changes from horizontal at the south end of the faulted zone to steeply south dipping at the north end of the exposure near the middle of the zone, indicating much of the displacement has been accommodated by folding and rotation of fault bounded blocks within the fault zone.

Clam Beach Terrace.

The Clam beach terrace is a late Holocene marine platform covered by a sequence of beach and dune sands containing a buried soil, layers of peat, and fossil trees. The platform is cut into faulted and folded late Pleistocene sediments. The shore line angle and landward part of the platform is presently several meters above highest water level, indicating the terrace has been raised at least several meters. Driftwood deposited in beach sands lying directly on the platform provide a ^{14}C age estimate for initial uplift of the terrace of 960-1257 yBP.

The dune sequences above the beach deposits are interpreted to have formed as a result of two (and possibly three) sudden (coseismic) uplift events. Each uplift event elevated the terrace platform and resulted in regression of the shoreline, exposing the adjacent seafloor and generating a source for the dune sand. The dune sequences are separated by a weak buried soil indicative of a period (interseismic) of non-deposition and weathering. The outer wood of fossil trees rooted in the buried soil provide ^{14}C ages of about 300 yBP.

Near the abandon sea cliff in the position of the back dune hollow the buried soil grades into a layer of peat, interpreted to reflect organic accumulation in the hollow during the period of soil development. The uppermost part of this peat also dates to about 300 yBP. Adjacent to the abandon sea cliff the peat is directly overlain by a landslide deposit derived from the sea cliff. The landslide tip and the seaward part of the peat layer is in turn overlain by a rhythmically bedded lacustrine mud composed of about 20 finning up layers, each interpreted to represent storm-wash sedimentation during one winter storm season. This lacustrine layer contains entombed marsh plants (Carix sp.) rooted in the peat and buried in upright growth position. The same type of fossil plants are crushed and buried beneath the landslide.

Layers of descidous plant leafs, mostly willows and alders, are present at the base and top of the lacustrine muds and along bedding surfaces in the overlying dune sands. These leaf layers probably represent the seasonal leaf fall during the autumn prior to the deposition of the muds, and the several years following the mud deposition.

Our interpretation of this sedimentary sequence is that the buried soil, peat, and trees were developed during the pre-seismic interval prior to an earthquake which elevated the terrace a second (or third) time about 300 years ago. During the earthquake, the old sea cliff failed, the resulting landslide partially filled the back dune hollow, impounding storm runoff during the succeeding winter. Within a few years the upper dunes were deposited, stabilized and the modern soil and vegetation cover began to developing at the present ground surface.

RETURN TO FREEWAY HEADED SOUTH.

13.4	Vista overlook, good view of the Mad River mouth and Clam Beach.
14.0	McKinleyville fault - a wide zone of distributed faulting results in the gentle sloping scarp with about 33 meters of vertical offset of the Patricks Point terrace The scarp is just south of the Co.airport on the left (east) side of the freeway.
16.5	South of the McKinleyville fault the Patricks Point terrace is relatively undeformed to about this location, where folding and warping of the terrace becomes apparent as the Mad River fault is approached.
17.2	**EXIT FREEWAY AT SCHOOL ROAD**, turn left at stop sign and cross freeway overpass.
17.5.	Turn left onto Windsor Avenue and park in the Church parking lot.

Stop 3, Day 1, Mad River fault.

The Mad River fault cuts the marine terraces at McKinleyville along four imbricate fault traces spaced several hundred meters apart, resulting in a zone of faulted and deformed terraces more than a kilometer wide (Figure 4). The multiple surface trace the vertical separation of the stage 5A (~83 ka) across the deformed zone at this location is about 40 meters. Trenches and limited stream bank and roadcut exposures along the fault in this vicinity show the fault has a shallow (20-30 degree) dip to the northeast. The late Quaternary slip rate for this fault, based on measurements of the

terrace offsets and the vertical separation of the base of the Falor Formation is estimated to be about 1.5-2.0 mm/yr.

Trenches at several locations across the most prominent scarp of the northern fault trace show considerable variation in faulting style. A single low angle thrust extending to the surface, a wide zone of conjugate faults and fractures similar to the beach exposure of the McKinleyville fault, and a tight overturned fold can all be observed at this location. Figure 5 shows the log of one trench which is expressed at the surface as a fold. In this trench, highly plastic Franciscan melange is folded into a sharp recumbent anticline. Beneath the overturned limb of the fold, a stack of at least six colluvial sheets are present. Each colluvial layer is capped by a weak buried soil. The colluviums were derived from the growing scarp with each sheet separated by a growth event of the fold. ^{14}C ages for detrital charcoal from the top of colluvium 4 and the base of colluvium 5 produced ages of about 10 ka, indicating 2 or 3 Holocene events on this trace of the Mad River fault.

17.7	**Return to U. S. 101 headed south.** Travel along the fault to the Mad River bridge.
19.5	Mad River Bridge. Cross bridge and cross late Holocene fluvial terraces of the Mad river. This area was inundated during the 1964 flood.
21.3	Leave late Holocene flood plain and climb onto late Pleistocene marine terrace.
22.0	Sunset Avenue. Humboldt State University is to the left (east) of the freeway. Continue straight ahead on U. S. 101 through Arcata. **TAKE SAMOA EXIT TO THE WEST,** continue ~ west on Samoa Blvd to the FOP parking area near the Slough .

STOP 4, Mad River Slough

Mad River slough and adjacent parts of northern Humboldt Bay are located in the axis of the Freshwater syncline, one of the large synclines of the Cascadia fold and thrust belt. Episodic sudden late Holocene subsidence of the axis of the Freshwater syncline has resulted in pulses of estuarine sedimentation around the margins of the northern end of Humboldt Bay. Intervening periods of salt marsh development has allowed for the accumulation of marsh peats on the top of each estuarine mud layer. The resulting stratigraphy contains a record of subsidence events interpreted to be coseismic and caused by large thrust earthquakes, possibly subduction zone events. Similar late Holocene marine mud and marsh peat stratigraphies are present at the south end of the bay and near the mouth of the Eel River, both located in large fold and thrust belt synclines.

Evidence for sudden subsidence at Mad River slough includes sharp contacts between the peats and overlying muds, entombed salt marsh plants in upright growth position in the overlying muds, and near the margins of the marsh, buried forests in growth position. Inspection of outer growth rings of these trees indicates robust growth through the last year of life and nearly simulations death (most trees either died in the same year or within several years).

In the Mad River Slough up to 5 buried peat layers have been identified in the upper 4 meters of sediments (Figure 6). Three of these are widespread and can be traced at low tide in tidal channel bank exposures continuously throughout the Mad River Slough area. ^{14}C age estimates for the tops of these widespread peats are about 300, 1100, and 1600 ybp. These ages are similar to ages for buried salt marsh peats found along the coasts of Oregon and Washington. An additional peat layer found at one location in the Mad River Slough produced an age of 540-1258 ybp. At several locations the 1100 ybp layer consists of two distinct peat horizons separated by 30 -50 cm of non-organic marine mud, suggesting the possibility that two subsidence events occurred over a short time interval.

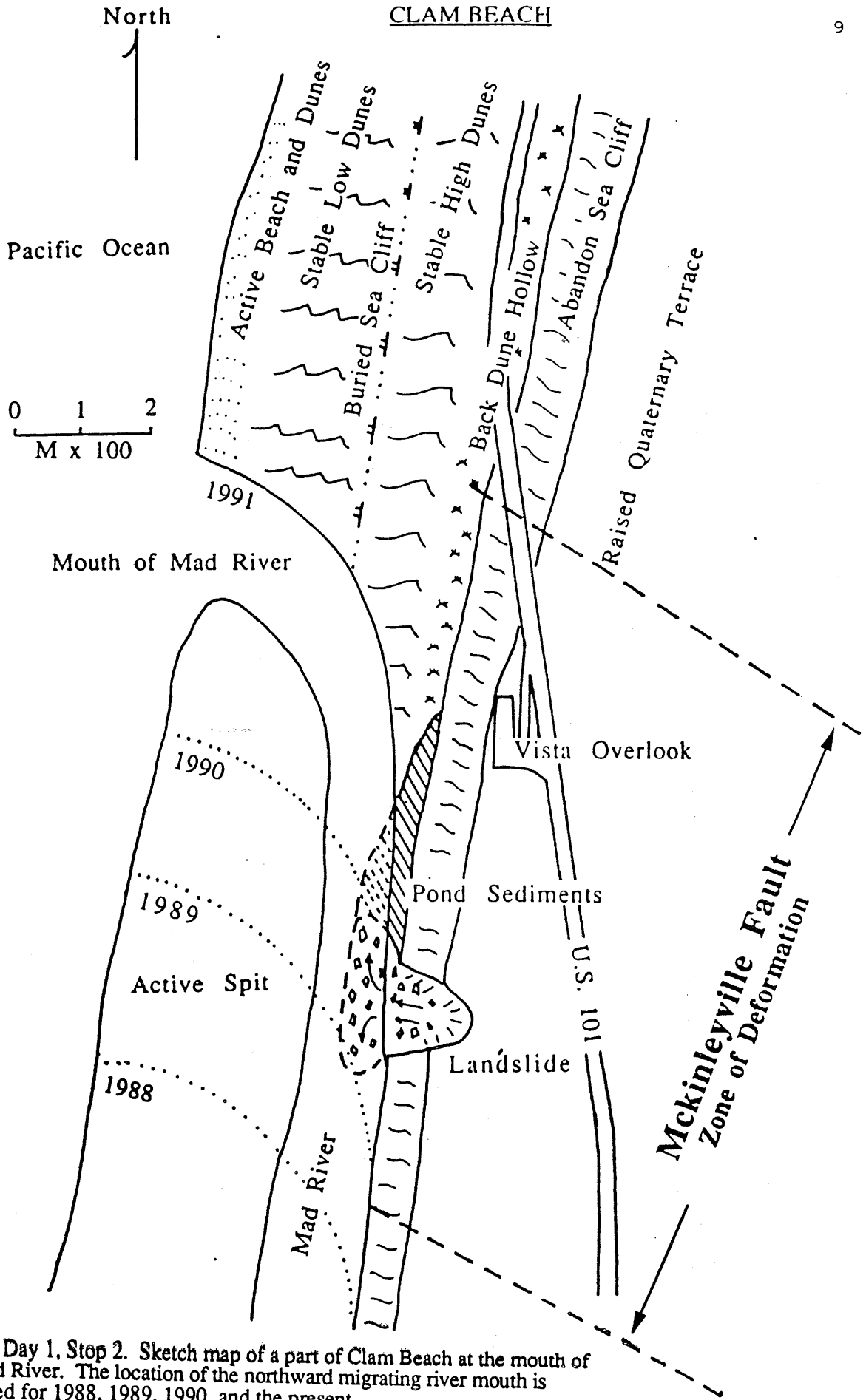

Figure 1: Day 1, Stop 2. Sketch map of a part of Clam Beach at the mouth of the Mad River. The location of the northward migrating river mouth is indicated for 1988, 1989, 1990, and the present.

CLAM BEACH STRATIGRAPHY

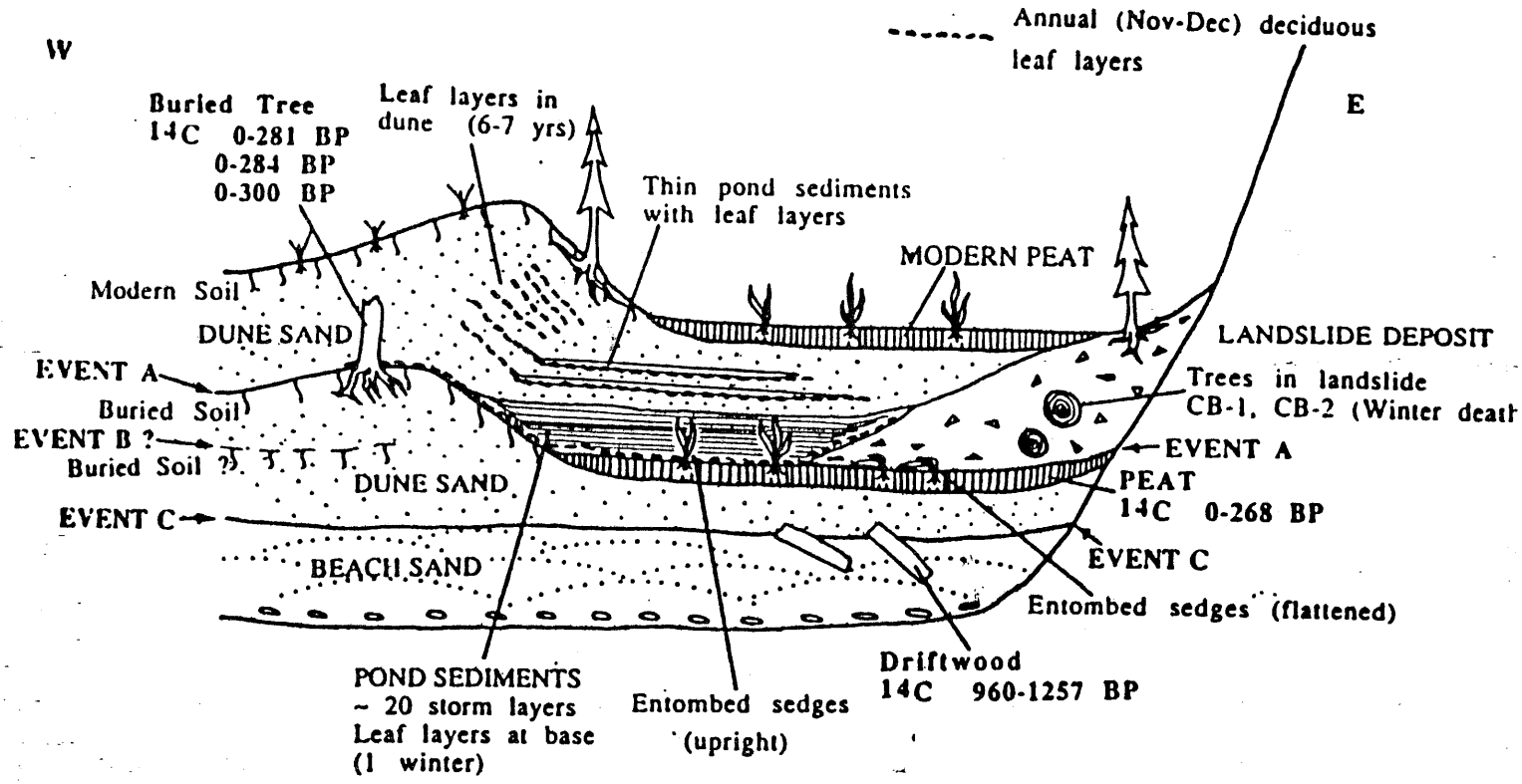

Figure 2: Day 1, Stop 2. Diagrammatic cross section of the cover sediments on the Clam Beach terrace at the mouth of the Mad River.

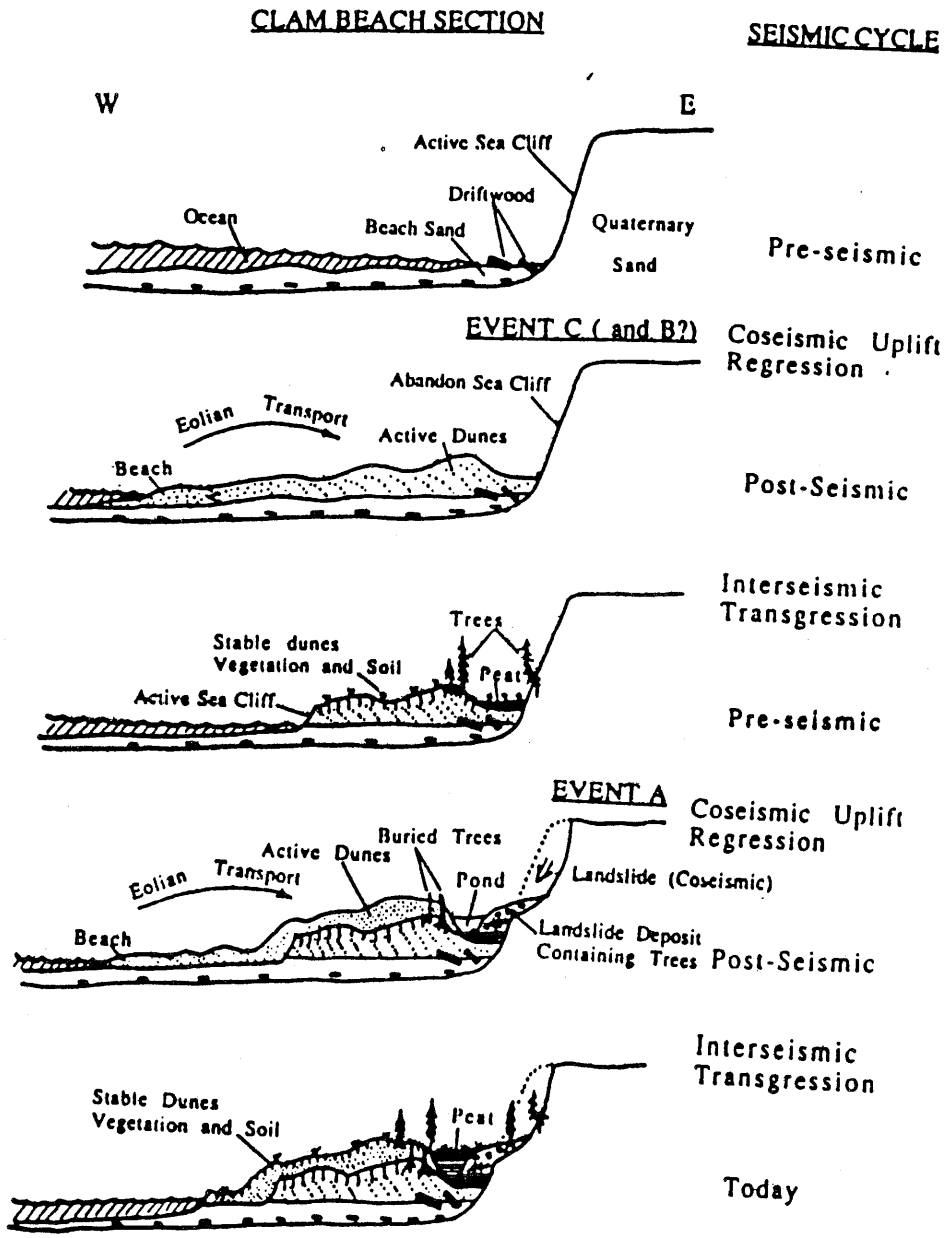

Figure 3: Day 1, Stop 2. Schematic diagrams of the development of the cover stratigraphy on the Clam Beach terrace.

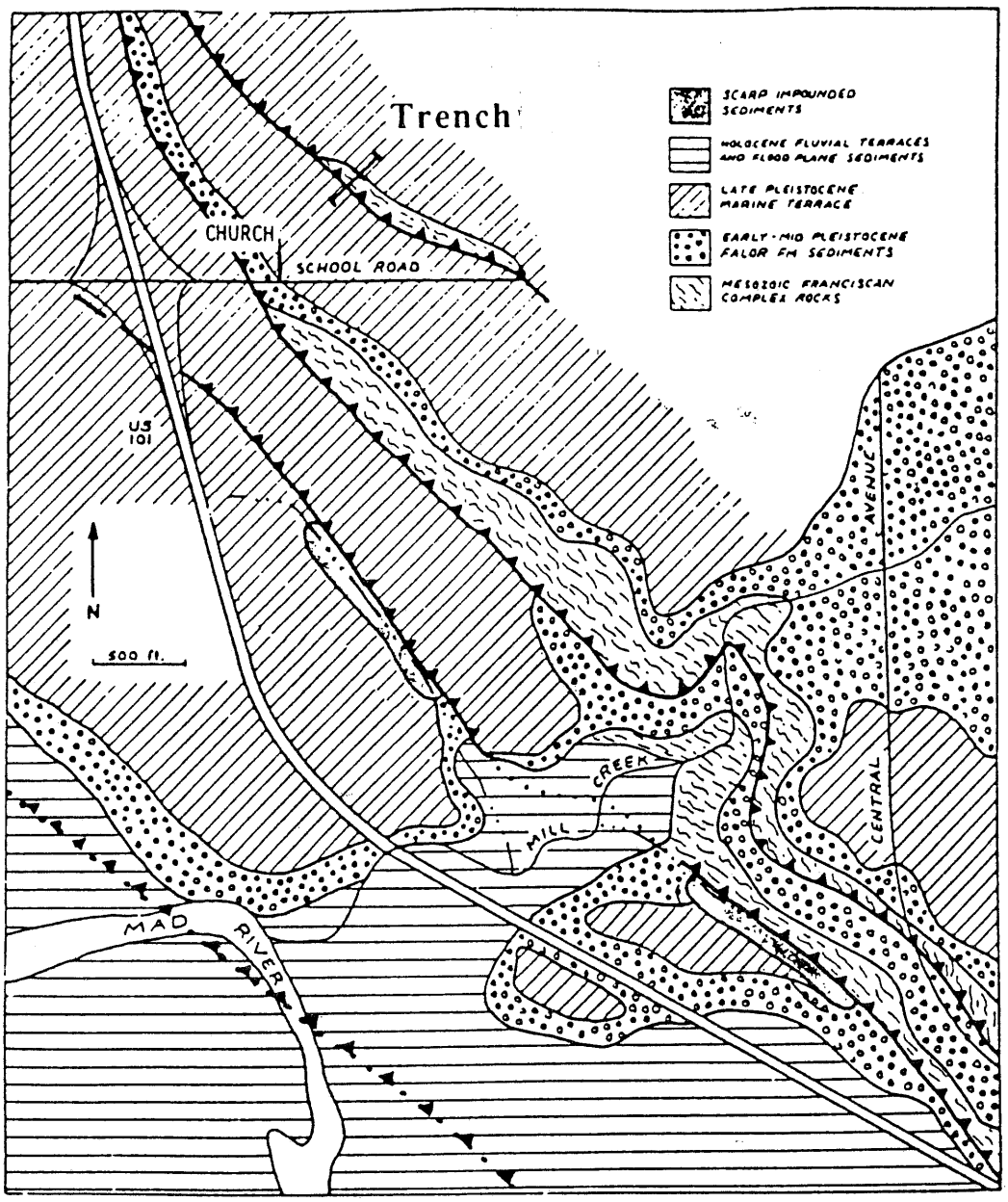

Figure 4: Day 1, Stop 3. Map of faulted late Pleistocene terraces at the Mad River fault in McKinleyville.

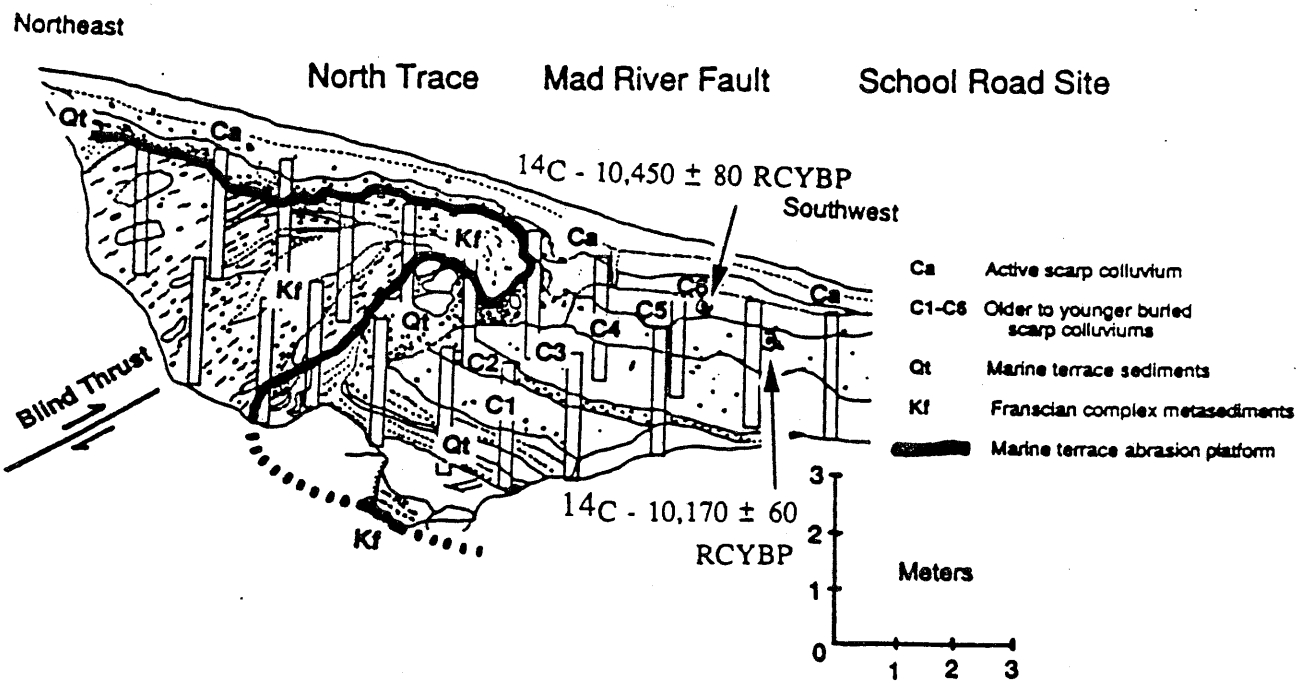

Figure 5: Day 1, Stop 3. Generalized trench log of the northern strand of the Mad River fault at McKinleyville.

CALIBRATED ^{14}C AGES - MAD RIVER SLOUGH

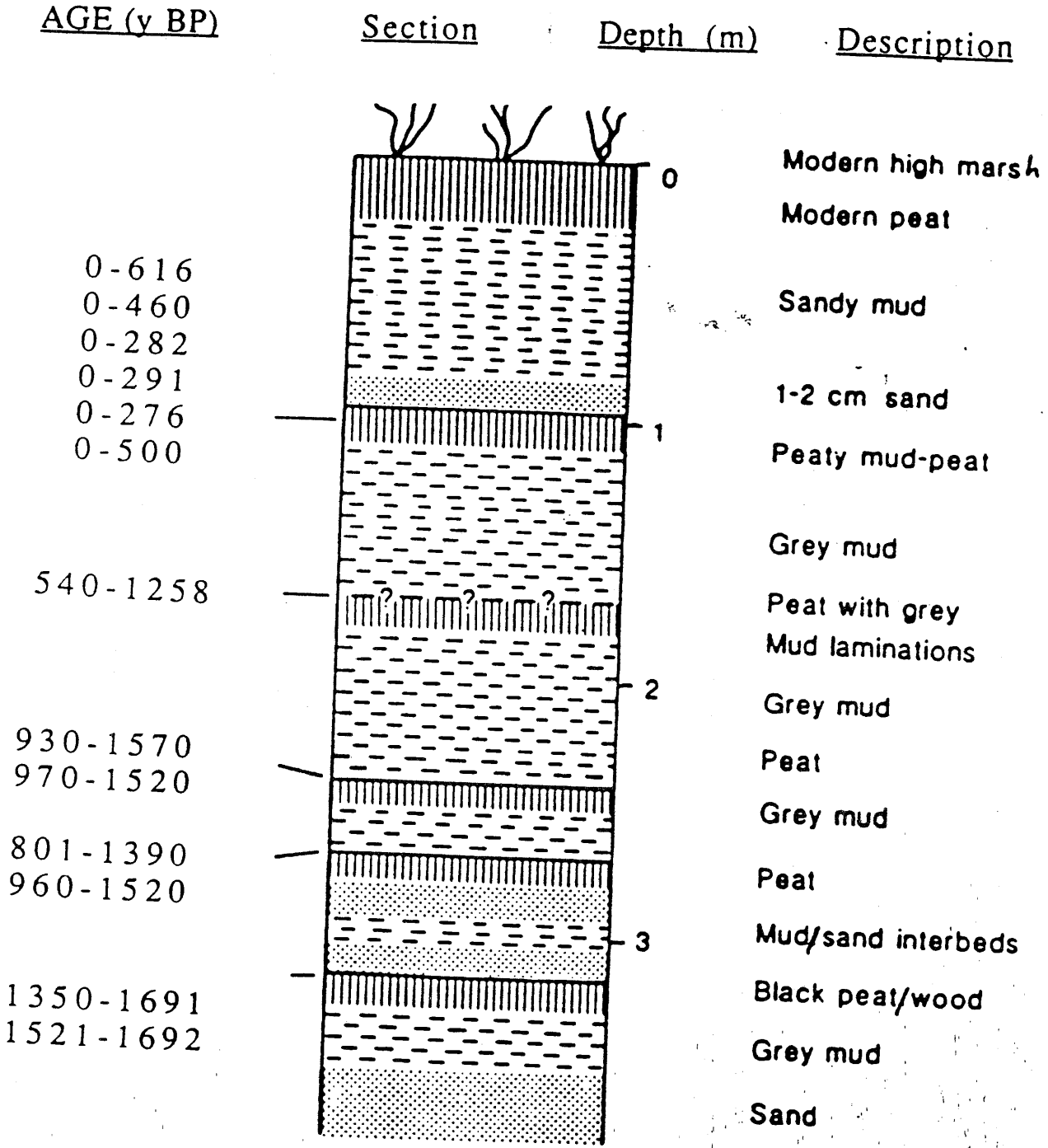

Figure 6: Day 1, Stop 4. Composite stratigraphic column and ^{14}C ages for buried salt marsh peats at the Mad River Slough, northern Humboldt Bay.

WE WILL TURN AROUND AT THIS POINT AND HEAD NORTH TO STOPS 5 - 7 FOR THE COMPLETION OF DAY 1

RETURN TO CAMPGROUND AND RESUME ROADLOG HERE ON DAY 2

22.4	The downtown Plaza of the city of Arcata is to the west of the highway
22.9	The escarpment most noticeable to the east, near the new ball field and the bright blue roof is the Fickle Hill Fault, part of the Mad River fault zone. This fault extends inland along the base of Fickle Hill, a large anticline in the tip of the upper thrust sheet. Fickle Hill is the large ridge southeast of Arcata.
23.5	To the west is the shallow Arcata Bay, a former deep water port. For TL dating of bay muds, see Berger (this volume). This part of Humboldt Bay occupies the axis of the Freshwater syncline. Marshes around Arcata Bay are underlain by buried peats and mud sequences interpreted to reflect coseismic subsidence during subduction zone earthquakes (see Valentine et al this volume.
29.1	Bridge over the Eureka Slough
29.4	Entering downtown Eureka, this is your <u>last opportunity to pick up supplies and gas</u>.
30.2	The highway is built on raised Quaternary marine terraces of unknown age
30.5	Here the highway is on Holocene bay fill
32.2	The Bayshore Mall is the shopping center on your right, This was tidal marshland prior to development.
33.1	Leaving Eureka and the last easy place to get gas or supplies
34.1	The Elk River Valley off to the east is formed at the base of the northwest trending Humboldt Hill Anticline (weather permitting non drivers may be able to spot a large TV tower high on the axis of this anticline). Older marine terraces are visable on the north side of the valley.
34.7	The surfaces to the east of the highway are raised marine terraces (from ~80 ka near the radio station tower to > 200 ka at the TV tower high on the anticlinal axis), these terraces are warped by the Humboldt Hill anticline
35.2	The Pacific Gas and Electric decommissioned nuclear power plant on the west. There is still natural gas fired turbines in production at this plant, utilizing the gas from the Table Bluff-Tompkins Hill anticline to the south.
37.5	Highway is along the Little Salmon fault for the next several miles. Humboldt Hill to the left is a large anticline above the thrust tip of the fault. Views to the southwest across the South Bay to Table Bluff. The South Bay occupies a large syncline and contains subsidence stratigraphy (see Valentine et. al. this volume). Table Bluff is the crest of a large anticline which folds late Pleistocene terraces.

37.5	Tompkins Hill overpass - collapsed during the 1980 M=7.0 earthquake.
38.2	The College of the Redwoods to the west along the trace of the Little Salmon fault.
39.4	South Bay Syncline, the Little Salmon fault remains at the base of the hills to the east
40.2	Intersection with Hookton Road is where Highway 101 starts up the hill on a warped marine terrace on the Table Bluff Anticline.
41.2	Top of the hill is also the structural top of the Table Bluff Anticline and in marine sediments which contain the Loletta Ash (Bend Pumice tuff ~ 325 ka, Sarna-Wojcicki, 1992) within a few kilometers east of here.
43.6	**TAKE THE EXIT TO FERNDALE OFF OF HIGHWAY 101** and proceed to Fernbridge
43.8	Stop sign - Go straight toward Ferndale.
44.5	Stop sign. Fernbridge - Turn right and cross the Eel River.
46.5.0	Eel River valley. The valley occupies the Eel River syncline. Near the mouth of the river stratigraphy indicative of coseismic subsidence is present (see Li, this volume.) This part of the valley was subjected to severe flooding in 1964.
48.0	Ferndale, a farming and tourist town. Turn right at the end of main street and continue to Centerville Beach (about 5 miles).

Stop 1, Day 2. Centerville Beach

At Centerville Beach we will examine the uppermost Wildcat Group and younger terrace deposits. Ogle (1953) mapped the terraces as Hookton Formation and provides the following description of this exposure:

"Approximately 420 feet (127 m) of ocherous, orange-brown, poorly consolidated, medium- to coarse-grained sandstones and pebble conglomerates. The beds are a few inches to over 20 feet thick, locally strongly cross-bedded, and somewhat lenticular. The grains are individually coasted with iron oxides. This unit overlies the Wildcat Group with an angular unconformity." (Ogle, 1953, p. 117).

On his geologic map, Ogle shows an angular discordance between the Hookton Formation and subjacent Rio Dell Formation of less than five degrees. The beach exposure of the Hookton Formation contains what we interpret as fluvial deposits, chiefly cobble to pebble conglomerates and sandstones with subordinate lenses of claystone that grade laterally into, or are channelled into and interstratified with, laminated sandstones. In places the conglomerates are imbricated, normally graded and consist almost entirely of common Franciscan clast lithologies such as graywacke, chert, greenstone and blueschist, similar to modern Eel River gravels. Sandstones and conglomerates are commonly arranged in couplets, with a sharp base, overlain by coarse-grained conglomerate grading up into cross-stratified sandstone. The lenticular nature of these couplets suggests deposition by aggregation of longitudinal bars in braided river channels. Sandstone very

likely accumulated in second and third order channels developed on bar crests, and clay drapes in abandoned channel segments.

The laminated sandstones contain stringers of well rounded Franciscan-derived clasts and occasional subvertical burrows. Laminations cross cut at low angles, indicative of swash cross-stratification developed in the vicinity of berm crests. Steep-sided conglomerate-filled channels may have originated in the littoral zone in response to erosion by rip currents. A marine origin for this lower unit suggests that it may be correlative with the Scotia Bluffs Formation, which is exposed a kilometer inland. If this is so, these deposits may in fact be Carlotta Formation, the uppermost unit in the Wildcat Group (see Moley, this volume). It is unfortunate that due to cliff erosion, a meter-thick zone of highly convoluted lamination, overlain disconformably by laminated sandstone, has vanished. It very likely had originated in response to earthquake shock, and thus would qualify as a 'seismite'. The April, 1992, earthquakes resulted in extensive rockfalls all along this seacliff.

Along the beach, a large debris slide that has developed along bedding in the upper Rio Dell Formation obscures the contact between the laminated sandstone described above and Rio Dell mudstone. This sort of land failure is common along steep seacliff that front exposures of the Wildcat Group at Centerville Beach. Many of these slides were reactivated during the April earthquakes. On the south side of the slide, Rio Dell rocks consist chiefly of highly bioturbated, crudely laminated sandy mudstone. Laminations are at the scale of decimeters and defined by changes in color tones from light to dark gray, which probably reflect variations in clay content. The mollusk *Pectin carinus* is common, and the condition of most shells suggests little transport after death. There are, however, some thin layers and lenses of shell hash with a sandy matrix which might have originated in conjunction with storm wave erosion of continental shelf sediments. This environment of deposition is supported by fossil assemblages in the upper Rio Dell Formation (Ogle, 1953). Some sandy lenses that apparently have escaped bioturbation exhibit wavy, low angle laminations that may have originated as hummocky cross-stratification. Others may be scour depressions formed by bottom fish.

Weather permitting, looking south at Centerville Beach one can see Franciscan seastacks that project seaward at the False Cape shear zone, the faulted base of the Wildcat Group.

RETURN TO CARS AND RETURN TO THE PETROLIA TURNOFF IN FERNDALE WHERE YOU CAN ONCE AGAIN FOLLOW A ROAD LOG. PROCEED WITH CAUTION OVER THE WILDCAT GRADE AND RECONVENE AT MERRITTS STOP #1 (SEE ROAD LOG BY MERRITTS AND DUNKLIN - MILE 28.2)

ROAD LOG FOR THE MATTOLE ROAD, FROM FERNDALE TO CAPETOWN, BEAR RIVER VALLEY.

Reset mileage to zero at start of the Mattole Road.

(* indicates an especially nice stop)

Mileage	# cars/pullout	Features of geologic interest
0.0	--	Start of Mattole Rd. at 'Capetown/Petrolia' sign in Ferndale. Fluvial conglomerates and marine sandstones of the Carlotta Fm exposed along the right side of road. WINDING NARROW ROAD--BE CAUTIOUS AND PARK OFF PAVEMENT!
0.2	2	Fluvial conglomerates and marine sandstones of the Carlotta Fm

		to the right. Within this formation there are at least three marine-nonmarine cycles represented (assuming no fault repetition). Conglomerates exhibit features characteristic of braided river sedimentation and are in many sites channeled into swash-cross stratified sandstones containing pebble stringers, interpreted as beach deposits. Pebble clasts are chiefly composed of such Franciscan Complex lithologies as graywacke, greenstone, chert and blueschist, similar to modern Eel River gravels. Marine-nonmarine cyclicity is very likely induced by glacial-eustatic sea level fluctuation.
0.9	2	Carlotta Fm conglomerate to the right.
*1.0	4	Carlotta Fm fluvial conglomerate channeled into marine sandstone to the right. Best exposure of these relationships along the Mattole Rd.
1.3	none	Carlotta Fm conglomerate channeled into marine sandstone to the right. Base of the Carlotta Fm.
*1.5	3	Scotia Bluffs Fm--swash-cross stratified sandstone containing pebble stringers to the right; interpreted as a beach deposit. Best exposure of this formation along the Mattole Rd.
1.7	2	Upper Rio Dell Fm. to the left. Cross-stratified medium bedded sandstone interpreted as a shoreface deposits.
*2.0	4	Upper Rio Dell Fm. to the right. Thick muddy sandstone underlain by shelly, heavily bioturbated mudstone interpreted as an inner shelf deposit. Portions of hummocky cross-stratified fine sandstone beds have in places survived bioturbation. Best exposure of this member of the Rio Dell Formation along the Mattole Rd.
2.6	2	Poor exposure of Middle Rio Dell mudstone to the left.
2.9	2	Poor exposure of Middle Rio Dell mudstone with a blocky fracture pattern to the left.
3.1	4	Poor exposure of Middle Rio Dell mudstone with a blocky fracture pattern to the left.
*3.6	4	Middle Rio Dell Fm turbidites containing faults and associated drag folds to the left. 2 parking spaces before and 2 after the roadcut. Best exposure of this member of the Rio Dell Formation along the Mattole Rd.
3.8	none	Middle Rio Dell Fm turbidites and fossiliferous mudstones to the left. Head of Guthrie Creek.
4.0	--	Corral on right.
4.2	3	Folded Middle(?) Rio Dell Fm turbidites to the left.

4.3	2	Lower(?) Rio Dell Fm turbidites to the left.
4.8	4	Thick lower(?) Rio Dell Fm turbidites to the left.
5.1	4	Eel River Fm mudstone to the left. In the distance to the south, one sees an end to forest cover that marks to contact of the Wildcat Group with the False Cape shear zone ('FCSZ').
5.2	--	Corral on left.
*5.4-5.6	many	Long roadcut on right of Eel River Fm mudstone and turbidites, some of which are rich in glauconite. Many faults cut bedding. Best exposure of the Eel River Formation along the Mattole Rd.
5.7	none	Appx. position of the contact between the Eel River and Pullen Formations. No good exposures of the Pullen exist on the Mattole Rd.
6.1	--	Intersection with Bunker Hill Ranch Rd to the left. This marks appx. base of the Pullen Fm, which is in contact with the Yager Fm according to Ogle (1953).
6.4	--	The position of the east-west trending Russ fault, which juxtaposes Yager Fm (north side) against rocks of the FCSZ, according to Ogle (1953). On Ogle's map, the width of the Yager Fm outcrop along the Mattole Rd. is 0.25 km, and widens to the east to appx. 1 km at the Scotia Eel River field trip stop (although K.R. Aalto and K. Moley feel the Yager outcrop is about half this width, based upon consideration of lithology and structural fabrics of west bank exposures). The Yager outcrop belt thins, then terminates appx 3 km west of the Mattole Rd, where the Wildcat Group is juxtaposed against the FCSZ along the Russ fault (Ogle, 1953). In this area, Yager rocks may in fact be tectonic blocks ('knockers') in the FCSZ. Where exposed, the Russ fault is near vertical.
6.8	--	Big barn on left
*7.1	2	Vista point. To the north (weather permitting), one can see Humboldt Bay flanked on the south by Table Bluffs, the northern margin of the Eel River syncline. In the foreground are a series hills whose flatiron morphology is controlled by east-west striking, north-dipping beds of the Wildcat Group on the southern margin of the Eel River syncline. Here on the thinning edge of the North American plate tilting is occurring in response to the northward driving of the Gorda wedge (Carver, this volume).The small hills in the Eel River valley bottom north of the river are sustained by growing anticlines associated with active thrust faults.
7.4	--	Sandstone knockers of the FCSZ to the right. The shear zone contains an assortment of phacoidal knockers suspended in sheared shale. Sandstone knockers are most abundant, but trace amounts of greenstone and chert are present along the coast at

		False Cape. Here and immediately north of Cape Mendocino, Neogene and Franciscan sandstones are structurally interleaved at both map, outcrop and thin section scale. Some faults that cut Neogene rocks contain sheared serpentinite. The FCSZ has developed in conjunction with Gorda wedge migration and extreme crustal shortening and structural imbrication of previously accreted Mesozoic and Cenozoic rocks. The near vertical foliation and sub-horizontal lineation that characterizes the shear zone probably originally formed in conjunction with subhorizontal shearing along a multitude of thrust faults during the early stages of structural imbrication of the upper plate leading edge, and structures have since been rotated to their present orientation as uplift occurred (see articles by Carver and Aalto, this volume). Indeed, larger isolated bodies of Neogene rocks such as those of the 'Bear River beds' may in fact be shear zone knockers.
7.7	--	Sandstone knocker to the right.
7.9	--	Sheared shale on the left. FSCZ landscape is strongly influenced by the susceptibility of shear zone matrix to mass wasting (note the prevalent hummocky topography, poor drainage and numerous slump scars and earthflows). Large knockers underlie many of the rounded knobs. Tree cover may be prohibited by widespread soil creep.
8.2	--	Sandstone knockers to the left.
8.4	2	Sandstone knockers to the left.
9.7	--	Sandstone knocker in roadcut on left.
10.0	--	Bear River Valley in foreground; Cape Mendocino to the southwest.
*12.8	4	Vista point. View of Bear River Valley with flights of Holocene terraces flanking the river. Late Pleistocene marine terrace gravels mantle the flat-topped ridges to the south.
13.8	--	Valley bottom.
14.1	--	Bear River bridge.

IF YOU HAVE BEEN USING THIS ROAD LOG, IT IS TIME TO SWITCH TO THE ROAD LOG BY MERRITTS AND DUNKLIN - THEIR MILEAGE 18.8 AT THE BRANSTETTER BRIDGE IS THE SAME POINT AS THIS MILEAGE 14.1 - BEAR RIVER BRIDGE.

We reconvene at the Merritts and Dunklin STOP 1, mileage 28.2 - McNutt Gulch/Mussell Rock. Parking will be a serious problem. We will have students and trip leaders helping you get to the right (west) side of the road and leaving the county road with only one lane left for public travel. We are walking south along the beach from this point. This was originally scheduled as a regular stop as indicated in the Merritts and Dunklin road log, it has since become the focus of an intense research effort relating to the uplifted terrace associated with the April, 1992 earthquakes.

REFERENCES CITED

Aalto, K.R., 1989, Geology of Patricks Point State Park, Humboldt County, northern California: California Geol., v. 42, p. 125-133.

Carver, G.A., 1985, Quaternary tectonics north of the Mendocino triple junction, in Kelsey, H.M., Lisle, T.E.,and Savina, M.E., eds., Redwood Country Guidebook: American Geomorphological Field Group 1985 Field Trip, p. 155-167.

Carver, G.A., 1987, Late Cenozoic tectonics of the Eel River basin region, coastal northern California, in Schymiczek, H., and Suchsland, R. , eds., Tectonics, Sedimentation and Evolution of the Eel River and Other Coastal Basins of Northern California: Pacific Sect., American Assoc. Petroleum Geol. Misc. Pub. 37, p. 61-72.

Kelsey, H.M., and G.A. Carver, 1988, Late Neogene and Quaternary tectonics associated with northward growth of the San Andreas transform fault, northern California: Jour. Geophys. Res., v. 93, p. 4797-4819.

Nilsen, T.H., and S.H. Clarke, Jr., 1987, Geological evolution of the late Cenozoic basins of northern California, in Schymiczek, H., and Suchsland, R. , eds., Tectonics, Sedimentation and Evolution of the Eel River and Other Coastal Basins of Northern California: Pacific Sect., American Assoc. Petroleum Geol. Misc. Pub. 37, p. 15-30.

Page, W.D., D.R. Packer, and T. Stephens, 1982, Speculations on the ages of the marine terraces and Quaternary marine deposits, Trinidad, California, in Harden, D.R., Marron, D.C., and MacDonald, A. , eds., Late Cenozoic History and Forest Geomorphology of Humboldt County, California: Friends of the Pleistocene Pacific Cell Guidebook, guidebook supplement.

Sarna-Wojcicki, A. M. Meyer, C. E., Nakata, J. K., Scott, W. E., Hill, B., Slate, J. L., Russell, P. C., 1988, Age and correlation of mid-Quaternary ash beds and tuffs in the vicinity of Bend, Oregon. in Scott, W. E. , Gardner, C. A., and Sarna-Wojcicki, A., eds., Guidebook, 1988 Friends of the Pleistocene, Pacific Cell, Field trip to the central Oregon High Cascades.

ROAD LOG FROM HIGHWAY 101 EXIT TO SATURDAY NIGHT CAMPSITE

D. J. MERRITTS and T. DUNKLIN

Mileage	Description of features along route
0.0	Exit to Fernbridge/Ferndale from 101 South in right lane.
0.2	Stop sign. Go straight.
0.7	Get in right lane at stop sign. Make a right turn and cross the Eel River on Fernbridge.
3.5	Crossing the Salt River.
4.4	Entering the quaint, Victorian village of Ferndale on Main Street.
5.1	Continue through the town of Ferndale until the intersection of Main Street and the Coast Road. Make a right turn.
5.2	Follow this road out of the town of Ferndale. You will come to a large wooden sign at the end of town which says "To Capetown/Petrolia". This points the way to Wildcat Road, a windy and narrow road which climbs over the mountains to the coastline. Follow the arrow on the sign and begin to climb the Wildcat grade.
6.5	Excellent view to the east of the Coast Ranges and the Eel River watershed.
6.8	Steeply dipping late Tertiary sediments on left.
8.6	View of Eel River to left, and of gently dipping late Tertiary sediments.
9.3	Excellent exposure of late Tertiary sediments on left.
9.4	View of the Pacific Ocean and Guthrie Creek to the right.
10.3-10.5	Late Tertiary sediments with numerous steeply dipping reverse faults on right.
11.2	Watershed to west (right) is Oil Creek.
12.1	Road pull-off to right has excellent view of Eureka, Humboldt Bay, and Table Bluff anticline to the north. Excellent photo point on a clear day.
12.7	Photo opportunity at pull-off on the right.
15.3	View to left upstream in the upper Bear River Valley. The remainder of the field trip on DAYS 2 and 3 will be spent in the coastal area between Cape Mendocino and Punta Gorda, which is encompassed in **Figures 1** and **Fig. 2**, topographic and geologic maps, respectively, of the area.
16.2	View to left of lower reach of Bear River Valley and the hamlet of Capetown.
16.9	View to left (upstream) of constricted reach of Bear River and a large Quaternary fan built into the valley from the South, downstream of the constriction.
17.8	After crossing the cattleguard, pull off to the right to view the mouth of the Bear River. Numerous marine and fluvial terraces can be seen. This land is part of the ranch of Joe Zanoni, a descendant of one of the original settlers in this region. Marine terraces are latest Pleistocene in age, and the uplift rate here is about 2.5 m/ky. Marine terrace ages and altitudes (Merritts and Bull, 1989; see Merritts et al, this volume) on the north side of the Bear River are as follows:

Altitude, m	Inferred Age, ka
41	29
72	40
94	45
118	53
141	59
162	72
183	81
197	100
211	118
240	200

18.0	Along the descending switchbacks watch for glimpses of the spectacular flights of terraces at the mouth of the Bear River, especially on the north side.
18.5	Road is built upon late Pleistocene and Holocene fluvial terraces.
18.8	Branstetter bridge.
19.8	Closed depression in topography to right. Interpreted as a sag pond along a fault or at the head of a landslide. Ranchowners have reported that the pond was once a large lake which has been infilled.
21.2	View to left of North Fork of Singley Creek. Note numerous landslides.
22.0	View to left of the mouth of Singley Creek. The mouth is comprised of a complex assemblage of Holocene fluvial and emergent marine terraces (**Figure 3**). Shells from the lowest Holocene marine terrace have ages of about 1.7 ka, while those from the second terrace have ages that range from about 3.3-3.8 ka. The third terrace probably correlates with a 6.5 ka terrace dated to the south, at Hair Seal Rock. We will see the inner edge (shoreline angle) of this terrace platform at **STOP # 1** today. See discussion of these terraces, and a coastal profile of marine terrace altitudes from Singley Flat to Hair Seal Rock, just north of the mouth of the Mattole River, in paper by Merritts et al, this volume (see especially Fig. 12 in that article).
22.2	Another excellent view of the terraces at Singley Flat.
22.5	House on the left is known as Ocean House, and was built by the late Joe Russ, a local rancher descended from one of the original ranch families in this area. Mr. Russ passed away in 1991. Between here and the next feature, at Devil's Gate, note the outcrops of pillow basalts on the left side of the road. Out of view to the right of and below the road is the 3.7 ka Holocene marine platform cut into the basalt.
24.2	To the right is Devil's Gate. This platform probably correlates with the 6.5 ka terrace dated to the south at Hair Seal Rock (**STOP # 1**). View to south of prominent escarpment at Punta Gorda (**Figure 4**) shows excellent, broad late Pleistocene terraces that range in age from 30 ka to 220 ka (see Merritts et al, this volume, especially Figure 8). These terraces and the soil profiles developed on them are the focus of **STOP # 3, DAY 3** (see below).
24.3	To immediate left is a view into an old quarry. At the back of the quarry wall the inner edges of several Holocene and late Pleistocene marine terraces are exposed.
27.0	Dune fields south of Davis Creek.
27.2	Domingo Creek, location of Domingo BenchMark used in survey of coastal terraces by Merritts et al, this volume.
STOP # 1 28.2	McNutt Gulch/Mussell Rock--approximate location of southern edge of subducted Juan de Fuca plate. Park along right side of road. We will hike south from here to Hair Seal Rock to view emergent Holocene marine terrace platforms and sites of shell samples for radiocarbon dates, inner edges (shoreline angles) of platforms, Holocene sea caves, paleodunes (see Fig. 11 in Merritts et al, this volume), landslides that have possibly been seismically induced, and late Holocene alluvial fans. Excellent view to south of Punta Gorda (**Figure 4**). See **Figure 5** for topographic map of area traversed during this short (2.0-2.5 km) hike.
	See Aalto article: Mattole River North Area Geology
30.5-31.5	Ancestral Mattole terraces. At least five terraces exist--all were cut by an ancestral Mattole that flowed westward through what is now McNutt Gulch. The Mattole was captured by a stream to the south, and now flows to the ocean about 5 miles south of its original exodus.
31.9	Town of Petrolia is to the left. Petrolia was the site of California's first oil well. Numerous gas wells still exist in the area. The town was originally

called Mattolia, after the Mattole Indians, but was renamed after the discovery of oil. Mattolia meant "clear water", as the Mattole once was.

32.8 Turn left on the Mattole Road, towards what used to be the Petrolia Store and Post Office. This landmark structure was tragically burned to the ground during the April, 1992, earthquakes.

33.7 George Lindley Bridge, crossing the Mattole River about 5 miles upstream from its mouth. To the left, below the bridge, is the famous Hideaway Restaurant, which serves excellent burgers, imported beer, etc.

34.2 View to left (north) of late Quaternary fluvial and marine terraces along the Mattole River. The sheep ranch is owned by Allan and Lois Gillespie. This is about the upstream extent of the 30 Ka sea-level highstand incursion. (See Figure 14, Merritts et al, this volume.)

37.2 Excellent fluvial terraces on right.

37.5 Indian Creek fan. View upstream of ridge with at least four late Quaternary terraces.

37.8 Lindley Bridge.

38.1 View of Mattole Restoration Council restoration work on right bank, Mattole River. Until this reach of the river (~18 km), the channel bed is dominantly alluvial, comprised of coarse gravel backfill associated with the present sea-level highstand, although up to 10 m of incision since ~6.5 ka has occurred. From ~16-40 km upstream (river miles), the channel is dominantly bedrock with a thin gravel veneer. Much bedrock is exposed beneath the gravel veneer. From ~40 km upstream to the headwaters, the channel is dominantly bedrock. The best fill terraces are exposed between 0 and 16 km, and are associated with sea-level highstands. The best strath terraces are exposed between 16 and 40 km, and are associated with sea-level lowstands. Few terrace remnants occur upstream of 40 km.

38.5 Bedrock exposed in channel.

38.9 A. W. Way County Park and Campground. We will camp at this park, on a spectacular meander bend with excellent exposures of strath terraces. On the third day of the field trip, participants have two field trip options:

STOP # 2: Head back to the coast to examine Pleistocene marine terraces and soil profiles (**Figure 6**) with Oliver Chadwick et al (see Chadwick et al, this volume). Excellent platforms with pholad borings are exposed in many gullies and creeks, and soils on terraces of at least four different ages, spanning over 200 ky, can be examined.

OR:

STOP # 3: Head upstream to examine numerous early to late Holocene strath terraces along the Mattole River that have been surveyed in great detail (from the mouth to 40 km upstream), and have been dated at multiple sites (see Merritts et al, this volume, Figures 14, 15, and 16). This part of the field trip will be led by Kirk Vincent, Thomas Dunklin, and Dorothy Merritts. It will focus on tectonic and eustatic controls on the longitudinal profiles of rivers, the late Quaternary history of the river and development of terraces, and the response of a large coastal stream to base-level change. It will also include discussion of seismically induced landslides and rockfalls from the August 1991 Honeydew earthquake, and the April 25, 1992, Petrolia earthquake.

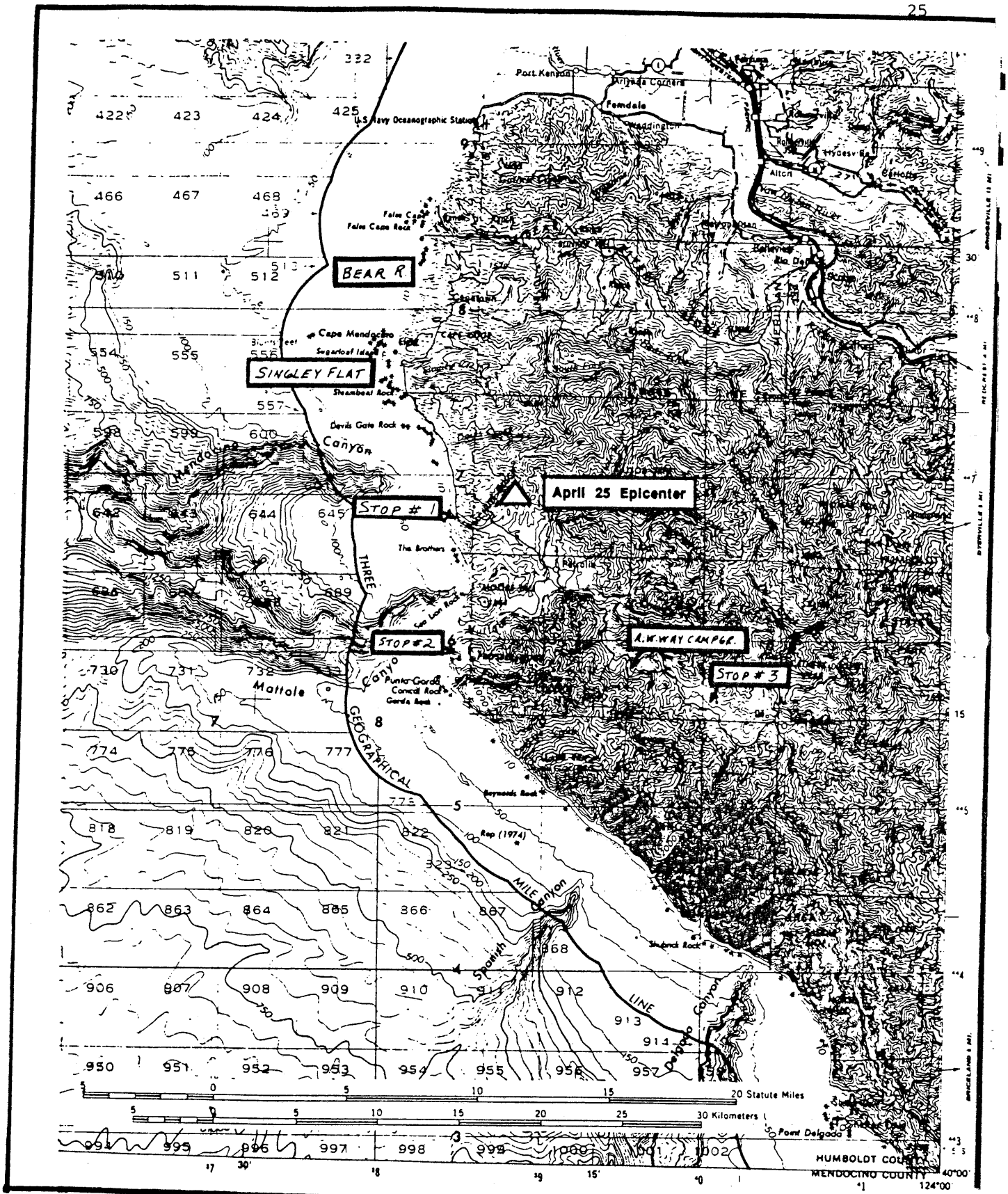

Figure 1. Location map for Days 2 and 3 of the field trip. The area visited during the optional backpack trip on Days 4 and 5 from Punta Gorda to Reynolds Rock is also covered on this map. (From Eureka 2° sheet, 1977, NK 10-10, contour interval 200 ft.)

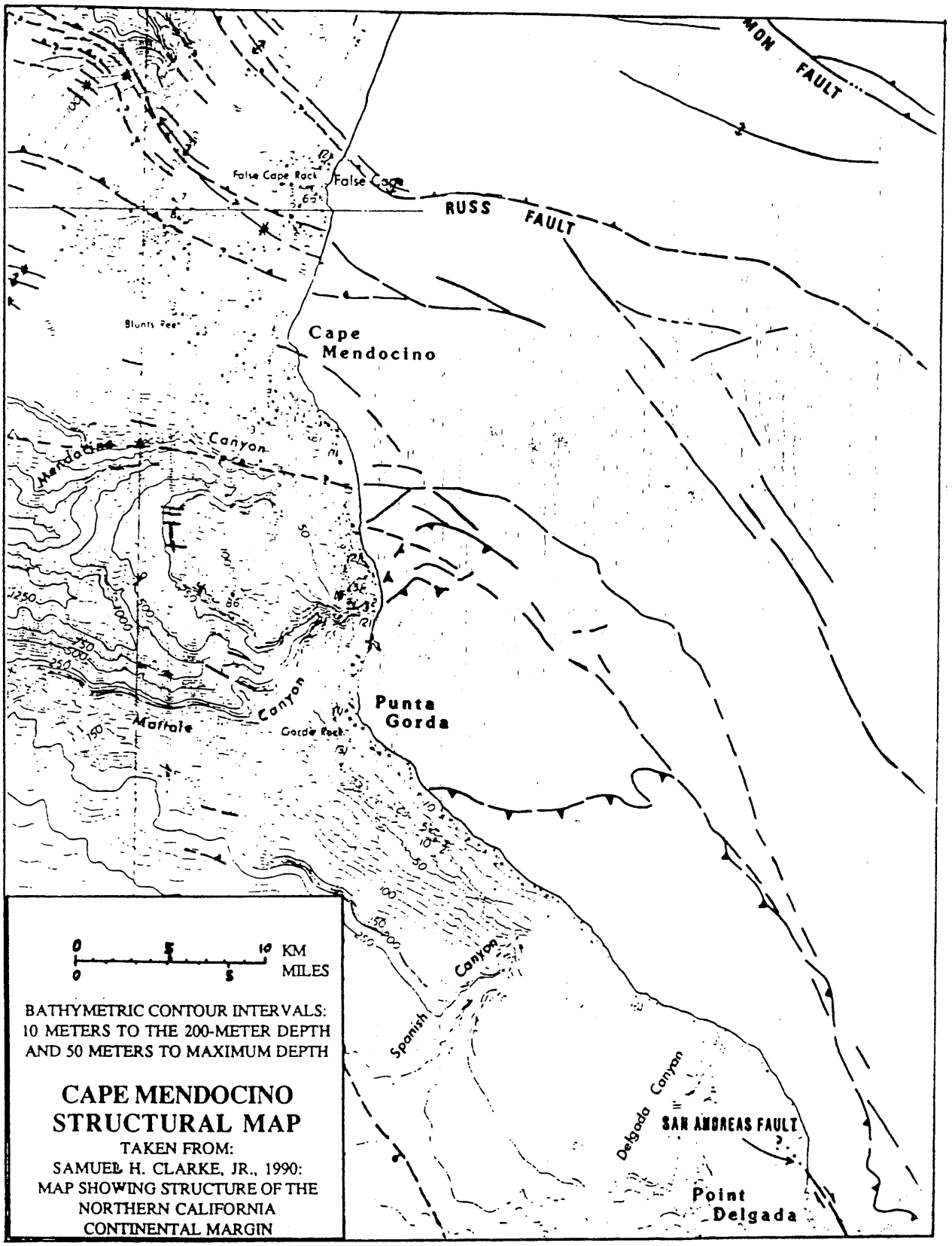

Figure 2. Structural map of area covered during Days 2 and 3 of the field trip. (From Clarke, 1990.) This map can be compared with Figure 1 to locate sites and stops.

Figure 3. Aerial view of Singley Flat, looking east. Singley Flat is a complex assemblage of mostly marine and some fluvial terraces, all mid- to late-Holocene in age (see discussion of radiometric dating by Lajoie, Merritts, and others in Merritts et al. this volume). Note three prominent Holocene terraces: A, 1.7 ka; B, ~3.5 ka; and C, 6.5 ka.

Figure 4. View to south of Punta Gorda escarpment from Hair Seal Rock (photo by W. B. Bull, 1987). Several late Pleistocene marine terrace remnants occur on the steep escarpment below 239 m, but much more spectacular, broad marine terraces occur above this altitude. White patches are beach sand cropping out along the outer edges of the marine terraces. Between 239 and 294 m, five marine terraces ranging in inferred ages from 100 to 240 ka, are well preserved. These terraces and soil profiles developed in their cover-bed deposits are the focus of **STOP # 2, DAY 3.**

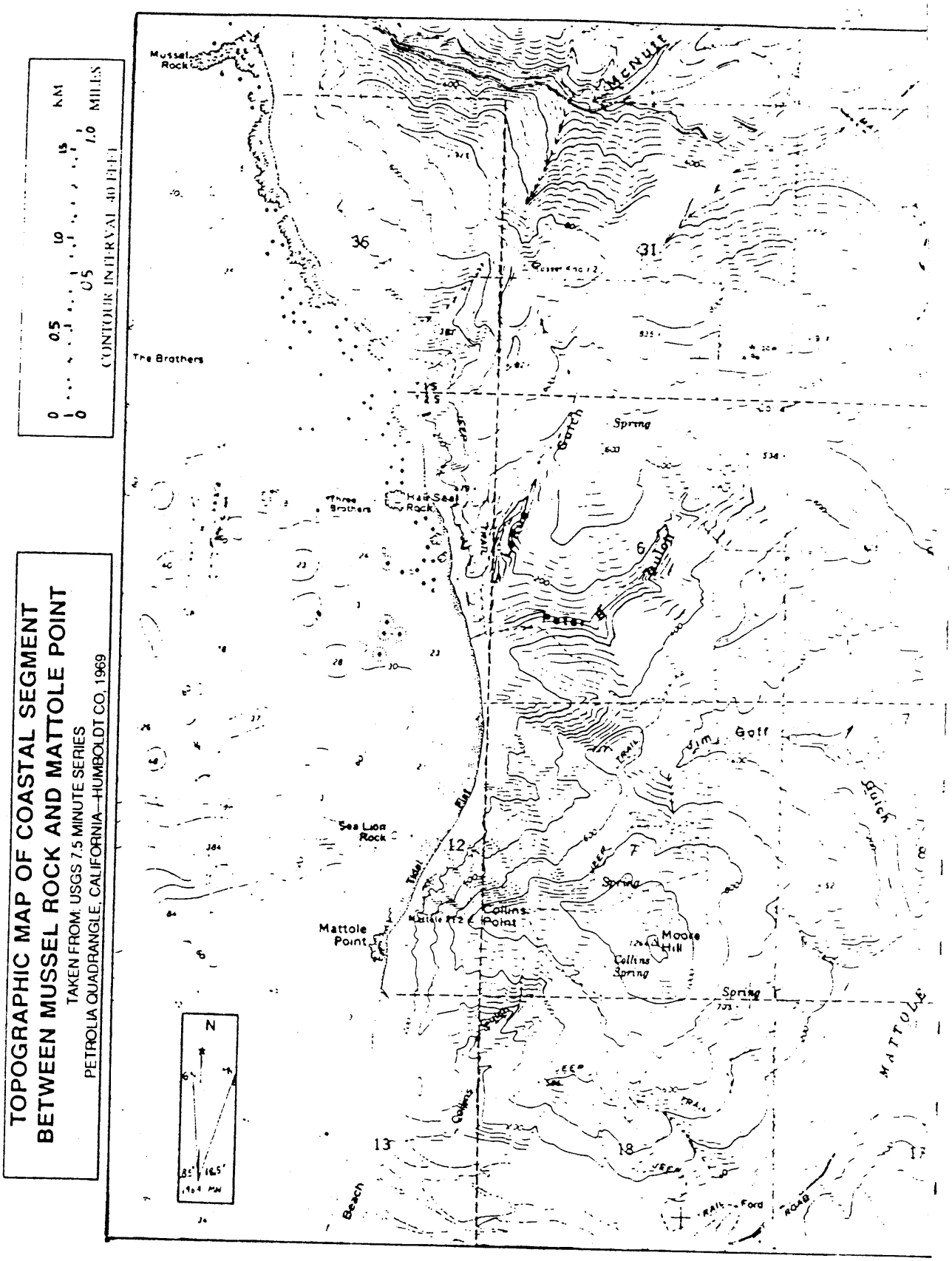

Figure 5. Topographic map of coastal area encompassed by hike at **STOP # 1, DAY 2** (Mussel Rock to Hair Seal Rock). Note that this part of the coastline is part of the crust of the North American Plate that directly overlies the rupture plane of the April 25, 1992, thrust fault earthquake (N32°W, 22° NE dip, rupture propagation to north, epicentral location on Figure 1.)

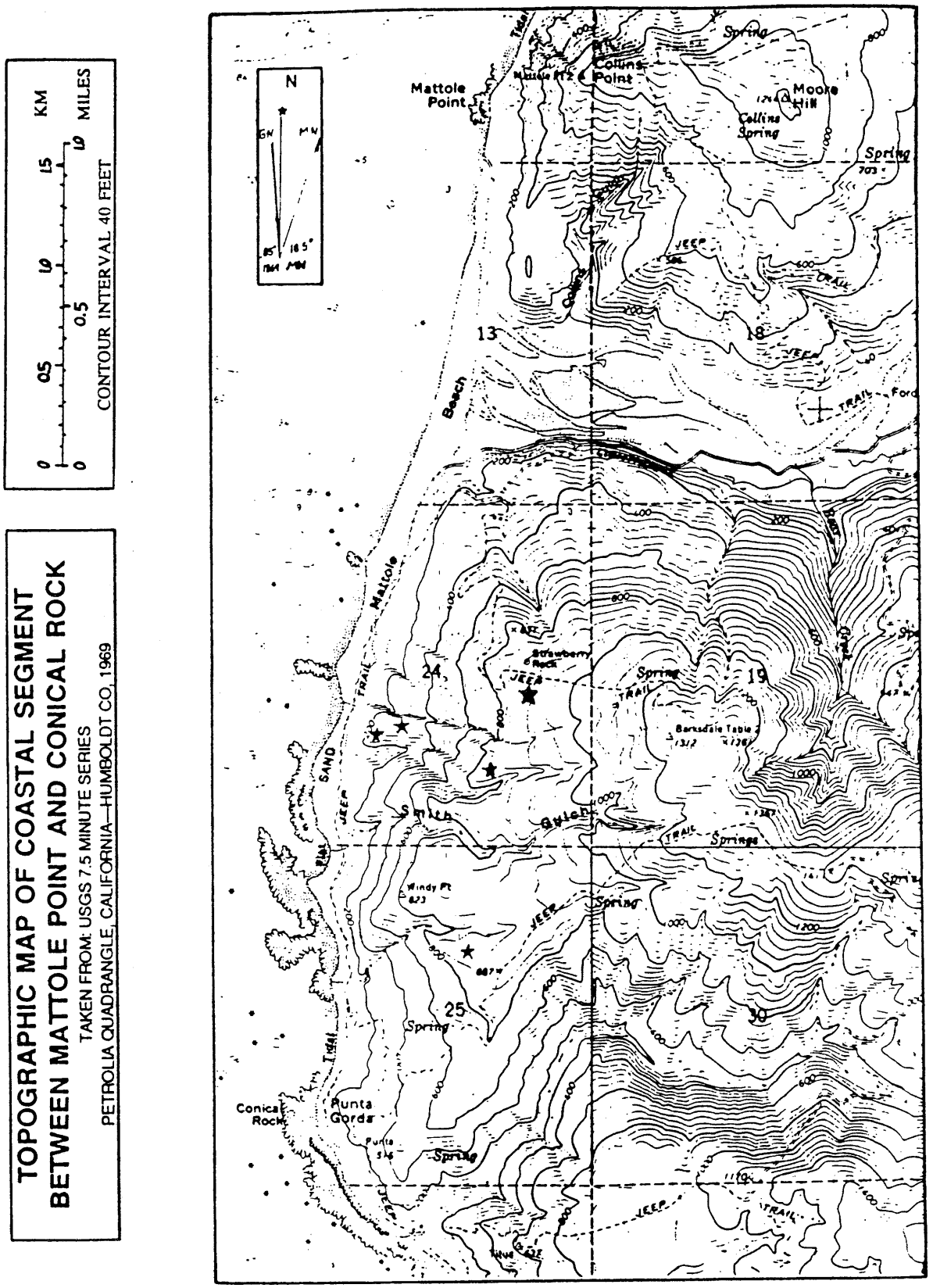

Figure 6. Topographic map of Pleistocene marine terraces at Punta Gorda, **STOP # 2, DAY 3**. Stars indicate location of soil pits.

Late Cenozoic Deformation on the Cascadia Subduction Zone in the Region of the Mendocino Triple Junction

G. A. Carver and R. M. Burke
Department of Geology
Humboldt State University
Arcata, California 95521

INTRODUCTION

Coastal California north of Cape Mendocino lies on the tectonically active convergent margin of the North American plate at the southern end of the Cascadia subduction zone (Csz). Since the Mesozoic the geologic development of this region of California has been dominated by plate convergence. During the last 140 ma subduction and resulting accretion has welded a broad complex of highly deformed oceanic rocks to the western margin of the North American plate and extended the edge of the continental lithosphere in northern California westward more than 200 km. These accreted rocks now compose the Franciscan complex which makes up the basement of the northern California coast region. For a more detailed description of the Csz tectonics and the lithologies involved, see Clarke and McLaughlin (this volume) and Aalto (this volume).

Late Pleistocene marine terraces are present along most of the coast north of Cape Mendocino for about 100 km to the vicinity of Big Lagoon, Humboldt County, California. The terraces are preserved as erosional remnants of raised shore platforms and associated cover sediments. The times of formation of the terraces are interpreted to have been glacio-eustatically controlled and coincident with late Pleistocene high sea level stands.

Differences in uplift rates for fault-bounded sections of the coast and variations in the rates of faulting and folding have resulted in differences in the number, age, and altitude distribution of marine terraces preserved at different locations along the coast. This, in turn, has resulted in an unique altitude-age relationship for the flights of terrace remnants on each fault bounded segment of the coast. Gaps in the terraces at Big Lagoon, Freshwater, and the Eel River valley reflect the location of late Pleistocene downwarping and/or subsidence. Holocene growth, both uplift and subsidence, of the fold and thrust belt is well documented by multiple ^{14}C dates of detailed stratigraphic sections.

Due to a virtual lack of datable materials in the older marine sediments, terrace ages have been estimated from the degree of soil development in the cover sediments and independently by applying uplift rate models to the unique altitudinal spacing for each flight of fault bounded terraces. Some of the younger soil age estimates are in reasonable agreement with ^{14}C ages, while experimental TL dating generally supports age estimates from both soils and the uplift model (see Berger, this volume). The goals of this paper are to introduce some of the regional tectonic

settings which are discussed in other papers of this volume, and to introduce, for comparis styles and rates of deformation in the 100 km section of the Cascadia Subduction Zone d north of the Mendocino Triple Junction

CASCADIA SUBDUCTION ZONE

The modern Csz extends from northwest of the northern end of Vancouver Island south to near Cape Mendocino in northern California (Figure 1). At the southern end of the Csz, relative plate motion is strongly oblique, but becomes more normal to the plate boundary to the north. Magnetic anomalies on the Gorda plate and global plate motion models show the rate of convergence between the Juan de Fuca - Gorda plates and the North American plate is between 2 and 4 cm per year while northward transport of the subducting oceanic slab and migration of the Mtj along the North American margin is about 4 to 5 cm per year (Engebretsen et al, 1985) (Figure 2).

The Gorda plate is generated at the Gorda rise, located some 200-300 km west of the subduction zone (Figure 2). Along the Csz the descending oceanic plates are youthful, especially the Gorda plate which at the trench ranges in age from about 5 ma (anomaly 3) at its north end to about 9 ma (anomaly 4) near the Mtj. The Gorda plate descends beneath the western edge of the North American plate at a shallow angle, about 10 degrees, to a depth of 30-40 km where the dip increases to 35-45 degrees (Walter, 1986; McPherson, 1989, this volume). The Csz deformation front is located at the base of the continental slope between 35 and 60 km offshore of northern California (Clarke, 1992). Landward of the deformation front the western edge of the North American plate is deforming across a 75-100 km wide fold and thrust belt made up of N-NW trending thrust faults and associated folds (Carver, 1987a; Clarke, 1992).

LATE NEOGENE TECTONICS

Late neogene rocks preserved along the northern California coast comprise a thick sequence of clastic marine and non-marine sediments which include the Wildcat Group (Ogle, 1953; see Aalto, this volume) and the Falor Formation (Manning and Ogle, 1950; Carver, 1987a; Aalto, this volume). These sediments were deposited in the regionally extensive Eel River basin, a broad forearc depocenter developed along the Csz (Nilsen and Clarke, 1987). The Wildcat Group and Falor sediments range in age from late Miocene and early Pliocene to early Pleistocene. The lower Wildcat Group sediments include the Pullen, Eel River, and lower Rio Dell formations, and are exposed primarily along the southern flank of the Eel River syncline, which we will traverse on day 2 of the FOP field trip. The lower Wildcat sediments are composed principally of fine grained sandstones, siltstones, and turbidities deposited in lower to upper bathyal open marine depositional environments (Ingle,1987; McCory, 1989)

The eastern margin of the neogene Eel River basin is not well defined. Isolated outliers of marine sediment , correlated to the Wildcat Group, are preserved in the northern California coast ranges near Garberville and in the Bridgeville area, 70 to 100 km inland from the present coast. East and north of these remnants of Eel River basin sediments, the Franciscan and Klamath rocks were eroded during the late tertiary to a low relief surface named the Klamath peneplain (Diller, 1902; see Stone, this volume). Developed into this erosion surface is a thick saprolite (Carver, 1987a) which is interpreted to represent deep weathering during a long interval of tectonic stability in a regionally extensive low relief landscape. This saprolite formed prior to the Quaternary uplift of the Klamath Mountains and Coast Ranges (see Aalto, this volume). In the upper Mad River Valley, the fully developed saprolite is overlain by early Pleistocene Falor formation sediments, constraining it's age to late neogene.

Upper Wildcat strata are widely distributed along the coast between the Eel River syncline and the Mad River Fault zone. These sediments represent an accumulation of course clastics in the non-marine and shallow marine depositional setting of the paleo-shoreline, shelf, and upper slope. The sequence of upper Wildcat Group sediments, up to 2.5 km thick on the south flank of the Eel River syncline, reflects shoaling of the Eel River basin (McCory, 1989; see the day 2 road log, this volume) and onset of regional marine regression along the northern California coast. Age estimates for the upper Wildcat sediments are constrained to late Pliocene and early Pleistocene by tephras, macro and microfossils, and paleomagnetics (Ingle,1976; Dott, et al., 1977; Kadama, 1979, Sarna-Wojcicki et al., 1987, 1991; Woodward-Clyde Consultants, 1980).

The regional structure of the Eel River Basin sediments and Klamath saprolite suggest their deposition predates the onset of intense folding and faulting which has characterized the north coast region during the late Quaternary. Strata within the lower Eel River basin sediments are generally conformable across large areas. Refraction profiles offshore show gentle low angle regional unconformities are present between the Pullen and Eel River formations and in the lower part of the Rio Del formation (Clarke, 1992). These unconformities reflect changes in deposition accompanied by gentle folding, but not major tectonism nor disruption of the forearc basin setting during the late neogene. Subduction of the Juan de Fuca plate during the late neogene appears to have occurred passively with little deformation of the accretionary margin in the northern California region. The extensive Eel River basin persisted with remarkably little change during this interval, and the continental margin in northern California maintained low relief and regional stability.

QUATERNARY TECTONICS

In contrast with the passive convergence which characterized the late neogene evolution of the northern California continental margin, the Quaternary history of the region has been marked by vigorous contractile deformation. Offshore, the regionally extensive Eel River basin in which the Wildcat Group sediments accumulated was disrupted and replaced by localized depocenters associated with rapidly growing folds and faults in the Csz fold and thrust belt. Inland uplift of the Klamath Mountains and Coast Ranges has elevated the Klamath saprolite surface and induced erosion and dissection, producing high local relief and rugged topography. Regionally, the onset of this intense deformation appears to follow deposition of the Rio Dell and Falor formations and therefore dates to about 1 MA. Possible plate scale events associated with the dramatic change in tectonics of the region include the passage of the Blanco fracture zone along the northern California continental margin and initiation of Gorda subduction. In the Cape Mendocino area the tectonics have been influenced by the approach of the Mtj.

The Csz fold and thrust belt includes systems of north-northwest trending east-northeast dipping reverse faults, fault generated anticlines, and broad north-northwest trending synclines that extend across a 70-80 km wide belt, situated along the western edge of the accretionary margin of the North American plate. Most of the fold and thrust belt is located offshore of the northern California coast, but the southern end of the belt extends onshore north of Cape Mendocino. During the mid- and late Quaternary, growth of the fold and thrust belt structures has controlled the geologic and geomorphic development of the north coast region.

The Csz fold and thrust belt contains two west-southwest convergent imbricate thrust systems. Offshore they extend along the Csz parallel to the coastline of southern Oregon. Seafloor mapping shows each fault system is composed of overlapping groups of right stepping en echelon faults. Individual faults in the thrust systems are less than 25 km to more than 75 km long. Acoustical profiling across these faults shows that they displace the Eel River basin sediments and extend downward into Franciscan basement to near the plate boundary (Clarke,1992). On shore in northern California, the two fault systems, the Mad River fault zone (MRfz) and the Little Salmon fault zone (LSfz), are separated by the 20-30 km wide Freshwater syncline, a major structure in the Gorda segment of fold and thrust belt(figure 2).

The MRfz forms the eastern part of the fold and thrust belt. Between the latitude of the Oregon border and Big Lagoon the fault system intersects the surface on the sea floor near the coastline. South of the mouth of the Klamath River the southeastern ends of several MRfz faults extend inland and offset Quaternary Gold Bluffs sediments (Kelsey and Carver, 1988). The principal

faults of the MRfz intersect the coast between Arcata and Big Lagoon (see the regional map, this volume). Included in the onshore part of the MRfz are the Big Lagoon, Trinidad, McKinleyville, Blue Lake, Mad River, Fickle Hill, and Greenwood faults, each a northeast dipping thrust. These thrusts offset late Pleistocene marine terraces along the coast and extend inland 40-50 km toward the southeast where they juxtapose Franciscan complex rocks over Falor and upper Wildcat sediments (Figure 3) (Carver, 1987a). The MRfz is about 25 km wide with the,principal imbricate faults spaced from 2 to 5 km apart. Anticlines developed on the tips of the upper thrust sheets have formed prominent ridges which dominate the topography. The largest of these are the Trinidad and Fickle Hill anticlines (shown on figure 5 and discussed at stop 1, day 1).

The LSfz traverses the southern end of Humboldt Bay and extends inland east-southeast about 40 km to near the rural town of Bridgeville. Offshore the LSfz includes a group of right steeping en echelon thrusts which define a 20-30 km wide zone along the outer edge of the fold and thrust belt. The offshore trend of the LSfz turns north-northwest and parallels the deformation front of the subduction zone (Clarke, 1992). The on land structures of the LSfz include the eastern segments of the Little Salmon and Table Bluff faults, the Yager fault, and the Table Bluff, Tompkins Hill, and Humboldt Hill anticlines. Near the coast, the folds and thrusts of the LSfz deform late Pleistocene and Holocene sediments.

Three large Quaternary synclines are present in the Csz fold and thrust belt in coastal northern California. The Freshwater syncline, located between the MRfz and the LSfz, extends onshore at Arcata Bay. The South Bay syncline lies in the LSfz at the south end of Humboldt Bay, and the large Eel River syncline, occupied by the Eel River valley, is situated on the coast south of the LSfz (see Li, this volume). These synclines are strongly asymmetrical with steeply dipping northeast limbs, broad planar flat floors, and gently dipping southwest limbs. Each of these folds has developed since deposition of the Falor-Upper Wildcat sediments and experienced substantial growth and axial subsidence during the late Quaternary (see Verhey, this volume).

Minimum estimates of total crustal shorting across the fold and thrust belt have been made from measurements of the thicknesses of Falor and Wildcat Group sediments faulted beneath Franciscan complex rocks (Figure 4). In the upper Mad River valley, more than 540 meters of Falor sediments have been overthrust by Franciscan rocks on the Trinidad fault, while the Blue Lake fault thrusts Franciscan rocks over a 930 meter thick deposit of Falor near the town of Korbel. The minimum estimated dip slip displacement across the MRfz, calculated from measured vertical separations of the Falor sediments on each fault is about 6 km. Vertical separation of the Rio Dell formation across the Little Salmon and Table Bluff faults, on the northeast side of the Eel River valley

exceeds 1800 meters, representing about 7 km of Quaternary dip-slip motion on the LSfz. Assuming this faulting was initiated at the end of deposition of the Falor and Rio Dell sediments about 700 ka to 1 ma, the minimum average rate of crustal shortening across the fold and thrust belt has been 13 to 19 mm/yr. Additional shortening has been associated with the growth of the Freshwater, South Bay, and Eel River synclines.

Estimates of late Quaternary slip rates for the MRfz and the LSfz are similar to the Quaternary rates derived from deformation measurements of the Eel River basin sediments. The late Quaternary rate estimates are based on vertical separation measurements of faulted marine terraces in the Trinidad-McKinleyville area for the MRfz (Figure 5) and at Humboldt Hill and Table Bluff for the LSfz. The age of the terraces are based on uniform uplift rate models for terrace flights at Trinidad and McKinleyville (Figure 6; see Merritts et al., this volume and references therein for a discussion of this method), soil development (Carver et al., 1985), and thermoluminesence dating (Berger et al, 1990: Berger, this volume). Terrace ages range from about 62 ka (Stage IVa, Chappel and Shackleton, 1986) to about 212 ka (stage VII) as discussed in the following section.

South of the Eel River syncline, the fold and thrust belt style of deformation changes to rapid regional uplift. Estimates of uplift rates based on the elevation of late Pleistocene marine terraces near Cape Mendocino are about 3 m/ka (Merritts and Vincent, 1989, Merritts et al., this volume). The marine terraces between Centerville and Cape Mendocino do not reflect the growth of large thrusts and associated anticlines during the late Quaternary (figure 5). This section of the coast includes broad belts of highly sheared shaley melange containing large fault bounded blocks of Franciscan complex rocks and neogene sediments, including the False Cape shear zone and the Bear River beds (Ingle,1976). This melange is interpreted to have formed by subduction driven accretion during the early evolution of the Csz. The rapid uplift of the Cape Mendocino area is attributed to the thickening of the underlying southern edge of the Gorda plate associated with the northward migration of the Pacific plate and the Mtj. The uplift has elevated the southern end of the accretionary margin and exposed recently accreted and deformed rocks in the tip of the accretionary wedge.

Focal mechanism studies and the distribution of seismicity in the area near Cape Mendocino indicate the south edge of the Gorda plate is undergoing N-S contraction (McPherson, 1989 and this volume) Assuming this uplift is driven by thrusting within the Gorda crust on thrusts with 30-45 degree dips, the Gorda-Pacific plate convergence across the eastern end of the Mendocino transform and thickened wedge of the Gorda plate is about 10 mm/yr. This deformation is akin to

the compressional bow wave of the advancing Pacific plate and reflects tectonics of the Mtj rather than the Csz.

The deformation of the Quaternary deposits of coastal northern California north of the Eel River reflects convergence of the subducting Gorda plate and resulting contraction of the North American plate margin. The en echelon arrangement of thrusts and folds in the LSfz and MRfz accommodates much of the right oblique component of relative plate motion. At the southern end of the Csz and in the Mtj region, lateral motion may also be taken up on the Eaton Roughs and Garberville faults (Kelsey and Carver, 1988) (figure 2). The orientation of the axis of Quaternary shortening in the North American margin as reflected in the trend of folds and faults is compatible with the convergence direction between the two plates. Intraplate faulting and clockwise rotation of the southern part of the Gorda plate result in increased obliquity in plate convergence to the south. This difference in the orientation of the convergence direction is reflected by the more east-west trend of the fold and thrust belt at it's southern end. Rates of contraction across the fold and thrust belt demonstrate strong coupling between the plates to depths of 25-35 km. The average crustal shortening rate of about 15-20 mm/yr suggests much of the 30 to 40 mm/yr of plate convergence accrues as permanent contraction in the upper plate of the subduction zone.

MARINE TERRACE AGE ASSIGNMENTS

No datable materials have been found in direct association with marine terraces in northern California north of Cape Mendocino, and age assignments have been made by comparing the altitude distribution of terraces in discrete terrace flights to a global high sea level stand chronology developed by Bloom et. al. (1974), and Chappell (1983), in accordance with the methods and assumptions discussed by Bull (1985) and Lajoie (1986) Terrace age assignments are based on the best matches between: (1) altitude sequences of local terrace remnants, and (2) unique terrace altitude sets produced by applying uniform average uplift rates to known ages and altitude of formation of New Guinea terraces (Chappell,1983).

In this study two reference sections, one near Trinidad (a flight of 12 terraces) and a second near McKinleyville (a flight of 8 terraces) were selected for terrace age assignments. For each of the two reference sections, terrace platform altitudes were plotted against a chronology of global high-sea level stand altitudes using tie lines between the two data sets. The slopes of these tie lines represent the inferred uplift rates for the tectonic block underlying the reference sections. Uplift rates were assessed for several potential age assignments at each reference section to test the validity of the constant uplift rate model and the best fit age assignment was selected for each reference section according to the methods proposed by Bull (1985), and Lajoie (1986). Based

on this analysis, the lowest emergent terraces at Trinidad and Mckinleyville are assigned an age of 64,000 years and the highest an age of 202,000 years (McKinleyville) and 240,000 years (Trinidad).

The correlation of terrace remnants along the coastline from Cape Mendocino to Big Lagoon is not immediately apparent from their topographic expression or elevation. However, groups of terrace remnants with obvious topographic continuity define Pleistocene shoreline profiles on individual tectonic blocks (figure 5). The number of preserved remnants and the elevations of these shoreline profiles vary greatly from block to block (figure 5), reflecting different uplift histories of each block. These variations in terrace deformational histories along the coast necessitate the use of a correlation tool without regard to topographic position. The correlation of terrace remnants across major faults and between tectonic blocks was based primarily on the degree of soil development exhibited in the terrace cover sediments. Soils were described and soil chronosequences were initially established for terrace flights at the age-assessment reference sections near Trinidad and Mckinleyville. Age assignments for other terraces along the coast were then established by correlation to the reference chronosequences.

TERRACE SOIL DEVELOPMENT

Terrace soils were described and sampled in hand dug pits averaging about 1.5 meters in depth at 39 sites along the coast between Cape Mendocino and Big Lagoon. Sites for the hand dug pits were chosen only after extensive hand auguring to verify that the soil sites were representative of the terrace surfaces. Samples were collected and analyzed for particle size distribution. Field descriptions were used to calculate profile development indexes (PDI's) in the manner outlined by Harden (1982) and Harden and Taylor (1983). When plotted against the assigned terrace ages, the PDI's along with individual field parameters and laboratory data clearly define a soil chronosequence, but with less precision than the total number of surfaces in any given terrace flight.

Based on field and lab data, the chronosequence at Trinidad and McKinleyville are differentiated into four age classes, I through IV (figure 7), less than the total number of terraces recognized in each reference section. Even though the chronosequence does not uniquely define each morphological surface, it does subdivide units at about the maximum capability of pedologic relative dating as estimated by Birkeland (1985). Soil age class I includes soils formed on terraces assigned ages between 64,000 and 83,000 years. Soil age class II includes soils formed on terraces assigned ages between 83,000 and 103,000 years. Soil age class III includes those soils formed on terraces assigned ages of either 120,000 or 130,000 years, and soil age class IV

includes all soils formed on terraces thought to be 200,000 years or older. Soils of age class I and age class II have many parameters which overlap, while age class IV could undoubtedly be further subdivided with additional work.

The soils in age class I are greatly influenced by eolian influx which is expressed by an increase in both silt and clay near the surface. The similarity in the trends of particle size distributions in the 15 profiles (figure 7) demonstrates the correlative value of this parameter. Many of these profiles indicate field evidence of erosion prior to the deposition of the eolian cap; however, no single mechanism of stripping has been identified and the work of Chadwick et al. (this volume) suggests no stripping has occurred on similar soils near Cape Mendocino. Smith (1983) suggests that the source and cause of the eolian cap on the lowest emergent terrace is the result of off shore desiccation during the latest low sea level stand about 18,000 years ago.

Many of the soils in age class II have weak to distinct textural B horizons and soils in age class III have argillic horizons with higher clay percentages to greater depths. It should be noted that soils of age class III are generally not completely exposed using hand dug pits.

While no single soil parameter can be utilized to place a terrace soil in a given age class, some parameters are definitely more age dependent than others, and several parameters of B horizons in these soils show trends related to the progressive development of argillic horizons through time. Utilizing just the B horizon thicknesses, the trend of the chronosequence can be recognized when these are plotted against the assigned terrace ages (figure 8A). The slope of the lines in figure 8 are typical of most of the soil data and suggest a greatly reduced pedologic discrimination beyond about 120 ka, in part an artifact of the shallow pits.

HOLOCENE TECTONICS AND PALEOSEISMOLOGY

Evidence for continued growth of the fold and thrust belt structures in the Holocene has been found at many locations along the north coast of California (figure 9). This evidence includes displacement on thrusts in the MRfz and LSfz, uplift at Clam Beach and along the coast near Cape Mendocino (see Dunklin, this volume; McPherson and Dengler, this volume), and subsidence of the axes of the Freshwater, South Bay, and Eel River synclines (see Li, this volume; Manhart, this volume; Valentine et al, this volume; and Verhey, this volume). The deformation appears to have occurred in sudden events interpreted as paleo-subduction zone earthquakes and may have involved multiple fold and thrust belt structures. Radiocarbon dating of several of these events shows recurrence at intervals of several hundred years in the latest Holocene.

Holocene displacement has been identified and ages for the faulting estimated using radiocarbon on the Little Salmon, Mad River, and McKinleyville faults. Youthful fault scarp morphology on the Trinidad, Blue Lake, and Fickle Hill faults suggest they also have experienced Holocene displacement. Offshore the Little Salmon, Trinidad, and several other faults in the MRfz have generated scarps on the sea floor which also suggest growth in the Holocene (Clarke, 1989). The most active structure appears to be the Little Salmon fault which deforms late Holocene sediments at the south end of Humboldt Bay (Clarke and Carver, 1992). Several faulting events have been interpreted from trench exposures across two traces of the fault which intersect the youthful floodplains of the Little Salmon and Salmon creeks. At these locations sequences of late Holocene overbank silts and buried soils are faulted and folded. Several individual slip events are reflected by onlapping and displacement characteristics of the floodplain stratigraphy. Estimates of the amount of fault slip for each of these events range from 4.5 to as much as 7 meters. C^{14} ages for these events indicate faulting occurred about 300, 800, and 1600 y BP. Average slip rates for the last 6 ky are about 6 to 10 mm/ yr. This slip rate is similar to the long term average rate of displacement across the fault since deposition of the upper Wildcat sediments and the late Pleistocene marine terraces.

Trenches across the Mad River fault at McKinleyville where the fault deforms a late Pleistocene marine terrace show overthrusted scarp derived colluvial wedges and buried soils interpreted to reflect faulting events in the late Pleistocene and Holocene (Carver, 1987b; see stop 3, day 1, this volume). Charcoal collected from the top of the third and base of the second buried colluvial wedge yielded C^{14} ages of about 10 ka, indicating the Mad River fault has generated at least three displacement events in the Holocene. On the McKinleyville fault near Blue Lake, where the fault offsets late Pleistocene fluvial terraces of the Mad River, C^{14} dating of faulted terrace sediments and colluvium indicate that 5 slip episodes of about 3 to 4 meters each have occurred during the last 25 Ky, with two of these more recent than 7400 yBP.

Holocene uplift is recorded along the coast at McKinleyville. This uplift has generated the Clam beach platform, an emergent Holocene marine terrace (see stop 2, day 1, this volume). Terrace cover sediments on the Clam beach platform are interpreted to record two sudden uplift events (Clarke and Carver, 1992). The first has been dated by C^{14} on driftwood contained in the terrace deposits on the platform at about 1100 yBP. Following this uplift event, eolian sand buried the raised terrace and beach. The second uplift event, about 300 yBP is interpreted to have generated a second sand dune sequence which buried the lower eolian blanket and associated weak soil developed in the lower dune surface. To the north near Trinidad, where the coast is cut into

resistant Franciscan rocks, emergent wave cut notches in offshore sea stacks probably also reflect sudden periodic uplift during the Holocene.

Along the coast between Centerville and Cape Mendocino Holocene uplift has generated incision of Holocene floodplain and alluvial fan sediments at the mouths of coastal streams (Johnson, this volume). South of Cape Mendocino raised late Holocene marine terraces extend along the coast southward to the vicinity of the triple junction. The uplift south of Centerville may reflect recent growth of the thickened wedge at the southern edge of the Gorda plate. Several episodes of uplift are indicated by multiple levels of raised beach berms and terrace platform in the Cape Mendocino area (Merritts and Vincent, 1989 and this volume; see also Dunklin, this volume; McPherson and Dengler, this volume).

Sudden events of subsidence of the axes of Freshwater, South Bay, and Eel River synclines have generated distinctive subsidence stratigraphy at Humboldt Bay and in the lower Eel River valley (Clarke and Carver, 1992; Vick, 1989; Valentine et al., 1991 and this volume; Li and Carver, in press; Li, this volume).The late Holocene sediments in these synclines include repeated sequences of intertidal mud which grade upward into peats composed of fossil salt marsh plants. The peats are sharply overlain by the intertidal mud of the next higher sequence, indicating submergence of salt marshes. Salt marsh plants rooted in the buried marsh surfaces are entombed in the base of the overlying intertidal muds, indicating sudden submergence. Foraminiferid associations indicative of high marsh environments are present in the uppermost peat strata, and associations of lower intertidal foraminiferid characterize the lower most mud layers (Shivelle et al., 1991, and C. Shivelle Manhart, this volume) .The abrupt change in microfossil associations also supports the sudden submergence hypothesis.

Fossil spruce trees in growth position are present beneath the upper intertidal mud layer in the Mad River Slough at the north end of Humboldt Bay (Vick, 1989) and in the lower Eel River valley (Li and Carver, in press; Li, this volume). Analysis of the annual ring patterns in these fossil trees supports the sudden submergence hypothesis for these areas. The width of annual rings in trees at both locations show normal growth to the last year of tree life followed by sudden tree death. Cross ring matching between seven of the fossil trees from the Mad River slough shows all died in a two year period.The annual ring patterns of spruce trees killed in Alaska as a result of coseismic subsidence and submergence during the 1964 subduction zone earthquake and the ring patterns of the Mad River slough trees are similar (G. Jacoby, per comm). Submergence recorded by the stratigraphy, fossil marsh plants, fossil trees, and foraminiferid associations in the synclines along

the coast at Humboldt bay and the Eel River valley is interpreted to reflect coseismic subsidence during large earthquakes generated on the southern part of the Csz.

Radiocarbon ages for subsidence events recorded in the syncline stratigraphy provide estimates for the timing of at least 7 late Holocene events. More than 60 C^{14} analysis have been obtained from the subsidence stratigraphy in the three synclines. The dating indicates subduction zone earthquakes occurred about 300, 800, 1100 (2 events), 1700, 2600, and 3000 yBP. The C^{14} ages are similar for all three synclines, and also correspond within the precision of conventional radiocarbon dating methods to the uplift events dated at Clam Beach and faulting episodes dated on the Little Salmon fault.

CONCLUSIONS

The geologic evidence of Quaternary growth of the fold and thrust belt structures in coastal northern California supports the interpretation that subduction is active at the southern end of the Csz.This contraction of the North American plate margin is normal to the direction of plate convergence and has occurred at rates that accommodate half or more of the plate motion predicted from global plate tectonic models. The upper plate deformation lies above the shallow dipping part of the subduction zone where the plate interface is between 5 and 30 km deep (McPherson, 1989, this volume). This part of the plate interface appears to be strongly coupled over geologic time scales, allowing plate motions to generate deformation in the upper plate.

The geologic record for the late Holocene indicates the Csz produces large earthquakes at intervals of several hundred years. Coseismic deformation has accompanied these earthquakes and includes uplift of the coastal region except in the cores of the major synclines where coseismic subsidence occurs. Some of these earthquakes also appear to be accompanied by large amounts of slip on faults in the upper plate above the megathrust, particularly the LSfz. Less frequent events also appear to generate slip of faults in the MRfz. Age estimates for the paleoseismicity at the southern end of the Csz are similar to estimates for coastal subsidence recorded in bays and estuaries on the Oregon and Washington coast (Atwater, 1987, Darienzo and Peterson, 1990, Grant and McLaren, 1987) and in the Puget sound region(Bucknam, 1990). This evidence of temporal coincidence of coseismic activity along the length of the Csz suggests the seismic character of the Csz is similar to other subduction zones where young oceanic crust is being subducted. These subduction zones, including Alaska, S. Chile, Colombia, Mexico, and SW Japan have historically generated great earthquakes and tsunamis, and resulted in coseismic deformation effecting large regions.

REFERENCES

Aalto, K. R., 1982, The Franciscan Complex of northernmost California: sedimentation and tectonics, *in Trench-Forearc Geology*, ed. J. K. Leggett, Geol. Soc. of London Special Pub. 10, p.419-432.

Atwater, B. F., 1987, Evidence for great Holocene earthquakes along the outer coast of Washington State, Sci. 236, p. 942-944

Atwater, T., 1970, Implications of plate tectonics for the Cenozoic tectonic evolution of western North America Geol. Soc. Am Bull. 81, p.3513-3536.

Atwater, T., 1989, Plate tectonic history of the Pacific and western North America, *in* Winterer, E. L., Hussong, D. M., eds., *The Eastern Pacific Ocean and Hawaii: Boulder , Colorado, Geol. Soc. Am. , The Geology of North America,* vol. N, p. 21-72.

Berger,G.W., Burke,R.M., Carver, G.A.,and Easterbrook, D. J., 1991, Test of Thermoluminesence dating with coastal sediments from northern California, Chem. Geol. [Isotope Section] 87, p. 21-37.

Birkeland, P. W., 1984, Soils and Geomorphology: New York, Oxford University Press, 372 p.

Birkeland, P. W., 1985, Quaternary soils of the western United States, *in* Soils and Quaternary Landscape Evolution (Boardman, J., ed.): Chichester, U. K., John Wiley and Sons, p. 303 - 324.

Blake, M. C. Jr., Jayko, A. S., and Howell, 1982, Sedimentation, metamorphism and tectonic accretion of the Franciscan assemblage of northern California, *in* Trench-Forearc Geology, ed. J. K. Leggett, Geol. Soc. of London Special Pub. 10, p.433-438.

Bloom, A. L., Broecker, W. S., Chappell, J., Matthews, R. K., and Mesolella, K. J., 1974, Quaternary sea level fluctuations on a tectonic coast: new Th/U dates from the Huon Peninsula, New Guinea: *Quaternary Research 4,* p.185 - 205.

Bucknam, R. C.,1990, Puget Sound paleoseismicity, *in* National Earthquake Hazards Reduction Program, Summaries of Technical Reports, 30, U.S.Geol. Surv. Open File Rpt. 90-334, p. 462-463.

Bull, W. B., 1985, Correlation of flights of global marine terraces *in* Tectonic geomorphology (Morisawa, M., and Hack, J., eds.): Binghamton Symposia in Geomorphology: International Series, 15, p. 129 - 152.

Burke, R. M., Carver, G. A., and Lundstrom, S. C., 1986, Soil development as a relative dating and correlation tool on marine terraces of northern California: *Geological Society of America Abstracts with Programs 18(2)*, p. 91.

Carver, G. A., 1987a, Late Cenozoic tectonics of the Eel River basin region, coastal northern California, *in* H. Schymiczek and R. Suchland, eds., *Tectonics, sedimentation and evolution of the Eel River and other coastal basins of northern California:* San Joaquin Geological Society Miscellaneous Publication 37, p.61-72.

Carver, G. A., Burke, R. M., and Kelsey, H. M., 1985, Quaternary deformation studies in the region of the Mendocino triple junction *in* Jacobsen, M. L. and Rodrigues,T.R.eds. *Summaries of Technical Reports, V, XXI, National Earthquake Hazards Reduction Program* ,U. S.Geol. Surv. Open File Rpt. 86-31, p. 58-62.

Carver, G. A., Burke, R. M., and Kelsey, H. M., 1986, Deformation of late Pleistocene terraces along the California coast north of Cape Mendocino: *Geological Society of America Abstracts with Programs 18(2)*, p. 93.

Carver, G. A., Stephens, T. A., and Young, J. C., 1982, Quaternary reverse and thrust faults, Mad River fault zone *in* Late Cenozoic history and forest geomorphology of Humboldt County, California, Guidebook for Friends of the Pleistocene 1982 Pacific Cell field trip, p. 93 - 100.

Carver, G. A., Stephens, T. A., and Young, J. C., 1983, Quaternary thrust and reverse faulting on the Mad River fault zone, coastal northern California: *Geological Society of America Abstracts with Programs 15* (5), p. 316.

Carver, G.A., 1987b, Geologic criteria for recognizing individual paleoseismic events in compressional tectonic environments, *in* Anthony J. Crone, ed. *Directions in Paleoseismology*, U. S. Geol. Surv. Open File Rpt. 87-673, p. 115-128.

Chapell, J., and Shackleton, N. J., 1986, Oxygen isotopes and sea level, Nature, 324, p. 137-140.

Chappell, J., 1983, A revised sea level record for the past 300,000 years on Papua New Guinea: a numerical calculation: *Quaternary Research 9,* p. 265 - 287.

Clarke, S. H. Jr., 1987, Geology of the California continental margin north of Cape Mendocino *in* Geology and resource potential of the continental margin of western North America and adjacent ocean basins - Beaufort Sea to Baja California (Scholl, D. W., Grantz, A., and Vedder, J. G., eds.): Circum-Pacific Council for Energy and Mineral Resources, Earth Science Series (in press).

Clarke, S. H. Jr., 1992, Geology of the Eel River basin and adjacent region: Implications for late Cenozoic tectonics of the southern Cascadia subduction zone and the Mendocino triple junction, Am. Assoc. Petroleum Geol. Bull , 76, 2, p.199-224.

Clarke, S. H. Jr., and Carver, 1992, Late Holocene tectonics and paleoseismicity, southern Cascadia subduction zone, Science, 255, p.188-192

Cox, A., and Engebretson, D., 1985, Changes in motion of the Pacific plate at 5 Myr BP, Nature, 313, p. 472-474.

Darienzo, M. E. and Peterson, C. D., 1990, Episodic tectonic subsidence of late Holocene salt marshes, northern Oregon coast, central Cascadia margin, U. S. A., Tectonics 9, p. 1-22.

Dickinson, W. R., and Snyder, W. S., 1979, Geometry of subducted slabs related to San Andreas transform, J. Geophy. Res., 87, p.609-627.

Diller, J. S., 1902, Topographic development of the Klamath Mountains, U. S. Geol. Survey Bull. 196, pp. 69.

Dott, J. M., Mead, J., and Stanton, R. G., 1977, Paleomagnetic stratigraphy of Pliocene Centerville Beach section, northern California, Earth and Planetary Sci. letters, 34, p. 381-386.

Engebretson, D. C., Cox, A., and Gordon, R. G., 1985, Relative motions between oceanic and continental plates in the Pacific basin, Geol. Soc. Am. Special Paper 206, 59 p.

Engebretson, D. C., Cox, A., and Gordon, R. G., 1985, Relative motions between oceanic and continental plates in the Pacific basin: Geological Society of America special paper 206, 59 p.

Grant, W. C., and McLaren, D. D., 1987, Evidence for Holocene subduction earthquakes along the Oregon coast, abs, EOS Trans. AGU, 68, p. 1469.

Harbert, W., and Cox, A., 1989, Late neogene motion of the Pacific plate, J. Geophys. Res., 94, p. 3052-3064.

Harden, J. W., 1982, A quantitative index of soil development from field descriptions: examples from a chronosequence in central California: *Geoderma 28,* p. 1 - 28.

Harden, J. W., and Taylor, E. M., 1983, A quantitative comparison of soil development in four climatic regimes: *Quaternary Research 20* (3), p. 342 - 359.

Harden, J.W., Sarna-Wojcicki, A.M., and Dembroff, G.R., 1986, Soils developed on coastal snd fluvial terraces near Ventura, California: U.S. Geological Survey Bulletin 1590 B, 34 p.

Ingle, J. C., 1976, Late neogene paleobathymetry and paleoenvironments of the Humboldt basin, northern California, in Fritsche, A. E., Ter Best, H. Jr., and Wornhardt, W. W. eds.: *The neogene symposium selected echnical papers on paleontoloy, sedimentology, petrology, tectonics, and geologic history of the Pacific coast of North America,* Soc.Economic Paleontologist and Mineralogist , Annual meeting, San Francisco, p. 37-61.

Ingle, J. C., 1987, The depositional, tectonic, and paleoceanographic history of the Eel River (Humboldt), Point Arena, and Bodega (Point Reyes) basins of northern California; a summary of stratigraphic evidence, *in* H. Schymiczek and R. Suchland, eds., *Tectonics, sedimentation and evolution of the Eel River and other coastal basins of northern California:* San Joaquin Geological Society Miscellaneous Publication 37, p.49-5

Jennings, C., 1977, Geologic map of California, 1: 750,000: California Division of Mines and Geology.

Kadama, K. P., 1979, New paleomagnetic results from the Rio Dell Formation, California, Am. Geophy. Union , Geophy. Res. Letters, 6, 4, p.253-256.

Kelsey, H. M., and Allwardt, A. O., 1983, Evidence for a major Quaternary fault zone in the Central Belt Franciscan Melange, northern California: *Geological Society of America Abstracts with Programs 15* (5), p. 316.

Kelsey, H. M., and Carver, G. A., 1986, Studies of Quaternary faulting through the analysis of small faults and fractures, north coastal California *in* National Earthquake Hazards Reduction Program, summaries of technical reports volume XXII, USGS open-file report 86-383.

Kelsey, H. M., and Carver, G. A., 1988, Late neogene and Quaternary tectonics associated with the northward growth the San Andreas transform fault, northern California, J. Geophy. Res. 93, p. 4797-4819.

Kelsey, H. M., and Cashman, S. M., 1983, Wrench faulting in northern California and its tectonic implications: *Tectonics 2,* p. 565 - 576.

Krantz, R. W., 1986, Orthorhombic fault patterns and three-dimensional strain analysis, northern San Rafael Swell, Utah: *Geological Society of America Abstracts with Programs 18* (2), p. 125.

Lajoie, K. R.,1986, Coastal tectonics *in* Active tectonics (Wallace, R. E., Chair) *in the series* Studies in Geophysics: Washington D. C., National Academic Press, p. 95 - 124.

Li, W. H. and Carver, G. A., in press, Late Holocene Subsidence in the Eel River syncline, northern California, abs, 1992 annual meeting Geol. Soc. Am, Cord. section, Eugene, Ore.

Manning, G. A., and Ogle, B. A., 1950, Geology of the Blue Lake Quadrangle, California, Cal. Div. Mines Bull 148, pp. 35.

Manning, G. A., and Ogle, B. A., 1950, Geology of the Blue Lake Quadrangle: California Department of Natural Resources, Division of Mines, Bulletin 148.

McCory, P. C., 1989, Late neogene geohistory analysis of the Humboldt basin and its relationship to convergence of the Juan de Fuca plate, J. Geophy. Res. 94, p. 3126-3138.

McKenzie, D. P., and Morgan, W. J., 1969, Evolution of triple junctions, Nature, 224, 5215, p. 125-133.

McLaughnin, R. J., 1983, Post middle Miocene accretion of Franciscan rocks, northwestern California, Geol. Soc. Am. Bull. 93,p. 595-605.

McPherson, R. C., 1989, Seismicity and focal mechanisms near Cape Mendocino, northern California: 1974-1984, Master Thesis, Humboldt State University, pp.75.

Merritts, D., and Vincent, K. R., 1989, Geomorphic response of coastal streams to low, intermediate, and high rates of uplift Mendocino triple junction region, northern California, Geol. Soc. Am. Bull. 101, p. 1373-1388.

Nilsen, T. H., and Clarke, S. H. Jr., 1987, Geologic evolution of the late Cenozoic basins of northern California,*in* H. Schymiczek and R. Suchland, eds., *Tectonics, sedimentation and evolution of the Eel River and other coastal basins of northern California:* San Joaquin Geological Society Miscellaneous Publication 37, p.15-29.

Ogle, B. A., 1953, Geology of the Eel River Valley area, Humboldt County, California, Cal. Div. Mines Bull 164, pp. 128.

Ogle, B. A., 1953, Geology of the Eel River valley area, Humboldt County, California: California Department of Natural Resources, Division of Mines, Bulletin 164.

Reches, Z., and Dieterich, J. H., 1983, Faulting of rocks in three-dimensional strain fields I. Failure of rocks in polyaxial servo-controlled experiments: *Tectonophysics 95,* p.111-132.

Riddihough, R., 1984, Recent movements of the Juan de Fuca plate system, J. Geophys. Res., 89, p.6980-6994.

Rockwell, T. K., Johnson, D. L., Keller, E. A., and Dembroff, G. R., 1985, A late Pleistocene-Holocene soil chronosequence in the Ventura basin, southern California, USA: *in* Geomorphology and Soils (Richards, K. S., Arnett, R. R., and Ellis, S., eds.): London, U. K., George Allen and Unwin, p. 309 - 327.

Sarna-Wojcicki, A. M., LaJoie, K. R., Meyer, C. E., Adam, D. P., and Rieck, H. J., 1991, Tephrochronologic correlation of upper neogene sediments along the Pacific margin, conterminous United States, Geol. Soc. Am. DNAG series K-12, p. 117-140.

Sarna-Wojcicki, A. M., Morrison, S. D., Meyer, C. E., and Hillhouse, J. W., 1987, Correlation of upper Cenozoic tephra layers between sediments of the western United States and eastern Pacific ocean and comparison with biostratigraphic and magnetostratigraphic age data, Geol. Soc. Am. Bull 93, p. 207-223.

Shevelle, C. D., Carver, G. A., and Valentine, D. W., 1991, Foraminiferid stratigraphy as evidence for great earthquakes on the Cascadia subduction zone in northern California, abs. Seismol. Soc. Am. and Geol. Soc. Am joint meeting, Abstracts with Programs, 23, 2, p. 97.

Smith, B., 1983, The McKinleyville "A" horizon: distribution and origin of an eolian soil cap: B. S. thesis, Humboldt State University, 28 p.

Soil Survey Staff, 1951, Soil survey manual: U.S. Department of Agriculture Handbook no. 18, 503 p.

Stuiver, M., and Reimer, P. J.,1986, A computer program for radiocarbon age calibration, Radiocarbon 28, p. 1022-1030.

Suppe, J., 1983, Geometry and kinematics of fault-bend folding: *American Journal of Science 283* (7), p. 684 - 721.

Tuttle, D. C.,1981, Investigation of methods for determining coastal bluff erosion: a report to the Sea Grant Program, Arcata, California, 161 p.

Upp, R. R., 1982, Holocene activity on the Maacama fault, Mendocino County, California: Ph.D. dissertation, Stanford University, 112 p.

Valentine, D. W., Carver, G. A., and Shivelle, C., 1990, Late Holocene stratigraphic evidence for rapid episodic subsidence, Humboldt Bay, California, abs. Geol. Soc. Am. Abstracts with Programs, 23, 1, p.42.

Vick, G. S., 1988, Late Holocene paleoseismicity and relative sea level changes of the Mad River Slough, northern California, Master Thesis, Humboldt State University, pp. 87.

Walter, S. R., 1986, Intermediate focus earthquakes associated with Gorda plate subduction, Bull. Seis. Soc. Am. 76, p. 583-588.

Wilson, D. S., 1989, Deformation of the so called Gorda plate, J. Geophy. Res. 94, p. 3065-3075

Woodward-Clyde Consultants, 1980, Evaluation of the potential for resolving the geologic and seismic issues at the Humboldt Bay Power Plant Unit No. 3, Appendices, Woodward-Clyde Consultants, Walnut Creek, California.

Woodward-Clyde Consultants, 1980, Evaluation of the potential for resolving the geologic and seismic issues at the Humboldt Bay Power Plant unit no. 3, appendix D: San Francisco, California, Woodward-Clyde Consultants, pp. 145.

FIGURES FOR CARVER AND BURKE ON FOLLOWING PAGES

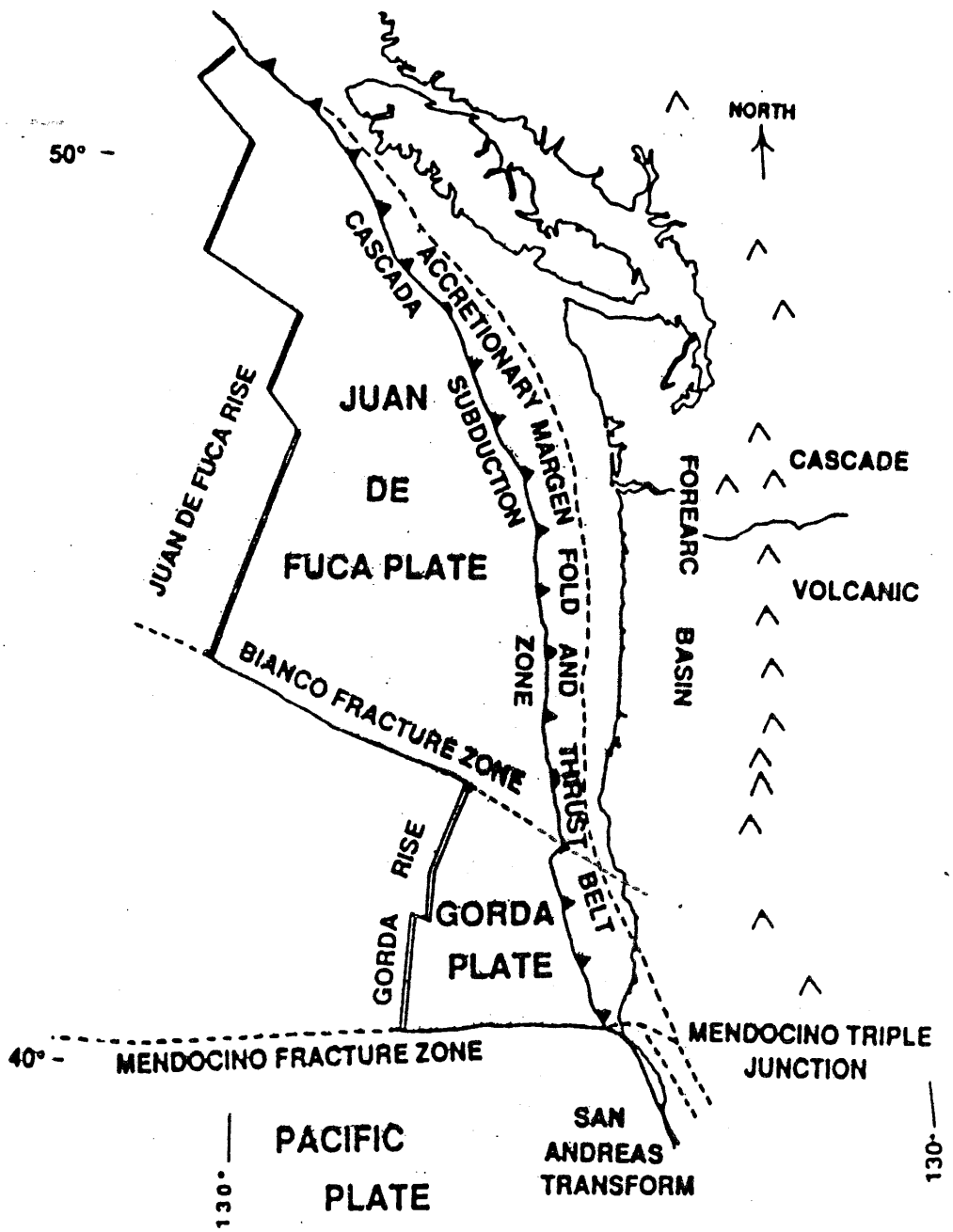

Figure 1. The modern Cascadia Subduction zone The Juan de Fuca-Gorda plates are obliquely subducting beneath the North American plate. A prominent fold and thrust belt is present in the western edge of the North American plate. This contractual system of faults and folds lies offshore except at the southern end of the subduction zone where the plate boundary approaches the coast.

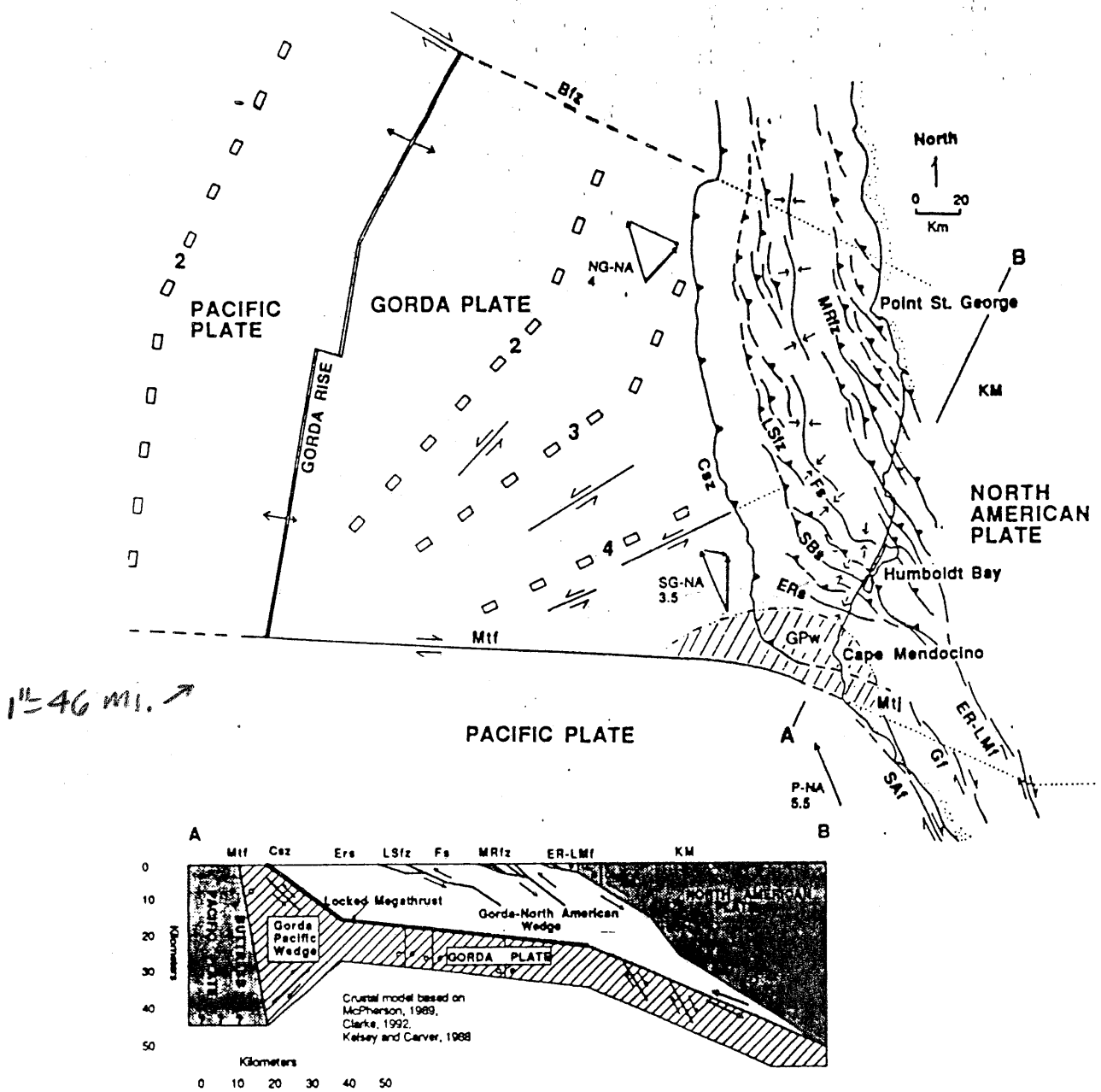

Figure 2. Plate tectonics map of the Gorda Plate and segment of the Cascadia subduction zone. lines of open rectangles indicate the position of sea floor magnetic anomalies which show rotation of the southern part of the plate and decreased spreading at the south end of the Gorda rise. These internal plate motions have resulted in decreased convergence at the south end of the subduction zone as shown by the vector-rate diagrams depicting northern Gorda (NG-NA), southern Gorda (SG-NA) and Pacific (P-NA) motions relative to a fixed North American plate. Convergence between the Gorda and Pacific plates results in compression and thickening of the southeast edge of the subducting oceanic slab and generated the Gorda-Pacific wedge. Symbols: Bfz-Blanco fracture zone, Mtf-Mendocino transform fault, Csz-Cascadia subduction zone, MRfz-Mad River fault zone, LSfz-Little Salmon fault zone, Fs-Freshwater syncline, SBs-South Bay syncline, ERs-Eel River syncline, Mtj-Mendocino triple junction, SAf-San Andreas fault. Gf-Garberville fault,ER-LMf-Eaton Rough-Lake Mountain fault, GPw-Gorda-Pacific wedge, KM-Klamath Mountains.

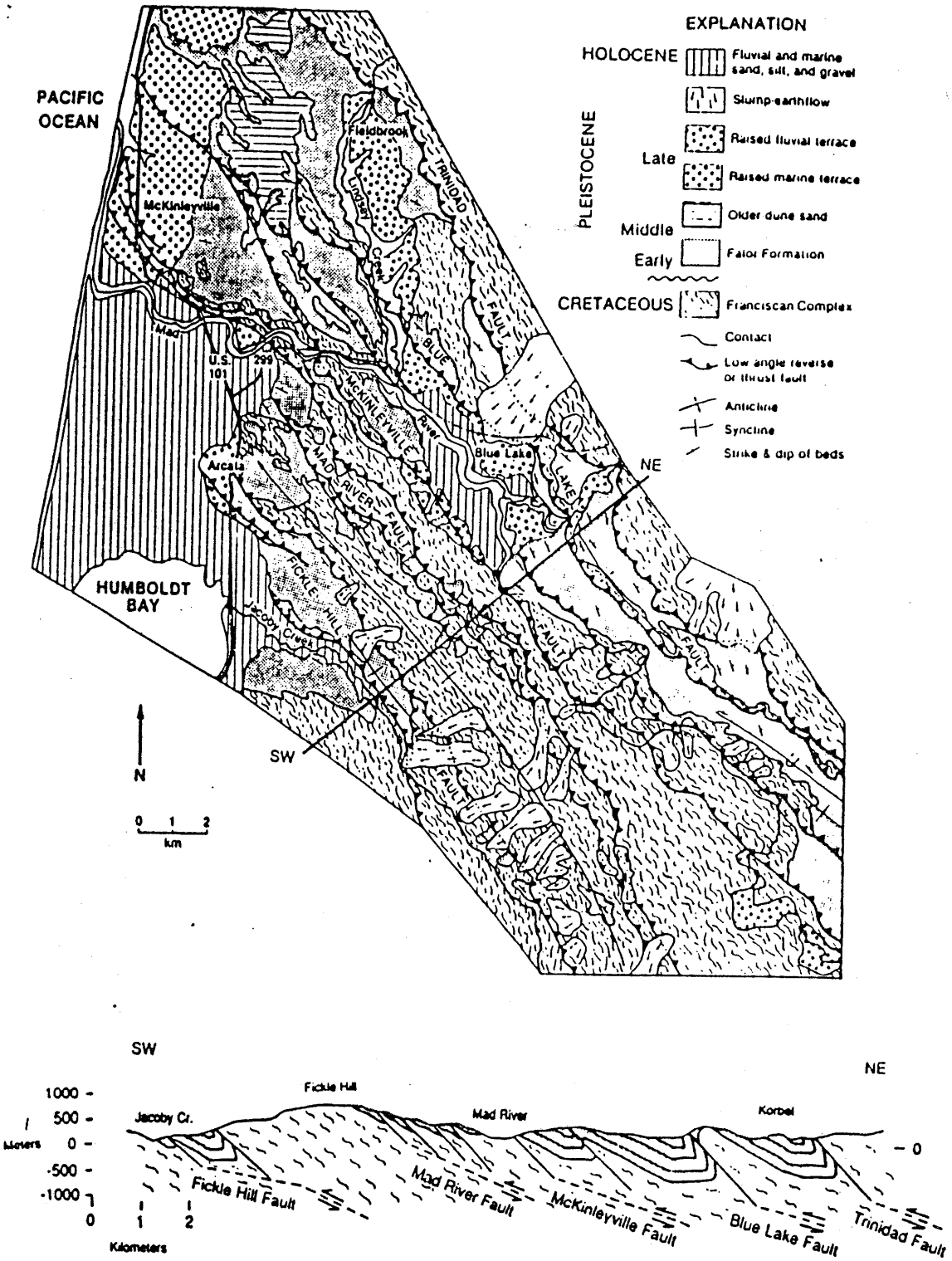

Figure 3. Geologic Map and cross section of the Mad River fault zone. Franciscan complex rocks have been thrust over Quaternary Falor Formation sediments on northeast dipping imbricate thrust faults.

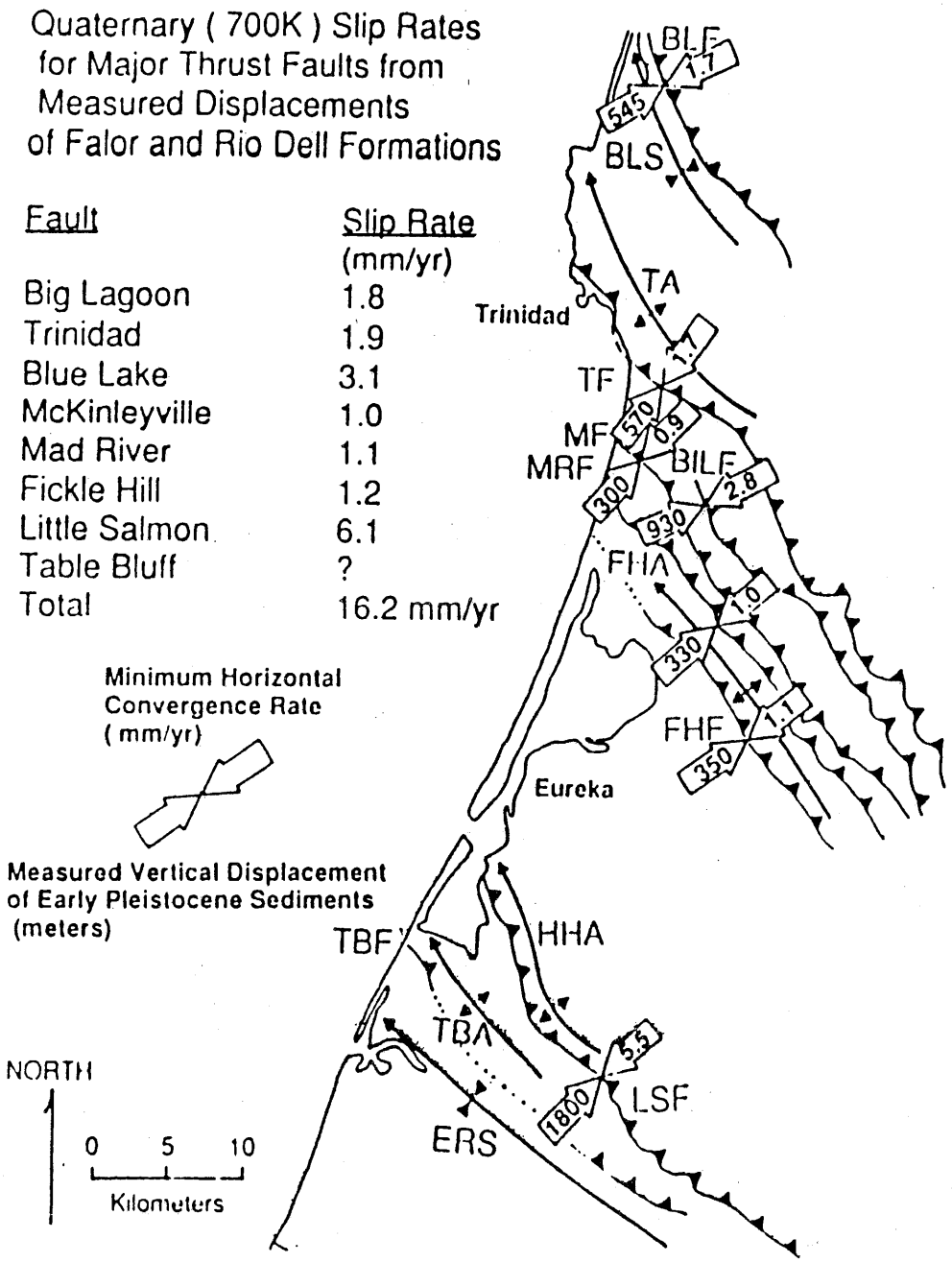

Figure 4. The amount and rate of growth of thrusts in the LSfz and MRfz since the deposition of the Falor and Rio Dell Formations can be estimated from measurements of the thickness of sediments thrust under Franciscan rocks. Numbers in northeast pointing arrows indicate sediment thickness in meters beneath the thrusts. Numbers in southwest pointing arrows show calculated horizontal convergence rates in mm/yr normal to the faults. Symbols: BLF-Big Lagoon fault, BLS-Big Lagoon syncline, TA- Trinidad anticline, TF-Trinidad fault, MF-McKinleyville fault, MRF-Mad River fault, BILF-Blue Lake fault, FHA-Fickle Hill anticline, FHF-Fickle Hill fault, HHA-Humboldt Hill anticline, LSF-Little Salmon Fault, TBF-Table Bluff fault, ERS-Eel River syncline.

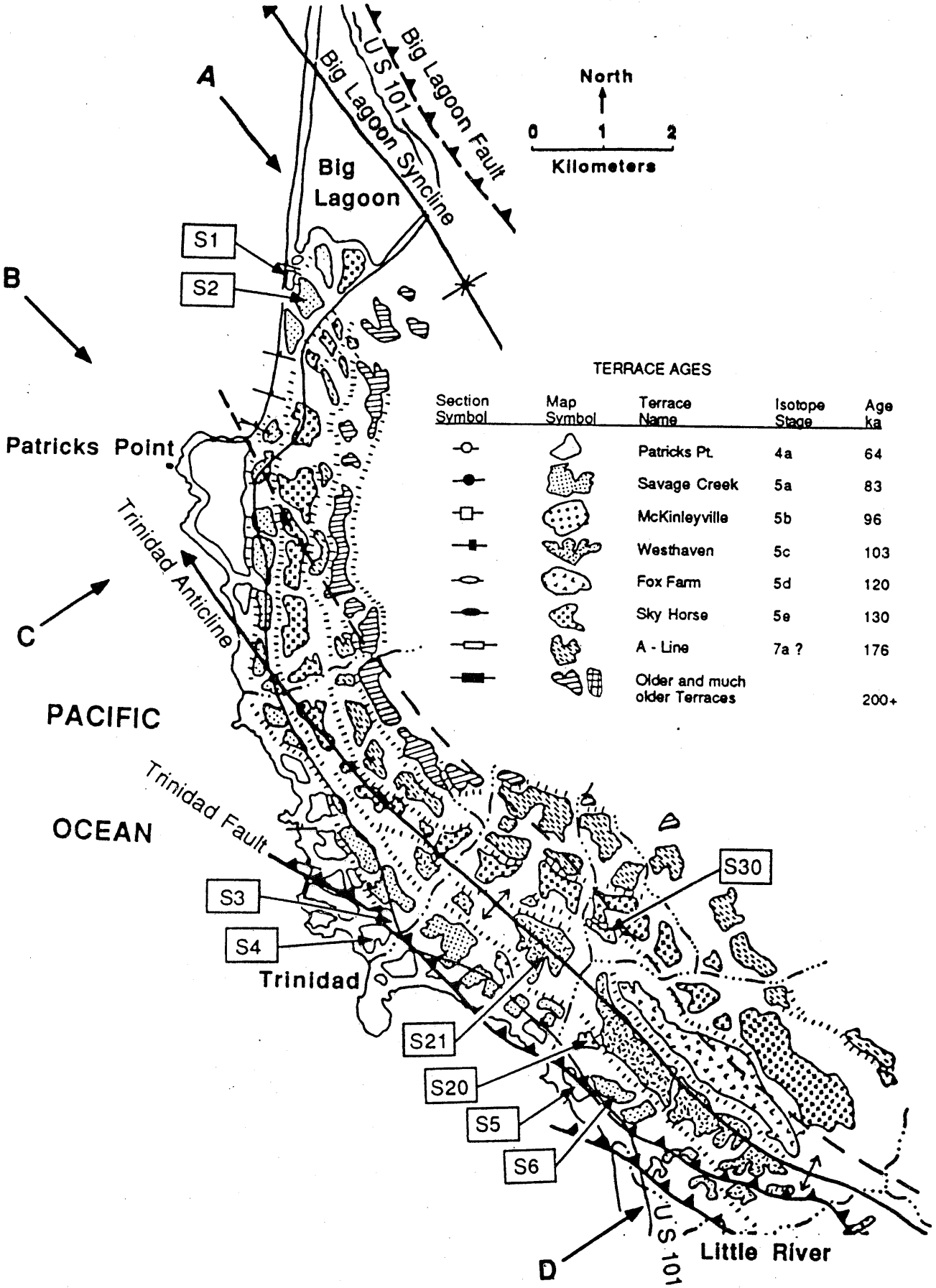

Figure 5. Map sheets and related cross sections (lower cross sections are shown with no vertical exaggeration) of raised, faulted, and folded late Pleistocene marine terraces between Big Lagoon and False Cape. Map segments are labeled A to L from north to south. Soil locations are given as S-#'s in the boxes, and cross section symbols for each age of terrace are given in the key near the northern portion of the map.

1" = 3265'

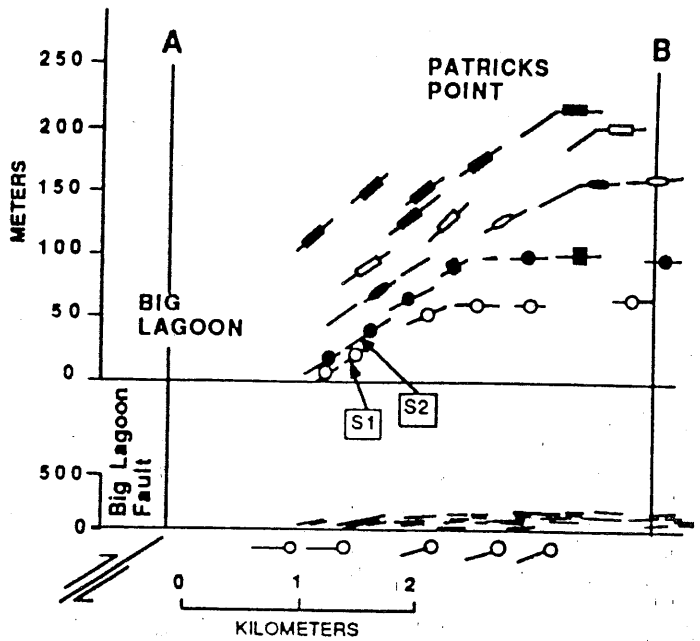
A
B
PATRICKS POINT
BIG LAGOON
METERS
250
200
150
100
50
0
500
0
Big Lagoon Fault
S1
S2
0
1
2
KILOMETERS

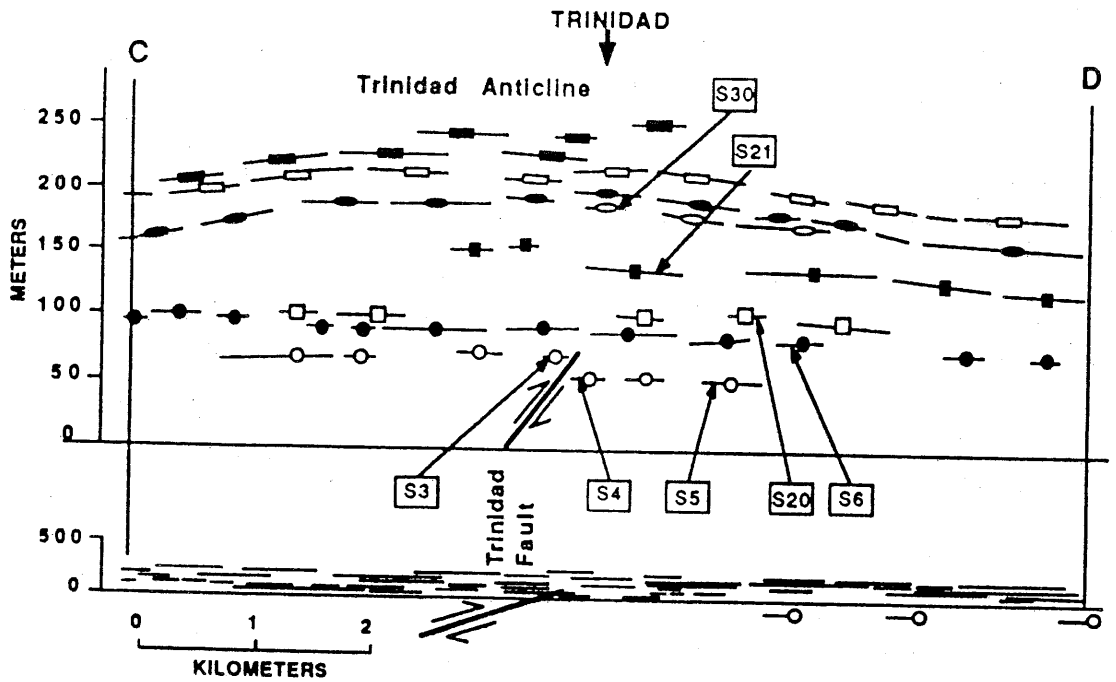
TRINIDAD
C
D
Trinidad Anticline
S30
S21
METERS
250
200
150
100
50
0
500
0
S3
S4
S5
S20
S6
Trinidad Fault
0
1
2
KILOMETERS

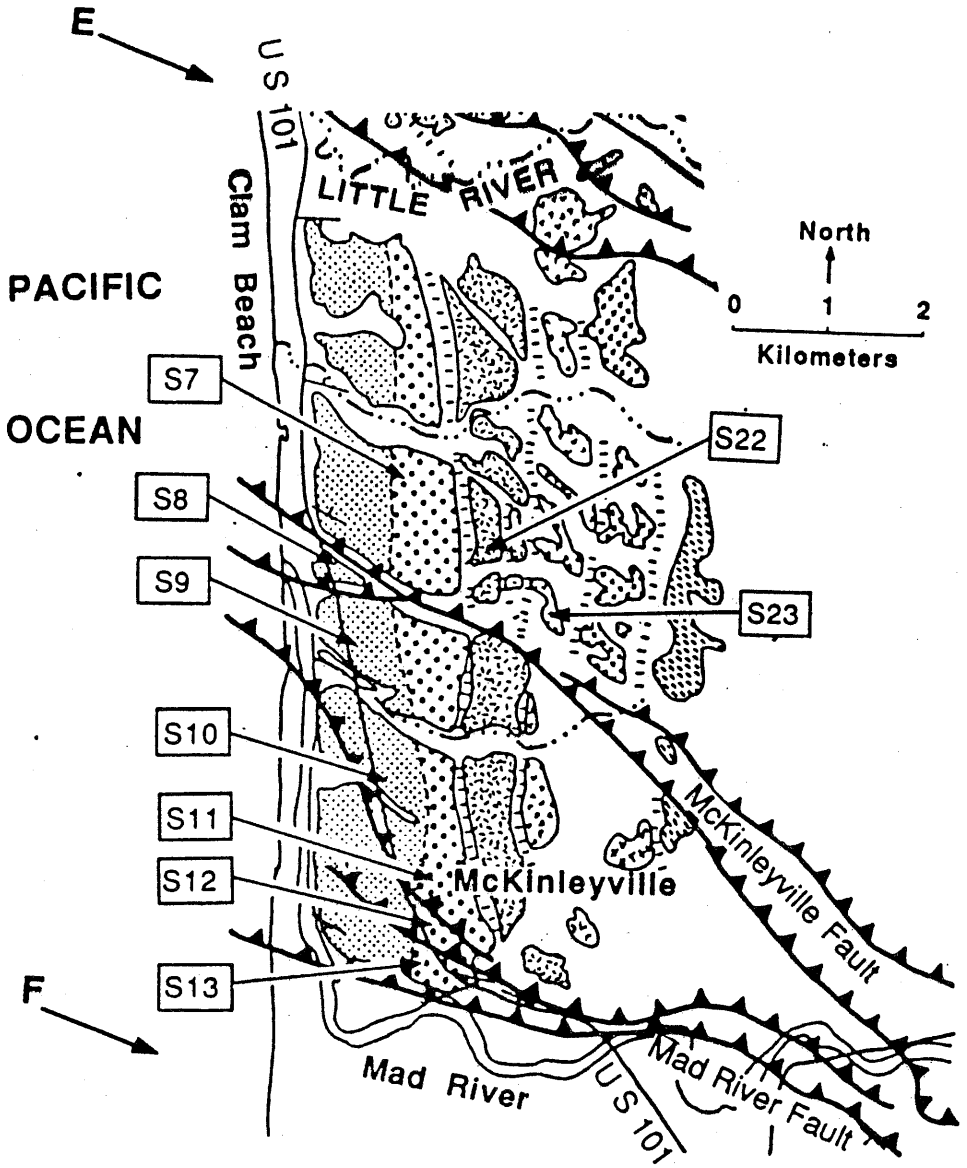
E
US 101
Clam Beach
LITTLE RIVER
PACIFIC
OCEAN
North
0 1 2
Kilometers
S7
S8
S9
S10
S11
S12
S13
S22
S23
McKinleyville
McKinleyville Fault
Mad River
US 101
Mad River Fault
F

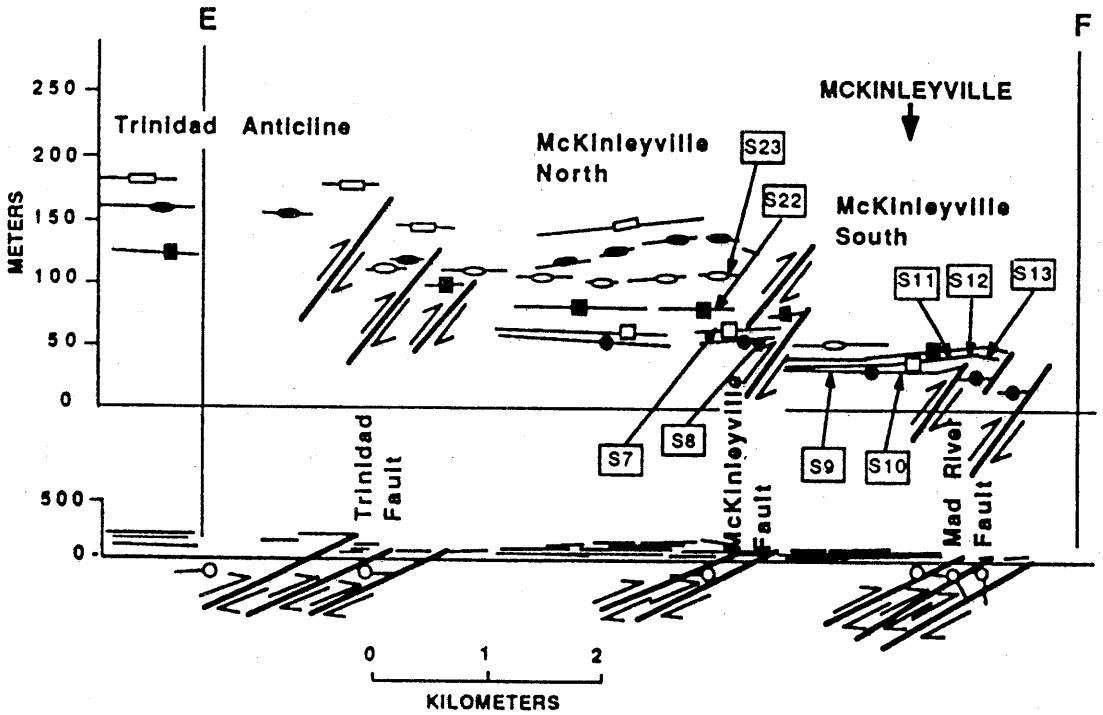
E
F
MCKINLEYVILLE
Trinidad Anticline
McKinleyville North
McKinleyville South
S23
S22
S11
S12
S13
S7
S8
S9
S10
METERS
250
200
150
100
50
0
500
0
Trinidad Fault
McKinleyville Fault
Mad River Fault
0 1 2
KILOMETERS

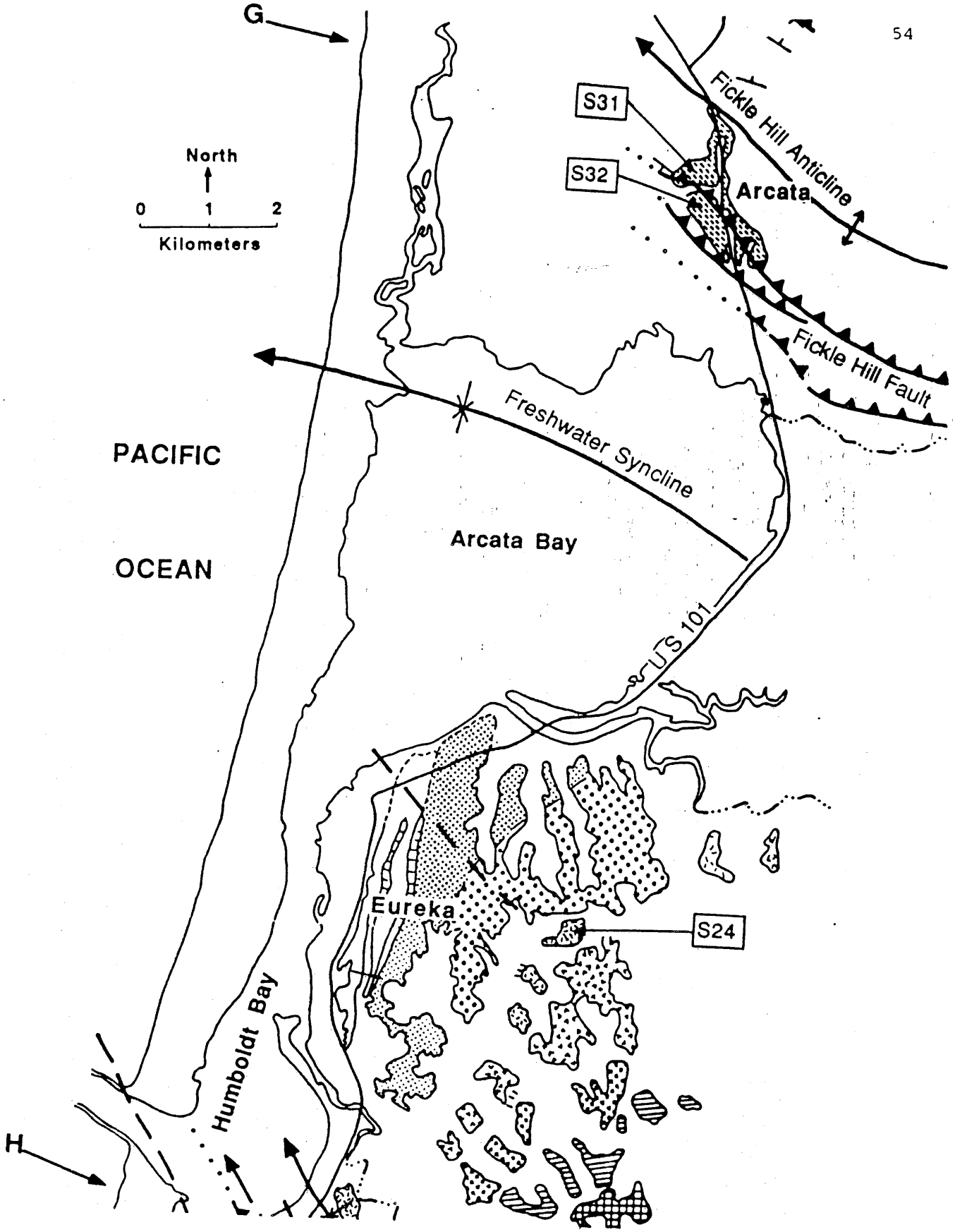
G
North
0
1
2
Kilometers
S31
S32
Arcata
Fickle Hill Anticline
Fickle Hill Fault
Freshwater Syncline
PACIFIC
OCEAN
Arcata Bay
US 101
Eureka
S24
Humboldt Bay
H

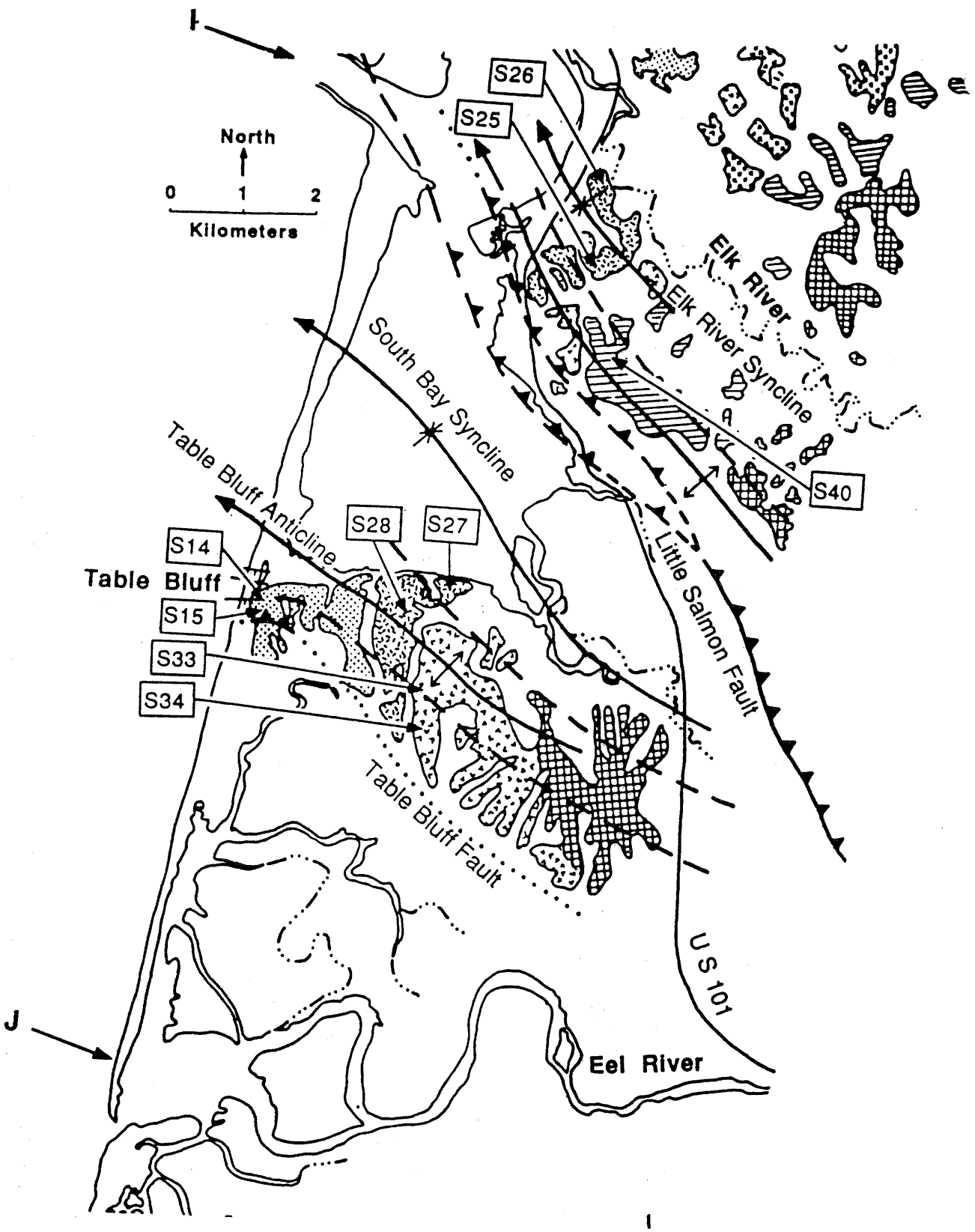
I
North
0
1
2
Kilometers
S26
S25
Elk River
Elk River Syncline
South Bay Syncline
Table Bluff Anticline
S40
S28
S27
S14
Table Bluff
S15
S33
S34
Little Salmon Fault
Table Bluff Fault
US 101
J
Eel River

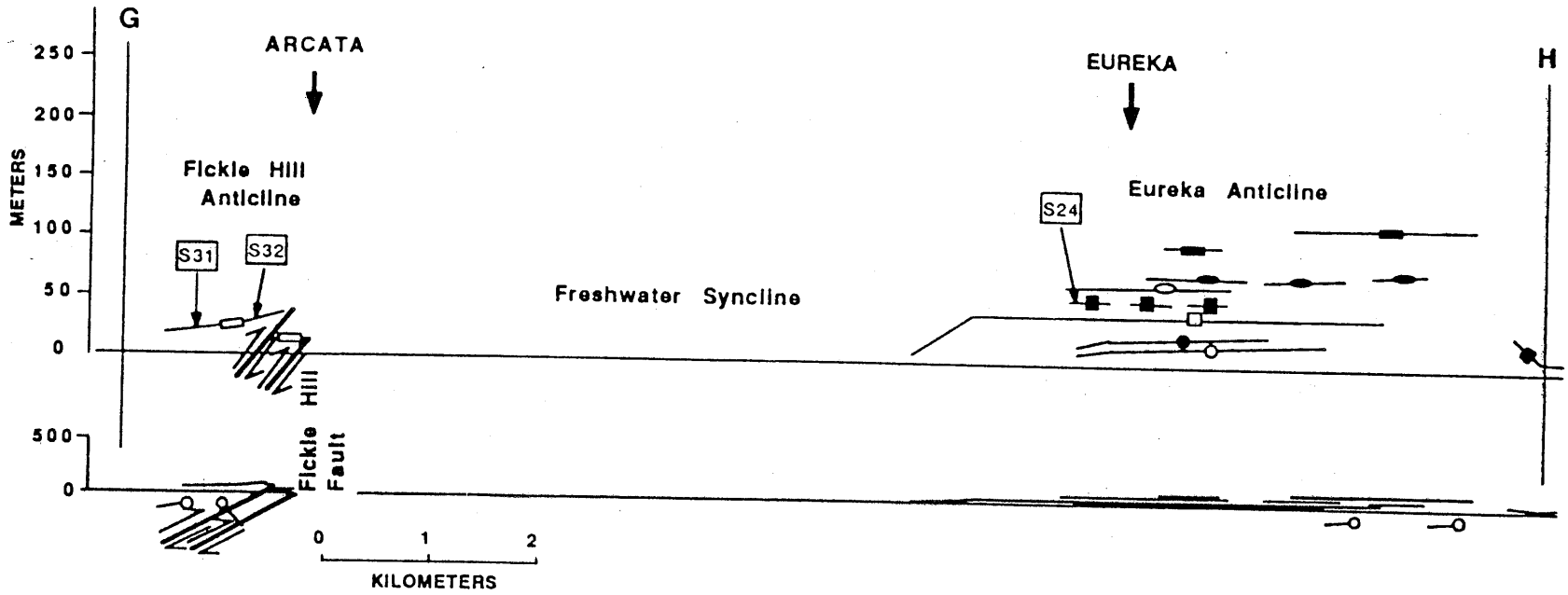
G
H
ARCATA
EUREKA
METERS
250
200
150
100
50
0
500
0
Fickle Hill Anticline
S31
S32
S24
Eureka Anticline
Freshwater Syncline
Fickle Hill Fault
0
1
2
KILOMETERS

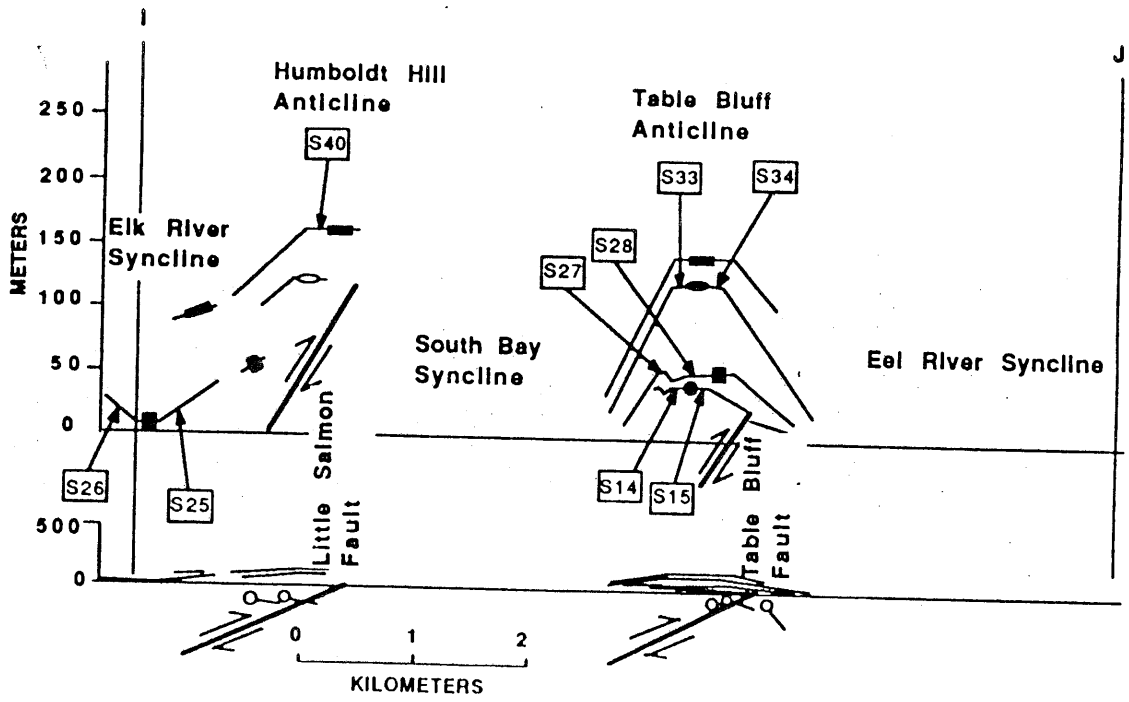
I
J
METERS
250
200
150
100
50
0
500
0
Humboldt Hill Anticline
S40
Elk River Syncline
S26
S25
Little Salmon Fault
South Bay Syncline
Table Bluff Anticline
S33
S34
S28
S27
S14
S15
Table Bluff Fault
Eel River Syncline
0
1
2
KILOMETERS

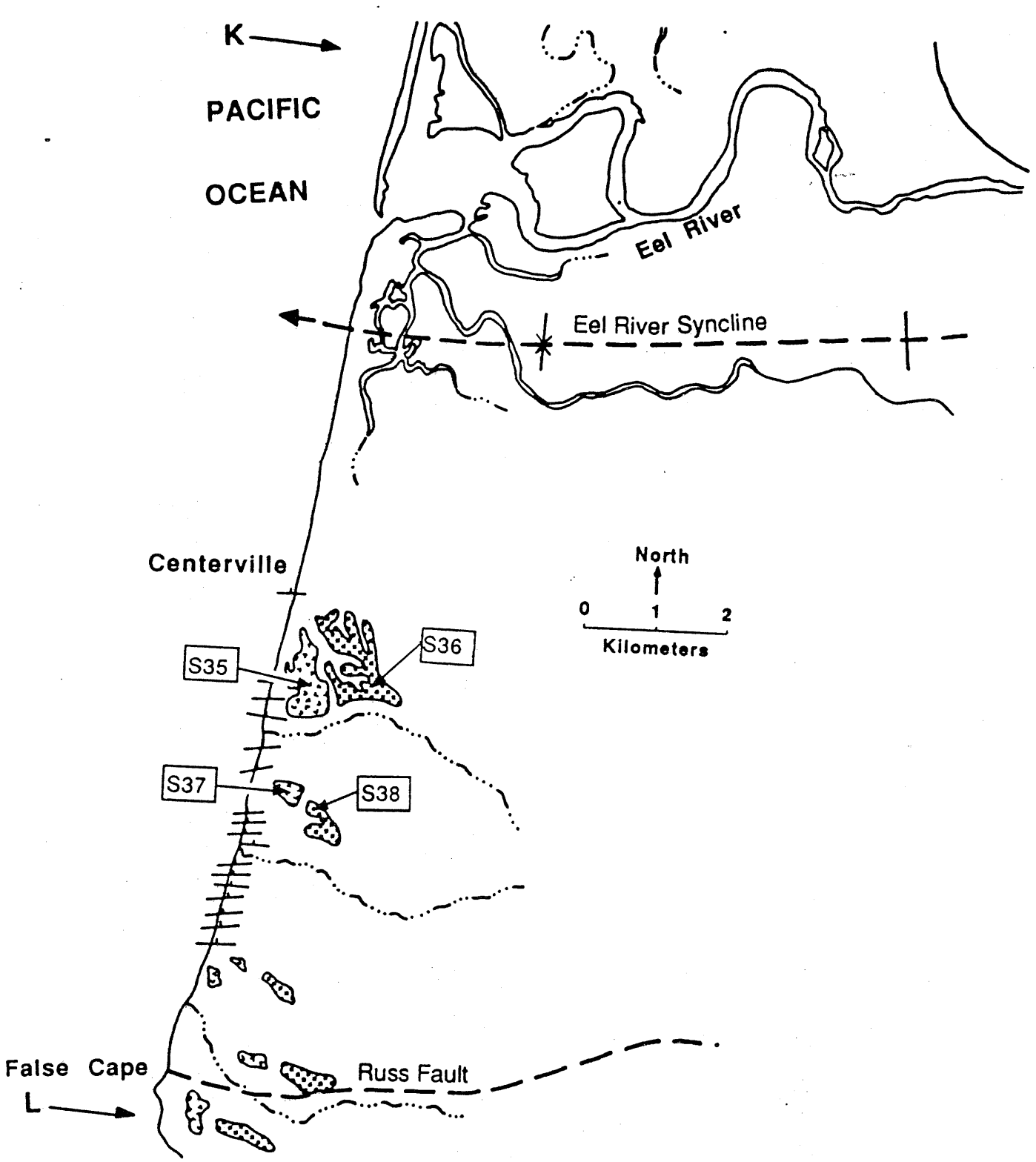
K
PACIFIC
OCEAN
Eel River
Eel River Syncline
Centerville
North
0
1
2
Kilometers
S35
S36
S37
S38
False Cape
L
Russ Fault

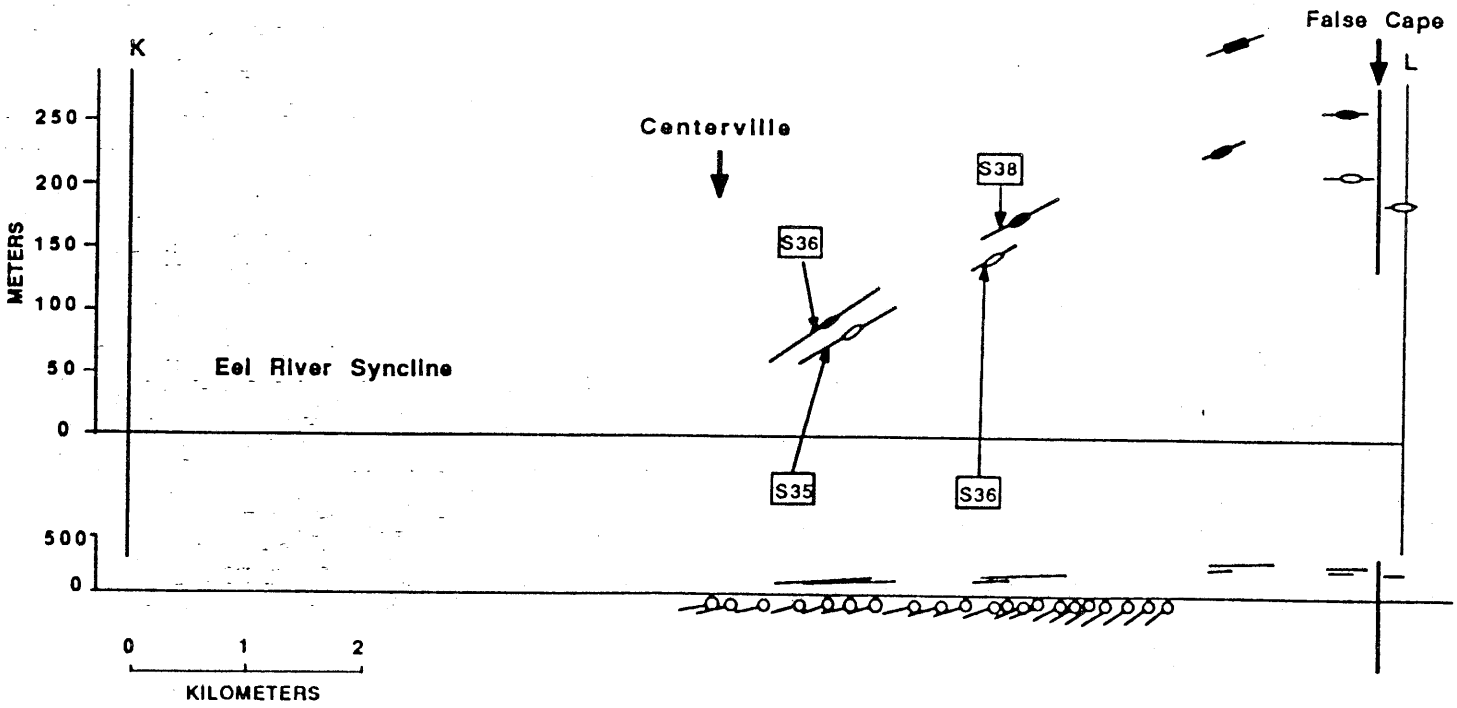
K
L
False Cape
Centerville
Eel River Syncline
S35
S36
S36
S38
METERS
250
200
150
100
50
0
500
0
0
1
2
KILOMETERS

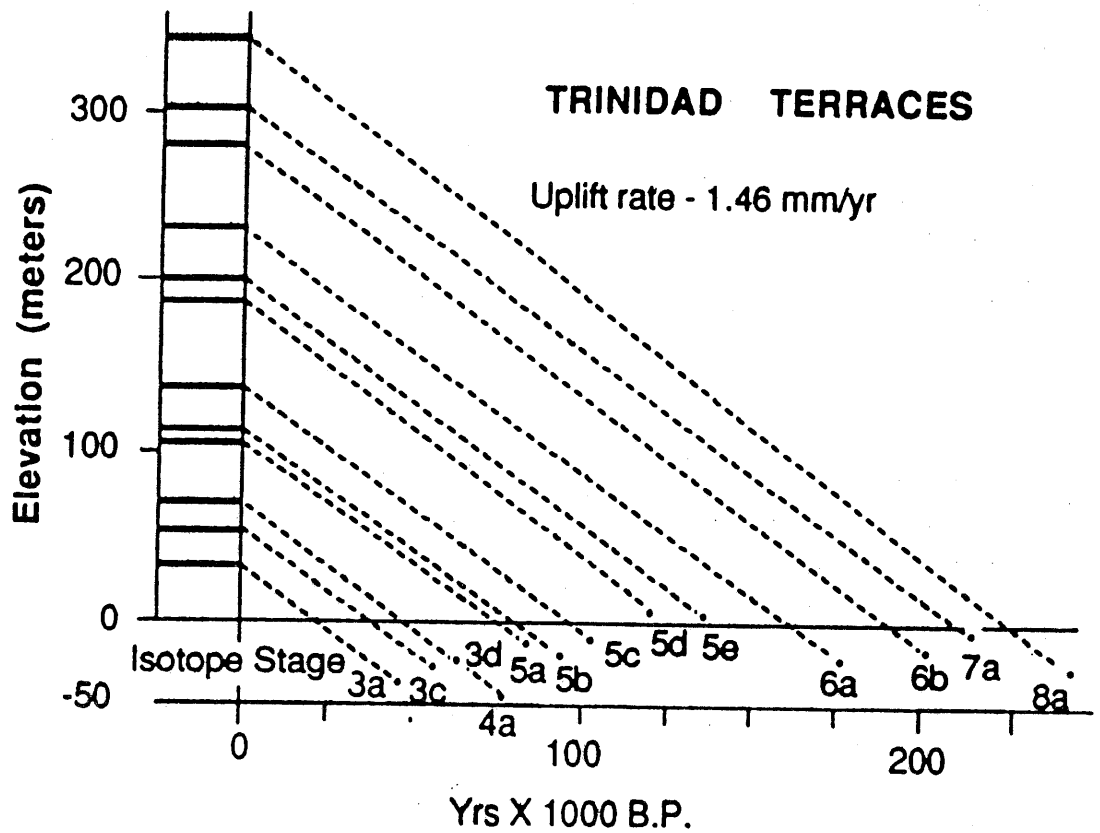

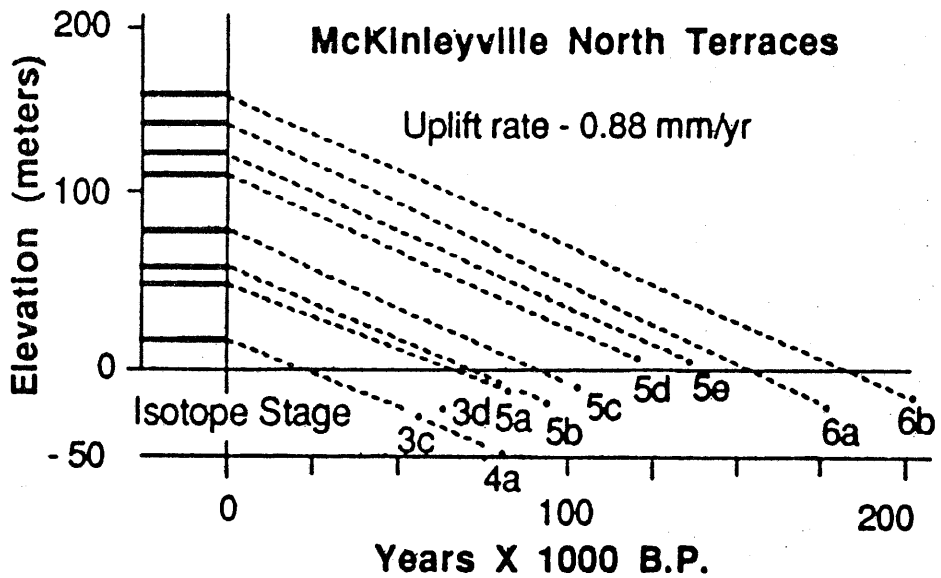

Figure 6. Uplift rate models for late Pleistocene marine terraces at Trinidad and McKinley ''le.

Soil Age Class I

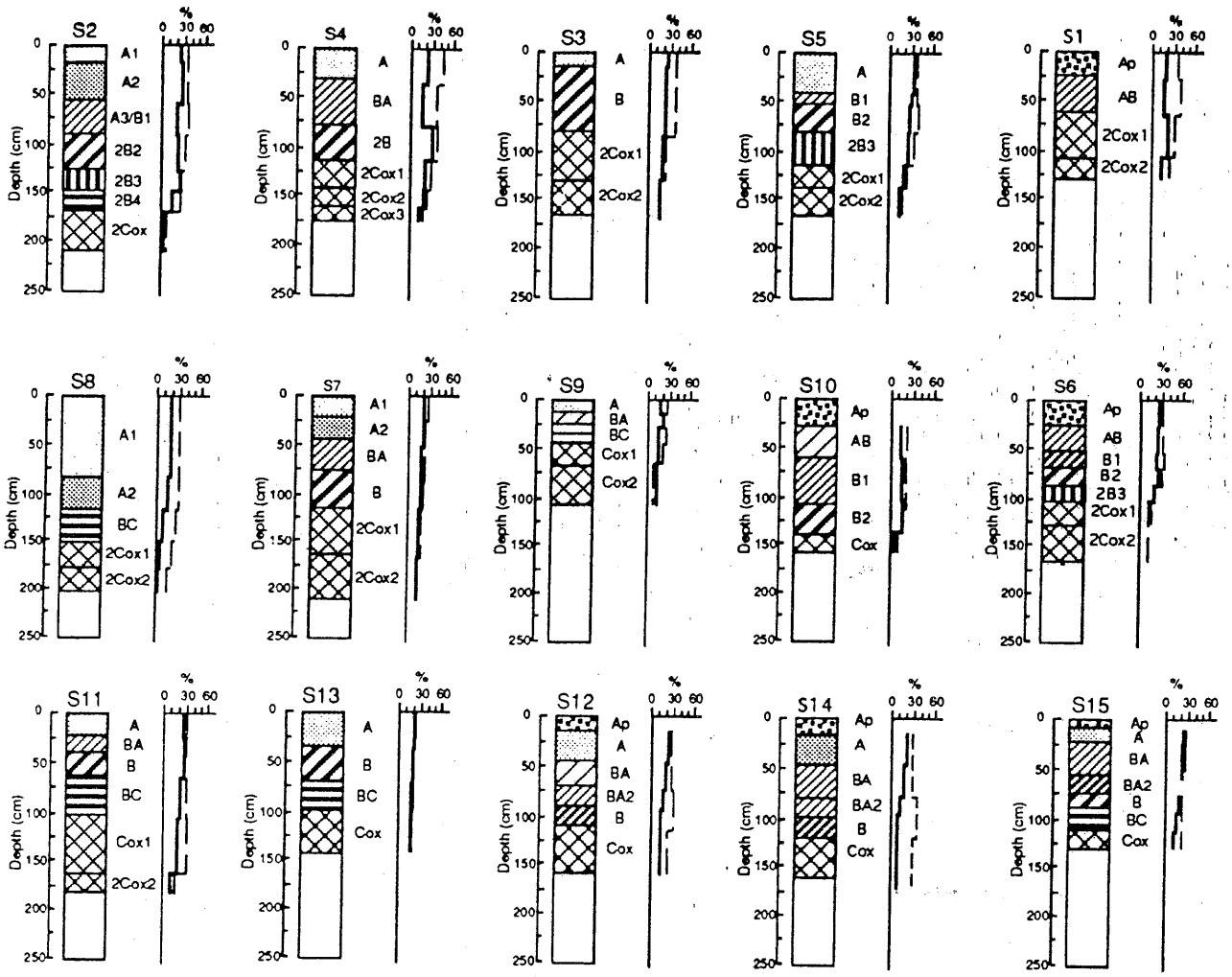

Figure 7. Schematic soil profiles for three soil age classes (I being the youngest) showing field horizonation and laboratory particle size distribution.

Soil Age Class II

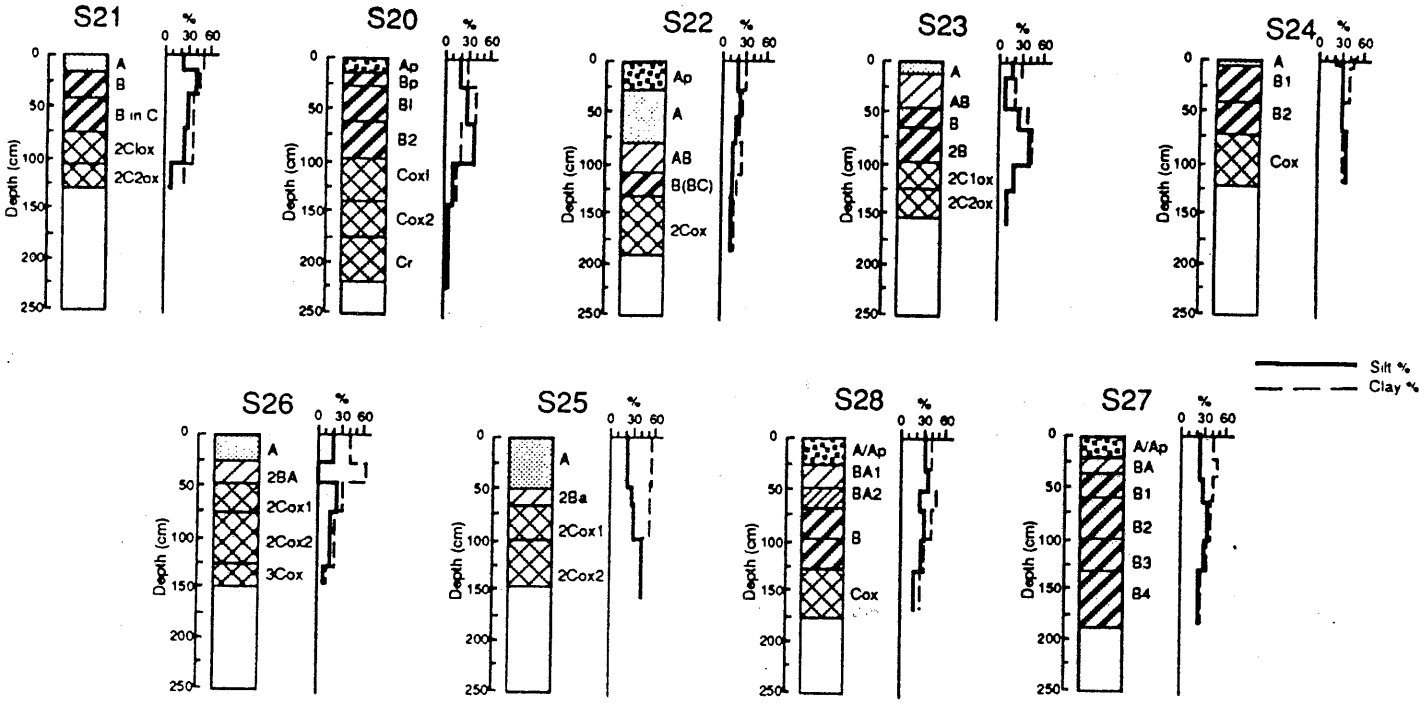

Soil Age Class III

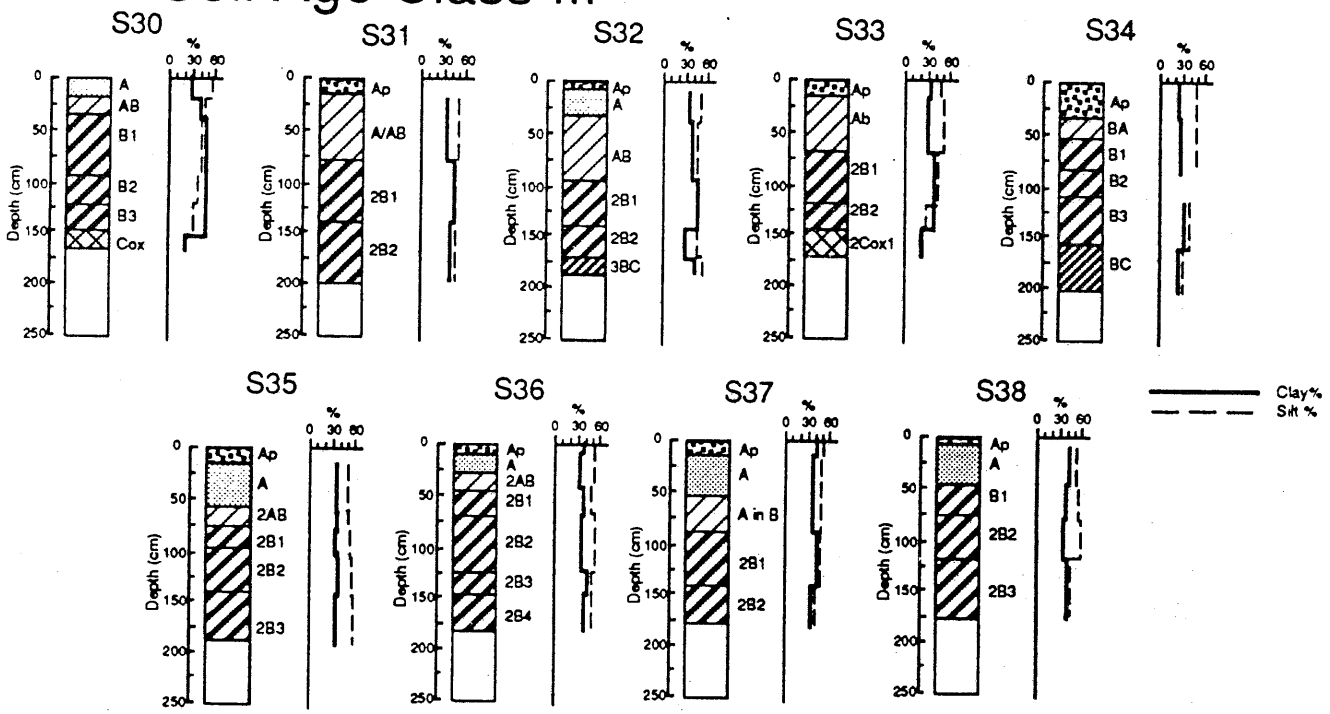

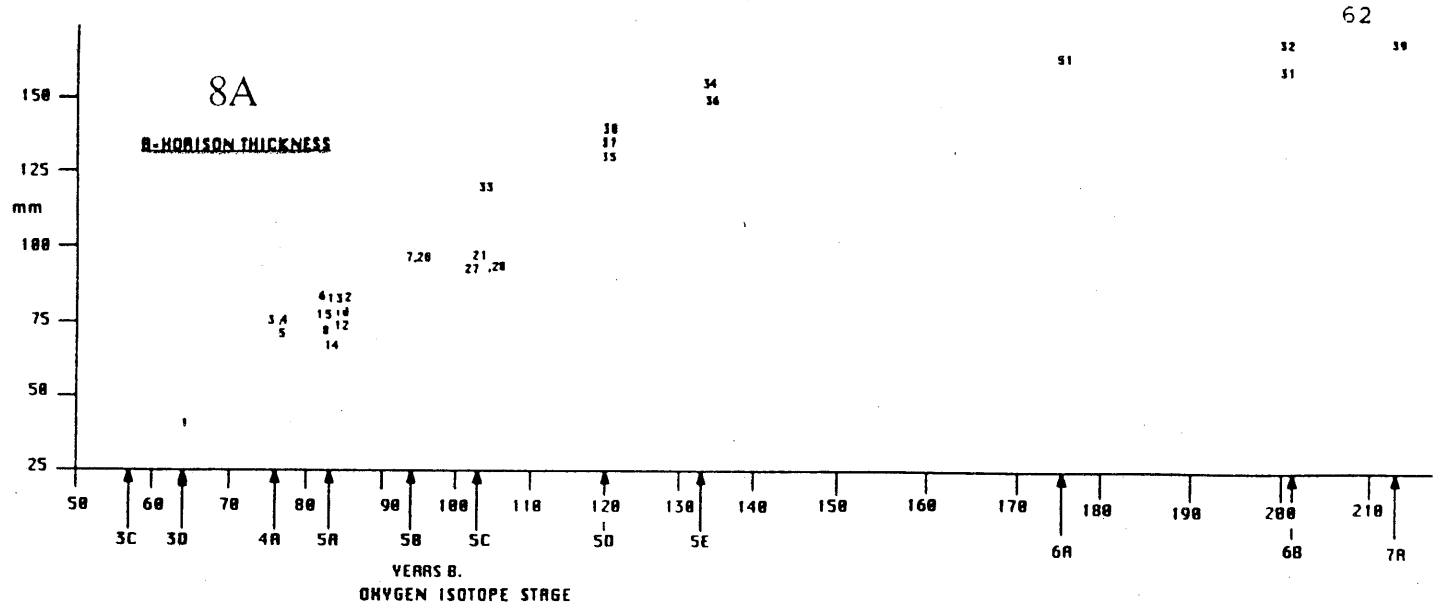

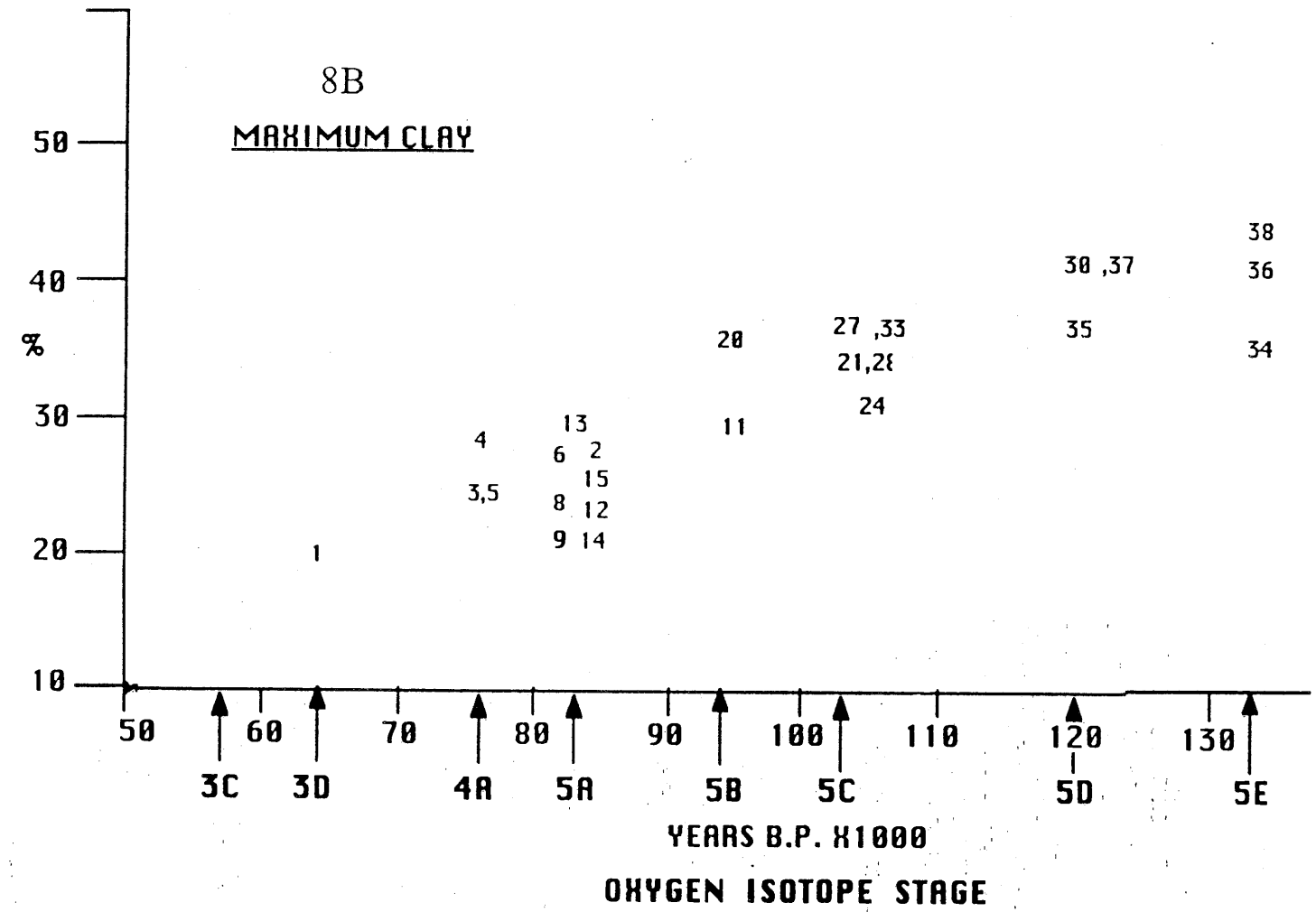

Figure 8. Selected soil data plotted against the terrace ages assigned by the uplift rate model.

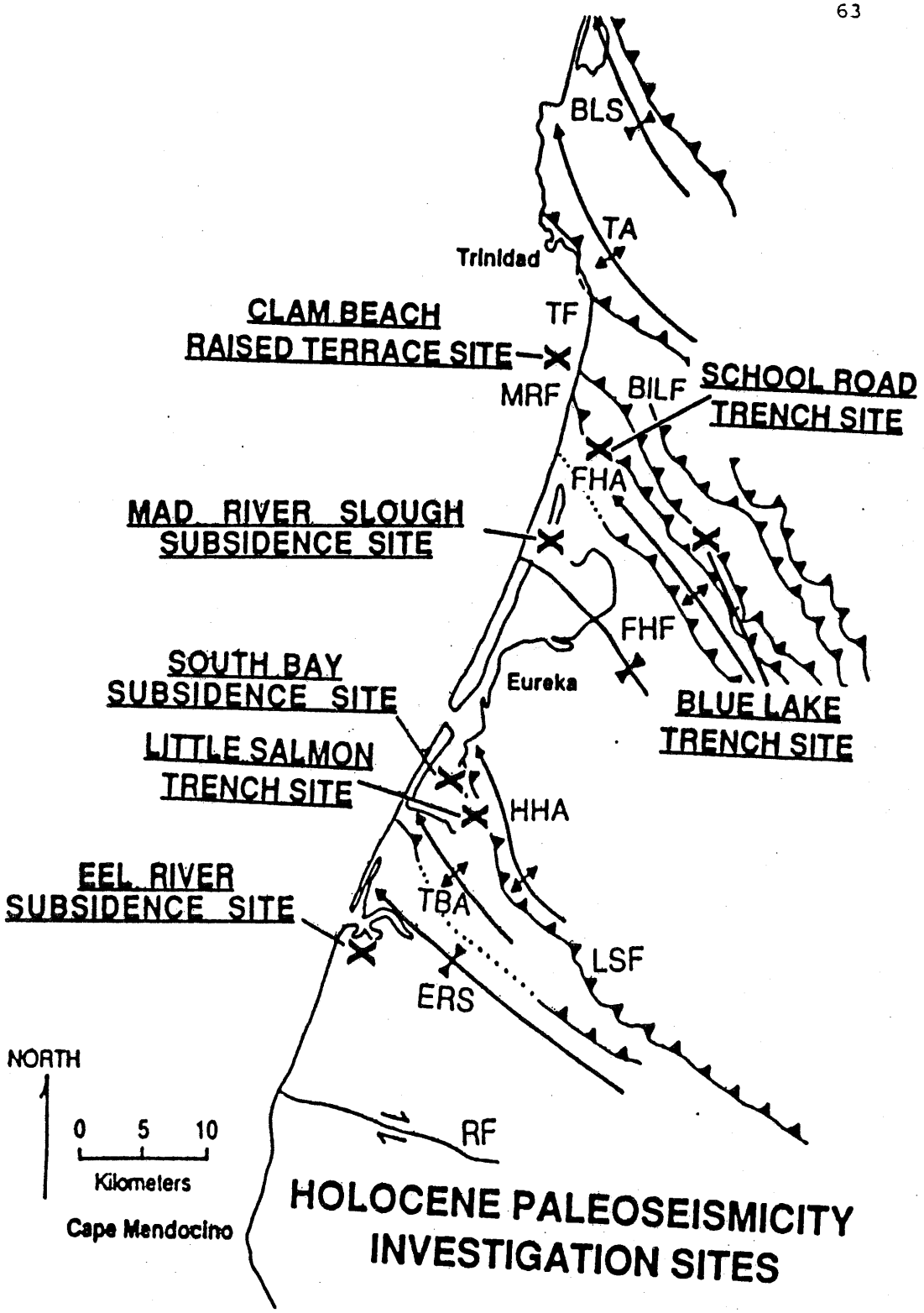

Figure 9. Location of late Holocene paleoseismic investigation sites in northern coastal California

NEOTECTONIC FRAMEWORK OF THE SOUTHERN CASCADIA SUBDUCTION ZONE - MENDOCINO TRIPLE JUNCTION REGION

Samuel H. Clarke, Jr.
Branch of Pacific Marine Geology
U.S. Geological Survey, MS-999
345 Middlefield Road
Menlo Park, California 94025

Robert J. McLaughlin
Branch of Western Regional Geology
U.S. Geological Survey, MS-975
345 Middlefield Road
Menlo Park, California 94025

Introduction

The Cascadia subduction zone (CSZ), the convergent boundary between the Ju de Fuca and North American crustal plates, extends for about 1,300 km from north of Vancouver Island, Canada, southward to the vicinity of Cape Mendocino, California. Along most of its length, the CSZ and overlying fold-and-thrust belt lie offshore; however, the southern end of the subduction zone converges with the coastline and extends onland in the Humboldt Bay region of northern California (Figure 1). Because the subduction zone is represented both offshore and onland in northern California, this region is uniquely fertile ground for the study of subduction zone tectonics, as offshore studies using acoustic-reflection techniques can be integrated directly with onland studies of structure, neotectonics, and paleoseismicity.

The accretionary fold-and-thrust belt of the southern Cascadia subduction zone (SCSZ) off northern California is 85-100 km wide and comprises at least two imbricate systems of north-northwest-trending, east-northeast-dipping thrust and reverse faults, fault-related anticlines and broad open synclines. This compressional domain is buttressed on the east by the Klamath Mountains and is underlain at depths of up to about 20-22 km by the east-dipping CSZ megathrust. A series of broad en echelon synclines centrally located in the fold-and-thrust belt extends onland in Arcata Bay as the Freshwater syncline (Figures 1, 2). The Freshwater syncline, together with smaller synclines that extend landward in the Humboldt Bay and Eel River Valley (Eel River syncline) areas, collectively form the structural expression of the late Cenozoic Eel River forearc basin.

Folds and faults in the southernmost part of the SCSZ south of Arcata Bay assume a west to west-northwest trend, with the intensity of deformation increasing southward toward the Cape Mendocino area. This change in trend is evident in the pronounced southeastward bend in the regional structural grain at the extreme south end of the SCSZ, and probably results from convergence of the relatively cold, rigid Pacific plate from the south, with consequent north-directed compression across the Mendocino fault, deformation of the southern Gorda plate, and uplift of the overlying Mesozoic and Cenozoic strata.

Basement rocks in the Eel River basin region are assigned to the Central and Coastal belts of the Franciscan Complex, which comprises a succession of tectonostratigraphic terranes ranging in age from Late Jurassic to (at least) late Eocene. Collectively, these terranes contain rock assemblages recording diverse histories including subduction, tectonic accretion, and large-scale lateral translation. Two upper Cenozoic depositional sequences of principally marine strata overlie Franciscan basement rocks onshore and offshore in this region. The older depositional sequence, early to middle Miocene in age, is assigned to the informally named Bear River beds of Haller (1980) and correlative units onshore and probably represents pre-forearc slope-basin and slope-blanket deposition. The younger sequence, late Miocene to middle Pleistocene in age, is assigned to the Wildcat Group and correlative units onshore and consists largely of forearc-basin fill. Strata of both depositional sequences have been tectonically interleaved in sheared Franciscan basement rocks in the vicinity of the Mendocino triple junction (MTJ).

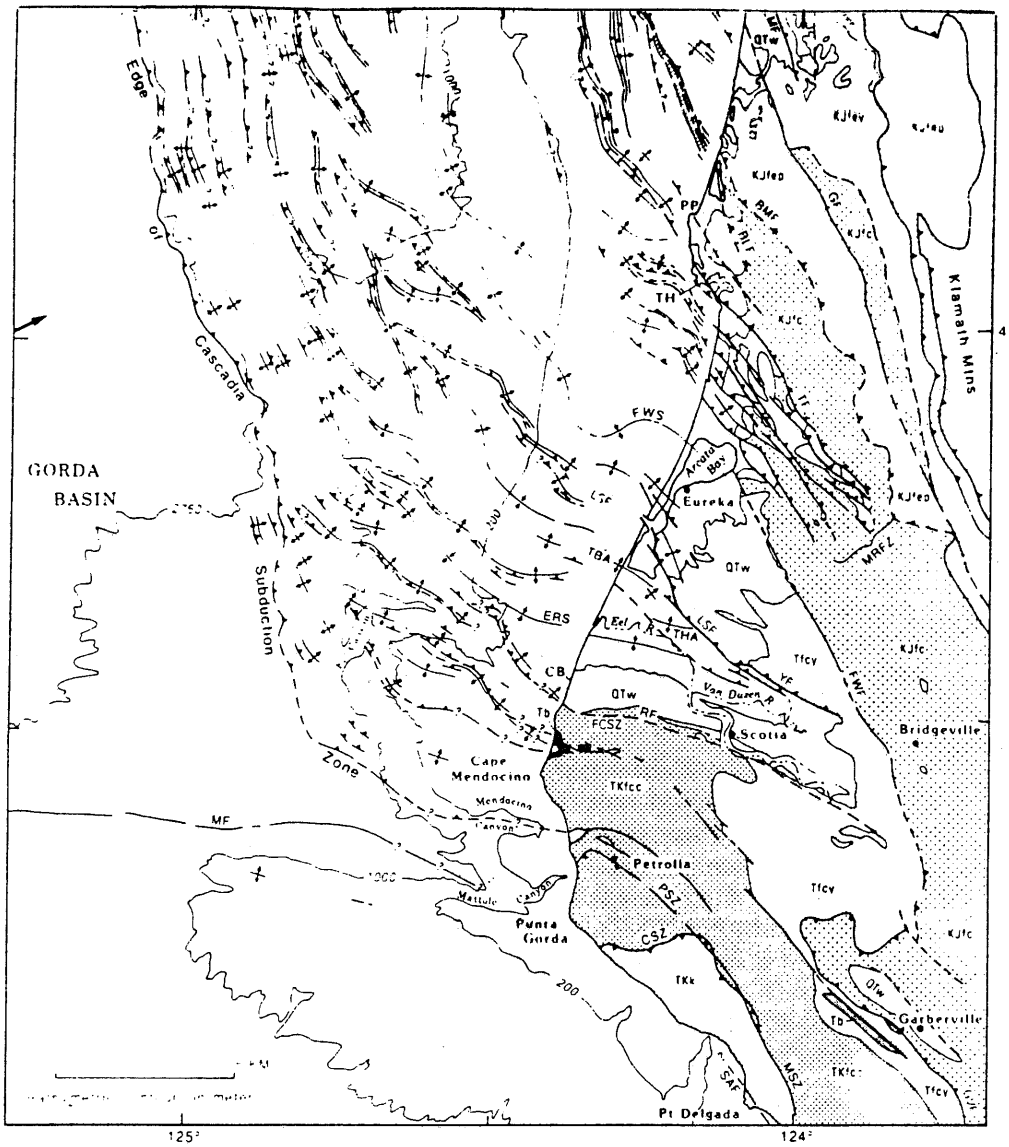

Figure 1 - Geologic and structural map of the southern Cascadia fold-and-thrust belt and Mendocino triple junction region. Rock units: KJfep = Cretaceous and Jurassic basement rocks of the Pickett Peak terrane of the Eastern belt, Franciscan Complex; KJfey = Cretaceous and Jurassic basement rocks of the Yolla Bolly terrane of the Eastern belt, Franciscan Complex; KJfc = Cretaceous and Jurassic basement rocks of the Central belt, Franciscan Complex; TKfcc = Paleogene and Cretaceous basement rocks of the Coastal terrane of the Coastal belt, Franciscan Complex; Tfcy = Paleogene basement rocks of the Yager terrane of the Coastal belt, Franciscan Complex; TKk = Tertiary and Cretaceous rocks of the King Range terrane; Tb = upper Tertiary rocks of the Bear River beds of Haller (1980) and correlative units; QTw = Quaternary and upper Tertiary rocks of the Wildcat Group and correlative units; unpatterned = mostly nonmarine, Quaternary deposits. Structural features: BLF = Big Lagoon fault; BMF = Bald Mountain fault (Bald Mountain-Big Lagoon fault zone offshore); CSZ = Cooskie shear zone; ERS = Eel River syncline; FCSZ = False Cape shear zone; FWF = Freshwater fault; FWS = Freshwater syncline; GF = Grogan fault; GVF = Garberville fault; LSF = Little Salmon fault; MF = Mendocino fault; MRFZ = Mad River fault zone; MSZ = Mattole shear zone; PSZ = Petrolia shear zone; RF = Russ fault; SAF = San Andreas fault; TBA = Table Bluff anticline; TF = Trinidad fault; THA = Tompkins Hill anticline; YF = Yager fault. Locations: CB = Centerville Beach; PP = Patrick's Point; TH = Trinidad Head; Hachured areas offshore indicate fault zones. Barbs are on upper plate of thrust and reverse faults. (Map reproduced from Clarke, 1992, Figure 2.)

Geologic Structure

Southern Cascadia Fold-and-Thrust Belt: The structure of the SCSZ fold-and-thrust belt in the southernmost part of the region is dominated by youthful thrust and high-angle reverse faults that trend generally west onshore and northwest offshore (Figure 1). Farther north in the offshore, major structures have a nearly north-south orientation. These structural trends reflect north- to northeast-directed stresses associated with northward migration of the MTJ and north-directed compression across the Mendocino fault in the southern part of the region, and east-northeast-directed compression associated with Gorda-North America plate convergence farther north.

Major youthful faults along the northeastern margin of the fold-and-thrust belt include the Mad River fault zone and faults that cut across the coastline between Patricks Point and Crescent City. The best documented of these fault systems is the Mad River fault zone which, onshore, forms a 10-km-wide set of at least five northwest-trending, northeast-dipping (10°-55°, commonly 20°-30°) imbricate thrust faults that have a history of late Quaternary activity (Carver, 1987; Kelsey and Carver, 1988). Detailed study of these faults indicates that displacement is almost entirely dip slip, with each of the principal thrusts accruing from 0.7 to 2.2 km of dip-slip displacement, mostly in middle and late Quaternary (Carver 1987). The Mad River fault zone extends offshore as a northwest- to west-northwest-trending zone of faults and short high-amplitude, west-plunging folds that are most prominent near Trinidad Head, where acoustic basement is shallow (Figure 1). Farther offshore they become obscure and may die out at depth. An exception is the Trinidad fault, the northeasternmost fault in the zone, which can be traced discontinuously north-northwestward for more than 50 km and which locally offsets the Franciscan basement surface at least 650 m, east side up (Figure 2a).

Thrust faults in the northeastern part of the forearc have been traced in offshore acoustic-reflection data into sole thrusts that extend to depths of as much as 14-16 km, which is within about 4 km of the top of the subducted Gorda plate (determined from seismicity data; Cockerham, 1984) in this region (Clarke, 1992). In map view, these thrust fault systems are approximately orthogonal to the direction of Gorda-North America plate convergence, and the imbricate blocks they bound follow the western margin of the Klamath Mountains (Figure 1). These fault systems are interpreted as a series of seaward-verging imbricate thrust fans that root at or near the Gorda-North America plate interface at depth, and that formed as a consequence of Gorda-North America plate convergence, with strong partial interplate coupling within the subduction zone. The fold-and-thrust belt is buttressed on the east by the rigid Klamath Mountains. Although oblique convergence between the Gorda and North America plates may result in minor right slip, such translational movement is clearly subordinate to convergence-related thrusting in this region and is unrelated to San Andreas transform motion.

Farther south, major structures that transect the coastline between Arcata Bay and Cape Mendocino have been traced northwestward onto the seaward margin of the forearc. These structures include the Little Salmon fault and the thrust-faulted Table Bluff anticline (and folds and faults associated with them), major thrust-bounded synclines (including the Eel River syncline), the Russ fault and False Cape shear zone, and thrust faults bounding the so-called Bear River syncline (Figures 1, 2b).

The Little Salmon fault is an active northwest-trending, northeast-dipping thrust associated with anticlinal folding. Late Holocene activity includes at least three displacements of 5 m or more during the past 1,700 years, and a corresponding slip rate of about 7-10 mm/year (Carver, 1987; Carver and Burke, 1987; Clarke and Carver, 1992).

2a.

2b.

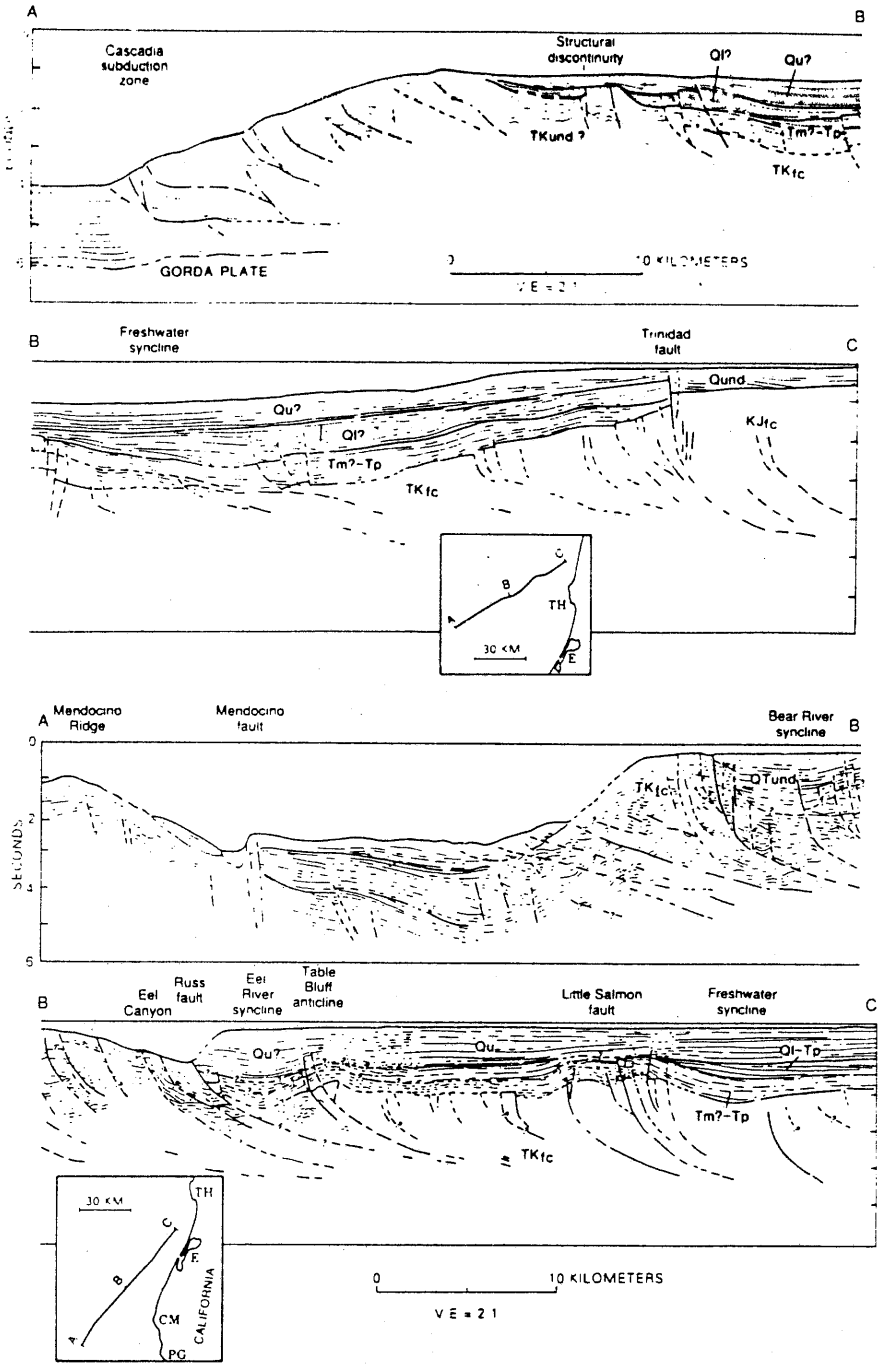

Figure 2 - Interpretation of acoustic-reflection profiles (time sections: time in seconds 2-way traveltime) (a) across the central Eel River basin, and (b) from the southern Eel River basin to Mendocino Ridge. Acoustic units: KJfc = Central belt, Cretaceous and Jurassic Franciscan Complex; TKfc = Coastal belt, Tertiary and Cretaceous Franciscan Complex; TKund(?) = Tertiary and Cretaceous strata, undivided, in the seaward part of the accretionary prism; Tm?-Tp = Miocene(?) and Pliocene strata equivalent in age to the lower part of the Wildcat Group; QTund = Quaternary and Tertiary strata, undivided, equivalent to Miocene and younger strata in the Bear River "syncline" on land; Ql-Tp = lower Quaternary and Pliocene strata equivalent in age to the upper part of the Wildcat Group; Ql? = lower(?) Quaternary strata equivalent in age to the upper part of the Wildcat Group; Qu = upper Quaternary strata equivalent to nonmarine deposits that postdate the Wildcat Group onshore; Qund = Quaternary strata, undivided. Locations: CM = Cape Mendocino; E = Eureka; PG = Punta Gorda; TH = Trinidad Head. (Sections reproduced from Clarke, 1992, Figures 6 and 7.)

Vertical separation of the base of the Hookton Formation of Ogle (1953) (0.6 ± 0.1 Ma) is about 320 to 565 m (Perkins and Coppersmith, 1980), and that of the Wildcat-Franciscan contact is about 2 km at Tompkins Hill (Wagner, 1980), about 9 km southeast of Humboldt Bay. Offshore, imbricated branches of the Little Salmon fault cut to or near the sea floor and offset the sea floor locally, and can be traced 45 km northwestward onto the seaward part of the modern accretionary prism (Figures 1, 2b).

The Table Bluff anticline and underlying thrust faults diverge obliquely from the footwall of the Little Salmon fault and also extend northwestward offshore for about 45 km (Figure 1). The Table Bluff fault apparently does not reach the surface on land. However, offshore, en echelon, thrust or reverse-faulted anticlines that deform the sea floor and on the flanks of which upper Quaternary strata thin and are warped attest to latest Quaternary structural growth and recent fault movement. The Table Bluff structural zone bounds the Eel River syncline along its northeast flank offshore until the syncline dies in the complex structure of the continental slope at a depth of 1,000-1,200 m (Figure 2b). It is noteworthy that half or more of the sedimentary section that overlies acoustic basement (Franciscan Complex) in the offshore Eel River syncline is late Quaternary in age and postdates the Wildcat Group onshore. This high rate of sedimentation (approximately 1,700 m/700,000 yr.) reflects both rapid late Quaternary source area uplift, and a very high rate of sediment supply to the offshore Eel River basin by the Eel River.

The Russ fault, which bounds the south flank of the Eel River syncline, was mapped by Ogle (1953) as a vertical to steeply south-dipping reverse fault on which major movement preceded deposition of the Wildcat Group. However, offshore elements of the Russ fault cut upper(?) Quaternary strata, and it is mapped as a northwest-trending, north-dipping thrust or reverse fault along the north side of Eel Canyon (Figure 2b). Study onland suggests that the fault may have formed as a seaward-vergent thrust on the North American accretionary margin, and that it has been steepened during northward-directed compressive deformation of the southern Eel River basin largely since middle Quaternary time (G. A. Carver, oral communication, 1990).

Farther south, acoustic-reflection data from the uplifted, highly sheared Franciscan bedrock platform off Cape Mendocino show that strata as much as 1,800 m thick and largely correlative with the Wildcat Group and Bear River beds are infaulted between two or more sets of prominent west-northwest-trending, north-northeast-dipping faults that extend offshore about 3-6 km north of Cape Mendocino (Figures 1, 2b). Thrust or reverse displacement is evident on the northern fault set. The southern set may be an offshore extension of the onshore Capetown fault zone. The position of these faults suggests that they formed as seaward-vergent thrusts that have subsequently been steepened by north-directed compression, analogous to the Russ fault to the north. This interpretation is supported by offshore mapping showing that both fault sets, together with the Russ fault, extend nearly 40 km northwestward into thrusts on the seaward-facing accretionary prism above the Cascadia subduction zone (Figure 1). This interpretation implies that upper Cenozoic deposits in the Bear River "syncline" onshore are infaulted remnants of slope and, perhaps, slope-basin deposits formed on the Neogene accretionary margin. Pervasively sheared and tectonically mixed rocks, including blocks of Wildcat-correlative shallow-to-deep marine strata as young as Pliocene (Ogle, 1953), that lie in the False Cape shear zone between the Russ fault and the Bear River "syncline" and farther south near Petrolia are also exposed remnants of this accretionary prism.

A discontinuity in structural trend that is locally expressed as a series of east-dipping high-angle faults extends northward along the northern California margin about 20 km landward of the SCSZ deformation front (Figures 1, 2a). West of this discontinuity, structures parallel the deformation front and are oblique to the direction of Gorda plate

convergence. East of the discontinuity, en echelon folds and faults have average trends that are oblique to the deformation front but orthogonal to the direction of Gorda plate convergence. The discontinuity also corresponds approximately to the western limit of North America plate seismicity (McPherson, 1989). Structures west of the discontinuity are interpreted as forming in young, offscraped Gorda plate cover sediment that lacks the strength to deform brittlely. Structures east of the discontinuity are interpreted as forming in the older, thickened part of the accretionary wedge that has acquired sufficient strength to transfer compressional stress from the subducting plate, to which it is coupled, upward through the overlying strata. The discontinuity may accommodate a component of right slip and approximates the western limit of strong interplate coupling in the SCSZ (Clarke, 1992).

Mendocino Triple Junction: The megathrust marking the seaward edge of the SCSZ does not join the Mendocino fault offshore, as commonly depicted, but instead extends east-southeastward around the south flank of the Eel River forearc and landward south of Cape Mendocino (Figure 1). The trace of the megathrust is clear in acoustic-reflection data southward and eastward along the North American margin to about 40°27'N/124°44'W, which is 20-25 km east-northeast of the commonly mapped location of the Mendocino triple junction (Clarke, 1990, 1992). It is tentatively extended 22 km farther east-southeast on these data to the north slope of Mendocino Canyon, and likely extends shoreward along the canyon to reach the coast about 10 km southeast of Cape Mendocino. This corresponds to the coastal location of the Petrolia shear zone (PSZ, Figure 1), which extends southeastward in Franciscan rocks to and along the northeast margin of the King Range (McLaughlin and others, 1982, 1988; Clarke, 1988, 1992). Near the coast, the Petrolia shear zone approximates the boundary between discordant structural domains, as shown by shear fabric orientation and fold trends in Franciscan rocks (McLaughlin and others, 1988, in press). Structures north of the shear zone strike northwest and dip northeast, consistent with shoreward extension of the accretionary margin overlying the SCSZ. Structures south of the shear zone parallel the northern and eastern boundaries of the King Range terrane (McLaughlin and others, 1988), consistent with their formation as a result of latest Cenozoic obductive accretion of the King Range terrane. Shoreward extension of the subduction zone and overlying accretionary prism is also consistent with shallow seismicity (Simila, 1980; McPherson, 1989), and is supported by the presence of outliers of Pliocene lower-slope deposits northwest of Petrolia (R. J. McLaughlin, personal communication, 1988). These strata, which are partly correlative with the Wildcat Group of the Eel River basin, formed at depths of 2,000 m or more and were elevated on the upturned landward extension of the accretionary prism, probably during northward-directed compression resulting from Pacific plate convergence.

The Mendocino fault extends on acoustic-reflection and GLORIA side-scan sonar records as a well defined single- or multi-strand fault eastward near the base of the Gorda Escarpment to 40°23'N/124°43'W, about 7 km west of the mouth of Mattole Canyon (Figures 1, 2b; Clarke, 1990, 1992). The fault is not clearly defined farther east, but could extend landward via Mattole Canyon to join the Cooskie shear zone (McLaughlin and others, 1982) (CSZ, Figure 1), which bounds the King Range along its northern margin. This interpretation is consistent with available offshore acoustic-reflection data, as well as with west-northwest-trending shear fabrics mapped in the Cooskie shear zone (McLaughlin and others, 1982, and in press), with the history of accretion and deformation determined for the King Range terrane (McLaughlin and others, 1982; Clarke, 1992), and with available earthquake focal mechanisms (Simila, 1980; McPherson, 1989). Alternatively, the Mendocino fault may exist as complex multiple breaks bounding imbricated slivers of Gorda and Pacific plate basement rocks and upper Cenozoic cover sediment in the highly deformed area offshore between Mattole and Mendocino Canyons (Figure 1).

This interpretation places the shallow crustal position of the Mendocino triple junction at the approximate intersection of the Petrolia and Mattole shear zones (Figure 1), near the hamlet of Honeydew. A more realistic conception of the near-surface expression of the triple junction is that it exists as a broad zone of deformation and rapid late Quaternary uplift that encompasses the region lying onshore and offshore between the allochthonous King Range terrane and the south flank of the Eel River syncline. Rocks exposed onshore between Petrolia on the south and the south flank of the Eel River syncline on the north are, by implication, upper Cenozoic counterparts of rocks that now underlie the seaward-facing accretionary prism of the SCSZ at water depths of 1,000-2,700 m. Similarly, strata offshore between the SCSZ and the Mendocino fault, and onshore between the Petrolia and Cooskie shear zones are Gorda basin sediments that are progressively more deformed eastward nearing the triple junction, an observation that is in accord with preliminary evidence offshore and on land.

Location of the Mendocino triple junction at the intersection of the Petrolia and Cooskie shear zones implies that the presently aseismic offshore strand of the San Andreas fault has been, or is being, abandoned, and that Pacific-North America plate relative motion is being accommodated in the upper crust along a fault or series of faults, possibly including the Mattole shear zone (MSZ, Figure 1), located east of the King Range terrane. Varied evidence supports a broad distribution of right slip in this region. Recent faulting at Whale Gulch, 10 km south of Point Delgada, may extend from the offshore San Andreas fault (McCulloch, 1987) into the Mattole shear zone (McLaughlin and others, 1982). Simila (1980) shows a focal mechanism (depth not reported) located on the east edge of the King Range that is consistent with right slip along a northwest-trending plane. Lawson and others (1908) reported landsliding, but not surface rupture, along the east side of the King Range, but undetected surface rupture has not been ruled out. Trilateration measurements (Lisowski and Prescott, 1989) indicate that, in the region south of Cape Mendocino, right-lateral shear is distributed across a 35- to 80-km-wide zone east of the San Andreas fault, with about half of the relative plate motion being accommodated by fault systems east of the King Range. More recently, Castillo and Ellsworth (submitted manuscript) conclude from seismicity data that right-slip in northern California is focused along the Maacama and Bartlett Springs fault zones, 30-60 km east-southeast of Point Delgada, and that the northern terminus of this motion lies near the surface projection of the southern edge of the subducted Gorda slab. Clearly, a major part of Pacific-North America plate relative motion is presently accommodated along faults that lie well east of the commonly depicted offshore location of the San Andreas fault.

The accretion history of the King Range terrane also suggests that the eastern edge of the Pacific plate lies well east of the offshore trace of the San Andreas fault. Alternative accretion histories were proposed for the King Range terrane by McLaughlin and others (1982): one involves King Range transport on the Farallon plate, with middle Miocene accretion to North America; the other involves Pacific plate transport with obductive accretion of the King Range in the late Cenozoic accompanying northwestward migration of the Mendocino triple junction. The first alternative, middle Miocene accretion, is not reflected in the generally fine-grained deep-water middle Miocene blanket deposits to the north and east of the King Range (Clarke, 1992). Latest Cenozoic accretion of the King Range terrane is favored by this and by the abundant evidence of Quaternary deformation in the southern Eel River basin; this scenario requires King Range terrane transport on the Pacific plate, which, in turn, implies that the Pacific-North America plate boundary lies along or beneath the eastern margin of the King Range.

Summary

Youthful tectonic activity related to Gorda-North America plate convergence indicates an active Cascadia subduction zone and strong partial interplate coupling. This activity is reflected in the northeastern part of the Eel River forearc basin by seaward-verging thrust and reverse faults that form imbricate thrust fans that extend downward to or near the Gorda-North America plate interface. A north-trending discontinuity in structural trends in the seaward part of the accretionary fold-and-thrust belt reflects the boundary between decoupled (to the west) and coupled (to the east) parts of the subduction zone. This discontinuity may accommodate a component of right shear related to oblique convergence but, elsewhere, strike-slip faulting is minor and transform-related translational faulting is absent. In the southernmost part of the SCSZ, major structures have been modified by northward encroachment of the Pacific plate and north-directed compression across the Mendocino fault.

The Cascadia subduction zone does not join the Mendocino fault at the commonly depicted offshore location of the Mendocino triple junction. Instead, the subduction zone extends southeastward around the southern Eel River forearc basin and shoreward along Mendocino Canyon to join the Petrolia shear zone on land. Similarly, the Mendocino fault probably extends shoreward to join the Cooskie shear zone on land. These two shear zones intersect northeast of the King Range, and the area of their intersection is the probable upper crustal location of the Mendocino triple junction.

Active San Andreas transform motion is probably being accommodated along fault zones, possibly including the Mattole shear zone, and the Garberville, Lake Mountain, Maacama and Bartlett Spring fault zones east of the King Range terrain, which is presently being obductively accreted to North America.

References Cited

Carver, G. A., 1987, Late Cenozoic tectonics of the Eel River basin region, coastal northern California, *in* H. Schymiczek and R. Suchland, eds., Tectonics, sedimentation and evolution of the Eel River and other coastal basins of northern California: San Joaquin Geological Society Miscellaneous Publication 37, p. 61-72.

Carver, G. A., and R. M. Burke, 1987, Late Pleistocene and Holocene paleoseismicity of Little Salmon and Mad River thrust systems, N.W. California--Implications to the seismic potential of the Cascadia subduction zone (abs.): GSA Abstracts with Program, v. 19, p. 614.

Castillo, D. A., and W. L. Ellsworth, Seismotectonics of the San Andreas fault system between Point Arena and Cape Mendocino in northern California: Implications for the development and evolution of a young transform: manuscript submitted to the Journal of Geophysical Research, February 1992.

Clarke, S. H., Jr., 1988, Late Cenozoic deformation of the California continental margin north of Cape Mendocino: Implications for Mendocino triple junction location (abs.): Geological Society of America Abstracts with Program, v. 20, p. A382.

Clarke, S. H., Jr., 1990, Map showing geologic structures of the northern California continental margin: U.S. Geological Survey Miscellaneous Field Studies Map MF 2130.

Clarke, S. H., Jr., 1992, Geology of the Eel River basin and adjacent region: Implications for late Cenozoic tectonics of the southern Cascadia subduction zone and Mendocino triple junction: American Association of Petroleum Geologists Bulletin, v. 76, p. 199-224.

Clarke, S. H., Jr., and G. A. Carver, 1992, Late Holocene tectonics and paleoseismicity, southern Cascadia subduction zone: Science, v. 255, p. 188-192.

Cockerham, R. S., 1984, Evidence for a 180-km-long subducted slab beneath northern California: Seismological Society of America Bulletin, v. 74, p. 569-576.

Haller, C. R., 1980, Pliocene biostratigraphy of California: American Association of Petroleum Geologists Studies in Geology, no. 11, p. 183-341.

Kelsey, H. M., and G. A. Carver, 1988, Late Neogene and Quaternary tectonics associated with the northward growth of the San Andreas transform fault, northern California: Journal of Geophysical Research, v. 93, p. 4797-4819.

Lawson, A. C., and others, 1908, The California earthquakes of April 18, 1906, Report of the state earthquake investigation commission: Carnagie Institution of Washington Publication Number 87, v. 1, p. 54-58.

Lisowski, M., and W. H. Prescott, 1989, Strain accumulation near the Mendocino triple junction, California: Eos, Transactions of the American Geophysical Union, v. 70, p. 1332.

McCulloch, D. S., 1987, Regional geology and hydrocarbon potential of offshore central California, *in* D. W. Scholl, A. Grantz, and J. G. Vedder, eds., Geology and resource potential of the continental margin of western North America and adjacent ocean basins -- Beaufort Sea to Baja California: Circum-Pacific Council for Energy and Mineral Resources, Earth Science Series, v. 6, p. 353-401.

McLaughlin, R. J., S. A. Kling, R. Z. Poore, K. McDougall, and E. C. Beutner, 1982, Post-middle Miocene accretion of Franciscan rocks, northwestern California: Geological Society of America Bulletin, v. 93, p. 595-605.

McLaughlin, R. J., W. V. Sliter, S. H. Clarke, Jr., D. S. McCulloch, N. O. Frederiksen, and D. C. Ingebretson, 1988, Implications of onshore and offshore structure for location and Cenozoic evolution of the Mendocino triple junction (abs.): Geological Society of America Abstracts with Program, v. 20, p. A382.

McLaughlin, R. J., W. V. Sliter, N. O. Frederiksen, W. P. Harbert, and D.S. McCulloch, in press, Plate motion recorded by tectonostratigraphic terranes of the Franciscan Complex in the vicinity of the Mendocino triple junction: U.S. Geological Survey Bulletin.

McPherson, R. C., 1989, Seismicity and focal mechanisms near Cape Mendocino, northern California, 1974-1984 [MS thesis]: Arcata, California, Humboldt State University,
75 p.

Ogle, B. A., 1953, Geology of Eel River Valley area, Humboldt County, California: California Division of Mines Bulletin 164, 128 p.

Perkins, M. E., and K. J. Coppersmith, 1980, Summary of plant site investigations, Appendix C, *in* Evaluation of the potential for resolving the geologic and seismic issues at the Humboldt Bay Power Plant Unit No. 3: prepared for the Pacific Gas and Electric Company by Woodward-Clyde Consultants, San Francisco, California, p. C1-C129.

Simila, G. W., 1980, Seismological evidence on the tectonics of the northern section of the San Andreas fault region, *in* R. Streitz and R. Sherburne, eds., Studies of the San Andreas fault zone in northern California: California Division of Mines and Geology Special Report 140, p. 131-137.

Wagner, J. R., 1980, Summary of regional stratigraphy and geologic structure, Appendix A, *in* Evaluation of the potential for resolving the geologic and seismic issues at the Humboldt Bay Power Plant Unit No. 3: prepared for the Pacific Gas and Electric Company by Woodward-Clyde Consultants, San Francisco, California, p. A1-A73.

LATE CENOZOIC SEDIMENT PROVENANCE AND TECTONIC EVOLUTION OF THE NORTHERNMOST COAST RANGES, CALIFORNIA

K.R. AALTO

Department of Geology, Humboldt State University, Arcata, CA 95521

ABSTRACT

Marine sandstones of the Lower-Middle Miocene Bear River beds, Upper Miocene-Lower Pleistocene Wildcat Group and Pliocene lower Falor Formation contain an average of 6% K-spar. $^{40}Ar/^{39}Ar$ laser probe analyses of Lower Pleistocene Wildcat Group micas yield ages of approximately. 52-57 Ma. Analyses of Pliocene Wildcat Group micas yield three groups of ages: approximately 66-75, 128.5, and 299-303 Ma. A logical source for the three younger groups are Cretaceous-Eocene plutonic rocks in Idaho, a source proposed for subjacent Eocene Yager Formation sandstones in the Coast Ranges by Underwood & Bachman (1986). The source of the older micas remains enigmatic, but may be reset Devonian Abrams Schist of the central Klamath Mountains.

Fluvial conglomerates and sandstones of the Upper Oligocene-Lower Miocene Weaverville Formation and Lower Pliocene Wimer Formation in the Klamath Mountains, the Upper Pleistocene upper Falor and Carlotta Formations in the Coast Ranges, and marine sandstones of the Lower Pliocene Wimer and St. George Formations in the Klamaths and Coast Ranges are derived largely from nearby basement rocks. Imbrication of western Weaverville Formation fluvial clasts indicates westerly flow of a major braided river. However, the deltaic facies of this formation is missing, due either to Miocene erosional stripping or removal by faulting. The eastern Weaverville Formation accumulated syntectonically in upper plate grabens above the regional LaGrange detachment fault. Initiation of LaGrange detachment faulting, Weaverville sedimentation and, possibly, Klamaths uplift is coeval with increased oblique convergence of oceanic and continental plates ca. 30 Ma, and with alkalic intrusive activity in the southwest Oregon and northwest California Coast Ranges. The intrusions may reflect an unrecognized rifting event which might have resulted from clockwise rotation of the Klamath Mountains and Coast Ranges provinces.

The Bear River beds accumulated at bathyal depths. Basal Wildcat Group sediments are fluvial to littoral. However, rapid submergence of the Coast Ranges region to bathyal depths (2-3 km) occurred following the initiation of Wildcat sedimentation. This abrupt bathymetric changes may relate to greater normal plate convergence ca. 9 Ma. Ca. 5 Ma the northwest Klamath Mountains were at sea level, as is indicated by presence of Wimer marine sediments on the present-day elevated erosion surface. Poorly dated, coarse fluvial conglomerates of the eastern Wimer facies may reflect local uplift and warping of this surface about a northwest-trending axis. Sediment shoaling, and onset of fluvial sedimentation in the Coast Ranges, may relate to the decreased plate convergence rate, lessening of angle of subduction and increased normal convergence ca. 1 Ma.

INTRODUCTION

The purpose of this paper is to relate sedimentation and sediment provenance of late Cenozoic sedimentary rocks to their tectonic setting of accumulation and the uplift history of the northernmost Coast Ranges of California. Brief descriptions of the various

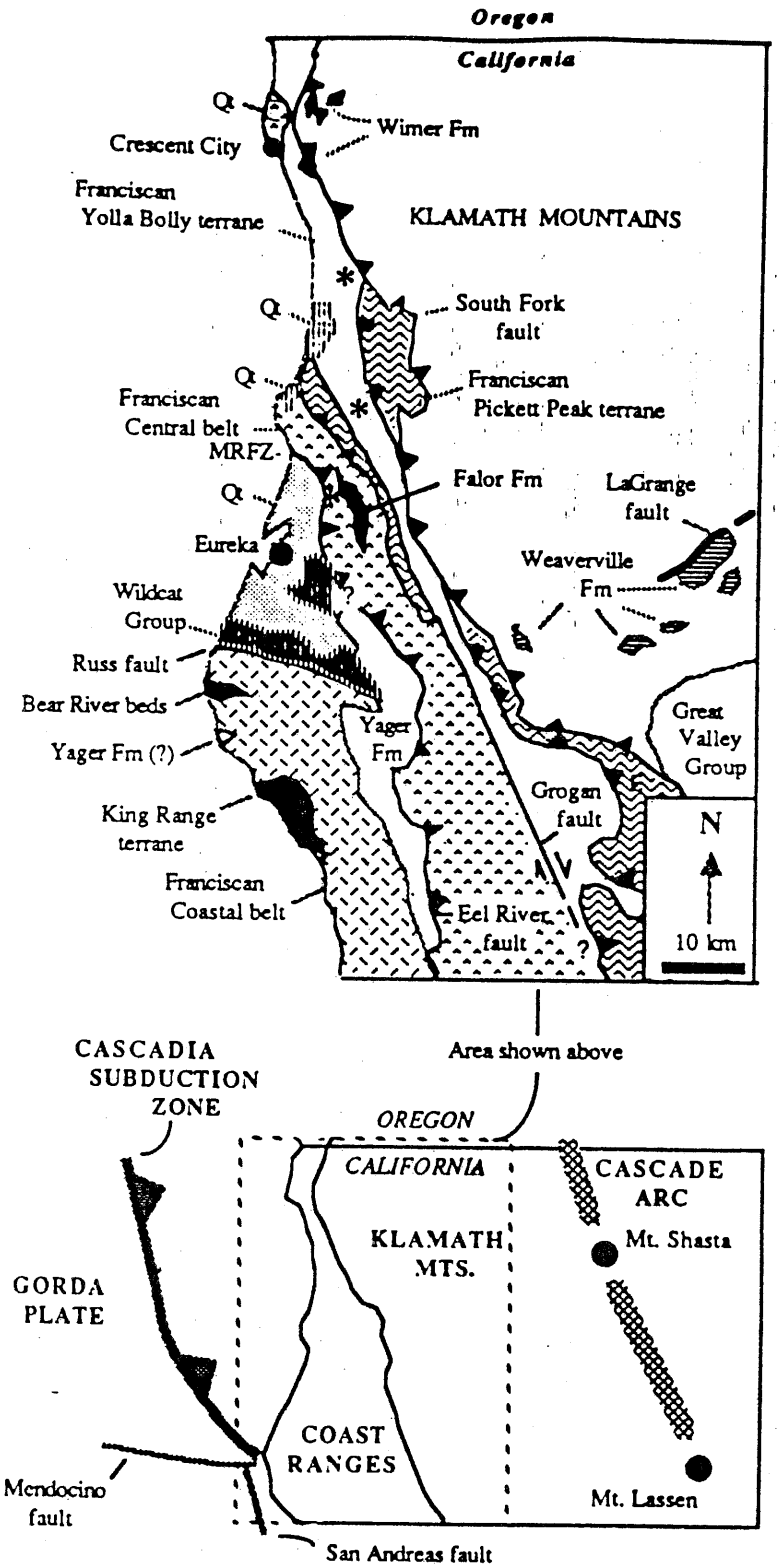

Figure 1. Generalized geologic map of northwestern California. Terrane nomenclature and distribution is from Blake *et al.* (1982, 1985a, 1985b), Miller and Aalto (1983) and Aalto (1989a). Plutons, many faults, Klamath geologic terranes and minor details, including and smaller outcrops of Cenozoic cover rock, are not shown. Patches of Weaverville formation discussed in the paper include: 1) the Weaverville area adjacent to the LaGrange fault, and 2) the Hyampom area adjacent to the South Fork fault. Only major faults dividing terranes are shown. The asterisks show the position of alkalic intrusive bodies coeval with LaGrange detachment faulting, with the size of the symbol proportional to the size of the body. Qt depicts late Pleistocene and Holocene terrace deposits

lithostratigraphic units within the field trip area will be presented with reference made to relevant literature. Detailed descriptions that relate to specific field trip stops are presented in the road log and several summary articles included herein. Age, depth of sediment accumulation, and stratigraphic and structural relationships among the Cenozoic lithostratigraphic units and tectonostratigraphic terranes shown in figure 1 are diagramatically portrayed in figures 2 and 3.

Late Cenozoic patterns of sedimentation reflect a long history of convergence between the Farallon and North American plates. This resulted in episodes of compressional and strike-slip faulting and rotation of fault-bounded blocks within the North American plate (Jayko and Blake, 1987; McCrory, 1989; Schweickert & Irwin, 1989). The northward migration of the Mendocino triple junction (Fig. 1; Kelsey and Carver, 1989) has resulted in changing stress regimes that are reflected in the neotectonic evolution of southern Humboldt County Gary Carver (this volume). The author will employ regional tectonic models developed by the aforementioned geologists to reflect upon the relationship between tectonics and sedimentation in northernmost California.

DESCRIPTION OF UNITS

Mesozoic - Early Cenozoic Basement Rocks

Franciscan Complex

Within many areas of the northernmost Coast Ranges of California, Cenozoic sedimentary rocks rest unconformably upon, or are in fault contact with, the late Mesozoic-Eocene Franciscan Complex. Unconformities are exposed beneath many marine and fluvial Plio-Pleistocene terrace deposits and will be visited on the field trip in the Trinidad-Patricks Point area. Franciscan rocks that are thrust faulted over terrace deposits will be seen within the Mad River fault zone (Carver, 1985, 1987; Kelsey and Carver, 1988).

Franciscan rocks within the field trip area correlate with those of both the late Mesozoic Franciscan Central and Eastern belts and late Mesozoic-early Cenozoic Franciscan Coastal belt (Blake, *et al.*, 1982; Jayko and Blake, 1987). Eastern belt rocks consist of foliated (textural zone 2 of Blake *et al.*, 1967) turbidite sandstones and argillite. Central belt rocks consist of abundant melange units that are intercalated with isoclinally folded, turbiditic broken formation units (*cf.* Hsü, 1974). Some melanges originated as olistostromes (large scale submarine mass flow deposits) that accumulated in a trench or inner trench slope basinal setting, seaward of the Mesozoic Klamath-Sierran arc and others by tectonic mixing in a subduction zone setting (Aalto, 1981, 1989b). Blake *et al.* (1985a, 1985b) suggested that these melanges were first deformed by early thrust faulting, and later by translation that occurred along regional strike-slip faults. Strike-slip faulting occurred in the early Cenozoic as the Kula-Farallon-North American triple junction migrated past northernmost California (Kelsey and Hagans, 1982; Aalto, *et al.*, 1988), and during the late Cenozoic accompanying the northward migration of the Mendocino triple junction (Kelsey and Carver, 1988).

The late Mesozoic Franciscan Eastern belt consists chiefly of schistose turbidites and argillite, interstratified with minor graphitic phyllite and tuff (Jayko and Blake, 1987). Within the field trip area, rocks of this belt are exposed along the coast in northern Patricks Point Park (Aalto, 1989b). These rocks, informally referred to as the "Patricks Point unit", differ greatly in their sedimentology from unfoliated Franciscan Central belt turbidites to the west (Aalto, 1976). The contact between rocks of the Eastern and Central belts at this site is interpreted as a reverse fault (Aalto, 1989b).

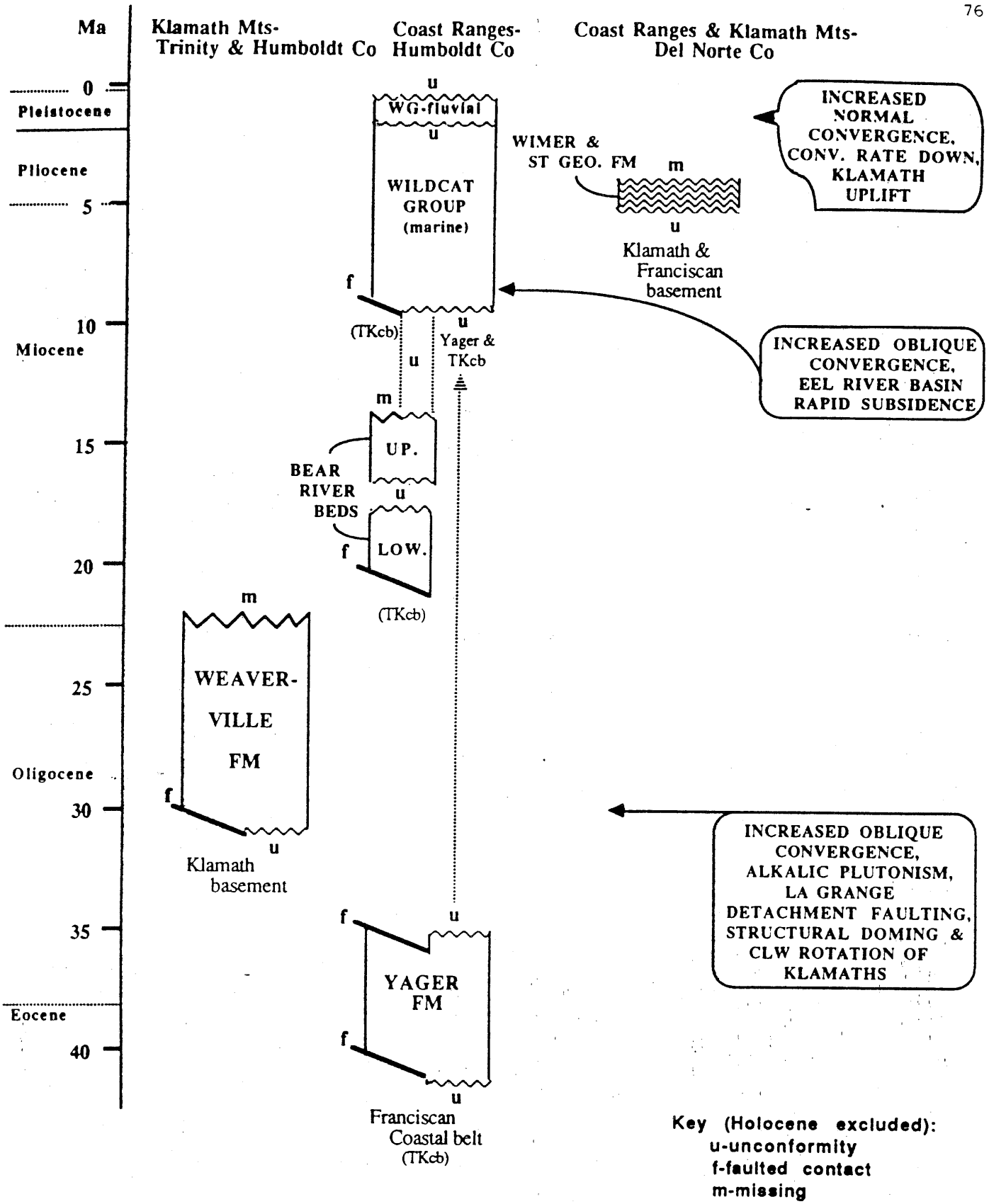

Figure 2. Time-stratigraphic chart relating Cenozoic cover rock stratigraphy to the possibly major regional tectonic events.

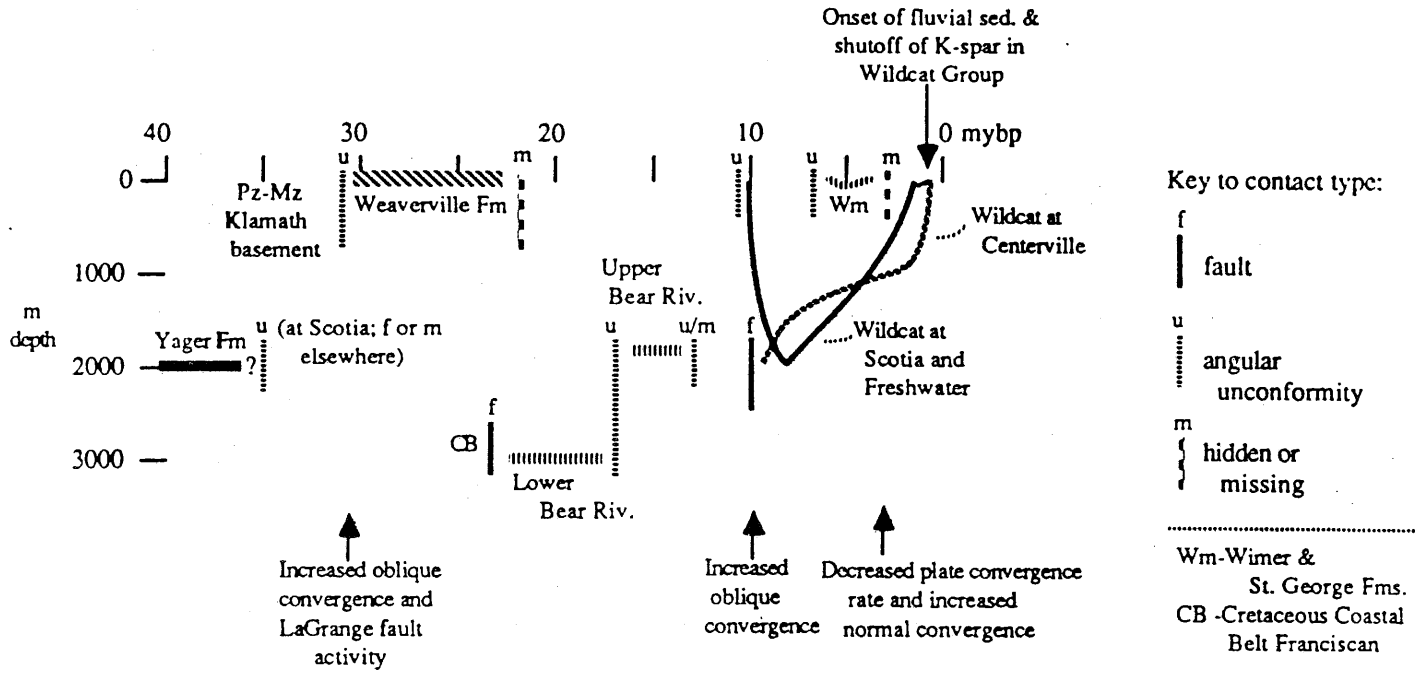

Figure 3. Summary bathymetric diagram showing water depth in which various formations accumulated through time. Holocene units are excluded. Data chiefly from McCrory & Ingle (1984), Ingle (1987) McCrory (1989) and Aalto, *et al.*, (1991).

The Central Franciscan belt consists of melange units and broken formation (tectonically disrupted turbidites). Broken formation units are intercalated with melange units in complex folds. Broken formation units sustain high relief while melanges fail in large debris flows that obscure contact relationships between the two. Melange units contain blocks of conglomerate, unfoliated graywacke, radiolarian chert, recrystallized limestone, blueschist facies metamorphic rock, greenstone and plutonic rock of ophiolitic affinity dispersed in scaly argillite (Aalto, 1981, 1982). Most graywackes are feldspathic litharenites (*cf.* Folk, 1974), rich in albitized plagioclase and aphanitic volcanic rock fragments.

Franciscan Coastal belt rocks consist chiefly of broken formation and are exposed along the coast and inland of Cape Mendocino (Fig. 1; Bachman, 1978; Underwood, 1983). Tectonized turbidites of the Coastal Franciscan belt, exposed south of Cape Mendocino, range in age from Late Cretaceous to Eocene (Kleist, 1974; Evitt and Price, 1975; O'Day, 1974; Bachman, 1978).

Yager Formation

The Paleocene-Eocene Yager Formation (also called a "terrane" or "complex") consists entirely of an unknown thickness of sediment gravity flow deposits and shales that are folded and faulted, but less tectonically disrupted than those of the Franciscan Complex (Ogle, 1953; Blake *et al.*, 1985a; Jayko and Blake, 1987). It is situated in the southern portion of the field trip area in fault contact with rocks of the Franciscan Central and Coastal belts (Fig. 1). Bachman (1978) and Underwood (1983) interpret the Yager Formation as deep-water, inner trench slope deposits that after deposition became structurally imbricated with Franciscan rocks.

Paleocurrent indicators and facies relationships demonstrate that Yager sediments were derived from the northeast and deposited in basins that developed on an inner trench slope during the last phase of Franciscan subduction (Underwood, 1983, 1985). Based upon the scarcity of Klamath rock types in Yager sediments, and comparison of the composition of Yager sandstones and modern Klamath River sands, Underwood and Bachman (1986) feel that the Klamath province was not a major sediment source for the Yager Complex. They envision sediment input from sources as distant as the Idaho batholith. At Scotia, lower Wildcat Group marine sediments overlie the Yager Formation in angular unconformity (Phillips and Aalto, 1989; Moley, 1991 and this volume).

Cenozoic Cover Rocks

Introduction

Cenozoic rocks that overlie the basement rocks discussed above and, in some instances, basement rocks of the Klamath Mountain province, include the Late Oligocene-Early Miocene Weaverville Formation (MacGinitie, 1937; Barnett, 1982), Lower to Middle Miocene "Bear River beds" (Ogle, 1953; Ingle, 1976, 1986) immediately north of Cape Mendocino, the Upper Miocene-Pleistocene Wildcat Group (Ogle, 1953; Haller, 1980) exposed south and east of Eureka, the Plio-Pleistocene Falor Formation (Manning and Ogle, 1950) exposed inland of Eureka, and the Lower Pliocene Wimer and St. George Formations (Back, 1957; Maxson, 1933; L. Stone, this volume) exposed along the coast and inland of Crescent City. Pleistocene sedimentary rocks equivalent in age to the upper Falor Formation are exposed along the coast from Patricks Point to Centerville Beach (field trip stops described herein). In addition, flights of Holocene marine and fluvial terraces that overlie these cover rocks (described in this volume by Carver, Burke and Verhey) are

discontinuously exposed throughout the field trip region. Detailed descriptions of many of these units are found in Schymiczek and Suchsland (1987).

Weaverville Formation

Although the Weaverville Formation does not crop out in the Coast Ranges, its presence in the Klamath Mountains immediately to the east of the field trip area (Fig. 1) is of interest in unraveling the sedimentary tectonic history of the region. Therefore, a brief description of this unit will be presented. More detailed descriptions are provided by MacGinitie (1937), Barnett (1982) and Phillips and Aalto (1989).

In preliminary work by Diller (1902), the Weaverville Formation was described as a series of continental Miocene sedimentary deposits overlying the 'Klamath peneplain', a regional erosion surface. Subsequent reconnaissance mapping of the southern Klamath Mountains confined the occupation of Weaverville deposits to a series of fault-bounded basins (Hinds, 1933; Irwin, 1960, 1963, 1981; Irwin *et al.*, 1985; Lydon and Klein, 1969). A paleobotanical study (MacGinitie, 1937) and a palynological study (Barnett,1982) have provided an Oligocene to early Miocene age constraint for the Weaverville Formation.

Recent work by Schweickert and Irwin (1986, 1989) suggests that Weaverville sediments accumulated in a series of grabens located on the upper plate of a regional detachment surface. They identify this feature as the shallow-dipping La Grange fault, which structurally bounds the northwestern edge of the Weaverville basin (Fig. 1). The relationship between this fault and the development of the Weaverville basin is examined by Phillips (1989).

In the Weaverville basin, which contains several hundred meters of Weaverville sediments, Phillips (1989) determined that facies distribution can be related to basin evolution. Lacustrine facies occur at the base of the sequence and are overlain by fluvial overbank sediment, punctuated by coarse channel fill deposits. These are, in turn, overlain by multistoried fluvial conglomerates intercalated with debris flow deposits which coarsen and thicken towards the La Grange fault and upwards within the section. Adjacent to the fault, slide breccias are interstratified with debris flow deposits.

Fluvial conglomerates exhibit a diverse assortment of clasts derived from eastern and central Klamath basement. Clast imbrication suggests a pronounced WNW paleoflow direction (note: due to an error, clast imbrication and structural data presented in figures 6 and 8 in Phillips and Aalto, 1989, should be rotated clockwise ~38 degrees). Slides and debris flows are comprised of detritus derived from rocks exposed in the footwall of the La Grange fault, as is evidenced by a restricted suite of locally-derived clast lithologies. Principal fractures strike NE, dip NW or SE and reflect NW-SE extension. Initiation of LaGrange detachment faulting, Weaverville sedimentation and, possibly, Klamaths uplift is coeval with increased oblique convergence of oceanic and continental plates ca. 30 Ma, and with alkalic intrusive activity in the southwest Oregon and northwest California Coast Ranges (Fig. 1 and 2; Aalto, *et al.*, 1991). Blake (1977) suggested that the intrusions reflect an unrecognized rifting event which might have resulted from clockwise rotation of the Klamath Mountains and Coast Ranges provinces.

In the Hyampom area adjacent to the Coast Ranges (Fig. 1), some 200 m of Weaverville Formation is preserved in a structural basin bounded by post-depositional NNE- and NW-trending, chiefly high angle, strike-slip faults. Clast imbrication and lithofacies among conglomeratic Weaverville sediments indicate that they were deposited by a west-flowing, coarse-bedload braided river. One must account for the absence of the

deltaic deposits that must have accumulated at the terminus of the Weaverville fluvial system. They could have been removed by erosion, as is suggested by the existence of a Yager-Wildcat unconformity at Scotia. It is also possible, however, to account for their absence structurally.

Most workers believe that the Grogan fault, a major right-lateral strike-slip fault situated west of Hyampom (Fig. 1; Aalto *et al.*, 1988), was active sometime during the early Tertiary (Kelsey and Hagans, 1982; Blake *et al.*, 1985; Cashman *et al.*, 1986). They estimate that a minimum of 75 km of offset occurred along the fault. Based upon overlap relations of the middle Eocene Tyee Formation on Coast Range basement in southwestern Oregon, Wells and Heller (1988) suggest northward transport of western Cordilleran terranes along faults such as the Grogan occurred prior to Tyee deposition. If, however, activity on the Grogan fault continued during and after Weaverville sedimentation, it is possible that the Weaverville delta could have been translated northwards. Although no rocks of this age are found onshore in California to the north, they might exist offshore in the subsurface, or might have been underthrusted after translation above the subducting Gorda-Farallon plate.

It is easier to account structurally for the absence of a Weaverville delta by invoking post-accretion crustal shortening within the Sierra-Klamath forearc. The contacts between several Franciscan terranes west of Hyampom are poorly dated regional thrust faults. These include the South Fork fault, along which Klamath rocks are thrust over Franciscan Pickett Peak terrane schist, the Redwood Mountain fault, along which the schist is thrust over unfoliated Eastern Franciscan Yolla Bolly terrane turbidites, and the Eel River fault, along which the Franciscan Central belt is thrust over the Yager Complex (Fig. 1; Irwin *et al.*, 1974; Jones *et al.*, 1978; Monsen and Aalto, 1980; Underwood, 1982; Bachman *et al.*, 1984; Aalto *et al.*, 1988; Aalto, unpublished mapping). The South Fork and Redwood Mountain faults are poorly dated. They predate the Grogan fault and deposition of the Neogene Wimer Formation (east of Crescent City). According to the latest estimates, these faults predate Weaverville sedimentation (Aalto and Harper, 1982; Blake and Jones, 1983; Jayko, 1983). The Eel River fault, however, appears to be younger.

From field relationships, Underwood (1982) determined that a minimum of 17 km of horizontal displacement occurred on the Eel River fault. Vitrinite reflectance data suggest that Yager sediments west of the fault suffered significant thrust burial, and that the Eel River fault is indeed a major structure (Underwood, 1985). Fault timing is constrained by the age of the dominant phases of Yager Complex folding, for folds are crosscut by the fault, and the maximum age of sediments that blanket the fault. Field relations concerning the latter require further evaluation. Although Plio-Pleistocene Wildcat rocks appear to blanket the fault both along the northeastern margin and south of the Eel River basin (Ogle, 1953; Underwood, 1982), field relations are complicated by younger contractional faulting (Menack, 1986; Kelsey and Carver, 1988). Underwood estimates that the Eel River fault developed sometime between the late Oligocene and middle Miocene, the paleontologically determined age of the Weaverville Formation.

The Eel River fault is a major post-accretion, out-of-sequence thrust whose origin reflects ongoing crustal shortening within an evolving Mesozoic-Cenozoic convergent plate margin. Episodes of shortening have occurred intermittently in northern California in areas north of the Mendocino triple junction since the initiation of the Franciscan-Great Valley-Sierran-Klamath arc-trench system during the late Mesozoic. During these episodes, coastal marine sediments were very likely underthrust beneath the Klamath plate. The deltaic facies of the Weaverville Formation may now lie structurally beneath a portion of the province.

"Bear River beds"

The Lower-Middle Miocene "Bear River beds" (Haller, 1980) consist chiefly of some 500 m of calcareous and siliceous mudstones and minor porcelanite and turbidite sandstone. Based upon paleontologic evidence, they are thought to have accumulated at lower bathyal depths on an inner trench slope (Fig. 3; Cushman, *et al.*, 1930; Haller, 1980; McCrory and Ingle, 1984; Chetelat and Ingle, 1987). These rocks strike east-west, are tilted moderately northwards, and are cut by chiefly east-west trending reverse faults. Bear River-age strata were folded and truncated along structural highs before deposition of the Wildcat Group (Clarke, 1987).

Immediately north of Cape Mendocino, this unit is faulted against Plio-Pleistocene marine shelf sediments that contain abundant shallow-water molluscs. These shelf sediments are meso- and microscopically structurally interleaved with Coastal Franciscan belt turbidites (Carver, *et al.*, 1990). Here Franciscan and Cenozoic marine rocks may be differented by the presence of fossils and abundance of potassium feldspar (Table 1) in the latter and lack of these and presence of zeolite and albite veins in the former. In this area, some fault-bounded phacoidal blocks, which are up to several km^2 in aerial extent, contain late Cenozoic strata that are relatively undeformed (Carver, *et al.*, 1990). The shear zone exhibits a pervasive, near-vertical, east-west-oriented foliation and subhorizontal lineation. Numerous east-west-striking faults exhibit apparent sinistral displacement according to fold data (Carver, *et al.*, 1990). The shear zone is interpreted to have formed by shallow underplating and tectonic interleaving of trench slope sediments and older Franciscan rocks during subduction. Faults and foliation may initially have formed subhorizontally within a developing accretionary wedge, and later uplifted and tilted northward as the wedge thickened in response to tectonic "end loading" that accompanied the northward migration of the Mendocino triple junction (Kelsey and Carver, 1988; McPherson, 1989; Carver, *et al.*, 1990; Carver, this volume).

Wildcat Group

The Wildcat Group (Ogle, 1953) constitutes the Late Miocene-Pleistocene sediment fill of the Eel River basin. McCrory (1989) feels that the Eel River basin formed rapidly near the base of an inner trench slope, in response to subduction of the Gorda plate, and that the initial accumulation of sediments occured at bathyal depths. Wildcat sediments were previously thought to have been derived from chiefly Coast Range sources to the southeast (Nilsen and Clarke, 1987). Aalto, *et al.* (1991) and Moley (this volume) feel that initial sediments that accumulated within the basin did so at shallow depths, that the Eel River basin is chiefly a structural basin formed in response to the northward migration of the Mendocino triple junction, and that some Wildcat sediments were derived from the northeast, possibly from Idaho. Moley (this volume) describes the formations that make up the group.

The marine portion of the Wildcat Group includes some 1,900-2,500 m of mudstone and subordinate sandstone that range in age from late Miocene to middle Pleistocene, arranged in an overall corasening-upward sequence (Ogle, 1953; Ingle, 1987; Nilsen and Clarke, 1987). Along the Eel River at Scotia, an angular unconformity separates tightly folded Yager turbidites and tilted, but relatively undeformed, late Miocene-early Pliocene Wildcat rocks. Above the unconformity are sandy shoreface deposits that contain locally derived Yager clasts, indicating that a certain amount of erosional stripping occurred in this region during post-Yager, pre-Wildcat time. Such stripping might account for the lack of older Wildcat rocks coeval with those found along the coast. East of Eureka, on the northeastern flank of the basin, facies relationships suggest that similar unconformities exist (K. Knudson, MS thesis in progress, Humboldt State Univ.). Paleontologic studies

suggest initial rapid basin subsidence to bathyal depths, followed by sediment infill and eventual influx of fluvial sediments by the middle Pleistocene (Ingle, 1976, 1987).

The nonmarine protion of the Wildcat Group is middle to late Pleistocene in age and consists of a series of fluvial clastic wedges that thin and intertongue with marine sediments to the west. Thickness of this section ranges from 800-1,000 m (Nilsen and Clarke, 1987). Marine-nonmarine cycles are probably glacioeustatic in origin. The Falor Formation (Manning and Ogle, 1950), which exists inland of the northeastern flank of the Eel River basin, isolated from it by basement rock uplifted along active thrust faults, is equivalent in age to the upper Wildcat Group. It consists chiefly of some 1,000 m of braidplain sediments (Carver, 1985), but does have a lower marine mudstone and sandy mudstone unit that may be correlative to the youngest marine Wildcat rocks exposed along the northeastern margin of the Eel River basin.

Wimer and St. George Formations

The St. George (Back, 1957) and Wimer (Maxson, 1933; Watkins, 1974) Formations are exposed, respectively, along the coast and inland of Crescent City (Fig. 1). Based on diatoms, they are thought to be early Pliocene in age (Stone, this volume). The St. George Formation consists of ~70 m of nearshore marine and bay sandstones and sandy mudstones arranged in a fining-upward sequence that unconformably overlies Franciscan rocks along the coast between Crescent City and Point St. George. This unit has been tilted northeast and contains numerous northeast-striking, steeply dipping joints and normal faults.

The Wimer Formation accumulated east of Crescent City on what now is an elevated, westward-tilting, erosion surface, the "Klamath peneplain" of Diller (1902). It consists of a western facies of ~15 m of fossiliferous mudstone, sandstone and pebble conglomerate, interpreted as tidal flat and estaurine deposits (Watkins, 1974; Stone, this volume), and an eastern facies of up to 21 m of coarse fluvial conglomerates and subordinate sandstones (Stone, this volume).

Late Pleistocene-Holocene units

Flights of marine and fluvial terraces are exposed throughout the coastal area of northern California and will be described in Carver (this volume) and the accompanying road log. They indeed contain a most interesting tectonic story and will be seen on the trip in the vicinity of Trinidad, Humboldt Bay and points south.

SANDSTONE COMPOSITION AND PROVENANCE

Table 1 provides compositional data for some of the Cenozoic units described above. Data for Franciscan and Yager rocks of this region are provided by Aalto (1989a) and Underwood and Bachman (1986). Moley (this volume) provides data for Wildcat Group sandstones. Of note is the high K-spar content of marine sandstones of the "Bear River beds", Miocene-Pleistocene Wildcat Group and Pliocene lower Falor Formation.

$^{40}Ar/^{39}Ar$ laser probe analyses (by P. Renne, Geochronology Lab., Inst. Human Origins, Berkeley) of late Pleistocene marine Wildcat Group micas yield ages of approximately. 52-57 Ma. Analyses of Pliocene marine Wildcat Group micas yield three groups of ages: approximately 66-75, 128.5, and 299-303 Ma (Aalto, *et al.*, 1991; Moley, this volume). A logical source for the three younger age groups are Cretaceous-Eocene plutonic rocks in Idaho, a source proposed for subjacent Eocene Yager Formation sandstones in the Coast Ranges by Underwood & Bachman (1986). The source of the

Table 1.-Framework modes for Cenozoic sandstones of the Klamath Mountains and Coast Ranges; given by formation and location, based on counts of 300 grains/thin section. Modes are those of Ingersoll, *et al.* (1984).

Ref.No.:	%QtFL	%QmFLt	%QpLvmLsm	%QmPK
		Weaverville Formation sandstones		
Weaverville basin (from Phillips, 1989):				
RC-4	10-6--84	1-6--3	10-39-38	2-98--0
RT-31	8-0--92	2-0--98	7-28-65	100-0--0
RT320	35-22-43	18-22-60	29-51-20	47-53--0
RESrd	80-10-10	59-10-31	68-24--8	86-14--0
SEC5M	37-17-46	21-17-62	25-37-38	56-44--0
SEC22	51-13-36	8-13--79	54-35-11	40-60--0
SEC35	45-10-47	31-10-59	20-41-39	76-24--0
SEC37	26-16-59	15-16-69	15-59-26	49-51--0
SEC42	10-9--81	1-9--89	10-65-25	13-87--0
SEC58	53-19-28	34-19-47	41-25-34	64-36--0
SEC67	21-11-68	14-12-75	9-41-50	56-44--0
SEC81	15-8--76	9-8--83	9-39-52	49-51--0
SEC91	23-10-67	5-10-85	22-36-43	31-69--0
SEC93	18-5--76	7-5--88	12-66-21	63-37--0
Reading Creek basin:				
RC-1	24-30-46	13-30-57	19-46-35	30-70--0
RC-2	48-5--47	30-5--65	28-26-46	86-14--0
Hyampom basin:				
HY-3	47-24-29	30-24-46	37-53-10	56-43--1
HY-5	49-20-31	35-20-45	32-66--2	64-32--0
HY-7	58-11-31	21-11-68	54-37--9	66-31--3
		St. George Formation sandstone		
SG-1	59-14-33	50-14-36	25-69--6	78-22--0
		Falor Formation sandstones		
Marine facies:				
F-5	45-39-16	31-39-30	47-47--7	44-47--9
Fluvial facies:				
F-1	37-50-13	23-50-27	52-30-19	32-18--0
F-2	40-13-47	17-13-70	33-14-53	57-43--0
F-3	51-32-17	30-32-38	55-18-26	48-52--0
F-4	57-15-28	25-15-60	53-13-33	63-37--0
		'Bear River beds' sandstones		
310-4	34-47-19	32-47-21	10-85--5	41-46-13
310-b	54-31-15	45-31-24	38-58--4	60-31--9
310-c	42-45-13	37-45-18	28-61-11	45-43-12
310-d	35-44-21	33-44-23	9-87--4	43-40-17
CM-2b	48-41-11	42-41-17	35-65--0	51-39-10
CM-2	41-43-16	38-43-19	16-84--0	47-43-10
CP-1	39-47-14	31-47-22	35-65--0	40-54--6
DS	40-47-13	36-47-17	24-76--0	43-48--9
DS-15	36-44-20	32-44-24	17-74--9	43-43-14

older micas remains enigmatic, but may be reset Devonian Abrams Schist of the central Klamath Mountains.

An Idaho source is compatible with the high K-spar content of these sandstones. Although K-spar is present in average abundances of 13% (in %QmPK detrital mode counts) among Franciscan Coastal belt sandstones of the northern Coast Ranges, and 10% among Yager sandstones (Underwood and Bachman, 1986), it is somewhat difficult to envision preservation of significant amounts of K-spar during recycling from these sources. An Idaho source provides an alternative worthy of consideration.

Fluvial conglomerates and sandstones of the Weaverville and Wimer Formations in the Klamath Mountains, the upper Falor and upper Wildcat Group sandstones in the Coast Ranges, and marine sandstones of the Lower Pliocene Wimer and St. George Formations in the Klamaths and Coast Ranges are derived largely from nearby basement rocks. This is reflected in their abundance of Klamath-derived lithologies and lack of K-spar (Table 1).

EPISODES OF SEDIMENT ACCUMULATION AND UPLIFT IN THE COAST RANGES AND KLAMATH MOUNTAINS

The Klamath Mountains province was sufficiently elevated to supply sediment to surrounding areas during the early Paleogene (Heller and Ryberg, 1983; Higinbotham, 1987; Aalto, 1988). By mid-Eocene, however, it was sufficiently reduced in elevation to allow rivers to cross the province, transporting arkosic sand from Idaho to marine basins in the Coast Ranges province of northern California and southern Oregon (Heller and Ryberg, 1983; Underwood and Bachman, 1986; see McKnight (1984) however, for a contrasting point of view).

Active uplift of the central Klamath region began during the Oligocene, accompanying development of the La Grange detachment fault (Schweickert and Irwin, 1989). Rivers of the Weaverville deposystem then transported sediment west to the Coast Ranges. During the Neogene much of the province was again reduced in elevation as the Klamath erosion surface, the "Klamath peneplain" of Diller (1902), developed.

The Bear River beds were deposited at 2-3 km water depth (Ingle, 1987, McCrory, and Ingle, 1984). At Scotia and Freshwater, basal Wildcat Group sediments are fluvial to littoral. However, rapid submergence of the Coast Ranges region to bathyal depths (2 km) occurred following the initiation of Wildcat Group sedimentation. Abrupt bathymetric changes may relate to a greater normal plate convergence rate ca. 9 Ma (Fig. 2 and 3; McCrory, 1989). Ca. 5 Ma the northwest Klamath Mountains were at sea level, as is indicated by presence of Wimer marine sediments on the present-day elevated erosion surface (Diller's 'Klamath peneplain'). Poorly dated, coarse fluvial conglomerates of the eastern Wimer facies may reflect local uplift and warping of this surface about a northwest-trending axis (L. Stone, in press). Sediment shoaling and onset of fluvial sedimentation in the Coast Ranges may relate to a decreasing plate convergence rate, lessening angle of subduction and increasing component of parallel convergence ca. 1 Ma (Fig. 2 and 3; Carver, *et al.*, 1986; McCrory, 1989). The uplift of 'Klamath peneplain' to elevations of as high as 1220 m may largely be a late Pleistocene-Holocene event.

Consideration of marine sediment provenance suggests that the Klamath Mountains were low during the Eocene, elevated during the Late Oligocene (possibly by clockwise rotation and structural doming associated with detachment faulting), low from Middle Miocene through Early Pleistocene, and rapidly elevated during the Late Pleistocene. Alternatively, marine sands may have traveled circuitously southward along the coast from fluvial systems in Oregon. Rapid down-dropping of the Eel River basin, followed by shoaling and fluvial input, is enigmatic, but may relate to large-scale plate interaction.

ACKNOWLEDGEMENTS

I thank past and present Humboldt State University graduate and undergraduate students for their contributions to our understanding of the Cenozoic sedimentary tectonic history of northwestern California, especially Keith Knudson, Harry Leland, Kathy Moley, Perri Phillips and Linda Stone. Thanks to Paul Renne for his invaluable argon-argon dating and to Kathy Moley for reviewing the manuscript.

REFERENCES CITED

Aalto, K.R, 1976, Sedimentology of a melange: Franciscan of Trinidad, California: Jour. Sed. Petrology, v. 46, p. 913-929.

Aalto, K.R., 1981, Multistage melange formation in the Franciscan Complex, northernmost California: Geology, v.9, p. 602-607.

Aalto, K.R., 1982, The Franciscan Complex of northernmost California: sedimentation and tectonics, in Leggett, J.K. ed., Trench-Forearc Geology: Geol. Soc. London Spec. Pub. 10, p. 419-432.

Aalto, K.R., 1988, Sedimentology of the Montgomery Creek Formation, Shasta County, California: California Geol., v. 41, p. 254-260.

Aalto, K.R., 1989a, Sandstone petrology and tectonostratigraphic terranes of the northwest California and southwest Oregon Coast Ranges: Jour. Sed. Petrology, v. 59, p. 561-571.

Aalto, K.R., 1989b, Geology of Patricks Point State Park, Humboldt County, northern California: California Geol., v. 42, p. 125-133.

Aalto, K.R. and Harper, G.D., 1982, Geology of the Coast Ranges in the Klamath and Ship Mountain quadrangles, Del Norte County, California: California Div. Mines Geol. Open-File Map QFR 82-16-SF, scale 1:62,500.

Aalto, K.R., Irwin, W.P., and Kelsey, H.M., 1988, Reconnaissance geologic map of the Pilot Creek quadrangle, Humboldt and Trinity Counties, California: U.S. Geological Survey Open-File Rpt. 88-363, scale 1:62,500.

Aalto, K.R., Moley, K., Knudsen, K.L., Stone, L., Phillips, P.A., and Renne, P.R., 1991, Sediment provenance and Cenozoic tectonic evolution of the central and western Klamath Mountains and northernmost Coast Ranges, California: Geol. Soc. America Abstr. Prog., v. 23, p. A137.

Bachman, S.B., 1978, A Cretaceous and early Tertiary subduction complex, Mendocino Coast, northern California, in Howell, D.G., and McDougall, K.A., eds., Mesozoic Paleogeography of the Western United States: Pacific Sect., Soc. Econ. Paleontologists Mineralogists Pacific Coast Paleogeography Symposium 2, p. 419-430.

Bachman, S.B., Underwood, M.B., and Menack, J.S., 1984, Cenozoic evolution of coastal northern California, in Crouch, J.D., and Bachman, S.B., eds., Tectonics and Sedimentation along the California Margin: Pacific Sect., Soc. Econ. Paleontologists Mineralogists Book 38, p. 55-66.

Back, W., 1957, Geology and ground water features of the Smith River plain, Del Norte County, Califronia: U.S. Geological Survey Prof. Pap. 1254.

Barnett, J.C., 1982, Palynology and paleoecology of the Weaverville Formation (Tertiary), northwestern California: M.S. thesis, Univ. Washington, 118p.

Blake, M.C., Jr., 1977, Tectonic significance of the Coyote Peak diatreme, Humboldt County, California (abs.): EOS Trans., v. 58, p. 1247.

Blake, M.C., Jr., W.P. Irwin, and R.G.Coleman, 1967, Upside-down metamorphic zonation, blueschist facies, along a regional thrust in California and Oregon: U.S. Geological Survey Professional Paper 575-C, p. 1-9.

Blake, M.C., Jr., Howell, D.G., and Jones, D.L., 1982, Preliminary tectonostratigraphic terrane map of California: U.S. Geological Survey Open File Rpt. 82-593, scale 1:500,000.

Blake, M.C., Jr., Jayko, A.S., and McLaughlin, R.J., 1985a, Tectonostratigraphic terranes of the northern Coast Ranges, California, in Howell, D.G., ed., Tectonostratigraphic Terranes of the Circum-Pacific Region: Circum-Pacific Council for Energy and Mineral Resources, Earth Sci. Series 1, p. 159-171.

Blake, M.C., Jr., Engebretson, D.C., Jayko, A.S., and Jones, D.L., 1985b, Tectonostratigraphic terranes in southwest Oregon, in Howell, D.G., ed., Tectonostratigraphic Terranes of the Circum-Pacific Region: Circum-Pacific Council for Energy and Mineral Resources, Earth Sci. Series 1, p. 147-157.

Carver, G.A., 1985, Quaternary tectonics north of the Mendocino triple junction, in Kelsey, H.M., Lisle, T.E. and Savina, M.E. , eds., Redwood Country Guidebook: American Geomorphological Field Group 1985 Field Trip, p. 155-167.

Carver, G.A., 1987, Late Cenozoic tectonics of the Eel River basin region, coastal northern California, in Schymiczek, H., and Suchsland, R., eds., Tectonics, Sedimentation and Evolution of the Eel River and Other Coastal Basins of Northern California: Pacific Sect., Am. Assoc. Petroleum Geologists Misc. Publ. 37, p. 61-71.

Carver, G.A., Burke, R.M., and Kelsey, H.M., 1986, Late Quaternary tectonics of coastal California north of the Mendocino triple junction (abs.): EOS Trans. v. 67, p. 1224.

Carver, G.A., Aalto, K.R., and McPherson, R.C., 1990, Tectonic processes at the Mendocino triple Junction: EOS Trans., v. 71, p. U41A-4.

Cashman, S.M., Cashman, P.H., and Longshore, J.D., 1986, Deformational history and regional tectonic significance of the Redwood Creek schist, northwestern California: Geol. Soc. America Bull., v. 97, p. 35-47.

Chetelat, G., and Ingle, J.C., Jr., 1987, Early Miocene foraminifera from the Centerville Beach Section, Humboldt (Eel River) basin, Humboldt County, California, in Barron, J.A., and Blueford, J., eds., Fourth Intern. Congress Pacific Neogene Stratigraphy, Abstr. Prog., p. 13.

Clarke, S.H., Jr., 1987, Late Cenozoic geology and structure of the onshore-offshore Eel River basin, northern California, in Schymiczek, H., and Suchsland, R., eds., Tectonics, Sedimentation and Evolution of the Eel River and Other Coastal Basins of Northern California: Pacific Sect., Am. Assoc. Petroleum Geologists Misc. Publ. 37, p. 31-40.

Diller, J.S., 1902, Topographic development of the Klamath Mountains: U.S. Geological Survey Bull. 196, 69p.

Evitt, W.P., and Price, S.T., 1975, Early Tertiary ages from the Coastal belt of the Franciscan Complex, northern California: Geology, v. 3, p. 433-436.

Folk, R.L.,1974, Petrology of Sedimentary Rocks: Hemphills Publishing Company, Austin, Texas, 1974.

Haller, C.R., 1980, Pliocene biostratigraphy of California: Am. Assoc. Petroleum Geol. Studies in Geology no. 11, p. 183-341.

Heller, P.L., and Ryberg, P.T., 1983, Sedimentary record of subduction to forearc transition in the rotated Eocene basin of western Oregon: Geology, v. 11, p. 380-383.

Higinbotham, L., 1987, Montgomery Creek Formation, Klamath Mountains, Shasta County, California: California Geol., v. 40, p. 130-138.

Hinds, N.E.A., 1933, Geologic formations of the Redding-Weaverville districts, northern California: California Jour. Mines and Geology, v.29, p.77-122.

Hsü, K.J., 1974, Melanges and their distinction from olistostromes, in Dott, R.H. , Jr., and Shaver, R.H., eds., Modern and Ancient Geosynclinal Sedimentation: Soc. Econ. Paleontologists and Mineralogists Spec. Pub. 19, p. 321-333.

Ingle, J.C., Jr., 1976, Late Neogene paleobathymetry and paleo-environments of the Humboldt basin, northern California, in Fritche, A.E., TerBest, H., and Wornardt, W., eds., The Neogene symposium: Pacific Sec., Soc. Econ. Paleont. Mineral., p. 53-61.

Ingle, J.C., Jr., 1986, Tectonic implications of Neogene marine deposits in the Cape Mendocino area, California (abs.): EOS Trans., v. 67, p. 1220.

Ingle, J.C., Jr., 1987, The depositional, tectonic, and paleo-oceanographic history of the Eel River (Humboldt), Point Arena, and Bodega (Point Reyes) basins of northern California; a summary of stratigraphic evidence, in Schymiczek, H., and Suchsland, R., eds., Tectonics, Sedimentation and Evolution of the Eel River and Other Coastal Basins of Northern California: Pacific Sect., Am. Assoc. Petroleum Geologists Misc. Publ. 37, p. 49-54.

Irwin, W.P., 1960, Geological reconnaissance of the northern Coast ranges and Klamath Mountains, California: California Div. Mines Geol. Bull. 179, 80p.

Irwin, W.P., 1963, Preliminary map of the Weaverville quadrangle, California: U.S. Geological Survey Min. Invest. Field Studies Map MF-576, scale 1:62,500.

Irwin, W.P., Wolfe, E.W., Blake, M.C., Jr., and Cunningham, C.G., Jr., 1974, Geologic map of the Pickett Peak quadrangle, Trinity County, California: U.S. Geological Survey Map GQ-1111, scale 1:62,500.

Irwin, W.P., 1981, Tectonic accretion of the Klamath Mountains, in Ernst, W.G., ed., The Geotectonic Development of California: Prentice-Hall, Englewood Cliffs, N.J., p. 29-49.

Irwin, W.P., 1985, Reconnaissance geologic map of the Hyampom quadrangle, Trinity County, California: U.S. Geological Survey Misc. Field Studies Map MF-1809, scale 1:62,500.

Jayko, A.S., 1983, Deformation in low-grade blueschists of the Eastern Franciscan belt, northern California: Geol. Soc. America Abstr. Prog., v. 15, p. 313.

Jayko, A.S., and Blake, M.C., Jr., 1987, Geologic terranes of coastal northern California and southern Oregon, in Schymiczek, H., and Suchsland, R., eds., Tectonics, Sedimentation and Evolution of the Eel River and Other Coastal Basins of Northern California: Pacific Sect., Am. Assoc. Petroleum Geologists Misc. Publ. 37, p. 1-12.

Jones, D.L., Blake, M.C., Jr., Bailey, E.H., and McLaughlin, R.J., 1978, Distribution and character of upper Mesozoic subduction complexes along the west coast of North America: Tectonophysics, v. 47, p. 207-222.

Kelsey, H.M., and G.A. Carver, 1988, Late Neogene and Quaternary tectonics associated with the northward growth of the San Andreas transform, northern California: Jour. Geophys. Res., v. 93, p.4797-4819.

Kelsey, H.M., and D.K. Hagans, 1982, Major right-lateral faulting in the Franciscan assemblage of northern California in late Tertiary time: Geology, v. 10, p. 387-391.

Kleist, J.R., 1974, Geology of Coastal belt Franciscan Complex near Fort Bragg, California: Ph.D. dissert., Univ. Texas, Austin, 133p.

Lydon, P.A., and Klein, I.E., 1969, Geology of the southeast quarter of the Trinity Lake quadrangle, Trinity County, California: California Div. Mines Geol. Map Sheet 12, scale 1:24,000.

MacGinitie, H.D., 1937, The flora of the Weaverville beds of Trinity County, California, in Eocene Flora of Western America, Carnegie Inst. Washington Contri. Paleontology, Publ.465, p. 83-151.

Manning, G.A., and Ogle, B.A., 1950, Geology of the Blue Lake quadrangle, California: Calif. Div. Mines Bull. 148, 36p.

Maxson, J.H., 1933, Economic geology of portions of Del Norte and Siskiyou Counties, northwesternmnost California: Calif. Jour. Mines Geol., v. 29, p. 123-135.

McCrory, P.A., 1989, Late Neogene geohistory analysis of the Humboldt basin and its relationship to convergence of the Juan de Fuca Plate: Jour. Geophys. Res., v. 94, p. 3126-3138.

McCrory, P.A., and Ingle, J.C., Jr., 1984, Neogene history of Humboldt basin of northern California and its relationship to convergence of the adjacent Gorda plate: Geol. Soc. America Abstr. Prog., v. 16, p. 588.

McKnight, B.K., 1984, Stratigraphy and sedimentology of the Payne Cliffs Formation, southwestern Oregon, in Nilsen, T.H., ed., Geology of the Upper Cretaceous

Hornbrook Formation, Oregon and California: Pacific Sect., Soc. Econ. Paleontologists Mineralogists Book 42, p. 187-194.

McPherson, R.C., 1989, Seismicity and focal mechanisms near Cape Mendocino, northern California: M.S. thesis, Humboldt State Univ., 75p.

Menack, J.S., 1986, Geology of the Neogene sedimentary rocks in Garberville, California: M.S. thesis, Cornell Univ., 231p.

Miller, S.G., and Aalto, K.R., 1983, Post-middle Miocene accretion of Franciscan rocks, northwestern California: a discussion: Geol. Soc. America Bull., v. 94, p. 1028-1029.

Moley, K., 1991, Petrology and basal contacts of the Wildcat Group, Eel River basin, Humboldt County, California: Geol. Soc. America Abstr. Prog., v. 23, p. A246.

Monsen, S.A., and Aalto, K.R., 1980, Petrology, structure and regional tectonics: South Fork Mountain Schist of Pine Ridge Summit, northern California: Geol. Soc. America Bull., pt. I, v. 91, p. 369-373.

Nilsen, T.H., and Clarke, S.H., Jr., 1987, Geological evolution of the late Cenozoic basins of northern California, in Schymiczek, H., and Suchsland, R., eds., Tectonics, Sedimentation and Evolution of the Eel River and Other Coastal Basins of Northern California: Pacific Sect., Am. Assoc. Petroleum Geologists Misc. Publ. 37, p. 15-30.

O'Day, M.S., 1974, The structure and petrology of the Mesozoic and Cenozoic rocks of the Franciscan Complex, Leggett-Piercy area, northern California: Ph.D. dissert.,Univ. Calif. Davis, 152p.

Ogle, B.A., 1953, Geology of the Eel River area, Humboldt County, California: Calif. Div. Mines Bull. 164, 128p.

Phillips, P. A., 1989, The Weaverville Formation: implications for tectonically controlled basin development in the central Klamath Mountains: unpubl. M.Sc. thesis, Humboldt State University.

Phillips, Perri, and Aalto, K.R., 1989, The Weaverville Formation: implications for tectonically controlled basin development in the central Klamath Mountains, in Colburn, I., Abbott, P., and J. Minch, eds., Conglomerates in Basin Analysis: Pacific Sect., Soc. Econ. Paleontologists Mineralogists Book 62, p. 81-98.

Schweickert, R.A., and Irwin, W.P., 1986, Tertiary detachment faulting in the Klamath Mountains, California: a new hypothesis: Geol. Soc. America Abstr. Prog., v. 18, p. 742.

Schweickert, R.A., and Irwin, W.P., 1989, Extensional faulting in southern Klamath Mountains, California: Tectonics, v. 8, p. 135-149..

Schymiczek, H., and Suchsland, R., eds., Tectonics, Sedimentation and Evolution of the Eel River and Other Coastal Basins of Northern California: Pacific Sect., Am. Assoc. Petroleum Geologists Misc. Publ. 37, 137p.

Underwood, M.B., 1982, The Garberville thrust-a contact of probable Miocene age within the Franciscan Complex, northern California: Geol. Soc. America Abstr. Prog., v. 14, p. 635-636.

Underwood, M.B., 1983, Depositional setting of the Paleogene Yager Formation, northern Coast Ranges of California, in Larue, D.K., and Steel, R.J., eds., Cenozoic Marine Sedimentation, Pacific Margin, U.S.A.: Pacific Sect., Soc. Econ. Paleontologists Mineralogists Book 28, p. 81-101.

Underwood, M.B., 1985, Sedimentology and hydrocarbon potential of the Yager complex, possible Paleogene source rocks in the Eel River basin of northern California: Am. Assoc. Petroleum Geologists Bull., v. 69, p. 1088-1100.

Underwood, M.B., and Bachman, S.B., 1986, Sandstone petrofacies of the Yager complex and the Franciscan Coastal belt, Paleogene of northern California: Geol. Soc. America Bull., v. 97, p. 809-817.

Watkins, R., 1974, Molluscan paleobiology of the Wimer Formation, Del Norte County, California: Jour. Paleontology, v. 48, p. 1264-1282.

Wells, R.E., and Heller, P.L., 1988, The relative contribution of accretion, shear and extension to Cenozoic tectonic rotation in the Pacific Northwest: Geol. Soc. America Bull., v. 100, p. 325-338.

DEPOSITIONAL/TECTONIC HISTORY OF THE PLIO-PLEISTOCENE CRESCENT CITY/SMITH RIVER, DEL NORTE COUNTY, CALIFORNIA

LINDA STONE
Dept. of Geology, Humboldt State University, Arcata, CA 95521

INTRODUCTION

The most complete site of Neogene deposition in the vicinity of northwestern California is the "Humboldt" or "Eel River" basin, an elongate offshore trough which received sediments from the late Miocene to the mid Pleistocene (Figure 1). An uplifted remnant of the northeastern portion of the basin is exposed in the vicinity of Crescent City and the Smith River (Figure 2). The deposits consist of the near-shore Saint George Formation and the estuarine/fluvial Wimer Formation.

WIMER FORMATION

The Wimer Formation has been preserved on flat topped ridges which are remnants of an erosion surface referred to as the "Klamath Peneplain" by Diller (1902) (Figure 2). The formation can be divided into two facies: a western marine facies and an eastern fluvial facies. The two facies are correlated based on proximity and their occupation of the same geomorphic surface.

Outcrops of the marine facies occur on Wimer Ridge, Bald Hill, and Lind Mine Ridge. At least 90% of the outcrops consist of fine-grained lithologies, primarily siltstone. Two minor lithologies are a silicified granule/pebble conglomerate and a coarse basal conglomerate. The fine-grained lithologies contain few sedimentary structures and appear to have been highly bioturbated. Fossiliferous horizons containing molluscan fauna diagnostic of a protected coastal mudflat environment occur throughout the fine-grained lithologies (Watkins, 1974). Based on the fossil assemblages, the deposits on Wimer Ridge and Bald Hill represent normal marine salinity conditions and those of Lind Mine Ridge represent brackish water conditions (Watkins, 1974). The fine-grained brackish water deposits overlie coarse-grained conglomerates which are matrix-rich, lack imbrication and contain siltstone rip-up clasts. This association suggests deposition in a fluvial/estuarine deltaic setting. Thin beds of silicified granule/pebble conglomerates occur on Wimer Ridge, Howland Hill, and Bald Hill and may represent fluvial or tidal surges triggered by storm or seismic events.

Several patches of fluvial conglomerates are preserved south and east of the marine facies (Figure 2). Deposits consist of pebble to boulder conglomerates, containing sub-rounded to rounded clasts derived from rocks of the Galice Formation, Josephine ophiolite and associated igneous rocks. Conglomerates on the west side of the Coast Range thrust also include clasts derived from the Franciscan Complex. Porphoritic latite clasts occur in two basal deposits on Lower Coon Mountain and Haines Flat. The only known source for the latite clasts are intrusions associated with the Mount Emily pluton, southwest Oregon.

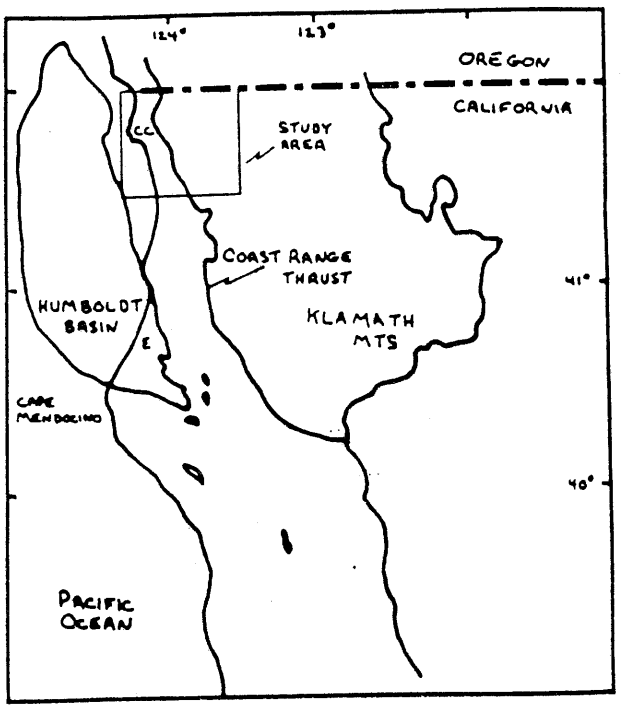

FIGURE 1. Location map of study area (CC=Crescent City, E=Eureka).

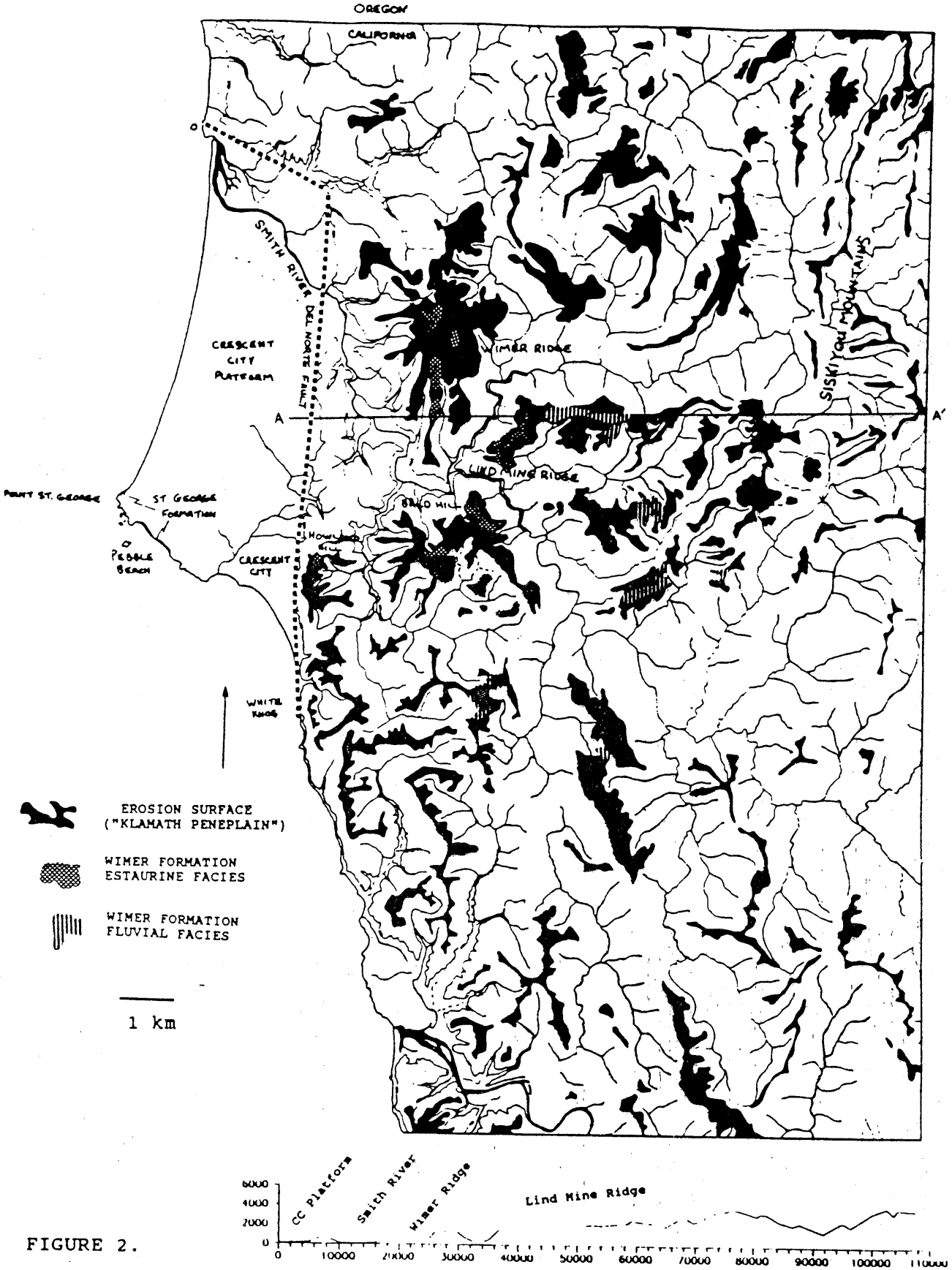

FIGURE 2.

Erosion surface, overlying deposits, drainage patterns and cross-section of study area.

Outcrops of the fluvial facies consist primarily of clast-supported, normally graded, massive to crudely bedded conglomerates which are consistent with deposition as gravel sheets on longitudinal and diagonal bars. The deposits contain minor amounts of interbedded silt and sand which are consistent with backswamp deposits, and overbank or drape deposits. The predominance of longitudinal and diagonal bars, is characteristic of very proximal, gravelly braided rivers.

Imbrication measurements indicate that the predominant paleoflow direction was to the north to northwest in accordance with the present day north-northwestern structural trend of the area. The river discharged into the Wimer estuary forming a deltaic environment in the vicinity of Lind Mine Ridge. However, imbrication in the latite-bearing unit indicates paleoflow of the basal deposits was toward the south. The northern source area of the latite clasts and the paleocurrent direction indicate that the basal deposits represents an older, south-flowing fluvial system.

ST. GEORGE FORMATION

The St. George Formation is exposed in wave cut cliffs along Pebble Beach just west of Crescent City. The northwest strike of bedding is roughly parallel to the beach and beds dip shallowly to the northeast. The deposits overlie rocks of the Franciscan Complex and are overlain by the late Pleistocene Battery Formation along a slight unconformity.

The St. George Formation consists of mudstone and sandstone and includes scattered pebbles and carbonized wood, and horizons containing fragmental molluscan shells. Although previously interpreted to have been deposited in a littoral environment (Back, 1957), the deposits lack the strong current bedforms and the coarse sand commonly associated with such environments. One of the few bedforms expressed in the St. George Formation is hummocky cross-stratification, which develops when large storm waves transport silt and fine sand from shorelines to the offshore, between fair-weather and storm wave base. The massive sandstones and mudstones most closely resemble an amalgamation of intensely bioturbated storm deposits. The inclusion of wood fragments, fragmental shells, and randomly oriented pebbles have been documented in other storm sequences (Dott and Bourgeois, 1982; DeCelles, 1987). The sediments were probably deposited during rare storms and were subsequently bioturbated during the relatively long periods between storms.

STRUCTURE

Based on geomorphic expression, offset of basement rocks and northeastern dip of the St. George Formation, previous investigators have suggested the existence of the Del Norte fault along the mountain front which delineates the eastern boundary of the Crescent City platform (Figure 2; Maxson, 1933; Back, 1957; Roberts and Dolan, 1977; Kilbourne and Mualchin, 1981). Prior to this investigation, the Wimer and St. George formations had been assigned respective ages of late Miocene and Pliocene based on the megafossil content (Watkins, 1974; Addicott, 1963). However, analysis of the diatom assemblages, which are more age diagnostic for this period, indicate an earliest Pliocene age for both formations (John Barron, written communication, 1988). Therefore, the near-shore, storm wave base, St. George Formation appears to be the western facies of the estuarine/fluvial Wimer Formation. At Pebble Beach the St. George Formation occurs at sea level. Toward the mountain escarpment, the most western occurrence of the Wimer Formation occurs just east of the escarpment at an elevation of 210 meters. Therefore, the two formations have been offset vertically by at least 210 meters.

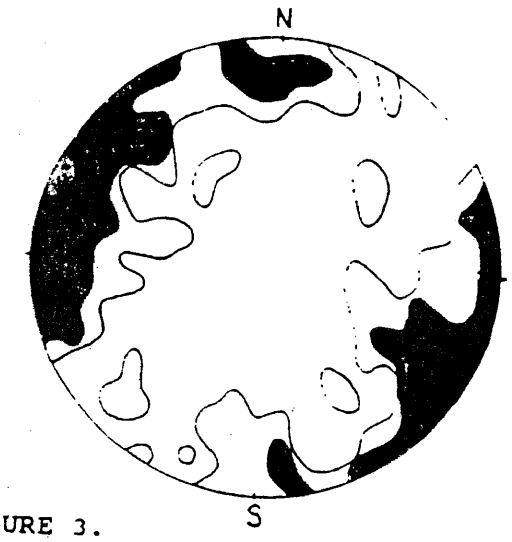

FIGURE 3.

Equal area lower hemisphere stereonet plot of poles to fracture planes in the St. George Formation, Pebble Beach, CA, N=234.

Offset of late Pleistocene deposits in the vicinity of Crescent City also support vertical movement along the Del Norte fault. A fluvial conglomerate on the east side of the escarpment has been correlated to late Pleistocene conglomerates in the subsurface of the Crescent City platform (Back, 1957), indicating that there has been a minimum of 40 meters of vertical offset since the late Pleistocene along this escarpment. Two kilometers south, a small alluvial fan deposit occurs on a steep slope approximately 55 meters above the upper surface of the modern fans. Further south, the escarpment intersects the coastline in the vicinity of White Knob where a wave-cut platform has been uplifted above sea level and vertical faults juxtapose Franciscan basement against young fan deposits and colluvium.

Offshore seismic data indicates that a northwest trending thrust fault with as much as 800 meters of vertical displacement of Pliocene and Pleistocene deposits projects into the coast at the mouth of the Smith River (Clarke, personal communication, 1988). The Del Norte fault may be an onshore expression of this thrust. Offshore of Point St. George, seismic data indicates a second thrust is associated with duplexing (Clarke, personal communication, 1988). This structure may be responsible for the uplift and the northeastern tilt of the St. George Formation.

The St. George Formation exposed along Pebble Beach contains extensive, well developed fractures. A total of 234 fractures were measured along Pebble Beach and poles were plotted on a lower hemisphere equal area net (Figure 3). The majority of the fractures are near vertical and strike northeast. The strikes vary broadly in the northeast/southwest direction, predominantly reflect SW/NE compression. During the last 5 Ma, the direction of convergence of the Gorda and North American plates has rotated counterclockwise from N48E to N23E (McCrory, 1989). The distribution of fractures in the St. George appears to reflect this rotation.

SUMMARY

Subsequent to the cessation of movement along the Coast Range thrust and prior to the Pliocene a surface of low relief formed in the vicinity of Crescent City/Smith River. The earliest Pliocene corresponded to a mild eustatic sea level rise (Haq et al., 1987) during which the St. George and Wimer formations were deposited on the erosion surface. Concurrent uplift of the Siskiyou Mountains to the east initiated the formation of braided streams in north-northwest trending valleys and blanketed older, south-flowing braided stream deposits. Subsequent to deposition, vertical movement along the Del Norte fault uplifted the Wimer Formation and the eastern block out of the zone of deposition. Uplift continued through the late Pleistocene and possibly into Holocene. Concurrently, the downdropped St. George Formation was tilted to the northeast along a northwest structural trend offshore of Point St. George (Point St. George fault). The St. George Formation was bevelled and partially eroded away during the formation of a wave cut platform and the late Pleistocene Battery Point Formation was deposited on that surface. Since the late Pleistocene, there has been continued uplift and slight tilting along the St. George fault.

REFERENCES CITED

Addicott, W.O., 1983, Biostratigraphy and Marine Neogene at Cape Blanco, southwestern Oregon, U.S. Geological Survey Professional Paper 0774-G, p. G1-G20.

Back, W., 1957, Geology and ground water features of the Smith River plain, Del Norte County, California: U.S. Geological Survey Water Supply Paper 1254. 76 p.

DeCelles, P.G., 1987, Variable preservation of middle Tertiary, coarse-grained, nearshore to outer-shelf storm deposits in southern California, Journal of Sedimentary Petrology, v. 57, p. 250-264

Diller, J.S., 1902, Topographic Development of the Klamath Mountains: U.S. Geologic Survey Bulletin 196, 69p.

Dott, R.H., Jr. and Bourgeois, J., 1982, Hummocky stratification: Significance of its variable bedding sequence, Geological Society of America, v. 93, p. 663-680.

Kilbourne, R.T., and Maulchin, L., 1981, Geology for planning: Crescent City and Sister Rocks 7 1/2' Quadrangles Del Norte County, California, U.S. Geological Survey Open File Report 81-1, 48 p.

Maxson, J.H., 1933, Economic geology of portions of Del Norte and Siskiyou Counties, northwesternmost California: California Journal of mines and Geology, v. 29, p. 123-135.

McCrory, P.A., 1989, Late Neogene geohistory analysis of theHumboldt basin and its relationship to convergence of the Juan de Fuca plate, Journal of Geophysical Research, v. 94, n. B3, p. 3126-3138.

Roberts, J.A., and Dolan, R., 1968, Coastal Geomorphology of the Smith River plain: Shore and Beach, April 1968, p. 4-11.

Watkins, R., Molluscan paleobiology of the Miocene Wimer Formation, Del Norte County, California: Journal of Paleontolrogy, v. 48, n. 6, p. 1264-1282.

Haq, B.U., Hardenbol, J., and Vail, P.R., 1987, The new chronostratigraphic basis of Cenozoic and Mesozoic sea level cycles, in Ross, C.A. , and Haman, D., eds, Timing and Depositional History of Eustatic Sequences: Constraints on Seismic Stratigraphy, Cushman Foundation for Foraminiferal Research, Special Publication No. 24, p. 7-24.

STYLE OF FAULTING AT THE SOUTHERN END OF THE CASCADIA SUBDUCTION ZONE

by
Robert C. McPherson
Geology Department
Humboldt State University
Arcata, California 95521

ABSTRACT

Three dimensional distribution of well-located seismicity is used to delineate the geometry of lithospheric plates comprising the Mendocino triple junction in northern California. After an understanding of the geometry of the plates is established, first motions of the best located earthquakes are analyzed to identify stress orientations within each plate. Using both the first motion data and the distribution of the earthquakes, the style of faulting within each plate is determined.

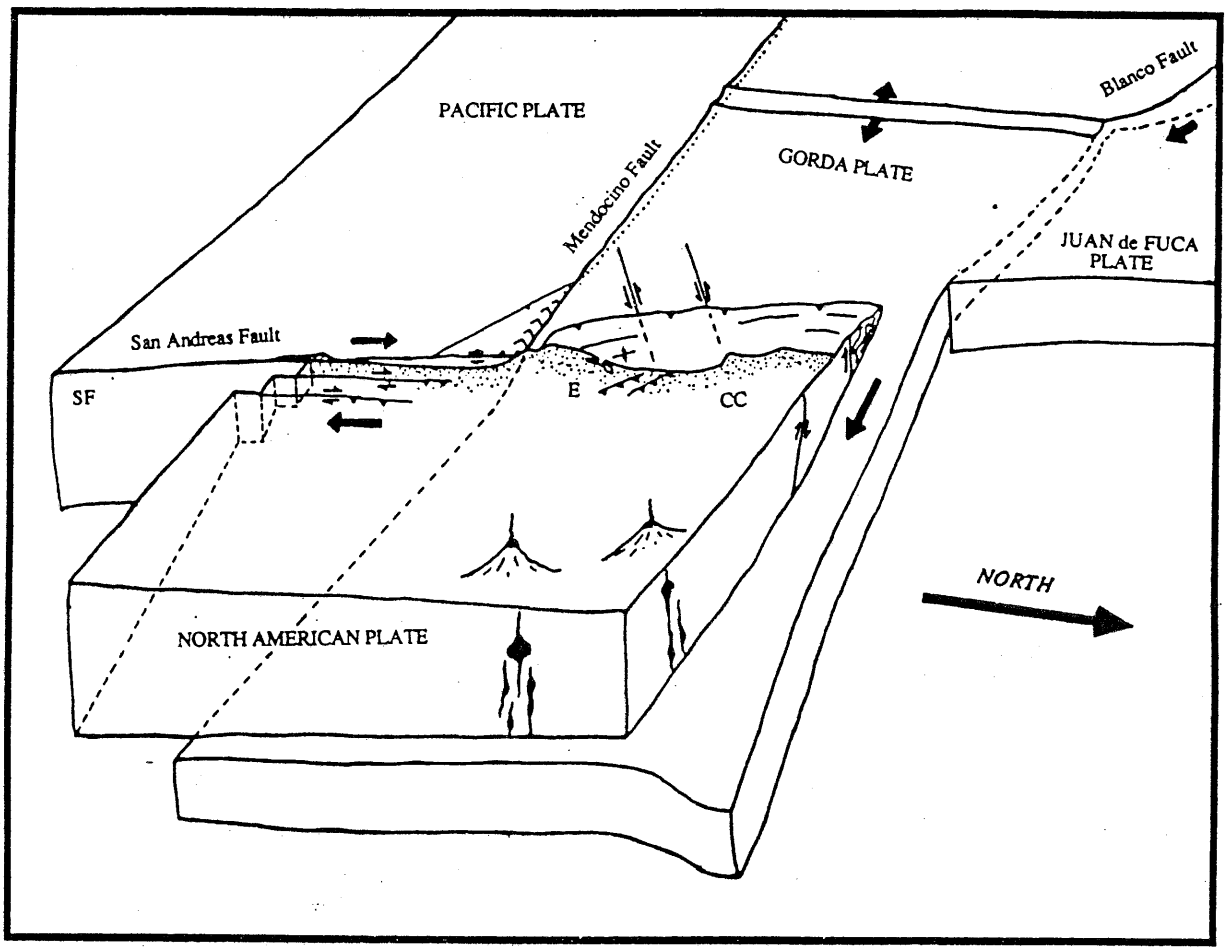

Figure 1. Cartoon showing the plates that make up the Mendocino triple junction. To the south the Pacific and North American plates slide past each other along a shear boundary that produces a series of parallel, right-lateral faults within the North American plate. The Pacific and Gorda plates meet along the Mendocino fault, an active vertical, right-lateral fault. The North American and Gorda plates converge with each other and form the southern edge of the Cascadia subduction zone. Abbreviations used in this Figure are: CC-Crescent City, E-Eureka, SF-San Francisco.

INTRODUCTION AND SUMMARY

The cartoon in Figure 1 summarizes the geometry of the three plates that form the Mendocino triple junction (MTJ). South of the triple junction, the North American and Pacific plates slide past each other in a shearing manner that produces a series of right lateral faults within the North American plate (Eaton, 1989, Kelsey and Carver, 1988). The Gorda plate forms offshore along the ridge (divergent arrows) and moves away from it, eventually descending to the east under the North American plate (bold arrow). This eastward motion of the Gorda plate away from the ridge produces right-lateral motion along the Mendocino fault and creates an accretionary prism with the sediments that are scraped off and piled up along the western edge of the North American plate (Clarke, 1992). Once the Gorda plate reaches a depth of 100-150km, water-laden sediments that have been dragged down along the interface between the North American and Gorda plates are heated up sufficiently to cause melting, which results in the beginning of the Cascade volcanic arc depicted by the two volcanoes in the cartoon (Lassen and Shasta). Notice that these volcanoes lie north of the southernmost edge of the Gorda plate.

The Humboldt Bay Seismic Network (HBSN) was installed in 1974 to investigate the tectonics in the region of the triple junction. All stations were on land and were located north, south and east of the triple junction. The HBSN recorded over 14,000 earthquakes ranging in magnitude from 0.0 to 7.2 from 1974-1984. The seismicity consisted primarily of Gorda and North American intraplate activity, with the Gorda plate earthquakes accounting for approximately 80% of the activity and over 90% of the actual strain energy released during this period. The intraplate Gorda seismicity patterns combined with the focal mechanism solutions were used as a basis to divide the Gorda plate into two provinces (McPherson, 1989ab): 1) the offshore region confined between the larger Pacific and Juan de Fuca plates and lying west of the MTJ and 2), that portion of the Gorda plate east of the triple junction and gently dipping under the North American plate.

The Gorda plate offshore is being shoved up against the Pacific plate along t Mendocino fault by the convergent motion of the Juan de Fuca plate from the north as w as the northwestward motion of the Pacific plate from the south. The influences of the larger plates' motions produce a north-south directed stress within the Gorda plate. response to this stress, the Gorda plate is failing along vertical, northeast trending, le lateral faults (Smith and others, 1981). These faults are capable of generating magnitu 7.0-7.5 earthquakes, the maximum magnitude being limited to this range by the strength the young Gorda plate. In addition to this style of deformation, the offshore portion of t Gorda plate is being thickened at its southern edge as it is crushed and sheared along t eastern Mendocino fault, where it is buttressed against the Pacific plate. Pieces of t Gorda plate may be broken off and wedged in this area in a vertical manner (Niazi a Karageorgi, 1992), and could be imbricated (Smith and others, 1992).

Once the Gorda plate moves east of the corner of the Pacific plate (i.e., the MTJ), thus no longer being confined and therefore removing the source of the north-south directed stress, the character of seismicity changes dramatically. In this region the intraplate earthquakes are primarily north-south oriented normal faults, with tension axes trending east-west and dipping at shallow angles to the east (McPherson, 1989a). In section the earthquakes appear as a 12km wide band, dipping eastward at about 11 degrees to a depth of 25-30km under the North American plate. The earthquakes in this region of the Gorda plate rarely have had magnitudes that exceed 4.0 in contrast to the larger earthquakes that occur in the region west of the MTJ. Also, east of the MTJ the southern edge of the Gorda plate trends eastward at about the latitude of the eastern end of the Mendocino fault (40.25^{o}).

The seismicity in the North American plate, which has a diffuse pattern in map view and covers the same area as the activity in the Gorda plate below it, occurs primarily on northwest trending reverse and oblique-slip faults as inferred from focal mechanisms. The compression axes for North American earthquakes were consistently horizontal and

oriented in a northeast direction. The northeast-directed compression in the North American plate which is parallel to the convergence between the Gorda and North American plates (Engebretsen and others, 1985, Nishimura and other, 1984), and the down slab tension determined for the Gorda plate earthquakes beneath the interplate thrust zone are consistent with features in other active subduction zones (Shimazaki, K. 1978). Although the movement of the Gorda plate has been found to be slowing down (Spence, 1987), the body forces within the plates are consistent with continuing subduction. The findings of this study indicate that contractional deformation is ongoing in the overriding North American plate, indicating that the Gorda and North American plates are presently coupled, and that their differential motion is dictating the orientation and style of youthful faulting in this region.

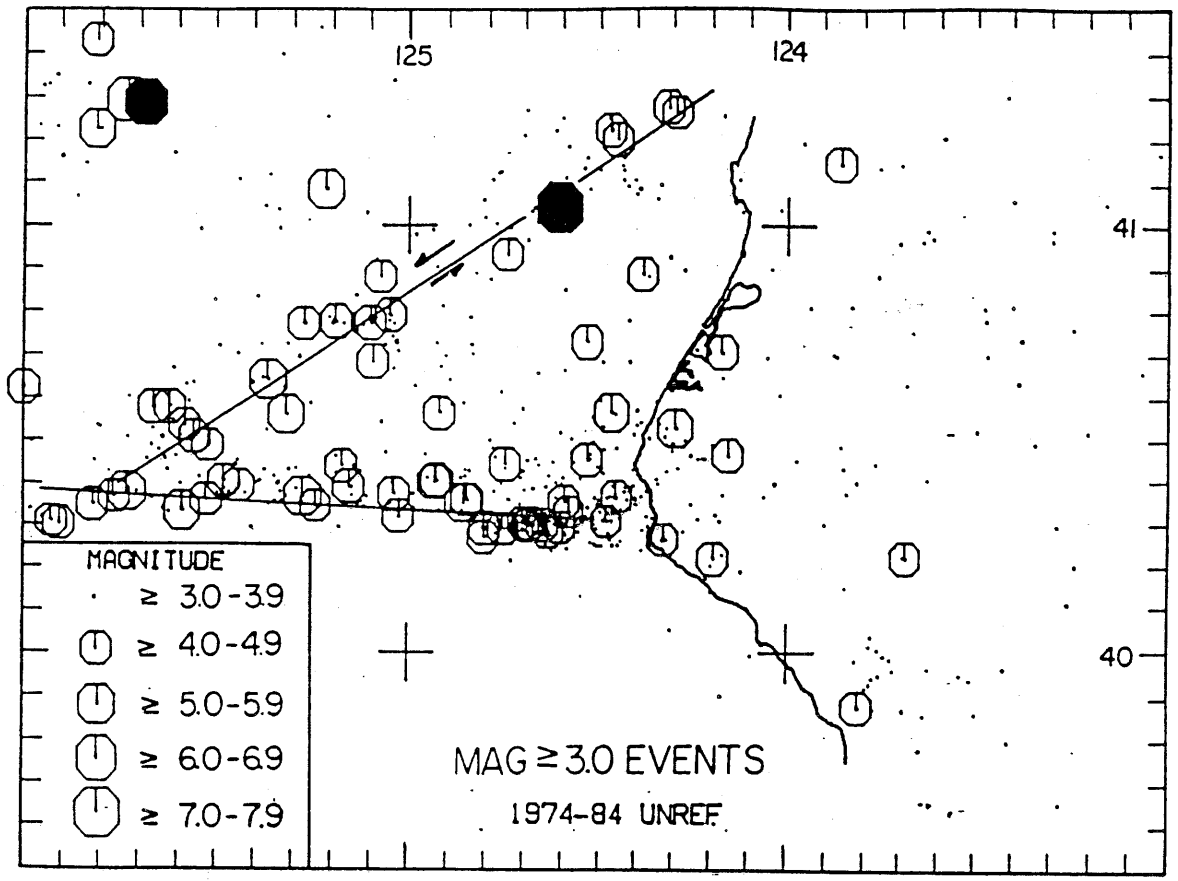

Figure 2. Map of epicenters of all earthquakes greater than M=3.0 located by the HBSN from 1974-84. Solid lines are drawn through the November 8, 1980, M=7.2 (intraplate) earthquake sequence and the Mendocino fault. Coastline is shown for reference.

DATA AND TERMS USED

The earthquakes used in this study were recorded by the Humboldt Bay Seismic Network, and were summarized in many technical reports written for Pacific Gas and Electric while I was at TERA Corporation. Most of the information here was garnered from a study by McPherson (1989a), in which a much more complete reference list is given of the technical reports. The earthquakes for this paper were relocated using the final 1-D layered model developed by Knapp (1982). A discussion about the development of the model and features of the seismicity located with this model are given in Smith and Knapp (1980) and Smith and others (1992).

The names used for geologic units and faults of the region is based on work done by Carver (in this volume) for the Humboldt Bay region, by Clarke and Carver (1991) and Clarke (1992) in the offshore region, and by McLaughlin and others (1982) and Kelsey and Carver (1988) for the region south of the MTJ.

MAP VIEWS OF SEISMICITY

North American Plate Seismicity

The activity within the North American plate consists of less than 20% of the activity located by the HBSN. Actual strain energy released within the North American plate is less than 10%, since the larger earthquakes occurred within (intra) the Gorda plate offshore and along the Mendocino fault (interplate activity between the Gorda and Pacific plates, see Figure 2). The magnitudes of the events ranged from 4.6 to less than zero, with 1481 well-located events shown in Figure 3. The seismicity was generally scattered over the whole region with some clustering and hints of northwest alignments. Seismicity in the North American plate generally coincides with the geographic distribution of the activity in the Gorda plate below it, indicating that the two plates are coupled and are influencing each other (see discussion below).

The map was constructed by assuming that the western edge of the North American plate is at the base of the continental slope and at a depth of 5km, i.e., a north-south line at 124° 45'. From this western edge all earthquakes that locate above a plane with a 11 degree eastward dip are displayed (see east-west cross section in Figure 6). Because this dipping plane is extended south past the Mendocino fault, it cuts through the eastern end of this east-west feature, and therefore some interplate events are displayed in this Figure (see trend labeled MF).

The densest cluster of events within the North American plate lies between the surface expresssion of the Russ Fault to the north and the False Cape shear zone to the south (labeled RF/FCSZ). The seismicity in this region appears to be aligned along a N75W trend, and the distribution in section is nearly vertical (see section C-C', Figure 7). The RF/FCSZ continued to be a source of small earthquakes throughout the ten-year study period, and the position of this activity lies directly above a cluster of similiarly intense activity within the Gorda plate (compare Figures 3 and 4). This concomitant relationship was interpreted as evidence that the Gorda and North American plates are coupled in this region.

A linear trend in seismicity that strikes N30W for approximately 30km developed in the southern part of the map (labeled GF). This group of events first appeared in 1979 as a swarm of 50 events in a 12-hour period, with the two largest events having been felt in the Garberville area as sharp jolts and having magnitudes of just over 3.5 (TERA, 1980, McPherson, 1989a). Depths of these events range from about 10-25 km, and they appear to have occurred along a near-vertical, northwest trending feature in the lower part of the North American plate. The orientation of this activity is similiar to the northwest lineations seen in the interplate seismicity further to the south, although the GF hypocenters are somewhat deeper (Eaton, 1988, McPherson, 1989).

The broad band of seismicity that comes on land near Punta Gorda represents interplate events associated with the Mendocino fault, and as mentioned above, are in this map because of the simplified, wedgelike selection used which cuts through the eastern end of this vertical fault. This lineation is significant in that it represents the eastward extention of the Mendocino fault as it approaches the coast in the vicinity of Punta Gorda. It continues to be presently active as evidenced by the aftershock sequence following the August 17, 1991 Honeydew earthquake (Oppenheimer, 1991, McPherson and others, 1991). It now seems likely that the Mendocino fault bends slightly to the south and comes on land in the vicinity of the Cooskie shear zone, as first proposed by Clarke (1992).

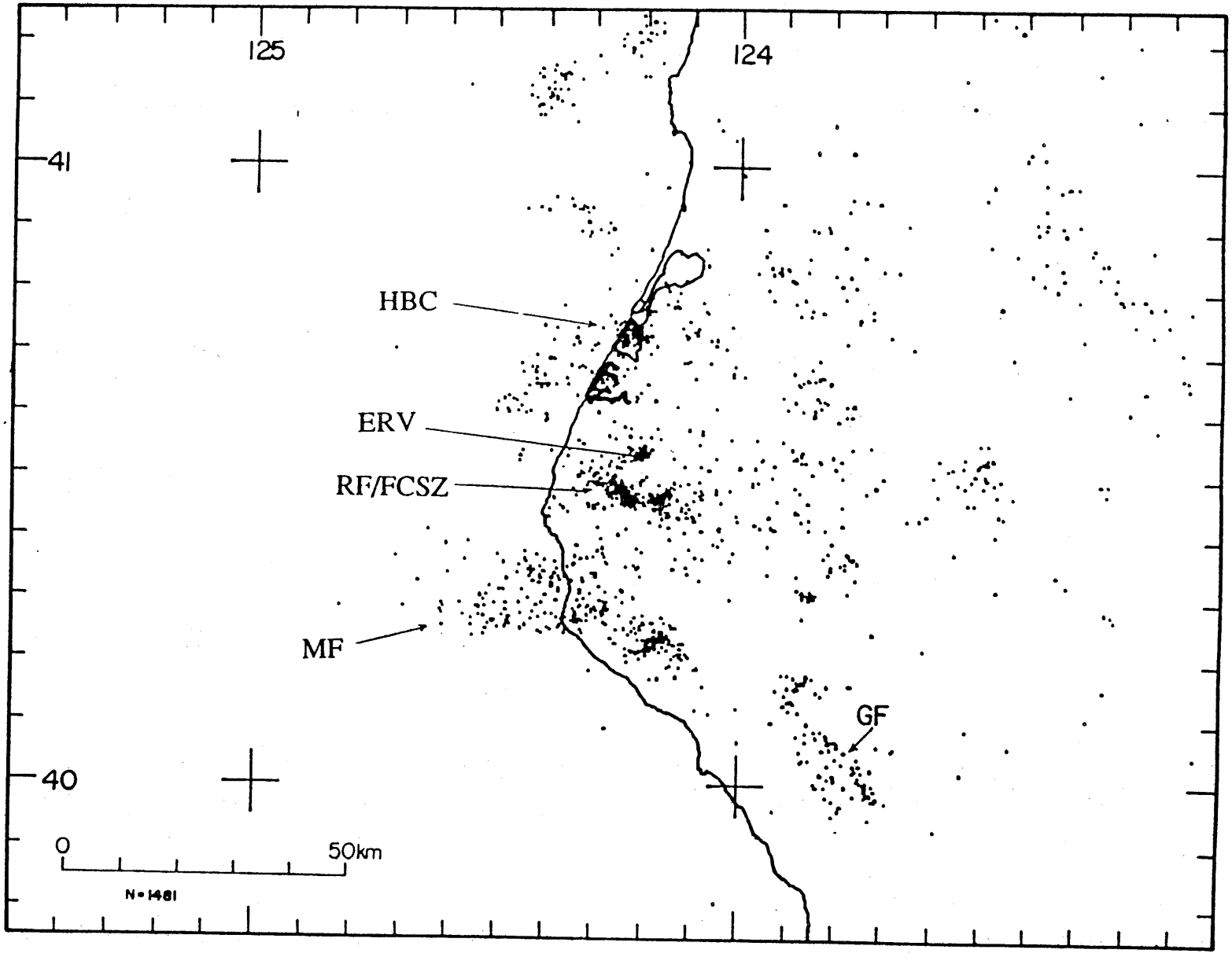

Figure 3. Map view of North American plate seismicity. There [illegible] 481 earthquakes displayed, ranging in magnitudes from 4.6 to zero. Abbreviations used: RF/FCSZ- Russ Fault/False Cape Shear Zone, HBC- Humboldt Bay cluster, GF- Garberville fault lineament, MF- [illegible] inc[illegible] ivi[illegible] E[illegible] /al[illegible] r.

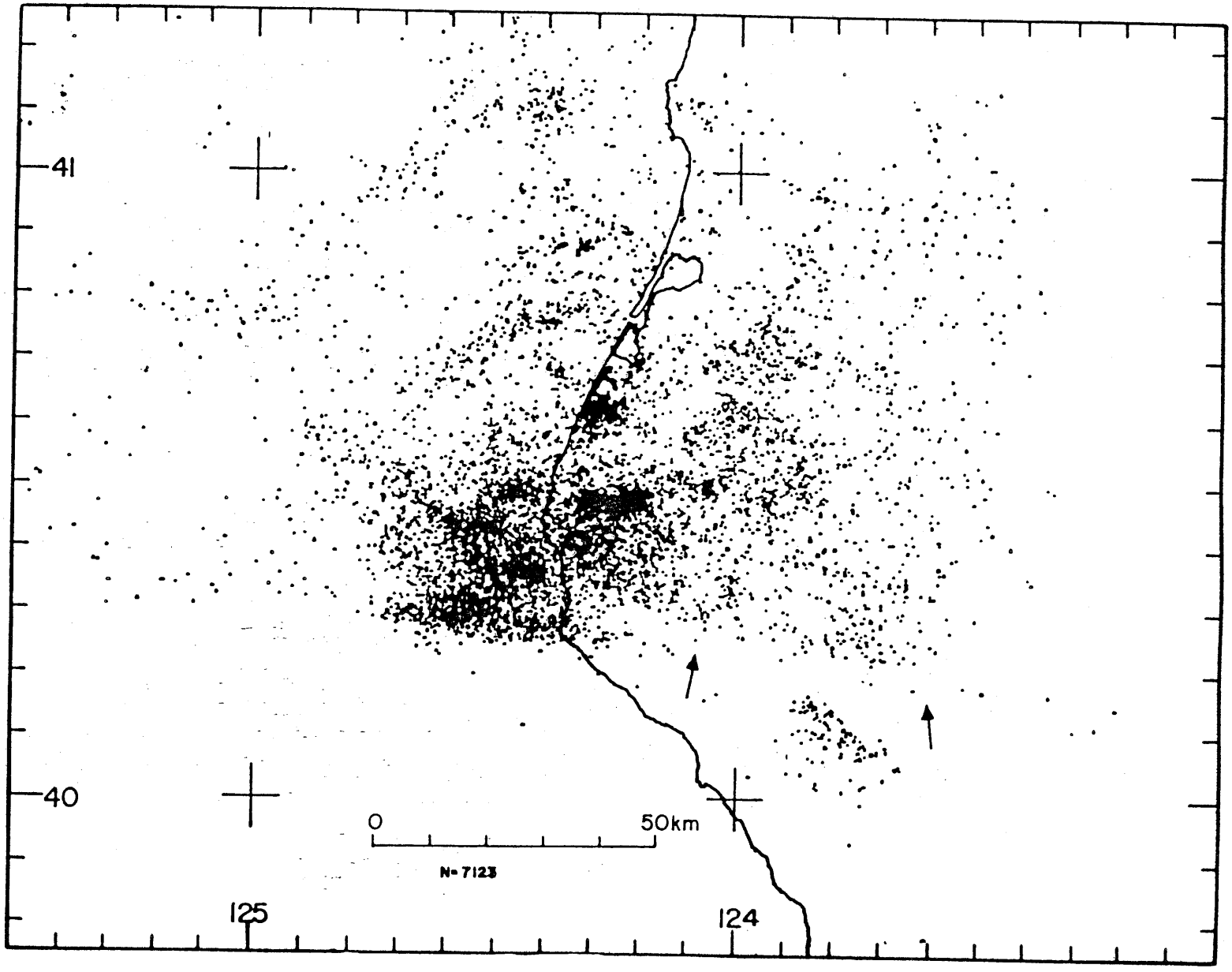

Figure 4. Map view of only Gorda plate seismicity. There are over 7000 earthquakes displayed in this map view that range in magnitude from 7.2 to zero. The arrows point to the southern edge of the Gorda plate. Notice the northeast-southwest alignments and clustering west of 124.15° as compared to the diffuse distribution of events east of this longitude, i. e., east of the MTJ. Abbreviations are the same as those used in Figure 3.

Gorda Plate Seismicity

The seismicity within the Gorda plate is displayed in plane view in Figure 4. Over 7000 earthquakes are displayed in this map, with the most striking feature being the dense concentration of events occurring within the Gorda plate just north of the corner of the Pacific plate. Within the southern portion of this cluster of events, there is an even denser cluster recognizable that has an east-west trend that comes onshore near Punta Gorda in the same vicinity as the shallow band shown in the previous map. Once again, this nearly east-west band represents Mendocino fault activity, and therefore is interplate motion between the Gorda and Pacific plates. This activity continues to the west, but because of the location quality chosen for this projection, events further offshore are not displayed because of their poorer location quality. During the existence of the HBSN, the Mendocino fault was a constant source of M= 5.5-5.7 events (see Figure 2, Dengler and others, 1992). The Mendocino fault activity extends to over 30km in depth along a near-vertical plane, and this is best seen in sections B-B' and C-C' in Figure 7.

Also, within this concentration of events is an even denser group of events that lies below the RF/FCSZ feature discussed above in the section on North American seismicity. As mentioned earlier, since the dense cluster appears in both plates, I think that this relationship indicates that there is coupling between the two plates.

Offshore, the distribution in Figure 4 hints of two northeast-southwest alignments, the one farther west being that which occurred during the November 8, 1980, M=7.2 event (Smith and others, 1981, TERA, 1981, see Figure 2). This earthquake had an aftershock distribution that extended for over 120km and had an estimated average 1 meter left-lateral offset along the strike of this trend (N50W, Lay and others, 1982). Because of the youth and thinness of the Gorda plate, this event is considered to be close to the largest that can be expected in the offshore region of this oceanic plate.

In the southernmost part of Figure 4, the cluster of earthquakes that have a diffuse northwest trend are believed to be associated with the lower portion of the North American plate, and specifically with the sequence labeled GF in Figure 2. Because of their northwest alignment and the uncertainty of the locations, these events are considered to be Pacific/North American events, and not Gorda plate events. If this interpretation is correct for the GF trend, the southern edge of the Gorda plate is marked by the abrupt cessation of events along a line running nearly east-west at approximately 40.25^{o} latitude, which is north of an earlier placement of the southern edge of the Gorda plate inferred from a gravity survey by Jachens and Griscom (1983).

CROSS SECTIONS OF THE SEISMICITY

East-West Section

The geometry of the Gorda plate as it moves eastward under the North American plate and the characteristics of the Mendocino fault are best seen in sections cutting through the seismicity shown in map view in Figures 2 and 3. Figure 5 shows a map view of all the seismicity, and the rectangles enclose the earthquakes that are used in the projections for Figures 6 and 7.

In the east-west section where over 6000 earthquakes are displayed, the top of the Gorda plate can be followed to the east as it dips gently at about 11° under the North American plate. In the western portion of this map, a double layer is apparent which changes to a diffuse band of seismicity when moving eastward and downdip. This change in the character from west to east reflects the change in provinces of the Gorda plate. In the western province, where the Gorda plate is squeezed between the Pacific and Juan de Fuca plates, the seismicity shows lineations trending northeast-southwest in the map view, as well as double layers in section. Once the Gorda plate passes the corner of the Pacific plate as it moves eastwards, the seismicity becomes more evenly distributed both in map and section projections. The focal mechanisms for intraplate earthquakes similiarly change their character across this same line, which occurs at about 124.15^{o} longitude (see Figure 7b).

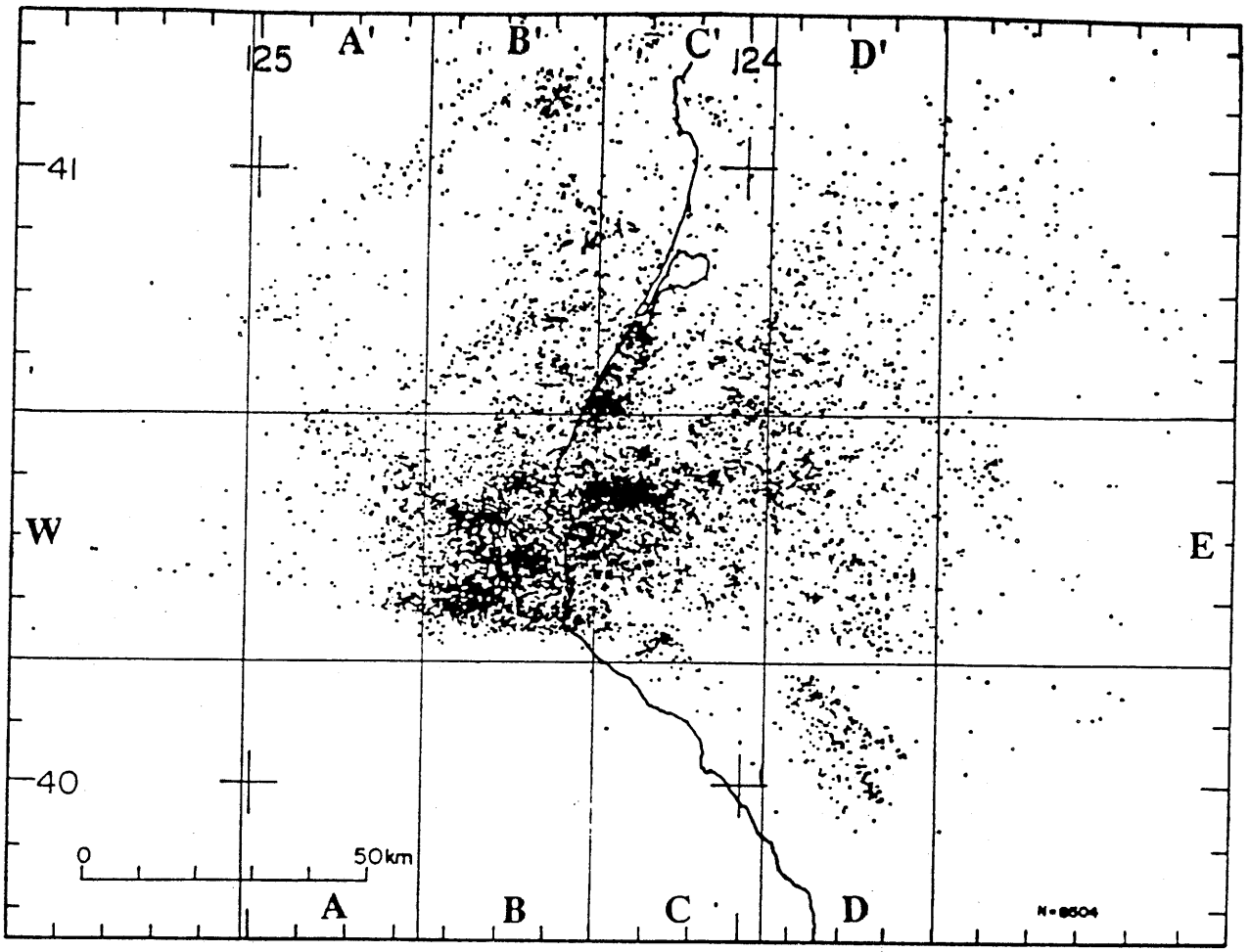

Figure 5. Map view of all the seismicity (Gorda + North American). There are over 8500 events displayed in this map. Rectangles enclose the earthquakes used in the sections presented in Figures 6 and 7.

One explanation for the double layer seen offshore is that the Gorda plate in this region is imbricated (Smith and others, 1992), with pieces of the brittle upper oceanic plate stacked on top of one another. The Gorda plate near the eastern end of the Mendocino fault does appear to be twice as thick when compared to its other regions (McPherson, 1989a), and there is additional evidence from a teleseismic delay study that some pieces may be breaking off and the plate itself has irregularities in it (Niazi and Karageorgi, 1992). As the Gorda plate moves eastward of the MTJ, it passes through a "tectonic die" (Smith and others, 1992), limiting its north-south length by the width of the die (the physical constraints established by the neighboring larger plates to the north and south).

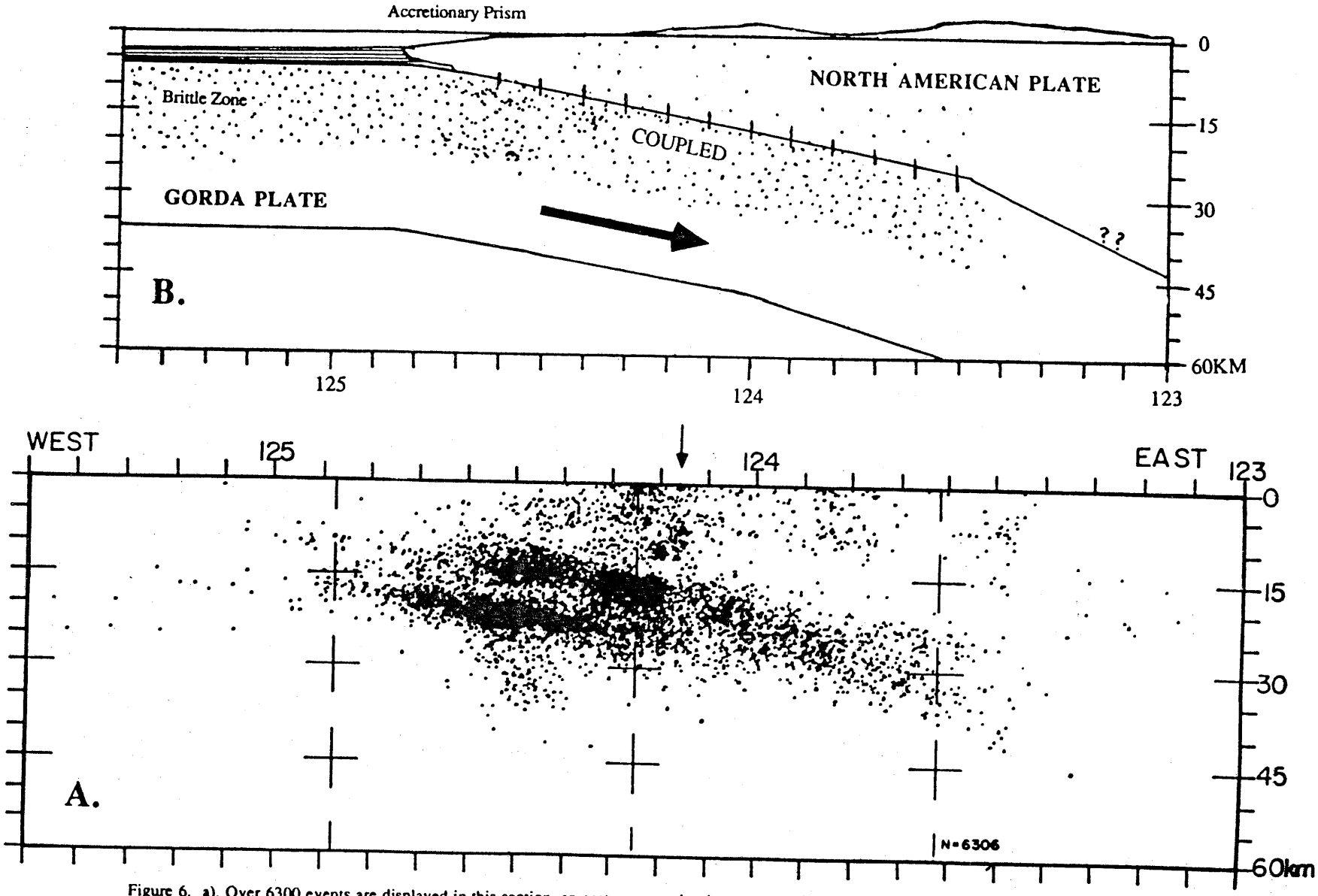

Figure 6. a). Over 6300 events are displayed in this section, an east-west section between 40.2°-40.6° latitude. The most striking feature in this section is the 12-15km wide band of earthquakes dipping 11-12° to the east, which represents brittle failure of the upper portion of the oceanic Gorda plate. Notice also the change in the character of seismicity east and west of 124.15° longitude (arrow), i.e., the MTJ. The double layer represents that region of the Gorda plate confined offshore between the larger Juan de Fuca and Pacific plates. The diffuse region of earthquakes lies east of the MTJ, or 124.15°. b). Interpretation of the cross section.

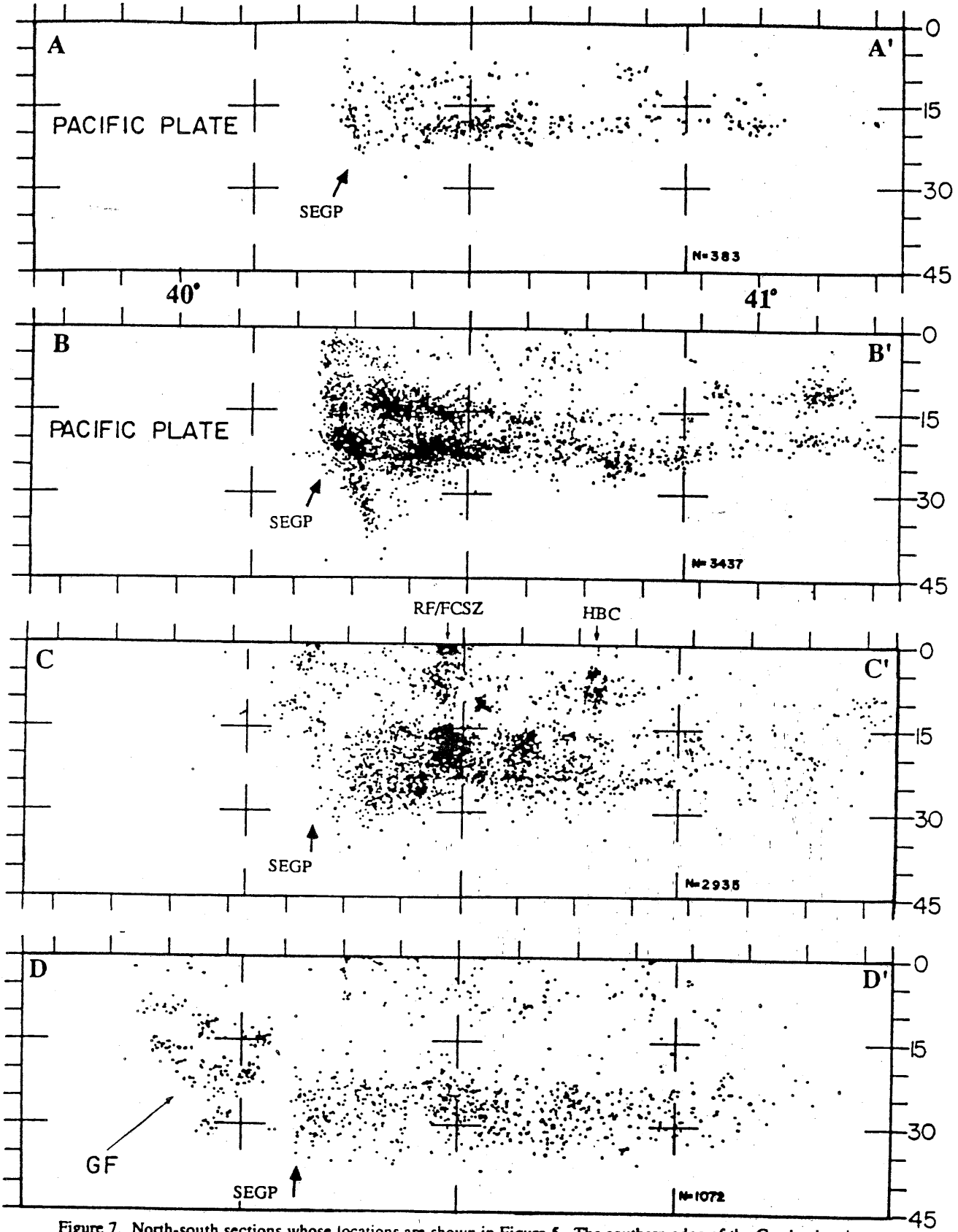

Figure 7. North-south sections whose locations are shown in Figure 5. The southern edge of the Gorda plate is shown by the arrow in each of the cross sections, with section D-D' being east of the influence of the Pacific plate. The southern edge of the Gorda plate is shown by the arrows labeled SEGP. Abbreviations used are the same as those defined in Figure 3.

North-South Sections

In the north-south sections shown in Figure 7, the Mendocino fault is a nearly vertical feature, with no underthrusting of the Gorda plate anywhere along the fault's extent (McPherson, 1989ab). Indeed, the Pacific plate acts as an unwielding obstacle, with all the deformation occurring within the Gorda plate, the younger, thinner and weaker of the two. As mentioned above, near the eastern extent of the Mendocino fault, the Gorda plate seems to thicken, possibly by imbrication. Niazi and Karageorgi (1992) found evidence for a sliver of the Gorda plate to be wedged in a vertical position near the easternmost Mendocino fault (see section B-B', Figure 7). It is in this region that several reverse earthquakes oriented along east-west trends have been located, a finding consistent with the thickening of the Gorda plate (TERA, 1981, McPherson, 1989a, Cockerham and others, 1990). Continuing eastward from the corner of the Pacific plate, the southern edge of the Gorda plate can be followed along an east-west line at just about the latitude of the easternmost Mendocino fault, i.e., 40.25° latitude (arrows labeled SEGP). The "cloud" of earthquakes that plots primarily above the Gorda/North American plate boundary (see section D-D' and Figure 3), was discussed above and interpreted to be related to the transform motion between the Pacific and North American plates. Also, notice the distribution of the earthquakes shown in section D-D', a diffuse band of seismicity which contrasts with the clustering and layering seen in sections further to the west.

FOCAL MECHANISMS

North American Plate

Focal mechanisms for North America sample the contractional region north of the Mendocino triple junction as described in Kelsey and Carver (1988). The geographic distribution of the mechanisms is shown in Figure 8a along with a summary of their P and T axes in Figure 8b. The focal mechanisms and summary plots of the P and T axes are upper hemisphere projections.

The mechanisms are primarily reverse faults with some events having components of oblique-slip or strike-slip motion consistent with near horizontal, north-northeast directed compression. This direction for the compression is parallel to the vector of convergence between the North American and Gorda plates (Engebresten and others, 1985, Nishimura and others, 1984). The preponderance of northwest-oriented reverse and oblique mechanisms agrees well with the youthful faults in the region around Humboldt Bay (see Carver, this volume).

Gorda Plate

The Gorda plate was divided into two regions based on focal mechanisms:

1). that portion of the Gorda plate west of the MTJ and,

2). that portion of the Gorda plate east of the MTJ (124.15°).

West of the MTJ the Gorda plate is responding to north-south directed compression by brittle failure along vertical, left-lateral, strike-slip faults (Smith and others, 1981, 1992, McPherson, 1989ab). First motions using both HBSN and teleseismic data repeatedly show the familar quadrantial pattern for intraplate Gorda earthquakes which is shown in Figure 9. In August of 1991, a series of left-lateral earthquakes occurred within the Gorda plate (Nabelek, 1991, Gee and others, 1991) that was both north and further west of the area that originally was found to be failing along left-lateral faults (Smith and other, 1981).

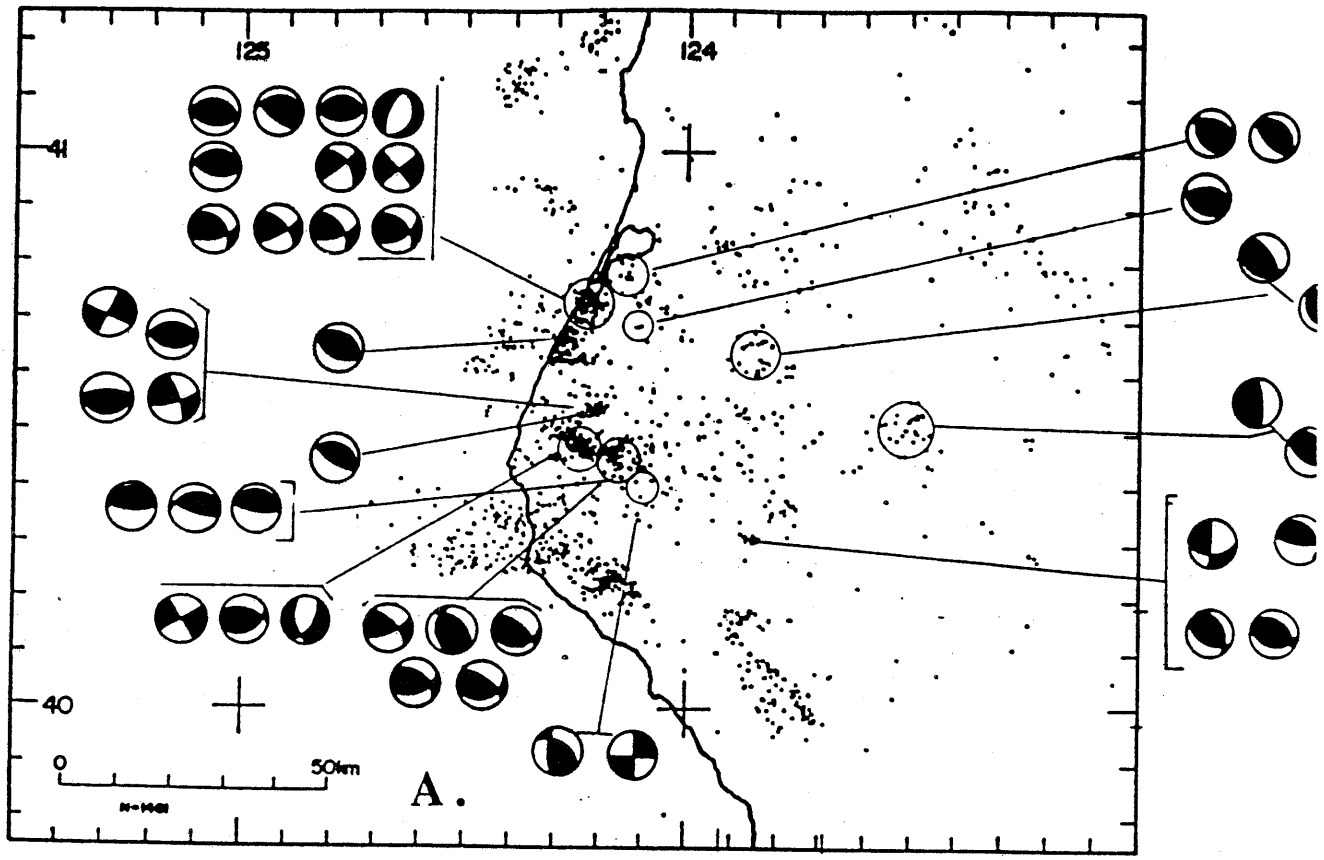

Figure 8. a). Selected focal mechanisms for the North American plate. The mechanisms are all upper hemisphere projections of primarily reverse and strike-slip earthquakes along northwest trends. b). Upper hemisphere plots of the P and T axes for North American earthquakes (from McPherson, 1989a).

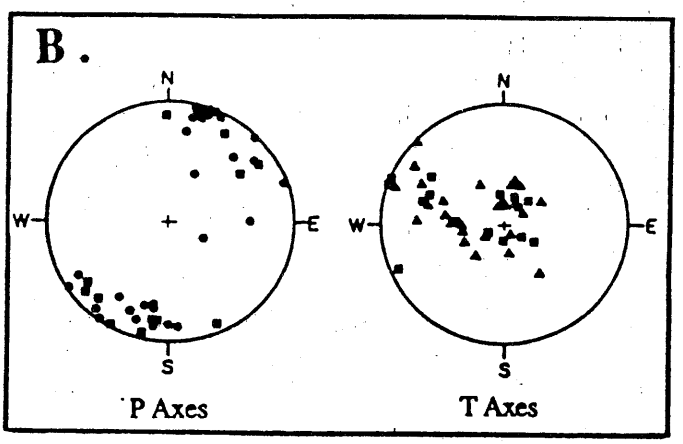

It now appears likely that most of the offshore region of the Gorda plate is failing in this manner and that the maximum earthquake that can be generated appears to be limited to 7.0-7.5 (Dengler and others, 1991, Smith and others, 1981).

East of the MTJ where the Gorda plate is dipping under the North American plate, the focal mechanisms dramatically change from strike-slip solutions to predominantly normal fault mechanisms (McPherson, 1989ab). This change is summarized in Figure 9, with the opposing bold arrows indicating east-west, down-dip tension. After the Gorda plate passes the MTJ to the east, the overprinting effects of the confinement offshore are removed and the subtle body forces related to subduction processes become discernable.

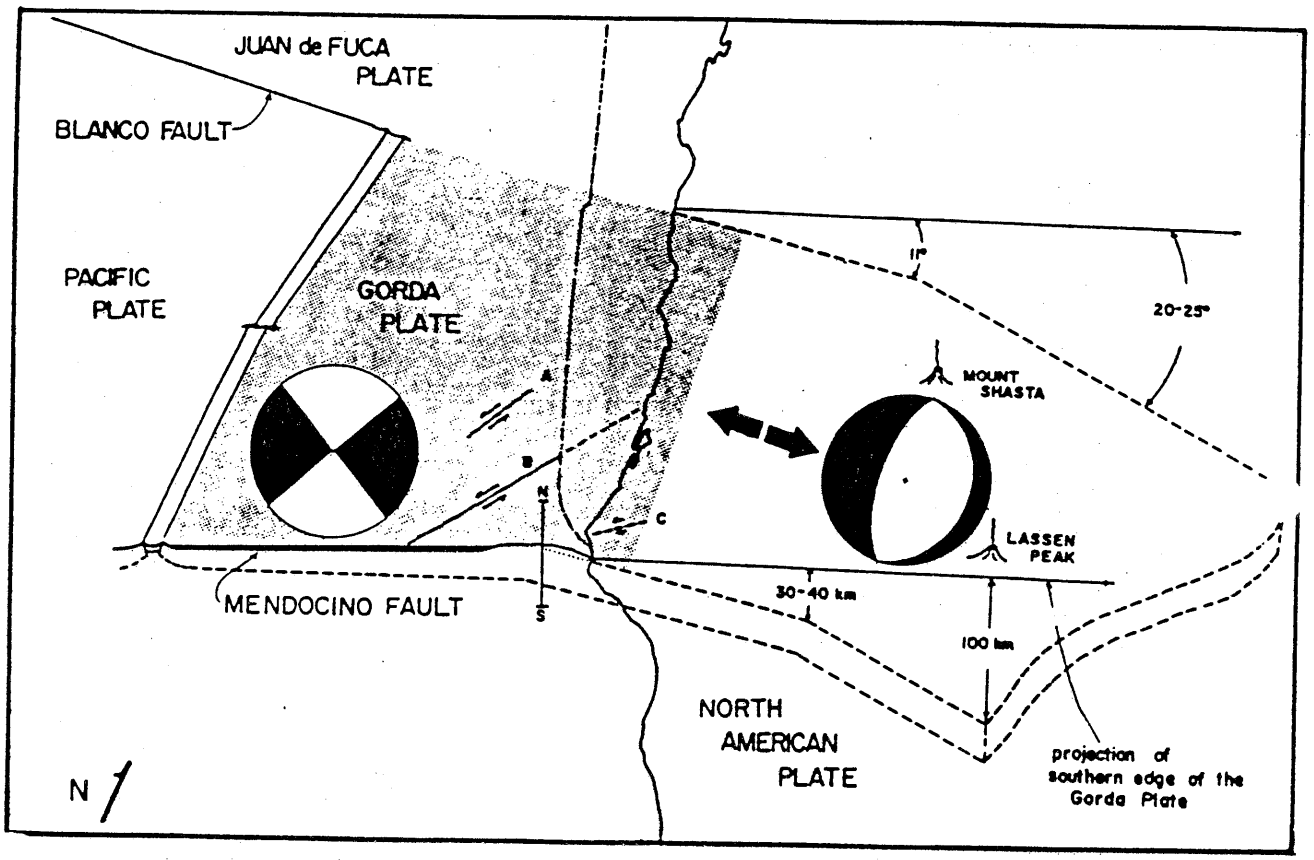

Figure 9. Summary of the Gorda plate regions based on focal mechanisms. West of the MTJ the mechanisms are mostly left-lateral, strike-slip faults along northeast-southwest trends. These faults are thought to occur along previous weaknesses in the plate. After the Gorda plate moves east of the MTJ, therefore no longer being confined between the Pacific and Juan de Fuca plates, the mechanisms change dramatically to normal events that are oriented north-south.

DISCUSSION

The Mendocino fault was shown to be a vertical fault for its entire length, with no underthrusting of the Gorda plate beneath the Pacific plate. Instead, the Gorda plate is being thickened along the eastern Mendocino fault as it is pushed and sheared against this unyielding barrier to the south. The Gorda plate, the weaker and smaller of the plates offshore, is deforming in response to the motions of its larger neighbors to the north and south. As the Gorda plate moves eastward, irregularities in its shape develop as it is shoved through a "tectonic die" imposed by the larger plates to the north and south. As a consequence of this squeezing, the plate is warping and pieces of its upper oceanic crust are broken off and wedged in various orientations near the MTJ. The seismicity along the Mendocino fault bends slightly to the south as it approaches the coastline, and comes onshore in the vicinity of the Cooskie shear zone. From there the southern edge of the Gorda plate can be followed eastward to about 123.5° longitude.

The North American plate seismicity, occurring at a much lower frequency than that in the Gorda plate, covers the same geographical area as the seismicity within the Gorda plate beneath it. This indicates that the two are coupled along the interface between them. Focal mechanisms for North American events are consistent with a northeast-southwest directed compression which is parallel to the covergence between the two plates. The evidence presently suggests that subduction is ongoing, albeit slowly, and is dictating the orientation and style of faulting in the North American plate in the vicinity of the MTJ.

REFERENCES

Clarke, S. H. Jr., G. Carver, Late Holocene tectonics and paleoseismicity, southern Cascadia subduction zone, Science, vol. 255, pp. 188-192, 1992.

Clarke, S. H. Jr., Geology of the Eel River basin and adjacent region: Implications for late Cenezoic tectonics of the Cascadia Subduction zone and Mendocino triple junction, Bulletin of AAPG, vol. 76, no. 2, pp. 199-224, 1992.

Cockerham, R., S. W. Smith, R. C. McPherson, S. H. Clarke Jr., Selected fault plane solutions and earthquake epicenters, Map 7b, California Continental Margin Geologic Map Series, 1989.

Dengler, L., G. Carver, R. McPherson, Sources of north coast seismicity, California Geology, vol. 44, March-April, 1992.

Eaton, J., Dense microearthquake network study of northern California, in J. J. Litehiser, ed., Observatory Seismology: An Anniversary Symposium on the Occasion of the Centennial of the University of California at Berkeley Seismographic Stations, University of California Press, Berkeley and Los Angeles, pp. 199-224, 1989.

Engebretsen, D. C., A. Cox, R. Gordon, Relative motion between oceanic and continental plates in the Pacific basin, GSA Special Paper 206, 59 pp., 1985.

Gee, L., R. Uhrhammer, B. Romanowicz, Source parameters and rupture characteristics of Gorda basin earthquakes and their tectonic implications, (Abstract) EOS, Transactions of the American Geophysical Union, vol. 72, p. 312, 1991.

Jachens, R., A. Griscom, Three-dimensional geometry of the Gorda plate beneath northern California, JGR, vol. 88, pp. 9375-9392, 1983.

Kelsey, H. M., G. A. Carver, Late Neogene and Quaternary tectonics associated with the northward growth of the San Andreas fault, northern California, Journal of Geophysical Research, vol. 93, pp. 4797-4819, 1988.

Knapp, J. S., Seismicity, crustal structure, and tectonics near the northern termination of the San Andreas fault, PHD Thesis, University of Washington, 1982.

Lay, T., J. W. Given, H. Kanamori, Long period mechanism of the November 8, 1980 Eureka, California earthquake, Bulletin of the Seismological Society of America, vol. 72, no. 2, pp. 439-456, April, 1982.

McLaughlin, R. J., S. King, R. Poore, K. McDougall, E. Buetner, Post-middle Miocene accretion of Franciscan rocks, northwestern California, Geological Society of America Bulletin, vol. 93, pp. 595-605, 1982.

McPherson, R. C., Seismicity and focal mechanisms near Cape Mendocino, northern California: 1974-1984, Masters Thesis, Humboldt State University, Arcata, Ca. 95521, 75pp, 1989a.

McPherson, R. C., Focal Mechanisms and seismicity at the southern end of the Cascadia subduction zone, GSA Program and Abstracts, Spokane, p. 66, 1989b.

McPherson, R. C., L. A. Dengler, D. Oppenheimer, 1991, Evidence of compressional tectonics in the King Range, California: the 1991 Honeydew earthquake, (abstract) EOS, Transactions of the American Geophysical Union, vol. 72, p. 315.

Nabelek, J., Parameters of Gorda plate earthquakes of July and August, 1991, (abstract), EOS, Transactions of the American Geophysical Union, vol. 72, p. 312, 1991.

Niazi, M., E. Karageorgi, Irregular geometry of the Gorda subduction and deep structure of the Eel River basin determined from teleseismic P delays, Tectonophysics, vol. 201, pp. 209-228, 1992.

Nishimura, C., D. S. Wilson, R. N. Hey, Pole rotation analysis of present-day Juan de Fuca plate motion, JGR, vol. 89, nB12, pp. 10283-90, 1984.

Oppenheimer, D. H., The 1991 M=6.0 Honeydew, California earthquake, (abstract) EOS, Transactions of the American Geophysical Union, vol. 72, p. 311, 1991.

Shimazaki, K., Correlation between intraplate seismicity and interplate earthquakes in Tohoku, northeast Japan, Bulletin of the Seismological Society of America, vol. 68, no. 1, pp. 181-92, 1978.

Smith, S. W., J. S. Knapp, The northern termination of the San Andreas fault, in Studies of the San Andreas fault zone in northern California, edited by R. Steitz and R. Sherburne, CDMG Special Report 140, pp. 153-164, 1980.

Smith, S. W., R. C. McPherson, N. I. Severy, Breakup of the Gorda Plate, (abstract) Earthquake Notes, vol. 52, p. 42, 1981.

Smith, S. W., J. S. Knapp, R. C. McPherson, Seismicity of the Gorda plate and the eastward jump of the Mendocino triple junction, submitted to JGR, 1992.

Spence, William, Implications of the slowing of subduction at Cascadia, Abstract, EOS, vol. 68, no. 44, pp. 1467-8, November 3, 1987.

TERA, Humboldt Bay Seismic Network progress report, October 28, 1979 to April 1, 1980, submitted to PG&E, 1980.

TERA, Trinidad offshore earthquake and aftershocks, submitted to PG&E, 1982.

HISTORIC SEISMICITY AND POTENTIAL SOURCE AREAS OF LARGE EARTHQUAKES IN NORTH COAST CALIFORNIA

L. Dengler, R. McPherson, G. Carver
Geology Department, Humboldt State University, Arcata, California 95521

INTRODUCTION

The north coast region of California in the vicinity of Cape Mendocino is one of the state's most seismically active areas, accounting for 25% of California's seismic energy release during the last 50 years (Gee and others, 1991). Coastal Humboldt County has been affected historically by earthquakes occurring on the San Andreas fault system, the Mendocino fault, and at the Mendocino triple junction and also by intraplate earthquakes within both the Gorda and North American plates. Over sixty of these earthquakes have produced damage since the mid-1800's (Table 1). Recent studies (Heaton and Hartzell, 1987; Clarke and Carver, 1992) indicate that north coastal California is also at risk of great earthquakes originating along the Cascadia subduction zone. Although the subduction zone has not generated great earthquakes in historic times, paleoseismic evidence suggests that very large earthquakes have been generated by the subduction zone in the recent prehistoric past.

HISTORIC SEISMICITY

Pattern of earthquakes

Table 1 summarizes regional historic earthquakes with Richter magnitudes ≥ 5.5, and/or Modified Mercalli intensities ≥ VI. Toppozada and others (1981) determined epicenter locations for pre-1900 events from the pattern of felt reports, and suggest errors may be 100 km or more. Although location errors of these early events are likely large, the record of damaging events after 1850 is probably fairly complete. The north coast area has had a widespread distribution of small logging and fishing towns throughout the last century and two to five newspapers have been in print at all times since 1850 (Toppozada and others, 1981). Offshore events which were not widely felt may not have been reported, but it is unlikely that any earthquakes causing significant damage have been missed. However, it is likely that intensity reports may not have been received from all areas and that Table 1 underestimates the peak intensity. In addition to incomplete reporting, we have found that it is difficult to differentiate between Mercalli intensities VII, VIII and IX in sparsely settled rural areas with wood frame construction. Lack of large structures, masonry construction, buried pipe lines and other Modified Mercalli 'indicators' make it possible that peak ir estimates may be off by one or two intensity levels for some earthquakes (Dengler and McP submitted).

In 1932, the University of California Seismographic Stations at Berkeley installed the first nor seismograph in Ferndale. Many of the events prior to 1932 were recorded by the Berkeley and Hamilton stations of the early Berkeley network (established in 1887). Because these stations ar away, instrument-determined epicenter locations prior to the establishment of the Ferndale station m uncertainties of 100 km or more (Urhammer, 1991). Event location gradually improved through middle part of the century as more instruments were installed. Berkeley established the Arcata st 1948 and the Fickle Hill station in 1968. However, the sparseness of stations and the complexities of local geology make it likely that locations of even onshore or near shore earthquakes as recently as the late 1950's may be in error by as much as 50 km (Knapp, 1982).

In mid 1974 a 16-station array of seismographs was installed in the region and operated by TERA Corporation as part of a seismic safety study for Pacific Gas and Electric Company's Humboldt Bay nuclear

power plant (TERA, 1977; Woodward-Clyde, 1980; McPherson and others, 1981; McPherson, 1989). Earthquakes recorded during the twelve years the array operated are the best located of the historic data set. After the network was disbanded, two of the stations were donated to the Berkeley network and have become part of the U. C. Seismographic Stations. In response to the damaging November, 198 earthquake, the U.S. Geological Survey established a network of telemetered instruments in the region, which continue to operate (Eaton, 1989). Recent onshore and near-offshore epicenters are likely to be located quite well, but locating events far offshore continues to be a problem due to the absence of ocean-bottom seismographs in the region.

Smith and Knapp (1980) published a number of relocations of the older earthquakes. They used the Joint Epicenter Determination technique which compares the seismic traces of a well-located recent event (recorded by both new and old seismic stations) to older events and simultaneously solved for a set of epicenter locations, origin times, and station corrections of the older events relative to the recent event. These relocated epicenters are thought to represent an improved estimate of the true location of the earthquake source.

Epicenters of the best located historic earthquakes (those after 1960 and Smith and Knapp's relocations) are shown in Figure 1. The majority are scattered throughout the southeastern portion of the Gorda plate and along the Mendocino fault. Earthquakes in the southern portion of the Gorda plate (such as 1984, 1954, 1941, and 1961) are difficult to distinguish between Mendocino fault and Gorda plate sources due to the imprecision in location. However, the majority of offshore earthquakes are clearly intraplate events. Aftershock data and fault plane solutions suggest that the Gorda plate earthquakes result from movement along northeast trending left-lateral strike-slip faults (TERA, 1977; Smith and others, 1981; McPherson, 1989). Mendocino fault earthquakes show predominantly right-lateral slip parallel to the trend of the fault with a few reverse-slip events in the vicinity of Cape Mendocino (Bolt and others, 1968; Simila and others, 1975; McPherson, 1989).

The epicenters of only eight earthquakes shown in Figure 1 fall within the onshore portion of the map. The January 1990, August 1991 and March 7, 1992 earthquakes were centered in the immediate vicinity of the triple junction (see McPherson and Dengler this volume). The April 25, 1992 M_s=7.0 earthquake was located just north of the August 17th event and is discussed in more detail below. Of the onshore earthquakes north of the triple junction, only the December 1954 earthquake is thought shallow enough to have occurred in the overriding North American plate (Tobin and Sykes, 1968; TERA, 1977; Smith and Knapp, 1980; Knapp, 1982). Hamilton (1975) suggested that this earthquake was associated with a fault in the Mad River fault zone, although lack of documented surface rupture and uncertainty about the type of faulting involved makes it impossible to confirm. The 23 km depth of the June 1975 earthquake (considered accurate to within a kilometer -TERA, 1977; Knapp, 1982) is clearly within the subducted portion of the Gorda plate beneath the North American plate. Over 80 % of well-located microearthquakes recorded by the Humboldt Bay seismic network during the period 1974 - 1984 occur at Gorda plate depths (McPherson, 1989), strongly suggesting that the Gorda plate is the main source for both onshore and offshore historic seismicity.

The April 25, 1992 Cape Mendocino earthquake is the only historic damaging event which may have resulted from thrusting along the Cascadia subduction zone. Prior to this earthquake, researchers had found no conclusive evidence within the historic record to suggest that such an event had occurred anywhere along

the subduction zone boundary from Cape Mendocino to Vancouver Island, B.C. during the last 150 years (Heaton and Kanamori, 1984; Heaton and Hartzell, 1987). Preliminary data suggest that the Cape Mendocino earthquake was the result of reverse slip along a shallow northeast dipping, northwest striking plane which coincides with the estimated location of the subduction zone boundary (Oppenheimer and others, 1992; Oppenheimer, 1992). This earthquake produced a tsunami recorded at tide stations in California, Oregon and Washington (NOAA, 1992) and preliminary investigations support coastal uplift from near Cape Mendocino to near the mouth of the Mattole River. This earthquake lends strong support to the seismogenic nature of the subduction zone; however it was a much smaller earthquake than the main portion of the locked zone is thought capable of producing (Clarke and Carver, 1992).

1906 San Francisco Earthquake

The 1906 San Francisco earthquake deserves special attention because it caused the greatest historic damage in the north coast region (with possible exception of the Cape Mendocino earthquake still under study) and the fault rupture was located south of Cape Mendocino. Lawson (1908) noted surface rupture (interpreted as fault displacement) in Shelter Cove, duration of strong ground motion in excess of 40 seconds throughout the Humboldt Bay region, and extensive damage to communities in the Humboldt Bay area and in southern Humboldt County. The Modified Mercalli intensities were at least VIII in Briceland, Eureka and Fortuna and may have reached IX in Petrolia and Ferndale (Toppozada and Parke, 1982). In Ferndale, not a chimney remained standing and brick buildings were badly damaged. Liquifaction features were observed in the Eel River Valley and around Humboldt Bay. Recurrence of a 1906 rupture is estimated between 200 to 400 years (Prentice, 1989).

Seismic frequency

Since the middle 1800's, the north coast region has experienced at least sixty earthquakes with peak Modified Mercalli intensities of VI, twenty-nine intensity VII's, eleven intensity VIII's and possibly, one IX (Figure 2). (Peak intensities associated with the Cape Mendocino earthquake are still under investigation, but initial damage estimates support MMI ≥VIII.) Intensity VII or greater events have recurred on average every five years, with the longest interval between such events just over thirteen years. The recurrence of Intensity VI or greater events has averaged two and a half years. Most of these events likely originated within the Gorda plate or along the Mendocino fault.

Figure 3 shows a composite intensity map of the north coast area since 1900. The map was constructed from the Modified Mercalli intensity data for the thirty four earthquakes marked by an asterisk in Table 1. For each of these earthquakes, communities reporting VI's or greater were marked on a map and the resulting pattern was contoured according to the number of times an area had experienced this level of intensity. Not surprisingly, communities in the coastal region near Cape Mendocino from Eureka to south of Petrolia have been damaged far more frequently than the rest of Humboldt or Del Norte Counties. The frequency decreases in roughly a radial pattern away from Cape Mendocino. The northern part of Humboldt County and all of Del Norte have been affected by earthquakes only rarely since 1900.

Historic seismicity combined with evidence from recent paleoseismic studies of the area (see other papers this volume) suggest six distinct sources of damaging earthquakes in the north coast region.

1. The Gorda Plate

location and style of faulting: intraplate, primarily offshore; left-lateral strike-slip faulting.
historic magnitudes of damaging earthquakes: 5 - 7.5.
historic peak intensities: VII - VIII.
recurrence: 5.5 years for intensities ≥VII (combined Mendocino fault and Gorda plate sources).
example: November 8, 1980 (surface wave magnitude 7.2).
special notes: accounts for majority of historic seismicity, most probable source of damage in the near future; primary impact to coastal communities of Humboldt County. Future events likely to be similar to known historic events, although greater intensities (IX) could result if rupture initiated within the subducted portion of the Gorda plate beneath the North American plate.

2. The Mendocino fault

location and style of faulting: plate boundary, offshore west of Cape Mendocino; primarily right-lateral strike-slip faulting, with reverse faulting near the Cape.
historic magnitudes of damaging earthquakes: 5 - 7.5?
historic peak intensities: VII - VIII?
recurrence: see above.
example: June 25, 1968 (local magnitude 5.9).
special notes: second most common source of historic earthquakes, primarily impacting communities near Cape Mendocino and those located in the Eel River Valley and Humboldt Bay areas.

3. The Mendocino triple junction

location and style of faulting: onshore and shallow, in the immediate vicinity of the triple junction; both reverse and strike-slip mechanisms likely.
historic magnitudes:of damaging earthquakes: 5.0- 6.0.
historic peak intensities: VIII.
recurrence: unkown.
historic example: August 17, 1991 (magnitude 6.0).
special note: recognized as a separate source of damaging earthquakes only after the 1991 earthquake. Raised Holocene terraces south of Cape Mendocino may have been produced by these types of earthquakes. If so, it suggests magnitudes of possibly 7.5 or larger, with the potential to significantly damage the more densely populated areas of the Eel River Valley and around Humboldt Bay.

4. The San Andreas transform system

location and style of faulting: plate boundary, onshore and near shore, south of triple junction; primarily strike-slip.
historic magnitudes of damaging earthquakes: 8.3.
historic peak intensities: VII to IX in southern Humboldt County.
recurrence: of 1906 San Andreas-type earthquakes 200-400 years.
historic example: April 18, 1906 (magnitude 8.3).
special note: less probable but potentially more damaging than (1) and (2) above. Primary impact in southern Humboldt County and Humboldt Bay areas.

5. The North American plate

location and style of faulting: intraplate earthquakes independent of slip on the subduction zone; onshore and shallow; primarily thrust faulting.
expected magnitudes: 6.5 to 8+.
expected peak intensities: ≥IX for thrust events.
recurrence: for thrust events, hundreds of years.
historic example: no historic large thrust earthquakes; December 21, 1954 magnitude 6.5 may have been associated with these faults.
special notes: less probable in near future than (1) and (2) above; much greater impact.

6. Cascadia Subduction Zone

location and style of faulting: plate boundary earthquakes with rupture both onshore and offshore; rupture length possibly 200 km or more; thrust faulting.
historic magnitudes: 7.0?
expected magnitudes: southern segment - 8.5; whole zone - 9 to 9.5.
expected peak intensity in Humboldt and Del Norte Counties: ≥X.
recurrence: 300-500 years.
historic example: no historic great subduction zone earthquakes; the April 25, 1992 magnitude 7.0 may have involved slip at the southern end of the zone.
special notes: less probable in near future than (1) and (2) above; most damaging of all potential sources with major damage to all communities overlying the subduction zone; likely to produce significant local tsunami hazard; potential for long period damage to populated areas inland and to the south of the subduction zone.

Acknowledgements: The predecessor of this paper was a section of the Humboldt State University Emergency Plan compiled by Kevin O'Dea. Sandra Potter compiled much of the intensity data for historic earthquakes and constructed the composite isoseismal map (Figure 5). She received support from CALEEP, the California Earthquake Education Project. The project was initiated and initially supported by a National Science Foundation Grant # 8950114 for undergraduate faculty teaching enhancement. Comments by Bud Burke and Tom Lisle on various stages of this manuscript were very helpful. Preliminary information on the April 25, 1992 Cape Mendocino Earthquake was provided by the USGS in Menlo Park, the California Strong Motion Instrumentation Program, The University of California at Berkeley Seismographic Stations, NEIS, NOAA. Special thanks to Dave Oppenheimer, Bob Urhammer, Greg Anderson, Sam Clarke, Thomas Dunklin, and Mike McGuire.

TABLE 1: NORTH COAST HISTORIC EARTHQUAKES OF MAGNITUDE ≥ 5.5 AND/OR INTENSITY ≥VI

LOCATION	DATE	Magnitude	Intensity	Lat. °N	Long. °W
Eureka area (wharf sank 4 feet)	23 Oct 1853	(5.7)	VII	40.80	124.20
Eureka (affected flow of streams, milk thrown from pans)	20 Mar 1855		VI		
Eureka	14 Jun 1857		VI		
Humboldt Bay (damage to plaster and chimneys)	13 Nov 1860	(5.7)	VII	40.80	124.20
Eureka (damaged brick houses, fissure near Fort Humboldt)	1 Oct 1865	(5.4-5.7)	VII-VIII	40.80	124.20
Petrolia (chimneys damaged in Rohnerville and Petrolia)	2 Mar 1871	(5.9)	VIII	40.40	124.20
Crescent City (damaged most buildings in Crescent City, landslides)	23 Nov 1873	(6.7)	VIII	42.00	124.00
Southeast of Eureka	30 Sept 1875	(5.8)	VII	40.70	124.00
West of Briceland (knocked down all chimneys in Petrolia)	9 May 1878	(5.8)	VIII	40.10	124.00
North of Hoopa	28 Jan 1884	(5.7)	V	41.10	123.60
Petrolia (chimneys down in Ferndale and Petrolia)	26 Jul 1890	(6.0)	VII	40.33	124.25
Near Miranda (chimneys down in southern Humboldt County)	30 Sep 1894	(5.6-5.8)	VII	40.30	123.70
Offshore Arcata (damaged mill in Eureka)	16 Apr 1899	(6.4)	VI	41.00	124.40
Offshore Eureka	9 Dec 1903		V-VI	40.80	124.20
*San Francisco(rupture began near San Francisco and extended north	18 Apr 1906	8.3	XI	37.70	122.50
possibly to Shelter Cove, damage throughout Humboldt Bay region)	VIII-IX in southern Humboldt Co. and Humboldt Bay region				
*McKinleyville (chimneys fell in Ferndale)	23 Apr 1906		VII	41.00	124.00
Offshore Eureka	11 Aug 1907		VI	40.80	124.20
*Eureka (chimneys fell)	18 Aug 1908	5.0	VII	40.83	124.17
*Petrolia (damaged chimneys)	18 May 1909		VIII	40.25	124.17
*West of Scotia (much damage in Rohnerville & Upper Mattole)	29 Oct 1909	6.4	VIII	40.58	124.17
Offshore Petrolia	19 Mar 1910	6	V	40.83	124.17
Offshore Cape Mendocino	31 Dec 1915	6.2-6.5	III	41.00	126.00
*West of Ferndale	5 Jul 1916	4.5	VI	40.58	124.25
Offshore Arcata	15 Jul 1918	6-6.5	VI	41.00	125.00
Eureka (chimneys fell)	15 Sep 1919		VI	40.80	124.20
Offshore Cape Mendocino	26 Jan 1922	6	I	41.00	126.00
*Offshore 60 km west of Arcata (felt in San Jose, OR, NV)	31 Jan 1922	7.3-7.6	VI	40.87	125.35
*Offshore Cape Mendocino (buildings damaged in Petrolia area)	22 Jan 1923	6.5-7.3	VIII	40.30	124.50
Offshore, west of Orick	4 Jun 1925	6	I	41.50	125.00
130 km west of Eureka	10 Dec 1926	6	I**	40.75	126.00
*Offshore of Arcata (chimneys fell, landslides)	20 Aug 1927	5	VIII	41.00	124.60
*Eureka (chimneys fell)	23 Sep 1930	5-5.5	VII	40.80	124.20
Offshore Cape Mendocino	11 Dec 1930	5	VI	40.08	124.50
Offshore Cape Mendocino	10 Mar 1931	5.6	V	40.00	125.00
Offshore Cape Mendocino	23 Aug 1931	5.3	VI	40.20	125.60
Offshore Eureka (chimneys damaged)	9 Sep 1931	5.8	VI	40.80	125.00
180 km west of Cape Mendocino	2 Mar 1932	5.6	I**	40.20	127.00
*Near Arcata (1 death, much damage in Eureka)	6 Jun 1932	5.9-6.4	VIII	40.87	124.02
90 km west of Trinidad	6 Jul 1934	6.5	I**	41.25	125.42
Offshore Cape Mendocino	2 Jan 1935	5.8	V	40.25	125.25
150 km west of Cape Mendocino	3 Jun 1936	5.8	V	40.16	126.45
Offshore Cape Mendocino (slight damage)	6 Feb 1937	5.7-5.8	V	40.50	125.25
*Southeast of Cape Mendocino (slight damage in Ferndale)	11 Sep 1938	5.5	VI	40.00	124.00
*Offshore Cape Mendocino (chimney damage)	19 Nov 1940	5.5	V-VI	40.75	124.90
Near Shelter Cove	20 Dec 1940	5.5	VI	40.00	124.00
*Offshore northwest of Cape Mendocino	9 Feb 1941	6.4-6.6	VI	40.70	125.40
Offshore Cape Mendocino	13 May 1941	6	V	40.30	126.40
*Offshore northwest of Cape Mendocino (chimneys damaged)	3 Oct 1941	6.4	VII	40.54	125.00
Offshore Cape Mendocino	19 May 1945	6.2	V	40.60	126.40
*Offshore Cape Mendocino (damage in Ferndale and Capetown)	18 Dec 1946	4.7	VI	40.30	124.60
Offshore Cape Mendocino	30 Mar 1947	4.6	VI	40.38	124.68
Offshore Cape Mendocino	27 May 1947	5.2	VI	40.40	124.70
*Offshore Cape Mendocino	23 Sep 1947	5.6	VII	40.40	125.20
150 km west of Orick	24 Mar 1949	5.9	II-III	41.30	126.00
*Offshore Cape Mendocino	14 Jan 1950	4.6	VI	40.22	124.42
*Petrolia	10 Mar 1951	4.1	VI	40.30	124.30
*Offshore Cape Mendocino, 16 km west of Petrolia	8 Oct 1951	5.8-6	VII	40.35	124.60
*Near Scotia (minor damage)	14 Nov 1951	4.9	VI	40.43	124.05
*20 km southwest of Petrolia (chimneys fell, foundation damage)	22 Sep 1952	5.2-5.4	VII	40.20	124.42
Offshore Cape Mendocino	25 Nov 1954	6.1-6.3	V	40.48	125.46
*20 km northeast of Arcata ($2,100,000 damages, 1 death)	21 Dec 1954	6.5-6.6	VIII	40.85	123.96
Offshore northwest of Cape Mendocino (slight damage in Ferndale)	11 Oct 1956	6	V	40.67	125.77
*Near Petrolia	24 May 1958	4.8-4.9	VI	40.30	124.02
Offshore, 90 km west of Trinidad	23 Jul 1959	5.8	IV	41.13	125.30
*Offshore Arcata (plaster fell at Eureka City Hall)	5 Jun 1960	5.7	VI	40.87	124.50
Offshore Cape Mendocino (felt in San Francisco and southern Oregon)	9 Aug 1960	6-6.2	V	40.32	127.07
Offshore 18 km west of Cape Mendocino (triggered landslide)	6 Apr 1961	5-5.5	VI	40.49	124.81
*Offshore Crescent City (slight damage)	23 Aug 1962	5.6	VI	41.84	124.39
Offshore northwest of Arcata (slight damage)	4 Sep 1962	4.9-5	VI	41.01	124.21
*Offshore 20 km west of Petrolia (slight damage)	10 Dec 1967	5.6-5.8	VI	40.58	124.58
*Offshore Cape Mendocino	26 Jun 1968	5.5-5.9	VII	40.29	124.67
*Near Petrolia (slight damage in Petrolia)	9 Aug 1973	4.9-5.0	VI	40.35	124.30
*Fortuna	7 Jun 1975	5.2-5.7	VII	40.51	124.27
Offshore150 km northwest of Eureka	26 Nov 1976	6.3	IV	41.30	125.70
*Offshore 25 km west of Arcata (pipes and windows broken in Eureka)	3 Feb 1979	5.2	VI-VII	40.92	124.42
*48 km w of Trinidad (bridge collapsed, 6 injured, $1,750,000 damages)	8 Nov 1980	6.9-7.4	VII	41.12	124.67
Offshore Cape Mendocino	24 Aug 1983	5.5	V	40.38	124.83
Offshore 250 km west of Eureka (felt from SF to Oregon)	10 Sep 1984	6.6	V	40.50	126.83
*Just offshore Cape Mendocino (2 events in 1 min., slight damage)	21 Nov 1986	5.1, 5.1	VI	40.37	124.44
*Just offshore Cape Mendocino (damage and rocksides in Petrolia)	31 Jul 1987	5.5	VII	40.42	124.41
Near Honeydew (caused damage in Honeydew and Petrolia)	16 Jan 1990	5.3	VII**	40.23	124.14
Offshore 80 km west - northwest of Crescent City	13 Jul 1991	6.7-6.9	V	42.14	125.61
Offshore 100 km west of Crescent City	*6 Aug 1991	5.9-6.3	V	41.73	125.39
Near Honeydew (chimney, foundation damage, landslides, well changes)	17 Aug 1991	6.0-6.2	VIII**	40.21	124.28
Offshore 100 km west of Crescent City	17 Aug 1991	6.9-7.1	V	41.61	125.51
South of Petrolia (foundation damage, landslides)	7 Mar 1992	5.3-5.6	VII**	40.23	124.29
5 km north of Petrolia ($61 million damages, 356 injuries, tsunami, uplift)	25 Apr 1992	7	≥VIII**	40.37	124.31
33 km west-northwest of Petrolia (add. damage, poss. foreshock below)	26 Apr 1992	6	VII**	40.44	124.58
25 km west of Petrolia (add. damage)	26 Apr 1992	6.5	VII-VIII**	40.40	124.56

Table 1. Sources for intensities, epicenter locations and magnitudes for individual events in this table can be found in Dengler and others, 1992. Intensities listed are the peak values reported.. Intensities for earthquakes marked by ** have been estimated by our examination of personal reports and newspapers or by our own surveys. A range of magnitudes given for a single event reflects different reporting sources and different ways of measuring magnitude.

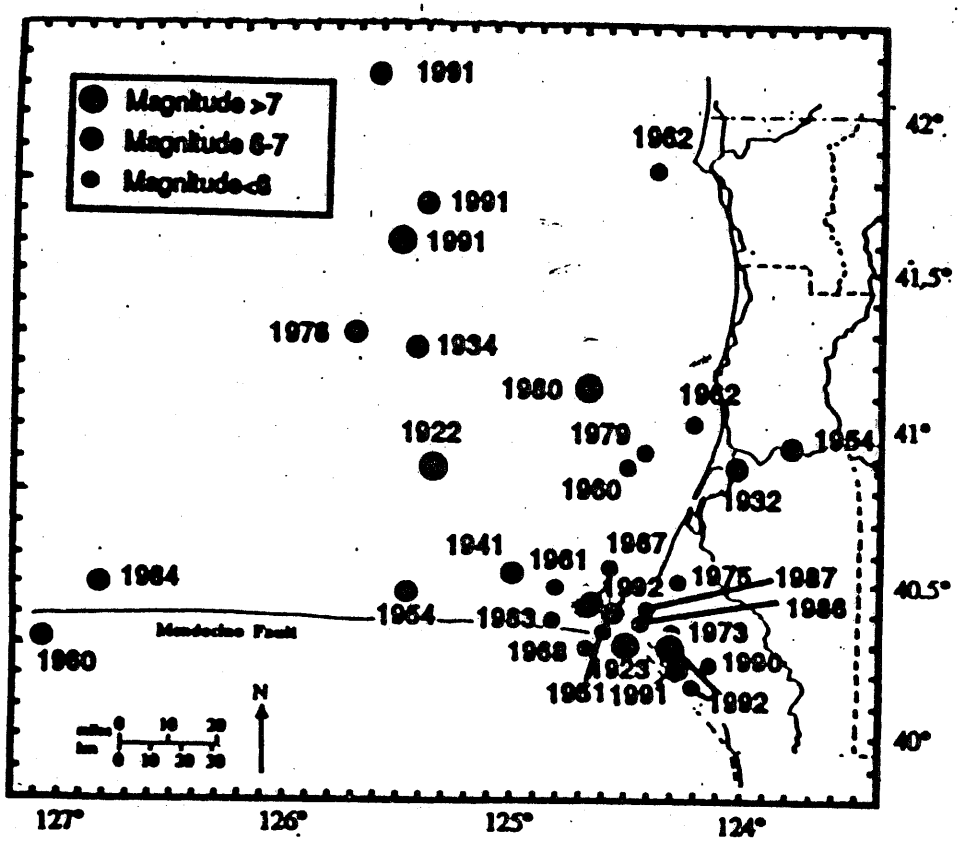

Figure 1. Epicenter locations and dates of best located north coast historic earthquakes of magnitude ≥ 5.5 and/or intensity ≥VI.

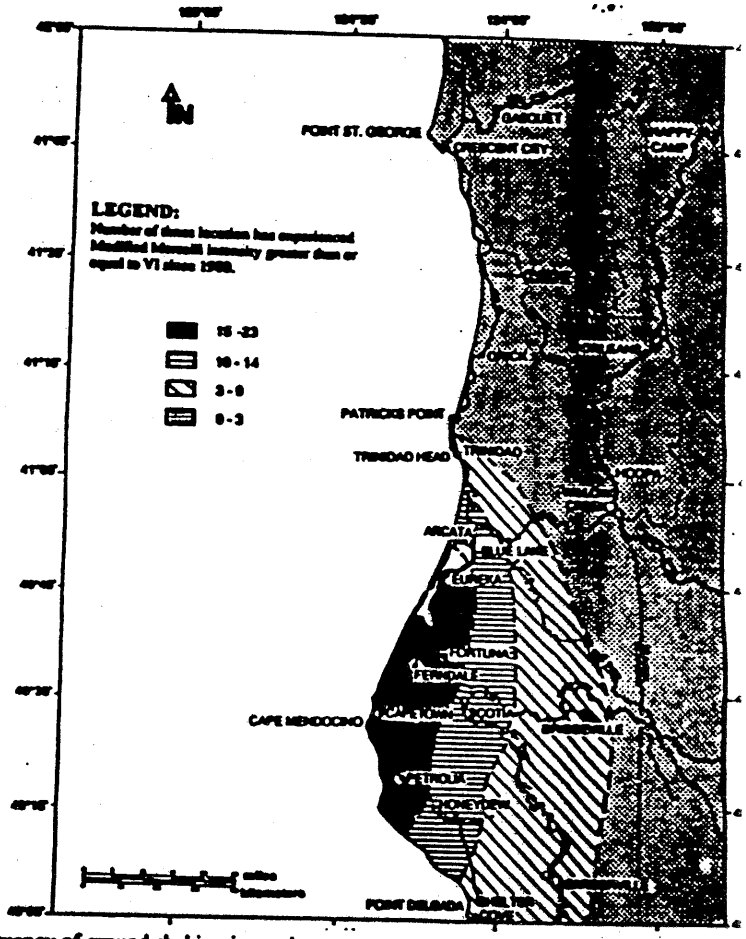

Figure 3. Cumulative frequency of ground shaking in north coast communities. Communities within the da area have experienced at least 15 earthquakes with ground shaking equivalent to or larger than VI on the Mod Mercalli Scale. Data compiled from 34 earthquakes since 1900 denoted by * in Table 1.

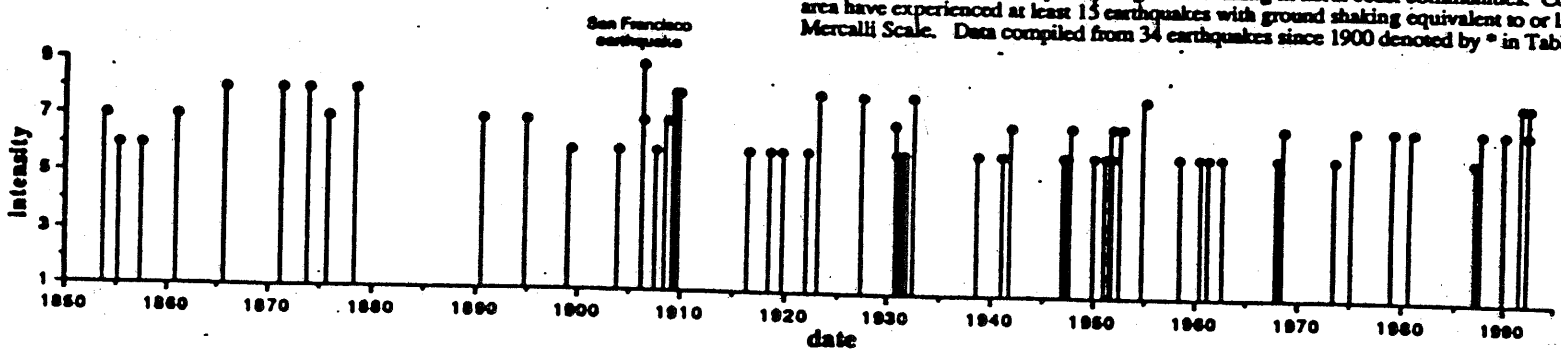

Figure 2. Frequency of historic earthquakes produ... Modifi... ca... nsi... VI ... abo...

REFERENCES

Bolt, B. A., Lomnitz, C., and McEvilly, T. V., 1968, Seismological evidence of the tectonics of central and northern California and the Mendocino Escarpment, Bulletin of the Seismological Society of America, v. 58, p. 1725-1767.

Clarke, S., and Carver, G., 1992, Late Holocene tectonics and paleoseismicity, southern Cascadia subduction zone, Science, vol. 255, p 188-192

California Strong Motion Instrumentation Program, 1992, Quick report on CSMIP Strong-Motion records from the Petrolia, California earthquakes of April 25, 26, 1992, CSMIP Report OSMS 92-04.

Dengler, L., Carver, G., McPherson, R., 1992, Sources of north coast seismicity, California Geology, vol. 44, April 1992.

Dengler, L., and McPherson, R., submitted, The August 17, 1991 Honeydew earthquake: a case for revising the Modified Mercalli scale in sparsely populated areas, Bulletin of the Seismological Society of America

Eaton J., 1989, Dense microearthquake network study of northern California, in J. J. Litehiser ed., Observatory Seismology: An Anniversary Symposium on the Occasion of the Centennial of the University of California at Berkeley Seismographic Stations, University of California Press, Berkeley and Los Angeles, p. 199-224.

Gee, L. S., Urhammer, R. A., and Romanowicz, B, 1991, Source parameters and rupture characteristics of the Gorda basin earthquakes and their tectonic implications, (abstract) EOS, Transactions of the American Geophysical Union, vol. 72. p. 312.

Hamilton, D., 1975, Geology of the Humboldt Bay region, unpublished report to thePacific Gas and Electric Co., San Francisco, California.

Heaton, T. H. and Hartzell, S. H., 1987, Earthquake hazards on the Cascadia subduction zone, Science, v. 236, p 162-168.

Heaton, T. H and Kanamori, H., 1984, Seismic potential associated with subduction in the northwestern United States, Bulletin of the Seismological Society of America, v. 75, p. 933-942.

Knapp, J., 1982, Seismicity, Crustal Structure and Tectonics near the Northern Termination of the San Andreas Fault, unpublished Ph.d dissertation, University of Washington, Seattle, 316 p.

Lawson, A.C., 1908, The California Earthquake of April 18, 1906, Carnegie Institute, Washington, D.C.

McPherson, R. C., 1989, Seismicity and Focal Mechanisms near Cape Mendocino, northern California, unpublished masters thesis, Humboldt State University, Arcata, California, 75 p.

McPherson, R. C., Smith, S. W., and Severy, N. I., 1981, The Humboldt Bay Seismic Network: 1974-1980, (abstract), Earthquake Notes, v. 52, p. 41-42.

NOAA, 1992, Personal Communication

Oppenheimer, D., 1992, Personal Communication, USGS, Menlo Park, CA 94025.

Oppenheimer, D., Reasenberg, P., Walter, S., Macgregor-Scott, N, Hirshorn, B., and Lindh, A., 1992, Weekly Seismicity Report, April 23-29, 1992, U.S. Geological Survey, Menlo Park, CA 94025.

Prentice, C. S, 1989, Earthquake geology of the northern San Andreas fault near Point Arena, California, unpublished Ph.d thesis, California Institute of Technology, Pasadena, California, 235 pp.

Simila, G. W., Peppin, W., and McEvilly, T. V., 1975, Seismotectonics of the Cape Mendocino, California area, Bulletin of the Geological Society of America, v. 86, p 1399-1406.

Smith, S. W., and Knapp, J. S., 1980, The northern termination of the San Andreas fault, Studies of the San Andreas fault zone in northern California, edited by R. Streitz and R. Sherburne, Spec. Rep. Calif. Div. Mines Geol., p. 153-164.

Smith, S. W., McPherson, R. C. and Severy, N. I., 1981, Breakup of the Gorda Plate, (abstract) Earthquake Notes, v. 52, p. 42.

TERA Corporation, 1977, Tectonic significance of large historic earthquakes in the Eureka region, September 9, 1977, unpublished report to the Pacific Gas and Electric Co., San Francisco, California.

Tobin, D. G., and Sykes, L. R., 1968, Seismicity and tectonics of the northeast Pacific Ocean, Journal of Geophysical Research, v. 73, p. 3821-3845,

Toppozada, T. R., and Parke, D. L., 1982, Areas damaged by California earthquakes 1900-1949, California Division of Mines and Geology Open-File Report 82-17 SAC.

Toppozada, T.R, Real, C. R. and Parke, D. L., 1981, Preparation of Isoseismal Maps and Summaries of Reported Effects for Pre-1900 California Earthquakes, California Division of Mines and Geology Open File Report 81-11SAC, 182 pp.

Urhammer, R. A., 1991, personal communication, Seismographic Station, University of California, Berkeley, CA, 94720.

Woodward-Clyde Consultants, 1980, Evaluation of the potential for resolving the geologic and seismic issues at the Humboldt Bay Power Plant Unit No. 3, Appendices, Woodward-Clyde Consultants, Walnut Creek, California.

Quaternary Tectonics and Topography, Mendocino Triple Junction

Dorothy Merritts, Geosciences Department, Franklin and Marshall College, Lancaster, PA
Thomas Dunklin, Geology Department, Humboldt State University, Arcata, CA
Kirk Vincent, Geosciences Department, University of Arizona, Tucson, AZ
Ellen Wohl, Department of Earth Sciences, Colorado State College, Fort Collins, Colorado
William B. Bull, Geosciences Department, University of Arizona, Tucson, AZ

Acknowledgements
Introduction
Background Information
Physiographic and Climatic Setting
Late Pleistocene Climate
Tectonic Setting
Evolution of the Mendocino Triple Junction
Uncertainties in Locating Plate Boundaries at the Mendocino Triple Junction
Geologic Setting: Accretionary Terranes
Late Quaternary Tectonics and Surface Uplift
Previous Work in the Region
Late Pleistocene Surface Uplift
Altitudinal Spacing Analysis of Marine Terraces
Spatial and Temporal Changes in Late-Pleistocene Uplift Rates
Holocene Surface Uplift
Ages and Deformation of Late-Holocene Marine Terraces
Paleoseismic Information from Emergent Holocene Marine Platforms
Recent Crustal Deformation
Historic Seismicity
Seismicity and Holocene Uplift
Strain Rates from Geodetic Surveys and Modelling
Geomorphic Indicators of Quaternary Uplift
Analysis of Small Coastal Streams
Multivariate Correlation Analysis
Spatial Variations in Morphologic Properties of Drainage Basins
Discussion of Morphologic Analyses
Discussion of Quaternary Tectonics
Mechanisms of Crustal Deformation and Mountain Building
Fluvial Response to Tectonism
The Response of Large Coastal Rivers to Base-Level Change
Fluvial Terraces, Base-Level Change, and the Graded Stream
Conceptual Model for Upstream Transmission of Base-Level Change
Terraces Along the Mattole River
Methods
Observations
Interpretation of Terrace Remnants
Conclusions Regarding Terraces and Base-Level Change
Fluvial Responses to Changing Patterns of Human Land Use, Mattole Watershed
Settlement and Logging History
Extent of Deforestation
Floods
Landslides
Conclusions

ACKNOWLEDGMENTS

It is not possible to list all the dozens--perhaps hundreds--of people who have helped one or more of the authors to accomplish the work outlined in this article. Gracious landowners, perceptive scientists, generous granting agencies, competent civil servants, hardworking and loyal students, energetic teenagers, and more friendly people than we've met anywhere else in the world have guided us, supported us, and joined us in our excitement in discovering the geologic wonders of California's Lost Coast over the past eight years. We can't name them all, but often think of them with gratitude and fond memories. The hardy pioneers of the Mattole and Bear River Valleys are individualistic and cautious, but gave us the benefit of the doubt and access to much land that holds invaluable clues to the triple junction's tectonics. Few at first believed that we--or anyone else--could possibly really want to do what we said we were up to, and we appreciate their trust. We hope that our work is someday of some help in their struggles to live in one of the most seismically active areas in North America. To the following landowners, we say THANK YOU!: Joseph Zanoni, Rus Chambers, Mr. and Mrs. Alan Gillespie, Jim Cooke, Bill McBride, Marry Etter, Jim Wilson, John Short, the late Joseph Russ, Sanford Lowry, Margie and Greg Smith, the Roscoe families, Kip Chambers, Hurky Lawrence, Don and Lorraine Etter, Randy Stemler, Jan Morrison, Ruth and Rex Rathbun, Ellen Tayor, Mike Evenson, Dick Scheinman, Buck and Alan Miner, and many more. We are indebted to several individuals at the Bureau of Land Management, the U. S. Geological Survey, and the Georgia-Pacific Lumber Company, who have offered generous technical, logistical, and advisory support. We are especially grateful to John Tinsley, Bob McLaughlin, Sam Clarke, Steve Ellen, and Jere Melo. We have received funding from many sources, and hope that the quality of our work proves worthy of that support. We thank the following for awards to Merritts: National Science Foundation (Doctoral Dissertation Improvement Grant # EAR-8405360; Research at Undergraduate Institutions Grants # EAR-89-04785 and 89-17116; Supplemental Grant # EAR-91-49176), the U. S. Geological Survey (Graduate Internship, 1984-1987; NEHRP grant #14-08-0001-G N2334,) the Geological Society of America (Fahnestock award), Franklin and Marshall College, and Sigma Xi. Finally, the first author would like to give a special thank you to the geology students who were inaugurated to field work and long field seasons with her in this mystic area: Stephanie Polaski, Rob Ticknor, George Dudkiewiscz, Rob Bruant, Jason Buchman, Lauren Hammack, Loren Ferdinand, Michael Polenz, and Ianya Rose. Many of the figures in this guide are the result of the creativity, cleverness, and willingness to work weekends of Michael Polenz and Rob Bruant.

INTRODUCTION

With their fringe of late-Quaternary marine and fluvial terraces, the unglaciated, northern California Coast Ranges provide a spectacular and relatively accessible area for studying Quaternary tectonics and topography. Geologic evidence indicates that some of the highest rates of uplift in North America occur here, at the juncture of the San Andreas fault (SAF) with the Cascadia Subduction Zone (CSZ; Fig. 1). The exact cause and mechanism of rapid uplift at this triple plate juncture--the Mendocino Triple Junction (MTJ)--are unknown. The narrow width of the fringe of Quaternary marine terraces along the base of the Coast Ranges makes it possible to use estimates of surface uplift derived from them to develop models of the mechanics of mountain building. Spectacular incised meandering rivers, such as the Bear, Mattole, and Eel, provide excellent opportunities to investigate fluvial response to base-level change. An unusual advantage for geologists is lack of development in this region. It is one of the few parts of the western United States without a coastal highway. It is, in fact, the rapi uplift and consequent ubiquity of mass movement that precludes highway development.

The region is also one of the most seismically active in California, accounting for mo

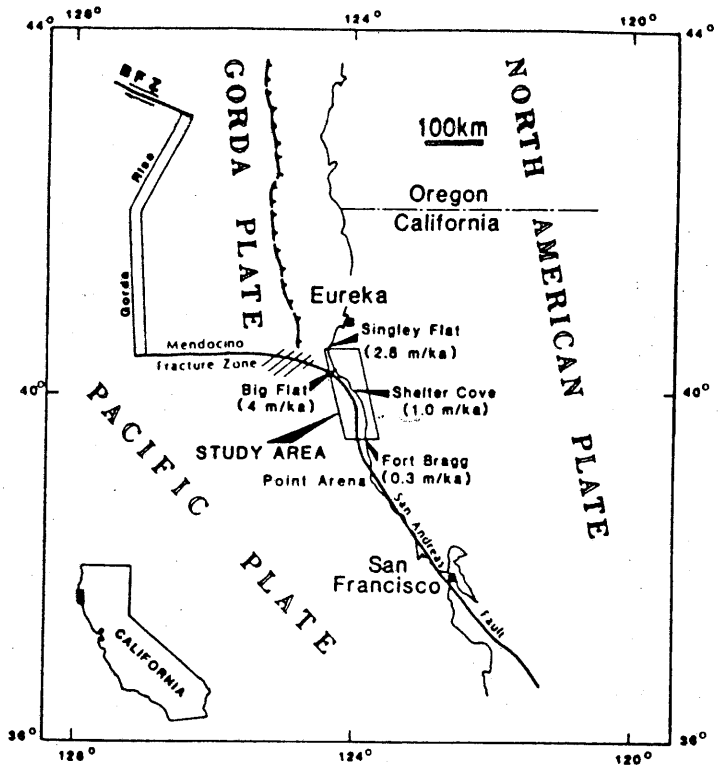

Fig.1. Location map, tectonic setting, and published rates of uplift of the Mendocino triple junction (MTJ) region, coastal northern California. The MTJ, shown in hachures, marks the juncture of the North American, Pacific, and Gorda plates. Uplift rates and their sources are discussed in the text. BFZ = Blanco Fracture Zone. See Fig. 4 for a three-dimensional view of this triple junction.

than 25% of the seismic energy released by all earthquakes in and near CA during the last 50 years (Gee et al, 1991). More than 35 earthquakes greater than Modified Mercalli Intensity VI have occurred in the immediate vicinity of the MTJ since 1850 (Dengler et al, unpub. manus.). Nevertheless, despite the seismic activity and the area's location along one of the most-studied faults in the world, the northern segment of the San Andreas is poorly understood. Because of the magnitude of the 1906 San Francisco earthquake (M_W=7.7) and intensity of ground shaking in northern California, the SAF is thought to have ruptured 450 km, from near San Francisco to the MTJ. However, no clear evidence of surface rupture associated with the 1906 earthquake, or any paleoearthquakes, has been obtained for the San Andreas north of Point Arena, where the surface trace of the fault goes offshore. The location and nature of the remaining 200 km of the SAF are unknown.

On the other hand, geomorphic evidence of crustal deformation probably associated with large-magnitude seismic events is clear: multiple Holocene strandlines emerge above sea level ~30 km south of the triple junction, and disappear below sea level about ~30 km north of it. Emergent Holocene marine platforms indicate that tectonic deformation is rapid and recent along the northern termination of the SAF and the southern termination of the CSZ. Holocene strandlines are common in the tectonically active Pacific Rim, especially along convergent plate margins; however, they are uncommon along transform boundaries such as the San Andreas. Historic large magnitude earthquakes along subduction zones in Japan, Alaska, and Chile have resulted in coseismic emergence of tidal platforms (Fujita et al, 1975; Plafker, 1969; Plafker and Savage, 1970). Questions of whether the emergent strandlines in northern California are coseismic or aseismic, and whether they are related to the SAF, the CSZ, or the migrating MTJ, are as yet unresolved. In this paper, we present evidence that they are seismic and are associated with the MTJ.

Land use in the MTJ region is predominantly ranching, practiced by a few close-knit, 5th-generation families descended from Portuguese, Italian, and Dutch settlers in the late 1800s. Large-scale logging did not occur until the late 1940s, just prior to the devastating high-magnitude floods of 1955 and 1964. Before then, large rivers in the region were spawning grounds for tens of thousands of salmon and steelhead trout. Since about 1960, however, fish populations have declined rapidly. Studies of fluvial response to change are now more critical than ever before, and geologists and geomorphologists have joined with ranchers, fishermen, loggers, and other local inhabitants to try to understand these fluvial systems and prevent further environmental degradation.

This paper synthesizes the tectonic, geomorphic, and land-use histories of the coastal ranges and valleys at the MTJ. Following a presentation of regional physiographic, climatic, tectonic, and geologic information, a detailed tectonic history proceeds from the Pleistocene to the Holocene, and ends with a discussion of recent strain rates and seismicity. Analysis of fluvial response to tectonism includes examination of both small coastal streams and much larger rivers. The paper concludes with a discussion of fluvial response to historic changes in the largest watershed in the region, the Mattole drainage basin. The Mattole River, one of the least--and most recently--developed for its size in California, has altered its pattern in the lower reaches from meandering to braided during the past several decades, and we present these changes in the context of simultaneous changes in forest cover and land use practices.

BACKGROUND INFORMATION

Physiographic and Climatic Setting

The rugged northwest-trending Coastal Ranges of the MTJ region are bounded on the west by the Pacific Ocean, and on the east by two large, northwest-flowing antecedent rivers, the Mattole and Eel (Fig. 2). The westernmost of California's Coast Ranges, the rugged 60-km long King Range, is located in this region. Its highest peak (King Peak) rises to 1246 m (4087 ft) within about 5 km (~3 mi) of the coastline, and is flanked by California's "Lost Coast", which can be accessed only on foot. The sinuous Mattole originates less than 5 km from the coast near Point Delgada, flows inland and north for 120 km, and exits north of the King Range. Twenty-four much smaller west- and southwest-flowing 3rd-order (blue-line) streams drain the King Range and adjacent hills along the coast (Fig. 3). Maximum relief along the major drainage divide separating these basins from the Mattole and Eel River basins increases northward from 300 m near Fort Bragg to 1246 m in the central part of the King Range. Hillslopes in all basins are generally steep and convex, and conducive to slope failure and rapid erosion.

The northern California coastal region has a cool, temperate, highly seasonal Mediterranean climate, characterized by mild, wet winters and a prolonged dry season. Local climatological data available from three coastal climatic stations (Eureka, Shelter Cove, and Fort Bragg) and one inland station (Honeydew) along the perimeter of the study area (Fig. 1 and 3; NOAA, 1985) are similar in that summers are cool, foggy, and dry; mean monthly temperatures vary less than 6° C throughout the year; mean annual temperatures are 12-14° C; and more than 90% of the mean annual precipitation of 1.0 m occurs as rain during mild winters. Climatic characteristics of the Fort Bragg and Eureka coastal stations are nearly identical (mean annual precipitation 1.00-1.02 m; mean annual temperature 12-14° C). Within the center of the study area, however, climate is modified by the orographic effects of the King Range. Measured mean annual precipitation (maP) at the coast at Shelter Cove is 1.65 m, and over the King Range crest at Honeydew it is 1.70-2.50 m.

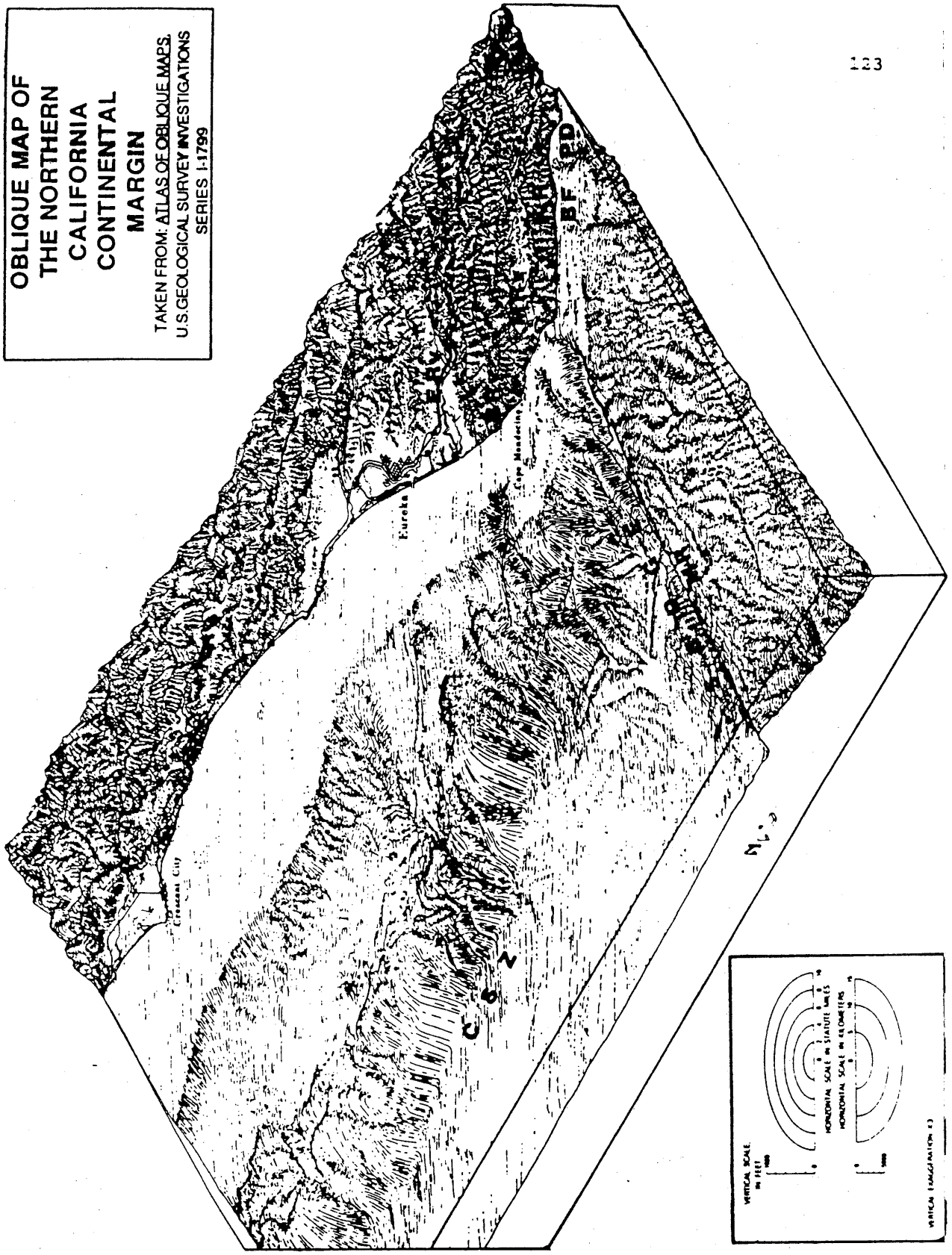

Fig.2. Oblique map of the continental margin along the northern California coast, from Point Delgada north to Crescent City. **PD:** Point Delgada; **KR:** King Range; **MR:** Mendocino Ridge; **SEDGE:** southern edge of "Gorda" plate; **MR:** Mattole River; **BR:** Bear River; **ER:** Eel River; **CSZ:** approximate location of Cascadia subduction zone. (From Alpha et al, 1988.)

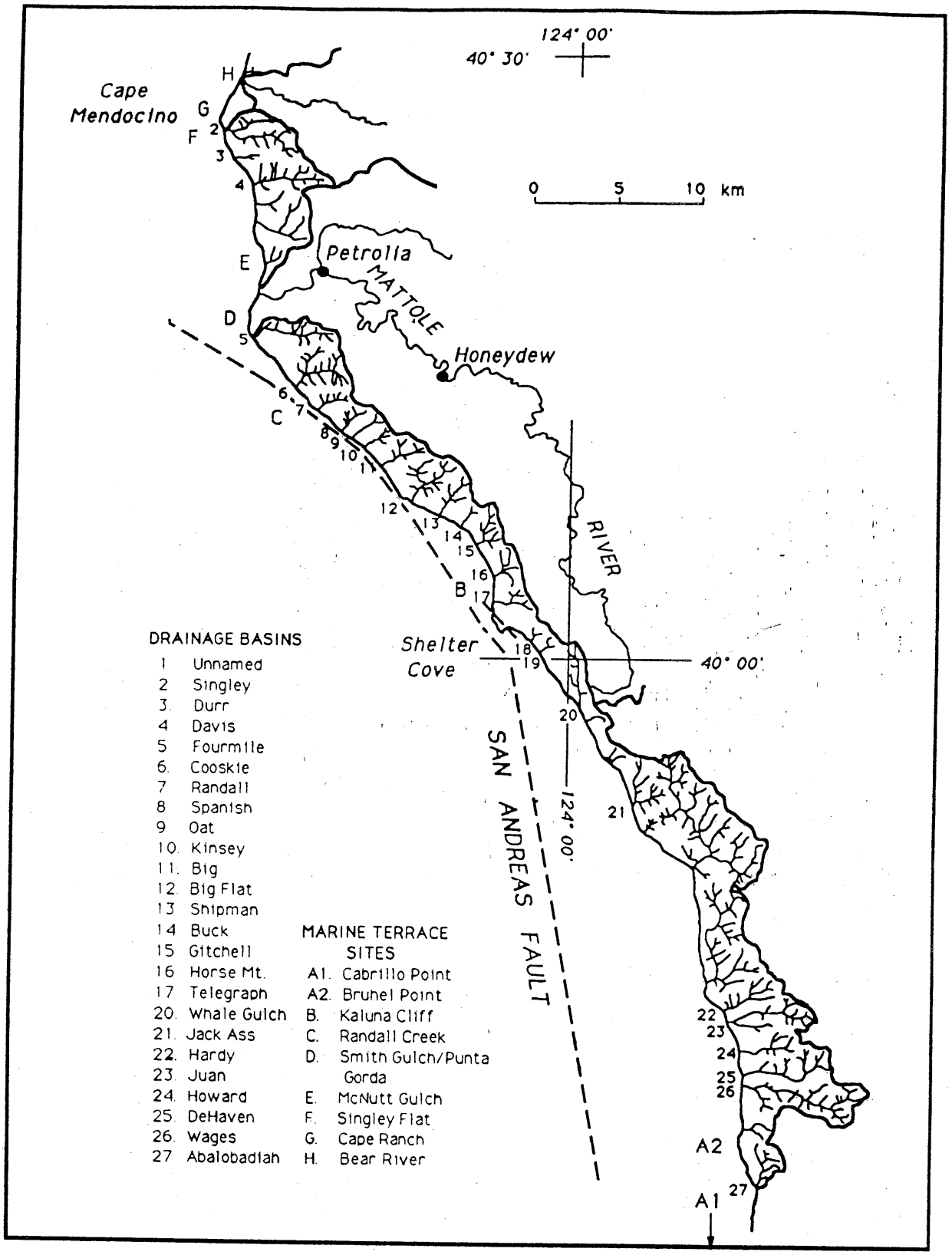

Fig. 3. Major drainage basins along coastal northern California. Drainage networks are taken from 7.5' topographic maps. Heavy lines are major drainage divides between west-flowing coastal drainages and larger inland drainage basins (Mattole and Eel). Only major trunk streams of the Mattole River basin are shown. Marine-terrace sites same as in Figure 7.

Late Pleistocene Climate

The late Pleistocene climate of northern coastal California was characterized by a series of cool-moist (glacial) and warm-dry (interglacial) alternations. These alternations were of a much lesser magnitude than those that produced the major climatic changes of glaciated and continental interior regions (Johnson, 1977). Climatic variations between glacial and interglacial periods were stabilized by maritime influences on intensities of temperature and precipitation gradients, and paleontological evidence indicates that the northern California coastal zone acted as an "ice-age refugium" for cold-sensitive faunal species displaced elsewhere (Johnson, 1977). During the most recent full-glacial climatic conditions at 18 ka, estimated sea-surface summer (August) temperatures (13° C) were similar to modern sea-surface summer temperatures (~13° C; <1° C difference); however, winter temperature gradients were intensified, and estimated full-glacial winter (February) sea-surface temperatures (7° C) were 4° C cooler than the modern winter temperature (11° C) (CLIMAP Project Members, 1981). Modern mean summer (August) and winter (February) temperatures onshore at both the Eureka and Fort Bragg stations are 13 and 8.5° C, respectively.

Tectonic Setting

Evolution of the Mendocino Triple Junction

Rapid uplift rates, pronounced relief, and high seismicity are the result of complex interactions among the plates joined along the migrating MTJ. The triple-junction-boundary between the North American, Pacific, and Juan de Fuca plates (Fig. 1) formed about 29 million years ago, when part of the ancestral spreading center of the Farallon (present-day Juan de Fuca) plate was subducted beneath the North American plate (NAP; Atwater, 1970; Dickinson and Snyder, 1979a and 1979b). Subduction of the Juan de Fuca plate has continued north of the triple junction, while south of it right-lateral shear between the Pacific and North American plates has developed into the San Andreas transform boundary (Fig. 4). The position of the MTJ migrates northward at the same rate as relative movement between the North American and Pacific plates (~56 mm/yr; Engebretson et al, 1985), and has been within the Fort Bragg to Cape Mendocino area for about two million years.

As the Juan de Fuca plate (JFP) moves northeastward relative to the NAP and is consumed by subduction, the length of the San Andreas transform boundary increases and a slab window develops beneath the NAP south of the MTJ (Fig. 4; Dickinson and Snyder, 1979a). The southern edge of the JFP trends due east along the Mendocino Fracture Zone (a right-lateral transform) towards Cape Mendocino until about 125° W, where the oceanic plate dips 11-15° beneath the NAP (Fig. 4). The top of the JFP has been inferred from magnetic data (Silver, 1971), seismic refraction and seismicity data (Smith and Knapp, 1980; McPherson et al, 1981, McPherson, 1989), gravity and magnetic data (Griscom, 1980; Jachens and Griscom, 1983), and earthquake tomography (Verdonck and Zandt, 1991). The subducted southern end of the JFP bends to the south and east, reflecting both north-south and northeast-southwest directed compression (Verdonck and Zandt, 1991). Isostatic gravity anomalies indicate that the southern edge of the subducted slab (SEDGE) changes strike after its plunge beneath the NAP, and trends S60°-80°E under the King Range from Punta Gorda towards Round Valley (Jachens and Griscom, 1983). The SEDGE is the northern boundary of the growing slab window. Growth of the slab window is associated with upwelling and juxtaposition of hot asthenosphere against cold lithosphere of the NAP, effective lithospheric thinning, thermal expansion of the crust, and isostatic flexural uplift (Furlong, 1984).

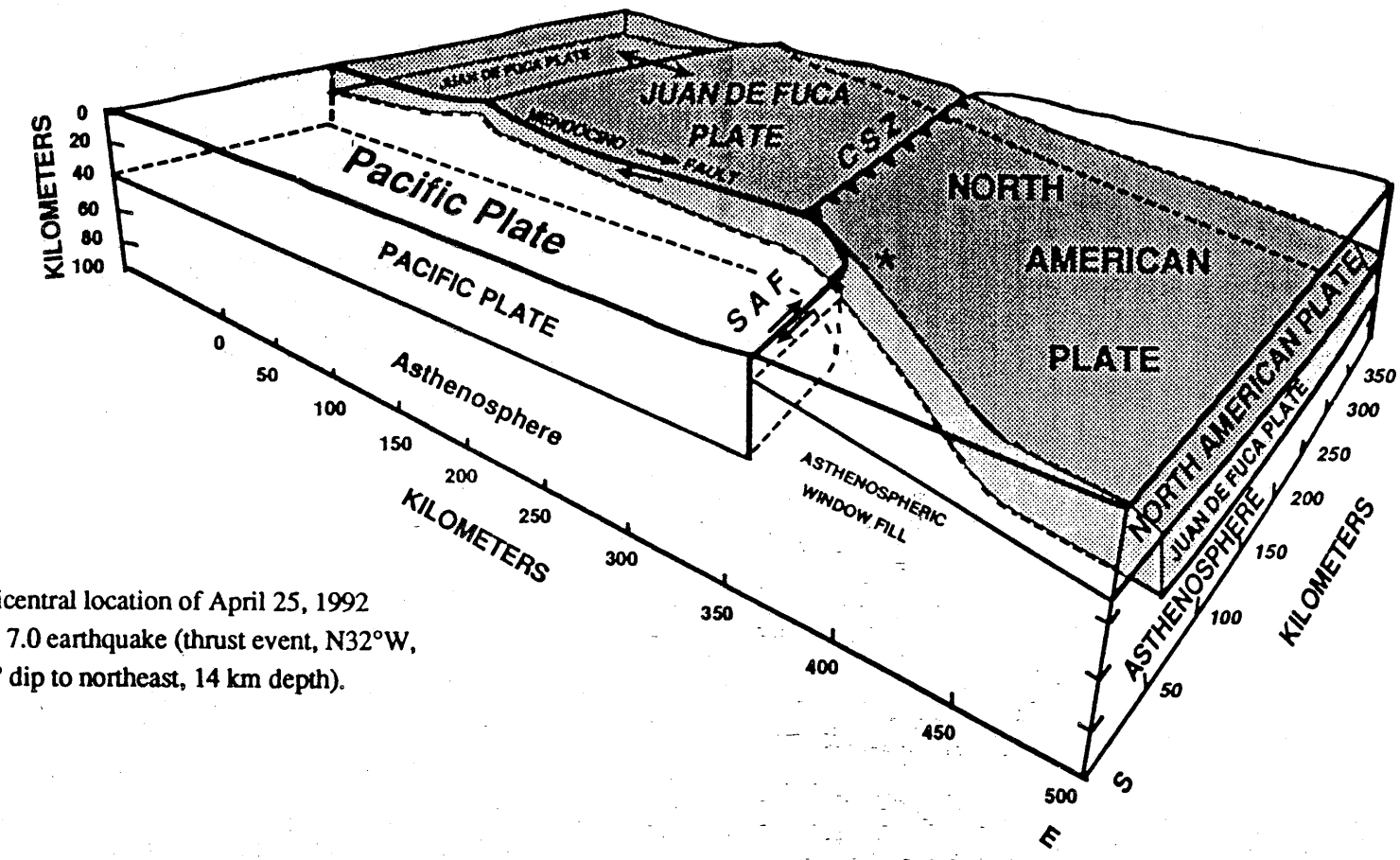

★ Epicentral location of April 25, 1992 Ms 7.0 earthquake (thrust event, N32°W, 22° dip to northeast, 14 km depth).

Figure 4. Three dimensional block diagram of the configuration of the Mendocino triple junction region. (Modified from Jachens and Griscom, 1983.)

Uncertainties in Locating Plate Boundaries at the Triple Junction

The locations of the SAF and transform boundary, the southern termination of the CSZ, and the MTJ itself are uncertain and controversial (cf., Griscom and Jachens, 1989; Clarke, 1992). Bathymetric data indicate that the offshore SAF can only be traced with certainty from Point Arena to Tolo Bank, just south of the town of Shelter Cove at Point Delgada (Fig. 1 and 3; Curray and Nason, 1967; Nason, 1968; Perry and Pryor, 1986). A region referred to as the Delgada-Gorda gap, in which no clear morphologic or seismic evidence of the San Andreas fault exists, stretches northward from Point Delgada to the MFZ (Perry and Pryor, 1986). Surface deformation onshore at the broad headlands at Point Delgada during the 1906 earthquake caused some workers to consider the possibility that the San Andreas comes onshore at the point, then passes offshore again to the north (Lawson et al, 1908; Brown and Wolfe, 1972). However, the northwest-trending surface breaks observed at Point Delgada after the 1906 earthquake were not clearly scarps associated with the main trace of the rupture, and other workers have considered them to be perhaps headscarps of landslides triggered during ground shaking (McLaughlin et al, 1983). On the basis of K-Ar dating of adularia veins (13.8 ±0.4 m. y) that cross one proposed bedrock fault trace, McLaughlin et al (1979a and 1979b) rejected the possibility of Quaternary movement along that segment (see also Beutner et al, 1980). Their work does not, however, reject the possibility of the existence of a segment of the plate boundary elsewhere near Point Delgada.

Dumitru (1991) has rejuvenated discussion of such a possibility with analysis of apatite fission-track ages and rock uplift histories of two northwest-trending accreted subterranes that are in contact at Point Delgada--the rugged, high-altitude King Peak and low-altitude Point Delgada subterranes of the King Range Terrane (McLaughlin et al, 1982; discussion below). Dumitru contends that 2-5 km of rock uplift and unroofing has occurred in the King Peak subterrane since about 1.2 Ma, whereas little or no uplift of the Point Delgada subterrane has occurred during the past 12 m. y. Consequently, he invokes vertical and lateral displacement along the boundary between the terranes to explain the differing uplift and thermal histories.

Part of the reason for uncertainty in locating the southern end of the CSZ and the MTJ itself in this region is the pervasive deformation of what Wilson (1989) calls the "so-called Gorda Plate". The Gorda Plate is the name given earlier (Silver, 1971) to that part of the JFP east of the Gorda Rise and between the Blanco and Mendocino Fracture Zones (Fig. 1). As Wilson (1986, 1989) has pointed out, no boundary occurs in the JFP north and south of the Blanco Fracture Zone, and consequently no basis exists for the naming of a separate plate. However, a sharp boundary does exist just south of the Blanco Fracture Zone between the rigid part of the JFP and a zone of high seismicity and complexly deformed material within the so-called Gorda Plate. Wilson (1986) recommends referring to this part of the JFP as the Gorda deformation zone.

The complexity of this deformation zone is attributed to a gradual change in absolute motion of the Pacific Plate between 5 and 3.2 Ma which resulted in the following:

1) a 20° clockwise rotation in relative motion between the Juan de Fuca and Pacific Plates (Cox and Engebretson, 1985; Harbert and Cox, 1989; Pollitz, 1986; Wilson, 1986);
2) transpression along the east-west trending MFZ because it was not reoriented;
3) shortening and deformation of magnetic anomalies in the southeastern corner of the JFP with respect to their counterparts in the Pacific Plate (Silver, 1971);
4) a southward decrease in spreading rate along the Gorda Rise (Jachens and Griscom, 1983); and
5) a decrease in rate of relative northward motion of the SEDGE.

As a consequence of these changes, north-northeast-directed transpression in this region has resulted in break-up of the Gorda Basin along northeast-striking left-lateral strike-slip faults (Eaton, 1981). This break-up accounts for most of the seismicity in the MTJ region.

The considerable complexity of the southern part of the JFP is illustrated in the geologic maps prepared by Clarke (1992) from interpretation of offshore continental margin seismic reflection profiles and from compilation of onshore mapping of the accretionary prism (part of this work is illustrated in Fig. 5). The continental margin north of Cape Mendocino consists of about 4000 m of late Cenozoic marine sediments deposited upon a basement comprised of rocks of the Mesozoic Franciscan Complex. Clarke (1992) describes two structural domains in this sedimentary basin: a southern part characterized onshore by west-trending thrust and high-angle reverse faults and offshore by similar structures that trend northwest; and a northern part comprised of north-trending folds and thrust faults. According to Clarke (1992),

> "This structural trend clearly reflects the influence of the north to northeast-directed stresses that are peculiar to the southern part of the region and do not correspond to structural trends farther north. Quaternary structures in the southern part of the basin probably reflect compression and uplift that are associated with the northward migration of the MTJ and Pacific plate, whereas farther north, the structural character appears to be primarily a reflection of Gorda-NAP convergence. In the north, structural trends are predominantly normal to the direction of Gorda plate convergence, and east-northeast-directed compression is indicated by reverse and thrust faulting." (p. 207-208)

Because of the structural complexity of the Gorda basin, the seaward edge of the CSZ is difficult to trace south of 40°27' N, but appears to bend to the east and follow the Mendocino Canyon (Fig. 2 and 5; Clarke, 1992). This is a dramatic change from past thinking that it joined the Mendocino fault, several tens of km offshore from Cape Mendocino. Clarke (1992) has tentatively postulated that the megathrust approaches the onshore region at the location of the east-southeast-trending Petrolia shear zone (PSZ), and that the more southerly Mendocino fault follows the Mattole Canyon to join the onshore Cooskie Creek shear zone (CCSZ). Clarke relies on mapping of these onshore structures (McLaughlin et al, 1988) to suggest that the location of the MTJ is inland along these shear zones, rather than offshore. As he notes, the PSZ marks the

> ". . . boundary between discordant structural domains, as shown by shear fabric orientation and fold trends within the Franciscan Coastal terrane. Structures of the domain to the north of Petrolia strike northwest and dip northeast, which is consistent with shoreward extension of the late Cenozoic subduction zone between the Gorda and North American plates and the overlying accretionary prism. Structures of the domain to the south of Petrolia parallel the northern and eastern boundary of the King Range terrane (McLaughlin et al, 1988)." (p. 209)

If Clarke's interpretation is correct, the accretionary prism overlying the southernmost Cascadia subduction zone extends onshore north of the town of Petrolia (the site of California's first oil well), and the position of the MTJ might be located at the junction of the PSZ and the CCSZ, north of the King Range. Based on this interpretation, Clarke redefined the MTJ:

> ". . . a more realistic concept of the MTJ is that it is a broad zone of deformation, centered near the town of Petrolia. . .[implying] . . . that the presently aseismic (e.g., Simila, 1980) offshore strand of the San Andreas fault between Point Delgada and Punta Gorda has been, or is being, abandoned, and that right-slip San Andreas motion is being taken up along a fault or faults, probably including the Mattole shear zone, located east of the King Range terrane." (p. 217)

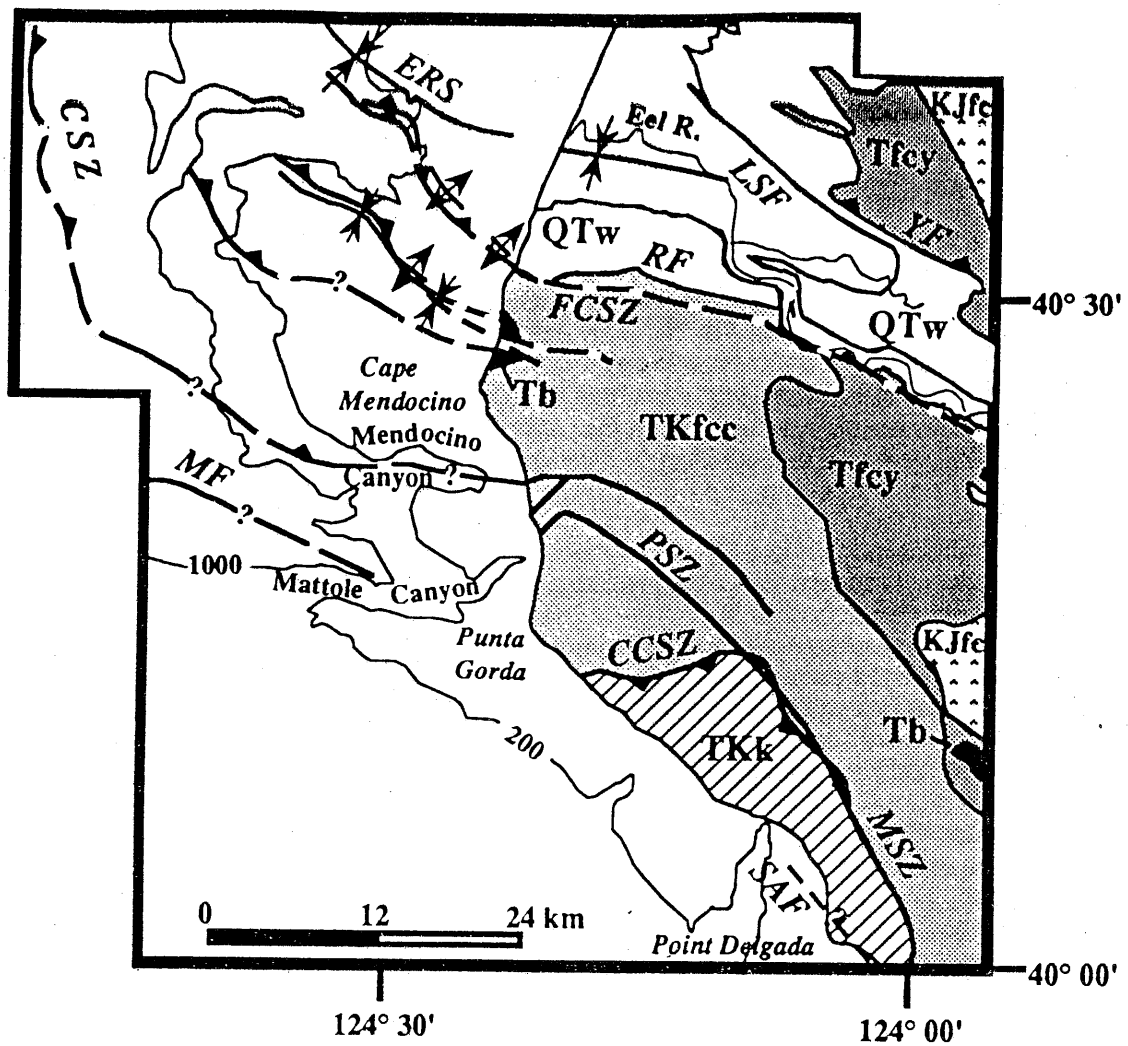

ROCK UNITS

KFfc	Cretaceous and Jurassic Central belt, Franciscan Complex
TKfcc	Paleogene and Cretaceous Coastal terrane of the Coastal belt, Franciscan Complex
TKk	Tertiary and Cretaceous King Range terrane
Tfcy	Paleogene Yager terrane of the Coastal belt, Franciscan Complex
Tb	Upper Tertiary Bear River beds of Haller (1980) and correlative units
QTw	-Quaternary and upper Tertiary rocks of the Wildcat Group and correlative units, mostly nonmarine

STRUCTURES

CCSZ	Cooskie shear zone	MSZ	Mattole shear zone
ERS	Eel River syncline	PSZ	Petrolia shear zone
FCSZ	False Cape shear zone	RF	Russ fault
LSF	Little Salmon fault	SAF	San Andreas fault
MF	Mendocino fault	CSZ	Cascadia Subduction Zone

Fig. 5. Onshore and offshore geology and structure of the MTJ region (from Clarke, 1992).

Geologic Setting: Accretionary Terranes

Rock units along this part of the NAP margin are part of the Franciscan assemblage of subduction-related deposits that formed within the convergent tectonic regime existing prior to passage of the MTJ. A broad shear zone (Cooskie shear zone) separates two northwest-oriented tectonostratigraphic units, the Coastal and King Range terranes (Fig.5; Beutner et al, 1980; McLaughlin et al, 1982; Mclaughlin et al, 1986). The larger Coastal terrane is composed dominantly of Paleocene to late Eocene turbidites (arkosic shale, siltstone, and sandstone) comprised of sediments derived from the inboard volcanic arc, with some coarse continental-margin detritus (Bachman, 1978; McLaughlin et al, 1982; Blake et al, 1985; McLaughlin et al, 1986). The Coastal terrane was accreted during normal convergence of the North American and Farallon plates from 40 to 25 m. y. ago (McLaughlin et al, 1986). Foraminifers, palynomorphs, and radiolarian chert contained in these rocks suggest a depositional origin no more than 600 km to the south (McLaughlin et al, 1986). Structural style is very nonuniform within the unit, and fabric varies from fairly coherent sandstone-rich rocks in the eastern part of the terrane to more disrupted, deformed, and sheared argillaceous rocks near the coast and eastern boundary of the King Range terrane (Blake et al, 1985).

Although the younger King Range terrane (early Tertiary (?) to mid-Miocene) is of similar lithologic and depositional origin to the Coastal terrane, its structural style differs (Beutner et al, 1980). The King Range terrane rocks generally are more structurally intact than those of the Coastal terrane, but grade to the east and north along the Cooskie shear zone (CCSZ) to melange of the Coastal terrane. According to McLaughlin et al (1986), the King Range terrane rocks originated as deep-water turbidite fan complexes in a trench-slope setting ". . . along the Farallon-North American plate boundary, but possibly as far as 450 km south of Cape Mendocino. . . The King Range terrane then was [rifted from the California margin], translated northward with the MTJ [and the Pacific Plate], and obductively reaccreted [during translation] in the early Pleistocene."

LATE QUATERNARY TECTONICS AND SURFACE UPLIFT

Previous Work in the Region

Styles and rates of Quaternary deformation vary spatially along the northern California coastline. North of the triple junction, northeastward-directed compression results in northwest-trending thrust faults and broad anticlinal folds (Carver et al, 1985, 1986; Kelsey and Carver, 1988; Clarke, 1992), and landward tilting of marine terraces (Adams, 1984). Local uplift rates as high as 1.5 m/ky, or possibly 2 m/ky, have been suggested from studies of marine terraces in Oregon and northern California, although rates less than 1 m/ky are more common (Adams, 1984; Carver et al, 1986). South of the triple junction, deformation along the SAF results from right-lateral shear with associated localized extension and transpression. Typical uplift rates along the central and southern California coast are 0.3 m/ky (Ku and Kern, 1974; Lajoie et al, 1979a, 1979b; Muhs, 1985; Lajoie, 1986a, 1986b). Locally, uplift rates are much higher, as at Ventura in the Transverse Ranges (6-10 m/ky: Lajoie et al, 1982; Lajoie and Sarna-Wojcicki, 1982), owing to oblique plate convergence and compression.

Unusually high rates of uplift also occur at and just south of the MTJ (Fig. 1). Early studies of Quaternary marine terraces in the MTJ region (Fig. 1, Table 1) determined that uplift rates span an order of magnitude, from the typical (for coastal California) low value of 0.3 m/ky near Fort Bragg (Kennedy et al, 1982) to at least 1 m/ky farther north at Whale Gulch and Shelter Cove (Hagemann, 1982; McLaughlin et al, 1983) to 4 m/ky at Big Flat 40 km south of

the triple junction and 2.8 m/ky at the triple junction at Cape Mendocino (Lajoie et al, 1982; Lajoie, 1986).

Table 1. Previously published radiometric dates for marine terraces in the MTJ region (see text for discussion of references).

Location (from South to North)	Reference	Feature dated and elevation above sea level	Age, ka	Material dated and method	Uplift rate, m/ky
Fort Bragg	McLaughlin et al, 1983, reference to Lajoie, K.R., 1981, unpub. data; Kennedy et al, 1982	Marine terrace deposits; inner edge platform 10 m	100 or 81	Molluscs, amino-acid racemization	~0.3
Whale Gulch	Hagemann, 1982;	Marine terrace deposits; platform 15 m	44 to >57	Fossil wood debris Carbon-14	>1.0 (?)
Point Delgada	McLaughlin et al, 1983	Marine terrace deposits; platform >7 m	44.8±1.3	Fossil wood debris Carbon-14	>1.0 (?)
Big Flat	Lajoie et al, 1982	9 beach ridges, up to 30 m	0.2 - 8.9	Molluscs Carbon-14	≤4.0-5.0
Cape Mendocino (Singley Flat)	Lajoie et al, 1982	8 marine terraces and beach ridges up to 12 m	1.7, 3.1 - 3.7	Molluscs, driftwood Carbon-14	≤2.8

Although identification of anomalously rapid rates of uplift which span an order of magnitude was exciting and has stirred much interest in the relation between rapid uplift and triple junction tectonics, problems inherent in comparing uplift rates derived from individual terraces of different ages at isolated sites underscores the need for much more work in the region. Three of the above noted uplift rates (the lowest rates) represent late Pleistocene time spans, while the remaining two (the highest rates) represent mid-late Holocene time spans. In addition, the late Pleistocene uplift rates are derived from age estimates that are poorly constrained. The 0.3 m/ky uplift rate at Fort Bragg is based on an amino-acid racemization age estimate of mollusks of ~ 80 or 100 ka, while the >1 m/ky uplift rates at Shelter Cove and nearby Whale Gulch are based on minimum radiometric dates of ~45 ka (minimum age, McLaughlin et al, 1983) for fossil wood from deposits overlying marine terrace platforms. In both cases, age estimates that are regarded as age minima were then correlated with times of sea-level highstands derived from radiometrically dated coralline marine terraces in New Guinea (Veeh and Chappell, 1970; Bloom et al, 1974; Chappell, 1983; Chappell and Shackleton, 1986). Finally, amounts of uplift were obtained by subtracting the altitudes of formation of the New Guinea sea-level highstands from the present altitudes of the northern California terraces.

Late Pleistocene Surface Uplift

Altitudinal Spacing Analysis of Marine Terraces

A dearth of datable materials has precluded development of an independent record of sea-level fluctuation for coastal California, so past workers have had to use the New Guinea marine terrace record to estimate uplift rates from *individual* dated terraces (e.g., McLaughlin et al, 1983). Another alternative in lieu of datable material is to examine *entire flights* of undated terraces (Bull, 1985; Bull and Cooper, 1986). The underlying premise of this method is that a given uniform rate of uplift will produce a unique altitudinal spacing and number of terraces that can be used to infer the ages of each terrace within the flight and the overall uplift rate (Fig. 6). Merritts (1987) and Merritts and Bull (1989) used this method to estimate terrace ages and determine long-term (330 ka) rates of inferred uplift of entire flights of terraces at the same

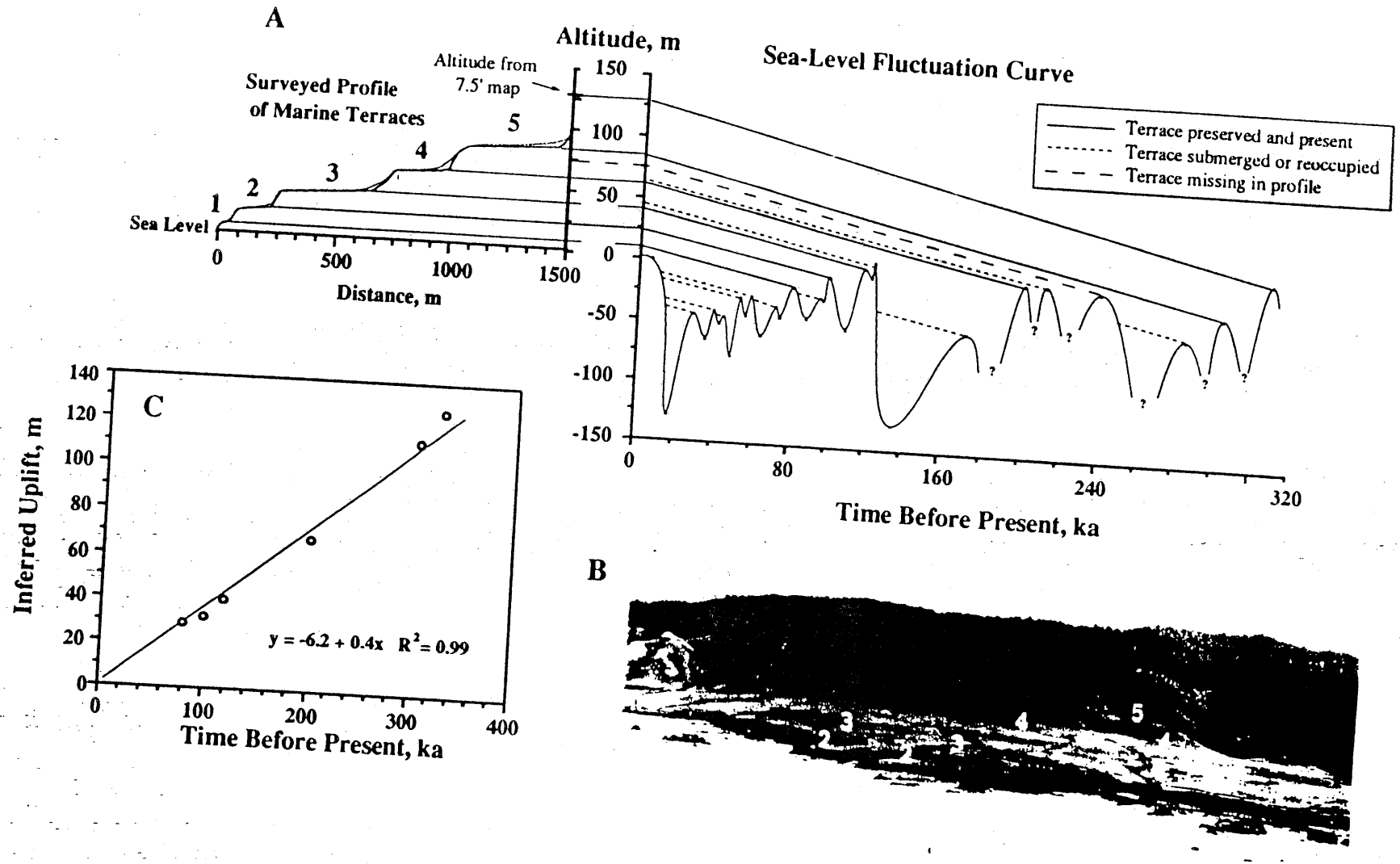

Fig. 6. A: Prediction diagram with glacioeustatic sea-level fluctuation curve and altitudes of marine-terrace remnants for Bruhel Point transect. B: Aerial view eastward of marine terrace flight surveyed at Bruhel Point, showing terraces 1-5 at 10 m, 23 m, 40 m, 61 m, and 86 m. C: Inferred uplift rate diagram that corresponds to prediction attempt in A. Equation beside curve is determined from linear regression analysis, and indicates an average uplift rate of 0.4 m/ka. (Survey data and altitudinal spacing analysis from Merritts and Bull, 1989. Sea level curve from Chappell, 1983, and Chappell and Shackleton, 1986.)

sites studied by previous workers in coastal northern California, and at numerous additional sites (Fig. 7). Their methods included two approaches to infer terrace ages and uplift rates. They first attempted to correlate terraces by surveying numerous adjacent flights of terraces, following individual terraces in the field, and comparing soil profile development on shoreline deposits mantling terrace platforms. Constrained by these correlations, they then used the altitudinal spacing of terrace inner edges within each flight to correlate individual terraces with global marine terraces dated elsewhere (methodology of Bull, 1985, and Bull and Cooper, 1986). The assigned terrace ages and inferred uplift rates obtained from the correlations can be viewed as predictions of the most probable ages, to be tested as further data are obtained.

Fourteen flights of terraces and numerous individual terraces were surveyed at sites between the Bear River and Cabrillo Point (Fig. 7). Surveys were generally accurate within ±1 m, but the precision of defining inner edge altitudes in the field commonly was ±2 m. Terrace preservation ranges from small (<10 m wide), flat bedrock benches with prominent inner edges and occasional shoreline deposits, to broad (10-400 m) bedrock benches mantled with 2-6 m of stratified marine shoreline deposits (Fig. 8). Shells of pholad clams in growth position are common on Holocene terraces, and pholad borings exist on many platforms up to 300 m in altitude. Terraces from Bear River to Punta Gorda (0-32 km, Fig. 8a) and from Bruhel Point to Mendocino Headlands (100-125 km, Fig. 6) can be tentatively correlated on the basis of their altitudes. South of 100 km, prominent, broad terraces with excellent platform exposures, known as the "Mendocino Staircase", can be followed nearly continuously for more than 20 km (Fig. 6). Between 32 and 100 km is a region known as California's "Lost Coast" because of its extremely rugged terrain and inaccessibility. The broad complex of terraces followed southward from Bear River to Punta Gorda and northward from Cabrillo Point to Westport disappears in the Lost Coast, but ridgelines are marked by occasional notched spurs and minor to prominent bedrock benches. Because of the sparsity of data, terraces between Randall Creek and Kaluna Cliff could not even be tentatively correlated based on altitudinal position.

A soils chronosequence was developed for relative age correlation of coastal terraces with shoreline deposits (Merritts et al, 1991). The prominent bench at Singley Flat (3259-3715 cal BP, see discussion of Holocene platforms below) is the only radiometrically dated terrace in the sequence. Amino-acid racemization of marine molluscan fauna from the 10-m terrace at MacKerricher State Park (near Cabrillo Point) suggests correlation with the 81 or 100 ka New Guinea terraces (Kennedy et al, 1982). Soil development (total weight of accumulated clay and iron and aluminum oxides, and clay mineralogy) on all the Mendocino terraces is pronounced; indeed, these soils are well-known for highly developed spodosols and associated pygmy forest ecosystems (Gardner, 1967; Jenny et al, 1969). Soil profiles on two of the lowest Mendocino terraces (23-m and 40-m) are similar in degree of development to those on three of the highest Punta Gorda terraces (261-m, 273-m, and 294-m). Soil development on the two lowest Punta Gorda soil sites (83-m and 111-m terraces) is substantially less than at any of the other sites, with exception of the Holocene soils at Singley Flat.

For each terrace flight, Merritts and Bull (1989) assigned ages and thus altitudes of formation to individual terraces by correlation with the New Guinea sea-level curve (ages and altitudes of formation tabulated by Bull from Chappell, 1983; Chappell and Shackleton, 1986; and Chappell, pers. comm. to Bull, 1986). The information presented above provided guidelines to assign ages to individual marine terraces during initial correlation attempts. For each correlation, graphs were plotted of inferred uplift (altitudes of local terraces minus their New Guinea altitudes of formation) versus inferred ages. The correlations were then evaluated for the most probable age assignments based on 1) the configuration of points on the inferred uplift-rate diagrams, 2) previously known terrace ages and soil profile development, and 3) the predicted correlation of coastal terraces based on altitudinal position.

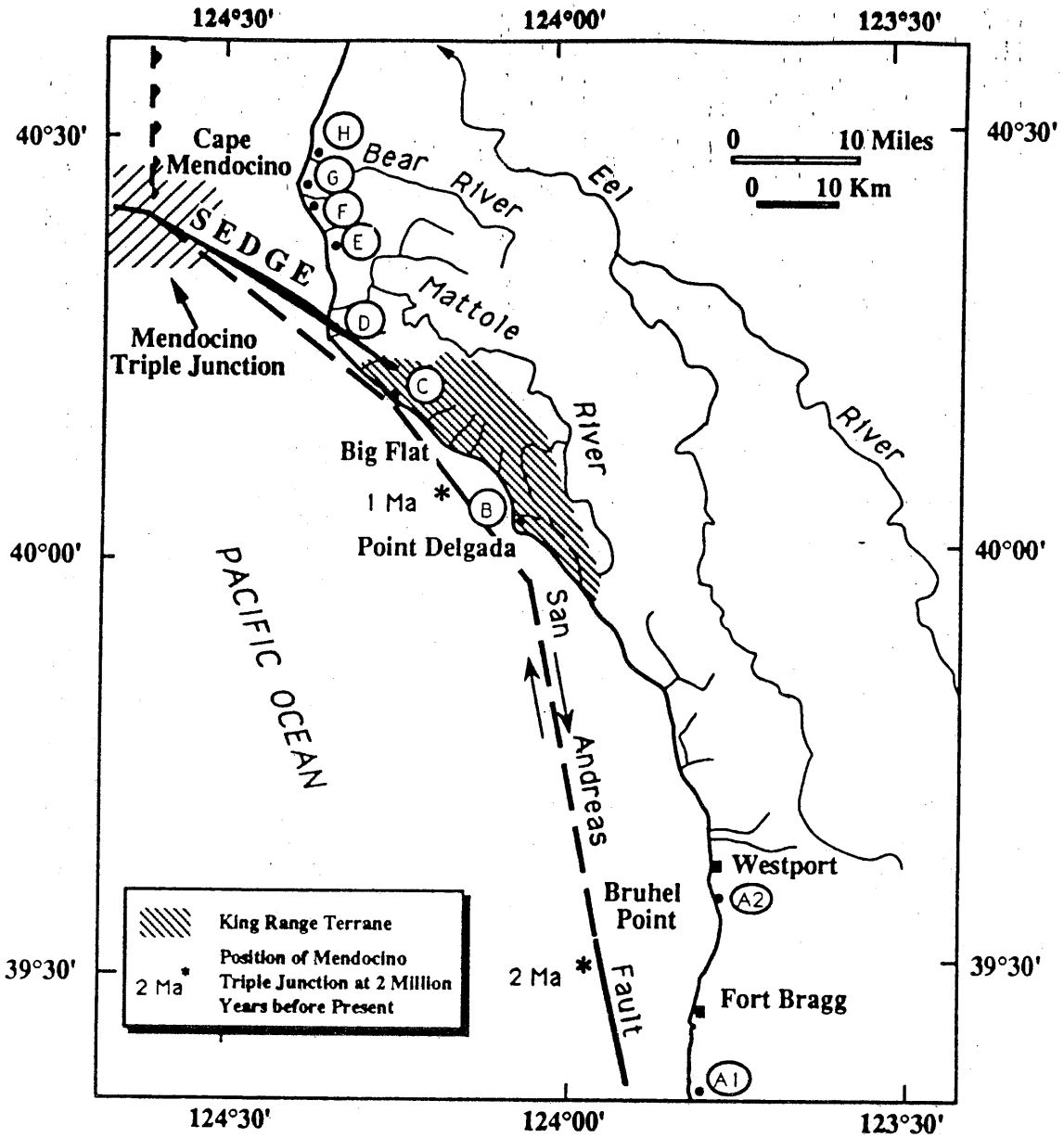

Fig. 7. Physiographic and geologic setting of coastal northern California and locations of flights of marine-terrace remnants used to infer rates of uplift. Boundary of the King Range terrane from Beutner and others (1980). Prior locations of the MTJ are indicated for 1 and 2 Ma. Marine-terrace sites: A1, Cabrillo Point; A2, Bruhel Point; B, Kaluna Cliff; C, Randall Creek; D, Smith Gulch/Punta Gorda; E, McNutt Gulch; F, Singley Flat; G, Cape Ranch; H, Bear River.

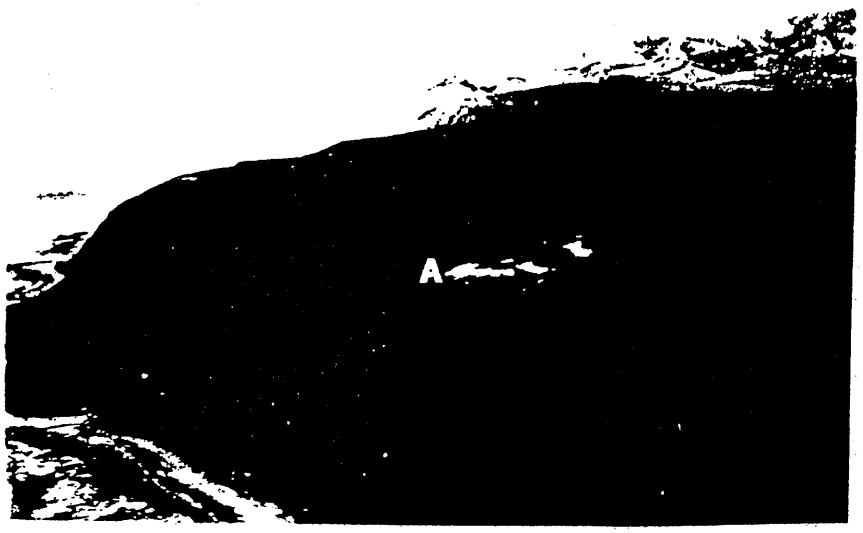

Fig. 8a. Aerial view northward along the coast from Punta Gorda to Cape Mendocino, showing site of surveys of marine terraces at Punta Gorda. Canyon in foreground is Fourmile Creek (stream # 5 in Fig. 3). A: White sand cropping out along outer edges of multiple marine terraces between approximately 239 and 294 m above sea level. Note steep escarpment below 239 m, and Holocene marine platform at base of escarpment. B: Emergent Holocene platforms exposed at Mussel Rock, the approximate location of the southern edge of the Cascadia Subduction Zone. C: Cape Mendocino and Singley Flat. Mouth of Mattole River is out of view, midway between Mussel Rock and Punta Gorda.

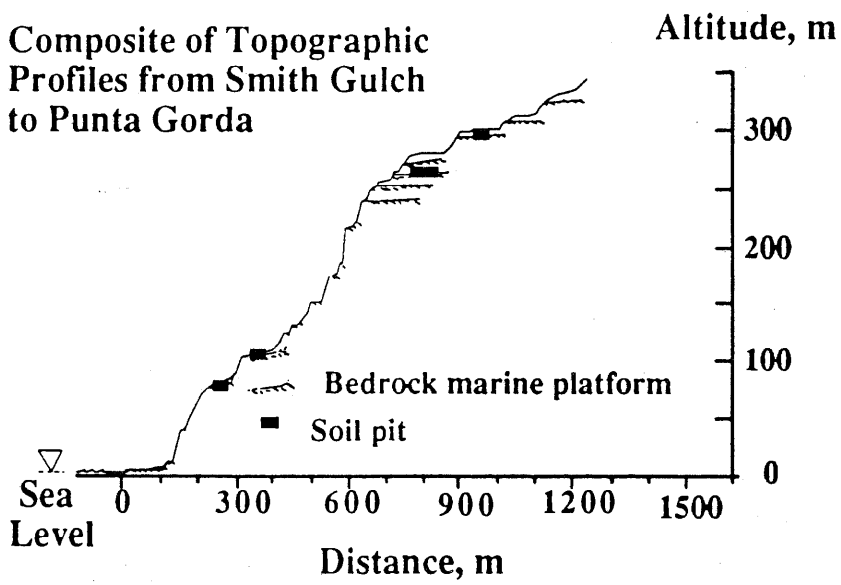

Fig. 8b. Composite topographic profile of multiple surveys of marine terraces between the mouths of Fourmile Creek and the Mattole River. Position of bedrock marine platform (hachures) is shown relative to surface topography of terrace tread. Soil pits were used by Merritts et al (1991 and in press) for work on soils chronosequences and mass balance analysis (see Chadwick et al, this volume).

The inner-edge altitudes of several prominent marine terrace platforms that we infer to be of the same age are plotted in Fig. 9. All altitudes are projected to a S60°E-trending line along the coast. At the time of formation, the inner-edges of a given marine platform were approximately subhorizontal. Deviation of such a datum from horizontal occurs due to deformation with time. Fig. 9 indicates (if the age estimates are correct) that surface uplift has been occurring in the MTJ region for at least 125 ky, and the greatest rates of uplift are in the King Range area, just south of the SEDGE. Rapid changes in the altitudes of terrace inner-edges near Randall Creek suggest that a structural boundary along which fault displacement is occurring exists between Punta Gorda and Randall Creek, in the vicinity of the Cooskie Creek shear zone (CCSZ). As discussed below, possible folding and faulting of emergent Holocene platforms has been identified at this same boundary.

Spatial and Temporal Changes in Late Pleistocene Uplift Rates

Inferred uplift rates derived from altitudinal spacing analyses of terraces by Merritts and Bull (1989) and from the terraces dated previously by other workers together define a distinct pattern of spatial variations in latest Pleistocene uplift rates when plotted along a S30°E coastal transect (Fig. 10). The pattern of differential tilt, which broadly resembles the cross-sectional shape of an anticline, is upwards towards the southern edge of the subducted Juan de Fuca plate slab (SEDGE), ~18 km south of Cape Mendocino.

One of several possible mechanisms for regional uplift is growth of a slab window south of the MTJ and associated juxtaposition of hot asthenosphere against cold lithosphere of the NAP (Furlong, 1984). The North American lithosphere responds to this thermal change and effective lithospheric thinning by thermal expansion of the crust and isostatic flexural uplift. The style of deformation can be modeled as regional time-transgressive flexure of a thin, unbroken elastic plate that would create higher uplift rates in the wake of the MTJ. Furlong's calculations of total uplift response 1 m. y. after triple junction passage is 1000-1300 m. At Point Delgada, the approximate location of the MTJ 1 m. y. ago and the SEDGE 0.6 m. y. ago, the present highest nearby altitude is 1000 m. The uplift rate determined from uplift of 1000 m over a 1 m. y. period (without correction for erosion) is 1.0 m/ky, close to that determined radiometrically by McLaughlin et al (1983) for the past 45 ka (>1.0 m/ky), and to that from altitudinal spacing analysis by Merritts and Bull (1989) for the past 330 ky (1.2 m/ky).

The area of highest uplift is about 12 km south of the SEDGE, suggesting a lag time of ~200 ky between passage of the MTJ and highest-uplift-rate response. The cause of rapid uplift seems to be migrating with the MTJ, resulting in a time-transgressive increase in uplift rates that moves northward in the wake of the MTJ. Results of the analysis by Merritts and Bull (1989) indicate temporal changes in late Pleistocene uplift rates that might be associated with passage of the MTJ and development of a slab window. Evidence of a change in uplift rates in the landscape from Randall Creek northward to the mouth of the Mattole is a prominent escarpment separating two contrasting parts of the landscape, and deep inner gorges along the lower reaches of coastal streams. At Punta Gorda, the topography above 239 m altitude resembles the broad staircase of marine terraces along the Mendocino coastline; below 239 m, a steep escarpment interrupted by small benches and notches--some with relict marine gravels--drops abruptly seaward (Fig. 8). Merritts and Bull (1989) suggested that a significant increase in uplift rates has occurred since the time of formation of the lowest broad terrace at about 239 m. Inner edge altitudes of 18 marine terrace remnants surveyed at five transects at Punta Gorda (Fig. 8b) revealed that no uniform uplift rate will produce such an altitudinal spacing; there seem to be too many terraces or too few highstands. Merritts and Bull were unable to generate an inferred-uplift rate diagram with any uniform uplift rate for this transect. After numerous correlation attempts, they obtained a correlation that consists of three segments, each with a

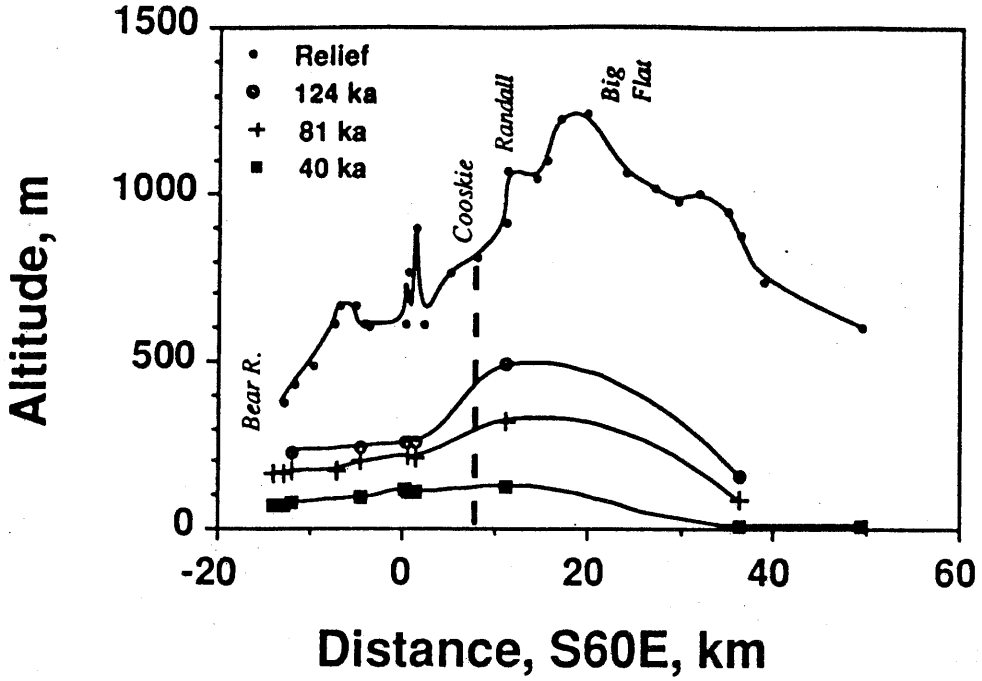

Fig. 9. Pattern of deformation of marine terraces along S60°E transect from ~Cape Mendocino to Bruhel Point; 0 km at ~ location of SEDGE. Dashed line is Cooskie shear zone.

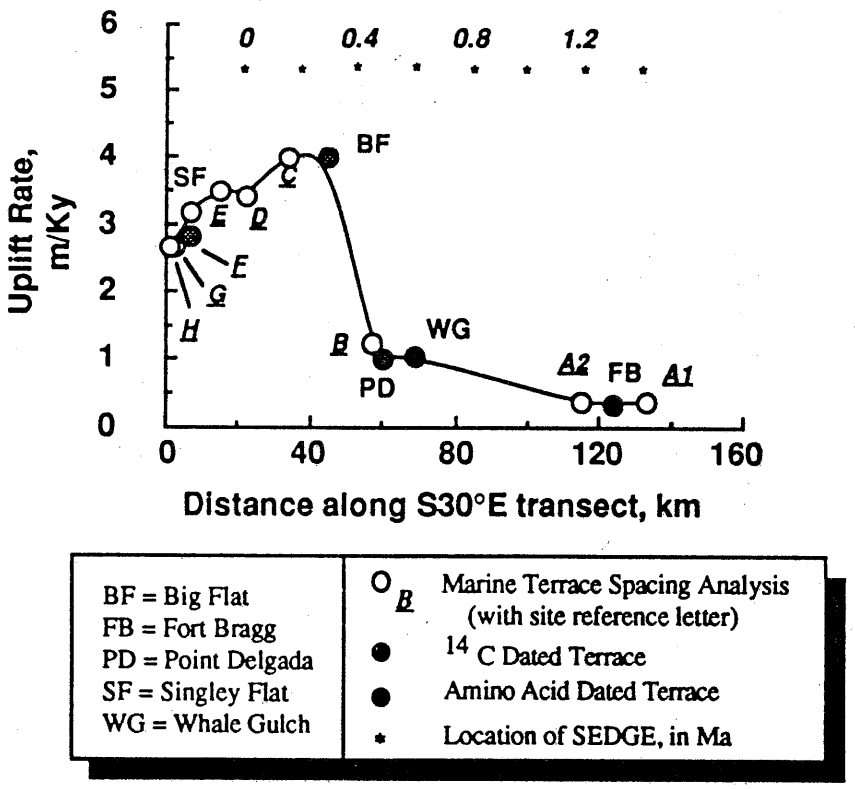

Fig. 10. Latest Pleistocene (<72 Ka) uplift rates plotted along S30°E transect from near Cape Mendocino (0 km) to Cabrillo Point (~120 km).

uniform uplift rate within that segment's time period: 0.4 m/ky from ~300-100 ka, 1.2 m/ky from ~100-60 ka, and 3.4 m/ky from ~60 ky to the present. The uplift rate for the broad terraces above 239 m is 0.4 m/ky, the same as the present rate at Mendocino Headlands (Fig. 6). The youngest segment indicates uniform uplift of 3.4 m/ky from ~60 ka to the present, consistent with Holocene rates estimated from dated terraces at Singley Flat (2.6 m/ky) to the north and Big Flat (4 m/ky) to the south (discussed below).

Accelerated uplift seems to occur both during and after passage of the triple junction, because times of increase in uplift rate, from <1 m/ky to 4 m/ky, are progressively younger towards the MTJ. Immediately north of the MTJ (Singley Flat to Bear River), inferred uplift rates have just begun to increase in the past ~70 ky, and have not yet reached maximum values of about 4 m/ky apparently associated with passage of the MTJ. Immediately south of the MTJ and directly above the northern edge of the slab window (from Punta Gorda to Randall Creek), inferred uplift rates began to increase from 0.7 to 4 m/ky about 120 ky ago at Randall Creek, and from 0.4 to 3.4 m/ky about 100 ky ago at Punta Gorda. At and south of Point Delgada, where the northern edge of the slab window passed about 600 ka, uplift rates have been uniform for at least 330 ky. More than 1.4 m. y. after passage of the southern edge of the subducted slab, at Bruhel and Cabrillo Points, uplift rates have been <0.4 m/ky for at least 330 ky. These results suggest that a drainage basin currently responding to rapid uplift near the MTJ may have been adjusted to low rates of uplift within the past several hundred thousand years. Conversely, farther south, a presently low uplift area may previously have been a rapid uplift area.

Holocene Surface Uplift

Ages and Deformation of Late-Holocene Marine Terraces

Studies of noncoralline (and hence, not easily dated) marine terraces are fraught with difficulties, unavoidable extrapolations, and interpretive despair. Because of our frustrations in working with emergent Pleistocene terraces in a region plagued by a dearth of datable materials, we began to focus on those features which would yield the most information with the least amount of ambiguity. The best preserved, most continuous, and most reliably and easily dated marine terraces in coastal northern California are the Holocene terraces (Fig. 11). Emergent Holocene marine terraces, although uncommon in the western United States, begin about 30 km north of the MTJ and occur almost continuously for ~60 km southward along the coast until they disappear ~7 km south of Big Flat (Merritts and Bonito, 1991; Merritts, unpub. mapping and data). The nearly continuous exposures across a major plate boundary of the inner edges of relatively easily dated features--which furthermore were approximately horizontal relative to the Earth's geoid at the time of formation--provide optimum conditions for obtaining a spatial pattern of surface deformation with which to compare to a variety of tectonic, geologic, and topographic features.

During preliminary work in 1990 and 1991, bedrock platforms, inner edges, and treads of emergent Holocene marine terraces were surveyed in detail with a total geodetic station along two 10-13 km segments of coastline (Fig. 12). Platform ages were obtained from multiple radiometric dates of shells found in growth positions (Merritts and Bonito, 1991). In addition, ages of marine deposits overlying the platforms were obtained from charcoal and shell debris at three sites. At least three emergent Holocene marine platforms occur at most sites. These platforms appear above sea level just south of a prominent shear zone that trends perpendicular to the coastline just north of Cape Mendocino (Fig. 12; False Cape Shear Zone). Platform inner-edge altitudes increase slightly from Cape Mendocino southward for ~13 km, then disappear (below sea level?) near another prominent east-west trending shear zone (Petrolia Shear Zone), near the mouth of the largest river in the region, the Mattole, and at the location of a large, offshore, submarine canyon, the Mattole Canyon (Fig. 2). Emergent Holocene

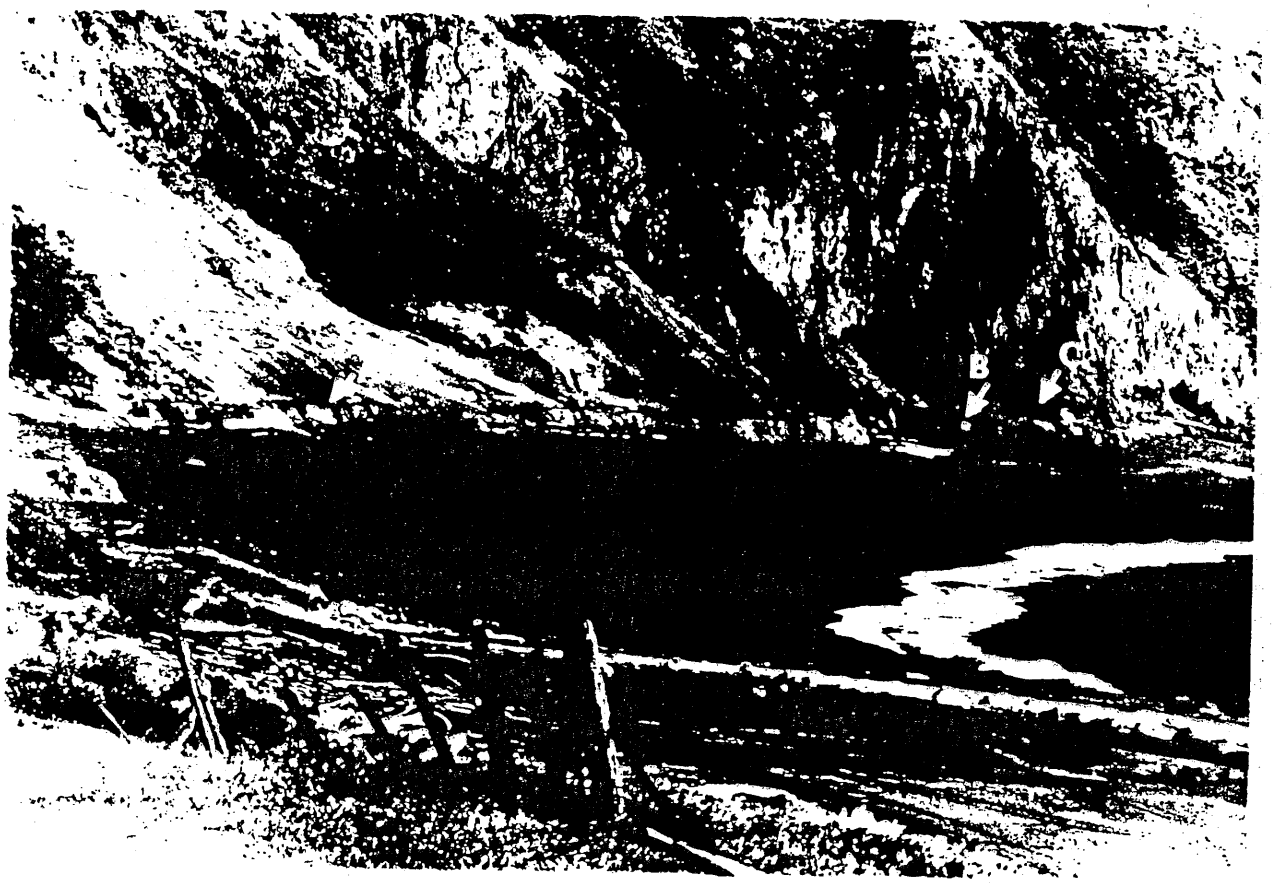

Fig. 11. Ground view of emergent Holocene (6179-6889 cal BP) platform at Hair Seal Rock. Features identified are as follows. **A**: Exposed platform overlain by Holocene dune sands; **B**: Inner edge of platform; **C**: marine sands overlying platform inner edge; **D**: Sea cave. (Photograph by W. B. Bull, 1987.)

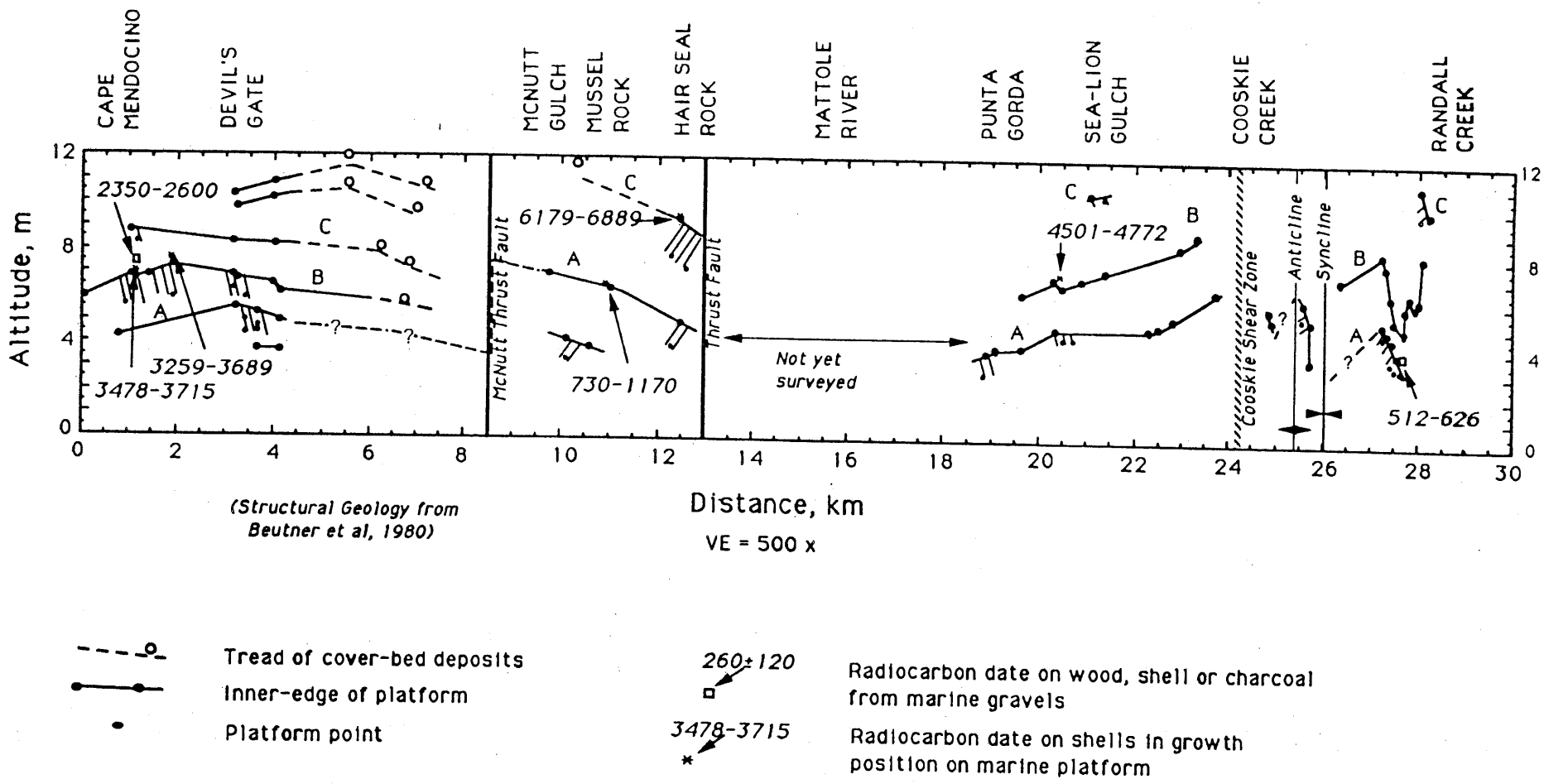

Figure 12. Surveyed altitudes of inner-edges and platform surfaces of emergent Holocene marine terraces projected along line subparallel to coastline. Hachured lines indicate relief on platform surface. Note that some radiocarbon dates are for shells found in growth positions on the platforms, while others are from charcoal or shells found in cover-bed sediments overlying the platforms.

platforms appear again several km south of the mouth of the Mattole River, and can be followed nearly continuously as bedrock exposures with minimal or nonexistent cover-bed deposits for 15 km from Punta Gorda to Randall Creek. From Randall Creek southward Big Flat (another 15 km), the coastline consists of large flats of interbedded alluvial fan and marine strata overlying emergent marine platforms. We plan to complete the surveying and dating of these terraces in 1992 (NEHRP Grant # 14-08-0001-G N2334).

The ages of Holocene marine terraces at these two stretches of coastline differ slightly (see Table 2 below; all ages are ± one sigma standard deviation). Maximum age ranges of shells found in growth positions from the three lowest Holocene platforms between Singley Flat and Hair Seal Rock are 730-1170 cal BP, 3259-3715 cal BP (2 dates), and 6179-6889 cal BP (shell samples GX-16209; GX-16210 and GX 1620; and GX-16205; Krueger Enterprises, INC., Geochron Laboratories Division; calibration reference Stuiver, Pearson, and Braziunas, 1986). The oldest terrace is probably the mid-Holocene pre-emergence terrace. We refer to these platforms as A, B, and C, from youngest to oldest. Only the two lowest platforms exposed between Punta Gorda and Randall Creek (Fig. 12) have been dated. Maximum age range for shells from a pebbly sand with abundant shell fragments immediately above the lowest platform is 512-626 cal BP (sample Beta-46742; Beta Analytic Inc.). Maximum age range for shells from borings (in growth position) in the next higher platform is 4501-4772 cal BP (sample Beta-46741; Beta Analytic Inc.). A third, higher platform that we have not yet dated also occurs. We refer to these platforms, again from youngest to oldest, as A, B, and C, and tentatively correlate them with the A, B, and C terraces north of Punta Gorda. Approximate age of formation of the A terrace is 730-1170 cal BP, as this date is from intertidal shells found in growth position on the platform. A minimum age for the A terrace is 512-626 cal BP, as this date is from shell debris deposited on the platform after it emerged above mean tide level. Ages of intertidal shells found in their growth positions from the B terrace north and south of Punta Gorda do not quite overlap, as the range in ages at Singley Flat is 3250-3715 cal BP, and that at Sea Lion Gulch is 4501-4772 cal BP. The age difference ranges from 786-1522 yrs, an amount that is within the limits of sources of error from such factors as correcting for reservoir carbon effects. Consequently, we tentatively correlate the two B terraces.

Each Holocene marine terrace platform is tilted, folded, and possibly faulted. Apparent offset of the terraces occurs immediately onshore at the southern termination of the CSZ, where a thrust fault is mapped (McNutt thrust fault of Miller, 1982; Miller and Aalto, 1983). Platforms cannot be traced across this structure, and sense of offset indicates motion is up on the south. Another locus of substantial folding and faulting occurs at the Cooskie shear zone, and indicates Holocene growth of fold structures mapped in the King Range rocks by Beutner et al (1980; Fig. 12). Strain fabric analysis at the Cooskie shear zone (Beutner, pers. comm., 1991) indicates vertical deformation.

Paleoseismic Information From Emergent Holocene Marine Platforms

From the following reasoning, we infer that the emergent Holocene marine platforms at the MTJ are probably coseismic:

1) Three platforms are tilted, folded, and faulted--if they were formed as a result of periods of intense storminess they would be subhorizontal.
2) Death assemblages of bivalve (*Pholadidae penitella*) communities with the same ages found in growth position on platforms at sites several km apart indicate sudden death over a large area.
3) Emergent platforms are local to the MTJ region; they emerge above sea level near Cape Mendocino, and can be followed almost continuously southward for about 60 km to Big Flat, where they disappear below sea level.

If platforms were uplifted during seismic events, their ages and present altitudes can be used to estimate maximum amount of uplift per event (assuming no interseismic strain) and an average uplift rate, as follows.

Table 2. Age estimates, altitudes, and uplift rates for emergent Holocene platforms.

Singley Flat to Hair Seal Rock:

Terrace #	±One Sigma Age Range, cal BP*	Maximum Altitude, m	Uplift per Event, m	Uplift Rate, m/ky
A	730-1170†	4.5	4.5	4.8
B	3259-3689† 3478-3715†	7.2	2.7	2.1
C	6179-6889†	10.5	3.3	1.6

Punta Gorda to Randall Creek:

Terrace #	±One Sigma Age Range, cal BP	Maximum Altitude, m	Uplift per Event, m	Uplift Rate, m/ky
A	>512-626§	7.0	7.0	<12.8
B	4501-4772†	9.0	2.0	2.0

* All ages calibrated with reference to Stuiver, Pearson, and Braziunas (1986).
† Radiocarbon ages of shells from platforms.
§ Radiocarbon ages of shells from sediments immediately above the platform.

An average amount of uplift per event is 3.1 m, and an average recurrence interval is ~2800 yrs. An average uplift rate (excluding terrace A from Punta Gorda to Randall Creek in the calculation, because its age estimate is a minimum for the platform) is 2.6 m/ky. For this same region, altitudinal spacing analysis of emergent Pleistocene strandlines results in an inferred uplift rate of 2.8-3.4 m/ky (Merritts and Bull, 1989).

Recent Crustal Deformation

Historic Seismicity

Although seismicity is high in the Cape Mendocino region, seismic evidence is difficult to interpret due to errors in locating epicenters (up to 50 km error for events located prior to the 1950s), and to complexities in interpreting focal mechanism solutions (Smith and Knapp, 1980). These difficulties result from poor station control, especially to the west and south, and from substantial lateral variations in seismic velocities. Since the 1970s, however, increased research on the seismicity of the region, relocation of epicenters, and new station coverage have resulted in a burgeoning seismic database (c.f., McPherson, 1989). In general, four seismic zones can be defined:

1) An offshore zone of high seismicity along the east-trending MFZ, with predominantly right-lateral focal mechanisms (Simila, 1980; Smith and Knapp, 1980).
2) A zone of scattered seismicity throughout the Gorda deformation zone, with mostly left-lateral focal mechanisms along northeast-trending faults (Eaton, 1981).

3) A zone of scattered onshore seismicity in the upper NAP in the Petrolia-King Range area, with right-lateral and thrust solutions along northwest-trending structures (Simila, 1980; McPherson and Dengler, 1991; Oppenheimer and Magee, 1991).
4) A zone of diffuse onshore seismicity from 12-30 km depth, in the subducted JFP, with strike-slip solutions along vertical structures (Smith and Knapp, 1980).

The axes of maximum compression stresses are generally north-south for all events in the vicinity of the MTJ. Interestingly, the northern San Andreas itself has been aseismic for most of this century since the 1906 event (Simila, 1980).

On August 17, 1991, and April 25, 1992, the largest historic earthquakes (M_L 6.0 and 6.9, respectively) recorded in the onshore MTJ vicinity occurred along or close to the Cooskie shear zone (Fig. 5 and 9). Focal mechanism solutions for the 1991 event indicate NE thrusting on a N45°W striking plane dipping 35-45°SW, at a depth of 12.3 km (McPherson and Dengler, 1991; Oppenheimer and Magee, 1991). The April 25, 1992 mainshock was also along a NW-trending reverse fault, at a depth of 11 km. Aftershock patterns suggest that the 1992 event was along a gently NE dipping plane, and was probably a subduction zone event. Seismic activity is still high, and numerous events with magnitudes from 3-6.5 have occurred after both events. The largest aftershock to date was the offshore April 26, 1992, 6.5 event, which occurred in the Gorda deformation zone along a N-NE-trending vertical strike-slip fault at a depth of ~20 km.

Seismicity and Holocene Uplift

As more data become available regarding the nature of onshore seismogenic structures, it might become possible to correlate them with the pattern of deformation recorded by emergent Holocene platforms along the coast. Furthermore, the surveys initiated by Merritts along the coast will be complete by the end of 1992, and a detailed picture of the pattern of Holocene deformation for the entire MTJ region will be available. At present, some speculations about the relations between emergent platforms and seismogenic structures are possible. First, for the reasons stated above, we consider the emergent platforms to be the result of coseismic uplift. Second, the platforms are tilted, folded, and faulted, and faulting at two localities coincides with mapped structures: the McNutt fault and the Cooskie shear zone (CCSZ). Offset at the McNutt fault indicates that motion is up on the south (Fig. 12). At the CCSZ, Holocene platforms are complexly folded and faulted. At this same location, we are unable to trace individual Pleistocene platforms to the south into the King Range, and late Quaternary uplift rates increase rapidly (Merritts and Bull, 1989). It is possible that Holocene motion along the CCSZ--which forms the northern and eastern boundaries of the King Range terrane--is similar to that of the August 1991 earthquake, characterized by thrust faulting to the northeast. This would explain the greater uplift rates of the King Range, and the increased folding and offset of Holocene platforms at the northern boundary of the King Range. Finally, the repetitive pattern of emergence and submergence of Holocene platforms along the coastline, combined with up-on-the-south motion at the McNutt fault and historic thrust-faulting along the CCSZ, leads us to propose that Holocene crustal deformation at the MTJ is due to imbricate thrust faulting and folding associated with N-S maximum compression stresses.

Strain Rates from Geodetic Surveys and Modelling

We can add yet another layer of information to the tectonic, geologic, geomorphic, and seismic database--strain rates and vertical velocity fields obtained from historic geodetic surveys (Lisowski and Prescott, 1989; Lisowski et al, 1991; Mitchell et al, 1991). Historic strain rates, like Pleistocene and Holocene uplift rates, increase rapidly towards the MTJ from both the north and south (Mitchell et al, 1991). South of the MTJ region, near Point Delgada,

maximum compression axes are oriented north-south, with 20-30 mm/yr of right-lateral shear strain and 10 mm/yr contraction (Lisowski and Prescott, 1989). To the north, compression axes rotate eastward, to ~N31°E between Cape Mendocino and Eureka, with uniaxial contraction and 15 mm/yr shortening.

Additional evidence regarding shear stresses has been obtained from modelling of the state-of-stress in the southern JFP (Jachens and Griscom, 1983; Wilson, 1986). Jachens and Griscom treated the southern JFP as an homogenous, isotropic, elastic plate and constructed a finite element model to analyze its state of stress. Their model (Jachens and Griscom, 1983) predicts highest shear stresses at the coast between Cape Mendocino and Punta Gorda, and north-south to northeast-southwest oriented maximum compressive stresses. Wilson's (1986) kinematic strain rate model of the southeastern part of the JFP also predicts maximum compressional strain rates (north-south) and hence maximum internal deformation at the easternmost end of the MFZ, where the space problem resulting from reorientation of the southern JFP is greatest.

GEOMORPHIC INDICATORS OF QUATERNARY UPLIFT

Analysis of Small Coastal Streams

The observations of anomalously high rates of surface uplift in the MTJ region were published in 1982 (Lajoie et al) and 1983 (McLaughlin et al), while the first author was developing a Ph. D. project in tectonic geomorphlogy at the University of Arizona (Merritts, 1987). With its spatially uniform climate and rock resistance, the area provided a unique opportunity to achieve the author's thesis objective: to define empirically the connection between *known* intensities of uplift and resultant morphological features for a given climate and rock type, then to develop hypotheses that relate morphogenesis to crustal movements. This work differed from most other studies in tectonic geomorphology, in that no Holocene fault scarps have been identified in the MTJ region, stream channels are bounded by bedrock and thus have little chance to adjust their geometries laterally, and mountain fronts are modified by coastal erosion. Furthermore, coastal California is a humid region with rapid erosion rates and dense forests, limiting both exposures and accessibility. The approach emphasized then, by necessity, was to compare three-dimensional morphological properties obtained from 1:24,000 topographic maps of twenty-five second- and third-order drainage basins that have evolved in areas of low(<1 m/ky), intermediate (1-3 m/ky), and high (>3 m/ky) rates of uplift (Fig. 3). Variables obtained with a digitizer for each drainage basin were stream length, drainage area, and channel slope of each first, second, and third-order stream segment. In addition, azimuthal orientation, from head to mouth, of each first-order stream segment was measured with a protractor.

This work led to several publications (c.f., Merritts and Vincent, 1989), and spawned much more work in the region on the relations between tectonics and topography (c.f., Merritts et al, 1991). Two of the methods used by Merritts and Vincent (1989) to compare morphologic variables between coastal basins are presented here. The first is a multivariate correlation analysis of linear, aerial, and vertical morphologic variables of each basin. The second is a spatial comparison of individual morphologic properties to the uplift rate curve of Fig. 10.

Multivariate Correlation Analysis

Fourteen morphologic variables were analyzed by Merritts and Vincent (1989) in an attempt to determine which variables are most highly correlated with uplift rate. The variables

of relief and uplift rate themselves have a correlation coefficient of 0.68, suggesting that relief--for which more data are available--is a reasonable proxy for uplift rates to compare its correlation with other drainage basin variables. The results of the correlation analysis indicate that relief and uplift rates have moderately high positive correlations with first- and second-order channel gradients (Pearson correlation coefficients). Increasingly higher order channel gradients have increasingly lower correlation coefficients with uplift rates and relief; correlation between uplift rate and first-, second-, and third-order channel gradients is 0.73, 0.60, and 0.33, respectively, and between relief and first-, second-, and third-order channel gradients is 0.73, 0.54, and 0.46, respectively. The variables of channel length, sub-basin drainage area, and drainage density have low correlations with uplift rate and relief, with the exception of channel length and area for first-order streams, which have moderately high negative correlations with uplift rate (-0.62 and -0.73, respectively), but no correlations with relief. Other correlations that are relevant to analysis of tectonic controls are the moderate to high negative correlations between drainage basin area (third-order area) and channel gradients (which increase in correlation with higher order streams). Interestingly, the variables of basin length, third-order stream length, and third-order basin area have low correlations with first-order channel gradient, thus negating the possibility that size of the drainage basin is the cause of steeper first-order gradients.

Spatial Variations in Morphologic Properties of Drainage Basins

In the second analysis of fluvial response to uplift, by Merritts and Vincent (1989) examined individual variables. The mean drainage basin value of each morphological property is projected onto the same S30°E coastal transect as the uplift rate curve of Fig. 10 (Fig. 13a). Individual planimetric properties (e.g., mean drainage basin density) vary little throughout the study area (Fig. 13b); however, vertical properties--especially maximum relief and mean drainage basin channel gradients--vary substantially (Fig. 13c). Planimetric network properties that appear to be largely insensitive to uplift rate and relief probably are more strongly related to lithologic and climatic conditions. Similarities in drainage density throughout the region, for example, suggest that the initial assumptions of effectively uniform climate and rock resistance are valid. The significance of the relief and channel gradient plots is that 1) the shape of each curve is similar to that of the uplift rate curve; 2) the greatest variation in channel gradients is among first-order streams, which vary from 7° to 24.4°, the lowest values being near Fort Bragg and Singley Creek, and highest values immediately north of Big Flat; and 3) variations in channel gradient decrease with increasing stream order, or power (Fig. 13c). The plot of second-order channel gradients shows a similar geographic pattern to that of first-order channels; channel gradients vary from 1.2° to 10.4°. Likewise, third-order channels have low gradients of 1.2° in the north, at Singley Creek, and of 0.9° in the south at DeHaven Creek, and high gradients of 3.4° and 5° at Spanish Creek and Big Creek, respectively (Fig. 13c). All three stream orders show channel gradients that gradually steepen towards Big Flat and Big Creeks from both the north and the south.

Discussion of Morphologic Analyses

The observed trends in channel gradients seem to correlate directly with spatial variations in uplift rates. With increasing stream order, and hence power, channel gradients are less altered by tectonism. We propose the following explanation. During rapid uplift, streams are rejuvenated, channels incise, stream gradients increase, and valley walls become oversteepened. Larger streams are able to maintain their profile forms through time by incising rapidly enough to adjust to lower base levels. Smaller tributaries are unable to incise an amount equal to the base-level fall, hence they accumulate the effects of net base-level fall over a period of time, and have steepest profiles in the areas of highest uplift rates. This conclusion

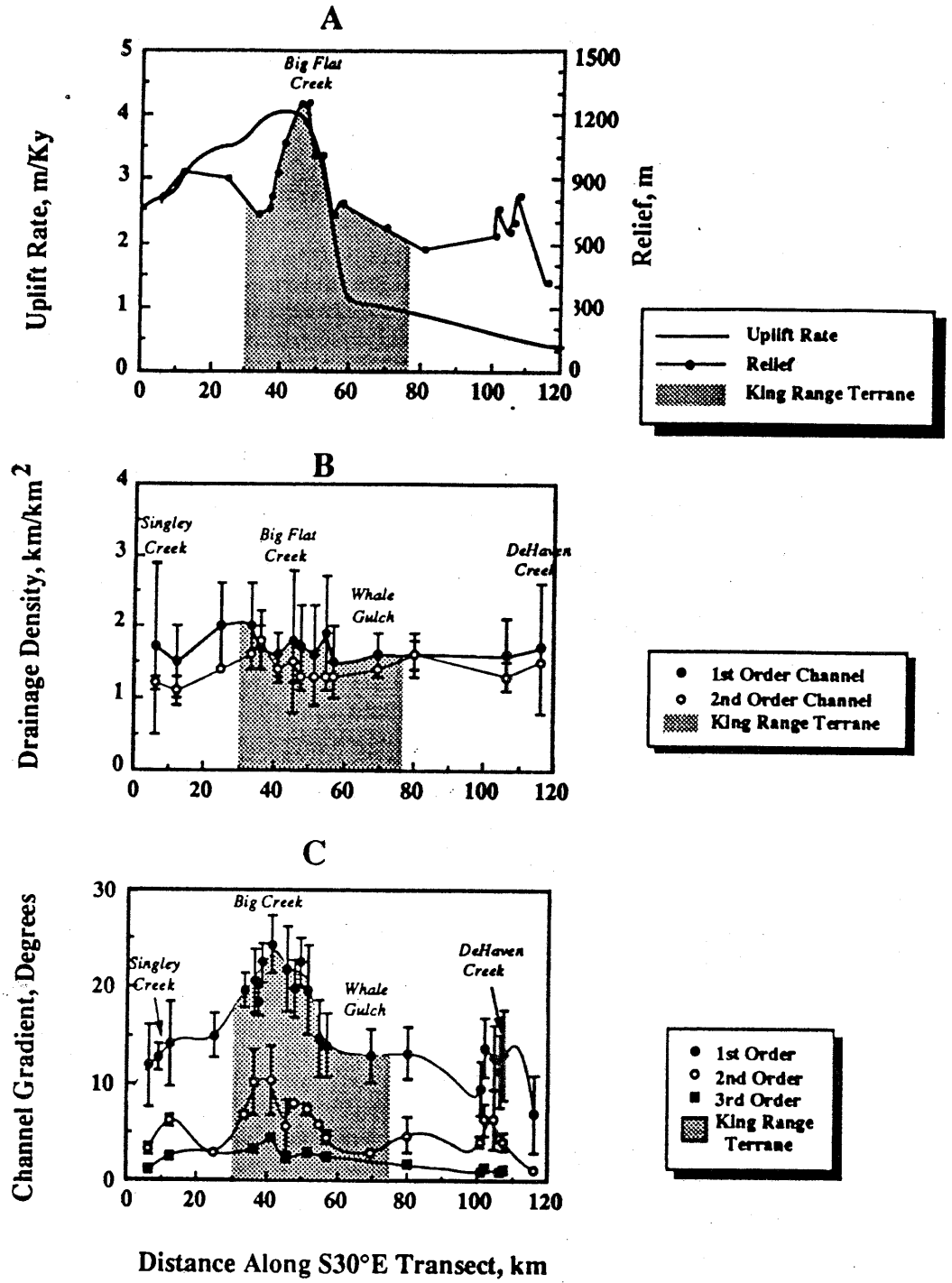

Fig. 13. A) Surface uplift rates and maximum relief; B) mean drainage density of first- and second-order sub-basins; and C) mean channel gradients of first-, second-, and third-order subbasins for each coastal drainage basin, along a S30°E transect from Cape Mendocino (0 km) to Fort Bragg (~120 km). Error bars are plus-or-minus one standard deviation.

suggests that studies of gradients of lowest magnitude streams will be most useful in identifying tectonically active areas.

Although the trends in mean channel gradients (Fig. 13c) might be related to increasing rock resistance or slightly higher precipitation in the center of the study area, we consider them to be a reflection of higher uplift rates for several reasons. First, although a difference in rock erodibility that would be great enough to cause a three- to five-fold increase in mean basin channel gradients should cause some variation in drainage density, no such change is observed (Fig. 13b). Second, channel gradients of all three orders increase regularly from Singley Creek to Big Creek, then decrease regularly from Big Creek to Telegraph Creek. Third, the geomorphic map of S. Ellen (unpub. USGS map; pers. comm., 1986) indicates that "soft" rocks dominate the Singley, Davis, Spanish, and Big Creek drainage basins, in which mean first-order channel gradients nonetheless increase from 11.9, to 14.2, 20.6, and 24.4°, respectively. Merritts and Bull (1989) have shown that inferred latest Quaternary uplift rates increase southward from 3.2 m/ky at Singley Creek, to 3.5 m/ky near Davis Creek, and to 4 m/ky near Spanish and Big Creeks. Finally, field evidence indicates that drainages in the high-uplift rate areas are subjected to rapidly falling base levels (or, rising land mass). The mouths and lower reaches of drainage basins in the highest uplift rate areas are narrow, v-shaped gorges and contain bedrock strath terraces which converge upstream (examples are prominent at Randall Creek, Kinsey Creek, Oat Creek, and Big Creek). These terraces are indicative of falling base level, not resistant rock types.

The most striking evidence that the trends in channel gradients are related to uplift rates is their correspondence to the uplift rate curve. The curves are roughly parallel with one another and with the gross topography of the mountain crest (Fig. 13a and 13c). The peaks of the uplift rate, first-order channel gradient, and maximum relief curves are not coincident, but lag behind one-another and behind the MTJ. Using a migration rate of 5.6 cm/yr (56 km/m. y.) for the MTJ, we calculate the following lag times for each response after passage of the subducted Gorda plate slab and development of a slab window: highest uplift rates---~160-290 ky; steepest first-order channel gradients---~290-620 ky; and highest maximum relief---~370-700 ky. Ranges in time periods are the result of uncertainties in the location of the SEDGE and MTJ. These calculated lag times are reasonable, in that accelerated uplift rates must occur over some finite time period in order to create steepened first- and second-order channel gradients, and to create substantial relief. In this case, ~130-330 ky of high uplift rates is required to create maximum channel gradients, and ~210-410 ky is required to create the maximum relief of the King Range.

DISCUSSION OF QUATERNARY TECTONICS

Mechanisms of Crustal Deformation and Mountain Building

By synthesizing the work done on Pleistocene marine terraces by Merritts and Bull (1989), on Holocene marine terraces by Merritts (Merritts and Bonita, 1991, and work in progress), and on geomorphic response of coastal streams to crustal deformation by Merritts and Vincent (1989), we have developed a number of constraints regarding the nature of deformation in the MTJ region:

1) the regional pattern of differential tilt, which broadly resembles the cross-sectional shape of an anticline, is upwards towards the edge of the subducted slab, ~18 km south of Cape Mendocino (Merritts and Bull, 1989);
2) the cause of rapid uplift seems to be migrating with the MTJ, resulting in a time-transgressive increase in uplift rates that moves northward in the wake of the MTJ (Merritts and Bull, 1989);

3) the area of highest uplift rates is about 9 km south of the present location of the southern edge of the subducted Juan de Fuca plate slab, suggesting a lag time of ~160-290 ky (range due to uncertainties in locating the MTJ) between passage of the MTJ and highest-uplift-rate response; (Merritts and Bull, 1989);
4) there is excellent correspondence among the spatial pattern of uplift rates, trends in mean 1st, 2nd, and 3rd order channel gradients, and the topography of the mountain crest (Merritts and Vincent, 1989), indicating that rapid uplift in association with the migrating triple junction has occurred for a long enough period to result in generation of the primary landscape morphology; and
5) an envelope map† of the highest parts of the topography in the MTJ region indicates that an imaginary upper surface resting on the landscape has the shape of an asymmetrical antiform that trends S30-60°E and plunges to the NW and SE, with the steep limb on the southwest. The crest of the antiform lies along the southern margin of the Mattole Valley, above and to the north of the estimated location of the SEDGE (Merritts, unpub. data from 1:62,500 topographic maps).

At least three models have been proposed to explain the cause(s) of rapid uplift at the MTJ. One of these is isostatic, a second is isostatic and thermal, and the third is geometric--i.e., based on the assumption of a space problem. We next consider these models in light of the tectonic and geomorphic observations presented above.

Jachens and Griscom (1983) determined from calculations of isostatic residual gravity anomalies that the coastal part of the NAP north of the SEDGE is isostatically imbalanced. They proposed that imbalance might be the result of the tendency of young, low-density oceanic lithosphere of the southern JFP to be buoyant and rise when subducted, and predicted greater uplift rates at and *north* of the SEDGE. The geomorphic data on marine terraces and drainage basin morphologies, however, indicate that late-Quaternary surface uplift rates are highest above and *south* of the SEDGE, and seem to be more a function of the lack of an underlying subducted plate than the presence of one.

Furlong (1984) has developed a model of thermo-mechanical response of the NAP to development of a slab window in the wake of the MTJ. This model--which treats the NAP as an unbroken elastic plate--predicts that asthenospheric upwelling associated with northward migration of the MTJ will result in warming of the basal NAP and consequent thermal uplift. A much greater mechanical response, however, is calculated to result from isostatic uplift of the NAP due to removal of the underlying subducted southern JFP slab. Total uplift response about 1 m. y. after development of a slab window is 1.2 km. The pattern and amount of tilt determined from marine platforms is in excellent agreement with this model, especially the observations that uplift rates have increased in the wake of the MTJ, and that highest rates of uplift occur south of the SEDGE, as is predicted by a model that invokes a time-dependent thermal and isostatic-mechanical response. A clear difference between the models presented by Jachens and Griscom (1983) and Furlong (1984) is that the former invokes the warmth (and resultant low density) of the southernmost JFP as a cause of uplift north of the SEDGE, while the latter invokes the greater warmth of the asthenosphere relative to the NAP as a cause of uplift south of the SEDGE.

One other proposed cause of deformation and surface uplift in the MTJ relies on compression and shortening due to plate geometries specific to the MTJ. Many have cited the geometry of the northern SAF itself, with its left-stepping restraining bend as it joins the MFZ, as a cause of transpression and rapid uplift, and have referred to similar bends and uplift

---

† An envelope map is a contour map of altitudes along drainage divides, and represents an upper limit for the landscape.

elsewhere in California, such as in the Ventura region (c.f., Dumitru, 1991). Other causes of rapid uplift might be the high shear stresses predicted to exist by Jachens and Griscom (1983) and Wilson (1986) in the Punta Gorda region as a result of reorientation of the southernmost Juan de Fuca plate during the past several million years (see discussion above). In both cases, these models predict greatest uplift rates in the areas with the greatest space problem--i.e., the corner of the Pacific Plate at Punta Gorda--and localized rapid rates of uplift rather than regional tilt. Our patterns of crustal deformation obtained from both Holocene and Pleistocene marine terraces indicate much greater deformation immediately south of SEDGE than north of it. We are unable to follow Pleistocene terraces south of Randall Creek into the King Range terrane, and Holocene terraces are extremely deformed between Cooskie and Randall Creeks, along the Cooskie shear zone which forms the northern boundary of the King Range terrane. These results are in excellent agreement with models based on space problems local to the King Range area.

Dumitru argues from apatite fission-track ages and lengths that rapid uplift is local to the King Range area, that at least 2-5 km of rock has been uplifted and unroofed, and that several tens of degrees of northeastward tilting have occurred in the past 1-2 m. y. (It should be noted that fission-track analyses yield amounts of rock uplift, not surface uplift. See, for example, discussion by Molnar and England, 1991.) Because his results indicate localized rock uplift of much more than 3 km, in contrast to Furlong's calculation of aerially extensive uplift of 1.2 km, Dumitru favors a model of localized compression and shortening due to space problems at the migrating triple junction. Furthermore, Dumitru has determined that the headland at Point Delgada, at the southwestern corner of the King Range, has had a vastly different thermal and tectonic history than the King Range, with vertical stability for the past 12 m. y. Consequently he infers that while the King Range rocks have been uplifted and unroofed during the past 1.2 m. y., the rocks at Point Delgada have only recently been translated to their present position, perhaps due to lateral motion along a strike-slip fault separating Point Delgada from the King Range. If a major strand of the San Andreas fault forms this boundary, and its slip rate is about 5.6 cm/yr, or 56 km/m. y., then the Point Delgada rocks could have moved from the southeast to their present location even as the King Range rocks were raised 2-5 km. However, this would require that a substantial amount of vertical offset (east side up) is also occurring along the proposed fault. If vertical motion is about 5 km in the past million years, the ratio of vertical to lateral motion is ~one to five.

At present, our geomorphic observations are not inconsistent with Dumitru's results from apatite fission track analyses; however, his results--as well as those of Furlong (1984)--explain only part of the pattern of uplift obtained from emergent marine platforms. This pattern indicates that in addition to rapid uplift rates south of SEDGE, moderate rates of surface uplift occur well north of the King Range, in fact as far as 32 km to the north, to the southern edge of the Eel River Basin at the False Cape Shear Zone. It also indicates regional tilt upwards to the south from False Cape to Punta Gorda, at the edge of the King Range, of 0.002°/ky. Because deformation becomes much more rapid and complex at and south of the northern edge of the King Range, it is probable that several mechanisms are causing rapid uplift between False Cape and Point Delgada.

We hope that the results of detailed surveying of Holocene marine platforms from False Cape to Point Delgada (a distance of more than 65 km; work in progress under a National Earthquake Hazards Reduction Program grant from the USGS to Merritts, 1992-1993) will enable us to fully evaluate the probable cause(s) of rapid surface uplift in this region. Until that work is completed, we can make some speculations on the causes of uplift based on our analyses of Pleistocene marine platforms, fluvial system morphologies, and regional elevations (envelope map and analysis of relief). We propose that the dominant control on regional uplift is somehow related to the position, trend, and migration rate of the SEDGE beneath the NAP. The actual mechanism(s) for this regional response could be isostatic imbalance of the NAP

north of SEDGE (Jachens and Griscom, 1983), thermal and mechanical uplift south of it (Furlong, 1984), and warping above the 1 km Mendocino Ridge (Jachens and Griscom, 1983). Regardless of the combination of causes, uplift is greatest at and just south of SEDGE, and has only recently begun to occur to its north. Superimposed on this regional uplift and tilt is localized shortening and vertical strain that is greatest south of the SEDGE, perhaps because of space problems due to late Neogene obduction of the King Range terrane, eastward relocation of the unstable MTJ, reorientation of the Juan de Fuca plate, or bends in the SAF.

FLUVIAL RESPONSE TO TECTONISM

The Response of Large Coastal Rivers to Base-Level Change

Earlier in this paper, we used tectonically sensitive elements of the landscape--first order tributaries to small coastal streams--to provide constraints for geodynamic models (see Merritts and Vincent, 1989). In this section, we do the converse. We examine the geomorphic response of large rivers to long-term base-level change, using tectonic information derived from marine terraces to provide control on rates of base-level change at the mouth of each river. We surveyed and radiometrically dated fluvial landforms along three large coastal rivers at the MTJ. Our approach is field-based, and differs from most other studies of the response of fluvial systems to base-level change, which generally fall into one of three categories:

1) analytical modelling;
2) physical modelling, e.g., flume studies; and
3) field studies of response of small alluvial streams to perturbation, such as land use change.

Few investigators have examined either bedrock rivers or large river systems, in part because appropriate technologies such as electronic distance meters and data loggers have only recently become available.

We recently surveyed in great detail the channels, bars, floodplains, and terraces of three large (up to 100-km long) bedrock rivers at the MTJ that are characterized by flights of marine terraces at their mouths, and fluvial terraces along much of their lengths. Up to 1300 points were surveyed on each river and projected in map view to a mid-valley axis to obtain longitudinal profiles. Rock type, climate, climatic history, and vegetation are similar for each, but uplift rates vary an order of magnitude, from 0.4 m/ky to ~3-4 m/ky. We focus on one of these rivers, the Mattole, in this paper. It is the largest (drainage basin area 655 km^2; trunk stream length 97 km), and is in the region of highest uplift rates (2.5-4.0 m/ky).

Our major objective is to better understand the interplay between base-level change and fluvial processes of bedrock incision and sediment deposition. Base-level change is the result of both tectonic/isostatic processes of upheaval, and eustatic processes of sea-level rise and fall. By working with a river for which approximate rates of base-level change through time are known, we hope to answer the following questions regarding the formation and significance of terraces.

- When and how does a river form and abandon a strath terrace? During sea-level highstands? Or lowstands? Or while sea level is rising or falling?
- Can terrace remnants along large meandering bedrock rivers be correlated in order to reconstruct past longitudinal profiles?
- Do terraces indicate that base-level change has occurred?
- How far upstream are effects of base-level change due to eustatics and/or tectonics transmitted?

- Do adjacent rivers have similar numbers and spacings of fluvial terraces that are synchronous?

Fluvial Terraces, Base-Level Change, and the Graded Stream

The mouth of each of the rivers investigated, at the Pacific Ocean, is characterized by spectacular flights of fluvial and marine terraces. Each of the marine terraces formed during a time of sea-level highstand during the late Quaternary Period. When viewing the mouth of one of these rivers, it is easy to imagine that the fluvial terraces merge with the marine terraces, and hence further to deduce that lateral valley floor planation--i.e., the formation of a strath surface--occurs during times of sea-level highstand. Abandonment due to vertical incision must occur then during times of falling base level, prior to sea-level lowstands. However, our detailed surveying and radiometric dating of fluvial and marine terraces for the Mattole and Bear Rivers indicate that such an interpretation, which seems reasonable to the average geomorphologist, is incorrect, as discussed below. Before presenting the results of our surveys and our interpretations of this information, we define a conceptual model of a graded river and its response to base-level change.

Conceptual Model for Upstream Transmission of Base-Level Change

In 1948, H. J. Mackin described a graded stream as one with a

> ". . . slope that will provide the velocity required for transportation of all the load supplied to it from above. . . [it] is a slope of transportation; . . . influenced directly neither by the corrasive power of the stream nor bedrock resistance to corrasion."

Mackin viewed the long profile of a graded river as an indication of a system in steady-state equilibrium, a system adjusted to the prevailing sediment load. Le Chatelier, a chemist, had earlier described the reaction of a system in equilibrium to a change:

> "If any stress is brought to bear on a system in equilibrium, a reaction occurs, displacing the equilibrium in a direction which absorbs the effect of the stress."

This reasoning could be interpreted by geologists to mean that if the level of water at the mouth of a stream is lowered (base-level fall) and the stream's gradient is increased as a consequence, the channel will incise in order to reduce its gradient to its previous level. Conversely, if base-level is raised and the stream's gradient is decreased, the channel will aggrade in order to increase its gradient. Geologists developed a number of questions from this basic model, such as "How is base-level change transmitted along a stream, and how far upstream is the effect of such a change transmitted." A more fundamental question, perhaps, was simply how one determines whether or not a stream is graded. Leopold and Bull (1979) answered this question by stating that a graded stream is one that is neither aggrading or degrading, according to the original ideas of Gilbert (1877).

In an active orogenic belt, one might suppose that no streams should be in equilibrium, as all are actively degrading. Merritts and Vincent (1989) disagreed, however, and suggested that a stream incising bedrock in response to an effective base-level fall may maintain a steady longitudinal shape by uniform incision along its length. According to this model, the size and power of a stream are of great importance in determining the ability of the stream to incise. For a given rate of uplift, smaller streams will be steeper than larger streams in order to maintain the power necessary to incise at a rate equal to that of the uplift rate. The stream is only able to incise uniformly if it is able to transmit all of the base-level change from its mouth upstream along its length. If a reach is encountered that has insufficient power to incise at an amount equal to the base-level fall, the bed altitude and consequently the gradient of that reach will

increase relative to the next downstream reach. At any given point, the altitude of the bed will change at a rate equal to the rate of uplift minus the rate of incision.

Many workers have considered Mackin's definition of a graded river and Le Chatelier's model of system response to change as an indication that terrace remnants along a river represent discrete events which acted to displace the system from equilibrium. For example, a fill terrace might represent an aggradational event in response to fluctuations in sediment loads due to climatic change, and abandonment of a strath terrace (cut surface in bedrock) might represent sudden movement along a fault or an increased rate of uplift. It is our contention here that we need to know more about fluvial response to change before we are able to infer from the terrace record that discrete events have occurred. To obtain such knowledge, we have conducted the investigation presented below. The following is our results of detailed surveying and radiometric dating along the Mattole River, and our analysis of the link between changes in base-level and the terrace record along its length.

Terraces along the Mattole River

Methods

Prominent terrace surfaces, or flats as called by the locals, are ubiquitous and seemingly continuous along the lower 40 km of the Mattole River downstream from Honeydew (Fig. 3). With a crew of 6-8 people, we spent about six weeks surveying these terraces and the active channel with a total geodetic station in the summer of 1991. Upstream of 40 km, the Mattole's upper reaches are distinctly different, as the river becomes a narrow, v-shaped bedrock gorge with few to no terraces. Survey data were plotted with a computer as a large-scale plan-view map and combined with field maps and notes to create a geomorphic and topographic base map. This map was then used to construct a mid-valley axial line. All points for long profiles were projected to this mid-valley line, and the distance to each point from the Pacific Ocean at the river mouth was measured with a digitizer. Distances and altitudes of each point were then plotted to construct long profiles for each terrace surface, the active channel bed, gravel bars, and the water surface (Fig. 14).

Observations

Several important features of the lower 40 km of the Mattole are illustrated in Fig. 14. First, both the channel bed (thalweg) and water surface profiles form straight, parallel lines† extending from modern sea level to the highest part of the river surveyed, at about 85 m altitude. The vertical difference between these two profiles indicates alternating pool and riffle sequences. The modern active channel is floored with gravel, unlike the bedrock upper reaches of the Mattole. We do not know the total thickness of the gravel veneer in the floor of the valley. We do know, however, that high-magnitude floods which occurred in 1955 and 1964 after more than a decade of extensive logging resulted in substantial widening of the channel as the outer edges of flats (terraces) were destroyed. As a consequence, deep pools were filled with gravel, and the present channel bed is smoother than that prior to the floods.

Second, terraces along the lower ~16 km of the river--where the valley is very wide--are comprised of alluvium (fill terraces) and bedrock exposures are rare, while terraces along the upper 16-40 km--where the valley becomes much more narrow--are dominantly bedrock, or strath surfaces (beveled surfaces cut in bedrock). The valley width decreases rapidly upstream of 40 km, and few to no terraces exist in the bedrock canyon. The treads of alluvial terraces

---

† Linear regression results are a) channel bed: $y = -1.30 + 0.002\,x$, $R^2 = 0.99$; b) water surface: $y = -0.81 + 0.002\,x$, $R^2 = 1.00$; c) top of active gravel bar: $y = 1.16 + 0.002\,x$, $R^2 = 0.99$.

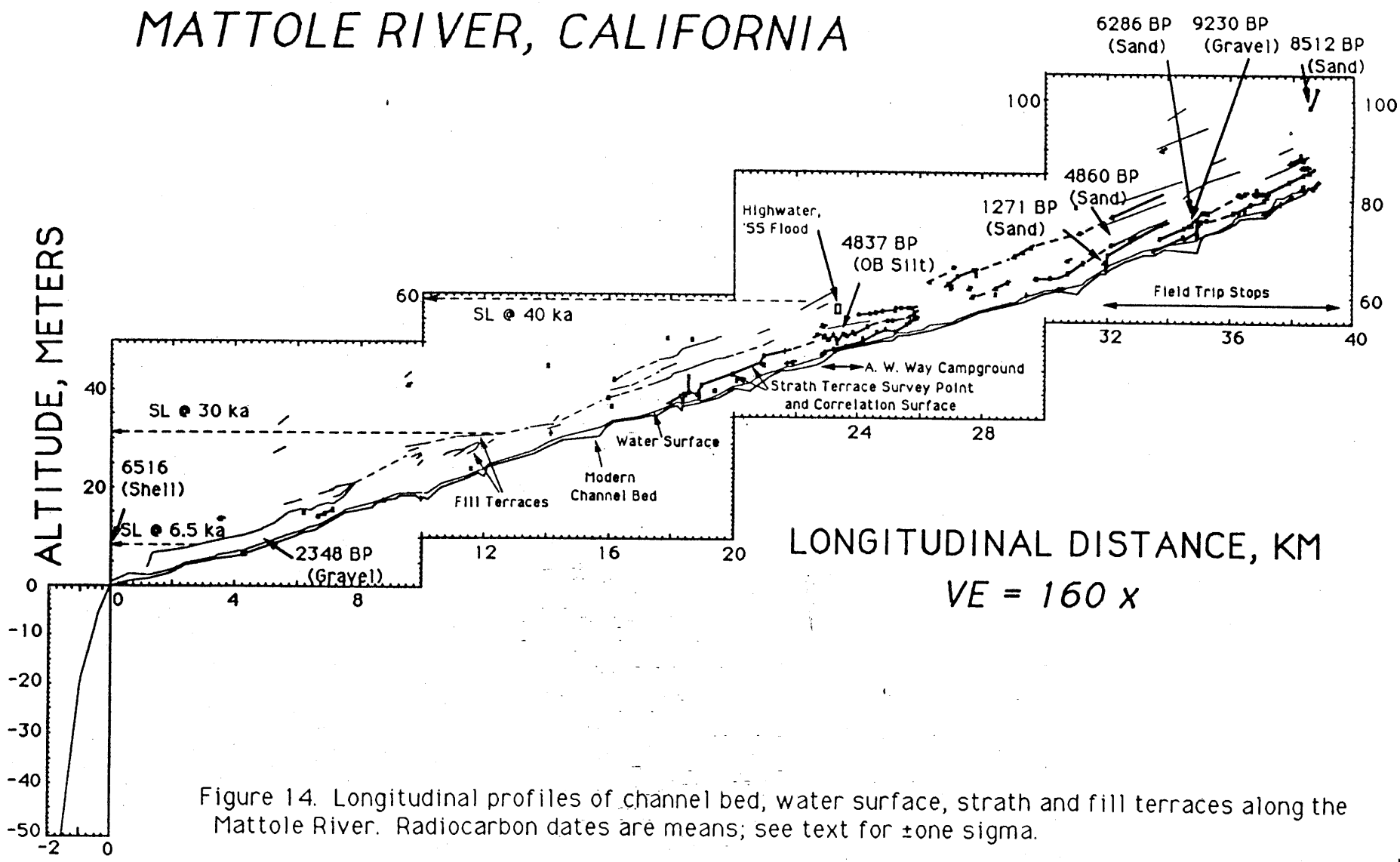

Figure 14. Longitudinal profiles of channel bed, water surface, strath and fill terraces along the Mattole River. Radiocarbon dates are means; see text for ±one sigma.

are indicated by fine lines, dashed where correlations of remnants are tentative, while the treads of bedrock terraces are indicated by both survey points (shown with an x) and heavy lines, again dashed where correlations of remnants are tentative. At most localities, strath terraces are overlain by 1-2 m of channel-bed gravels, which in turn are overlain by 1-2 m of overbank fine-grained sands and silts. Samples for radiometric dating were obtained from both types of deposits. From about 16 km upstream, fine lines indicating the treads of gravel deposits on Fig. 14 are actually the treads of fluvial material overlying strath terraces.

Finally, note that strath terraces are parallel to one another, but are steeper than the modern channel bed and do not merge with marine terraces at the river mouth. The positions of the 30-Ka and 40-Ka marine terraces are obtained from surveys at Punta Gorda just south of the mouth of the Mattole (Fig. 8b). The position of a Holocene marine terrace (the preemergence terrace), dated via a shell from the platform (6179-6889 cal BP; see discussion above), is from the survey at Hair Seal Rock immediately north of the mouth (Fig. 12). Horizontal projection of the altitudes of the two youngest marine terraces (6.5 Ka and 30 Ka terraces) coincides remarkably with prominent, gently sloping fill terraces along the river. In contrast, strath surfaces appear to project downstream into the modern channel bed, forming a series of imbricated benches that emerge from the channel, one after the other, as one follows the river upstream.

Interpretation of Terrace Remnants

We make the following assumptions and interpretations of the results of the Mattole survey and radiometric dating, which are very similar to our results for the next river to the north, the Bear (Merritts et al, 1991), but are not discussed in detail here. We assume that coarse bouldery gravels overlying strath surfaces are channel-bed gravels that were left lying upon the inactive bedrock floor of the channel after abandonment due to incision. These deposits are roughly synchronous with the time of formation of the strath surface. In contrast, cumulic fine-grained deposits which cap the gravels post-date the time of strath formation by up to several thousand years, and are the result of flood events that were large enough for the river stage to top the terrace deposits. Radiometric dating of such alluvial sequences on the Bear and Mattole Rivers indicates that overbank sands and silts can be as much as 3000 years younger than the underlying gravels at a given locality. For example, at km 34, a log <1 m above a strath in channel bed gravels yielded an age of 9230±290 BP (USGS Sample # 2225). Samples of charcoal from thin beds of sand directly above the gravel, 2 m above the strath, yielded ages of 5907-5945 cal BP and 6191-6298 cal BP (USGS Samples # 2224 and 2226; calibration procedure of Stuiver and Becker, 1986, and Pearson et al, 1986). The older date is a minimum age for the strath, but is probably much closer to its age than a date from overbank deposits. Channel-bed gravels provide an upper limit on the altitudinal position, and a minimum limit on the time of formation, of the channel floor associated with the strath. The overbank deposits are also useful, in that they provide an approximate age and an upper limit for the altitudinal position of the channel bed that flooded to deposit the fine material.

A maximum height for the altitudinal position of the Mattole River channel during the ~6.0-6.5-Ka highstand is reconstructed from five "anchor" points along the river's length (Fig. 15). At the downstream end, we anchor the profile at the horizontal projection of the altitude of the marine platform dated at 6179-6889 cal BP, where it coincides with the break in slope in the alluvial fill terrace. At the upstream end of the river, at km 35, we anchor the profile below the overbank sand deposits that date at 6191-6298 cal BP and 5907-5945 cal BP. Between these endpoints, we project the 6.5-Ka profile below overbank deposits at two sites that yield dates from near the tops of the deposits of 4913-4981 or 4821-4890 cal BP (Beta Analytic Inc.; Sample # 47149), and 4529-4989 cal BP (Beta Analytic Inc.; Sample # 46475; calibration procedure of Pearson et al, 1986). We assume that deposits that are 6.5 Ka in age would exist below the younger overbank deposits.

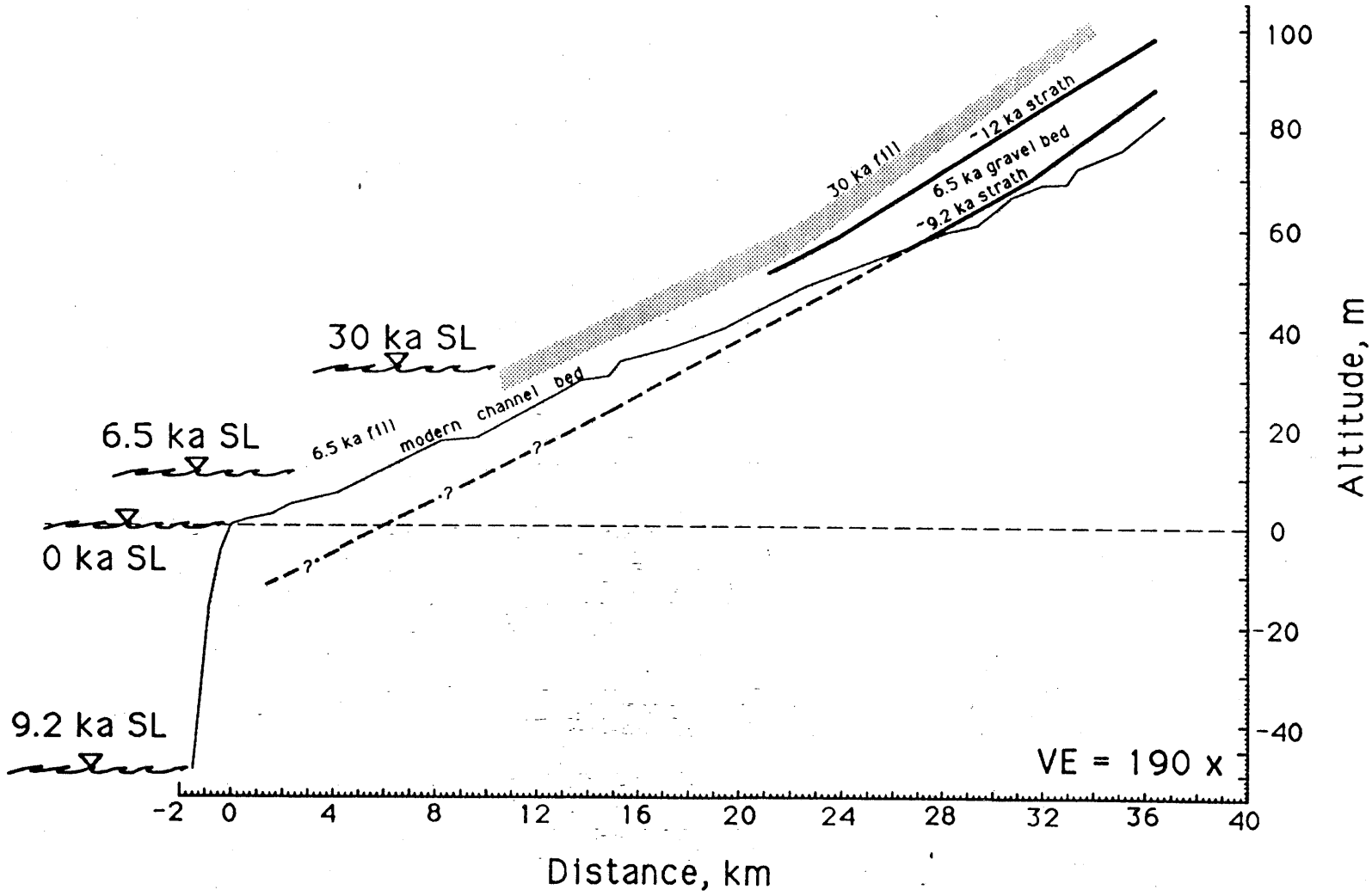

Figure 15. Interpretation of paleoprofiles of Mattole River from 30 Ka to the present. Stippled patterns represent alluvial backfill. Heavy lines are remnants of strath terraces from Figure 14. The 9.2 Ka strath is tentatively projected beneath the modern gravel streambed and downstream toward the altitude of the sea-level lowstand at that time.

We use similar reasoning to reconstruct long profiles for the 30-Ka, 12-Ka, and 9.2-Ka profiles of the Mattole River (Fig. 15). In addition, we tentatively correlate intermediate strath surfaces to indicate altitudinal positions of the channel bed between these times. The radiometric date of 8568-8422 cal BP (Beta Analytic Inc., Sample # Beta-46479; calibration procedure and intervals from Linick et al, 1985; Stuiver et al, 1986; Kromer et al, 1986; and Linick et al, 1986) for charcoal from the base of the overbank deposits at km 39 indicates that the underlying strath formed more than ~8.5 ky ago, and perhaps as much as 11 or 12 ky ago if overbank deposition postdates strath formation by as much as 3 ky. It also indicates that a channel existed below that altitude at ~8.5 Ka, and flooded to that level at that time. We assume an approximate age of 12 Ka for this strath. The steep gradient on this surface is a function of projection of the terrace surface along a curved meander bend to the mid-valley axial line. The original path of the channel was probably more sinuous than that of our mid-valley line, hence the gradient would have been less. We estimate that the position of the channel which flooded this high strath at 8.5 Ka was below the level of the prominent strath at 35 km, from which a log in the basal gravels yielded a date of 9230±290 BP.

From constraints regarding the position of the mouth of the Mattole River during sea-level highstands, and from estimates of its channel-bed altitudinal position at different times between 30 and 6 Ka, we are able to reconstruct the vertical path of the Mattole in space with time as it responded to eustatic and tectonic changes in base level at its mouth (Fig. 15). Because the present is a time of high sea-level, while most of the last 125 ky has been a time of low sea level, the mouth of the Mattole has experienced dominantly base-level fall as the coast rises due to tectonic uplift. The most recent sea-level highstand was 30 ky ago, at ~ -44 m, and caused inundation and backfilling of what is now the lowermost 12 km of the mouth of the Mattole (Fig. 14). (Note that the land mass has been uplifted about 76 m since that time, and the relative position of the past highstand is 32 m above modern sea level.) Between 30 and 6.5 Ka, sea-level reached its lowest stand at ~ -130 m in altitude at ~15 Ka. During this time period, bedrock in the river mouth was removed by deep incision, and numerous strath terraces that dip more steeply than the modern backfilled channel were formed. Between 15 Ka and 6.5 Ka, sea-level rose rapidly in response to global melting of ice sheets and valley glaciers. Although the rate of eustatic rise exceeded that of tectonic uplift, sea level was still low relative to its position at 30 Ka, and it was not until about 6.5 Ka that strath terraces at the mouth of the river were submerged and buried during backfilling. We tentatively project these strath terraces beneath the channel bed downstream to the coast, indicating the approximate position of sea level about 9.5 Ka, taking into account the rate of tectonic uplift.

During the time of maximum sea level altitude at ~6.5 Ka, an erosional marine terraced formed at the coast, but inundation of the incised valley mouth gorge--from which much bedrock had already been removed--was associated with aggradation that extended about 40 km upstream. The resulting deposit decreased rapidly in thickness, from at least 21 m at the mouth to less than 4 m at km 39. This tapering gravel wedge buried numerous strath terraces which had formed during the relative sea-level lowstands. The river has been incising since about 6.5 Ka due to tectonic uplift of about 1-2 m/ky, or about 9 m, and consequently it has exhumed these older late-Pleistocene to early Holocene strath terraces that were partially buried during the early Holocene sea-level rise.

Conclusions Regarding Terraces and Base-Level Change

At this point we can go back to the questions posed earlier regarding the origin and meaning of fluvial terraces. First, "Can terrace remnants along the Mattole River, a large meandering bedrock river, be correlated in order to reconstruct past longitudinal profiles?" The answer is, with much difficulty. We surveyed the Mattole over a period of six weeks, with a work crew of 6-8 people and a total geodetic station with a range of 2 km. We had the advantage of computer technology to facilitate generation of maps and long profiles. We found

abundant exposures and datable material. Thanks to numerous Mattole Valley residents, we had complete access to all sites. Over 1300 points were surveyed over a distance of 40 km. Despite all this, many of our correlations are uncertain, for the following reasons:

1) Strath terraces may be buried by subsequent fill terraces.
2) Strath surfaces are incised during their abandonment, hence in places one strath becomes two or three different straths. Although this tells us much about the processes of strath formation, it means that individual surfaces are time transgressive.
3) Datable material in the gravels and sands above the straths provides minimum ages for the time of strath formation, and can span a long time period if the strath remains within the zone of overbank deposition. Base-level rise after strath formation can result in overbank deposition long after the original strath formed.

In particular, we consider the correlation of strath remnants to be an arbitrary activity because response to eustatic and tectonic base-level fall results in continuous incision and adjustment along what might be viewed as a subhorizontal folded paper fan (Fig. 16a), not episodic incision punctuated by periods of base-level stability and lateral valley floor beveling. The latter model has been assumed by many past workers, including ourselves (c.f., Merritts and Vincent, 1989); however, our detailed results for two rivers, the Bear and the Mattole, have caused us to reevaluate our earlier models.

Why then, do prominent terraces occur along the Mattole, with exposures of straths that appear to be flat and aerially extensive? Shouldn't a river that is continually incising leave only a v-shaped valley without terrace remnants? The answer is in the size and power of the river, and consequently the valley width. If a meandering channel is incising sideways and downwards along what can be imagined as a continuous folded fan it will remove parts of individual folds during its sideways sweeps, and leave remnants that appear to be continuous, individual surfaces. The size and valleyward slope of the remnants will be a function of the original slope of the bedrock valley floor toward the thalweg. This slope is controlled by the ratio of the rate of lateral migration to the rate of vertical incision. If the ratio is very large the slope will be gentle, and broad strath surfaces will be formed (Fig. 16 b). If the ratio is small, steep, narrow surfaces will be formed (Fig. 16c). Any terrace remnant that can be followed is a time line, but it represents a line that could be traced along one of the folds in the subhorizontal fan (Fig. 16a). The time of formation of the tread of the remnant is synchronous with that of the fold surface, but the time of formation of the riser is synchronous with the sideways sweep of the river that removed the rest of the fold surface. The greater the rate of lateral migration relative to vertical incision, the wider the valley and the greater the likelihood of formation and preservation of broad strath surfaces. The fact that few terraces occur in the bedrock gorge farther upstream in the Mattole valley indicates that the fan has become very narrow and compressed due to dominantly vertical incision with little lateral component, or meandering (Fig. 16d).

This model leads us to conclude that strath terraces will only form along certain special parts of a stream. This special location is upstream of the effects of a bobbing sea-level surface, and far enough downstream from the headwaters that stream power is in excess of that needed to transport the prevailing sediment load and to overcome resistance elements impinged upon the flowing water by the irregular bedrock floor and walls of the valley. In a downstream direction, total stream power along the Mattole increases as numerous large tributaries join the trunk stream, consequently the power available for lateral erosion increases. Because this widens the active valley floor and decreases the longitudinal gradient of the river, power per unit area actually remains the same as that upstream, or might even decrease (unpubl. data, Vincent, Merritts, and Wohl). If only base-level fall occurred, the river would probably form large strath surfaces all the way to its mouth. The combination of tectonic uplift and eustatic sea-level fall has resulted in deep incision and formation of steep strath surfaces that were

We use similar reasoning to reconstruct long profiles for the 30-Ka, 12-Ka, and 9.2-Ka profiles of the Mattole River (Fig. 15). In addition, we tentatively correlate intermediate strath surfaces to indicate altitudinal positions of the channel bed between these times. The radiometric date of 8568-8422 cal BP (Beta Analytic Inc., Sample # Beta-46479; calibration procedure and intervals from Linick et al, 1985; Stuiver et al, 1986; Kromer et al, 1986; and Linick et al, 1986) for charcoal from the base of the overbank deposits at km 39 indicates that the underlying strath formed more than ~8.5 ky ago, and perhaps as much as 11 or 12 ky ago if overbank deposition postdates strath formation by as much as 3 ky. It also indicates that a channel existed below that altitude at ~8.5 Ka, and flooded to that level at that time. We assume an approximate age of 12 Ka for this strath. The steep gradient on this surface is a function of projection of the terrace surface along a curved meander bend to the mid-valley axial line. The original path of the channel was probably more sinuous than that of our mid-valley line, hence the gradient would have been less. We estimate that the position of the channel which flooded this high strath at 8.5 Ka was below the level of the prominent strath at 35 km, from which a log in the basal gravels yielded a date of 9230±290 BP.

From constraints regarding the position of the mouth of the Mattole River during sea-level highstands, and from estimates of its channel-bed altitudinal position at different times between 30 and 6 Ka, we are able to reconstruct the vertical path of the Mattole in space with time as it responded to eustatic and tectonic changes in base level at its mouth (Fig. 15). Because the present is a time of high sea-level, while most of the last 125 ky has been a time of low sea level, the mouth of the Mattole has experienced dominantly base-level fall as the coast rises due to tectonic uplift. The most recent sea-level highstand was 30 ky ago, at ~ -44 m, and caused inundation and backfilling of what is now the lowermost 12 km of the mouth of the Mattole (Fig. 14). (Note that the land mass has been uplifted about 76 m since that time, and the relative position of the past highstand is 32 m above modern sea level.) Between 30 and 6.5 Ka, sea-level reached its lowest stand at ~ -130 m in altitude at ~15 Ka. During this time period, bedrock in the river mouth was removed by deep incision, and numerous strath terraces that dip more steeply than the modern backfilled channel were formed. Between 15 Ka and 6.5 Ka, sea-level rose rapidly in response to global melting of ice sheets and valley glaciers. Although the rate of eustatic rise exceeded that of tectonic uplift, sea level was still low relative to its position at 30 Ka, and it was not until about 6.5 Ka that strath terraces at the mouth of the river were submerged and buried during backfilling. We tentatively project these strath terraces beneath the channel bed downstream to the coast, indicating the approximate position of sea level about 9.5 Ka, taking into account the rate of tectonic uplift.

During the time of maximum sea level altitude at ~6.5 Ka, an erosional marine terraced formed at the coast, but inundation of the incised valley mouth gorge--from which much bedrock had already been removed--was associated with aggradation that extended about 40 km upstream. The resulting deposit decreased rapidly in thickness, from at least 21 m at the mouth to less than 4 m at km 39. This tapering gravel wedge buried numerous strath terraces which had formed during the relative sea-level lowstands. The river has been incising since about 6.5 Ka due to tectonic uplift of about 1-2 m/ky, or about 9 m, and consequently it has exhumed these older late-Pleistocene to early Holocene strath terraces that were partially buried during the early Holocene sea-level rise.

Conclusions Regarding Terraces and Base-Level Change

At this point we can go back to the questions posed earlier regarding the origin and meaning of fluvial terraces. First, "Can terrace remnants along the Mattole River, a large meandering bedrock river, be correlated in order to reconstruct past longitudinal profiles?" The answer is, with much difficulty. We surveyed the Mattole over a period of six weeks, with a work crew of 6-8 people and a total geodetic station with a range of 2 km. We had the advantage of computer technology to facilitate generation of maps and long profiles. We found

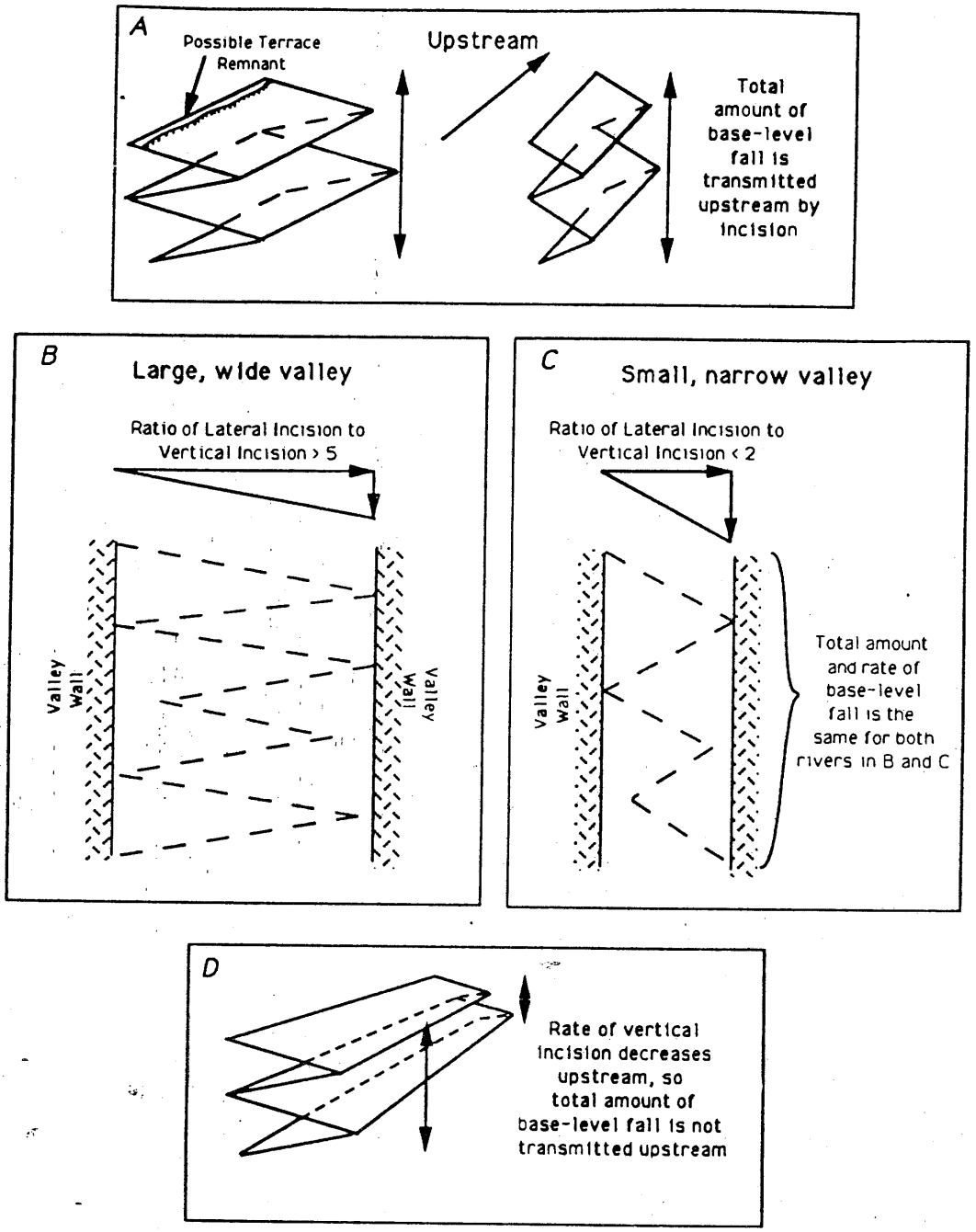

Figure 16. Model of strath terrace development along a meandering bedrock river. A. Folded "fan" to illustrate vertical pathway of an incising, meandering river with time. Path on right is for smaller stream with steeper valley gradient. Total amount of base-level fall is the same for both the large and small rivers, and is fully transmitted upstream by incision. B and C. Front face of folded fan at mouth of river to illustrate ratio of lateral to vertical incision. River in C is smaller than river in B, but amount and rate of base-level fall are the same for both rivers. D. Upstream pinching of folded fan illustrates the merging of strath surfaces that indicates decreasing rate of vertical incision upstream, and hence only partial transmittal of base-level fall.

graded to sea levels much lower than that at present, and might extend all the way to the coast (Fig. 15). However, high frequency fluctuations of sea-level at the mouth also result in episodic backfilling when the water surface rises above the level of the lowest, most recently formed strath. The lower 16 km of the Mattole is dominated by deposits from such backfilling. The rate of tectonic uplift determines whether or not older, buried strath terraces are exposed at present. A river in a region of lower rates of surface uplift, such as the Ten Mile River to the south in the Fort Bragg area, seems to have no strath terraces, because the zone of backfilling extends upstream to the zone of canyon formation, and no special, intermediate zone of strath formation is exposed (Merritts et al, 1989). One can envision the Ten Mile as forming along a folded fan like the Mattole, but the reduced amount of base-level fall over a given time period results in a "compressed" fan in which strath surfaces are pinched close together.

Our second question was "When and how does a river form and abandon a strath terrace? During sea-level highstands? Or lowstands? Or while sea level is rising or falling?" Both strath and fill terraces are the result of base-level change. Fill terraces are formed during times of relative sea-level rise (i.e., rate of sea-level rise >> rate of uplift), while strath terraces are formed during times of relative sea-level fall, which has been most of the past 125 ky. For a given rate of uplift, the size and power of a river controls its ability to erode laterally in addition to vertically, and consequently determines whether or not broad strath surfaces are likely to be formed and preserved. The smaller the river, the fewer the strath surfaces and the greater their spacing (vertically). At some critical size threshold--for a given uplift rate--no strath surfaces will be formed or preserved.

These answers result in a striking conclusion: abandonment of strath terraces does not indicate that sudden base-level change has occurred, nor does it even require that uplift occurs. Rather, straths can form solely as a result of eustatic base-level fall; however, without tectonic uplift, they are not likely to have been exhumed during the present sea level highstand. Exposures of straths formed during sea-level lowstands are not likely at present, during a time of very high sea level, unless at least 1-2 m/ky of tectonic uplift and consequent incision has occurred in order to exhume the older straths. The effects of relative sea-level rise (fill terraces with nearly horizontal surfaces) are found well upvalley in the Mattole and Bear Rivers. A fill terrace associated with the most recent highstand (~6.5 ka) is found at 4-5 km, and aggradation of the channel bed in response to this filling occurs up to ~36 km upstream. Incision associated with relative sea-level fall also occurs far upstream, at least 40 km in the case of the Mattole River, which has a trunk stream length of 97 km, and at least 25 km upstream in the Bear River, which has a trunk stream length of 44 km.

Adjacent rivers with the same uplift rate do not have similar numbers, spacings, and ages of strath terraces because these landforms are not the result of regional or instantaneous events, but rather are part of a time-continuum that represents constant adjustment to changing sea-level. The degree of adjustment, or fine-tuning, depends upon the power of the river. A larger river is more likely to create one large surface over a long period of time, while a smaller river creates many merging, steep straths that are difficult to separate from one another (Fig. 16). However, adjacent rivers do have fill terraces associated with sea-level highstands that are the same age. The downstream end of such a deposit for the present sea-level highstand can be used to estimate an approximate amount of late-Holocene uplift, as its altitude is roughly equal to the amount of incision that has occurred at the river mouth since the highstand stabilized.

FLUVIAL RESPONSES TO CHANGING PATTERNS OF HUMAN LAND-USE, MATTOLE WATERSHED

In order to asses fluvial responses to Holocene climatic change and tectonism, one must first consider the more recent fluvial adjustments to changing patterns of human land use. This is often difficult, as the signals left by such changes can be so extensive as to go practically

unnoticed by researchers new to an area. Historical information and personal accounts can be very useful in distinguishing many of the effects of the changes in land use. In the Mattole Valley, a shift in land use practices happened rather abruptly in the 1940s, and was soon followed by the 1955 and 1964 floods, both extreme magnitude events. The combination of the two, that is, the initiation of extensive road-building and deforestation followed by extreme storm events, led to a series of physical, hydrological and biological changes that would be considered catastrophic on a geologic time scale. In brief, the changing patterns of land-use resulted in extensive channel aggradation of both the mainstem of the Mattole and its tributaries, and a dramatic increase in the long-term frequency and magnitudes of landsliding and erosional processes. Ultimately, these changes led to the destruction of salmonid spawning and rearing habitat for enough years to severely impact and reduce fish populations.

Settlement and Logging History

The history of human land-use in the Mattole Valley can be divided into four distinct phases: 1) prior to 1850: pre- and early European contact, with land-use almost exclusively by the Mattole Indian groups and a few early European settlers; 2) 1850's to 1940's: post-contact/ early settlement years/range-land conversion and oil days 3) 1940's to mid 1970's: industrial timber period/range-land conversion; 4) modern era: period of recovery/restoration.

The actual impacts of the first two phases are difficult to quantify, since very few detailed characterizations or photographs exist for comparative purposes. However, a number of historical and ethnographic studies give at least a general sense of the types of land-use activities conducted over the past few centuries. Even prior to the arrival of European settlers, residents of the Mattole actively manipulated their environment. It is well documented that the Mattole Indians regularly burned large portions of land in order to maintain optimum hunting grounds and vegetative characteristics. Huge fires were observed near Cape Mendocino by the French explorer Jean Francois Galoup de la Perouse in 1786. He interpreted the fires to be of volcanic origin, but subsequent travelers from the same time period recorded regular patterns of burning by Indian groups (Roscoe, 1985). Large scale burning was also common following the arrival of European settlers in the 1850's, when the dominant land use gradually shifted to cattle ranching. From the ranchers' perspective, burning patches of timber was an effective means of converting unusable forest to productive rangeland. Oil was probably recognized by the Mattole Indians long before the arrival of the settlers, but it was the new immigrants who brought in the first oil company agents in 1864. Fourteen registered wells were dug in the area in the next three years, but only one ever produced much oil. The first shipments of oil left the valley in 1865 on mule. Although oil companies attempted more operations in the next six decades, not more than a few hundred gallons of oil ever left the area.

Road construction at this time is thought to have steadily increased, but roads were still limited to hauling materials in and out of the valley. Dynamite and horse drawn graders were the primary means of constructing roads through the steep and rugged terrain, so access to these areas was limited largely to travel on foot or horseback. Not until road construction and timber harvesting reached its peak following the mid 1940's, were the activities of humans thought to have severely upset the sensitive equilibrium that existed between the rapid rates of tectonic uplift, the geologically unstable terrain, the humid climate, and the ubiquitous processes of mass movement.

Following the post-war housing and industrial boom, demand for timber production grew, and Douglas fir became recognized as a valuable wood for construction purposes. Furthermore, the design and construction of heavy machinery made it possible to punch roads into steep and remote areas. The development of gas-powered chainsaws, logging trucks, yarders and caterpillar tractors enabled logging operations rapid entry into and exploitation of remote areas. Prior to these developments, many operations were limited to locations where

rail lines could be readily constructed. Landowners were willing to sell the trees on their land to supplement their income and to open up more land for grazing purposes, as well as to reduce the taxes they were required to pay on all standing timber. Timber harvest permits cost only one dollar in the early days (1940's to early 50's), but permits were often never checked, and site or road inspections were almost unheard of (Chambers, 1992). Harvesting occurred essentially without regulation , and without concerns for water quality or cumulative impacts. During the wet winters, when it was too muddy to operate machinery on the steep hillslopes, it was commonplace for machinery operators to push debris into tributaries in order to turn them into corridors for transporting logs (Chambers, 1992). Logs were then felled directly into the stream channel where the caterpillar tractor awaited, or were flushed out when debris dams broke either intentionally or by accident. Needless to say, these techniques destroyed many reaches of stream channels for many species, and acted as sediment storage sites to blow out at a later date. Many low order tributaries are today still choked with saw-cut logs and debris.

Little concern was given to constructing stream crossings or maintaining original drainage patterns, and subsequently, both small and moderate-sized landslides became commonplace. Many logging crews came down from Oregon, simply to cut and run; their main objective was to get the logs off the hill, loaded on the trucks, and out of the valley. Therefore, many roads were used for one season and then abandoned. The abandoned skid trails and roads existing today are innumerable, and although many of them have already blown out, there remain large areas still far removed from a state of hillslope equilibrium.

Extent of Deforestation

While the Mattole Valley remains relatively undeveloped in regard to population expansion, its land area has been extensively impacted by industrial timber harvest during the past five decades. The Mattole Restoration Council (MRC) conducted a detailed mapping project utilizing 1: 20,000 scale aerial photos from 1941-1942, Humboldt County timber harvest records, 1984 aerial photos enlarged to 1: 5,000, and extensive field work in order to determine the extent of the impact. They estimated that approximately 75% of the Mattole originally consisted of timberland, and that approximately 91% of the original old-growth coniferous forests had been logged between the years 1947 and 1988 (MRC, 1989). If we assume that 80% of the original timberland consisted of coniferous old-growth forest, then at least 55% of the total acreage of the Mattole Watershed was directly impacted by timber harvest practices and associated road building. Numerous studies have shown the relationships between road building and use, methods of timber harvesting, and accelerated erosion rates (Amaranthus et. al., 1985; Beschta, 1978; Megahan and Kidd, 1972;Brown and Krygier, 1971; Reid and Dunne, 1984), as well as the relationship between increases in water-yield following extensive vegetative removal (Rothacher, 1970). It follows that the combination of extensive deforestation and hasty road construction would have severe cumulative impacts when combined with extreme storm events such as those which occurred in 1955 and 1964.

Floods

While the flood of December, 1964, was the most severe storm to hit in recorded history throughout most of northern California, this was not the case in the Mattole Valley. The 1955 flood hit the Mattole the hardest--unfortunately near the peak years of timber harvest. Maximum discharge in 1955 reached 90,400 cubic feet per second (cfs), relative to mean winter peak discharges of 15,000 to 40,000 cfs. Flood waters overtopped the bridge immediately upstream of A. W. Way county park and flooded many of the hay-fields in the lower Mattole. Old-timers recall at least 4 feet (1.5 m) of water on the broad floodplain known as Chamber's flat immediately downstream of the George Lindley bridge, near Petrolia. Fence lines were in some places ripped up, and in others buried in up to 0.3-1.0 meters of fine sediment. Pieces of farm machinery were buried in place to the point that no sign was left of

them; some were extracted after the mud dried. Overall, sedimentation on floodplains was variable, but today, the upper 1.0-2.0 meters of most flood plains and low terraces consists of homogeneous packages of fining upward sequences of fine sediment. Riparian vegetation was carried away, and large amounts of bank erosion and channel re-alignment were witnessed throughout the valley.(Smith, 1991). The river channel suffered extensive aggradation with debris, rocks and fine sediment, and many of the old-timers favorite swimming holes were mostly filled in. A photograph taken sometime in the 1920's(?) from a site near the George Lindley Bridge shows two very large rocks with a swimmer atop one. Russell Chambers, an octogenarian rancher/ ex-logger/ road builder clearly remembers swimming in that hole when he was in grammar school. Today that reach is a broad shallow alluvial one, with no place to swim. Aggradation at the Lindley bridge is therefore thought to be on the order of at least 3 to 4 meters. The 1964 flood reached a peak discharge of 78,500 cfs, and was viewed by locals as a significantly less damaging flood event, but it likely compounded the effects of the 1955 flood. Damage resulting from each flood was estimated at roughly one million dollars, and primarily consisted of damage to roads and bridges, fences, livestock,and mill-yards, which lost significant amounts of lumber in each flood(State of California, 1973). One person drowned in the 1955 flood, when the house he refused to leave was swept away.

Landslides

Evidence for large pre-historic landslides and debris flows is extensive in the Mattole Valley. Broad alluvial fans comprised of debris-flow deposits are common in both the upper and lower valley near the towns of Petrolia and Honeydew. Large boulders in the mainstem of the Mattole and in the middle of floodplains, as well as streambank exposures of angular alluvium are evidence of large slides that perhaps dammed the river. Some of these exposures, such as the one at the mouth of Indian Creek downstream from the Elwynn Lindley bridge are superposed by at least 3 meters of fluvial deposits, and thus provide some indication of the age of the slide.

Examination of the 1941-42 aerials shows that the majority of landslides in the watershed occur along the Mattole mainstem and its major tributaries, especially on the outside bends of meanders. Very few slides are visible on the forested slopes of the valley in '41 aerials except along the steep western slopes of the King Range, where coastal retreat constantly works at the toes of broad unstable slopes. Examination of the 1981 1:12,000 aerials show a greatly increased number of landslides of varying scales located mostly in the upper reaches of small drainage basins. Some of these slides are visible from the Mattole road. Field studies of these slides, and comparison of the pre and post -impact aerial photos indicate that although the slides occur in the vicinity of mapped shear zones of known geologic instability, the ultimate failure of the slides can often be directly attributed to human activities on the hillslopes. A good example of this is the Honeydew slide, which failed catastrophically in April 1983 following a period of intensive precipitation . Over 111 inches of rain fell in the Honeydew area between December and March, with 31 inches falling in March. Madrone (1983) examined a sequence of air-photos from the years 1941, 1963,1966,1974, and 1983 that showed the rates of timber harvesting and their effects on the slopes. In 1941 the first signs of rangeland conversion are evident, but there are few signs of large-scale logging operations. By 1963 skid and haul roads are visible and the upper slopes of the drainage basin are in the process of being harvested. By '66 the haul roads are notably larger, and skid roads traverse the entire drainage basin. The first signs of mass wasting are in the '74 photo, where approximately 55% of the drainage basin has been logged. In this photo the mainstem of the Mattole is already showing signs of being pushed away from the mouth of the slide basin. By 1983, 185 acres of the 400 acre watershed slid into or slumped toward the Mattole river, resulting in a 20-25 foot deep dam which lasted for nearly two years. Steensen (1987) estimated approximately 430,000 cubic yards of mud and rock were deposited in the debris fan

at the toe of the slide. He estimates another 103,000-400,000 cubic yards on the opposite hill will be mobilized due to the shifting of the mainstem channel from the right to the left bank.

The Honeydew Slide is the largest landslide event in the Mattole Valley to occur in recent history, and appears to be the result of extensive ground disturbance on a geologically unstable area, combined with one season of heavy precipitation (the 1983 water year had the highest recorded precipitation since 1974). Nested debris levees outside of the active slide channel indicate that the slide has been mobilized in the past hundreds to thousands of years, but the slide appeared to be in a stable condition in the early 1940's. The activities occurring between the 1940's and the 1980's are not entirely responsible for the mobilization of the slide, but they are likely to have greatly accelerated the processes leading to its ultimate failure.

Large scale landsliding has been a key player in the geomorphic evolution of the Mattole Valley. Historic accounts of seismically triggered slides (e.g. 1906), record what has likely been a repeated phenomenon. At least 3 significant landslides have been recorded since the March 7, 1992 Petrolia Earthquake (M_L =5.3). A quake on the order of a great subduction event would clearly have widespread geomorphic effects in this type of terrain.

CONCLUSIONS

Historic changes to fluvial and hillslope environments can present disturbing problems for researchers studying Quaternary fluvial geomorphology. Recent aggradation and subsequent changes in channel pattern in the Mattole River have formed a subtle overprint on the landscape that masks indicators of other geologic processes. The shift to a more braided channel in the lower six kilometers of the river resulted in over 50 acres of fill-terraces being cut back, or eroded completely. At least 30 acres of "hayfields" supporting barns and a dairy ranch in 1941 are now completely gone. The sedimentary history recorded in their stratigraphy washed away with them. Low strath terraces downstream of 30 km are probably buried at numerous locations by a few meters of active channel gravels, thereby removing them as data points from inclusion in the long-profile study.

Some of the biologic effects are felt over a more widespread area, and are more difficult to characterize. At present, much of the ongoing research and work taking place in the Mattole Valley is directed toward river restoration and salmonid habitat enhancement. Groups like the Mattole Restoration Council (MRC) and the Mattole Salmon Group are dealing most directly with the effects of changing patterns of land-use. The MRC has documented many of these in *The Elements of Recovery,* published in 1989. This document serves as an inventory of upslope sources of sediment and summarizes the history of landuse throughout nearly the entire watershed. We close with an eloquent quote from the preface of this thoughtful document.

> "Erosion is as common an aspect of life in the Coast Ranges as Pacific sunsets. As the mountains rise up out of the soft ocean bottom, a tenuous and fluid equilibrium is established--most of each year's uplift is washed or shaken back into the sea. An inch of soil which took a hundred years to build can wash away in a single storm unless held in place by grasses, shrubs, and trees. The streams and rivers are conduits for all this material on its way downhill. Yet under conditions of equilibrium, no more sediment enters the stream than can be easily stored or quickly transported through the system. The Mattole in prehistoric times was able to move thousands of yards of sediment each year and still be called "clear water," the meaning of the word Mattole in the native tongue. . . It doesn't take much to create a disturbance in such a delicately balanced system. . . So far, the land is resilient and the processes of recovery are marvelous to watch. . . Creeks which have been buried in twenty feet of rubble cut their way down to bedrock again--a geological age imitated in forty years. Really, we could all just leave for two hundred years and it would be hard to tell we had been here. . . . But we don't want to leave, and neither do we want to think of ourselves as despoilers of the land. . . As inhabitants working to restore natural systems, we will learn to see the healing processes and to align ourselves with them. It's time now for human populations to become one of the elements of recovery." (Freeman House, Project Coordinator, The Mattole Restoration Council.)

REFERENCES

Adams, John, 1984, Active deformation of the Pacific northwest continental margin: Tectonics, **3**, p. 449-472.

Alpha, Tau Rho, Detterman, Janis S., and Morley, James M., 1988, Atlas of oblique maps: A collection of landform portrayals of selected areas of the world: U. S. Geological Survey Misc. Investigations Series **I-1799**.

Amaranthus, M.P.,and R.M. Rice, N.R. Barr, R.R. Ziemer, 1985, Logging and forest roads related to increased Debris slides in Southwestern Oregon: Journal of Forestry, **83**, no.4, pp 229-233.

Atwater, T., 1970, Implications of plate tectonics for the Cenozoic tectonics of western North America: GSA Bulletin, **80**, p. 3513-3536.

Bachman, S. B., 1978, A Cretaceous and early Tertiary subduction complex, Mendocino coast, northern California, *in* J.K. Leggett (ed.), Trench-forearc geology: Sedimentation and tectonics on modern and ancient active plate margins: Geological Society of London Special Publications, **10**, p. 401-418.

Beschta, R.L., 1978, Long-term patterns of sediment production following road construction and logging in the Oregon Coast Range: Water Resources Research, **14**, p. 1011-1016.

Beutner, E.C., McLaughlin, R.J., Ohlin, H.N., and Sorg, D.H., 1980, Geologic map of the King Range and Chemise Mountain Instant Study Areas, northern California: U.S. Geological Survey Miscellaneous Field Studies Map MF-**1196-A**, scale 1:62,500, 1 sheet and explanation.

Blake, M.C., Jr., Jayko, A.S., and McLaughlin, R.J., 1985, Tectonostratigraphic terranes of the northern Coast Ranges, California, *in* Howell, D.G., ed., Tectonostratigraphic terranes of the Circumpacific region: Earth Science Series, v. **1**, Circumpacific Council for Energy and Mineral Resources, p. 159-171.

Bloom, A.L., Broecker, W.S., Chappell, J., Matthews, R.K., and Mesolella, K.J., 1974, Quaternary sea-level fluctuations on a tectonic coast: New 230Th/234U dates from the Huon Peninsula, New Guinea: Quaternary Research, **4**, 185-205.

Brown, R. D., Jr., and Wolfe, E. W., 1972, Map showing recently active breaks along the San Andreas fault between Point Delgada and Bolinas Bay, California: U. S. Geological Survey Misc. Field Invest. Map, I-681.

Brown, G.W., and J.T. Krygier, 1971, Clearcut logging and sediment production in the Oregon Coast Range: Water Resources Research, **7**, p. 1189-1198.

Bull, W.B., 1985, Correlation of flights of global marine terraces: *In*: M. Morisawa and J.T. Hack (Editors), Proceedings of the 15th Annual Geomorphology Symposium, State University of New York at Binghamton. Allen and Unwin, 129-152.

Bull, W.B., and Cooper, A.F., 1986, Uplifted marine terraces along the Alpine Fault, New Zealand. Science, **234**, p. 1225-1228.

Carver, G.A., Burke, R.M., and Kelsey, H.M., 1985, Quaternary deformation studies in the region of the Mendocino Triple Junction: U.S. Geological Survey Open-File Report 86-31, p. 58-62.

Carver, G.A., Burke, R.M., and Kelsey, H.M., 1986, Deformation of late Pleistocene marine terraces along the California coast north of Cape Mendocino: GSA Abstracts with Programs, v. 15, n. 5, p. 316.

Chambers, R, 1992, personal communication, Petrolia, CA.

Chappell, J.M., 1983, A revised sea-level record for the last 300,000 years from Papua New Guinea: Search, **14**, p. 99-101.

Chappell, J.M., and Shackleton, N.J., 1986, Oxygen isotopes and sea level: Nature, **324**, p., 137-140.

Clarke, S. H. Jr., 1992, Geology of the Eel River Basin and adjacent region: American Association of Petroleum Geologists Bulletin, **76**, no. 2, p. 199-224.

Climap Project Members, Andrew McIntyre, Leader LGM Project, 1981, Seasonal reconstructions of the Earth's surface at the last glacial maximum: GSA, Map and Chart Series, **36**.

Cox, A., and Engebretson, D., 1985, Change in motion of Pacific Plate at 5 Ma: Nature, **313**, p. 472-474.

Curray, J. R., and Nason, R. D., 1967, San Andreas fault north of Point Arena, CA: GSA Bulletin, **78**, p. 413-418.

Dickinson, W.R., and Snyder, W.S., 1979a, Geometry of subducted slabs related to San Andreas transform: JGR, **87**, p. 609-627.

Dickinson, W.R., and Snyder, W.S., 1979b, Geometry of triple junctions related to San Andreas transform: JGR, **84**, n. B2, p. 561-572.]

Dumitru, Trevor, 1991a, Major Quaternary uplift along the northernmost San Andreas fault, King Range, northwestern CA: Geology, **19**, no. 5, p. 526-529.

Eaton, J. P., 1981, Detailed study of the November 8, 1980, Eureka, CA, earthquake and its aftershocks (abstract): EOS Trans. AGU, **62**, p. 959.

Ellen, Steven, 1986, Unpubl. geomorphic map of coastal northern California: 1:100,000.

Engebretson, D.C., Cox, A., and Gordon, R.A., 1985, Relative motions between oceanic and continental plates in the Pacific basin, Spec. Pap. Geol. Soc. Am., **205**, 59 p.

England, P. and P. Molnar, 1990, Surface uplift, uplift of rocks, and exhumation of rocks: Geology, **18**, p. 1173-1177.

Fujita, N., Fujii, Y., and Tada, T., 1975, Crustal effects of a heavy offshore earthquake in eastern Hokkaido, Japan: Tectonophysics, **29**, p. 523-528.

Furlong, Kevin P., 1984, Lithospheric behavior with triple junction migration: an example based on the Mendocino triple junction: Physics of the Earth and Planetary Interiors, **36**, p. 213-223.

Gardner, R.A., 1967, Sequence of podzolic soils along the coast of northern California: Ph.D. thesis, University of California, Berkeley, 236 p.

Gee, Lind S., Uhrhammer, Robert A., and Romanowicz, Barbara, 1991, Source parameters and rupture characteristics of the Gorda basin earthquakes and their tectonic implications (abstract): EOS Trans. AGU, **72**, p. 312.

Gilbert, G.K., 1877, Geology of the Henry Mountains (Utah); U.S. Geographical and Geological Survey of the Rocky Mountain region: Washington, D.C., U.S. Government Printing Office.

Griscom, Andrew, 1980, Aeromagnetic interpretation of the Mendocino triple junction, in Studies of the San Andreas fault zone in northern California: California Division of Mines and Geology Special Report **140**, p. 121-127.

Griscom, Andrew, and Jachens, Robert C., 1989, Tectonic history of the north portion of the San Andreas fault system, CA, inferred from gravity and magnetic anomalies: JGR, **94**, no. B3, p. 3089-3099.

Hagemann, M.F., 1982, Origin and uplift of a pair of late Quaternary marine platforms near Cape Mendocino, California: GSA Abstracts with Programs, **17**, n. 6, p. 359.

Harbert, William, and Cox, A., 1986, Late Neogene motion of the Pacific Plate: JGR, **94**, no. B3, p. 3052-3064.

Jachens, Robert, and Griscom, Andrew, 1983, Three-dimensional geometry of the Gorda plate beneath northern California: JGR, **88**, no. B11, p. 9375-9392.

Jenny, H., Arkley, R.J., and Schultz, A.M., 1969, The pygmy forest-podzol ecosystem and its dune associates of the Mendocino coast: Madrona, **20**: 60-74.

Johnson, Donald Lee, 1977, The late Quaternary climate of coastal California: evidence for an ice age refugium: Quaternary Research, **8**, p. 154-179.

Kelsey, H.M., and Carver, G.A., 1988, Late Neogene and Quaternary tectonics associated with northward growth of the San Andreas transform fault, northern California: JGR, **93**, no. B5, p. 4797-4819.

Kennedy, G.L., Lajoie, K.R., and Wehmiller, J.F., 1982, Aminostratigraphy and faunal correlations of late Quaternary marine terraces, Pacific Coast, U.S.A.: Nature, **299**, p. 545-547.

Kromer, B., Rhein, M., Bruns, M., Schock-Fischer, H., Munnich, K. O., Stuiver, M., and Becker, B., 1986, Radiocarbon calibration data for the 6th to the 8th Millennia BC: Radiocarbon, **28**, no. 2B, p. 954-960.

Ku, T.-L., and Kern, J.P., 1974, Uranium-series age of the upper Pleistocene Nestor Terrace, San Diego, California: GSA Bulletin, **85**, p. 1713-1716.

Lajoie, K.R., Kern, J.P., Wehmiller, J.F., Kennedy, G.L., Mathieson, S.A., Sarna-Wojcicki, Yerkes, R.F., and McCrory, P.F., 1979a, Quaternary marine shorelines and crustal deformation, San Diego to Santa Barbara, California, *in* Abbott, P.L., ed., Geological Excursions Southern California Area: San Diego State University, p. 3-15.

Lajoie, K.R., Weber, G.E., Mathieson, S.A., and Wallace, J., 1979b, Quaternary tectonics of coastal Santa Cruz and San Mateo Counties, California, as indicated by deformed marine terraces and alluvial deposits, *in* Weber, G.E., Lajoie, K.R., and Griggs, G.B., eds., Coastal tectonics and coastal geologic hazards in Santa Cruz and San Mateo Counties, California: GSA Guidebook.

Lajoie, K.R., and Sarna-Wojcicki, A.M., 1982, Late Quaternary coastal tectonics in the central and western Transverse Ranges, southern California: GSA Abstracts with Programs, **14**, n. 4, p. 179.

Lajoie, K.R., Sarna-Wojcicki, A.M., and Ota, Y., 1982, Emergent Holocene marine terraces at Ventura and Cape Mendocino, California- -indicators of high tectonic uplift rates: GSA Abstracts with Programs, **14**, n. 4, p. 178.

Lajoie, K.R., 1986a, Coastal Tectonics, *in* Wallace, R., panel chairman, Active Tectonics: Studies in Geophysics Series, Geophysics Research Forum, National Academy Press, p. 95-124.

Lajoie, K. R., 1986b, Rapid tectonic uplift near the Mendocino triple junction recorded by emergent marine strandlines (abstract): EOS Trans. AGU, **67**, no. 44, p. 1224.

Lawson, A. C., et al, 1908, The California earthquake of April 18, 1906: Report of the State Earthquake Investigation Commission: Carnegie Institute, Washington, Publication **87**, 3 vols., 1 atlas.

Leopold, Luna, and Bull, William B., 1979, Base level, aggradation, and grade: Proc. of the American Philosophical Soceity: **123**, p. 168-202.

Linick, T. W., Suess, H. E., and Becker, B., 1985, La Jolla measurements of radiocarbon in south German oak tree-ring chronologies: Radiocarbon, **27**, no. 1, p. 20-32.

Linick, T. W., Long, A. Damon, P. E., and Ferguson, C. W., 1986, High-precision radiocarbon dating of bristlecone pine from 6554 to 5350 BC: Radiocarbon, **28**, no. 2B, p. 943-953.

Lisowski, M., and Prescott, W. H., 1989, Strain accumulation near the Mendocino triple junction, CA (abstract): EOS Trans. AGU, **70**, no. 43, p. 1332.

Lisowski , M., et al, 1991, (abstract): GSA Abstracts with Programs, **23**.

Mackin, J.H., 1948, Concept of the graded stream: GSA Bulletin, **59**, p. 463-512.

Madrone, S.G, 1992, personal communication, Redwood Community Action Agency, Eureka, CA.

Mattole Restoration Council, 1988, Distribution of old growth coniferous forests in the Mattole River Watershed, map: MRC, Petrolia, CA.

Mattole Restoration Council, 1989, The Elements of Recovery: an inventory of upslope sources of sedimentation in the Mattole River Watershed: Mattole Restoration Council, Petrolia, CA.

McLaughlin, R.J., Sorg, D.H., Morton, J.L., Batchelder, J.N., LeVeque, R.A., Heropoulos, C., Ohlin, H.N., and Norman, M.B., II, 1979a, Timing of sulfide mineralization and elimination of the San Andreas fault at Point Delgada, California: EOS (American Geophysical Union Transactions), **60**, p. 883.

McLaughlin, R. J., Sorg, D. H., Ohlin, H. N., and Heropoulos, Chris, 1979b, Base and precious metal occurrences along the San Andreas fault, Point Delgada, CA: U. S. Geological Survey Open-File Report **79-589**, 11p.

McLaughlin, R.J., Kling, S.A., Poore, R.Z., McDougall, Kristin, and Beutner, E.C., 1982, Post-middle Miocene accretion of Franciscan Rocks, northwestern California: GSA Bulletin, **93**, p. 595-605.

McLaughlin, R.J., Lajoie, K.R., Sorg, D.H., Morrison, S.D., and Wolfe, J.A., 1983, Tectonic uplift of a middle Wisconsin marine platform near the Mendocino triple junction, California: Geology, **11**, p. 35-39.

McLaughlin, R. J., 1983, Reply to Discussion of "Post-middle Miocene accretion of Franciscan rocks, northwestern California", by S.G. Miller and K.R. Aalto: GSA Bulletin, **94**: p. 1029-1031.

McLaughlin, R. J., Sliter, W. V., and Frederiksen, N. O., 1986, Plate motions recorded by tectonostratigraphic terranes adjacent to the Mendocino triple junction (abstract) EOS Trans. American Geophysical Union, **67.**

McLaughlin , R. J., Sliter, W. V., Clarke, S. H., Jr., McCulloch, D. S., Frederiksen, N. O., and Ingebretson, D. C., 1988, Implications of onshore and offshore structure for location and Cenozoic evolution of the Mendocino triple junction (abstract): GSA Abstracts with Program, **20**, p. A382.

McPherson, R. C., Smith, S. W., and Severy, N. I., 1981, The Humboldt Bay seismic network, 1974-1980 (abstract): Earthquake Notes, **52**, p. 41.

McPherson, R. C., 1989, Seismicity and focal mechanisms near Cape Mendocino, northern California, 1974-1984: Master's thesis, Humboldt State University, CA, 75 p.

McPherson, R. C., and Dengler, L. A., 1991, Evidence of compressional tectonics in the King Range, CA: the 1991 Honeydew earthquake (abstract): EOS Trans. AGU, **72**, no. 44, p. 315.

Merritts, Dorothy, 1986, Late Quaternary tectonism in coastal northern California, Mendocino triple-junction region: a geomorphic approach [abstract]: EOS Trans. AGU, **67**, p. 1224.

Merritts, Dorothy J., 1987, Geomorphic response to late Quaternary tectonism, coastal northern California, Mendocino triple junction region: unpublished Ph. D. dissertation, Univ. of Arizona, 190 p.

Merritts, Dorothy, and Bull, W. B., 1989, Interpreting Quaternary uplift rates at the Mendocino triple junction, northern California, from uplifted marine terraces: Geology,.**17**, 1020-1024.

Merritts, Dorothy, and Vincent, Kirk, 1989, Geomorphic response of coastal streams to low, intermediate, and high rates of uplift, Mendocino triple junction region, northern California: GSA Bulletin, **11**, p. 1373-1388.

Merritts, Dorothy, Wohl, Ellen, and Vincent, Kirk R., 1989, Comparison of flights of fluvial terraces among nearby bedrock rivers with different rates of base-level fall, coastal northern California: GSA Abstracts with Programs, **21**, no. 6, p. A-40.

Merritts, D. J., and Bonita, J, 1991, Patterns and rates of crustal deformation, northern termination of the San Andreas transform boundary: GSA Abstracts with Programs, **23**, p. 78.

Merritts, D. J., Chadwick, O.A., and Hendricks, D.M., 1991, Rates and processes of soil evolution on uplifted marine terraces, northern California: Geoderma, **51**, p. 241-265.

Merritts, Dorothy, Chadwick, Oliver, Hendricks, D. M., Brimhall, George, and Lewis, Christopher, in press, Mass balance approach to interpreting processes of soil formation on a flight of late Quaternary marine terraces, northern California: GSA Bulletin.

Miller, S. G., 1982, Petrology and structure of the coastal Franciscan from the Mattole River to Mussel Rock, northern CA: B. Sc. thesis, Humboldt State Univ., CA, 40 p.

Miller, S. G. and K. R. Aalto, 1983, Discussion of "Post-middle Miocene accretion of Franciscan rocks, northwestern California", by McLaughlin et al: GSA Bulletin, **94**, p. 1028-1029.

Miner, A., 1992, personal communication, Petrolia, CA.

Mitchell, C. E., Weldon, R. J., II, Vincent, P., and Pittock, H. L., 1991, Active uplift of the Pacific northwest margin: EOS Trans. AGU, **72**, no. 44, p. 314.

Muhs, Daniel R., 1985, Amino-acid age estimates of marine terraces and sea levels on San Nicolas Island, California: Geology, **13**, p. 58-61.

Nason, R. D., 1968, San Andreas fault at Cape Mendocino, *in* Dickinson, W.R., and Grantz, A., eds., Conference on Geologic Problems of San Andreas Fault System: Stanford Publications in Geological Sciences, **11**, 231-241.

National Oceanic and Atmospheric Administration (1985), Local climatological data, annual summaries: Environmental Data Service, National Climatic Center, Dept. Commerce, Washington, D.C.

Oppenheimer, D. H., and Magee, M. E., 1991, (abstract): EOS Trans. AGU, **72**, no. 44, p. 311.

Pearson, G. W., and Stuiver, M., 1986, High-precision calibration of the radiocarbon time scale, 500-2500 BC: Radiocarbon, **28**, no. 2B, p. 839-862.

Perry, R. B., and Pryor, D. E., 1986, Bathymeric evidence for the San Andreas fault north of Point Arena: EOS Trans. AGU, **67**, no. 44, p. 1215.

Plafker, G., 1969, Tectonics of the March 27, 1964 Alaska earthquake: U.S.G.S. Professional Paper 543-I, 74 p.

Plafker, G. and J. C. Savage., 1970, Mechanism of the Chilean earthquakes of May 21 and May 22, 1960: GSA Bulletin, **81**, p. 1001-10030.

Pollitz, F. F., 1986, Pliocene change in Pacific plate motion: Nature, **320**, 738-741.

Puls, Robert W., 1985, Soils of the King Range National Conservation Area (western slope), Humboldt County, California: prepared for the Bureau of Land Management, Contract No. Ya551-Ct3-340079, 119 p.

Reid, L. M. and T. Dunne, 1984, Sediment production from forest road surfaces: Water Resources Research, **20**, no. 11, p. 1753-1761.

Roscoe, J., 1985, Ethnohistory of the Mattole: unpublished report, Humboldt State University, Arcata, CA.

Rothacher, J., 1970, Increases in water yield following clear-cut logging in the Pacific Northwest: Water Resources Research, **6**, no. 2, p. 653-658.

Selby, M.J., 1980, A rock mass strength classification for geomorphic purposes: with tests from Antarctica and New Zealand: Zeitschrift fur Geomorphologie, v. 24, no. 1, p. 31-51.

Shreve, R.L., 1967, Infinite topologically random channel networks: Journal of Geology, v. 75, p. 178-186.

Silver, E. A., 1971, Tectonics of the Mendocino triple junction: GSA Bulletin, **82**, p. 2965-2978.

Simila, G. W., 1980, Seismological evidence on the tectonics of the northern section of the San Andreas fault region, *in* Studies of the San Andreas Fault Zone in Northern California, edited by R. Streitz and R. Sherburne: Spec. Rep. Calif. Div. Mines Geol., **140**, p. 131-137.

Smith, A., 1991, personal communication, Honeydew CA.

Smith, Stewart W., and Knapp, John S., 1980, The northern termination of the San Andreas fault, in Studies of the San Andreas fault zone in northern California: California Division of Mines and Geology Special Report 140, p. 153-164.

State of California, 1973, Character and Use of Rivers, Mattole River: Resources Agency, Department of Water Resources, Division of Resources Development, Memorandum Report.

Steensen, D.L. 1987, Honeydew Slide Study: summary report: Prepared for Mattole Watershed Salmon Support Group, Petrolia CA.

Stuiver, M. and Becker, B., 1986, High-precision decadal calibration of the radiocarbon time scale, AD 1950-2500 BC: Radiocarbon, **28**, no. 2B, p. 863-910.

Stuiver, M., Pearson, G. W., and Braziunas, T. F., 1986, Radiocarbon age calibration of marine samples back to 9000 Cal yr BP: Radiocarbon, **28**, no. 2B, p. 980-1021.

U.S. Geological Survey WSP 1650-A, B, Floods of December, 1955 -January, 1965 in the Far Western States, parts 1 (description), and 2 streamflow data).

U.S. Geological Survey WSP 1866-A,B, Floods of December, 1964 - January, 1965 in the Far Western States, parts 1 (description), and 2 (streamflow data).

Veeh, H. H., and Chappell, J., 1970, Astronomical theory of climate chaneg: Support from New Guinea: Science, **167**, p. 862-865.

Verdonck, D., and Zandt, G., 1991, Structure of the Mendocino triple junction from local earthquake tomography: EOS Trans. AGU, **72**, no. 44, p. 315.

Wilson, D.S., 1986, A kinematic model for the Gorda deformation zone as a diffuse southern boundary of the Juan de Fuca plate: JGR, **91**, p. 10,259-10,270.

Wilson, D. S., 1989, Deformation of the so-called Gorda plate: JGR, **94**, no. B3, p. 3065-3075.

Thermoluminescence dating of coastal sediments near Eureka

Glenn W. Berger

Department of Geology, Western Washington University,

Bellingham, WA 98225-9080

ABSTRACT

Accuracy tests of the thermoluminescence (TL) sediment-dating method show that estuarine mud, beach/terrace sediments, and dune sand and interbedded soils are suitable targets for TL dating under some conditions. Application of TL dating to unknown-age shallow marine mud at a Mad River site gave an age of 176±33 ka, and a nearshore deposit at the Southport Landing site yielded a TL date of 119±33 ka. These first results for this region suggest that this dating method is useful for some Pleistocene coastal deposits.

INTRODUCTION

Numerical dating methods that can reach beyond the usual ~40 ka limit of ^{14}C dating are needed to provide accurate estimates of deformation rates, and thereby a fuller understanding of the neotectonic processes operating in regions such as represented in Figure 1. Berger et al. (1991) applied the fine-grain partial-bleach TL sediment dating technique (Aitken, 1985; Berger, 1988) to several modern, independently dated and unknown-age deposits from sites shown in Figure 1. Their objective was to test the TL-zeroing assumption under local conditions, and to apply resulting TL procedures to a few older sediments that had no independent age control.

The basic principles of (unheated) sediment dating by TL are that: insolation dramatically reduces the light-sensitive TL component in mineral grains before burial, after burial a light-sensitive TL signal builds up in each grain at a constant rate from exposure to ambient low-level ionizing radiation, laboratory measurements of TL induced and modified with calibrated radiation sources and simulated or natural daylight exposures, yield a TL signal proportional to the burial time.

RESULTS

Eolian Sediments

Many of the marine terrace remnants in NW California are capped by eolian sediments (dune sand or silt). Figure 2 shows the Holocene site at the mouth of the Mad River (Fig. 1) used in the TL zeroing tests for dune environments. This sand-dune sequence rests on a marine abrasion platform cut across Pleistocene sediments. Extensive cross bedding in the sand indicates an eolian origin and the composition of the well-sorted, fine sand suggests a short transport distance from a nearby beach.

The two TL samples from this site yielded TL ages in accord with the radiocarbon chronology. These results therefore suggest that the TL zeroing assumption has been reasonably satisfied for the 4-11 μm grains in this dune sand and buried soil.

At the Patricks Point site (Fig. 1) the upper 8-10 meters of sediment above a marine abrasion platform consist of cross-bedded, well-sorted, fine-to-coarse grained dune sand with several interbedded paleosols. Figure 3 summarizes the TL and ^{14}C dating results for pre-Holocene dune sand and buried soil from the upper portion of the Patricks Point section. There is good agreement among the TL and ^{14}C results for the upper samples. Because the lowest sample (PAT-7) was collected from a protruding bench that is believed to have been exhumed within the last few years, this sample may have been contaminated by younger fine-silt grains from higher in the bluff. These results suggest that dune sands or soils formed in those sands, and capped by additional sands, appear to represent a suitably "closed" system for fine-grain TL dating.

Estuarine Mud

Fossiliferous mud and bioturbated sand at the top (~35-40 m ASL) of the Mad River bluffs section (Fig. 1) is interpreted by Miller and Morrison (1988) as backbar sediments, consisting of slough-margin sandflats and muddy slough deposits. Abundant in-situ fossils indicate a shallow-water, marine, estuarine depositional environment, probably similar to the present one at Arcata Bay. A 176±33 ka TL age for the mud at ~40 m ASL in the Mad River bluffs is the first direct age determination for these deposits and is consistent with the soil correlation age of ~70 ka (Burke, unpublished soils course data) for the soil cut into the upper sediments.

Beach/Terrace Sediments

The Southport Landing, Table Bluff, and Centerville Beach sites (Fig. 1) have beach and nearshore sediments lying on abrasion platforms that have been uplifted. The zeroing assumption for beach sediments was tested with a sample from the surf zone of Agate Beach, and a TL zero-point age of ~5 ka was measured. A quarry cut into a marine terrace at Southport Landing exposes nearshore sediments resting on an abrasion platform. Clay/silt lenses interbedded with pebbly sand and gravel just below the abrasion platform were sampled for TL dating. A TL date of 119±31 ka was obtained for this Southport Landing sample (SPLQ-1), which is consistent with the correlative age estimate of ~80 ka for the marine terrace surface (Carver et al., 1985). Because the sampled unit was below the abrasion platform of that terrace, its age should be somewhat older than the 80 ka age assumed for the platform. Unlike this sample, the TL samples from the Table Bluff and Centerville Beach sites failed the equivalent-dose plateau test, and so did not yield acceptable TL dates.

CONCLUSIONS

With careful sample selection, one can date capped dune sands and associated buried soils using the fine-grain TL method. Estuarine mud is a good target for TL dating, as also shown by Berger (1990) and Berger et al. (1990). The single reliable TL result (119±33 ka, Southport Landing) from the three sampled beach/marine terrace deposits suggests that further application of TL dating methods to such sediments would be fruitful.

REFERENCES

Aitken, M. J., 1985, Thermoluminescence dating: New York, Academic Press, 351 p.

Berger, G. W., 1988, Dating Quaternary events by luminescence, *in* Easterbrook, D. J., ed., Dating Quaternary sediments: Geological Society of America Special Paper, 227, p. 13-50.

Berger, G. W., 1990, Effectiveness of natural zeroing of the thermoluminescence in sediments: Journal of Geophysical Research, v. 95, p. 12,375-12,397.

Berger, G. W., Luternauer, J. L., and Clague, J. J., 1990, Zeroing tests and application of thermoluminescence dating to Fraser River delta sediments: Canadian Journal of Earth Sciences, v. 27, p. 1737-1745.

Berger, G. W., Burke, R. M., Carver, G. A., and Easterbrook, D. J., 1991, Test of thermoluminescence dating with coastal sediments from northern California: Chemical Geology (Isotope Geoscience Section), v. 87, p. 21-37.

Carver, G. A., Burke, R. M., and Kelsey, H. M., 1985, Quaternary deformation studies in the region of the Mendocino triple junction: *in* Jacobsen M. L. and Rodriquez, T. R., eds., Summaries of technical reports, National Earthquake Hazards Reduction Program, v. XXI, p. 58-62.

Miller, W., and Morrison, S. D., 1988, Marginal marine Pleistocene fossils from near mouth of Mad River, northern California: Proceedings of the California Academy of Sciences, v. 45, p. 255-266.

FIGURE CAPTIONS

Figure 1. Location of TL sampling sites.

Figure 2. Schematic stratigraphic section of exposures near the mouth of the Mad River, with TL and ^{14}C dates (converted to calendar years).

Figure 3. Schematic stratigraphic section at upper Patricks Point site, with TL (all in ka) and ^{14}C dates.

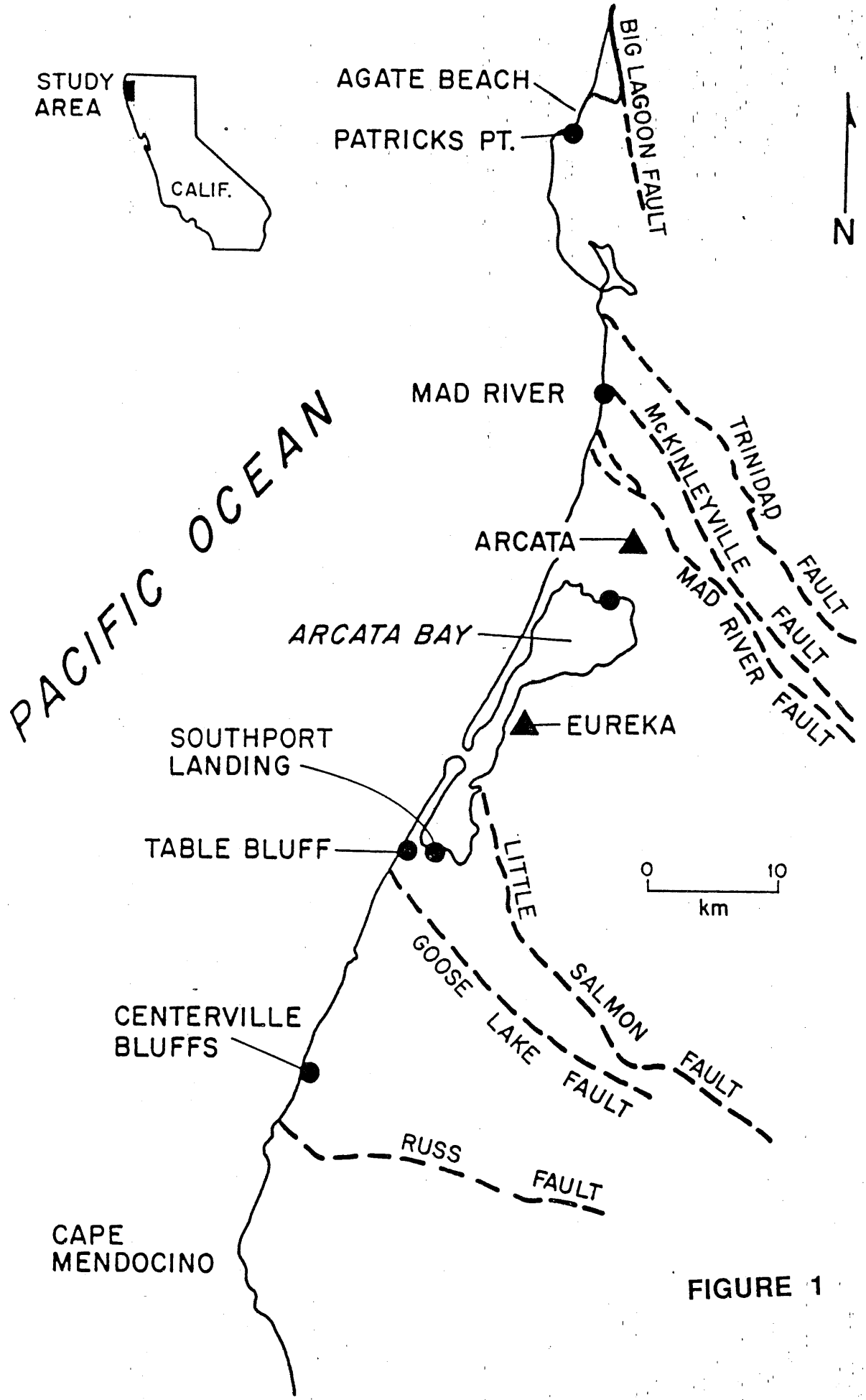
STUDY AREA
CALIF.
AGATE BEACH
PATRICKS PT.
BIG LAGOON FAULT
N
MAD RIVER
McKINLEYVILLE FAULT
TRINIDAD FAULT
MAD RIVER FAULT
PACIFIC OCEAN
ARCATA
ARCATA BAY
EUREKA
SOUTHPORT LANDING
TABLE BLUFF
LITTLE SALMON FAULT
0 10
km
GOOSE LAKE FAULT
CENTERVILLE BLUFFS
RUSS FAULT
CAPE MENDOCINO

FIGURE 1

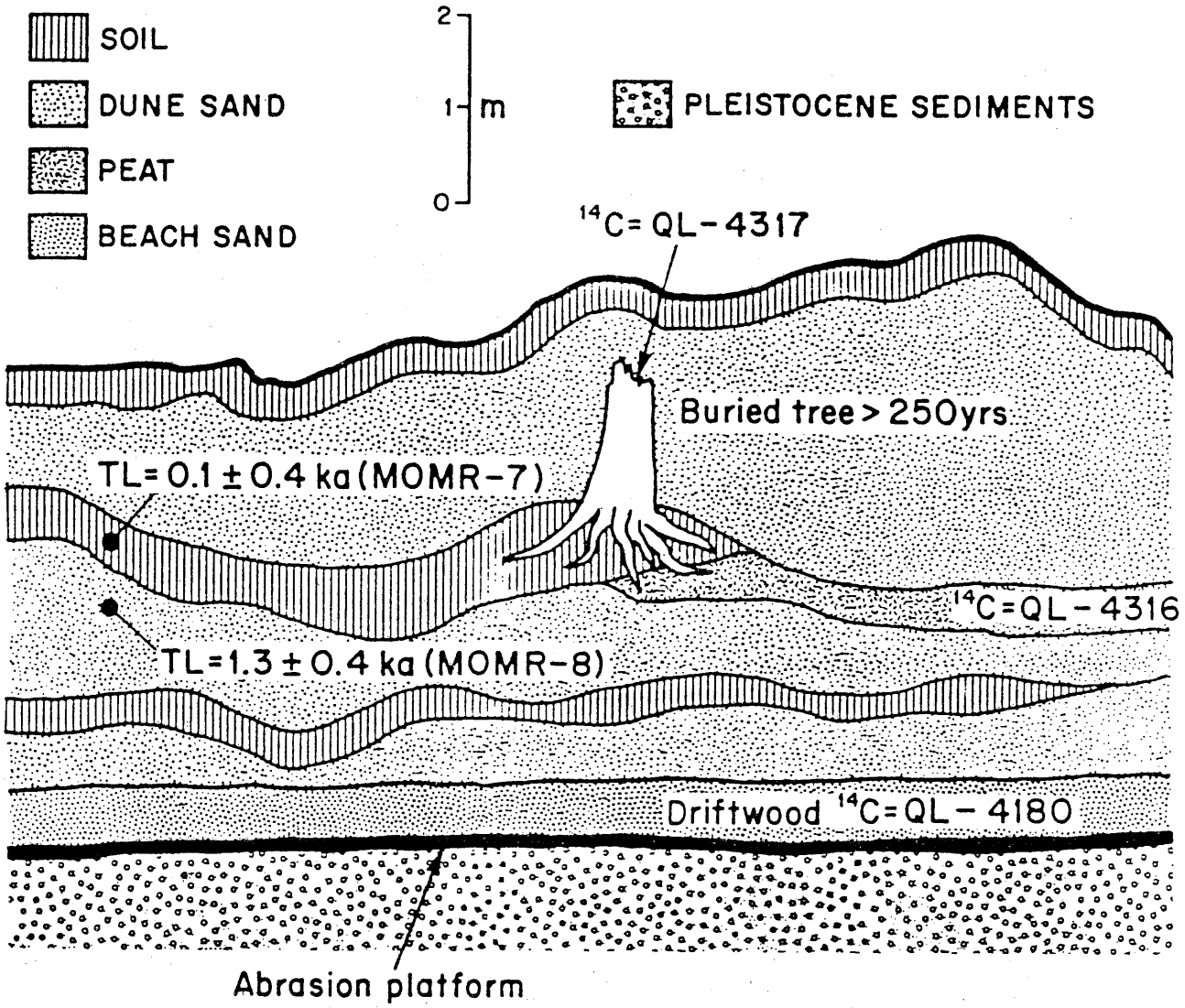
SOIL
DUNE SAND
PEAT
BEACH SAND
2
1
0
m
PLEISTOCENE SEDIMENTS
14C= QL-4317
Buried tree > 250yrs
TL= 0.1 ± 0.4 ka (MOMR-7)
14C=QL-4316
TL=1.3 ± 0.4 ka (MOMR-8)
Driftwood 14C=QL-4180
Abrasion platform

FIGURE 2

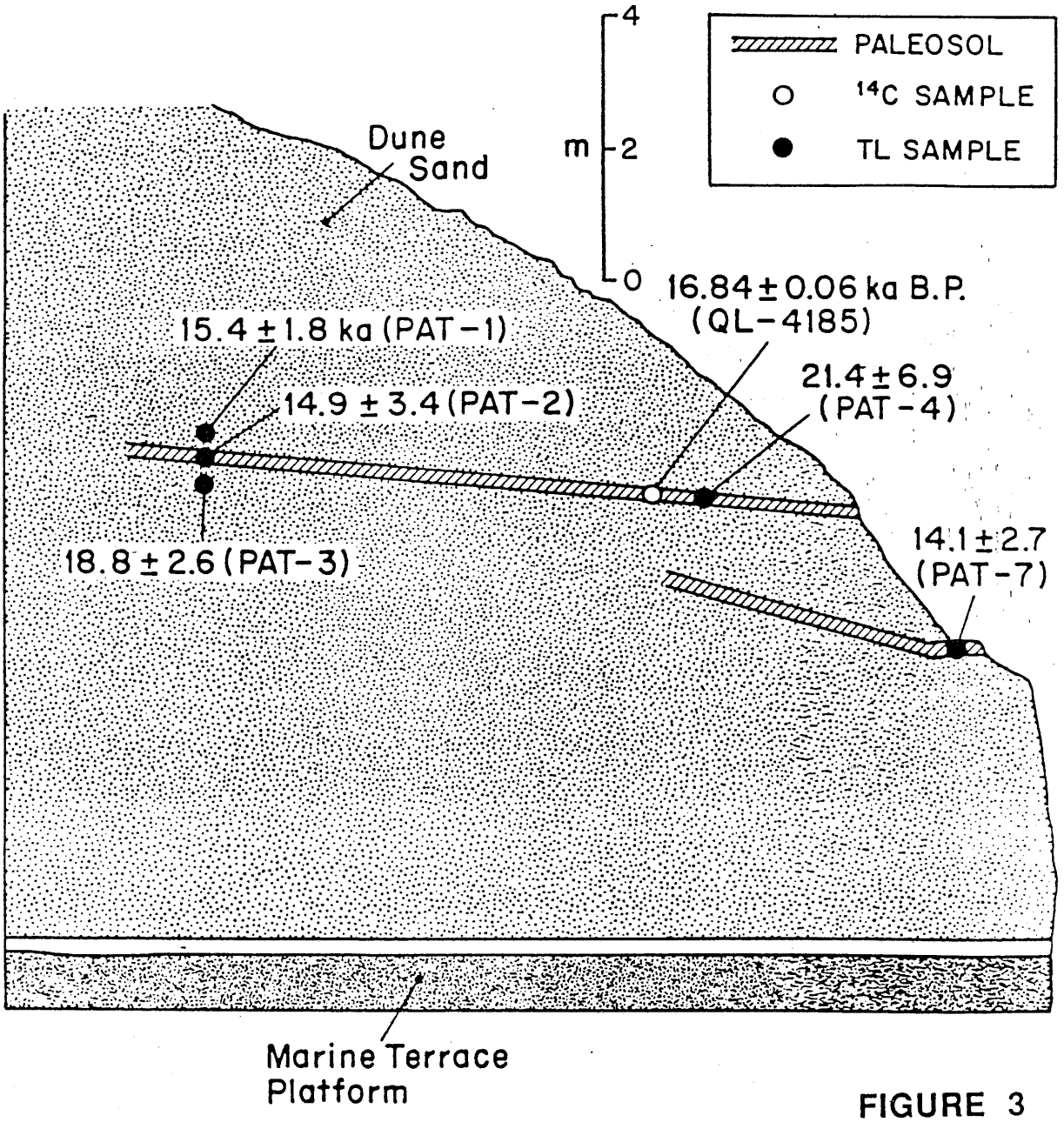
PALEOSOL
^{14}C SAMPLE
TL SAMPLE
4
m 2
0
Dune Sand
16.84 ± 0.06 ka B.P. (QL-4185)
15.4 ± 1.8 ka (PAT-1)
14.9 ± 3.4 (PAT-2)
21.4 ± 6.9 (PAT-4)
18.8 ± 2.6 (PAT-3)
14.1 ± 2.7 (PAT-7)
Marine Terrace Platform

FIGURE 3

SEDIMENTOLOGY AND STRATIGRAPHY OF THE MOUTH OF MAD UNIT, HUMBOLDT COUNTY, CALIFORNIA

Erik W. Harvey Eileen M. Weppner
Department of Geology
Humboldt State University
Arcata, CA 95521

INTRODUCTION

Northward migration of the mouth of the Mad River has produced extensive new exposures along the eastern bank. Included in this exposure is an unconformity bour unit consisting of Pleistocene marine and estuarine deposits. Since this unit was first studied (Miller and Morrison, 1988), the extent of the exposure has increased to reve complex sequence of depositional facies. The unit is informally named the Mouth of unit (Harvey and Weppner, 1992). An informal name is used for two reasons: 1) onl exposure of the Mouth of Mad unit is known at this time, and 2) extensive folding and faulting in northern coastal California make correlation of units difficult. Four distinctive depositional facies can be delineated within the unit, representing nearshore marine and shallow bay environments. Abundant fossil, primarily mollusks, are present in the upper and lower facies. The purpose of this paper is to describe the Mouth of Mad unit and to interpret its depostitional history. We also attempt to correlate the unit with other Pleistocene deposits that have been described in the same region.

STUDY AREA AND METHODS

The Mouth of Mad unit is exposed in the bluffs along the east bank of the Mad River, extending from 250 m south of the Highway 101 vista point to 100 m north of Widow White Creek (Fig. 1). The bluffs reach a maximum height of approximately 30 m at the north end of the exposure and decrease steadily to the south. South of the bluffs the deposits are covered by vegetation, but presence of the unit is suggested by shell material in the beds of small tributary creeks along the river.

Samples were collected from the bay deposits for analysis of fossil content. Six samples were soaked overnight in 10% sodium hexameta phosphate solution and then washed on a 2 mm screen. After drying, the fossils were identified using the literature of west coast mollusks (Abbott, 1974; Grifith, 1975; Abbot and Dance, 1982; and Kozloff, 1987). One additional sample from the lowest sand facies, collected by Gary Carver, was examined and the fossils identified. Descriptions of bed thickness, sediment texture, and physical sedimentary structures are drawn from our field observations made in the fall and winter of 1991-92.

STRATIGRAPHY

The Mouth of Mad unit contains four depositional facies, representing a sequence of nearshore marine and shallow bay environments (Fig. 2). The unit is bounded by unconformities; it is underlain by a paleosol, and overlain by younger late Pleistocene terrace deposits (Fig 2). The majority of the unit consists of unconsolidated sand and gravel, but some mud is found at the top.

The lowest facies (Fig. 2) is a well-sorted, subangular to subrounded, light olive gray (5 Y 5/2) fine sand. Scattered pebbles and pebble stringers occur near both the upper and lower contacts. A basal muddy gravel bed contains the clam *Tresus* sp. in living position is found above the paleosol. Trough cross-bed sets, approximately 20 cm thick, are poorly

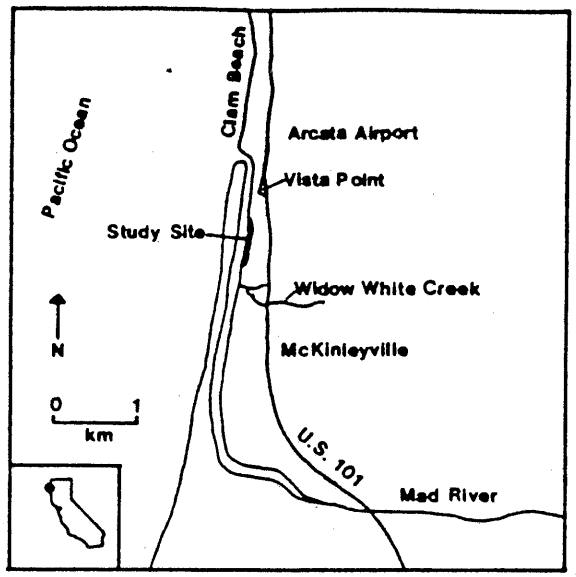

Figure 1. Location of the study site.

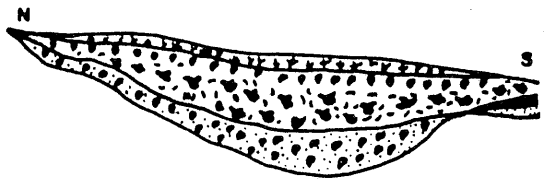

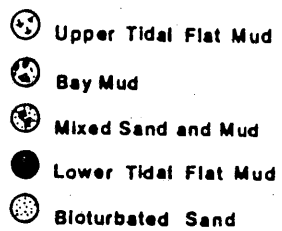

Figure 4. Lateral variation within the bay facies of the Mouth of Mad unit.

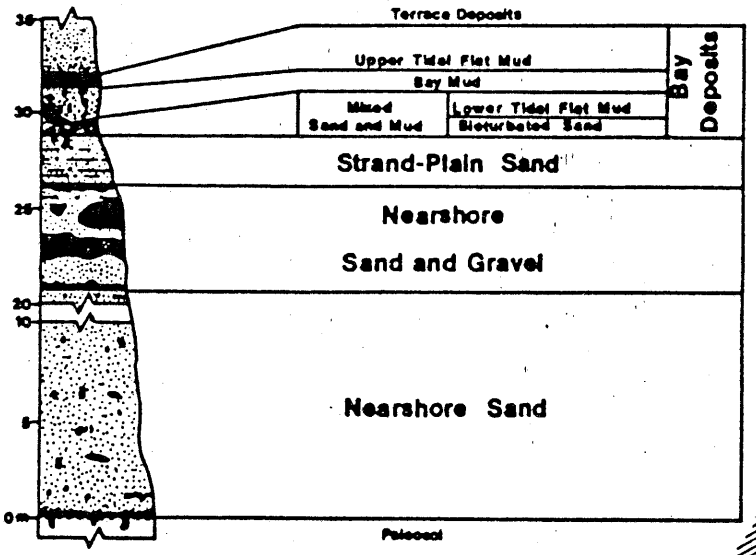

Figure 2. Generalized stratigraphic column for the Mouth of Mad unit.

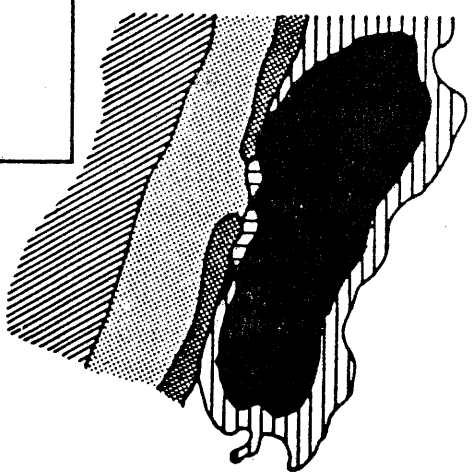

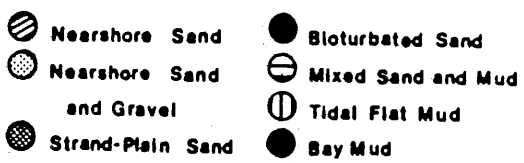

Figure 3. Depositional environment model for the Mouth of Mad unit.

visible throughout the facies. Occasional vertical burrows 10-15 cm in diameter (?*Ophiomorpha*) are also present. A single fossil sample from within the sand near the contact with the muddy gravel contains the gastropod *Olivella biplicata* (Sowerby, 1825) and fragments of the sand dollar *Dendraster* sp. Abrasion of the gastropod shells and fragmentation of the sand dollars suggests transport, probably by waves and currents.

Nearshore sands grade upward to an interbeded sand-and-gravel facies (Fig. 2). Scattered pebbles occur near the top of the nearshore sand and increase in frequency upward until small gravel stringers are found. The contact between the two facies is defined here as the lowest laterally continuous gravel bed. The sand interbeds are similar in composition to the subjacent nearshore sand. Gravels consist of poorly to very poorly sorted, subangular to subrounded, moderate yellow brown (10 YR 5/4). gravel in a fine to medium sand matrix. Pebbles average approximately 15 mm in diameter, but reach a maximum diameter of 9 cm. Gravel occurs in lenses and tabular beds. Normal grading and high-angle or trough cross-beds are present in most of these gravel beds. Some of the gravels contain imbricated mud clasts, the mud clasts being 6-10 cm in length. Gravel beds increase in thickness to a maximum of 63.5 cm in the middle of the facies, but decrease to single-pebble thickness at the upper and lower contacts. The highly irregular lower boundaries of the gravel beds show evidence of scour and fill. The pohysical structures within the sand beds changes gradually to parallel lamination near the top of the facies.

Above the last laterally continuous gravel bed is a well-sorted, subangular to subrounded, moderate yellow brown (10 YR 5/4), fine to medium sand (Fig. 2). The sand occurs in plane-parallel lamination 1-4 mm thick. Pebble stringers occur near the lower contact. Near the upper contact with the bay deposits, burrows increase in abundance. The most prominent of these burrows is 8-10 cm wide and extends to 1 m below the contact with the overlying bay deposits. One such burrow contained the clam *Tresus* sp. in living position.

The bay deposits are further divided into five subfacies (Figs. 2 and 4) based on sedimentologic and faunal differences. Lateral variation among the subfacies is extensive (Fig. 4). A bay separated from the ocean by a migrating sand spit is proposed as the original depositional setting (Fig. 3).

Near the southern end of the exposure the lowest subfacies division is a heavily bioturbated sand (Figs. 2 and 4). The sand is a well-sorted, subangular to subrounded, moderate yellowish brown (10 YR 5/4), fine to medium sand. Bioturbation has apparently eliminated all original physical sedimentary structures. An increasing abundance of burrows marks the contact with the subjacent strand-plain sand. This highly fossiliferous deposit contains the bivalves *Protothaca staminea* (Conrad, 1837), *Tresus* sp., and *Saxidomus gigantea* (Deshayes, 1839), and small amounts of transported plant material, possibly eel grass. Also found are transported fragments and whole shells of the bivalves *Ostrea lurida* Carpenter, 1864 and *Macoma nasuta* (Conrad, 1837), and the gastropod *Bittium eschrichtii* (Middendorf, 1849). Transportation is indicated by abrasion of the shells, although their generally intact condition indicates a short distance of transport.

Where it occurs, the bioturbated sand is always overlain by an olive gray (5 Y 4/1), finely laminated mud (Figs. 2 and 4). This mud contains no shells, but has abundant plant fragments, which may be eel grass.

Where the lower tidal flat mud and bioturbated sand are absent, a poorly sorted, subangular to subrounded, light brown (5 YR 4/4-5/6) clay-rich sand deposit occurs (Figs 2 and 4). Bioturbation has thoroughly mixed what was likely a backshore sand with bay mud from above. The clay content of this subfacies increases toward the upper contact with

the bay mud subfacies. This deposits contains abundant fossils, including the bivalves *Ostrea lurida*, *Clinocardium nuttali* (Conrad, 1837), *Tresus* sp., *Saxidomus gigantea*, and *Protothaca staminea*; the gastropods *Acteocina culcitella* (Gould, 1852) and *Tricolia* sp.; the cirriped *Balanus* sp.; crustacean appendages; and plant fragments. Also found are the transported gastropods *Bittium eschrichtii* and *Odostomia nota* Dall and Bartsch, 1909.

Overlying both the mixed sand and mud, and the lower tidal flat mud, is an olive gray (5 Y 4/1) mud, some sand is present near the upper contact with the upper tidal flat mud (Figs. 2 and 4). Abundant fossils and bioturbation have formed a shell hash with no obvious structure. The dominant fossil is *Ostrea lurida*, which occurs in small clumps that were originally part of an oyster garden. Also present are the bivalves *Macoma nasuta*, *Protothaca staminea*, and *Clinocardium nuttalli*; the gastropods *Acteocina culcitella* and *Mitrella gausapata* Gould, 1850; the polyplacophoran *Mopalia* sp.; the cirriped *Balanus* sp.; crustacean appendages; and plant fragments. The transported component includes the bivalve *Saxidomus gigantea* and the gastropods *Diodora aspera* (Rathke *in* Eschscholtz, 1833) and *Tricolia* sp. The clam *Tresus* sp. is found in place near the upper contact where the sand content is greater.

At the top of the Mouth of Mad unit, underlying the younger late Pleistocene terrace deposits, is another tidal flat mud (Figs. 2 and 4). This mud is considerably thicker than the lower tidal flat mud and the upper 20 cm is deeply weathered to a moderate reddish brown color (10 R 4/6). This mud also contains abundant plant material, which is again likely to be eel grass.

DISCUSSION

Depositional Environments

The trough cross-beds, normal grading, and the presence of fragmented sand dollars suggests a high-energy environment seaward of a beach swash zone for the nearshore sand and nearshore sand and gravel facies. This likely corresponds to the outer rough to inner rough zones of Clifton et al. (1971) (Fig. 3). The thick gravel beds suggest winter storm deposits, while the smaller lenses were probably formed by rip currents (Leithold and Bourgeois, 1984).

The thin essentially flat and planar lamination of the strand-plain sand facies suggest a swash zone (Clifton, 1969) such as found on a beach or sand spit. A spit is likely to have developed during a more gradual regressive phase. Sand spit deposits appear to occur near the southern end of the exposure, while beach deposits occur to the north (Fig. 3).

The gradational lower contact of the bioturbated sand subfacies with the strand-plain sand and the sandy texture suggest a backshore area near a tidal flat (Fig. 3). This backshore sand was likely colonized by burrowing invertebrates following encroachment by the bay. The resulting biological activity destroyed the original physical sedimentary structures.

The fine laminations, in the both the lower and the upper tidal flat mud subfacies and the possible presence of eel grass suggest a tidal flat bordering a bay or estuary (Fig. 3). The upper tidal flat mud appears to have formed landward of the bay, with the lower mud forming along the backshore of a spit or beach.

The sedimentary texture and fauna of the mixed sand an mud facies, and the gradual increase in bioturbation in the upper portion of the strand-plain sand suggest a transition between backshore and bay deposits without the formation of a tidal flat (Fig. 3). This

transition would occur near the inlet of a bay or where the migration of a spit allowed a change of environments without the development of a tidal flat environment. A tidal flat would form along the backshore of a spit up to a point near the end where water depth and biological activity produces deposits similar to the bioturbated sand (Fig. 3). With lowering sea-level or porgradation, the depositional environment would change from a sand spit to a bay, producing a mixed sand and mud deposit. When the spit migrates, the limit of tidal flat formation will also migrate covering the sand before bay mud can be incorporated into it. (Fig. 3).

The fauna and texture of the bay mud subfacies suggest a shallow protected bay that received occasional sand input owing to storms topping a protective spit (Fig. 3).

Age and Correlation

All of the fossils present in the Mouth of Mad unit appear to be extant, whereas older deposits in the area, such as the Falor Formation and the Wildcat Group, contain extinct species. This indicates that the Mouth of Mad unit is very young. A single thermoluminescence date was obtained for the upper tidal-flat mud by Berger et al. (1991). Their estimate for the age of the mud is 176+/-33 ka. This age estimate is supported by a soil correlation age of 70 ka for a soil formed on the overlying terrace deposits (Berger et al., 1991, p.34). these dates and the fossil evidence suggest a late Pleistocene age for the Mouth of Mad unit (proposed solely on fossil evidence by Miller and Morrison, 1988).

The extensive folding and faulting in the region (Carver, 1989; Carver et al., 1986; Clarke and Carver, 1992) makes correlation over even short distances difficult. Evenson (1959) mapped the pre-terrace units in the vicinity of the study area as part of the Hookton Formation. The formation name "Hookton" was used by Ogle (1953) to describe post-Wildcat Group deposits south of Eureka and north of Fortuna. The lithologic variability in this formation, which includes gravel, sand, and mud of marine and terrestrial origin, and the lack of continuous exposure, make carrying the name outside the type area difficult to justify.

Carver (1985) mapped deposits in the banks of streams that erode the margin of Dow's Prairie as the early to middle Pleistocen Falor Formation. The apparent age of the Mouth of Mad unit makes it younger than the Falor, and therefore not equivalent.

Several fossiliferous Pleistocene localities in the area were studied by Kennedy (1978, pp. 190-265), and Roth (1979). Kennedy reported dates for many of the deposits using amino acid racemization from Wehmiller, Kennedy, and Lajoie (1977) and Wehmiller et al. (1977). The date reported for the Marine lenses of the Hookton formation, or "Hookton marine", in the Eureka-Fields Landing area was 175+/-35 ka, or oxygen isotope stage 7 (Wehmiller, Kennedy, and Lajoie, 1977). This date suggests a possible time equivalence between the "Hooton marine" and the Mouth of Mad unit. This cannot be confirmed however, owing to the lack of continuos exposure between the Hookton type are and the mouth of the Mad River. Other localties dated include Elk head (stage 11 or 13, most likely 11), the Crannel beds of Kohl (1974)(stage 11, 13 or 15), Trinidad Head (stage 11,13, or 15, most likely 13), and Moonstone Beach (stage 21). Therefore, it would appear that all of these deposits are significantly older than the Mouth of Mad unit.

ACKNOWLEDGEMENTS

We would like to thank Dr. William Miller, for his advice, support, and help in editing this manuscript. We would also like to thank Dr. Raymond "Bud" Burke and Dr. Gary Carver for their helpful suggestions and encouragement.

REFERENCES CITED

Abbott, R.T. 1974. American seashells, 2nd. ed. Van. Norstrand Reinhold Co., New York. 633 pp.

Abbott, R.T. and S. P. Dance. 1982. Compendium of Seashells. E. P. Dutton, Inc., New York. 410 pp.

Berger, G.W., Burke, R.M., Carver, G.A. and Easterbrook, D.J. 1991. Test of thermoluminescence dating with coastal sediments from northern California. Chemical Geology. 87:21-37.

Carver, G.A. 1985. Quaternary tectonics north of the Medocino Triple Junction: the Mad River Fault Zone. Pp. 155-167 *in* Redwood Country, M.E. Savina, ed. American Geomorphological Field Group Field Trip Guidebook.

_____. 1989. Active convergent tectonics in northwestern California: in Sedimentation and tectonics of western North America; Vol. 2, Geological evolution of northern Coast Ranges and western Klamaths; in the collection field trips for the 28th International Geologic Congress, Americal Geophysical Union, Washington, D.C. p. 64-82.

Carver, G.A., R.M. Burke, and H.M. Kelsey. 1986. Deformation of late Pleistocene marine terraces along the California coast north of Cape Medocino. GSA, Abstracts with Programs 18:93.

Clarke, S.H. and G.A. Carver. 1992. Late Holocene tectonics and paleoseismicity, southern Cascadia Subduction Zone. Science 255:188-192.

Clifton H.E. 1969. Beach laminations-nature and origin. Marine Geology. 7:553-559.

Clifton H.E., R.E. Hunter, and R.L. Phillips. 1971. Depositional structures and processes in the non-barred high energy nearshore. Journal of Sed. Pet. 41:651-670.

Evenson, R.E. 1959. Geology and ground-water features of the Eureka area, Humboldt County, California. Water-Supply Paper 1470, U.S. Geological Survey. 80 pp.

Griffith, L. M. 1975 The Intertidal Univalves of British Columbia. Handbook 26, British Columbia Provincial Museum, Victoria. 101 pp.

Harvey, E.W. and E.M. Weppner. 1992. Plestocene marginal marine sediments near mouth of Mad River, Humboldt county, California. (In Press) .

Kennedy, G.L. 1978. Pleistocene paleoecology, zoogeography, and geochronology of marine invertebrate faunas of the Pacific northern coast. Ph.D. Dissertation, University of California, Davis. 824 pp.

Kozloff, E. N. 1987. Marine Invertebrates of the Pacific Northwest. University of Washington Press, Seattle. 511 pp.

Leithold,E.L. and J. Bourgeois.1984. Characteristics of coarse-grained sequences deposited in nearshore, wave-dominated environments- examples from the Miocene if south-west Oregon. Sedimentology 31:749-775.

Miller, W.C., and S.D. Morrison. 1988. Marginal marine Pleistocene fossils from near mouth of Mad River, northern California. Proc. Cal. Academy of Sci. 45(10):255-266.

Ogle, B.A. 1953. Geology of the Eel River Valley area, Humboldt County, California. California Division of Mines and Geology Bulletin 154. 128 pp.

Roth, B. 1979. Late Cenozoic marine invertebrates from northwest California and southwest Oregon. Ph.D. Dissertation, University of California, Berkeley. 803 pp.

Wehmiller, J.F., G.L. Kennedy, and K.R. Lajoie. 1977. Amino acid racemization age estimates for Pleistocene mareine deposits in the Eureka-Fields Landing area, Humboldt County, California: E.S. Geol. Surv., Open-File REpt. 77-157: 1-25, figs 1-2, tables 1-2.

Wehmiller, J.F., K.R. Lajoie, K.A. Kvenvolden, Etta Peterson, D.F. Belknap, G.L. Kennedy, W.O. Addicott, J.G. Veddeg, and R.W. Wright. 1977. Correlation and chronology of Pacific Coast marine deposits of the continental United States by fossil amino acid stereochemistry- technique evaluation, relative ages, kinetic model ages, and

Late Holocene Stratigraphy and Paleoseismicity, Humboldt Bay, California

David Valentine[1]
Greg Vick[2]
Gary Carver[2]
Christine Shivelle Manhart[2]

[1] Dept, of Geological Sciences, University of California, Santa Barbara, CA 93106. Internet: dwv@magic.ucsb.edu
[2] Dept. of Geology, Humboldt State University, Arcata, California 95521

Summary

Late Holocene stratigraphy representing rapid episodic subsidence due to large magnitude earthquakes is found in synclines of Humboldt Bay, California. These synclines are onshore structures associated with the Cascadia subduction zone fold and thrust belt, which bends eastward in Northern California. In the axes of the synclines, repeated sequences of intertidal muds overlying tidal-marsh to wetland peat deposits represent episodes of rapid submergence followed by gradual emergence. Observations of the contacts between the peats and overlying muds are abrupt (<1 cm). The rapid submergence is interpreted to represent coseismic subsidence associated with large magnitude earthquakes. The evidence for these submergence events is found within both the northern Freshwater syncline and the southern South Bay syncline.

Radiocarbon dating indicates at least eight rapid episodic subsidence events during the past 3500 years. Rapid episodic events have occurred for the following age ranges: 0-300, 500-800, 1050-1350 (2 events), 1600-1900, 2450-2600, 2800-3300, 3200-3400. There are indications of additional events back to 4500 years, with ages of 3700-3900 and 4000-4300. The age ranges of the subsidence events are similar to ages for paleoseismic events from the Little Salmon fault. Great earthquakes occurring on the underlying Cascadia subduction zone megathrust may have accompanied the Humboldt Bay paleoseismic events.

Geomorphology of Humboldt Bay

Humboldt Bay comprised of three compartments: Arcata (or North) Bay, Entrance Bay, and South Bay (Figure 1)[1]. These regions are filled river valleys, which correspond to structural synclines. At the northern boundary is the Fickle Hill anticline and fault, and the Southern Boundary is the Table Bluff anticline. The northern most bay, Arcata Bay, correlates with broad shallow Freshwater syncline, which can be traced in the offshore stratigraphy and contains an accumulation of Holocene shelf sediments [2-4]. Separating Arcata Bay from Entrance Bay, is the Eureka Anticline, uplifting at approximately 0.3 mm/yr. Entrance Bay correlates with the Elk River syncline, which lies between the transition of the Little Salmon fault to the North Spit fault. The Humboldt Hill anticline and the Little Salmon Fault separate Entrance Bay from South Bay. The South Bay correlates with the informally named South Bay syncline which contains a thick accumulation of Holocene shelf sediments [2-4].

Beginning in the late 1800's, diking of the saltmarshes for agricultural land greatly altered the form of Humboldt Bay. The original extent of the tidal-marsh and wetlands was reduced from approximately 8700 acres to approximately 970 acres [5]. Soil formation behind the dikes has restricted the investigations the present tidal-marsh surfaces, and tidal channel exposures.

Relative Sea-level Estimates from Lithology

We use lithologic changes in the stratigraphy to identify changes in depositional elevations and environment. These elevations are related to the geomorphology of an estuary or bay which can be broken into zones: wetlands/forest, tidal marshes, mudflats and tidal channels. The wetlands/forests are low lying areas which may be inundated once or twice a year, but are mainly freshwater environments. These represent deposits only located near the fringes of the region. The tidal marshes can be broken into two or three zones which represent about 1.5 meters of vertical range, although the range varies for each estuary. For the Humboldt Bay region, marsh is broken into three zones, a low marsh, a mixed marsh, and a high marsh [3, 6]. The mudflats are located below the edge of the low marsh. Although the mudflat may be broken in
and a high mudflat [1], there is no lithologic
might allow for the discrimination in stratigraph

Each environment has an approximate ve
reference water level [7, 8]. Wetlands/fo
elevations above higher high water (HHW). Ir
regions, the high-marsh deposits accumulate
mean high water (MHW)[9], and represent c
MHW and HHW. The low marsh usually extend
to mean tidal level (MTL). The mudflats rep
below MTL. Nelson [9] reports uncertainties o
the estimate of MHW.

Peat horizons can be broken into zones u
Plants with a restricted growth range are
lithologic studies. An example for Humboldt
stricta which has a growth range of about 0.6 meters [6]. Stratigraphic studies by Vick [3] use *Grindelia stricta* as a high-marsh indicator fossil. The dense woody root of *Grindelia stricta* is easily preserved, and is the preferred material for radiocarbon dating.

Late Holocene Stratigraphy

The stratigraphy of the late Holocene in Humboldt Bay is repeated lowland horizons covered by intertidal sediments. This stratigraphy was first noted by Thompson [1] who attributed it to the erosion and accretion processes of saltmarshes found along the margins of Humboldt Bay.

The stratigraphy found in Humboldt Bay contains evidence for rapid submergence in the form of entombed tidal-marsh plant fossils, and in place *Picea* (spruce) stumps [3, 10, 11]. The growth rings in the *Picea* stumps show vigorous growth until death indicating that they were not strained by slow sea-level rise, or saltwater intrusion. This vigorous growth until death is interpreted to represent rapid submergence into the intertidal zone. Other evidence for rapid submergence are mid to high tidal-marsh plant fossils entombed in the overlying intertidal sediments.

The sediments overlying the horizons contain evidence for rapid deposition[3]. This allows for the preservation and entombment of the plant fossils. The contacts between the intertidal and the with the underlying peat horizons are usually abrupt (<0.5 cm), and can be traced for many tens of meters. The intertidal sediments sometimes contain *Triglochin martima* rhizomes, indicating a low marsh environment. These sediments gradually grade into new tidal marsh and wetland horizons.

Localities

No location contains a complete stratigraphic sequence for all events. This is attributed to the nature of the tidal-marsh morphology, tidal channel erosion, and extent of tidal-marsh growth.

Mad River Slough

Up to four sequences of horizons representing the last 2000 years are found in tidal exposure at Mad River Slough (see

Vick, this Volume)[3]. These horizons are found in tidal exposure and core. The upper horizon is traced along the 5.5 km length of Mad River Slough. At the lower end of the Mad River Slough, this horizon is a high marsh horizon containing *Grindelia stricta* fossils, while at the upper end the it contains in situ *Picea* stumps. The horizons are the same with the age constraints of radiocarbon dating, with and age of approximately 300 BP.

Jacoby Slough

Jacoby Slough contains evidence of three horizons, with two exposed at MLLW (Figure 2). The lowest dated horizon, Horizon 2, contains high marsh plant fossils, and is covered by intertidal sediment which grade into horizon 1. The age of horizon 2 is 766-1410 (JC-D-230-2). Horizon 1 contains *Grindelia stricta* at several sites. Horizon 1 has an age of 0 - 426 cal YBP (JC-D-115).

Eureka Region

The Eureka area contains evidence for two recent horizons, and a series of horizons older than Mad River Slough (Figure 3 and 4). Horizon 1 is found in tidal exposure near highway 101, and Second slough. Horizon 2 is found in tidal exposure on Daby and Gunther islands, and in core at second slough. The older horizons are found in first slough.

At First Slough, a horizon overlies a soil in one exposure (Column Bridge, Figure 4). This horizon can be traced for several tens of meters before becomes covered by sediment within the tidal channel. The underlying soil disappears rapidly, indicating that the soil may mantle a protecting ridge. The lowest horizon is a freshwater peat, with organic content of greater than 50%, which are dated at greater than 3989-4419 cal BP. This freshwater peat is covered by a tidal-marsh peat, which could represent a gradual sea level rise, or a rapid submergence. The tidal-marsh horizon is covered by intertidal sediments which grade into a sequence of two horizons.

South Bay

In South Bay, there are few areas undisturbed marsh areas, and high sedimentation rates in the tidal channels leaves little tidal exposure. From cores, South Bay contains several horizons (figure 5). The correlations are tentative, it is hard to correlate the stratigraphy due to the distances between sites. There are no continuous tidal channel exposures present, and the upper portions of the stratigraphy have been disturbed. An in progresses core transect across South Bay indicates that these are distinct horizons which can be traced laterally. The most prevalent horizon at about 4 meters below present marsh horizons, horizon 4, is dated at about 2339-2769 cal BP, and contains *Grindelia stricta* fossils in some localities.

Paleoseismicity

We can not use radiocarbon dating to discriminate gradual submergence, from rapid submergence, because the resolution of the dating technique is in the approximate range of short term sea-level fluctuations. We use the stratigraphy to discriminate rapid submergence events. The rapid submergence events are believed to be due to coseismic subsidence of the marsh and wetland surfaces into the intertidal zones. The lithology and radiocarbon support that the submergence events have occurred repeatedly during the late Holocene.

There is a close correlation between the paleoseismic events for the Little Salmon Fault and Clam Beach and the events found within the stratigraphy. The stratigraphy extends the paleoseismic record. By using the stratigraphy, we conclude that there have been 8 paleoseismic events in the past 3500 years and 10 for the past 4500 years (Figure 6; Table 1).

Event Y

Event Y is prevalent in the stratigraphic record, and has limiting dates of 1810 AD (historic record) and the last event on the Little Salmon Fault (290-690 BP; LSF 430) [12].

Event X

Event X is found in both the Eureka and South Bay, its age is constrained by events on the Little Salmon Fault. Two events have occurred on the Little Salmon Fault in the last 1000 years, one at less than 290--690 cal BP (LSF 430), and one at 530-1173 cal BP (LSF-S22) [12]. This event can be identified in the stratigraphy of South Bay. The age and stratigraphic separation of three horizons, one 60 cm (0-291 cal BP; HS1-689), a second at 155 cm (540-690 cal BP; HS-A-155-ave), the third at 275 cm (1081-1310; HS-B-275), is an indication that the ages that fall into this zone are not an artifact of the calibration. Daby island contains one horizon with dates that fall in this range (510-670 cal BP, Wood-C-70-1). Although this event is not widely preserved as a tidal-marsh or wetland horizon, it can be supported by other evidence.

Event U and Event V

Events U and V can be distinguish by the stratigraphy of Mad River Slough, but are not distinct events based on radiocarbon ages. Dates from other areas correlate with this time frame, but they cannot be properly placed into either event category. This tightly space group of distinct events is bracketed by movement on the Little Salmon Fault (530-1173 cal BP; LSF-S22)[11], and the stratigraphy at MRS-3 (MRS-2-205{1007-1520} stratigraphically above MRS-3-G305{970-1518}). It is believed that Event U and Event V occurred approximately 100-150 years apart, and at least one was a regional of the event.

Event T

Event T is separated stratigraphically from event U in Mad River Slough. This is the lowest horizon found in the slough, and ages around 1592-1498 cal BP (MRS-3-3689). Evidence for event T is found in Eureka Slough region and South Bay. Fault slip of 1820-2039 cal BP (LSF-6) on the Little Salmon Fault is the upper age limit of this event.

Event Q

Event Q is represented in South Bay, and horizons in First slough. In South Bay, age of 1611-1947 Cal BP overlies the horizon dated at 2349-2749 cal BP. The age constraints of these horizons are poor. The presence of the horizon in First slough, helps support event Q. The horizon representing Q is found between 360-425 cm is extensive, and is found at near every site.

Events P and O

Events P and O are supported by the stratigraphy in Eureka and South Bay. The deep stratigraphy of the South Bay is poorly documented, and has problems with age control, but it appears that there is a comparable number of horizons/events in both the SB-E, SB-A. There is evidence for two events in South Bay, following Event Q, and there is evidence for one in First Slough. For South Bay, an undated horizon lies between Event Q, and the lower horizon dated at 2782-3469 cal BP. For First slough, reversed radiocarbon ages leads to inconclusive evidence. The upper horizon is PAY-300 (2212-2769 cal BP), and the base of this peat is PAY-365 (2783-3379 cal BP), but PAY-395 (2359-2922 cal BP) dated younger than this horizon. Stratigraphic evidence suggests that these are separate horizons. Pay-395 is a clean horizon, and is separate from PAY-365. Pay-430 (3145-3546 cal BP) may be separate from PAY-395, but if the date on Pay-A-365 is correct, then they may be the same horizon, or could be horizons relating to event P and event O.

Event M and L

These are the oldest horizons in First slough (ES-E-645, 3705-4151 cal BP; ES-E-695, 3989-4419 cal BP). The lowest horizon is a wetland peat, which is covered by a saltwater peat. This could represent sea-level rise, the breaking of a berm, or coseismic subsidence. This tidal-marsh horizon has an abrupt

upper horizon indicating rapid submergence. Two out of three cores to this depth penetrated this sequence. The third penetrated intertidal sediments. We interpret the wetland marsh/tidal marsh/intertidal sediments to represent two events.

No Characteristic Earthquake

The concept of a characteristic earthquake with an estimated recurrence interval and magnitude is not applicable to the southern end of the Cascadia Subduction Zone based on our record of paleoseismicity for the past 4500 years. The period between events range from 100 years to 900 years with an average of 426 years (Table 1). It would be hard to develop a prediction for this region based on these ten events.

Clarke and Carver [11] propose possible magnitudes for events along the southern end of the Cascadia subduction zone: A magnitude 7.2 for the Little Salmon Fault, and a magnitude 8.3 for the southern end of the Cascadia subduction zone. At present, we cannot discount the possibility of either or both events occurring.

Conclusions

1) Wetland horizons covered by intertidal sediments represent evidence for rapid episodic submergence events. Evidence for 10 submergence events in the past 4500 years are found within the late Holocene stratigraphy of the Humboldt Bay.
2) These horizons are submerged coseismically during earthquakes associated with the southern end of the Cascadia subduction zone fold and thrust belt. Therefore these horizons provide a paleoseismic record for the past 4500 years. We believe we have complete record of five events for the past 1800 years. Longer records of 8 events for the past 3500 years, and ten events for the past 4500 may be incomplete.
3) The timing of the events do not follow a characteristic earthquake model, interval range in from 100 to 900 years. Therefor, we believe the concept of a recurrence interval is not applicable to the southern end of the Cascadia subduction zone.

References

1. Thompson, R.W., *Recent sediments of Humboldt Bay, Eureka, California.* 1971, Petroleum Research Foundation
2. Clarke, S.H., *Geology of the Eel River basin, and adjacent region--implications for late Cenozoic tectonics of the northwestern California continental margin and Mendocino triple junction.* American Association of Petroleum Geologists Bulletin, 1992. **76(2)**:199-224.
3. Vick, G., *Late Holocene paleoseismicity and relative vertical crustal movements, Mad River Slough, Humboldt Bay, California.* 1988, Humboldt State University:
4. Borgeld, J., *Holocene stratigraphy and sedimentation of the northern California continental shelf.* 1985, University Of Washington: 177 pp.
5. Shapiro and Associates, *Final Humboldt Bay wetland review and baylands analysis.* 1980, Submitted to Corps of Engineers, San Francisco; Shapiro and Associates, Seattle, WA: 3 volumes.
6. Eicher, A.L., *Salt marsh vascular plant distribution in relation to tidal elevation, Humboldt Bay, California.* 1987, Humboldt State University, Arcata, California: 78 pp.
7. van de Plassche, O., *Definitions of sea level and sea-level change derived from (fossil) natural evidence,* in *Late Quaternary sea-level changes,* Q. Yunshan and Z. Songling, Editor. 1987, China Ocean Press: Beijing. p. 43-45.
8. Sheenan, I., *Fladrian sea-level changes in the Fenland. II--tendencies of sea-level movement altitudnal changes, and local and regional factors.* Journal of Quaternary Science, 1986b. **1**: 155-180.
9. Nelson, A.R., *Holocene tidal-marsh stratigraphy in south central Oregon--evidence of localized subsidence in the Cascadia subduction zone,* in *Quaternary coast of the United States: marine and lucustrine systems, SEPM Special publication no. 48,* C.P. Fletcher and J.F. Wehmiler, Editor. 1992a,
10. Valentine, D.W., Late Holocene Stratigraphy As Evidence For Late Holocene Paleoseismicity Of The Southern Cascadia Subduction Zone, Humboldt Bay, California 1992, Humboldt State University: p. 99.
11. Clarke, S.H. and G.A. Carver, *Late Holocene tectonics and paleoseismicity, southern Cascadia Subduction Zone.* Science, 1992. **255**: p. 188-192.
12. Carver, G.A., G.S. Vick, and R.M. Burke, *Holocene Paleoseismicity of the Gorda Segment of the Cascadia Subduction Zone.* Geological Society of America Abstracts with Programs, 1989. **21**(5): p. 64.
13. Radiocarbon dates are calibrated using Stuvier and Remier, 1986, with a two standard deviation interval, and no laboratory error

14. This project has been supported by California Sea Grant project numbers RCZ-86 and RCZ-87. Land Access was provided by Humboldt Bay National Wildlife Refuge.

Event	Estimated Age interval	Estimated Age	Estimated Years between events
Y	0-300	216	
X	500-800	650	434
V	900-1250	1100	450
U	1050-1350	1300	100
T	1600-1900	1600	300
Q	2450-2600	2500	900
P	2800-3300	2900	350
O	3200-3400	3300	400
M	3700-3900	3900	600
L	4000-4300	4200	300

Events	Recurrence Interval	Standard Deviation
X to T	321	162
X to O	419	243
X to L	426	224

Table 1. Paleoseismic events, and recurrence interval calculation for the southern end of the Cascadia subduction zone. A separation of 100 years was assigned to event pair UV. The actual separation is unknown.

Map of Humboldt Bay

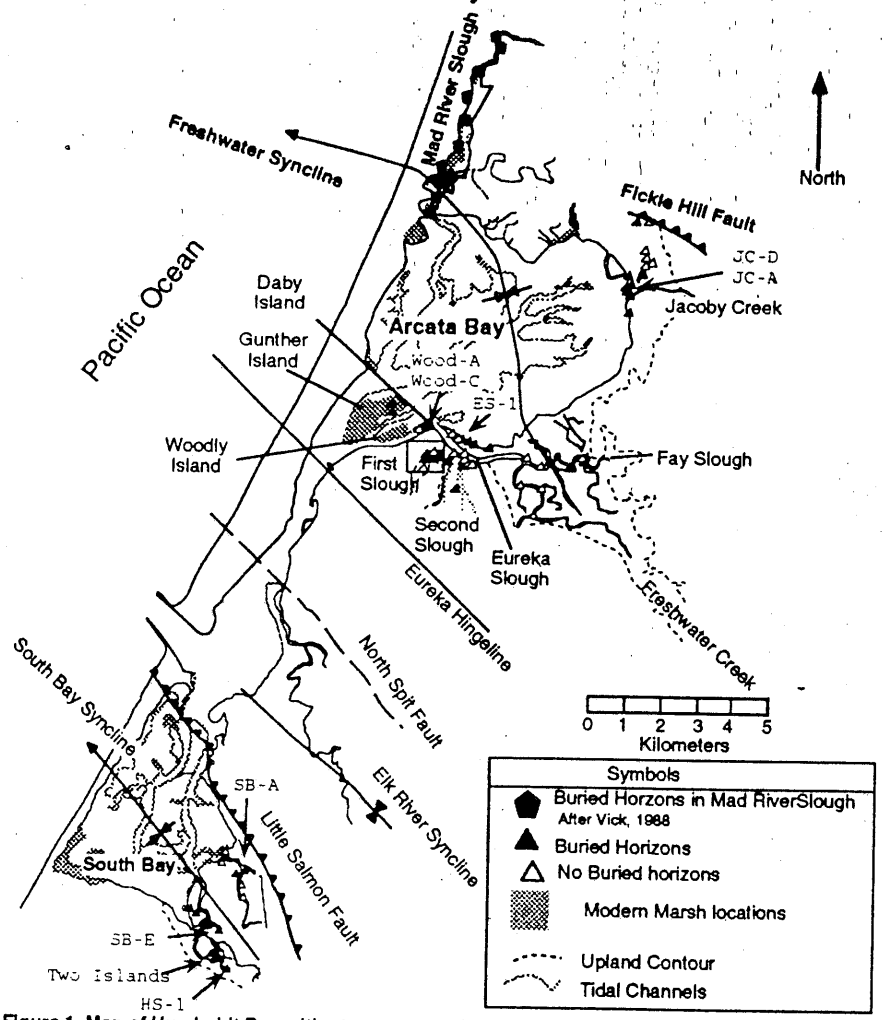

Figure 1. Map of Humboldt Bay with structures, and sample localities.

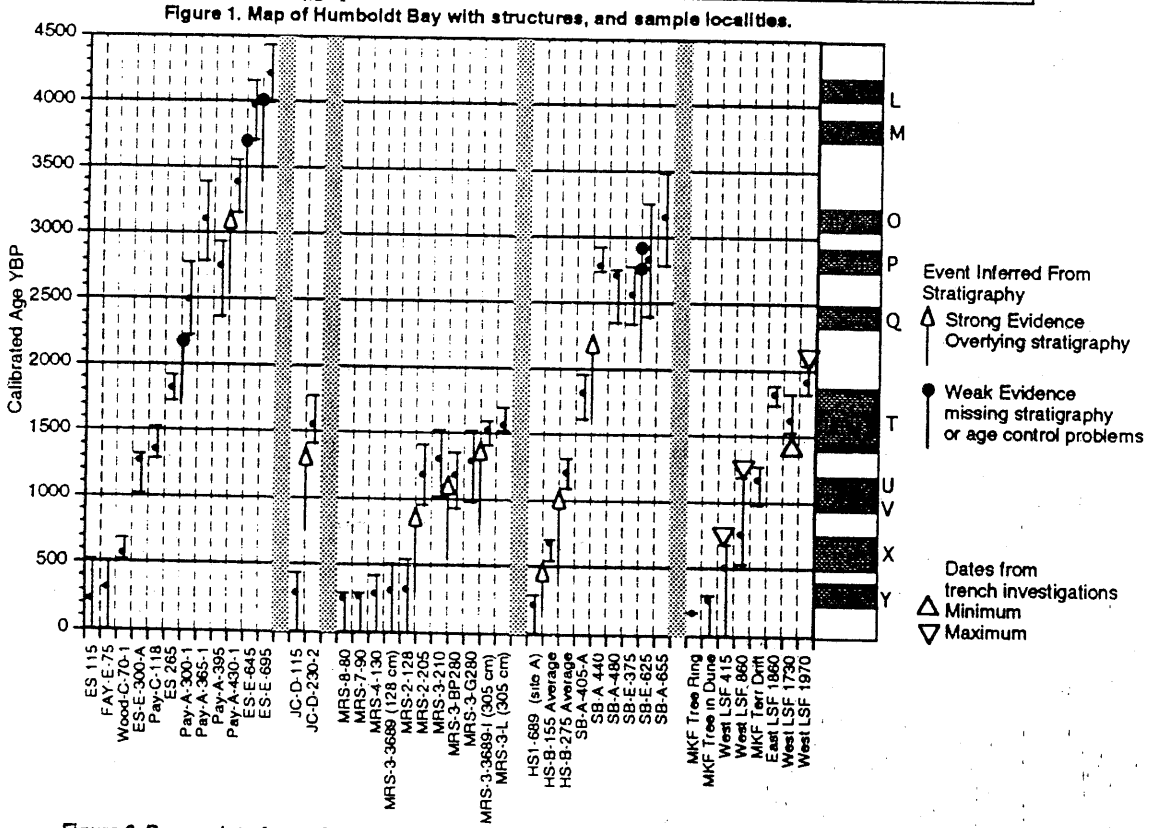

Figure 6. Range plot of ages from Humboldt Bay and vicinity. Arrows indicate strong evidence for a subsidence event. Round balls indicate weak evidence for coseismic subsidence.

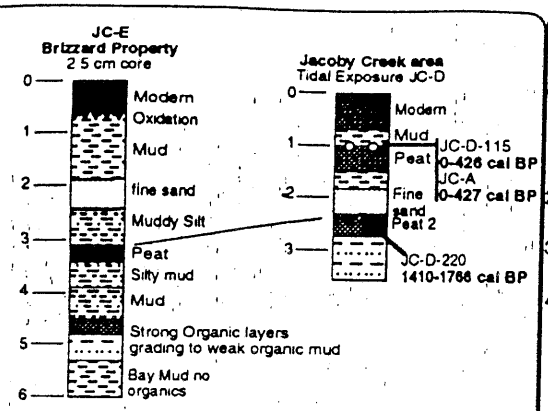

Figure 2. Stratigraphic Columns from Jacoby Creek.

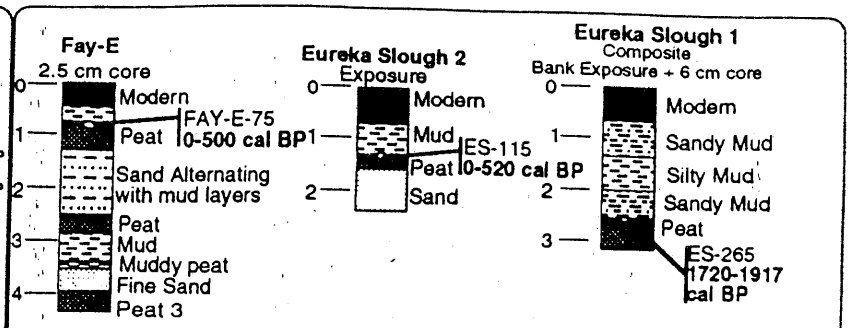

Figure 3. Stratigraphic Columns from the Eureka Region.

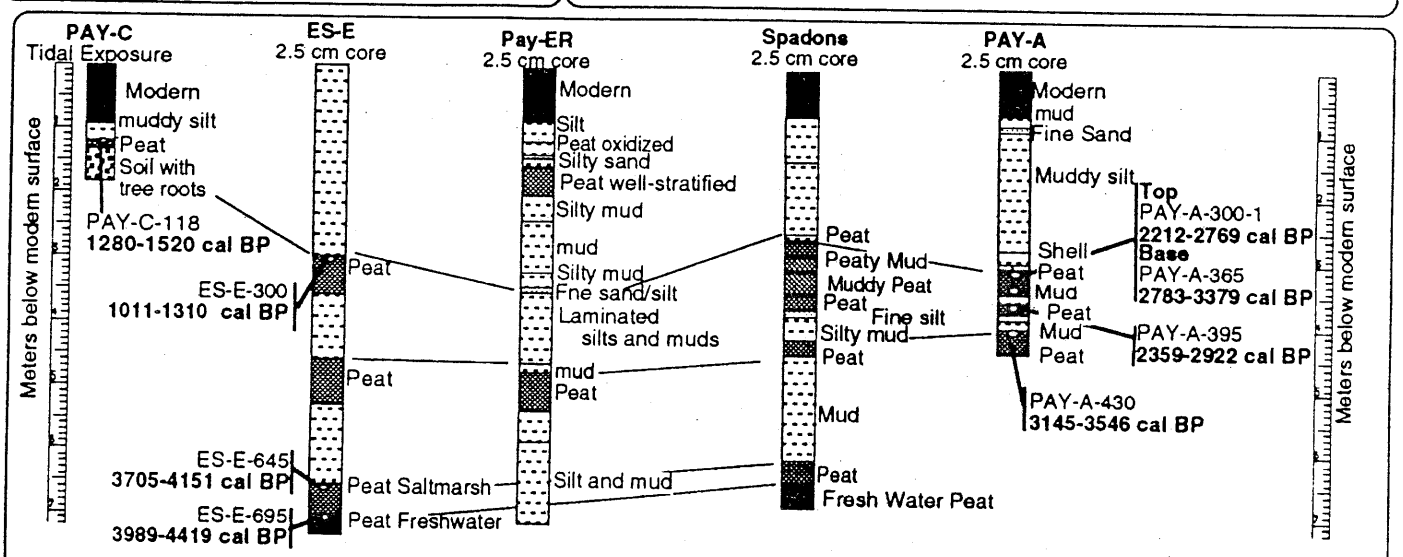

Figure 4. Stratigraphic columns from First Slough, Eureka.

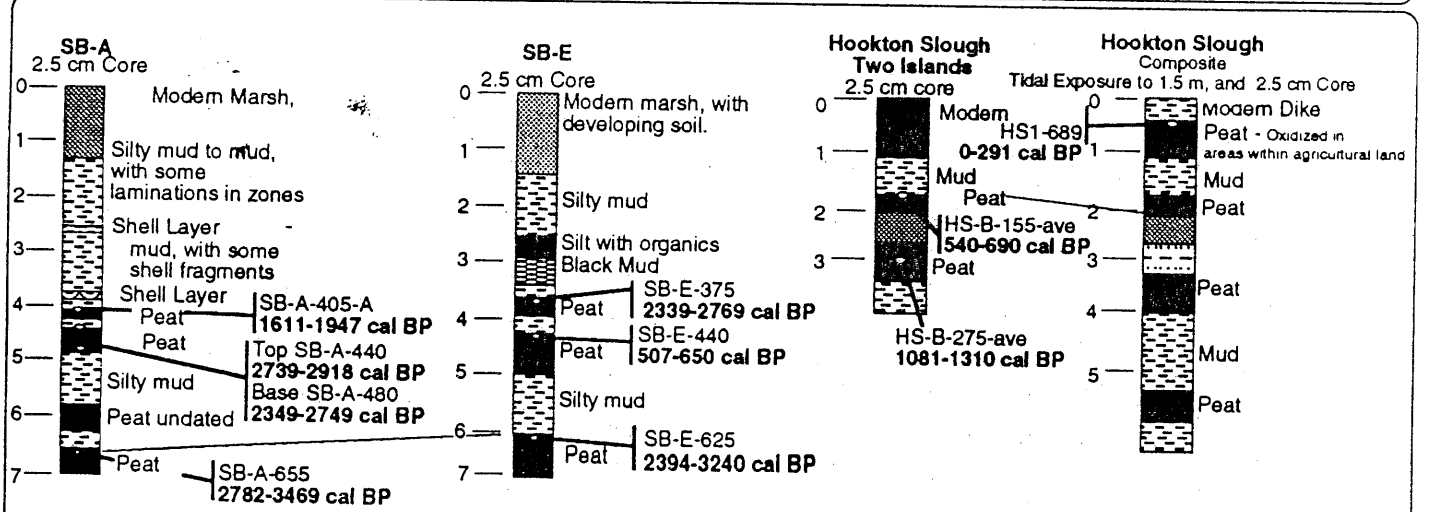

Figure 5. Stratigraphic Columns from South Bay.

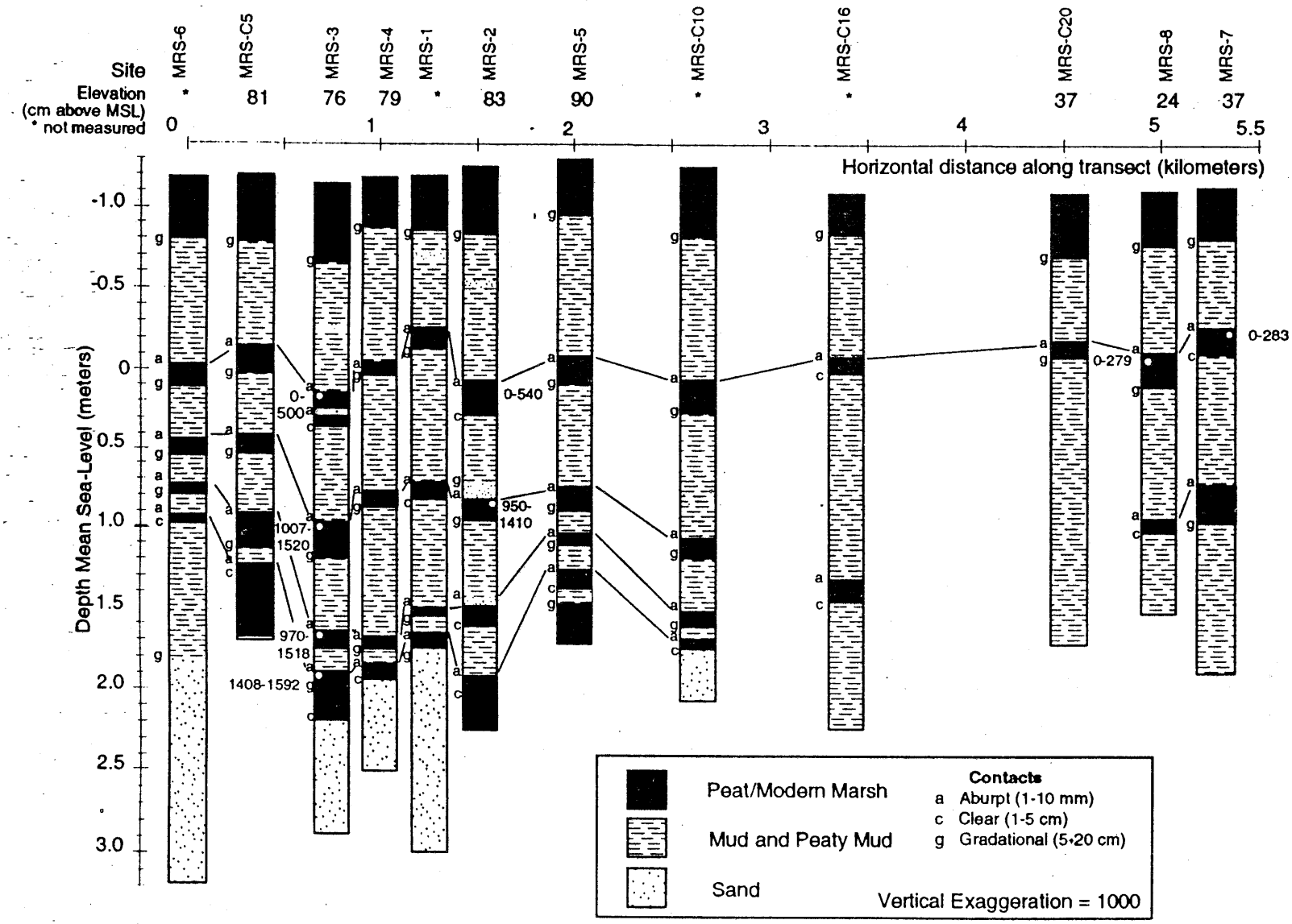

Figure 17. Generalized stratigraphic sections of the upper Holocene sediments of Mad River Slough. All ages reported as calibrated years before present (modified from Vick, 1988)

High-Resolution Foraminiferid Stratigraphy as Evidence for Rapid, Coseismic Subsidence: Preliminary Results

Christine Shivelle Manhart
Geology Dept., Humboldt State University,
Arcata, California 95521

ABSTRACT

A series of three Holocene peat horizons, one of which is a closely spaced couplet, are found at several locations along the margins of Humboldt Bay, northwestern California. These peats are found at the Mad River slough on the north edge of the northern compartment of the bay. The modern and stratigraphic distributions of salt marsh foraminiferids are being studied to determine changes in relative sea level caused by tectonic events on the Cascadia subduction zone. Preliminary studies of modern salt marsh foraminiferid distribution on the east coast of Canada and New England define two to three narrow zones in the marsh relative to sea level. The studies indicate that small scale changes in paleo-sea level could be determined by identifying modern associations, determining the zone in the marsh that association represents, and showing the chang the marsh zones over time. The upper surface of the first buried peat at Mad River sl shows a foraminiferid association indicative of a position near the higher high water boundary. Three centimeters above this horizon,within a massive bed of intertidal m an association was discovered that lived between the mean tidal level and mean high Considering the elevation of these tidal datums at Mad River slough, this change in foraminiferid association corresponds to a potential magnitude of subsidence of betw 0.4 and 1.3 m within the span of time necessary to deposit 3 cm of sediment.

INTRODUCTION

Buried peat horizons have been widely observed at various locations in the Pacif Northwest, including Humboldt Bay (Fig. 1). These horizons represent past salt marsh environments that have been indundated by bay waters and buried by intertidal muds. Repeated sequences of salt marsh peat and intertidal mud have been interpreted as to result from subsidence events associated with earthquakes on the Cascadia subduction zone (CSZ) (Atwater, 1987; Darienzo and Peterson, 1990; Valentine and others, 1990; Atwater and Yamaguchi, 1991; Shivelle and others, 1991; Clarke and Carver, 1992). Radiocarbon dates of the peat horizons found in the vicinity of Humboldt Bay have been obtained and used to correlate horizons between locations.

Preliminary studies of modern salt marsh foraminiferid distribution on the east coast of Canada and New England define two to three narrow zones in the marsh relative to sea level. The studies indicate that small scale changes in paleo-sea level could be determined by identifying modern associations, determining the zone in the marsh that association represents, and showing the changes in the marsh zones over time. At Humboldt Bay, foraminiferid stratigraphy is being used to define the environment of deposition, both immediately before and after a subduction event, and in the intervening "interseismic" period. It was hoped that the the distribution of modern salt marsh foraminiferid associations would be sufficiently distinct to allow very small scale changes in relative sea level to be defined. Relative sea level changes on the Pacific Northwest coast are reflections of the response of the land surface to the strain accumulation and release during the seismic cycle. While it was determined that the resolution of the distribution data of

modern foraminiferid associations will not allow for this kind of detailed analysis, it is possible to estimate the order of magnitude of subsidence. Additionally, preservation problems prevent using this technique for making interpretations of peat horizons found at depths greater than approximately two meters.

Previous Work

Several recent studies of the distribution of modern salt marsh foraminiferid species have described using the modern distributions to infer paleo-sea level changes (Scott and Medioli, 1980a, 1986; Patterson, 1990). Sudden, relatively large, changes in sea level could be used as evidence to support the repeated occurrance of great earthquakes on the CSZ (Atwater, 1987; Vick, 1988; Clarke and Carver, 1992). Episodes of sudden subsidence should appear in the stratigraphic record as abrupt changes in the marsh zone as inferred from salt marsh foraminiferid associations. These associations are extremly sensitive to environmental factors related to elevation (with reference to some tidal datum). Work by Scott and others (Scott and Medioli, 1980a,b,1986;Scott and Martini, 1982) over the last ten years have greatly increased the level of understanding of how salt marsh foraminiferids react to changes in elevation. While most of this work was concentrated primarily on the North American east coast, it is becoming clear that the same effects are observable on a global scale. Salt marshes everywhere contain a remarkably low diversity of foraminiferid species. The same 6 - 10 species are the dominant components of all salt marshes (Scott and Medioli, 1980a). At the higher zones of salt marshes (to within a few centimeters of the HHW datum), the foraminiferid association is composed almost entirely of *Trochammina macrescens*. It is the lack of variation in the composition of the association found at the highest elevation of the marsh, as well as the low elevational range in which it is found, that allow for the use of foraminiferid distributions as sea level indicators. If this association is found then sea level can be accurately inferred. The low marsh association shows more variation between different marshes, but within a particular marsh the associations are fairly easy to distinguish. Changes in sea level can theoretically be tracked by analysizing foraminiferid associations and identifying the marsh zone fthey represent in repeated sequences of peat and mud deposits.

RESULTS

It is impossible to interpret past community compositions without understanding a modern analogue. To this end, a study of the modern marsh at the mouth of the Mad River slough was undertaken in 1989 (Fig. 1). The patterns observed were consistent with those found by other workers. *Trochammina macrescens* dominated the composition of the upper reaches of the marsh; *Miliammina fusca* dominated the composition of the lower reaches. These species and others occurred in the transitional zone (Fig. 2; Shivelle and others, 1991). It was difficult to determine the elevation of the upper boundary of the salt marsh associations because of an extensive network of dikes built around the turn of the century that completely surrounds the northern compartment of the bay Because of this, there are few areas where the highest zone of the marsh can be found. Therefore, the upper elevational limit of the marsh and the composition of the foraminiferid association inhabiting this zone are difficult to determine. This uncertainty results in increasing the possible range of a predicted magnitude of subsidence.

Equipped with information concerning the modern marsh foraminiferid distribution, the examination of a section in outcrop was attempted. The section selected for study is located approximately 1 km from the mouth of the Mad River slough (Fig. 1). This location was chosen for several reasons. The contacts between the upper peat horizons and the overlying mud deposits were exceptionally sharp. Also, a series of three buried peat horizons were accessible during extremely low tides. Moreover, several radiocarbon dates

on plant macrofossils had been obtained previously (Vick, 1988). These dates allowed the peat horizons to be correlated in different parts of the slough and also provided an estimate of the time span represented by each peat/mud sequence. The dating of the first buried peat horizon at this location is equivical. While it has a radiocarbon date of approximately 800 ybp, it correlates stratigraphically with peats in other locations that date at approximately 300 ybp. If the 800 ybp date is correct, the prevelant 300 yr horizon is absent at this location. Since the 300 ybp horizon is extremely continuous throughout this area, its absence seems unlikely. It is more probable that the 800 ybp date is incorrect. To test this, additional plant material has recently been submitted for analysis, but until the results are known it is uncertain how this stratum should be interpreted. A second horizon, dates approximately 1300 ybp (Vick, 1988).

Figure 3 shows the vertical distribution of marsh foraminiferid associations at Mad River slough. The upper surface of the peat contained a *Trochammina macrescens* association signifying that it was created at an elevation very close to HHW (approximately +1.3 m mean tidal level, MTL; tidal datums from National Ocean Service, 1981-1985). Three centimeters above the contact, a horizon that contained 50 % *T. macrescens* and *Trochammina inflata* and 50 % *M. fusca.* was sampled. This stratum was formed at some elevation between MTL and mean high water (MHW). At the Mad River slough (in this study), MTL is the 0.0 datum and MHW corresponds to an elevation of +0.9 MTL. This foraminiferid distribution represents a magnitude of subsidence that is the difference in elevation between HHW and MTL. This results in an estimated range in the magnitude of subsidence of 0.4 - 1.3 m in the span of time needed to generate 3 cm of intervening sediment.

At a depth of 180 cm below the modern marsh surface, a horizon was found that contained an association having 40 % *T. macrescens*, 45 % *T. inflata*, and 15 % *M. fusca* (Fig. 3). This composition indicates a depositional elevation fairly high in the marsh, probably near MHHW (+0.9 m MTL). Above this horizon, at 175 cm, the association was composed of 60 % *T. inflata* and 40% *M. fusca* , which indicates deposition somewhat lower in the marsh (probably MHW, or slightly lower). While these datums may not indicate a spectacular change of elevation, it is interesting because the shift in relative abundances does not to correspond to a buried peat horizon. The next lower buried peat horizon at this location has been dated at approximately 1300 ybp (Vick, 1988). Recently, the section of the outcrop that contains this horizon was resampled. An extremely weakly developed peaty mud was noted 12 cm above the 1300 yr horizon. This was approximately the position of the horizon containing the high marsh association. A problem arises in interpreting the significance of this horizon because of the questionably date for the first peat horizon. Two possible interpretations result for the anomolous high marsh association: (1) it represents a peat surface where the plant material was not preserved and for this reason has gone unnoticed in other locations; and (2) it represents the 800 ybp horizon that is preserved discontinuously.

LIMITATIONS

The stratigraphy for the first (and possibly the second, from youngest to oldest) buried peat horizons were extremely clear in demonstrating that a significant amount of subsidence occurred in a relatively short length of time, there are some problems, however, with the use of this technique at lower stratigraphic levels. When the lower horizons in the section were studied it appeared that deposits with associations dominated by *M. fusca* were conspicuously absent. It is unclear at this time whether this is simply owing to a problem with uneven sampling density in the lower levels of the outcrop, or if there is some unspecified taphonomic process at work here. It was noted in buried salt marsh deposits on barrier islands off the coast of Georgia, that the relative abundance of *M. fusca* also

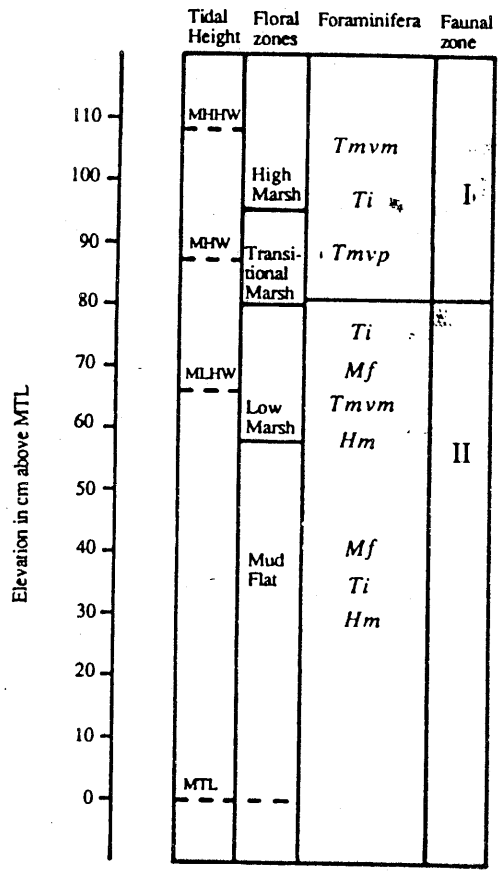

Figure 2. Distribution of the modern salt marsh foraminiferid species. Species names are abbreviated as follows: *Tmvm* = *Trochammina macrescens* var. *macrescens*; *Ti* = *Trochammina inflata*; *Tmvp* = *Trochammina macrescens* var. *polystoma*; *Mf* = *Milliammina fusca*; *Hm* = *Haplophragmoides manilaensis*. Discriminant analysis of data from various modern marsh locations around the northern compartment of Humboldt Bay yielded two distinct associations for the faunal zone labelled II. Inadequate elevational control between these different locations have thus far prevented determining the elevation at which the lower association predominates.

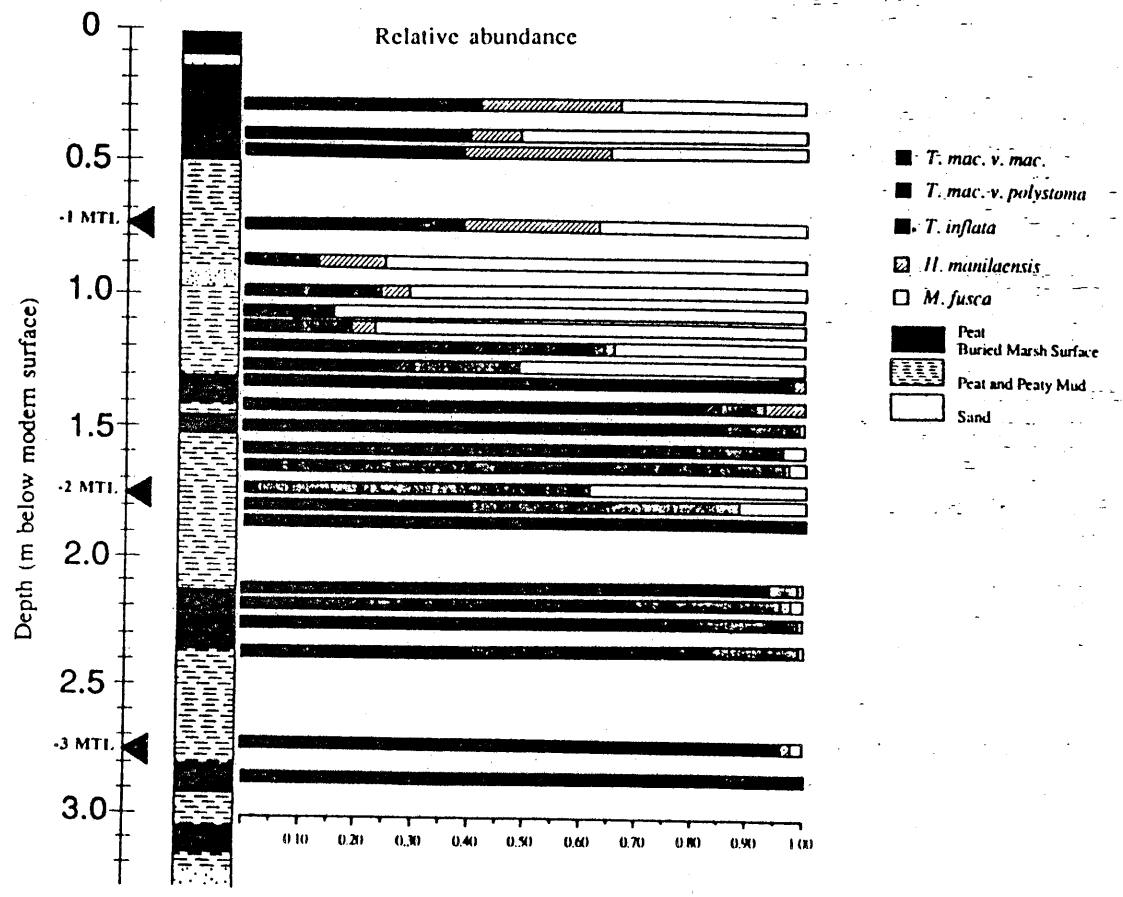

Figure 3. Relative abundance of foraminiferid species in relation to the depth at which the horizon was found. Stratigraphic column is from Valentine (1990) after Vick (1988).

decreased markedly with depth (Goldstein, 1988). This was determined to be the result of a bacterial degradation of the calcitic cement used in construction of the test (Goldstein, personal communication, 1992). In Georgia the change in relative abundance caused by taphonomic damage was noticed at depths of less than 10 cm below the modern surface. Although this taphonomic effect is first noticed at Humboldt Bay at depths much greater than in Georgia, the difference in depth could possibly be related to climate. The implication is that the data from lower horizons is unreliable owing to possible taphonomic biasing.

Using high-resolution foraminiferid biostratigraphy to estimate magnitudes of subsidence at Humboldt Bay is proving to be more difficult and less precise than envisioned based on the original east coast studies of salt marsh foraminiferid distribution. Salt marsh plant and foraminiferal zone boundaries on the west coast seem to correlate to both high and middle marsh zones on the east coast (Patterson, 1990; Jennings and Nelson, 1992). The wide vertical range in elevation of the high and low marsh zones at Mad River slough, as well as those studied in Oregon (Jennings and Nelson, 1992) limit the precision to which the magnitude if subsidence can be determined. With the low marsh association in this study found over a wide elevational range, only the minimum amount of subsidence can be calculated with any precision. There is also a problem with obtaining reliable control on the modern distribution of the marsh foraminiferids in Humboldt Bay that has resulted from diking of almost the entire margin of the slough. This limits precision in determining the maximum elevation at which salt marsh foraminiferids are found.

CONCLUSIONS

Although the technique of using the distribution of modern salt marsh foraminiferid associations to interpret the recent history of relative sea level is not as straightforward as initially predicted, it is not without merit. Useful information about the approximate magnitude of subsidence events can still be determined. The sea level changes inferred from foraminiferid association changes corroborate lithostratigraphic, structural, and radiometric data. Additionally, it appears that foraminiferid association analysis can be used to demonstrate relative sea level changes in an intertidal environment that may not be represented by a well developed peat horizon.

Future research will concentrate on the changes found in the peat/mud deposits representing the most recent seismic cycle along the length of the Mad River slough and correlated upstream. Concentrating on the most recent deposits will circumvent problems caused by taphonomic biasing. Correlating individual relative sea level changes over a longitudinal profile provides evidence that the change is related to a regional event rather than to natural processes of marsh accretion and erosion.

ACKNOWLEDGEMENTS

This paper is funded in part by a grant from the National Sea Grant College Program, National Oceanic and Atmospheric Administration, Department of Commerce, under grant number NA89AA-D-SG138, project number R/CZ-88, through California Sea Grant College Program, and in part by the California State Resources Agency. The views expressed herein are those of the author and do no necessarily reflect the views of NOAA or any of its sub-agencies. The U.S. Government is authorized to reproduce and distribute for governmental purposes. Research has also been supported by the National Earthquake Hazards and Reduction Program of the U.S. Geological Survey. Early work on the distribution of modern salt marsh foraminiferid associations was supported by the Humboldt State University Marine Laboratory Summer Research Institute, 1989. I would

like to thank David Valentine and Gary Carver for help in the field and Wen-Hao Li and Laurie Thom for help with processing samples. Comments by William Miller improved this paper.

REFERENCES CITED

Andersen, H., 1953, Two new species of Haplophragmoides from the Louisiana Coast,Contributions to the Cuhman Foundation for Foraminiferal Research, v. 4, p. 21-22.

Atwater, B.F., 1987, Evidence for great Holocene earthquakes along the outer coast of Washington State Science v. 236, p. 942-944.

Atwater, B.F and Yamaguchi, D.K., 1991, Sudden, probably coseismic submergence of Holocene trees and grass in coastal Washington State, Geology v. 19, P. 706-709.

Clarke, S.H., Jr. and Carver, G.A., Late Holocene tectonics and paleoseismicity, Southern Cascadia subduction zone, Science v. 255, p. 188-192.

Eicher, A.L., 1987, Salt Marsh Vascular Plant Distribution in Relation to Tidal Elevation, Humboldt Bay, California, Unpublished M.S. Thesis, Humboldt State University, Arcata, California, 86 pp.

Goldstein, S.T., 1988, Foraminifera of relict salt marsh deposits, St. Catherines Island, Georgia: taphonomic implications, Palaios v. 3, p. 327-334.

Jennings, A.E. and Nelson, A.R., 1992, Foraminiferal assemblage zones in Oregon tidal marshes -- relation to marsh floral zones and sea level, Journal of Foraminiferal Research v. 22, p. 13-29.

National Ocean Service (National Oceanic and Atmospheric Administration), 1981-1985, Tidal benchmark sheets for Humboldt Bay: Mad River Slough.

Patterson, R.T., 1990, Intertidal benthic foraminiferal biofacies on the Fraser River Delta, British Columbia: Modern distribution and paleoecological importance, Micropaleontology v. 36, p. 229-244.

Phleger, F.L., and Walton, W.R., 1950, Ecology of marsh and bay foraminifera, Barnstable, Mass., American Journal of Science v. 248, p. 214-294.

Scott, D.B. and Martini, I.P., 1982, Marsh foraminifera zonations in western James and Hudson bays, Le Naturaliste Canadien, v. 109, p. 399-414.

Scott, D.B. and Medioli, F.S., 1980a, Quantitative Studies of Marsh Foraminiferal Distributions in Nova Scotia: Implications for Sea Level Studies, Cushman Foundation for Foraminiferal Research, Special Publication No. 17. 58 pp.

Scott, D.B. and Medioli, F.S., 1980b, Living vs. total foarminiferal populations: their relative usefulness in paleoecology, Journal of Paleontology v. 54, p. 814-831.

Scott, D.B. and Medioli, F.S., 1986, Foraminifera as sea-level indicators, ***in*** Sea-Level Research: A Manual for the Collection and Evaluation of Data, O. van de Plassche (ed) Geo Books, Norwich, Great Britain, pp 435-457.

Shivelle, C.D., Carver, G.A., and Valentine, D.W., 1991, Foraminiferid stratigraphy as evidence for great earthquakes on the Cascadia subduction zone in Northern California, Geological Society of America, Abstracts with Programs v. 23, p. 97.

Valentine, D.W., Carver, G.A., and Shivelle, C.D., 1990, Late Holocene stratigraphic evidence for rapid episodic subsidence, Humboldt Bay, California, Geological Society of America, Abstracts with Programs, v. 22, p.A23.

Vick, G.S., 1988, Late Holocene Paleoseismicity and Relative Sea Level. Changes of the Mad River Slough, Northern Humboldt Bay, California, Unpublished M.S. Thesis, Humboldt State University, Arcata, Calfornia, 87 pp.

Mattole River North Area Geology

K.R. Aalto, Dept. of Geology, Humboldt State Univ., Arcata CA 95521

Along the coast, between the Mattole River and the Mattole shear zone (Fig. 1), there are two very distinct rock units (Miller, 1982; Miller and Aalto, 1983). The northern unit, interpreted as Coastal belt Franciscan complex, consists of a pervasively sheared, boudinaged, tightly folded broken formation composed of conglomerate, pebbly sandstone, and subordinate argillite, gray ribbon chert, and grayish-white limestone. The limestone is recrystallized and occurs in boudins up to 0.5 m thick and 2 m long, intercalated with sandstone and argillite. The sandstone/shale ratio of the northern unit is on the order of 20:1. Bedding features are difficult to discern, however, Miller and Aalto (1983) recognize facies characteristic of proximal sediment gravity flow deposits and interpret the depositional setting to be that of a high-energy inner submarine fan.

Conglomerates have rounded clasts as much as 3 cm long, consisting chiefly of gray, green, and black chert; graywacke; gray to black porphyritic volcanic rock; and milky vein quartz (Miller, 1982). Point counts of medium- to fine-grained, texturally immature sandstones give the following detrital modes: Q-24, Qm-10, Qp-14, F-30, P-25, K-5, Lt-60 and Ls+Lv-46. Sandstones have been metamorphosed to the prehnite-pumpellyite facies in the vicinity of faults and shear zones within this unit. Veins of quartz, calcite and aragonite are present. This unit is bordered on the south by the northeast-trending Petrolia shear zone (Fig. 1). The contact between the two is gradational, marked by increased shearing and faulting as the shear zone is approached from the north. To the north lies the east-west-trending Mattole shear zone, with which contact is not exposed. Within the shear zones, there are widely scattered, ellipsoidal boudins of graywacke (also pillow basalt in the Mattole shear zone) encased in pervasively sheared argillite characterized by subvertical foliation..

The southern unit (Fig. 1; Miller and Aalto, 1983) is mapped on the Redding Sheet of the Geologic Map of California as undifferentiated Tertiary marine rock. This unit is unfossiliferous, highly indurated, and in the field *appears* similar to typical Yager Formation in lithology and degree of deformation. This unit consists of thin-bedded sandstone and shale, with an overall sandstone/shale ratio of approximately 1:2 to 1:3. Sandstone beds are most commonly non-channeled, tabular and laterally continuous. They exhibit base-cut-out Bouma sequences. Minor channelized, thick, lenticular sandstones exist. Repetitious thinning-upward sequences with prevalent slump-folded, chaotic intraformational intervals and the abundance of shale suggest a submarine slope depositional setting.

Point counts on fine- to medium-grained sandstones give the following detrital modes: Q-38, Qm-21, Qp-17, F-32, P-28, K-4, Lt-46, and Ls+Lv-29. The northern and southern units could have the same magmatic arc source terrane with the southern unit sandstone composition reflecting a greater degree of arc dissection (Miller, 1982). The southern unit abuts the Petrolia shear zone and is folded into an open, northeast-trending syncline. It is possible that this unit rests unconformably upon rocks of the shear zone, however, the contact is obscured by debris flows. If, as is suggested by the state of deformation, the northern unit is part of an accretionary wedge, the southern unit might be a slope deposit draping this wedge which later might have been tectonically kneaded into previously underplated and/or offscraped sediments (Miller and Aalto, 1983).

Within the Mattole shear zone there are scattered outcrops of semi-indurated, fossiliferous mudstone and sandstone, determined paleontologically to be late Miocene in age (Miller and Aalto, 1983). Recent work by Carver and Aalto (papers in this volume) in shear zones north of Cape Mendocino shows that Neogene sandstones are tectonically interleaved with Franciscan rocks from the mesoscopic to microscopic scale. Thus the prevalence of shear zones containing

lithostratigraphic units of varied age, lithology and state of stratal disruption may be characteristic of upper plate rocks in the Mendocino triple junction (MTJ) region. Shear zone genesis very likely involves a long and complex deformation history beginning with accretionary wedge genesis, followed by further tectonic disruption and uplift as the triple junction approaches and terminating with strike-slip fault deformation following the northward passage of the MTJ.

Approximately 1 m of coastal uplift occurred along the coast in the area of figure 1 following the April, 1992, earthquakes. Based upon regional extent of uplift to the north and south of this area, it appears that none of the mapped faults were reactivated. The uplift, however, provides a graphic and exciting illustration of how the abrasion platform carved into seacliffs of the northern unit might have been uplifted early in the Holocene.

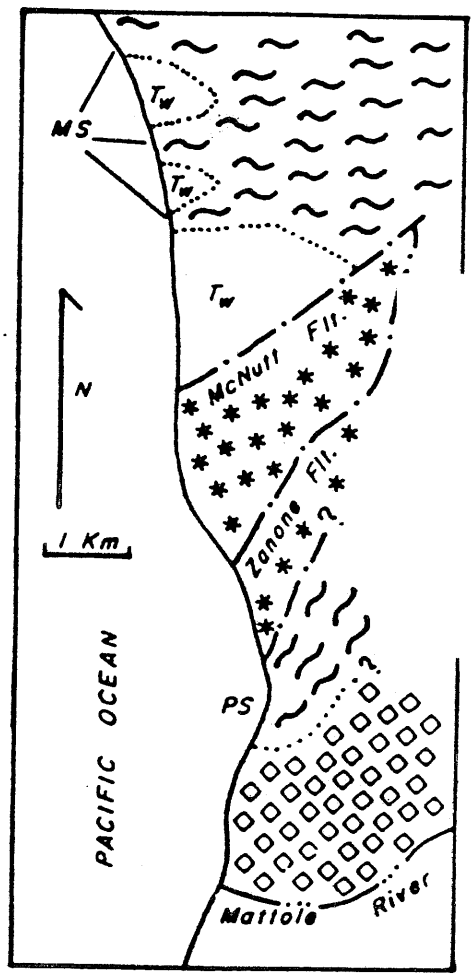

Figure 1. Geology north of the Mattole River. The generalized coastal geology is depicted as follows: Wildcat Group equivalent rocks by "Tw", northern unit by asterisks, southern unit by diamonds, and shear zones by wavy dashes. MS indicates the Mattole shear zone; PS indicates the Petrolia shear zone. Geology from Miller (1982) and Nason (1968).

References cited

Miller, S.G., 1982, Petrology and structure of the coastal Franciscan from the Mattole River to Mussel Rock, northern California: *unpublished B.Sc. thesis, Humboldt State Univ.*, Arcata, CA, 40p.

Miller, S.G., and Aalto, K.R., 1983, Post-middle Miocene accretion of Franciscan rocks, northwestern California: a discussion: *Geological Society of America Bulletin*, v. 94, p. 1028-1029.

Nason, R.D., 1968, San Andreas fault at Cape Mendocino, *in* Dickinson, W.R., and Grantz, A., eds, Conference on geologic problems of San Andreas fault system, proceedings: *Stanford Publications in Geological Sciences*, v. 11, p. 231-241.

LOCAL EFFECTS OF 1991-1992 EARTHQUAKE SEQUENCE

Thomas Dunklin, P.O. Box 106, Petrolia, Ca 95558
(707) 629-3478

The earthquakes of April 25 and 26, 1992 are the most recent in a series of damaging events in the Petrolia and Honeydew areas. Damages from these events were the greatest relative to past earthquakes based on historical accounts and physical evidence. A few old ranch houses were destroyed, and some tombstones in the Petrolia Pioneer Cemetary were damaged or destroyed. Some of the damaged ranch houses and tombstones date back to the late eighteen hundreds. Most local residents and old-timers characterize this sequence as the largest and most destructive series of events in their memory. In addition to the April 1992 earthquakes, the events of January 16, 1990, August 17, 1991, and March 7, 1992 all produced effects of Intensity VII or larger.

Geomorphic Effects of Recent Earthquakes

Although no surface rupture has been identified, geomorphic indicators of strong shaking are widespread. Liquifaction features, ridge failures (Sakungen ?), all scales of landslides, road cracking and fill failures, and localized small extentional cracking features have been mapped in the area between the town of Honeydew and Ferndale. Most notable of all these features is the regional uplift pattern along the coast resulting from the August 25 thrust event.

Liquifaction Features

Sand-blows were identified and mapped from the mouth of the Eel river to the mouth of the Mattole River. They were also identified at a few locations at the mouths of sandy coastal streams. Features vary from scattered circular vents to linear fissures up to 100 meters in length. They often appear as en echelon crack systems across low gravel bars and floodplains. Near the mouth of the Mattole, anomalously large gravels (dia.= 2.2 cm) were blown out of the vent, and were found on the flanks of the sand-blow cone. Stratigraphically, the gravels overlie extensive fluvial silt deposits, and are strikingly different from the more typical sand and silt-sized sediments discharged from the vent. Sand-blow features were found as far inland as Honeydew, near the mouth of Bundle Prairie Creek, where sand-blows were formed in both the August 17, 1991 "Honeydew Earthquake", and the March 7, 1992 "Petrolia Earthquake."

Landslides

Hundreds of small landslides were triggered across the effected area, and at least 12 significant landslide features have been identified and mapped. Some features, such as the landslides at McNutt Gulch and Clear Creek (near Petrolia) present continued geologic hazards to travellers. Most slides identified are to some extent associated with the county road system or to the many miles of logging roads constructed throughout the area. The most dramatic slide is located approximately one kilometer east of the George Lindley Bridge near Petrolia, near the mouth of Clear Creek. It was moderately effected by the August 17 event, and then catastrophically released during the event of March 7, resulting in partial blockage of the

road. Storms following this event caused continual activity at this site for weeks to follow, and the road was closed on numerous occasions. The events of April 25 and 26 brought down the greatest volume of material, and again completely blocked the road on a few occasions. Many smaller slides have been identified along the Mattole River, and in the inner gorges of many small coastal or tributary streams. Some streams, such as Singley Creek were temporarily dammed by slides that crossed the channel. These features exist at all scales, and require further examination. Sliding is common in this area during winter storm events, and distinguishing between seismically triggered slides and moisture triggered slides requires extensive field work. At present this is difficult since many of the logging roads needed to reach remote areas are impassable due to fill failures, slumps, or rockslides.

Road Cracking

Road cracks are common in the area between Honeydew and Bear River. Between the Bear River and Ferndale there are some zones of cracking , but their frequency is much less common. Many of the cracking sites are reactivations of the August and March events which respectively shook Honeydew and Petrolia the hardest. New sets of notable cracks were formed in the April event along Lighthouse road, and on the road between McNutt Gulch and Ocean House. A zone of cracks following the ridge road on Cape Ridge was followed for approxmately 8 kilometers, and follows an orientation defined by a set of cracks crossing a beach berm near Cape Mendocino. These areas are all on private property, and require written permission for access.

Ridge Failures and Extensional Features

Cracks along ridge-tops showing horizontal separation and in places uphill facing scarps have been identified in only a few locations. A few paired extensional features have also been identified that have graben-like characteristics. One such feature cuts across a linear marsh, which was instantly drainded following the April 25 event.

Uplift

The uplift pattern resulting from the April 25 thrust event is at present being closely studied. Anomalously low tides were recognized by local residents in the days following the quake, but it took two weeks for the biological organisms to die off. Local fisherman and abalone divers estimate between three and five feet of uplift in the presumed maximum uplift area, and marine ecologists estimate roughly one meter of uplift based on the communities effected. Reconaissance mapping of bleached (dead) seaweeds, and dead mussel beds shows an apparent maximum uplift zone in the area between Devils Gate and Mussel Rocks, with uplift appearing to decrease in both directions from this zone. There is a strikingly high zone of uplift in the region north of Cape Mendocino, but it is currently uncertain whether this uplift is tectonic, or associated with a large rotational slump of a previously mapped landslide area. Merritts et al. will be resurveying Holocene platform elevations between Shelter Cove and the Bear River to examine the patterns of uplift.

Weathering and Soil Development on Marine Terraces along the Lost Coast of California.

Oliver A. Chadwick, Dorothy M. Merritts, & David M. Hendricks.

We have taken advantage of the detailed geomorphic work of Dorothy Merritts and Bill Bull to conduct studies that seek to describe the genesis of soils along this part of the California coast. In contrast to the work of Burke and Carver - who use soils to differentiate groups of terraces - we use terrace stratigraphy to define soils of differing age. We have sampled soils on terraces that range in age from 3.9 ka to 240 ka. The enclosed packet of tables and figures is taken from a series of papers referenced below. Copies of these papers are available from Oliver Chadwick. During the field trip, we will discuss the tables and figures in the context where they can best be appreciated - the sampling localities.

Merritts, D.M., O.A. Chadwick, D.M. Hendricks, G. H. Brimhall, and C.J. Lewis. 1992. The mass balance of soil evolution on late Quaternary marine terraces, northern California. Geological Society of America Bulletin (accepted).

Brimhall, G.H., O.A. Chadwick, C.J. Lewis, W. Compston, W.E. Dietrich, M. Power, D. Hendricks, and J. Bratt. 1992. Deformational mass transport and invasive properties of soil geomembranes. Science 255: 695-702.

Merritts, D.M., O.A. Chadwick, and D.M. Hendricks. 1991. Rates and processes of soil evolution on uplifted marine terraces, northern California. Geoderma 51: 241-275.

Chadwick, O.A., G.H. Brimhall, and D.M. Hendricks. 1990. From a black to a gray box - a mass balance approach to understanding soil processes. Geomorphology 3: 369-390.

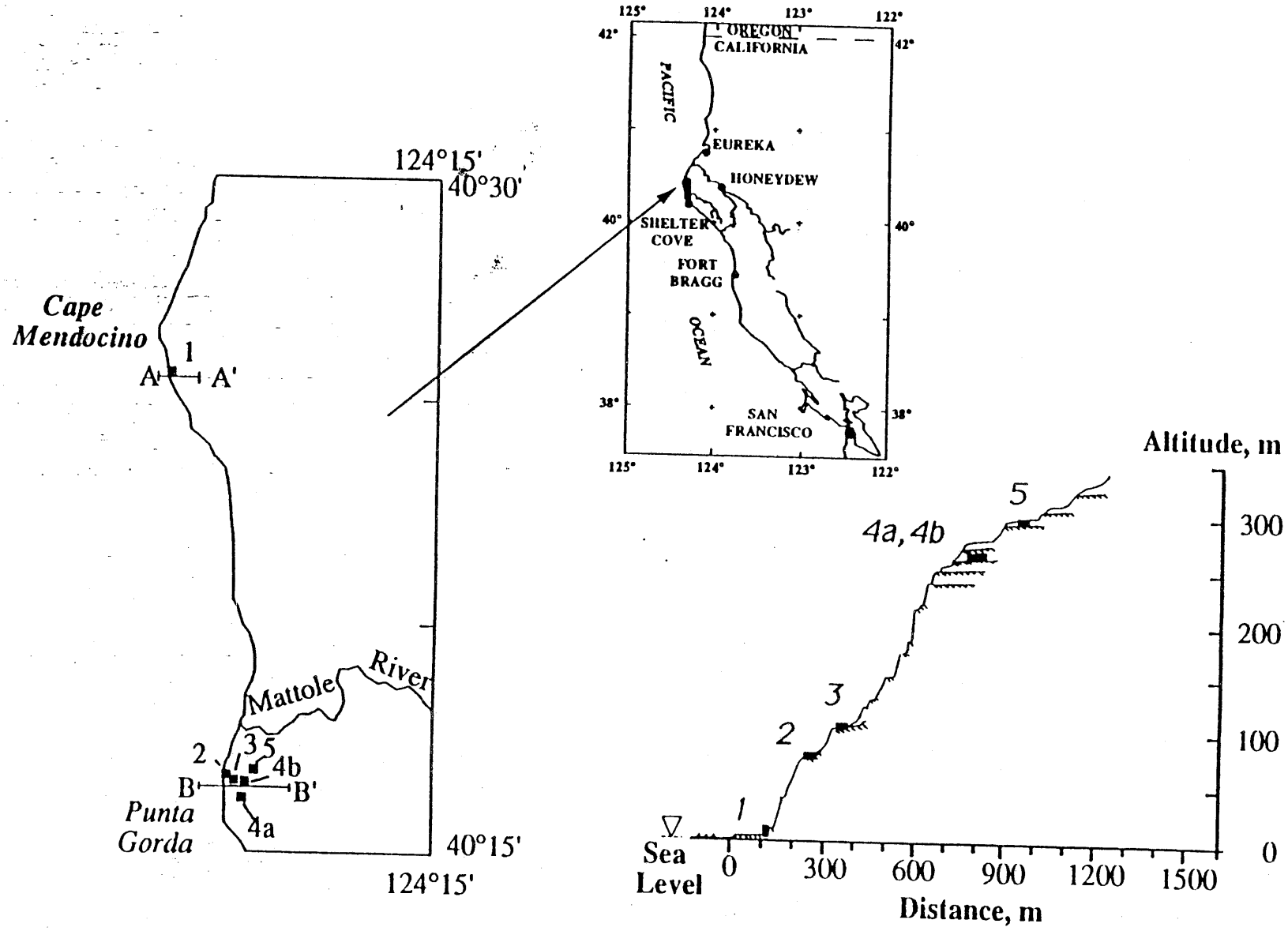

Composite of Topographic Profiles of
ine Terraces Surveyed at A-A' and B-B'

TABLE 1 GENERAL DESCRIPTIONS OF SOIL SITE CHARACTERISTICS.

Soil Site Number	Terrace Age, ky*			Platform Inner-Edge Altitude, m	Terrace Tread Slope, degrees	Soil Class†	Vegetation
1	3.9	+0.1	-3.9§	7	3	1	Grass
2	29	+5	-15	78	2-8	2	Grass
3	40	+5	-15	111	4	3	Grass
4a	124	+5	-15	261	2-4	4	Grass
4b	124	+5	-15	261	2-3	4	Grass
5	240	+15	-20	297	2-4	5	Grass

*Unless otherwise noted, terrace ages are inferred from correlation of marine platforms with global sea level highstands. (See Merritts and Bull, 1989, for discussion and methods.)

†Soil Families:

1--Sandy, mixed, mesic Entic Hapludoll
2--Coarse-loamy, mixed, mesic Typic Hapludoll
3--Fine-loamy, mixed, mesic Pachic Haplumbrept
4-Fine-loamy, mixed, mesic Pachic Haplumbrept
4-Fine-loamy, mixed, mesic Pachic Haplumbrept
5--Fine, mixed, mesic Typic Hapludalf

§Terrace age determined by radiometric dating of organic matter and shells (see text for discussion).

TABLE 2. Field descriptions of Cape Mendocino-Punta Gorda soils.

Horizon	Depth to base of horizon, cm	Texture	Color (Wet)	Mottles	Mottle Color (Wet)	Consistency (Wet)	Structure	Clay and Organic Films	Nodules
Pedon 1--3.9 ka									
A1	22	ls	2.5Y3/2	--	--	so,po	sg	none	--
A2	48	ls	2.5Y3/2	--	--	so,po	sg	none	--
A3	65	ls	10YR3/2	--	--	so,po	sg	none	--
ABs	80	ls	10YR3/2	1ff	--	so,po	1msbk	none	3mp, Mn
2Bs1	97	sl	7.5YR4/6	--	--	ss,sp	2mabk	1 n br	3mp, Mn
2Bs2	115	sl	10YR4.5/2	--	--	so,po	1fsbk	none	--
2C	>125	sl	2.5Y3/2	--	--	so,po	m/1msbk	none	--
Pedon 2--29 ka									
A	8	sl	10YR2/1.5	--	--	ss,sp	1mgr	none	--
AB1	23	sl	10YR2/1	--	--	ss,sp	1fsbk	none	--
AB2	38	sl	10YR2/1	--	--	ss,sp	1f-msbk	none	--
AB3	56	sl	10YR2/1	--	--	ss,po	1mabk	none	--
Bw1	74	sl	10YR2/1	--	--	ss,po	1mabk	1 n br	--
Bw2	94	sl	10YR2/1	--	--	ss,sp	m	1 n br	--
Bw3	114	sl	10YR2/1	--	--	s,sp	m	1 n po pf	--
Bw4	135	sl	10YR2.5/1	--	--	s,p	m	2 mk po;2 n br	--
2Rr	>135	weathered graywacke bedrock		--	--	--	--	--	--
Pedon 3--40 ka									
A1	5	l	10YR3/1	--	--	ss,sp	1f-vfsbk;1mgr	none	--
A2	13	l	10YR2/2	--	--	ss,sp	1f-vfsbk;1mgr	none	--
AB1	30	l	10YR2/2	--	--	s,sp	1mabk	2 n po pf br	--
AB2	43	l	10YR2/2	--	--	s,sp	1f-vfsbk	2 n po pf br	--
AB3	53	l	10YR2/2	--	--	s,sp	1f-vfsbk	2 n po pf br	--
Bw1	74	l	10YR3/2	--	--	s,sp	1msbk	2 n pf	--
Bw2	104	vkl	10YR4/3	--	--	s,sp	2mpr/2mabk	3 mk po pf	--
BC1	147	vkl	10YR5/4	cd	--	ss,sp	m	2 n po pf	--
Ccv	173	vgsl	10YR5/4	--	10YR5/8	ss,sp	m	none	--
2Rr	>173	weathered graywacke bedrock		--	--	--	--	--	3p,Mn + Fe
Pedon 4a--124 ka									
A1	19	cl	10YR2/2	--	--	s,p	1fsbk;2mgr	none	--
AB1	44	cl	10YR2/1	--	--	s,p	2f-msbk;2mgr	1 n po pf	--
AB2	61	cl	10YR2/2	--	--	s,p	2f-msbk	2 mk po pf	--
Bw1	97	cl	10YR5/5	1cd	10YR5/8	s,p	2f-mpr	2 mk po pf br	--
Bw2	132	l	10YR6/6	1cd Fe;1fp Mn	7.5YR5/6, 6/8	s,p	2f-mabk;2mpr/3mabk	3 mk po pf br	--
Bw3	182	l	10YR6/6	2md Fe;2cd Mn	10YR5/8	s,p	2mabk	3 k po pf br	--
BC1	270	gl	10YR6/4	3md Fe	10YR5/8	ss,sp	m	2 k po pf	1 fd Mn
BC2	320	scl	5Y6/1	--	--	s,p	--	--	--

Horizon	Depth to base of horizon, cm	Texture	Color (Wet)	Mottles	Mottle Color (Wet)	Consistency (Wet)	Structure	Clay and Organic Films	Nodules
Pedon 4b--124 ka									
A1	16	l	10YR2/1	--	--	ss,ps	2mfsbk + 2mfgr	none	--
A2	49	l	10YR2/1	--	--	ss,ps	1,2mfsbk	none	--
A3	65	l	10YR2/1	--	--	ss,ps	2mfsbk	none	--
A4	108	l	5YR3/2	--	--	s,ps	2mfabk + sbk	1mk po art + org	--
AB	131	cl	10YR4/4	--	--	s,p	2mfabk + sbk	1 mk po	--
Bw1	156	cl	--	cd Fe	7.5YR5/8	s,p	2mabk	1 n po + br sg	--
Bw2	183	l	2.5Y6/6	cd Fe	10YR5/2	s,p	2mfabk	1 n po + br sg	--
Bw3	204	cl	2.5Y6/4	3md Fe	10YR6/8	ss,po	m	none	--
2BC1	241	gsl	2.5YR6/4	--	--	so,po	m	none	--
2BC2	265	vgsl	10YR5/4	--	--				
Pedon 5--240 ka									
A1	15	cl	10YR2/2	--	--	s,p	2msbk	none	--
A2	33	cl	10YR2/2	--	--	s,p	2f-msbk/2mgr	none	--
AB1	63	l	10YR3/2	--	--	s,p	2f-mabk/2mgr	2 mk po pf	--
AB2	90	cl	10YR2/2	--	--	s,p	2f-mabk/2mgr	2 mk po pf	--
Bw	128	cl	10YR3/2	--	--	s,p	2f-mabk	2 mk po pf	--
Bt	173	c	10YR6/4	--	--	s,vp	3cpr/3cabk	3 k po pf	--
Bg	200	l	10YR5/4	1cd Fe; 1cg	10YR6/8, 6/2	s,p	3abk	3 k po pf	1 cd Mn
Bs1	231	l	7.5YR5/8	40-60%Fe ce	10YR6/2	s,p	m	3 k po	3md Mn
Bs2	246	l	7.5YR5/8	--	--	s,p	m	3 k po	2-3fd Mn
BCg	257	l	2.5Y6/4	--	--	s,p	m	3 k po	--
BC	282	sl	10YR5/3	2cd Fe	7.5YR5/8	s,sp	m	3 k po	--

Abbreviations according to USDA Soil Survey Staff, 1975.
*Textures are estimated from field estimates and laboratory measurement of % clay.
†ce = cement

Table 3: Selected laboratory measurements of Cape Mendocino-Punta Gorda soil and parent material properties.

Horizon	Depth, cm	% Gravel	% Sand	% Silt	% Clay	% Organic Carbon	ph, H_2O	% Fed	% Feo	% Fep	% Alo	% Alp
Parent Material--0 ka												
Mean	--	7.3	96.1	2.9	1.0	--	7.5	0.50	0.39	--	0.20	--
Standard Deviation	--	12.2	1.7	1.2	1.2	--	--	0.04	0.06	--	0.03	--
Pedon 1--3.9 ka												
A1	22	0.0	91.3	6.6	2.1	0.93	6.69	0.34	0.29	0.06	0.11	0.04
A2	48	0.0	94.9	3.9	1.2	0.28	7.20	0.36	0.33	0.07	0.13	0.05
A3	65	0.0	94.3	4.5	1.2	0.24	7.40	0.33	0.24	0.05	0.07	0.03
ABs	80	0.0	89.5	7.9	2.6	0.40	7.31	0.48	0.40	0.05	0.11	0.03
2Bs1	97	0.0	77.1	20.1	2.8	0.53	7.12	2.89	1.73	0.11	0.09	0.02
2Bs2	115	0.1	78.5	16.6	4.9	0.40	7.28	0.35	0.26	0.04	0.09	0.03
2C	>125	0.0	76.7	18.3	5.0	0.26	7.08	0.28	0.16	0.03	0.08	0.02
Pedon 2--29 ka												
A	8	0.4	78.0	14.6	7.5	4.88	5.42	0.64	0.34	0.16	0.17	0.13
AB1	23	1.6	79.5	13.1	7.4	2.84	5.45	0.69	0.35	0.17	0.18	0.16
AB2	38	1.2	80.5	12.4	7.1	2.53	5.67	0.62	0.39	0.18	0.18	0.18
AB3	56	2.0	83.5	9.8	6.7	2.08	5.83	0.70	0.40	0.19	0.19	0.18
Bw1	74	1.1	82.9	10.4	6.7	1.77	5.92	0.66	0.37	0.22	0.18	0.21
Bw2	94	1.7	84.2	9.4	6.9	1.38	6.13	0.63	0.35	0.17	0.16	0.17
Bw3	114	5.4	78.3	10.1	9.6	1.39	5.92	0.72	0.35	0.17	0.20	0.17
Bw4	135	9.4	67.2	16.7	16.1	1.43	5.72	0.77	0.39	0.17	0.25	0.19
2Rr	>135	weathered	graywacke	bedrock	--	--	--	--	--	--	--	--
Pedon 3--40 ka												
A1	5	11.4	51.6	28.4	20.0	5.96	4.79	1.26	0.37	0.21	0.30	0.26
A2	13	7.5	47.5	30.4	22.1	4.83	4.94	1.23	0.34	0.22	0.30	0.26
AB1	30	8.3	42.0	36.3	21.7	3.29	4.91	1.27	0.35	0.26	0.34	0.33
AB2	43	7.5	49.9	26.7	23.4	2.89	5.23	1.35	0.37	0.29	0.36	0.36
AB3	53	10.8	49.4	29.5	21.1	2.78	5.09	1.43	0.37	0.32	0.36	0.39
Bw1	74	10.4	49.3	28.3	22.4	1.66	5.29	1.60	0.32	0.29	0.38	0.34
Bw2	104	43.2	39.7	38.1	22.2	0.89	5.31	1.22	0.23	0.15	0.32	0.24
BC1	147	38.6	47.2	35.7	17.1	0.78	5.42	1.25	0.23	0.14	0.30	0.22
Ccv	173	70.9	60.5	28.8	10.7	0.33	5.36	1.43	0.36	0.06	0.22	0.14
2Rr	>173	weathered	graywacke	bedrock	--	--	--	--	--	--	--	--

Table 3 (Continued.)

Horizon	Depth, cm	% Gravel	% Sand	% Silt	% Clay	% Organic Carbon	ph, H_2O	% Fed	% Feo	% Fep	% Alo	% Alp
Pedon 4a--124 ka												
A1	19	3.3	31.5	46.2	31.5	6.33	4.82	1.83	0.70	0.52	0.88	0.75
AB1	44	4.1	33.1	45.5	33.1	4.93	5.12	1.90	0.69	0.54	0.87	0.81
AB2	61	3.6	31.9	45.9	31.9	4.01	5.26	1.90	0.72	0.50	0.87	0.73
Bw1	97	2.9	28.9	44.3	28.9	0.74	5.67	1.63	0.60	0.20	0.73	0.40
Bw2	132	1.7	26.7	54.8	26.7	0.27	5.17	1.67	0.39	0.06	0.42	0.22
Bw3	182	2.8	18.4	52.0	18.4	0.16	5.19	1.50	0.55	0.03	0.32	0.14
BC1	270	3.9	19.6	52.5	19.6	0.06	5.22	1.33	0.47	0.01	0.24	0.08
BC2	320	--	10.6	43.9	10.6	0.27	--	--	0.12	0.04	0.22	0.12
Pedon 4b--124 ka												
A1	16	5.0	38.3	39.0	22.7	6.69	5.08	1.53	0.77	0.44	1.01	0.74
A2	49	5.0	36.3	40.3	23.4	5.09	5.11	1.63	0.84	0.50	1.07	0.78
A3	65	5.0	37.4	40.4	22.2	4.90	5.09	1.63	0.84	0.49	1.03	0.81
A4	108	5.0	36.3	40.2	23.4	3.21	5.34	1.64	0.89	0.51	1.08	0.79
AB	131	5.0	30.6	39.5	29.8	1.84	5.36	1.57	0.82	0.43	1.07	0.72
Bw1	156	5.0	29.3	43.1	27.6	0.81	5.39	1.60	0.63	0.27	1.12	0.60
Bw2	183	5.0	33.2	38.9	27.9	0.54	5.46	1.05	0.30	0.10	0.97	0.46
Bw3	204	5.0	30.1	36.5	33.4	0.16	5.32	1.53	0.17	0.05	0.58	0.30
2BC1	241	20.0	74.1	18.6	7.3	0.29	5.26	0.29	0.11	0.01	0.79	0.25
2BC2	265	35.0	86.8	7.7	5.5	0.27	5.25	0.86	0.45	0.05	0.80	0.25
Pedon 5--240 ka												
A1	15	1.7	26.1	42.7	31.2	6.03	5.31	2.00	0.64	0.48	0.72	0.64
A2	33	1.9	24.1	43.2	32.7	5.34	5.26	2.01	0.64	0.52	0.77	0.69
AB1	63	3.3	29.0	45.4	25.6	4.44	5.35	2.00	0.69	0.51	0.80	0.73
AB2	90	4.3	22.0	45.4	32.6	3.27	5.43	1.94	0.65	0.51	0.74	0.64
Bw	128	1.0	25.9	45.7	28.4	1.82	5.57	1.91	0.64	0.50	0.71	0.64
Bt	173	0.9	21.9	38.0	40.1	0.15	5.09	2.13	0.10	0.04	0.25	0.11
Bg	200	5.6	42.1	34.2	22.7	0.04	5.33	1.39	0.09	0.01	0.14	0.05
Bs1	231	23.0	43.3	34.2	22.5	0.04	5.78	4.61	0.56	0.03	0.18	0.06
Bs2	246	2.1	37.1	37.5	25.4	0.02	5.62	4.19	0.45	0.02	0.15	0.04
BCg	257	5.6	48.9	33.0	18.1	0.01	5.84	0.39	0.06	0.00	0.09	0.03
BC	282	17.4	64.5	25.2	10.3	0.01	6.20	0.41	0.11	0.01	0.11	0.05

TABLE 4. CHEMICAL PROPERTIES OF BEACH SAND PARENT MATERIAL.

Total element analysis for present beach sand:

	Si (wt%)	Al (wt%)	Fe (wt%)	Na (wt%)	Mg (wt%)	Ca (wt%)	K (wt%)	Ti (wt%)	Zr (wt%)	P (wt%)
Mean	36.16	5.44	2.41	1.02	0.78	0.77	0.51	0.36	0.01	0.01
S. D.	1.12	0.35	0.23	0.09	0.13	0.10	0.05	0.05	0.001	--
No. of Samples	12	12	12	12	12	12	12	12	12	1

Relative ranking of X-ray diffraction peak intensities for beach sand, <2 mm crushed:

Quartz	Plagio-clase	Chlorite	Kaolinite	Mica	Vermi-culite	Smectite	Chloritic intergrade
Large	Large	Medium	Small	Trace	*	*	*

*Mineral form looked for, but not found.

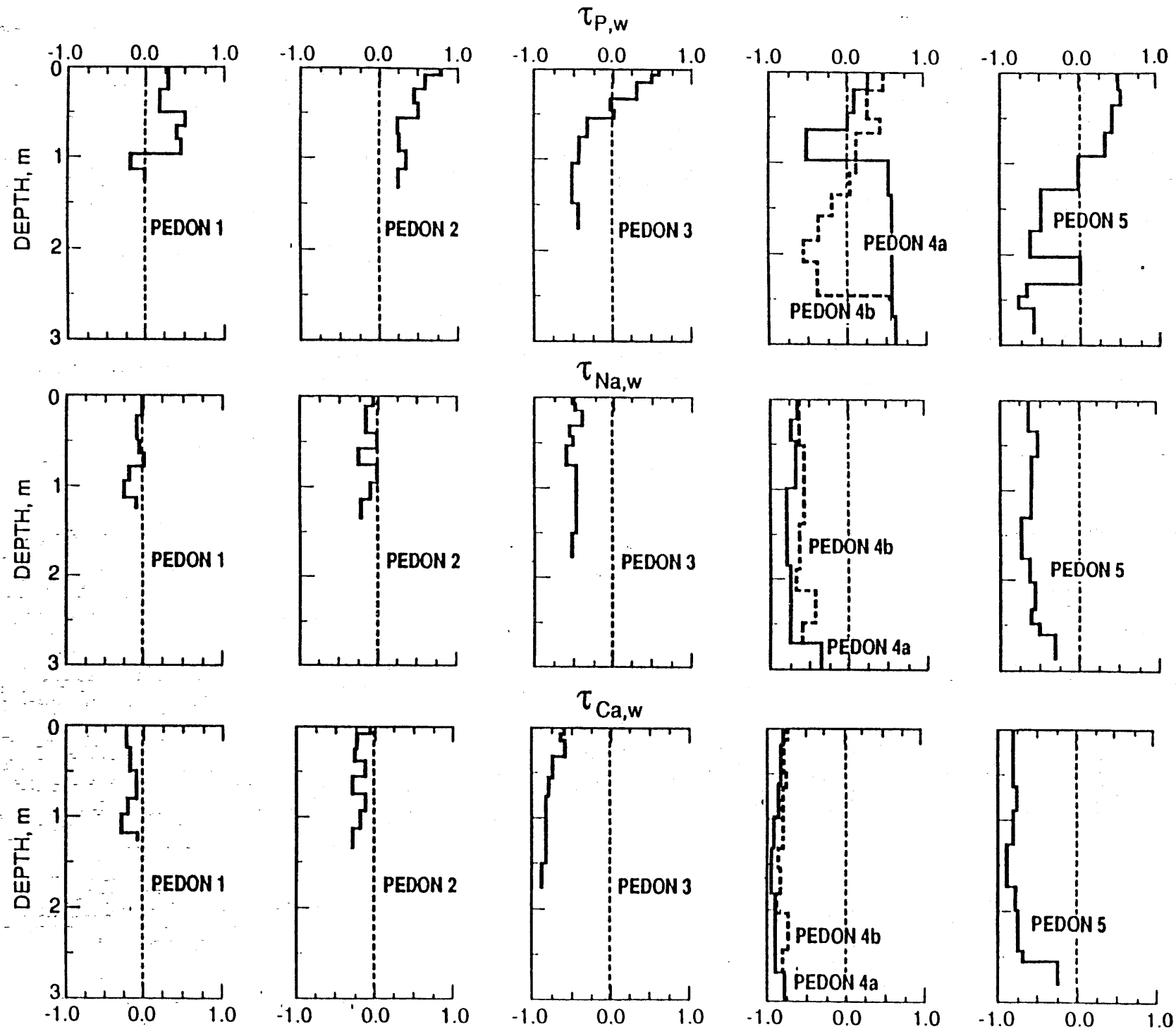
$\tau_{P,w}$
$\tau_{Na,w}$
$\tau_{Ca,w}$
DEPTH, m
-1.0
0.0
1.0
0
1
2
3
PEDON 1
PEDON 2
PEDON 3
PEDON 4a
PEDON 4b
PEDON 5

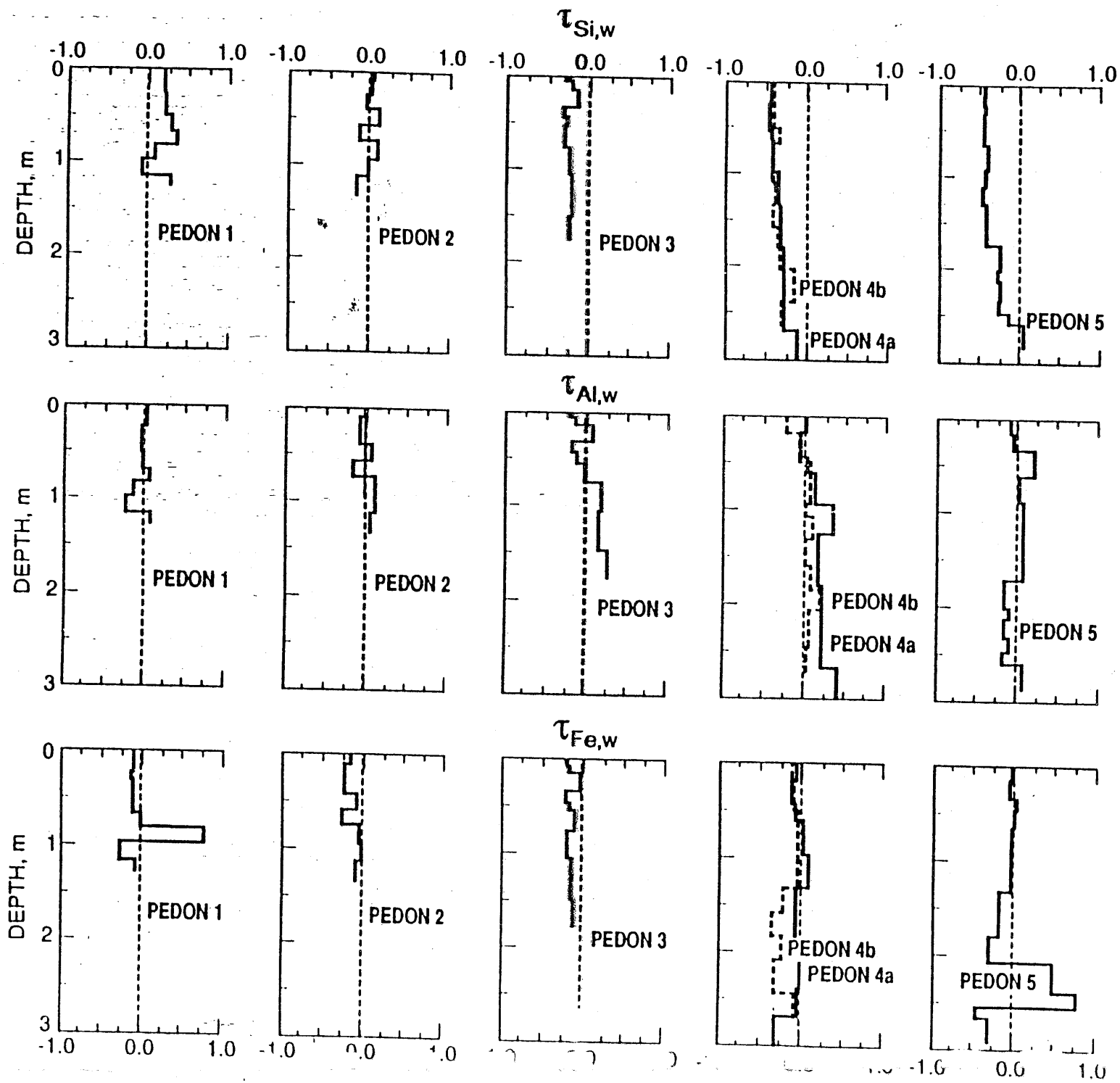
$\tau_{Si,w}$
$\tau_{Al,w}$
$\tau_{Fe,w}$
DEPTH, m
-1.0
0.0
1.0
0
1
2
3
PEDON 1
PEDON 2
PEDON 3
PEDON 4b
PEDON 4a
PEDON 5

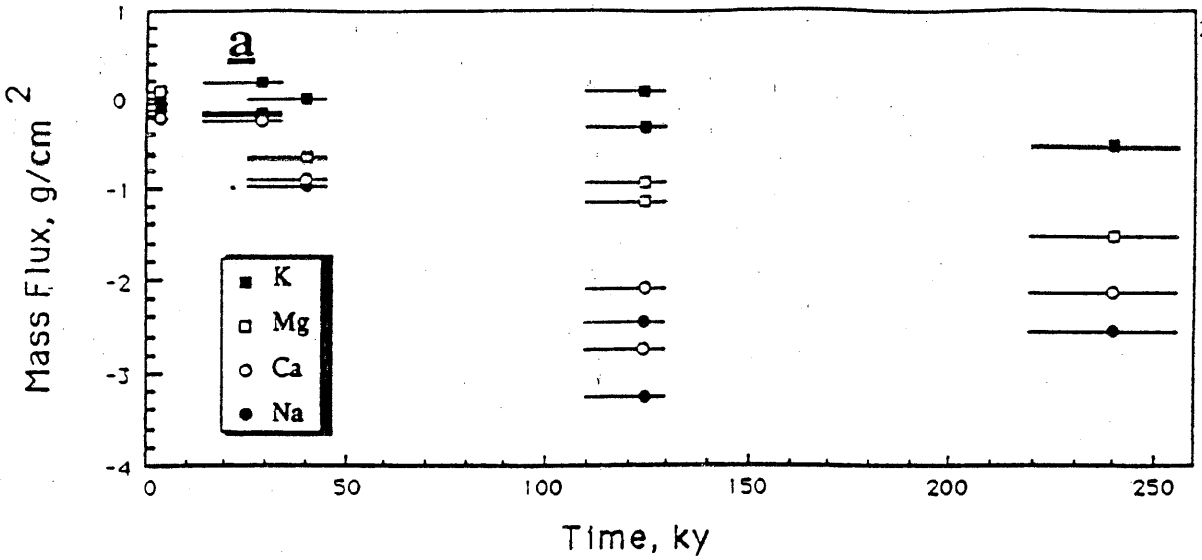
a
Mass Flux, g/cm 2
Time, ky
K
Mg
Ca
Na
1
0
-1
-2
-3
-4
0
50
100
150
200
250

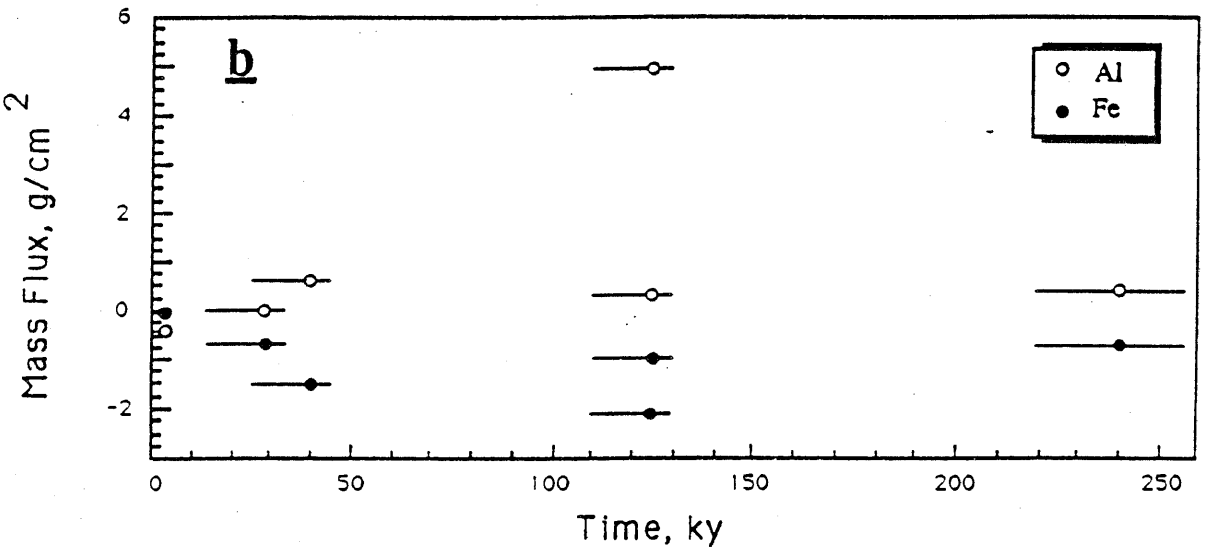
b
Mass Flux, g/cm 2
Time, ky
Al
Fe
6
4
2
0
-2
0
50
100
150
200
250

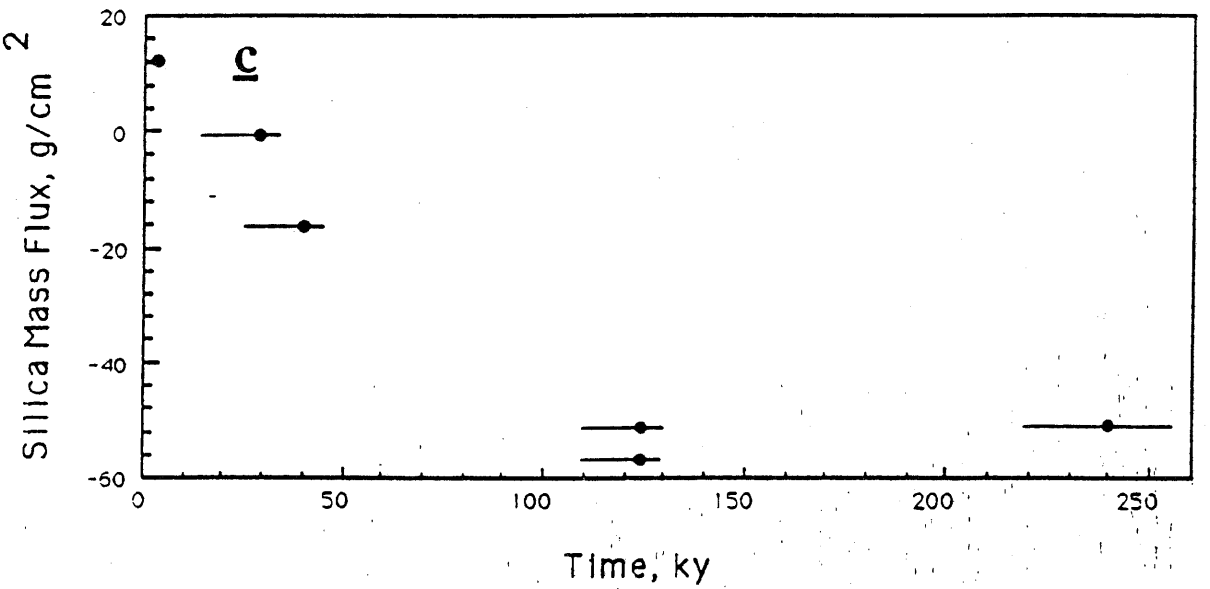
c
Silica Mass Flux, g/cm 2
Time, ky
20
0
-20
-40
-60
0
50
100
150
200
250

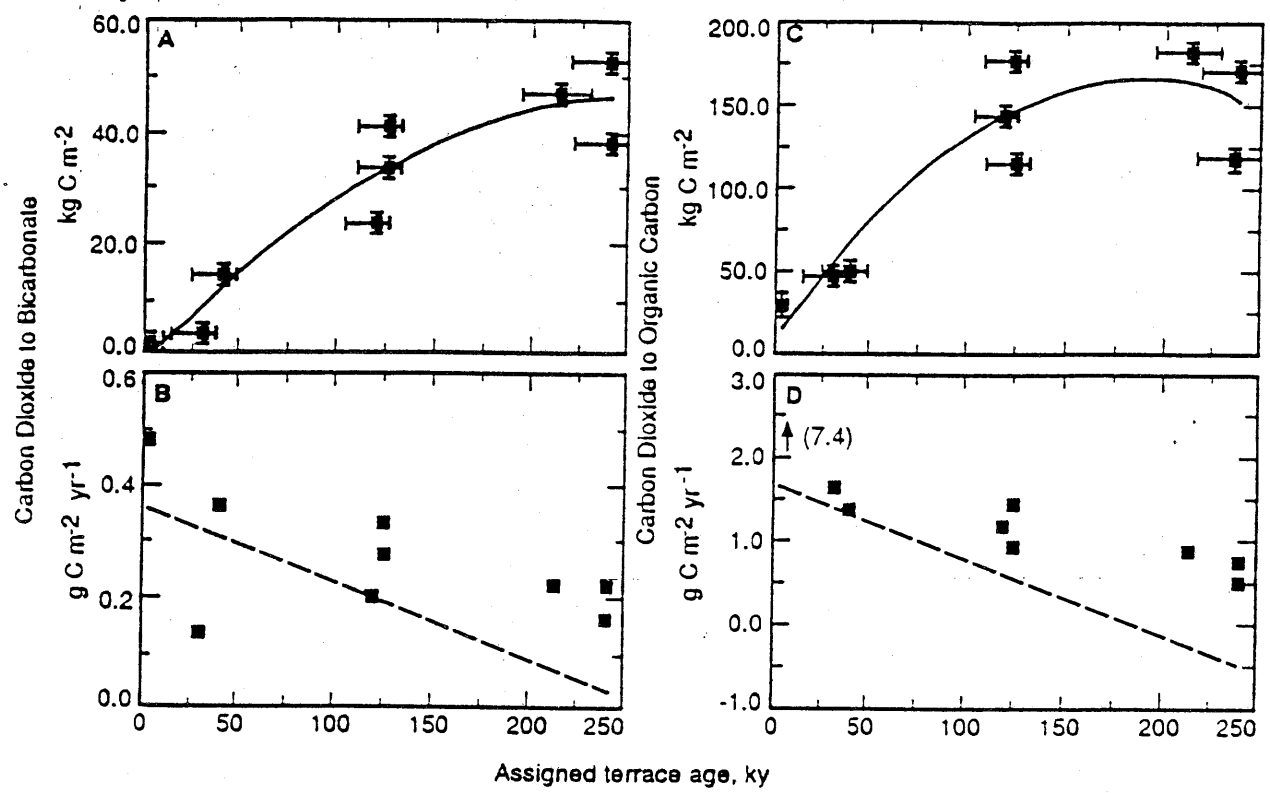
A
B
C
D
Carbon Dioxide to Bicarbonate
Carbon Dioxide to Organic Carbon
kg C m-2
g C m-2 yr-1
(7.4)
Assigned terrace age, ky

HORNBLENDE GRAIN ETCHING AS A RELATIVE DATING TECHNIQUE ON MARINE TERRACES OF NORTHERN CALIFORNIA

BEVIS, Kenneth A., Department of Geosciences, Oregon State University, Corvallis, OR 97331

ABSTRACT

This paper evaluates the use of hornblende grain etching as a relative dating technique on marine terraces of northern California. The variability in the degree of etching of hornblende grain samples collected from these surfaces is assessed by determining a hornblende etching index for each sample, then comparing the mean, standard deviation, and variance of each sample. The variability among samples from a single terrace, and between samples from separate terraces is statistically analyzed using the two sample T-test and ANOVA methods at a 5% significance level. Results indicate there is little variability in etching within a sample and between samples from a single terrace, but significant variability exists between samples located on surfaces separated by time intervals of approximately 30,000 years. Regression analyses compare the mean value of the hornblende etching index from each terrace to the assigned age of the terrace. Results indicate the rate of hornblende etching expresses a chronofunction for the marine terrace sequence that best fits a linear relationship.

INTRODUCTION

Quaternary tectonism along the northern California coast is expressed in uplifted and deformed marine terrace sequences located between Cape Mendocino and Big Lagoon, Humboldt County (Fig. 1)(Carver et al., 1986). Ages of marine terraces are estimated by correlation of the altitudinal distribution of flights of marine terrace surfaces with a world-wide chronology of high sea levels (Bloom et al., 1974; Chappel, 1983) as discussed by Bull (1985) and Lajoie (1986). Sequences including seven terrace surfaces with assigned ages of 76, 94, 103, 120, 133, and 214 ka are used in the investigation. These ages were supported by relative age estimates obtained from an analysis of soil development on the

marine terraces (Carver et al., 1986). The maximum thickness of the B horizon, the percentage of clay in the soil profile, and the profile development index (Harden, 1982) were used to distinguish fourage groups among the terraces, consisting of surfaces withages from 64-83, 83-103, 120-133, and greater than 202 ka.

The purpose of this paper is to evaluate the use of hornblende grain etching as a relative dating technique on marine terraces of northern California. Evaluation of this technique is accomplished in three steps: 1) the characteristics of the hornblende grains from several terraces are examined and expressed quantitatively by an index based on the degree of grain etching; 2) a statistical analysis of the variability among samples from a single terrace and between terraces is determined to assess the extent to which t degree of hornblende grain etching parallels the interpreted ages of the marine terra stratigraphy; and 3) the mean hornblende grain etching indices for each surface a compared with the assigned ages of the marine terraces in a regression analysis determine whether the data best fit a linear or logarithmic function.

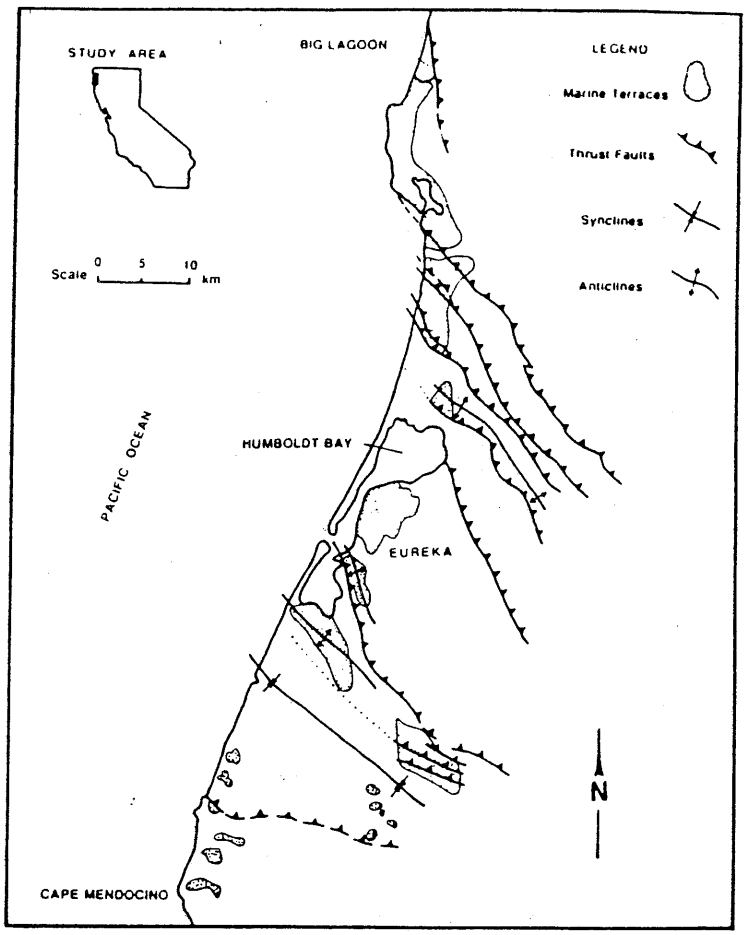

Figure 1. A map showing the location of marine terraces along the northern coast of California between Cape Mendocino and Big Lagoon and their relationship to active tectonic features.

METHODS

Field and laboratory experiments in a variety of environments and deposits have shown that the rate of hornblende etching is related to the rate of soil development, which in turn depends on five factors; topography, climate, vegetation, parent material, and time (Gillam

et al., 1977; Locke, 1979 and 1986; Berner and Schott, 1982; and Hall and Martin, 1986). The significance of these soil forming variables lies in their effect on the amount and chemical composition of water that passes through the soil, and thus is available for chemical interaction with the heavy mineral grains.

The study area and sampling program for this investigation were chosen to minimize changes in these factors. Rapid rates of soil formation on the marine terrace deposits are favored by nearly level topography which has undergone little post-depositional modification, well drained loamy textures, an isomesic temperature regime, high average annual precipitation in a xeric moisture regime, high rates of eolian influx of salts and fine mineral material, and intense forest bioturbation. These factors are nearly uniform throughout the distribution of marine terrace remnants. Thus, the effects of climate, vegetation, parent material, and topography are considered constant and time becomes the dominant variable influencing the degree of etching of the mineral grains in the soil. Hornblende grains were initially selected for this study because they are the most abundant heavy mineral making up the the mafic portion of sandy marine terrace deposits of northern Califoria and because the weathering environment was considered condusive to the rapid formation of features (etch pits and cockscomb terminations) on these grains used to develop a scale of hornblende etching (Table 1).

Samples were collected from the B horizon of three soil profiles on each of seven terrace surfaces with assigned ages of 76, 83, 94, 103, 120, 133, and 214 Ka (Carver et al., 1986). The B horizon is the zone of maximum weathering in the soil profile, and pre-sumably best represents the maximum hornblende etching in the soil. This sampling technique allows for more control over the rate of etching development from one sampling site to another for pur-

TABLE 1
HORNBLENDE ETCHING SCALE a

Etching Class	Etching Index Value	Criteria for Etching Classifications: Prism Sides	Prism Ends	Grain Shape
Unetched	1	Faces smooth and reflective; Edges straight	No cockscomb terminations	Subhedral to anhedral
Slight	2	Shallow pitting; Very shallow grooves	Very short terminations	Subhedral to anhedral
Moderate	3	Pitting more extensive; Grooves on most surfaces	Terminations longer, extend into sides	Obviously modified
High	4	Coalescence of pits; Deep grooves	Terminations very long, extend into sides	Very irregular
Extreme	5	Coalescence of pits; Deep grooves	Terminations very long, may be acicular	Extremely irregular; holes common

a - Modified from the Heavy Mineral Etching Scale by Gillam et al. (1977).

poses of comparison, rather than randomly sampling horizons (that may weather less rapidly) or collecting a bulk sample from the soil profile. Laboratory preparation of the samples for heavy mineral extraction and the identification of hornblende grains is adapted from Gillam et al. (1977). The heavy mineral separation followed the procedure outlined in Singer and Janitsky (1986).

A total of 50 hornblende grains from the fine sand fraction are counted for each sample. Each mineral grain is assigned an etching index between 1 and 5 based on the degree of grain etching from least to most etched, and a mean etching index value for the sample is derived. The criteria of Gillam et al.(1977) modified for hornblende grains is used to determine the degree of grain etching (Table 1). The etching scale allows each index value to represent significant variation from the next. Where classification of the index is difficult, grains are systematically assigned to the next lower value to avoid over estimating the true degree of etching for the sample.

TABLE 2
HORNBLENDE ETCHING INDEX VALUES BY SAMPLE

Terrace Age	Sample No.	N	Mean	S.D.	Var.
76Ka	1	50	2.14	0.90	0.95
	2	50	2.24	0.87	0.93
	3	50	2.18	0.87	0.93
83Ka	1	50	2.18	0.87	0.93
	2	50	2.16	0.93	0.96
	3	50	2.06	0.87	0.93
94Ka	1	50	2.14	0.93	0.96
	2	50	2.18	0.96	0.98
	3	50	2.26	0.92	0.96
103Ka	1	50	2.72	1.09	1.04
	2	50	2.62	0.97	0.98
	3	50	2.68	1.02	1.01
120Ka	1	50	3.06	0.94	0.97
	2	50	3.04	1.05	1.02
	3	50	2.98	0.96	0.98
133Ka	1	50	2.98	1.04	1.02
	2	50	3.04	0.90	0.95
	3	50	3.00	0.97	0.98
214Ka	1	50	3.72	0.95	0.97
	2	50	3.64	1.06	1.03
	3	50	3.70	1.00	1.00

RESULTS

To evaluate the use of hornblende grain etching as a relative dating technique, the mean etching index of the samples was quantitatively compared, and related to the age assigned to each terrace. The variability within each sample was assessed by its mean etching index, and associated standard deviation and variance (Table 2). The index means show relatively little variation with a progressive increase in value as the age of the terrace remnants increase, while the standard deviation and variance remain essentially constant. The

variability among the three samples from a single terrace was statistically analyzed using the two sample T-test (Table 3a) and ANOVA (Table 3b) methods at a 5% significance level. These results indicate the mean etching index values among the samples from a single terrace are statistically similar.

The average mean etching index for each group of three samples from a single terrace was calculated (Table 4). The variability between terraces was assessed using these means and the two sample T-test and ANOVA statistical analyses at a 5% significance level (Table 5). Significant increases in the mean etching index values for separate terraces occur between the 94 and 103 Ka surfaces, 103 and 120 Ka surfaces, and 133 and 214Ka surfaces. The etching values obtained for the 76, 83, and 94Ka terraces were statistically similar, as well as those of the 120Ka and 133Ka terraces.

TABLE 3a
RESULTS OF TWO SAMPLE T-TEST'S BY SAMPLE a

Terrace Age	Null Hypothesis	Accept	Reject
76Ka	1 = 2	•	
	1 = 3	•	
	2 = 3	•	
83Ka	1 = 2	•	
	1 = 3	•	
	2 = 3	•	
94Ka	1 = 2	•	
	1 = 3	•	
	2 = 3	•	
103Ka	1 = 2	•	
	1 = 3	•	
	2 = 3	•	
120Ka	1 = 2	•	
	1 = 3	•	
	2 = 3	•	
133Ka	1 = 2	•	
	1 = 3	•	
	2 = 3	•	
214Ka	1 = 2	•	
	1 = 3	•	
	2 = 3	•	

a - Two Sample T-test's were determined at a significance level of 5%, n-2 degrees of freedom, and a null hypothesis that the mean value of the hornblende etching index for each sample from a single terrace was equal.

TABLE 3b
RESULTS OF ANOVA'S BY SAMPLE a

Terrace Age	Null Hypothesis	Accept	Reject
76Ka	1 = 2 = 3	•	
83Ka	1 = 2 = 3	•	
94Ka	1 = 2 = 3	•	
103Ka	1 = 2 = 3	•	
120Ka	1 = 2 = 3	•	
133Ka	1 = 2 = 3	•	
214Ka	1 = 2 = 3	•	

a - ANOVA'S were determined at a significance level of 5%, k(n-1) degrees of freedom, and a null hypothesis that the mean values of the hornblende etching index for all samples from a single terrace are equal.

Regression analyses were preformed on the mean hornblende etching indices from each terrace, comparing their values to the assigned ages of each marine terrace (Fig. 2). The analyses indicate that the rate of hornblende etching fits either a linear relationship (Fig. 2a) or a logarithmic relationship (Fig. 2b) with little difference in the correlation coefficients (R^2). Figure 2a suggests that hornblende etching begins soon after deposition of the marine terrace sands and occurs at a relatively constant rate through time. This

relationship agrees with field and experimental studies conducted by Berner et al. (1980), Schott et al. (1981), and Berner and Schott (1982). The alternative regression curve presented in Figure 2b suggests that etching does not become recognizable using this technique until approximately 40,000 years have past, while the rate of hornblende etching exponentially decreases through time. This relationship is supported by logarithmic rates of hornblende etching obtained from field studies by other investigators (Gillam et al., 1977; Locke, 1979 and 1986; Hall and Martin, 1986). However, these latter studies were conducted in more continental settings, while this investigation is in a maritime environment. Climatic conditions on the northern coast of California are probably more conducive to rapid etching of hornblende grains which may account for the observed differences in etching rates. In either case (linear or logarithmic), the relationship for the portion of the curve with data control predicts nearly identical ages for a given hornblende etching index.

TABLE 4
HORNBLENDE ETCHING INDEX VALUES BY TERRACE

Terrace Age	N	Mean	S.D.	Var.
76Ka	150	2 19	0 88	0 94
83Ka	150	2 13	0 89	0 94
94Ka	150	2 19	0 93	0 96
103Ka	150	2 67	1 02	1 01
120Ka	150	3 03	0 98	0 99
133Ka	150	3 01	0 97	0 98
214Ka	150	3 69	1 00	1 00

CONCLUSIONS

When hornblende etching development was compared to assigned terrace ages, a fourfold grouping of surfaces could be discerned, including ages of 76 to 94 ka, 103ka, 120 to 133 ka, and 214 ka. The results from this paper are very similar to the age groups obtained using other relative dating parameters (Carver et al., 1986), implying that the hornblende etching index can also be used to define a chronosequence for the marine terraces of northern California.

TABLE 5
RESULTS OF TWO SAMPLE T-TEST'S AND ANOVA'S BY TERRACE a

Terrace Age	76ka	83Ka	94Ka	103Ka	120Ka	133Ka	214Ka
76Ka	-	A	A	R	R	R	R
83Ka	-	-	A	R	R	R	R
94Ka	-	-	-	R	R	R	R
103Ka	-	-	-	-	R	R	R
120Ka	-	-	-	-	-	A	R
133Ka	-	-	-	-	-	-	R
214Ka	-	-	-	-	-	-	-

a - Both tests were determined at a significance level of 5%, and a null hypothesis that the mean value of the hornblende etching indices for each group of three samples from separate terraces was equal (A) - Accept, (R) - Reject

A linear function seems to best represent the relationship between the degree of hornblende grain etching and the length of time the grains have spent in the soil weathering environment. Regression analyses indicate a logarithmic curve can also be fitted to the data, but climatic conditions are probably more conducive to weathering in this maritime environment then the lower portion of this curve would indicate. The initially rapid rates of etching that remain relatively constant through time suggested by the linear etching relationship probably are related to greater rates of weathering on the northern coast of California.

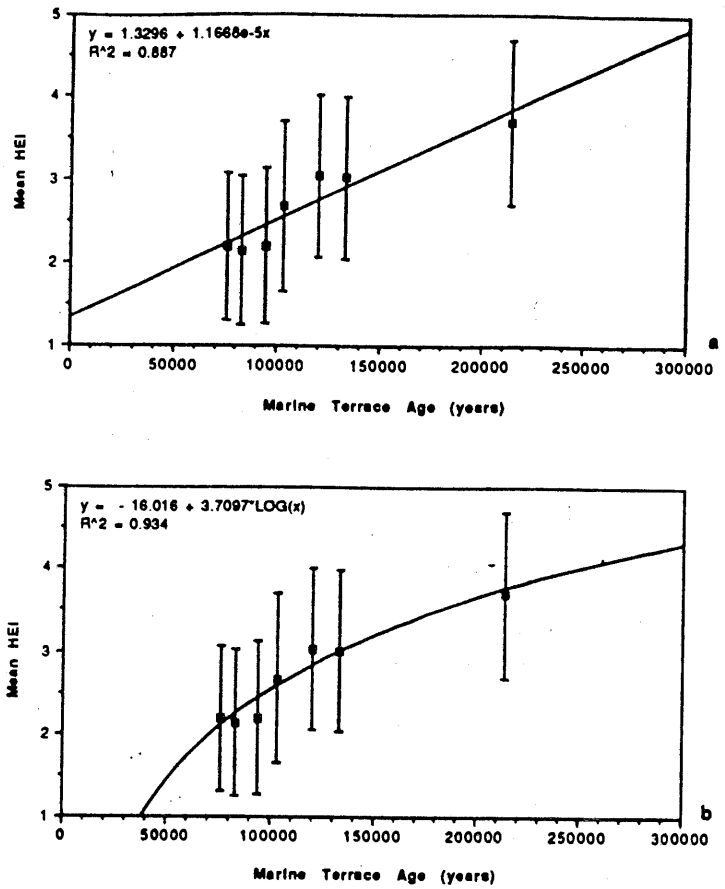

Figure 2. Regression analyses displaying a linear (2a) and a logarithmic (2b) relationship between the mean hornblende etching index of each marine terrace and the ages assigned to these surfaces in northern California.

Hornblende etching is clearly a useful technique for indicating the relative age of marine terrace deposits in northern California, and may be a useful technique for correlation between marine terrace sequences along the northwest coast of the United States and western coast of Canada, where environmental influences on the rate of hornblende etching are consistent with those of northern California. Obviously no single parameter should be used to differentiate between these surfaces, but this technique is shown to be a valuable addition to the relative dating techniques currently available for marine terrace dating and correlation.

REFERENCES

Berner, R. A., and Schott, J. (1982). Mechanism of pyroxene and amphibole weathering II: Observations of soil grains. American Journal of Science, 282, 1214-1231.

Berner, R. A., Sjoberg, E. L., Velbel, M. A., and Krom, M. D. (1980). Dissolution of pyroxenes and amphiboles during weathering. Science, 207, 1205-1206.

Bloom, A. L., Broeker, W. S., Chappell, J., Matthews, R. K., and Mesolella, K. J. (1974). Quaternary sea level fluctuations on a tectonic coast: new Th/U dates from the Huon Peninsula, New Guinea, Quaternary Research, 4, 185-205.

Bull, W. B. (1985). Correlation of flights of global marine terraces, in: Tectonic geomorphology, Morisawa, M. and Hack, J. eds., Binghamton Symposia in Geomorphology: International Series, 15, 129-152.

Carver, G. A., Burke, R. M., and Kelsey, H. M. (1986). Quaternary deformation in the region of the Mendocino Triple Junction, Final Report, U.S.G.S. National Earthquake Hazard Reduction Program.

Chappell, J. (1983). A revised sea level record for the past 300,000 years on Papua, New Guinea: a numerical calculation, Quaternary Research, 9, 265-287.

Gillam, M. L., Ensey, C., Page, W. D., and Blum, R. L. (1977). Heavy mineral etching in soils from the Merced and Truckee areas, California, in: Soil Development, Geomorphology, and Cenozoic History of the Northeastern San Joaquin Valley and Adjacent Areas, California: A Guidebook for the Joint Field Session of the American Society of Agronomy, Soil Science Society of America, and the Geologic Society of America, p. 230-244.

Hall, R. D., and Martin, R. E. (1986). The etching of hornblende grains in the matrix of alpine tills and periglacial deposits, in: Rates of Chemical Weathering of Rocks and Minerals, ed. by Colman, S. M., and Dethier, D. P., Academic Press, Inc., p. 101- 128.

Harden, J. W., 1982, A quantitative index of soil development from feild descriptions: examples from a chronosequence in central California, Geoderma, 28, 1-28.

Lajoie, K. R. (1986). Coastal tectonics, in: Active tectonics, Wallace, R. E., ed., in the series: Studies in Geophysics, Washington D. C., National Academic Press, p. 95-124.

Locke, W. W. (1979). Etching of hornblende grains in Arctic soils: An indicator of relative age and paleoclimate, Quaternary Research, 11, 197-212.

Locke, W. W. (1986). Rates of hornblende etching in soils on glacial deposits, Baffin Island, Canada, in: Rates of Chemical Weathering of Rocks and Minerals, ed. by Colman, S. M., and Dethier, D. P., Academic Press, Inc., p. 129-145.

Schott, J., Berner, R. A., and Sjoberg, E. L. (1981). Mechanism of pyroxene and amphibole weathering I: Experimental studies of iron-free minerals, Geochem. Cosmochim. Acta., 45, 2123-2135.

Singer, M. J. and Janitsky, P. (1986). Field and laboratory procedures used in a soil chronosequence study. U. S. Geological Survey Professional Paper 1648, 49pp.

Geology and Stratigraphy of the Freshwater Creek Watershed, Humboldt County, California

by Keith Knudsen*

The 60 to 70 square kilometer Freshwater Creek watershed encompasses previously unmapped terrain in coastal Humboldt County. It is located east-southeast of Arcata Bay between 2 previously mapped areas. The area to the north was mapped by G. Carver of Humboldt State University (Carver, Stephens and young, unpublished; Kelsey and Carver, 1988). The region south of Freshwater Creek basin was mapped by B. Ogle (Ogle, 1953). Both of these areas contain Neogene sediments deformed by northwest-trending folds and thrust faults. The purpose of this study was to develop a detailed geologic map and cross-section (Figure 1) of the area and to correlate the Neogene stratigraphy of the Freshwater Creek watershed with that described by Carver, Ogle, Ingle (Ingle, 1987) and others.

Figure 1 is an approximately 10 kilometer long, north-70-east-trending cross section of the Freshwater Creek area. Two major northwest-trending, northeast-dipping faults are diagrammed. The Freshwater fault is a reverse fault which places rocks of the Jurassic through Cretaceous Franciscan Central belt against those of the Eocene Yager Formation. Lower Pliocene fault activity is documented by at least 100 meters of vertical offset of a 4.88±0.21 Ma volcanic ash. The Greenwood Heights fault is a previously unmapped northwest-trending, northeast-dipping, reverse or thrust fault which places Central belt Franciscan rocks against Pleistocene Wildcat Group sediments and vertically offsets basal Wildcat sediments a minimum of 450 meters. Both of these faults are interpreted to result from the stresses imposed by oblique subduction of the Gorda-Juan de Fuca oceanic plate beneath the North American plate.

The Wildcat Group, a sequence of predominantly marine mudstone, siltstone, and sandstone, is divided into two units in the Freshwater Creek drainage basin. The lower Wildcat unit consists of open marine deposits which are no older than Late Miocene and are chronostratigraphically equivalent to the lower Rio Dell, Eel River and Pullen Formations described to the south by Ogle (1953), Ingle (1987) and others (Figure 2). The upper Wildcat unit, which contains nearshore, bay and fluvial facies, is Plio-Pleistocene in age and is interpreted to be correlative to the Falor Formation described to the northeast by Manning and Ogle (1950) and Carver (1987).

To the northeast of the Greenwood Heights fault the lower Wildcat unit is not found and the upper unit of the Wildcat group rests directly on heavily saprolitized Franciscan Central belt rocks, while on the downthrown block of the fault the upper unit rests on the lower unit of the Wildcat (Figure 1). The northeastern, upthrown block was thrust above sea level such that the lower unit of the Wildcat could be eroded and a saprolite could develop on Franciscan rocks prior to deposition of the upper unit of the Wildcat (Figure 3).

This portion of the Eel River basin, a broad forearc basin encompassing a large percentage of the continental shelf as well as southwestern Oregon and northwestern California, subsided rapidly to middle bathyal depths during the Miocene. It then proceeded to shoal and was filled by Wildcat Group sediments during the early Pleistocene (Figure 3). Evidence suggests that the margin of the Eel River basin extended farther to the east than previously thought.

*This work was done while Keith was a graduate student at Humboldt State University. He is presently employed by Balance Hydrologics, 1760 Solano Ave, Suite 209, Berkeley, CA, 94707.

References

Carver, G.A., 1987, Late Cenozoic Tectonics of the Eel River Basin Region, Coastal Northern California: in Tectonics, Sedimentation and Evolution of the Eel River and Associated Coastal Basins of Northern California, eds. Schmiczek, H. and Suchsland, R., by San Joaquin Geological Society.

Carver, G.A., T.A. Stephens and J.C. Young, in press, Quaternary Geologic Map of the Mad River Fault Zone, Humboldt County, California.

Ingle, J.C. Jr., 1987, The Depositional, Tectonic, and Paleoceanographic History of the Eel River (Humboldt), Point Arena, and Bodega (Point Reyes) Basins of Northern California; A Summary of Stratigraphic Evidence: in Tectonics, Sedimentation and Evolution of the Eel River and Associated Coastal Basins of Northern California, eds. Schmiczek, H. and Suchsland, R., by San Joaquin Geological Society.

Kelsey, H.M. and G.A. Carver, 1988, Late Neogene and Quaternary Tectonics Associated with Northward Growth of the San Andreas Transform Fault, Northern California: J. Geophys. Res., vol. 93, pp. 4797-4819.

Manning, G.A. and B.A. Ogle, 1950, Geology of the Blue Lake Quadrangle California, Bull. Calif. Div. Mines, 148, 36 pp.

Ogle, B.A., 1953, Geology of the Eel River Valley area, Humboldt County, California, Bull. Calif. Div. Mines, 164, 128 pp.

GEOLOGIC CROSS SECTION OF THE FRESHWATER CREEK WATERSHED
HUMBOLDT COUNTY, CALIFORNIA

by Keith Knudsen
1990

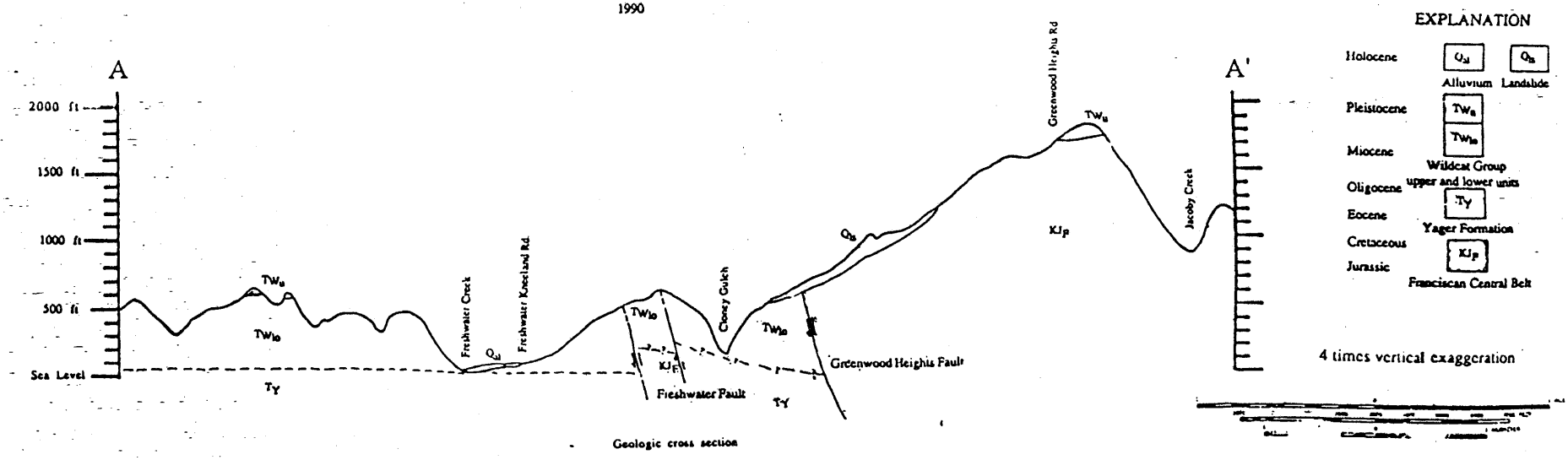

Figure 1

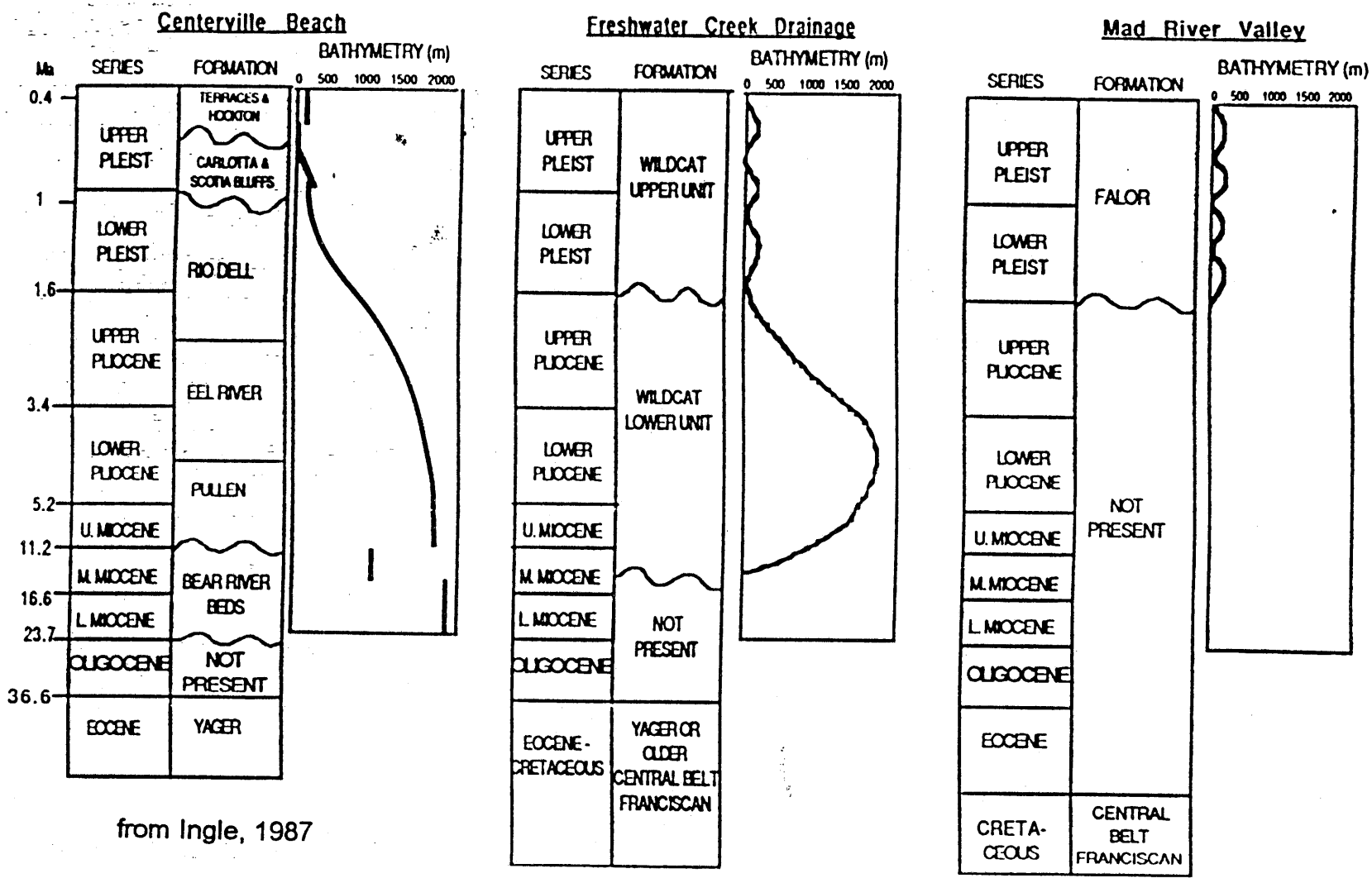

Correlation of Regional Stratigraphy

Figure 2

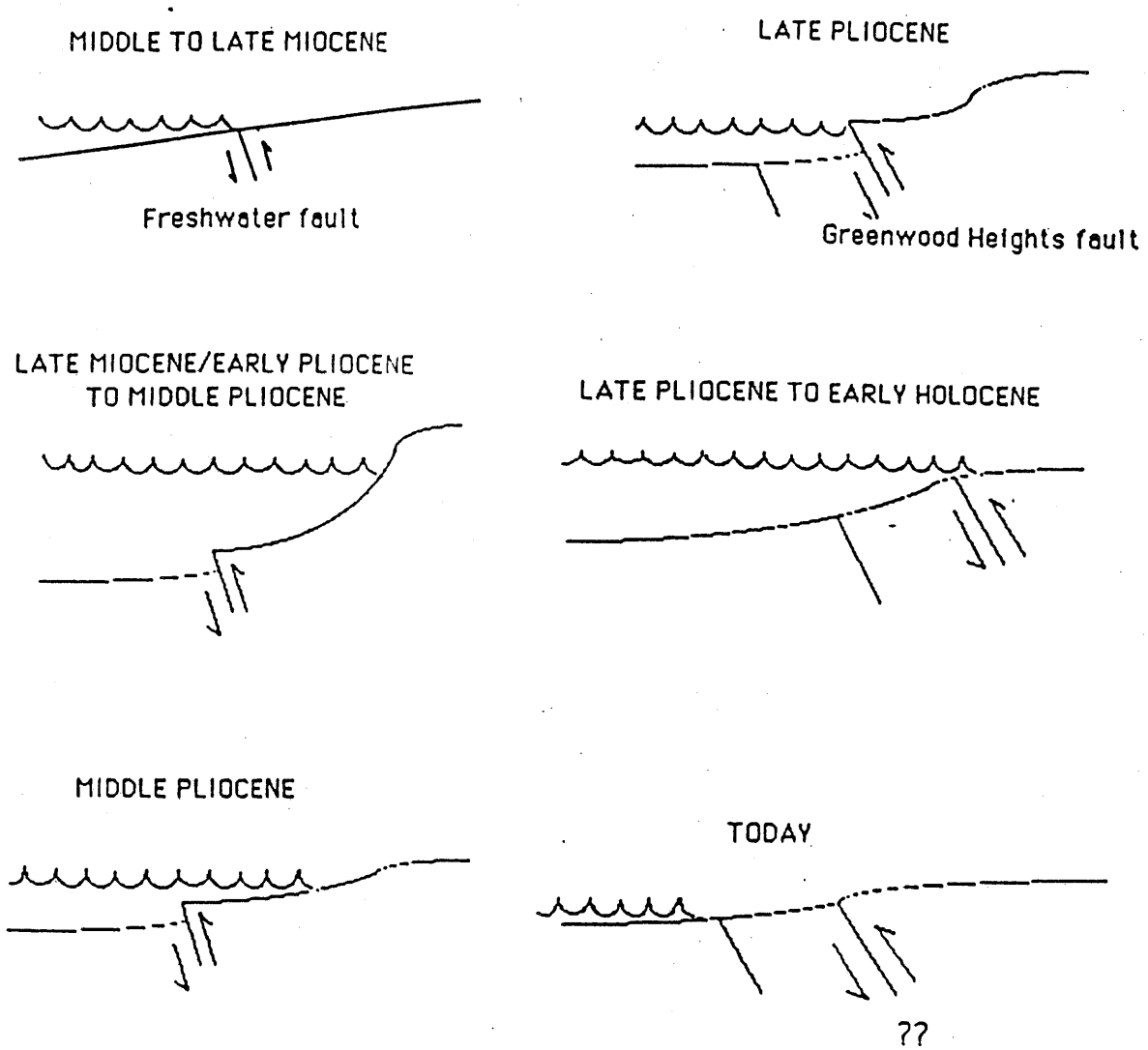

Cartoon depicting likely evolution of the Freshwater Creek region of the Eel River Basin

Figure 3

ANALYSIS OF PROFILES OF STREAMS THAT CROSS A PORTION OF THE LITTLE SALMON FAULT, HUMBOLDT COUNTY, CALIFORNIA

Andrea Stein
Corps of Engineers, Sacramento District
1325 J St., Sacramento, CA 95814

Introduction

The Little Salmon fault is a thrust fault associated with the southern terminous of Cascadia Subduction, where the fold and thrust belt intersects the northern California Coast between Big Lagoon and Cape Mendocino (Figure 1) (Carver, 1987). The Little Salmon fault is a northwest trending, northeast dipping (20°-30°) thrust fault with at least 4.3 to 7 km Quaternary dip slip (Carver and Burke, 1988). Stratigraphic data collected from exploratory trenches in the fault zone near the study area indicate late Quaternary and late Holocene displacements (Woodward-Clyde Consultants, 1980; Carver and Burke, 1988). For this study profiles of small streams that cross a portion of the Little Salmon fault near southern Humboldt Bay were analyzed to obtain information on the style of deformation of the fault in that area.

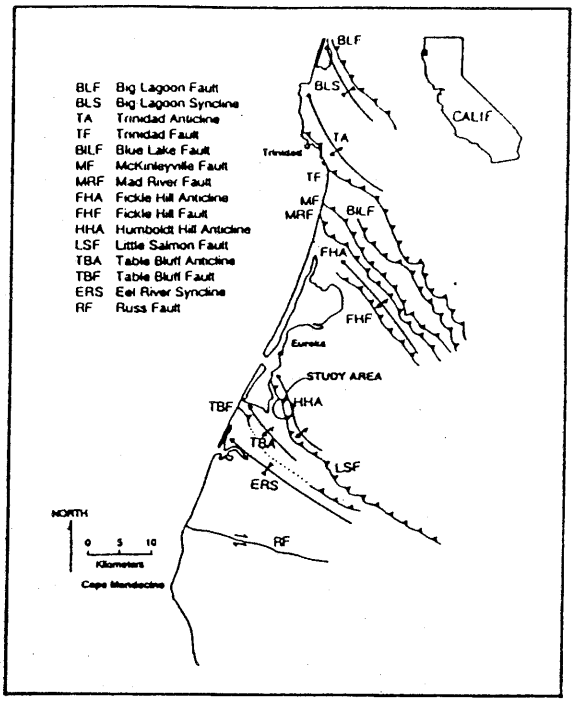

Figure 1. Map showing location of study area and major late quaternary structures on the coast of northern California. From Carver and Burke, 1988.

Background and Methods

The use of stream profiles as analytical tools is based on the generalization that the longitudinal profiles of most graded streams are smooth concave-up curves, (Leopold and Bull, 1979), and their logarithmic profiles can be approximated by a straight line. Deviations in shape or steepness from the graded profile indicate relatively recent changes in one or more of the factors that affect the profile, such as discharge, tectonics, sediment load, and bed lithology (Hack, 1960). In areas where the other factors can be held constant, deviations in the profiles can be interpreted as indicators of tectonic activity (for ex. Merritts and Vincent, 1989; McKeown,et al, 1988).

Profiles of eleven small streams in the study area were plotted three different for analysis (Figure 3). For each stream profile shown on Figure 3 the top plot i arithmetic plot, and the bottom one is the semilog plot. The middle plot is that of st

gradient (SL) index of stream segments versus length. Hack (1973) developed the SL index as a semi-quantitative method of analyzing the slopes of different segments of the same stream. The SL index of a stream segment is calculated as shown on Figure 2. It is the slope of a stream segment, normalized to the distance of that segment from the headwaters of the stream. The arithmetic and SL plots are annotated with geologic contacts and faults, as mapped in the field.

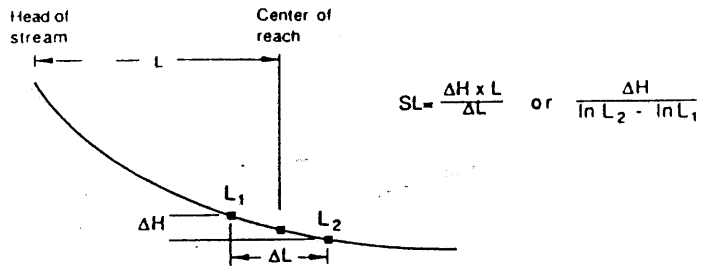

Figure 2. Calculation of the stream gradient (SL) index for a stream segment. Modified from Hack, 1973.

Results and Interpretations

The shapes of the longitudinal profiles vary from roughly concave to nearly straight. The slopes of the profiles are generally steeper in the bedrock and more shallow in the alluvium, despite the ubiquitous decrease in slope along the lengths of the streams. This is illustrated on the plots of SL index. The values of the SL indices rise nonuniformly from the headwaters of the streams through the bedrock, and abruptly drop at the bedrock/alluvium boundaries. This trend is mimicked on the semilog plots. Their shapes can be described as a backwards, stretched "S". The discrepancy in steepnesses between the alluvial and bedrock portions of the profiles may indicate that they have not been subjected to the same forces of uplift. Indeed, the location of the west trace of the Little Salmon fault roughly corresponds to the bedrock/alluvium contact on most of the profiles. Uplift along the fault has occurred recently enough to not allow the streams to become graded to their new tectonic conditions.

Two traces of the Little Salmon fault have been mapped in the study area (Ogle, 1953; Carver and Burke, 1988; Stein, in prep.). The eastern trace is crossed by all of the streams shown of Figure 3, except First and Spring Creeks. The western trace is crossed by all of the streams except Joe's, Nunes and South Creeks. Gradient highs in the profiles are clearly illustrated by the SL index plots. Most of the profiles show moderate gradient highs in the bedrock portions of the profiles where they cross the eastern trace. The western trace is located in the alluvial portions of all of the profiles that cross it. Some show quite anomalous gradient highs there (Patti's, First, Holgerson, and Swiss Hall Creeks, and Willow Brook). Landslide and Spring Creeks exhibit distinct swales at the western trace of the fault. Considering that the western trace anomalies are located in the alluvial portions of the streams, and yet are generally comparable or greater in magnitude than the anomalies at the eastern trace, it can be concluded that the western trace is younger and/or more active than the eastern trace.

In summary, the slightly oversteepened profiles of the bedrock portions of the streams that cross the Little Salmon fault suggest that the area east of the western trace

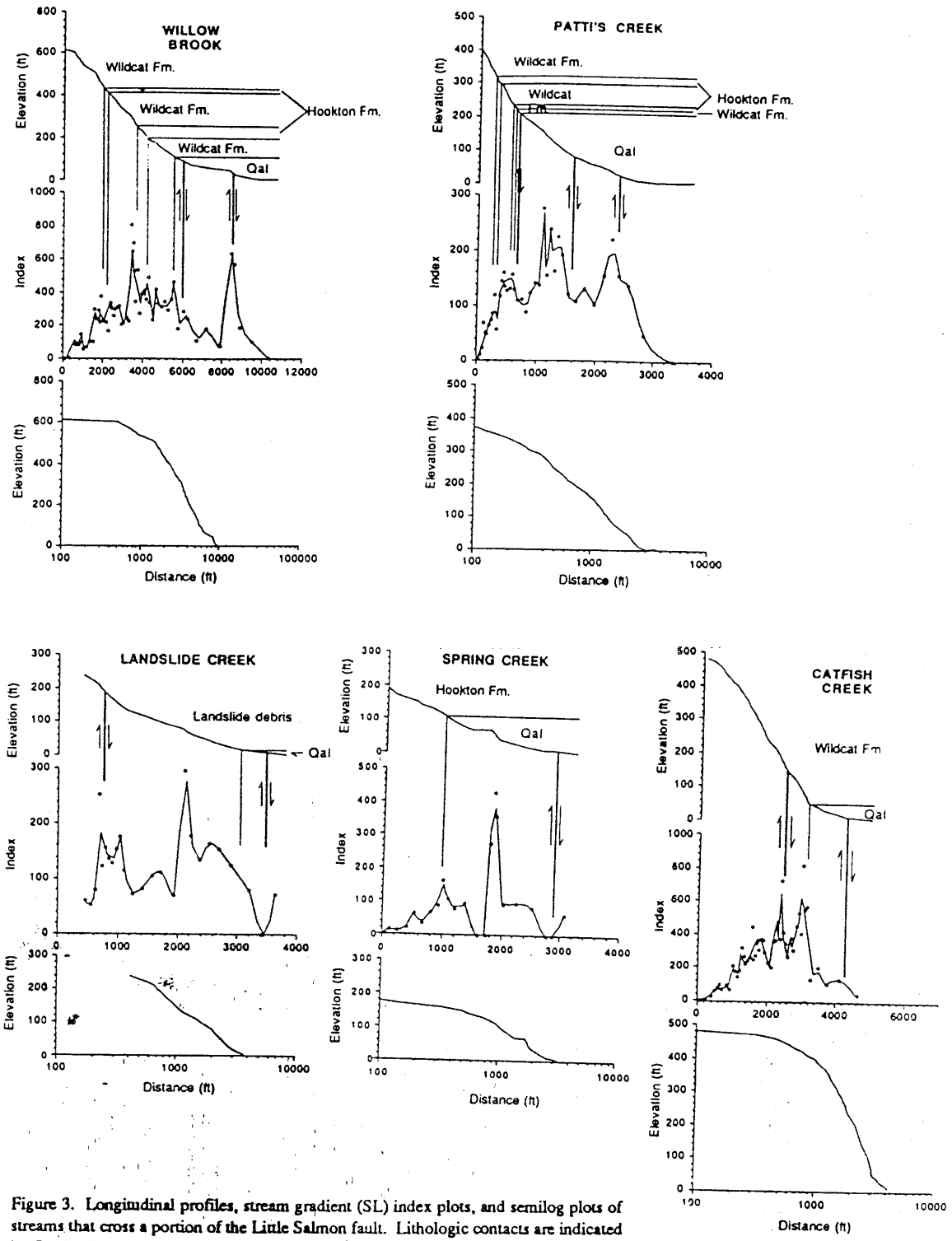

Figure 3. Longitudinal profiles, stream gradient (SL) index plots, and semilog plots of streams that cross a portion of the Little Salmon fault. Lithologic contacts are indicated by fine horizontal lines, and fine vertical lines between the longitudinal profiles and SL index plots. The Wildcat and Hookton Formations are poorly indurated late Tertiary and Quaternary mudstones, sandstones and minor conglomerates. Faults are shown as thick vertical lines, with arrows indicating relative direction of movement.

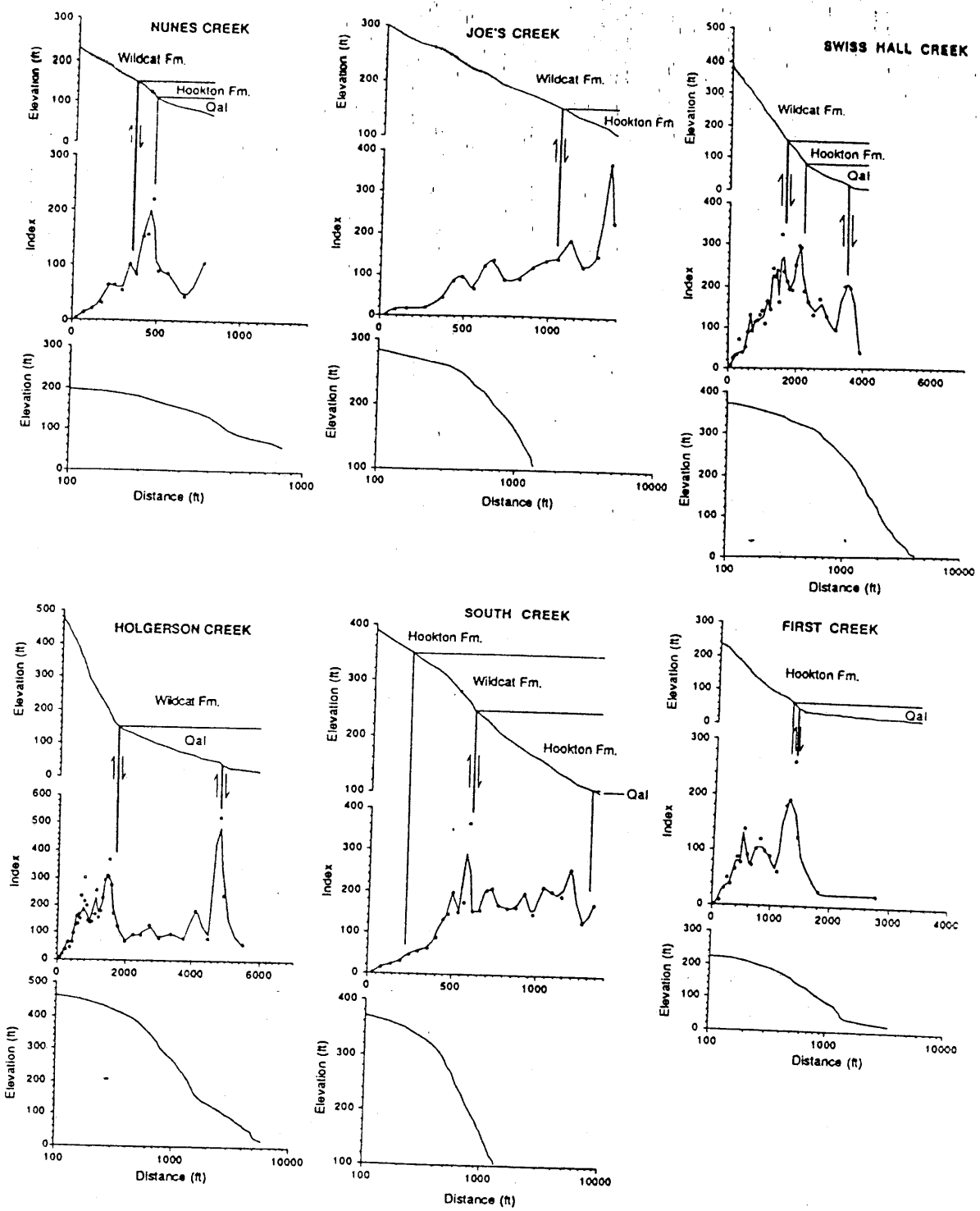

Figure 3. Continued

of the fault is undergoing, or has recently undergone, uplift along the fault. The magnitude of the gradient anomalies in the profiles where they cross the eastern and western traces suggests that more recent uplift has occurred along the western trace.

References

Carver, Gary A., 1987, Late Cenozoic tectonics of the Eel River Basin region, coastal northern California, *in* Schymiczek, H. and Suschsland, R., eds., Tectonics, sedimentation, and evolution of the Eel River and associated coastal basins of northern California: San Joaquin Geological Society Miscellaneous Publication #37.

Carver, Gary, and Burke, Raymond, 1988, Final Report, Trenching investigations of northwestern California faults, Humboldt Bay region: Report for U.S. Geological Survey Grant 14-08-0001-G1082.

Hack, John, 1960, Interpretation of erosional topography in humid temperate regions: American Journal of Science, v. 258-A, p.80-97.

____, 1973, Stream profile analysis and stream gradient index: U.S. Geological Survey Journal of Research, v. 1, no. 4, p. 421-429.

Leopold, L. B., and Bull, W. B., 1979, Base level, aggradation, and grade: Proceedings of the American Philosophical Society, v. 123, no. 3, p. 168-202.

McKeown, F. A., Jones-Cecil, M., Askew, B. L., and McGrath, M. B., 1988, Analysis of stream profile data and inferred tectonic activity, Eastern Ozark Mountains Region: U.S. Geological Survey Bulletin 1807, 39 p.

Merritts, D., and Vincent, K. R., 1989, Geomorphic response of coastal streams to low, intermediate, and high rates of uplift, Mendocino triple junction region, northern California: Geological Society of America Bulletin, v. 101, p. 1373-1388.

Ogle, B. A., 1953, Geology of the Eel River Valley area, Humboldt County, California: California Division of Mines and Geology Bulletin 164, 128 p.

Woodward-Clyde Consultants, 1980, Evaluation of the potential for resolving the geologic and seismic issues at the Humboldt Bay Power Plant Unit No. 3: unpub. report to Pacific Gas and Electric Company: Woodward-Clyde Consultants, San Fransisco, California.

TERRACE FORMATION AND DEFORMATION ON YAGER CREEK
Humboldt County, California[1]

Presented by:
Kevin M. O'Dea[2]

INTRODUCTION

A complex of fluvial terraces near the confluence of Yager Creek and the Van Duzen River in coastal northern California provides a well preserved geomorphic record of late Pleistocene and Holocene fluvial and tectonic activity at the southern end of the Cascadia Subduction Zone (CSZ). The terraces can be observed as obvious and distinct geomorphic surfaces on Highway 36 between the towns of Carlotta and Hydesville in Humboldt County, California (Figure 1). The formation and preservation of the terraces provide an opportunity to investigate geomorphic response to active tectonics near the Mendocino Triple Junction and stream adjustment to changes in the late Pleistocene climate of coastal northern California.

Eight of the surfaces ($Qtyc_1$ through Qyc_7 and Qr) form a flight of terraces trending parallel to and west of the south-flowing lower reach of Yager Creek. The terrace flight rises over 70 meters above the active channel and is cut by four east-west trending, north facing linear fault scarps. These faults cannot be traced with confidence beyond the limits of the Yager Creek terrace flight. Higher terrace surfaces (Qi_1, Qi_2, and Qh) have an east-west trend, subparallel to and north of the Van Duzen River, and occur on both the east and west sides of the Yager Creek valley.

The lower reach of the creek cuts through Tertiary and Pleistocene deposits of the Wildcat Group of the Eel River basin and younger Pleistocene and Holocene alluvuim. In general, the stream can be described as having a steep gradient, cobble-bedded, straight to slightly sinuous, entrenched channel with side and diagonal bars.

TECTONIC AND STRUCTURAL SETTING

The terraces at Yager Creek are located less than 30 km northeast of the Mendocino triple junction, the transform-transform-trench intersection of the North American, Pacific, and Gorda lithospheric plates. An active fold and thrust belt forming an accretionary prism within the western edge of the North American plate extends parallel and inboard of the Cascadia Subduction Zone. The accretionary prism extends southward along the present coastline to near the Eel River where the structural trend bends eastward. The study area is near the southern and eastern limits of the region of contractile tectonics (Kelsey and Carver, 1988) associated with the fold and thrust belt of the Cascadia Subduction Zone.

Within the study area, several major structural features are known to be active in the late Quaternary. The Little Salmon Fault forms the approximate northern boundary of the study area. Approximately 7,000 meters of dip slip displacement has occurred in the last 700,000 years along this low -angle reverse fault (WCC, 1980). North of the Little Salmon fault, the Yager fault forms a splay of the Little Salmon fault. Between these two northeast dipping faults, Ogle (1953) interpreted a tight, overturned isoclinal syncline developed in Wildcat sediments. South of and subparallel to the Little Salmon Fault, the mapped axis of the Wolverton syncline cuts across the northern edge of the Yager Creek terrace flight. Near Carlotta, this fold is asymmetric with its northern limb overturned (Ogle, 1953; Wagner, 1979) and may represent an example of fault propagation fold on the lower plate of the Little Salmon Fault.

---

[1] *Humboldt State University Master's thesis in preparation*

[2] *BASELINE Environmental Consulting, 101 H St., Petaluma, CA 94952*

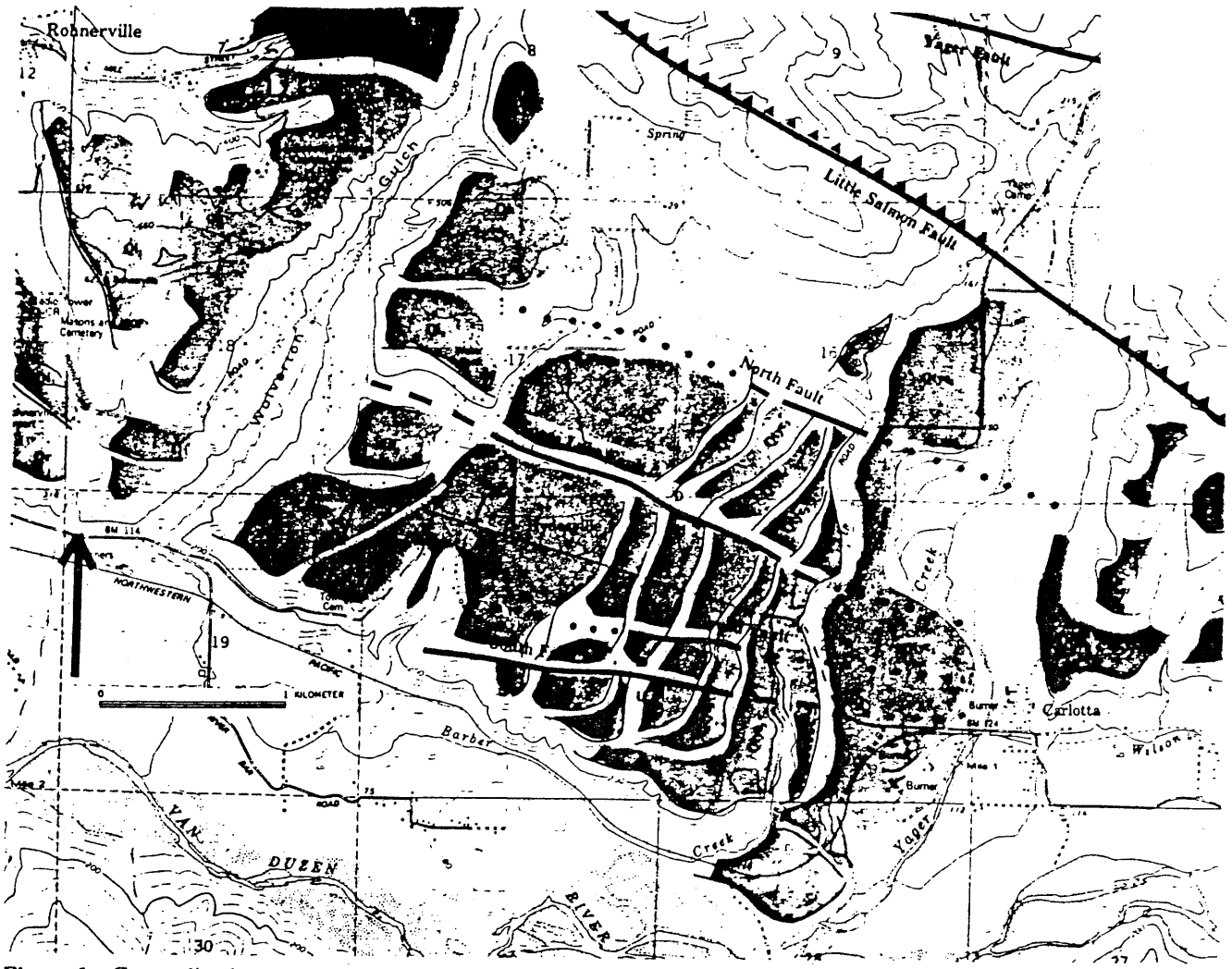

Figure 1. Generalized geomorphic map of the lower Yager Creek Valley showing principal drainages, faults and terrace remnants (dark shaded areas).

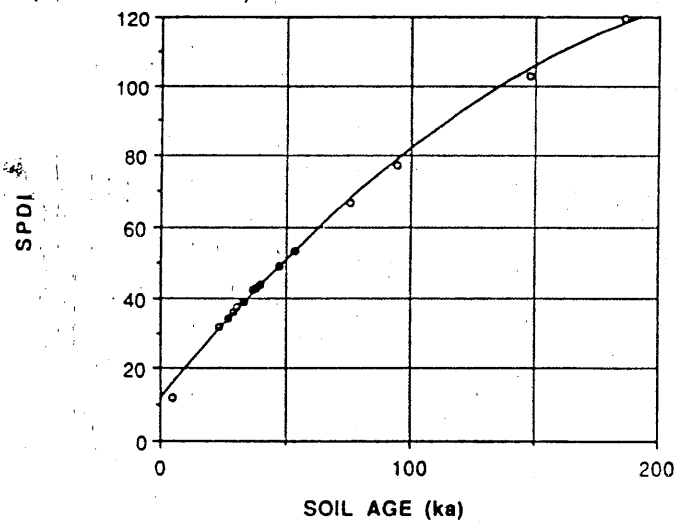

Figure 2. Soil age estimates for Yager Creek terrace soils. Age estimates are based on the soil profile development indices (SPDI) for the Yager Creek soils and SPDI-age relationships from the Merced soil chronosequence (Harden, 1982).

Further to the south, in the approximate center of the Yager Creek terrace flight, the Goose Lake Fault transects the terrace surfaces. The fault is expressed as a north facing scarp which displaces at least four of the Yager Creek terraces ($Qtyc_7$ through $Qtyc_3$). In an exploratory trench, the offset on the fault was identified along steeply north-dipping bedding planes in the Carlotta Formation. Late Pleistocene to Holocene displacement on the fault is indicated by faulting and warping of lacustrine sediments dated at 16,100±110 and 8,716±195 C14 years (WCC, 1980). A less well expressed and unnamed fault has been identified approximately 800 m north of and subparallel to the Goose Lake fault. The fault, called the "North" fault in this study, forms a north-facing fault scarp and mole track along the eastern 400 m of its expression on a relatively young Yager Creek terrace ($Qtyc_3$).

South of Highway 36 and north of the Van Duzen River bluffs, another unnamed fault transects the terrace surfaces (WCC, 1980). This fault (referred to in this study as the "South fault") is expressed by a well developed and well preserved fault scarp on the Yager Creek terraces south of Highway 36 in Hydesville. The north-facing scarp of this fault is erosionally modified but distinct on the Yager Creek terraces $Qtyc_7$ through $Qtyc_3$. A fourth fault, the Tread fault, is evidenced by displacement of the $Qtyc_5$ and $Qtyc_4$ terraces. This fault is subparallel and approximately 250 meters north of the South fault.

RELATIVE AGE ESTIMATION TECHNIQUES

Soil Profile Development

Similarities in topography, vegetation, climate and parent materials and the geomorphological chronology provided by the Yager Creek terrace flight encouraged the application of a soil chronosequence as a relative dating tool. Soil pits were excavated on each of the terrace surfaces of the Yager Creek terrace flight (Qtyc1 - Qtyc7) and on the older, higher terraces, Qi1, Qi2 and Qh. The field descriptions and particle size analysis of the soils formed on the terrace surfaces show a progressive increase in the degree of soil development for successively older terraces. The soils reflect an isomesic soil temperature regime, a udic soil moisture regime and the characteristics of the fine-grained (silt loam) fluvial overbank deposits on which the soils have developed. The soils progress from inceptiols on the younger terrace surfaces to ultisols on the older terraces.

The degree of soil profile development for each terrace was defined using the "Soil Profile Development Index" (SPDI) (Harden, 1982). Soil age was estimated for the Yager Creek/ Van Duzen River terraces by comparison of the calculated SPDI of their surface soils to the SPDI - surface age relationships suggested by data gathered from terraces along the Merced River in central California (Harden, 1982). The results of a comparison of age calibrated soil chronosequences from four different climatic regimes (Harden and Taylor, 1983) suggest that the rate of soil development is primarily an age dependent process. Although there are significant differences in the climates, vegetation and parent materials for these two areas, the Merced River data presents a calibrated chronosequence within the broadly defined Mediterranean climate of California. The SPDI values calculated for the Yager Creek soils and soil age estimates based on the Merced chronosequence are presented in Figure 2.

Terrace Surface Uplift and Attitudinal Spacing

The flight of well-expressed terraces on the middle and south structural blocks of the lower Yager Creek valley record seven major terrace formation episodes. A terrace riser identified on the middle block below the Qr terrace tread identifies an eighth and initial incision of the Yager Creek channel. The number of prominent terrace formation events recorded on the middle structural block coincides with the number of high sea level stands in the last 83 Ka. On the basis of soil development, the relative age estimates for the Yager Creek terraces suggest that a reasonable correlation can be made between the timing of fluvial terrace formation events and high sea level stands. Making the assumption that terrace formation is nearly coincident with high sea level stand ages, the approximate tectonic uplift rate can be estimated by the attitudinal spacing of the fluvial terraces. In Figure 3, the height of the terrace surfaces above Yager Creek in each structural block is plotted against time, assigning high stand ages to terrace surfaces. Regression analysis of the data plotted in this manner show strong correlation between high sea level stand ages and the altitudinal position of the terraces above Yager Creek. The slopes of the regression lines can be interpreted as the uplift rate of the structural blocks of the terrace flight. The uplift

rate (0.8 to 1.2mm/yr) is comparable to estimates of uplift rate determined for marine terraces on the coast at Centerville Beach 25 km west of the study area.

Comparison of Soil Development and Altitudinal Spacing Age Estimates

The geomorphic chronology described by the Yager Creek - Van Duzen River terrace complex supports the temporal trends identified by the relative age estimating techniques. The increasing age of the terraces is documented by increasing soil development of the surface soils and the altitudinal spacing of the terrace surfaces. Plotting terrace age as estimated by the degree of soil development ("soil age") against terrace age determined by attitudinal spacing ("uplift age") indicates correlation between the results of these two age estimating techniques (Figure 4). A group of data points plot below the regression line, reducing the strength of the correlation. These data points represent soil ages calculated from soil profiles (TP-5, TP-8, TP-9, TP-12) in which soil development extended beneath the contact between fine grained overbank deposits and cobbly channel deposits. The anomolously young soil ages for these profiles are an apparent artifact of the effective reduction of soil development properties caused by removal of translocated clay from the profiles.

FAULT DISPLACEMENTS AND INFERRED SLIP RATES

The age estimate techniques provide an opportunity to evaluate the slip rates for the South and Goose Lake faults which transect the Yager Creek terrace flight. Poor preservation of the terraces north of the North fault precludes determination of faulting activity on the North and Tread faults using the geomorphic analysis presented in this study. The plots in Figure 3 demonstrate that whereas uplift of the entire area has occurred, slip along the east-west trending faults can be documented. Observable offset across the "South" and Goose Lake Faults indicates that the uplift rate of the terraces varies between the "south", "middle" and "north" structural blocks of the terrace flight defined by these faults.

The altitudinal spacing analysis indicates the terrace flight uplifted at progressively higher rates southward across each of the faults. The difference in uplift rates across the "South" and Goose Lake Faults is approximately 0.2 mm/yr with the uplift rate being higher on the southern side of the faults. This variable uplift defines long term slip rates on the faults.

Terrace tread offsets measured from topographic profiles of the Yager Creek terraces provide an estimate of the total amount of offset that has occurred since each terrace was abandoned by a stream incision event (Figure 5). The difference between the amount of offset recorded on adjacent terrace treads indicates the amount of offset that occurred between the timing of the incision events. The slope of the trend between each terrace formation event documents that the slip rate on these faults has varied between <0.1 mm/yr to 0.4 mm/yr. The upper limit of this range appears to characterize a periods of increased activity on both the South faults during the occupation of $Qtyc_4$ and $Qtyc_5$ (64 to 47 ka) and on the Goose Lake fault between 64 to 76 ka and 57 to 47 ka. The initiation of faulting apparently began and terminated earlier on the Goose Lake fault compared to the South Fault. The apparent lack of fault offset on terraces younger than 47 ka along the Goose Lake fault and 40 ka along the South fault may indicate reduced fault activity. Alternatively, the low estimated slip rates and rapid geomorphic processes within the area (including floodplain deposition and scarp degradation) may combine to obscure surface expression of faulting on the younger terrace surfaces.

DISCUSSION AND CONCLUSIONS

Mechanism and Timing of Terrace Formation

The estimates of relative age of the Yager Creek terrace surfaces infer that terrace formation events are in phase with climatic maxima. Consideration of the possible influences on channel stability suggests that, the response of the streams to hydrologic conditions caused by climatic change is the most significant control on channel incision. Whereas climatic change appears to be the primary control on terrace formation, the active tectonic uplift of the area is responsible for preservation of the terrace surfaces. The inference that stream incision and abandonment occur during climatic maxima is supported by a hydrologic model for stream response to climatic change.

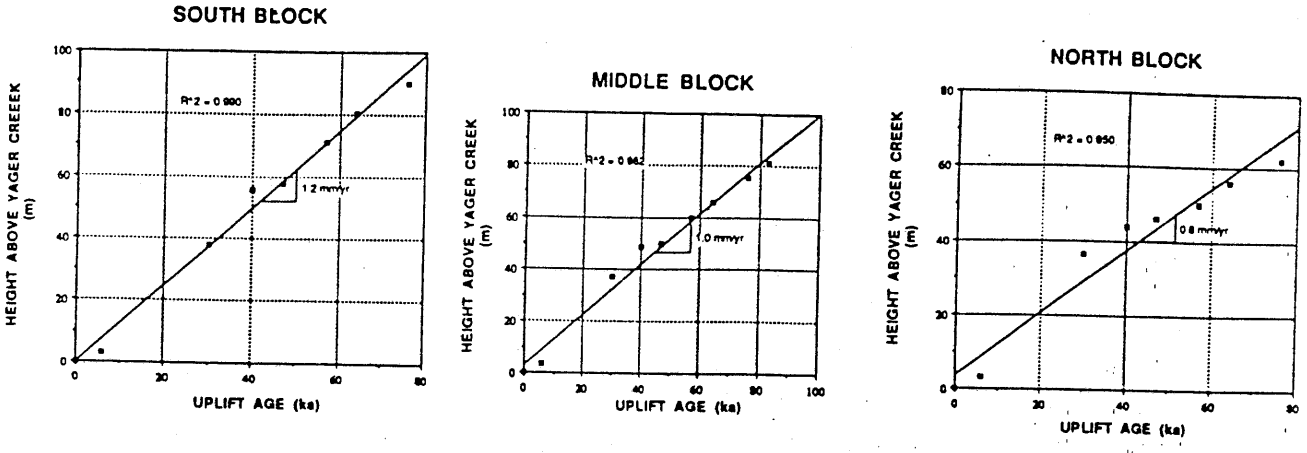

Figure 3. Altitudinal spacing of Yager Creek terraces. The heights of terrace treads above the active channel of Yager Creek are plotted against the age of Quaternary high sea level stands (Chappell, 1983). Differences in the inferred uplift rate for each structural block of the terrace flight indicate slip rates for the South and Goose Lake faults which define the blocks.

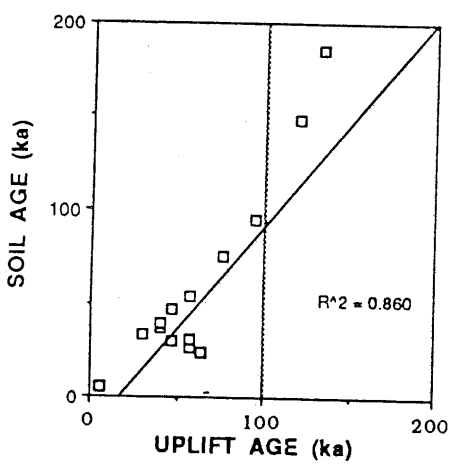

Figure 4. Comparison of age estimation techniques applied in the Yager Creek terrace study. Soil age estimated by comparison to SPDI - age relationships from the Merced chronosequence (Hardin, 1982).

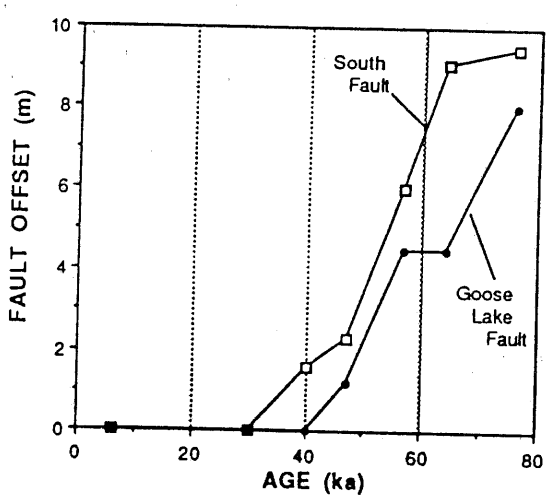

Figure 5. Terrace tread offset on Yager Creek terraces along the south and Goose Lake faults. The ages of terrace surfaces are estimated for $Qtyc_1$ through $Qtyc_7$, by comparison of soil age and altitudinal spacing analysis.

The model is contingent on qualified assumptions which connect thresholds of hillslope stability to the response of streams to changes in sediment load. Evaluation of Quaternary climatic change in coastal Pacific Northwest area suggest that climatic minima were characterized by decreased temperature, increased precipitation and intensification of storms (Johnson, 1977). The intensification of storms during the transition periods from climatic minima to climatic maxima (and presumably throughout the minima) may have caused increased frequency of slope failures and aggradation of stream channels in the Pacific Northwest (Reneau and others, 1990). As climate ameliorated toward the climatic maximum, relative slope stability and decreased sediment load delivery to the streams would promote the potential for stream incision. The tendency toward incision would be exacerbated by the continued tectonic uplift of the region.

Structural and Tectonic Interpretation

The orientation of the structures in the area and the sense of displacement of the North, Goose Lake, Tread and South Faults supports the interpretation of these structures as shallow-seated, active, flexural slip faults formed on the north limb of an uplifted overturned syncline. The syncline may represent a fault-bend fold developed on the lower plate of the Little Salmon Fault, the major active regional thrust fault. The axis of the proposed syncline is coincident with the axis of the eastern end of the Eel River Synclinorium.

Analysis of recent seismicity (McPherson, 1988) and geodetic data suggest that the current state of stress in the region of the southern end of the Cascadia subduction zone is northeast- southwest compression. The faults with the lower Yager Creek valley are oriented nearly perpendicular to the direction of maximum compression. The possibility of continued strain accumulation and release on the structures within the study area is consistent with the neotectonics of the region.

ACKNOWLEDGEMENTS

Sincere thanks are extended to the powers responsible for the beauty and wonder of the tectonic geomorphology in the region of the MTJ. Respect is due to previous workers, especially B. A. Ogle and C. R. Wagner, for providing the geologic framework used to focus this study. Special thanks to Gary Carver, Bud Burke, Frank Bickner, Greg Vick, and Bob Busch for insightful input throughout the study.

REFERENCES CITED

Harden, J. W., 1982. A quantitative index of soil development from field descriptions: examples from a chronosequence in central California, Geoderma, 28: p.1-28.

Harden, J. W., and Taylor, E. M., 1983. A quantitative comparison of soil development in four different climates: Quat. Research, v. 20, p. 342-359.

Johnson, D. L., 1977. The late Quaternary climate of coastal California: evidence for an Ice Age refugium, Quaternary Research, V. 8, p. 154-179.

Kelsey, H. M., and Carver, G. A., 1988. Late Neogene and Quaternary tectonics associated with the northward growth of the San Andreas transform fault, northern California: Journ. of Geophysical Research, v. 93, n. B5, p. 4794-4819.

McPherson, R., 1988. Seismicity of the Humboldt Bay Area, unpublished master's thesis, Humboldt State University.

Ogle, B. A., 1953. Geology of the Eel River valley area, Humboldt County, California, Bull. Calif. Div. Mines Geol., 164, 128pp..

Reneau, S. L., Dietrich, W. E., Donahue, D. J., Jull, A. J., and Rubin, M., 1990. Late Quaternary history of colluvial deposition and erosion in hollows, central California Coast Range: Geological Society of America Bulletin, v. 102, p. 969-982.

Wagner, C. R., 1979. Unpublished geologic map of the Hydesville 7.5' quadrangle.

Woodward-Clyde Consultants (WCC), 1980. Evaluation of the potential for resolving the geologic and seismic issues at the Humboldt Bay power plant unit no.3, Appendices A and B, San Francisco, CA.

THE LATE HOLOCENE SUBSIDENCE STRATIGRAPHY IN THE EEL RIVER SYNCLINE, NORTHERN CALIFORNIA

LI, WENHAO

Deptartment of Geology, Humboldt State University
Arcata, Ca 95521

ABSTRACT

Late Holocene stratigraphy, interpreted to represent at least 5 cycles of intertidal sedimentation punctuated by sudden episodes of submergence, have been investigated in the lower part of the Eel River Delta, about 15 km south of Humboldt Bay in northern California. The sediments consist of estuarine muds that grade upward into peats muds, peats containing salt marsh plant fossils, and at two locations weak soils containing rooted stumps of spruce trees. The estuarine muds contain foraminiferid associations dominated by the lower intertidal *Miliammina fusca*. These muds are in sharp contact with underlying salt marsh peats that contain high marsh foraminiferid associations, dominated by *Trochammia macrenscens*. The change in foraminiferid associations occurs across a stratigraphic distance of no more than 7 mm at the contact between the peats and overlying muds, reflecting sudden changes from upper intertidal to lower intertidal depositional environments. Convectional C-14 age estimates for the fossil trees and marsh peats indicate ages for the sudden submergence episodes of about 300, 800, 1200, 1500 and 2000 ybp (calendar years before present). We interpret the most likely cause for the sudden changes in sedimentation and foraminiferid association during the late Holocene to be coseismic subsidence resulting from earthquakes on the southern part of the Cascadia subduction zone.

INTRODUCTION

The Eel River delta is located in the axis of the Eel River syncline (Ogle 1953). This syncline is one of the largest broad open folds in a group of NW-SE trending thrust faults and folds associated with the southern part of the Cascadia subduction zone (Carver 1988; Clarke 1990). Arcata Bay and South Bay and parts of Humboldt Bay, are situated in synclines similar to the Eel River syncline. Investigations of the buried salt marshes in Humboldt Bay (Vick 1988; Valentine personal communication 1991) have revealed a sequence of at least 5 buried marsh surfaces interpreted to reflect coseismic subsidence of the axis of these synclines in the last 1700 ybp. Age estimates for these buried peat layers, based on multiple C-14 analyses, are about 300, 800, 1100, 1300, and 1700 ybp. Several older layers in Humboldt Bay are presently being studied.

The physical stratigraphy, biostratigraphy, and radiocarbon ages for the buried peats and forests in the Eel River delta are similar to those found in Humboldt Bay. The buried marsh peat sequences in Humboldt Bay, and similar buried peat and mud sequences in bays along the Oregon and Washington coasts (Atwater 1987, 1988; Darienzo 1988, 1990; Peterson 1989; Grant 1987, 1988; Nelson 1988, 1991), are all interpreted to result from coseismic and interseismic elevation changes associated with the seismic cycles of the Cascadia subduction zone. In the coastal regions of Alaska and Chile, very similar intertidal marsh sequences were also identified to result from the historic great subduction Zone earthquakes. The preliminary results of this reconnaissance study of the late Holocene sediments in the Eel River syncline suggest the fold has deformed during the several previous subduction zone earthquakes.

In this study, hand auguring, bank exposures, and vibracore sections were used in the investigation of the shallow stratigraphy of the Eel River delta. About 50 sites were sampled by hand auguring, 12 bank exposures were studied along the Eel River, Salt River and their tributaries, and three vibracore sections were obtained from either side of the Eel River.

RESULTS

Five sedimentation cycles were found in cores of the uppermost about 4 m of delta sediments. Each cycle consists of, from bottom to top; peat or soil in sharp contact with o sand (locally) and mud, which grades upward into peaty mud and then peat or soil. locations, the buried soil contains rooted spruce trees. They are interpreted to reflect a lon of stability or gradual uplift followed by sudden subsidence. In each cycle the sudden sul resulted in submergence of the delta surface and burial of subaerial plant communities intertidal muds. The total of the sudden subsidence and the gradual elevation adjustmen followed resulted in about 0.5-2 meters of net subsidence in each event.

The five sudden subsidence events are strongly supported by foraminiferal evide overlying estuarine muds contain the lower intertidal foraminiferid associations domi *Miliammina fusca*. The underlying salt marsh peats contain high marsh foraminiferid ass dominated by *Trochammia macrenscens*. The change in foraminiferid associations occurs stratigraphic distance of no more than 7 mm, constrained by the sampling interval. Fig. 1 shows that the distribution of the percent foraminiferid associations reflect the sudden change of depositional environment interpreted from the stratigraphic column (ER-VCC).

The five subsidence events have been dated by radiocarbon analysis of eighteen samples collected from buried peats and stumps. The uppermost event is represented by the first buried peat layer in the vibracores of the south section and the buried weak soil with rooted stumps exposed at two locations along both banks of the Eel River near Cock Robin Island. Dates for this event average about 300 ybp. Dates from the second to fifth buried surfaces, represented across much of the outer delta by salt marsh peats buried beneath intertidal muds, produced age estimates of 800, 1200, 1500 and 2000 ybp respectively (see fig. 1, for the stratigraphic positions of the buried peat or soil layers).

DISCUSSION

One of the principal types of geological evidence of changes in the elevation of the ground in coastal areas is the stratigraphy that results from submergence of supertidal vegetated ground surfaces (Atwater 1987). In stratigraphic sections, these surfaces are recognized by organic rich layers containing plant fossils and microfossils indicative of environments above the elevation of tidal influence. When such organic rich layers, generally peaty mud or peat, are found buried beneath intertidal or subtidal mud, submergence is indicated.

Four major processes can generate the buried vegetation layer reflecting submergence. They are: 1) changes (rise) of eustatic sea level, 2) sediment compaction, 3) river channel migration, or rapidly deposited big floods or alluvial fans, and 4) coseismic and/or interseismic subsidence and/or uplift. Buried peat sequences resulting from coseismic subsidence are clearly different from those formed by interseismic or non-tectonic processes in the type of sedimentary structures, thickness, distribution, and development of the sequences. Sudden submergence typical of coseismic deformation results in abrupt and sharp contacts between the overlying mud or sand and the buried organic layer. The submergence of some vegetation layers in Eel River delta, as Nelson (1991) found in Oregon, seems too widespread, too large, and too sudden to be attributed to any process but coseismic subsidence.

The sudden change of foraminiferid associations further supports that the burial of the salt marsh peats was the result of coseismic subsidence. Because foraminifera live only in salt water, fresh water can be excluded as a cause of the burials. The time over which the foraminiferid associations changed, represented by Less than 7 mm of sediment, was probably very short, perhaps only a few months, because Eel River has the highest suspended sediment in the United State. Only a coseismic subsidence event could cause such a rapidly change in relative sea level.

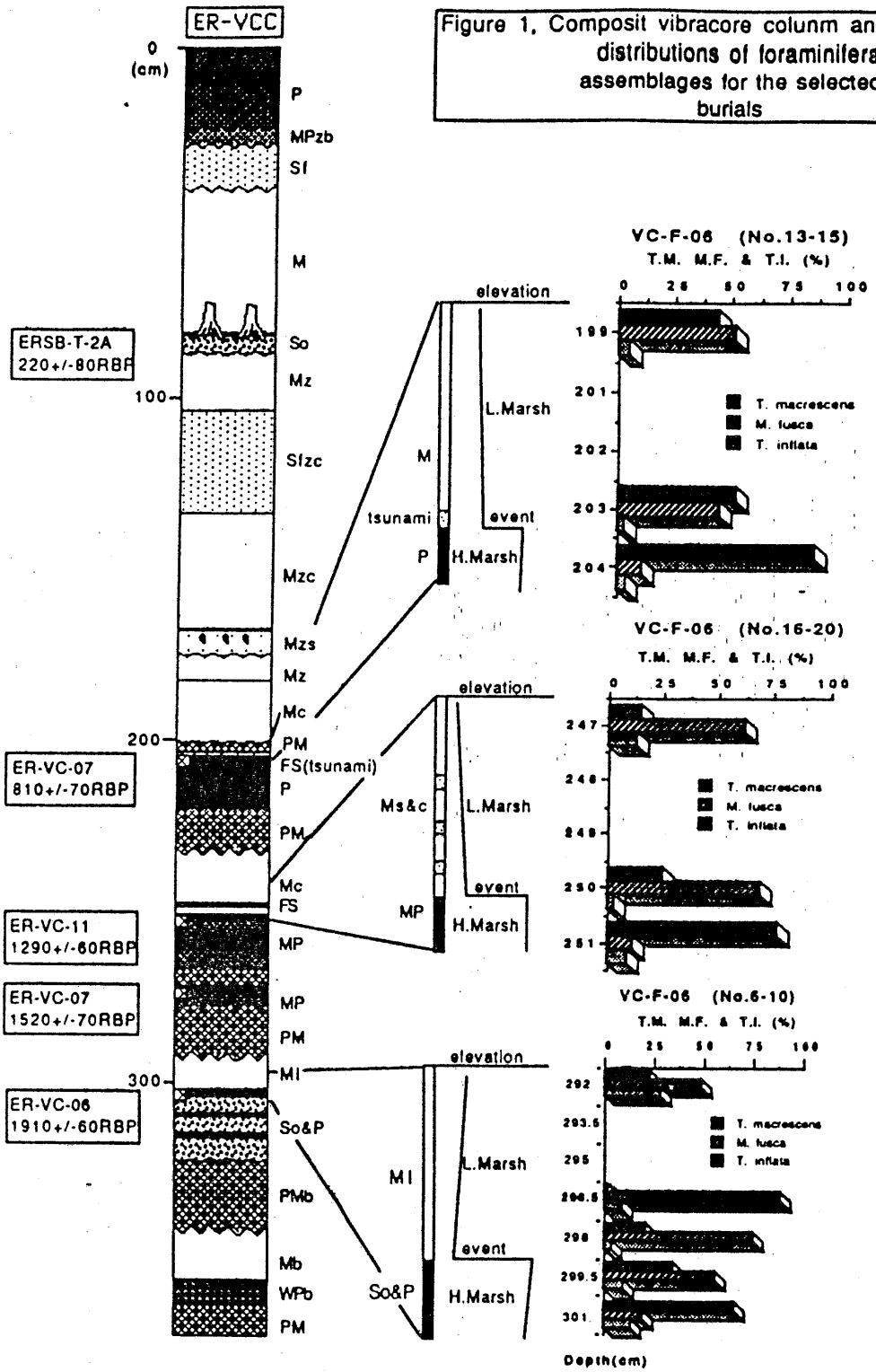

Figure 1. Composit vibracore colunm and distributions of foraminiferal assemblages for the selected burials

The ages and depths of the buried peat layers at several sites allow determination of net subsidence rates for the Eel River delta. Radiocarbon age for the second buried peat, based on two analyses in core ER-VC-06 and ER-VC-07, is 800+/-70 RCYBP (radiocarbon year before present). This peat is generally about 1.2 to 2.2 meters below the present ground surface and about the same elevation below present high tide level, yielding a net subsidence rate of 1.5-2.75 mm/yr. The third buried peat layer, located about 1.8-2.8 meters below the surface, was dated at 1200+/-80 RCYBP, yielding an average subsidence rate of 1.5-2.3 mm/yr. The fourth buried peat layer is about 0.3-0.5 m below the third peat layer and was dated at about 1500+/-70 RCYBP, yielding a subsidence rate of 1.4-2.2 mm/yr. The fifth peat layer found at about 300 cm below the ground surface, dates to about 2000+/-80 RCYBP, resulting in an average subsidence rate of 1.5 mm/yr (Fig. 1).

CONCLUSIONS

1. The Eel River delta has been an area of net subsidence in the late Holocene. Average subsidence rates have been about 1-3 mm/yr.

2. Most or all of the subsidence occurred suddenly during five or more events. Gradual elevation changes between these sudden subsidence events resulted in less than 1-2 meters of net permanent subsidence.

3. C-14 ages for the five events interpreted to represent sudden subsidence are about 300, 800, 1200, 1500 and 2000 ybp.

4. The sudden subsidence events were probably associated with coseismic slip on the southern part of the Cascadia subduction zone.

5. The sudden changes of foraminiferid associations across the upper sharp contact of the buried peat layers adds to evidence of coseismic subsidence by indicating sudden change of the depositional environment.

REFERENCE

Atwater, B. F.,1987, Evidence for great Holocene earthquakes along the outer coast of Washington State: Science, v.236, p942-944.

Atwater, B. F.,1988, Buried Holocene wetlands along the JohnsRiver, southwest Washington: in Holocene Subduction in the Pacific Northwest. A symposium sponsored by the Quaternary Research Center, University of Washington, Seattle.

Carver, G. A.,1987, Late Cenozoic tectonics of the Eel River basin region, coastal northern California, in Tectonics, Sedimentation and Evolution of the Eel River and other Coastal basins of Northern California, Sau Joaquin Geological Society Bakersfield, California.

Carver, G. A. and R. M. Burke,1988, Late Holocene paleoseismicity of the southern end of the Cascadia subduction zone. EOS, v.68(44), p1240.

Clarke, S. H.,1990, Geological structures, Northern California continental margin. The U. S. Geological Survey.

Clarke, S. H. and G. A. Carver,1991, Late Holocene tectonic and paleoseismicity, sorthern Cascadia subduction zone. GSA Abstracts with Programs, v.23(2).

Darienzo, M. E. and C. D. Peterson,1988, Episodic tectonic subsidence record in Late-Holocene salt marshes, Northwest Oregon. EOS, v.68(44), p1239.

Darienzo, M. E.,1989, Evidence for and implications of small-scale (<1m) tectonic subsidence in salt Marshes of Alsea Bay, Oregon, central Cascadia margin. EOS, v.69, p1331.

Darienzo, M. E. and C. D. Peterson,1990, Episodic tectonic subsidence of late Holocene salt marshes, northern Oregon coastal Cascadia margin. Tectonics, v.9(1), p1-22.

Grant, W. C. and D. D. Mclaren,1987, Evidence for Holocene subduction earthquakes along the Northern Oregon coast. EOS, v.68(44), p1239.

Grant, W. C. (1988). Evidence for late Holocene subduction earthquakes recorded in tidal marsh deposits along the Nehalem and Salmon River, Northern Oregon. Holocene Subduction in the Pacific Northwest. A symposium sponsored by the Quaternary Research Center, University of Washington, Seattle.

Nelson, A. R.,1988, Implications of late Holocene salt-marsh stratigraphy for great earthquake recurrence along the coast of south-central Oregon. in Proceedings of Conference XLII. U.S. Geological Survey Open-File Report 88-541,. p149-151.

Nelson, A. R. and S. F. Personius,1991, Great earthquake potential in Oregon and Washington, in An overview of recent coastal geologic studies and possible segmentation of the central Cascadia subduction zone. USGS Open File #91-441-A.

Ogle, B. A.,1953, Geology of Eel River Valley area, Humboldt County, California. California Div. Mines.

Peterson, C. D. and M. E. Darienzo,1989, Potential evidence of subduction zone tectonics from stacked peat horizons in late Pleistocene coastal terraces of the northern Cascadia margin. EOS, v.69,p1331.

Scott, D. B. and F. S. Medioli,1980, Quantitative studies of marsh foraminiferal distributions in Nova Scotia, implications for sea level studies. Cushman Foundation for Foraminiferal Research.

Vick, G. S., 1989, Late Holocene paleoseismicity and relative sea level changes of the Mad River Slough, Northern Humboldt Bay, CA. Humboldt University, Arcata, CA.

An Investigation of Active Tectonics Along the Southern Limb of the Eel River Syncline

By: Mark Verhey [1,2]

Abstract

The altitudinal spacing of late Quaternary fluvial terraces along the southern limb of the Eel River syncline in coastal northern California provides a record of recent tectonic movements at the southern margin of the Cascadia subduction zone. I examined soils formed on Eel River terraces ranging from recent to greater than 100 ka. Based on soil morphology, I recognized three terraces. Mapping and reconstruction of the longitudinal profile of these terraces shows a general increase in elevation to the north, indicating a northward tilting or southward increase in the rate of uplift. This pattern is interrupted near the confluence of the Eel and Van Duzen Rivers by faulting and folding associated with the east-west-trending Grizzly Bluff anticline.

Introduction

The Eel River syncline (ERS) is a major east-west-trending structural depression in coastal northern California that contains more than 3000 m of late Neogene sediments (Ingle, 1976). These deposits form the southern margin of a much larger basin, the northwest-trending Eel River basin, which lies offshore for most of its length, extending into southern Oregon (Clarke, 1992). Rapid uplift of the southern basin margin has exposed nearly the entire basin fill and has deformed the overlying flight of late Quaternary terraces.

I mapped and reconstructed the longitudinal profiles of Eel River terraces along the southern limb of the ERS by excavating, sampling, and describing 10 soil profiles. I also surveyed the profiles and relative elevations of terrace treads to accurately establish terrace spacing relationships. All soil sites are on gently sloping surfaces (1-4 degrees), are moderately well-drained, have similar vegetation (perennial grasses), and contain relatively homogeneous parent material.

Background and Geologic Setting

The southern limb of the ERS is located in a tectonically dynamic area between two disparate tectonic regimes. To the north, late Quaternary deformation is dominated by

[1] HSU Geology Dept, Arcata, CA. 95521
masters thesis in prep

[2] Busch Geotechnical Consultants, Arcata CA. 95521

northwest-trending, northeast-dipping thrust faults and folds that have accommodated as much as 8 km of crustal shortening (Carver, Burke, and Kelsey, 1986). To the south, late Quaternary deformation is complicated by the movements of three lithospheric plates, the Pacific, Gorda, and North American plates, which meet at the Mendocino Triple Junction less than 30 km south of the ERS.

The late Miocene to Pleistocene Wildcat Group (Ogle, 1953) is well exposed along the southern limb of the ERS and consists of five formations (Figure 1). Lower Wildcat sediments (Pullen, Eel River, and Rio Dell Formations) consist primarily of mudstones and siltstones deposited at depths as great as 2000 m (Ingle, 1976). These marine sediments are succeeded by a shallow marine sandstone of the Scotia Bluff Formation, and chiefly fluvial conglomerate and sandstone of the Carlotta Formation. Unconformably overlying the Wildcat are nearshore, fluvial, lagoon, and bay deposits mapped by Ogle (1953) as the Hookton Formation. Quaternary terraces cut into the eroded surface of the Wildcat are faulted and folded, so attest to ongoing deformation.

Logs of gas wells on the northern side of the valley show that the Table Bluff and Tompkins Hill anticlines (Figure 2) are fault propagation folds formed above large thrust faults (Carver, 1987). The topography of the terraces on these folds is a subdued expression of the structure. To the northeast, trench excavations across the Little Salmon fault show repeated displacement of Holocene sediments. Measured vertical displacement of early Pleistocene sediments across the Little Salmon fault indicate a late Quaternary slip rate of about 5-7 mm/yr (Clarke and Carver, 1992). Bounding the ERS to the south is the False Cape shear zone (Ogle, 1953), marked by the east-west-trending Russ fault.

Terrace Formation and Longitudinal Profile

Based on soil morphology, I defined three ages of terraces that I mapped along the Eel River from east of Ferndale to Rio Dell. The highest terrace in the flight is the large and widespread Rohnerville Formation (Ogle, 1953). Below the Rohnerville terrace is the Weymouth terrace (informally named), which occurs only at Rio Dell and in the foothills east of Ferndale. The lowest terraces are located on the Eel River plain and the inside of meander bends and do not have differentiated soils, although there are at least three distinct elevations. Absolute ages of terraces are unknown due to an absence of datable material. However, if the timing of terrace formation is coincident with warm-dry climatic cycles (see O'Dea, this guidebook), then the Rohnerville terrace is probably equivalent to oxygen isotope stage 5e, or about 120 ka.

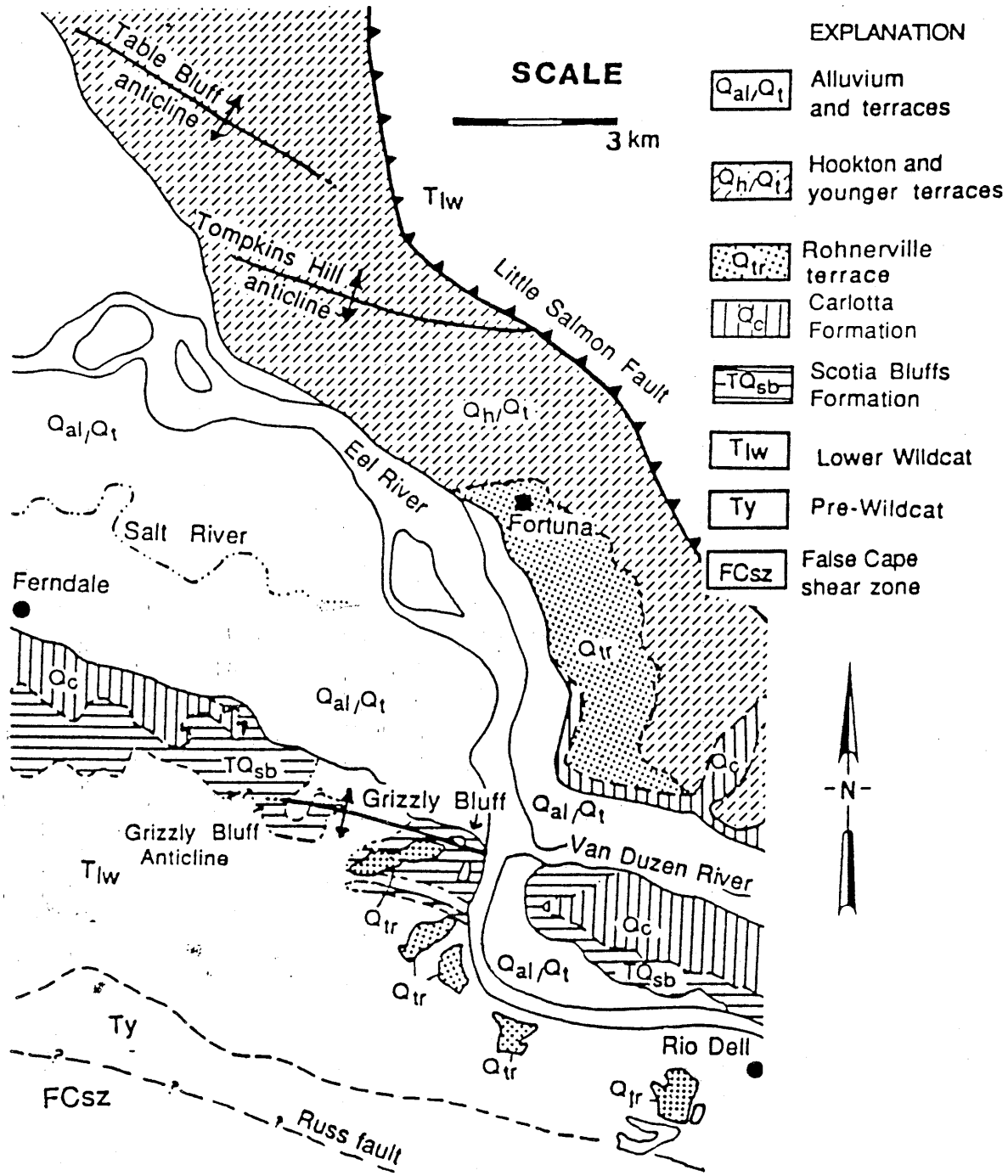

Figure 1. Generalized geologic map of the Eel River valley showing major structures, the location of Eel River terraces, and geographic locations described in text (modified from Ogle, 1953; Wagner, 1982). Grizzly Bluff anticline is shown at a larger scale in figure 2.

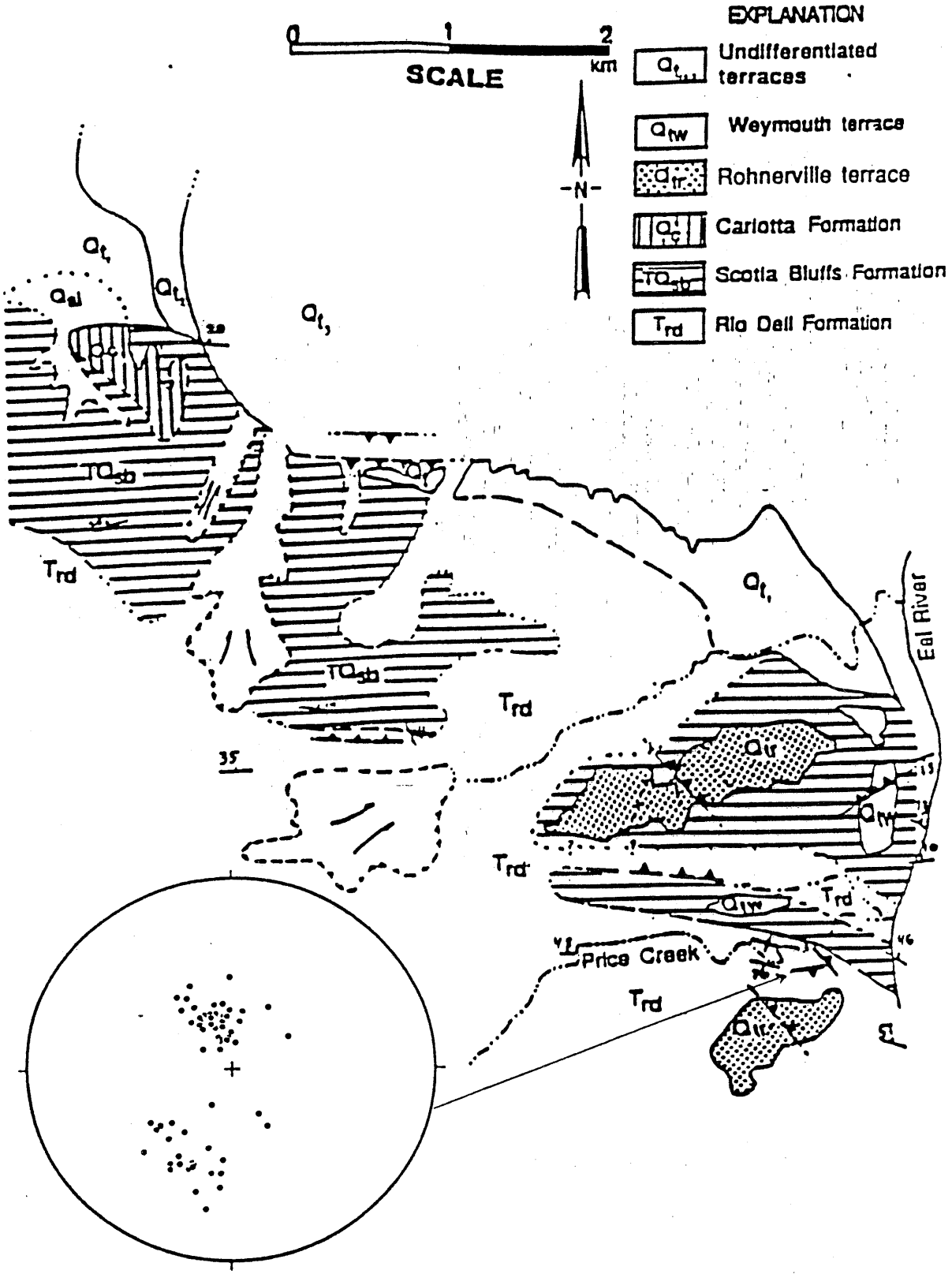

Figure 2. Geologic map of Grizzly Bluff anticline and stereoplot of poles of meso-scale faults exposed at Price Creek.

The longitudinal profile of the Rohnerville terrace indicates a pattern of a northward decrease in elevation. At Rio Dell the Rohnerville terrace is located at 213 m above sea level. Less than one km to the north it is as low as 100 m. Near the confluence of the Eel and Van Duzen Rivers the flight of terraces is faulted and folded over the Grizzly Bluff anticline. Across Price Creek the Rohnerville terrace is displaced down to the south by 70 m, giving the group of faults to the north a collective late Quaternary slip rate of about 1.3 mm/yr (assuming 35 degrees dip of fault plane and 120 ka age for Rohnerville terrace).

Style of Faulting and Surface Deformation

Thrust faults along the southern limb of the ERS are best expressed in the massive, cliff-forming sandstone of the Scotia Bluff Formation and where the faults intersect a terrace. Two roads that transect the eastern side of Grizzly Bluff allow access to excellent exposures of some of the thrusts that deform the overlying terraces. The surface deformation of the Weymouth terrace at Grizzly Bluff consists of south-facing scarps trending about N50E, and a south dip of the terrace treads. The outcrop expression of the faults is widely spaced faults (about 10 m apart) oriented at about N50E, 40 NW, separating unfaulted blocks of sandstone and conglomerate. Tracing a conglomerate bed through the zone of faulting indicates that bedding locally dips south, coincident with the south dip of the overlying terrace, indicating the youthfulness of the deformation.

Displacement at Price Creek has occurred as small amounts of slip (<50 cm) on many conjugate thrust faults (Figure 2) that form a distinctive rhombohedron pattern in outcrop across a zone at least 100 m wide. The dip of Pleistocene strata in the fault zone changes from nearly horizontal north of the fault to vertical and steeply south-dipping within the zone of faulting. The symmetry of the conjugate faults indicates a N10E direction of shortening.

Timing of deformation

Two outcrops, one at Price Creek and the other at Grizzly Bluff, support the contention that deformation of the Grizzly Bluff anticline began greater than 1 Ma ago. A bank exposure at Price Creek (Figure 3) reveals angular blocks of siltstone, probably derived from the older Rio Dell Formation, incorporated into the younger Scotia Bluff Formation. At Grizzly Bluff, a large thrust fault (0.33 m- thick gouge) displaces near-horizontal massive sands, but is truncated by a south-dipping conglomerate. The fault extends into the conglomerate and produces a small amount of displacement, but not as much as would be expected according to the thickness of the gouge, suggesting that

significant slip occurred prior to erosion of the surface, deposition of the conglomerate, and continued displacement.

These exposures indicate that deformation and growth of the Grizzly Bluff anticline began during deposition of the Scotia Bluff Formation. The age of the Scotia Bluff Formation at Price Creek is constrained by the Rio Dell ash, a 1.2-1.3 Ma ash bed found in the upper Rio Dell Formation at Centerville Beach, but in the middle of the Carlotta Formation at Scotia Bluffs, about 10 miles to the east (Wagner, 1980).

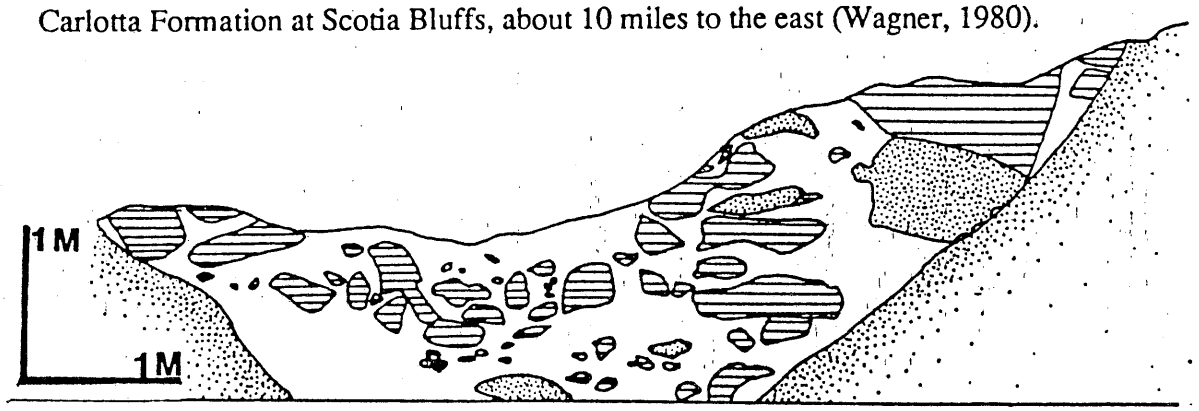

Figure 3. Line drawing of bank exposure in Price Creek with blocks of siltstone (line pattern), and sandstone (stippled pattern) in a matrix of intact shells and medium sand (area without pattern). The surrounding material is massive, fine-grained Scotia Bluff sandstone.

Summary

The southern limb of the ERS is deforming by nearly north-south directed crustal shortening. Differential rates of uplift along the southern limb result in a general northward decrease in elevation of equivalent terrace treads. However, near the confluence of the Eel and Van Duzen Rivers, the Rohnerville and Weymouth terraces are faulted and folded over an east-west-trending anticline located above previously unrecognized thrust faults. The youthfulness of this anticline is evidenced by a similar south dip of terrace treads and Pleistocene bedrock. Thrust faults exposed in bedrock below the terraces coincide in location, orientation, and sense of slip with the surface deformation, indicating that the topography of terrace treads is a subdued expression of the structure. The zone of faulting is more than 100 m wide and consists of many small faults, sometimes occurring as single traces, and other times as conjugate sets. Unconformities within the Scotia Bluff Formation at Grizzly Bluff and Price Creek indicate that the onset of deformation of the Grizzly Bluff anticline is greater than 1 Ma. However, most of the deformation must be recent because the Scotia Bluff Formation at Grizzly Bluff was only mildly folded prior to deposition of the Rohnerville terrace.

REFERENCES

Carver, G.A., R.M. Burke, and H.M. Kelsey, 1986, Late Quaternary Tectonics of Coastal California North of the Mendocino Triple Junction: EOS, vol. 67, no. 44, Nov. 4, 1986.

Carver, G.A., 1987, Late Cenozoic Tectonics of the Eel River Basin Region, Coastal Northern California: in Tectonics, Sedimentation and Evolution of the Eel River and Associated Coastal Basins of Northern California, eds. Schymiczek, H. and Suchsland, R., by San Joaquin Geological Society.

Clarke, S.H. Jr., 1992, Geology of the Eel River Basin and Adjacent Region: Implications for Late Cenezoic Tectonics of the Southern Cascadia Subduction zone and the Mendocino Triple Junction: AAPG Bull, v. 76, p. 199-224.

Clarke, S.H. Jr., and G.A. Carver, 1992, Late Holocene Tectonics and Paleoseismicity, Southern Cascadia Subduction Zone: Science, v. 255, pp 188-192.

Ingle, J.C., Jr., 1976, Late Neogene Paleobathymetry and Paleoenvironments of the Humboldt Basin, Northern California, in, Fritche, A.E., Terberst, H., and Wornardt, W. (eds.), The Neogene symposium. Soc. Econ. Paleont. Mineral., Pacific sec., pp 53-61.

Ogle, B.A., 1953, Geology of the Eel River Valley area, Humboldt County, California: Bull. Calif. Div. Mines, 164, 128 p.

Wagner, J.R., 1980, Summary of regional stratigraphy and geologic structure, in Evaluation of the potential for resolving the geologic and seismic issues at the Humboldt Bay Power Plant Unit no. 3, appendix A, Woodward-Clyde Consultants, Walnut Creek, California, pp A1-A73.

SOIL CHRONOSEQUENCE AND TECTONIC UPLIFT RATES OF FLUVIAL TERRACES NEAR GARBERVILLE, CALIFORNIA

by
Frank Bickner
LACO Associates

INTRODUCTION

Within the Northern California Coast Ranges, the geomorphology of the South Fork Eel River (SFER) has been effected by rapid tectonic uplift, eustatic sea level changes, climatic change and high sediment yields. As a result, complex sequences of Quaternary terraces are present along much of the river's length.

Using quantitative data based on weathering and soil development phenomena, a soil chronosequence has been developed on a well preserved flight of terraces at the Mitchell Ranch near Garberville, California (Figure 1). A soil chronosequence is the evaluation of the strength of soil development as a function of time in order to estimate the relative and numeric ages of the fluvial deposits and strath surfaces. This soil chronosequence provides a basis with which to correlate similar geomorphic surfaces elsewhere in northwestern California. Tentative ages of the terraces are based on relative soil development and a simplified constant incision/uplift rate model.

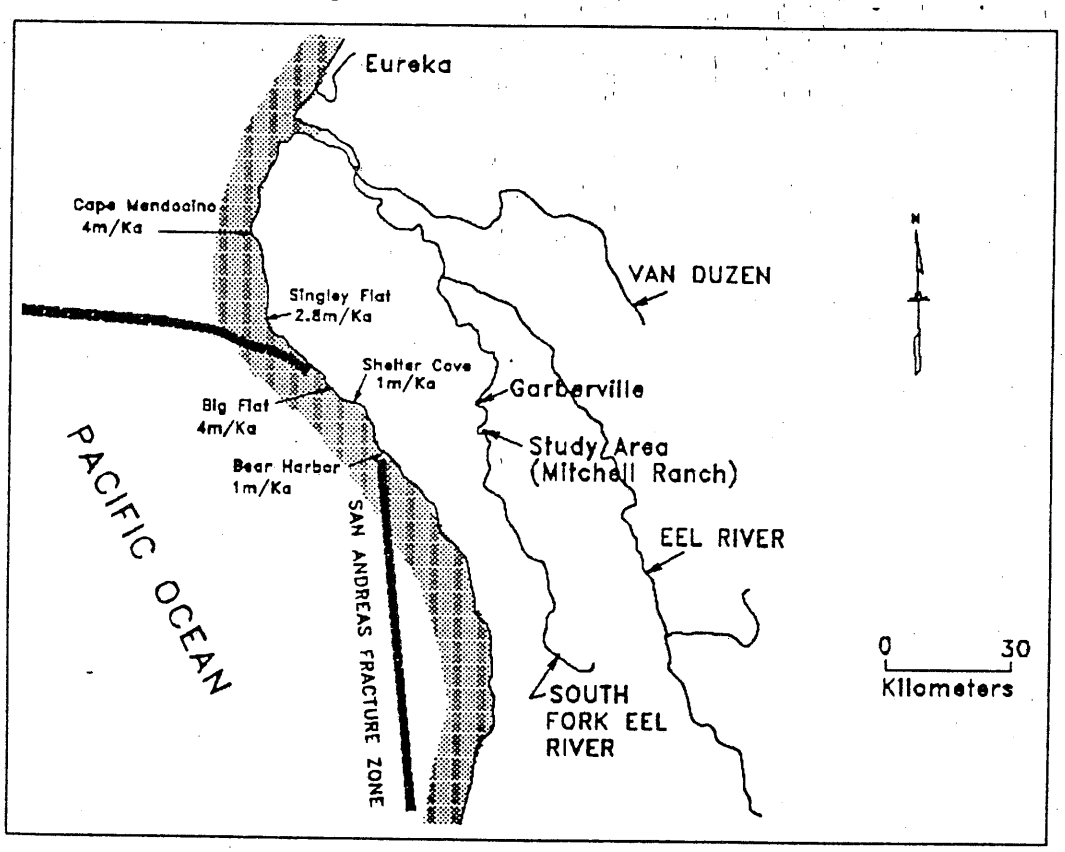

Figure 1. Location map, tectonic setting, and published rates of uplift in coastal northern California, near the Mitchell Ranch study area.

A nested terrace sequence of fourteen surfaces step upwards from the SFER at the Mitchell Ranch (Figure 2; Bickner, 1985). This sequence of terraces is well suited to the study and development of a soil chronosequence because: 1) the terrace surfaces are spatially distinct;

2) the alluvial parent material is compositionally similar; 3) the depositional stratigraphy for the terrace deposits is similar; 4) soils occur as surface soils and most have not had appreciable profile rejuvenation; 5) magnetic susceptibility of the terrace soils provides supporting evidence for the relative soil development ages and a tentative age of 104 Ka - 117 Ka (thousands of years before present); 6) the relative soil development and topographic data suggest that the terraces and soils can be grouped into age-classes.

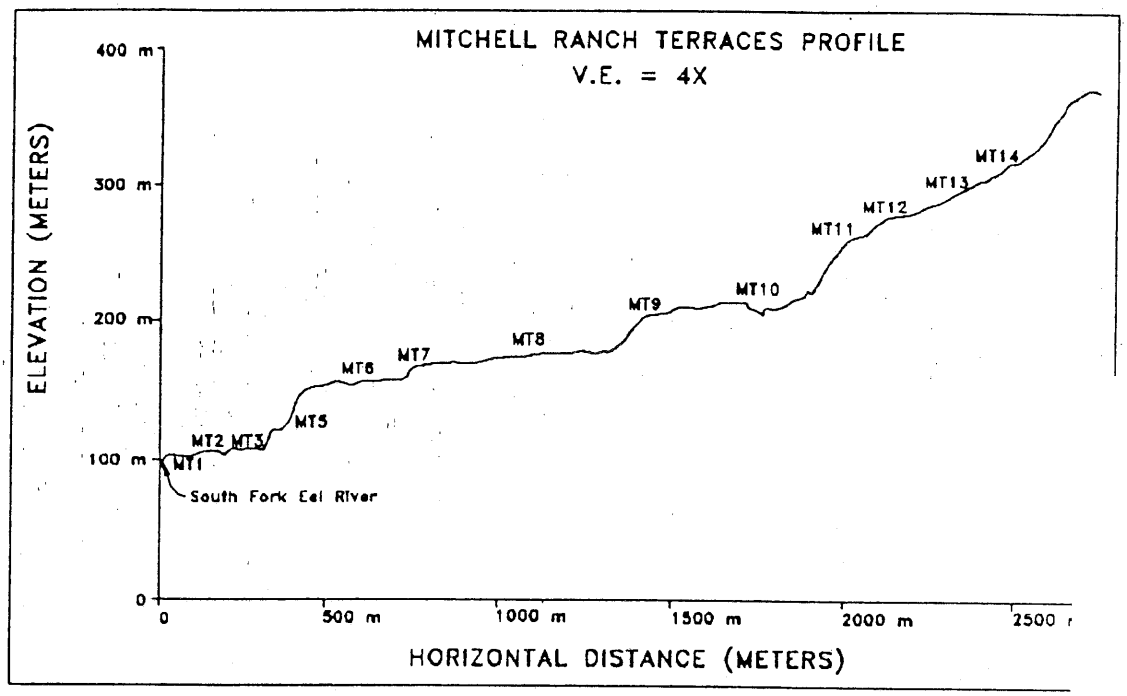

Figure 2. Cross sectional profile of Mitchell Ranch terracs.

The purposes of this study were to: 1) establish whether soils develop systematically with terrace elevation (and therefore, age); 2) estimate the ages of Holocene and Pleistocene fluvial terrace deposits where numerical age control is lacking; 3) use the soil development ages of the terrace deposits along with topographic elevation of the surfaces to estimate rates and timing of tectonic uplift; 4) compare fluvial terrace surface uplift rates locally to uplift rates estimated from emergent marine terraces regionally; 5) determine whether soils developed on fluvial terraces at the Mitchell Ranch can be used to identify and correlate fluvial terraces elsewhere in northwestern California.

The study consisted of terrace mapping along the SFER from near Garberville (Figure 1) downstream to the confluence with the Eel River, excavation, description and sampling of soil pedons at the Mitchell Ranch portion of the mapped area. Quantitative textural analyses of selected soils were performed. Soil Profile Development Indexes (SPDI) for the fluvial terrace soils were calculated from the field descriptions.

GEOLOGY

Field mapping (Bickner, 1984) shows that the sequence of nested terraces near Garberville on the Mitchell Ranch are the most complete and preserved sequence of discontinuous terrace remnants in the SFER (Figure 3).

Geomorphic mapping (Bickner 1977, 1985) shows that other terrace sites exist on the SFER, Eel River, and Van Duzen River (O'Day, this volume; Kelsey, 1977), Mattole River (Merrits and Vincent, 1989) and the Trinity River (Bickner, 1992). Some of these terrace sets may

be time correlative to those along the SFER, in particular, with those studied in detail at the Mitchell Ranch.

Strath surfaces associated with fluvial terraces in the SFER are cut into the Tertiary Central Belt Franciscan Melange, late Tertiary Yager Formation and Neogene Wildcat Formation sediments. The Wildcat Formation sediments (Kimtu Unit and Garberville Unit) may be as young as early Pleistocene in the Garberville area (Menach, 1986), which suggests that the present SFER basin may be younger than mid-Pleistocene (1 Ma).

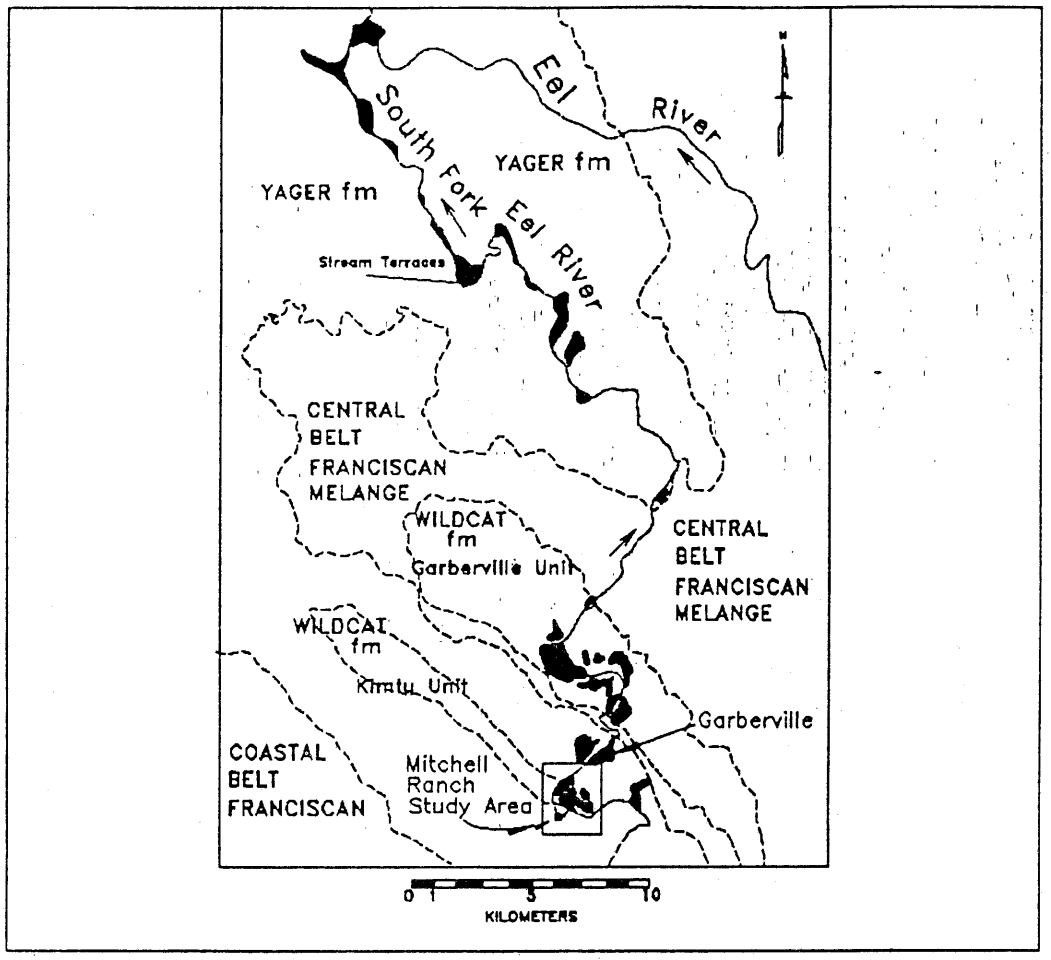

Figure 3. Geologic map and terrace locations along a portion of the South Fork Eel River.

MITCHELL RANCH STUDY AREA

Elevations (in meters) of the terraces measured relative to the adjacent bedrock SFER channel are shown in Table 1. Terraces MT1-MT3 are channel fill deposits with modern flood cut surfaces. Terraces MT4- MT10 are predominantly gently sloping (0-4%) bedrock strath slip-off surfaces, covered by lag gravels and overbank deposits. These terraces (MT4-MT10) have well preserved depositional surfaces, separated by steep cut scarps. The upper terraces (MT11-MT14) are highly eroded and weathered and consist of poorly preserved bedrock strath surfaces and fluvial deposits.

TECTONIC SETTING

Convergence and subduction has resulted in regional tectonic uplift (Figure 1) of marine terraces along coastal northern California with ranges from 0.3 to 4 m/ky (meters / thousand

years) from Fort Bragg north to Cape Mendocino (Merrits and Vincent, 1989; Hageman, 1984; McLaughlin and others, 1983; Lajoie, 1982).

The tectonics in the area is presently dominated by crustal deformation, the result of a right lateral shear environment south of the Triple Junction (McPherson, this volume; Kelsey and Carver, 1988). Within the Mitchell Ranch area, this deformation is apparently being taken up, in part, by possible right slip along the Garberville fault zone (Kelsey and Carver, 1988) and by uplift (Bickner, 1985).

RELATIVE SOIL DEVELOPMENT

The SPDI (Harden, 1982) is an indicator of the relative degree of the soil profile development (Table 1). The SPDI is based on the field descriptions modified by laboratory textural data. Field properties examined in this study include: rubification (dry and moist colors), clay films, pedologic structure and total texture (texture plus wet consistence). The different properties are assigned numerical values based on the amount of change relative to the assumed parent material characteristics. For comparative purposes, the SPDI values were normalized to a common depth of 260 cm to adjust for differences in deposit thickness (after Harden, 1982).

Factors of parent material were controlled by selecting a study site with unconsolidated deposits of sandy to sandy loam textures of graywacke lithologies. This is mineralogically similar to the parent materials in the Merced (Harden, 1982, Harden and Taylor, 1983), Ventura (Rockwell, 1983) and Mattole chronosequences (Merrits and Vincent, 1989). These similarities make soil development comparisons possible.

Parent material deposits at the Mitchell Ranch are represented by modern active channel sediments. The modern channel bank consists of basal imbricated lag gravel and coarse sand that grade upward to bedded fine gravel and sand. The higher energy gravel and sand is capped by fine grained overbank flood deposits of loamy sand to silty loam composition. The stratigraphy and depositional fabric of the active channel bank profile is representative of the deposits in all of the higher terraces with exception to MT11-MT14.

RESULTS AND DISCUSSION

Tables 1 and 2 summarize the soil development data for relative dating and show correlations based on relative dating and the SPDI based on Harden's methodologies. Estimated ages are based on soil profile development correlations to regionally dated alluvial terraces. These data suggest that the terraces can be grouped into six age-classes, as follows: age-class 1, recent alluvium; age-class 2, 3.5 Ka - 8.3 Ka; age-class 3, 29 Ka - 48 Ka; age-class 4, 75 Ka - 80 Ka; age-class 5, 100 Ka - 120 Ka and age-class 6, greater than 300 Ka.

Local tectonic uplift rates were estimated with a constant incision/uplift rate model using coastal uplift rates to the west of the study area (Figure 1). These coastal uplift rates are assumed to be similar to the uplift rates at the Mitchell Ranch. The predicted age of a stream terrace at the Mitchell Ranch is a product of its altitudinal spacing above the channel and a given uniform uplift rate. Uplift rates between 0.5m/ky and 4m/ky were evaluated in the constant incision/uplift rate model. Age estimates based on coastal uplift rates for the terrace surfaces are shown in Tables 1 and 2. Age estimates predicted from uplift rates for the terraces were compared to the relative soil development predicted ages (Harden's Merced and Ventura Chronosequence, 1982, 1983) and a terrace formation climate model. This comparison suggests that the most reasonable ages from the constant incision rate model are extrapolated from 1m/ky. This rate compares well to uplift rates along the coast west of the study area (Figure 1).

There is a strong relationship between 1) the elevation of the terraces, 2) ages estimated from the relative soils development, and 3) the SPDI predicted ages. In general, soils at the

Mitchell Ranch appear to develop systematically with elevation and therefore, age.

TABLE 1. CALCULATED SPDI AND PREDICTED AGE FOR TERRACES AT THE MITCHELL RANCH

				PREDICTED AGES					
				SOIL DEVELOPMENT AGE		UPLIFT RATE AGE			
TERRACE NUMBER	ELEV (m)	SPDI UNADJUSTED	SPDI ADJUSTED	UNADJUSTED	ADJUSTED	$1m/10^3yr$	STAGE	$2m/10^3yr$	STAGE
MT 14	310	50.78	214.45			310,000		155,000	
MT 12	274	45.17	138.97			274,000		137,000	
MT 10	108	62.47-69.92	60.5	97,000	114,000	108,000	5C	54,000	3C
MT 9	97	46.81	61.07	66,000	80,000	97,000	5B	48,000	3B
MT 8	65	27.90	49.19	31,400	75,000	65,000		32,000	
MT 7	62	23.62	38.71	25,000	48,000	62,000		31,000	2A
MT 6	50	19.84	31.58	19,000	29,000	50,000	3B	25,000	
MT 5	10	15.21	17.53	13,500	8,300	10,000		5,000	1A
MT 4	8	11.63	7.42	9,200	3,500	8,000	1A	4,000	

TABLE 2. PREDICTED UPLIFT RATE FROM ELEVATION / SOIL AGE

TERRACE NO.	ELEV(m) / AGE(Ka)	SOIL INDEX UPLIFT RATE (m/ky)
MT 10	108/114	0.9
MT 9	97/80	1.2
MT 8	65/75	0.9
MT 7	62/48	1.3
MT 6	50/29	1.7
MT 5	10/8.3	1.2
MT 4	8/3.5	2.3

REFERENCES CITED

Bickner, F. R., 1977, Geologic reconnaissance of a portion of the Eel River near Alderpoint, California, unpublished California Department of Water Resources, Northern District, Memorandum Report. 22pp.

Bickner, F. R., 1985, Relative dating and geologic interpretation of thirteen fluvial terraces of the Eel River, northern California: Geological Society of America Abstracts with Programs, v.

Bickner, F. R., 1992, in progress, Water quality assessment of the Hoopa Valley Indian Reservation, U. S. Environment Protection Agency.

Carver, G. A., Burke, R. M., and Kelsey, H. M., 1985, Quaternary deformation studies in the region of the Mendocino triple junction: U. S. Geological Survey Open-File Report 86-31,p.58-62.

Hagemann, M. F., 1984, Origin and history of an emergent late Quaternary marine terrace sequence near the Mendocino triple junction, California [masters thesis]: Los Angeles, California, California State University.

Harden, J. W., 1982, A quantitative index of soil development from field descriptions: examples from a chronosequence in central California: Geoderma, v. 28, p.1-28.

Harden, J. E. and Taylor, E. M., 1983, A quantitative comparison of soil development in four climatic regimes: Quaternary Research, v.20, p.242-359.

Kelsey, H M., 1977, Landsliding, channel changes, sediment yield and land use in the Van Duzen River basin, north coastal California 1941-1975 [PhD. dissert.]: Santa Cruz, California, University of California.

Kelsey, H. M. and Carver, G. A., 1988, Late Neogene and Quaternary tectonics associated with the northward growth of the San Andreas Transform Fault, northern California: Journal of Geophysical Research, v.93, p.4797-4819.

Lajoie, K. R. Sarna-Wojcicki, A. M., and Ota, Y., 1982, Emergent Holocene marine terraces at Ventura and Cape Mendocino, California-Indicators of high tectonic uplift rates: Geological Society of America Abstracts with Programs, v.14,no.4,p.178.

Menack, J. S., Geology of the Neogene sedimentary rocks in Gaberville, California, 1986, [M. A. thesis], Cornell University.

Merrits, D. and Vincent, K. R., 1989, Geomorphic response of coastal steams to low, intermediate, and high rates of uplift, Mendocino triple junction region, northern California: Geological Society of America Bulletin, v.101, p.1373-1388.

McLaughlin, R. J., Lajoie, K. R., Sorg, D. H., Morrison S. D., and J. A. Wolfe, 1983, Tectonic uplift of middle Wisconsin marine platform near the Mendocino triple junction, California: Geology, v.11, p.35-39.

Rockwell, T. K., 1983, Soil chronology, geology, and neotectonics of the north central Ventura basin, California [PhD. dissert.]: Santa Barbara, California, University of California.

INTERPRETATION AND CORRELATION OF HOLOCENE COASTAL DEBRIS FLOW FANS NEAR THE MENDOCINO TRIPLE JUNCTION

· Ralph Johnson, Humboldt State University, Arcata CA, 95521

Abstract

South of Cape Mendocino debris flow fan complexes at stream mouths are partially preserved on top of emergent Holocene marine platforms. Complexes usually consist of nested fans; younger, smaller fans are inside older, larger fans. No surface channels were observed on, or buried channels in any fans, and no buried soils were found. The morphologic and stratigraphic evidence indicates that each fan represents a discrete, short lived aggradation event.

Fans were correlated using soil relative dating with some help from a few radiocarbon dates. Four fan age classes are distinguishable. Fans in the three oldest classes represent major mass wasting events which occurred during the period between about 1000 and 6000 years before present. The youngest class contains fans representing smaller, more frequent events. If major mass wasting events occur simultaneously in most drainage basins, then evidence for three such events in the last 6000 years is preserved in the study area fans. Possible causes are extreme precipitation events, large earthquakes, or fires followed by heavy precipitation. The author favors the earthquake hypothesis, because (1) it is almost certain that very large earthquakes have struck the area in the past, resulting in the emergence of marine platforms; (2) it is well documented that large earthquakes cause extensive mass wasting; and (3) the inferred fan building event frequency is consistent with the probable frequency of those earthquakes.

Introduction

The Mendocino triple junction (MTJ) is an uncommonly dynamic area for coastal-fluvia geomorphology. High rates of deformation, uplift, seismicity, and precipitation combi with eustatic sea level changes have resulted in some of the most dynamic coastal strean geomorphic environments found anywhere in the world. The present geomorphology a stream mouths around the MTJ is the result of mid and late Holocene uplift, stream inci and drainage basin mass wasting superimposed on effects of the early Holocene sea lev rise. Rapid uplift in the Holocene has resulted in emergent marine platforms along muc the coastline around the MTJ, and these provide a site for sediment storage during fluvi aggradation events. Many streams have deposited debris flow fan complexes on these platforms and the description, interpretation, correlation, and age estimation of these is objective of this paper.

The fans studied are found at intermittent, first, and second order stream mouths between Cape Mendocino and Spanish Flat (Figure 1). High uplift rates have produced a steep, rugged topography throughout the area. From Cape Mendocino southward, uplift rates appear to increase steadily from 2.8 m/ky (meters per thousand years) at Singley Flat to 4-5 m/ky at Spanish Flat (Lajoie et al., 1982; Merritts and Bull, 1989; Merritts, 1991). The coastal geomorphology of the study area consists of emergent Holocene marine platforms backed by paleo sea cliffs, interrupted by strips of actively retreating rocky coastline.

The bedrock of the study area consists mainly of accreted terranes of the Franciscan coastal belt. They are lithologically similar, consisting mainly of sandstone, shale, and argillite turbidites (Ogle, 1953; Nason, 1968; Beutner et al., 1980; McLaughlin et al., 1982). These rocks are moderately resistant except for several major shear zones, where they compose a very weakly resistant melange. There is also some Tertiary Wildcat Group-like mudstone in the area between the Mattole River mouth and Davis Creek which is either overlying or is tectonically incorporated into the Franciscan rock.

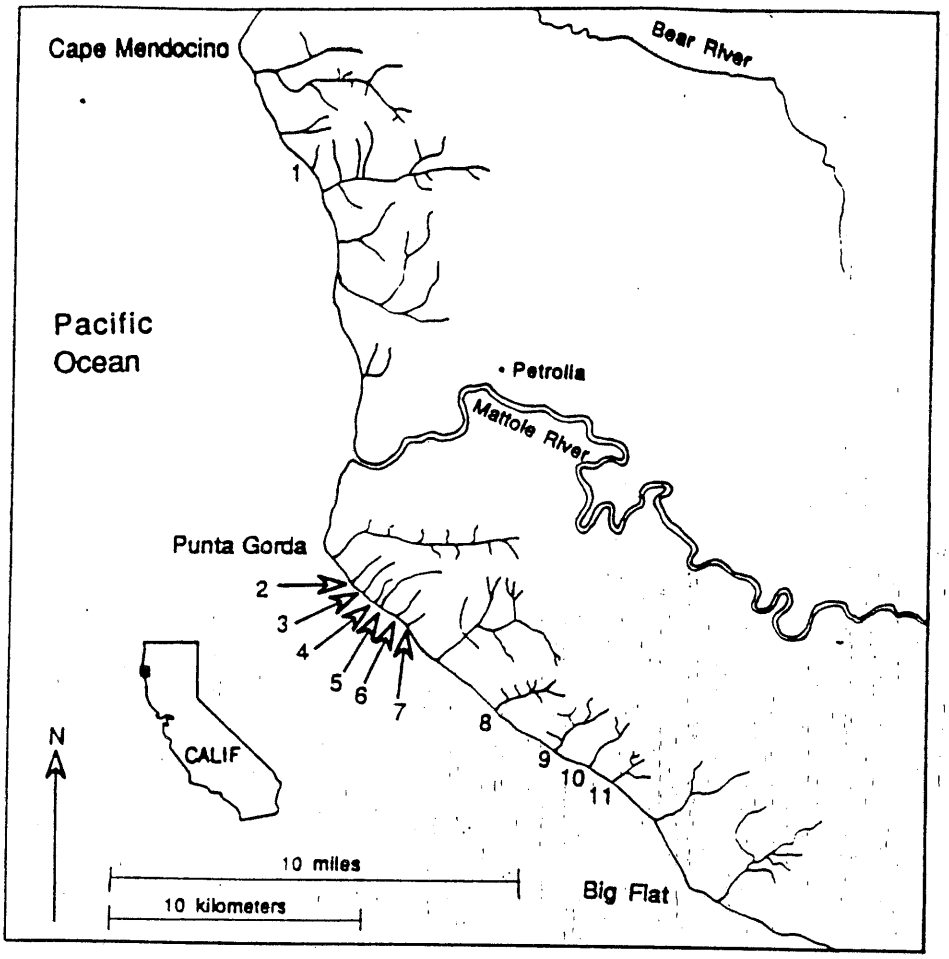

Figure 1. Study area fan locations: 1 = Clay Cr; 2 = Slab Cr; 3 = Willow Cr; 4 = Sea Lion Gulch North; 5 = Sea Lion Gulch; 6 = Johnny Jack Cr; 7 = Barn Cr; 8 = Randall Cr; 9 = Spanish Cr; 10 = Oat Cr; 11 = Kinsey Cr.

Fan Morphology, Sedimentology, and Stratigraphy - Observations and Interpretations

The fan complexes usually consist of nested fans (Figure 2); younger, smaller fans are inside older, larger fans. Fan apex heights range from a few meters to as high as 40 meters, oldest fans being highest. Most fans have been truncated by wave action at their distal edges; older fans are truncated further from the present shoreline than younger fans. No surface channels were observed on, or buried channels in any of the fans, and no buried soils were found.

Individual fans are usually composed of debris flows of fairly uniform thickness and inferred viscosity . Fluid flow fans are clast supported and well stratified with thin flows, while viscous flow fans are matrix supported and poorly stratified. The smaller, steeper drainage basins produce the more viscous flows, with higher clay content.

The morphology and stratigraphy of the complexes indicates that fans are built during rapid, short lived aggradation events, and are then quickly incised as streams return to base level. Fans are eroded between events by channel migration during high flows. Larger fans represent major mass wasting episodes--perhaps the result of earthquakes, infrequent extremely large storms, or the occurrence of large storms following fires.

Figure 2. Fan remnants at Sea Lion Gulch. The oldest fan is preserved as a ridge of debris flow material (right center of photo). The youngest fan is preserved only as a terrace inset into the middle aged fan.

Fan Age Correlation

Inter-drainage basin fan age correlation was conducted to estimate the number and frequency of major mass wasting events in the study area. Two dating methods were used to correlate fans: soil relative dating and radiocarbon dating. Radiocarbon dating is obviously the preferred method for this objective; however, finding wood in the fans proved to be difficult . Wood was occasionally found in the smaller, young fans, but was only found in one of the larger, older fans. This is partly due to the better exposure of young fans (freshly exposed by stream incision and wave erosion) and partly due to the differing nature of the small and large fans: Smaller fans are probably the result of floods and therefore contain a higher proportion of woody debris cleared from channels. Four fans were dated by radiocarbon and the results are shown in Table 1.

Because few fans could be radiocarbon dated, soil relative dating was relied upon for most correlations. Though the particle size distribution of the parent material varies among the fans, there is an obvious progression in soil development and depth from younger to older fans. Youngest soils (less than a few hundred years old) have only a weak A horizon at best, less than 45 cm deep. I label these class I soils. Class II soils have an A/C profile with a weak to moderately developed A horizon less than 75 cm thick. Class III soils have an A/C profile with a moderately developed A horizon up to 90 cm thick containing more clay (developmental) than class II soils; there is very little evidence of clay translocation. The two oldest fans in the study area appear to have A/Btj/C profiles. I label these soils class IV. The Btj horizon is suggested by clay enrichment below the A horizon (clay films few and thin). The clay enrichment may simply be a parent material variation; however,

Fan Name	Radiocarbon age, years before 1950	Calendar age, years before 1950	Lab Number
Sea Lion Gulch North #3	4150±60	4981-4912 4889-4409	Beta-44498
Johnny Jack Cr	90±60	430-357 330-0	Beta-44497
Big Slide Basin	50±50	300-0	Beta-44496
Oat Creek	130±60	460-0	Beta-44495

Table 1. Fan radiocarbon dating summary. Radiocarbon dates were calibrated using a microcomputer program obtained from the University of Washington (Stuiver and Reimer, 1986). The calendar year range covers the 95% confidence interval, including a lab multiplier of 1.6.

one of these fans, located at Sea Lion Gulch, is clearly older than an adjacent class III fan, based on its geomorphic position.

The above four soil classes were used to group the fans and soil development and available absolute dates (from fans and emergent platforms) were used to estimate class ages. The results are shown in Table 2.

Soil class	I	II	III	IV
Approximate age (calendar years)	0-500	1000-3000	3000-5000	4000-6000
Stream fans	Kinsey Cr(4) Oat Cr (3) Spanish Cr(3) J. Jack Cr (3) Clay Cr (1)	Kinsey Cr (1) Willow Cr (1) Sea Lion G N (1) Sea Lion G (1) Clay Cr (1)	Willow Cr (1) Randall Cr (1) Sea Lion G N (1) Sea Lion G (1) Slab Cr (1)	Sea Lion G (1) Barn Cr (1)

Table 2. Debris flow fan age classes

Stream names are used for the fans; the numbers in parentheses indicate the number of fans in the same class at the stream location. Note that class I contains multiple fans (events) at most locations; none of these events were as large as those of classes II-IV. The age range for class I fans is based on radiocarbon dates and soil development. The age range for class II fans is an estimate based on their soil development relative to classes I and III. The age range for class III fans is based on soil development, the radiocarbon date from the class III Sea Lion Gulch north fan, and a date of 4409-4819 ybp (calendar years before 1950) on a shell in a platform a few hundred meters north of Sea Lion Gulch (Merritts, 1992; personal communication). The platform can be traced beneath the class II and class III fans at Sea Lion Gulch. The age range for class IV fans is based on soil development; its maximum is limited by the approximate date of the Holocene transgression culmination.

Based on my correlation results, I can state that three or more major mass wasting events probably occurred in the study area over about the last 6000 years. If the fans which are correlated in classes II-IV were deposited simultaneously,then evidence for only three such events is preserved. I feel that the simultaneity hypothesis is reasonable, since it is likely that given an extreme precipitation event or a large earthquake, many drainage basins will be affected. However, since soil relative dating may fail to distinguish some fans which

were actually from separate events, the hypothesis cannot be disproven using this technique. Also, because there are only two class IV fans and because only one location (Sea Lion Gulch) has fans from each of classes II-IV, the importance of the oldest event is less certain.

I find the idea of very large earthquakes causing these mass wasting events compelling. We are almost certain that large Holocene earthquakes occurred here, resulting in the uplifted shore platforms; it is well documented that large earthquakes cause extensive mass wasting; and the inferred fan event frequency is consistent with the probable frequency of those earthquakes--Merritts (1991) reports a 1300-2200 year Holocene periodicity of platform uplifting events just south of Cape Mendocino. Flood flows may have been necessary to evacuate earthquake caused slides from the drainage basins, but these can be expected on a high enough frequency (less than 20 years) to have little effect on the earthquake record in fans. Not all large earthquakes are expected to be represented in the fan record; large earthquakes occurring during dry seasons, especially during droughts, may not have caused landsliding sufficient to be preserved in the fan record.

Conclusions

Deposition of stream mouth debris flow fans is possible where streams exit the mountain front onto emergent Holocene marine platforms. Larger fans are the result of major mass wasting events in the drainage basins. Correlation of fans has produced four age classes, the three oldest representing major mass wasting events which occurred between about 1000 and 6000 years ago. If major mass wasting events occur simultaneously in most drainage basins, then three such events are recorded in study area debris flow fans.

References Cited

Beutner, E.C., McLaughlin, R.J., Ohlin, H.N., and Sorg, D.H., 1980, Geologic Map of the King Range and Chemise Mountain instant study areas of northern California: U.S. Geological Survey Miscellaneous Field Studies Map MF-1196-A, scale 1:62,500.

Lajoie, K.R., Sarna-Wojcicki, A.M., and Ota, Y., 1982, Emergent Holocene marine terraces at Ventura and Cape Mendocino, California--indicators of high tectonic uplift rates: Geological Society of America Abstracts with Programs, v.14, p.178

McLaughlin, R.J., Kling, S.A., Poore, R.Z., McDougall, K., and Beutner, E.C.,1982, Post-middle Miocene accretion of Franciscan rocks, northwestern California: Geological Society of America Bulletin, v.93, p.595-605

Merritts, D.J., 1991, Patterns and rates of crustal deformation, northern termination of the San Andreas transform boundary: Geological Society of America Abstracts with Programs, v.23, no.2, p.78

Merritts, D.J., and Bull, W.B., 1989, Interpreting Quaternary uplift rates at the Mendocino triple junction, northern California, from uplifted marine terraces: Geology, v.17, p.1020-1024

Nason, R.D., 1968, San Andreas fault at Cape Mendocino, in Dickinson, W.R., and Grantz, A., eds., Conference on Geologic Problems of the San Andreas Fault System, Proceedings: Stanford University Publications in Geological Sciences, v.11, p.231-241

Ogle, B.A., 1953, Geology of the Eel River valley area, Humboldt County, California: California Division of Mines Bulletin 164, 128p.

Stuiver, M., and Reimer, P.J., 1986, A computer program for radiocarbon age calibration: Radiocarbon, v. 28, p.1022-1030

THE HONEYDEW EARTHQUAKE OF AUGUST 17, 1991: EVIDENCE OF COMPRESSIONAL TECTONICS AT THE MENDOCINO TRIPLE JUNCTION

Robert C. McPherson, Lori A. Dengler
Geology Department, Humboldt State University, Arcata, California 95521

INTRODUCTION

On August 17 at 12:29 pm PDT, a magnitude 6.2 earthquake occurred in the immediate region of the Mendocino triple junction. It was the largest land-based earthquake to occur in the continental United States during 1991. This earthquake is important because: 1) It was the largest earthquake located on land in the vicinity of the triple junction in this century. 2) The shallow depth of focus (12 km) suggests a previously unrecognized source for damaging earthquakes in the region, which has now produced three damaging earthquakes in slightly over a two year period[1]. 3) The earthquake produced a conspicuous zone of northwest oriented surface cracks which coincided with a previously recognized shear zone. 4) The epicentral region has undergone a very high rate of Quaternary uplift and the proposed style of faulting for the Honeydew earthquake is consistent with uplift of this region. 5) A large region surrounding the epicenter experienced changes in ground water and stream flow related to the earthquake.

GEOLOGIC SETTING

The Honeydew earthquake was located at the Mendocino triple junction, the region where the Gorda, Pacific and North American plates meet (figure 1). To the northwest of the triple junction, the southern end of the Cascadia subduction zone bends eastwards and comes onshore in the vicinity of the Petrolia Shear Zone (Clarke 1992). The boundary between the Gorda and Pacific plates, the Mendocino fault, can be followed eastwards along the base of the Gorda Escarpment offshore to about 124° 45' longitude, but further landward its location becomes less certain (Clarke 1992). Seismicity trends of shallow earthquakes (McPherson, 1989; Oppenheimer, 1991) suggest that the Mendocino fault follows the Mattole River Canyon and eventually joins up with the Cooskie shear zone as proposed by Clarke (1992). Therefore, two of the boundaries between the three plates that comprise the triple junction come on shore near two previously recognized on land shear zones, the Cooskie and Petrolia Shear zones.

The third plate boundary, which lies between the Pacific and North American plates, has historically been defined in northern California by the surface rupture of the San Andreas fault during the 1906 earthquake (Lawson, 1908). The 1906 surface rupture can be traced northward from San Jose to Pt. Arena. North of Pt. Arena the San Andreas fault is thought to run offshore, intersecting land just south of Pt. Delgada (Griscom,1973, McCulloch, 1989). The San Andreas fault's location is less well known north of Pt. Delgada, and may either run parallel and near to the coastline curving westwards to join the Mendocino Fault (McCulloch, 1989), or come on land southeast of Pt. Delgada to join with the Mattole Shear Zone (McLaughlin and others, 1988). The boundary between the Pacific and North American plates is distributed across a broad zone of faults that run parallel to and east of the San Andreas fault, and the 1906 surface rupture defines the western margin of this diffuse transform boundary (Kelsey and Carver, 1988; Eaton, 1989).

---

[1] Magnitude 5.3 earthquakes occurred in the same area on January 16, 1990 and March 7, 1992. Both earthquakes produced peak intensities of VII.

Because of the uncertainties in the plate boundaries in the triple junction region, the Mendocino triple junction cannot be considered a single point. Rather it is a region bounded to the northeast by the Petrolia Shear zone, to the south by the Cooskie Shear zone, and to the west by the coastline (figure 1). The epicenter of the Honeydew earthquake is located within this region, and must therefore be considered a triple junction event.

South of the Mendocino triple junction region are the rocks of the King Range Terrane, with peaks reaching over 1200 meters (4000 ft) within a few miles of the coast. McLaughlin and others (1982) have suggested that the King Range Terrane was obducted on to northern California along a southwest dipping reverse fault as recent as two million years ago. Since then, the area has undergone folding and uplift. The uplift is recorded in suites of marine terraces along the western margin of the King Range and mountains to the north (Lajoie and others, 1982; McLaughlin,et al., 1983; Merrits and Bull. 1989) and fluvial terraces to the east near Garberville (Bickner, 1992). Studies using fission tracks (Dimitru. 1990) and stream profiles (Merrits and Vincent, 1989) corroborate the late Holocene history of rapid uplift in the region.

THE AUGUST 17TH EARTHQUAKE

The Honeydew earthquake was felt as far away as San Francisco and Sacramento, 300 km to the south and produced strong ground shaking (intensity IV or greater) over an area of nearly 10,000 sq. km (Mcpherson and others, 1991). Violent ground motion in the epicentral area lasted for six to ten seconds, strong enough to cause some people to fall to the ground and shake debris from both live and dead trees. As the shaking subsided, dense clouds of dust were observed rising from a multitude of rockfalls and reactivated landslides by local residents and numerous startled fisherman offshore.

In the two weeks following the earthquake, we undertook field studies to investigate the effects of strong motion in the epicentral area. Initial reports of damage were light and our original interest in studying this earthquake was based on its onland and shallow location, rather than the reported effects. Mapping of surface features and damaged structures on 7 1/2 minute quadrangle sheets was conducted primarily along all roads in the area starting 2 days after the earthquake. Numerous residents of the area were interviewed and many invited us to look at features on their property. The region cover most detailed field mapping is shown in figure 2.

Description of Damage

Structural damage was concentrated in a 5 km radius zone centered near the town of Hone was most prevalent in homes inadequately tied to foundations and mobile homes on post a block foundations. We interviewed or received survey responses from fifty three resider Honeydew, Wilder Ridge, Panther Gap and Petrolia area. Of these, thirty-three reported som structural damage, and minor structural damage was reported as far away as Ettersburg. A dozen structures in the Panther Gap, Wilder Ridge, and Honeydew areas moved off their foundations resulting in considerable structural damage. Properly constructed homes, with attention given to shear bracing and properly bolted to continuous foundations suffered little or no structural damage.

At least fifteen chimneys were reported down or damaged in the Petrolia - Honeydew area. Incidence of chimney damage, however, was lower than for many previous earthquakes. Residents of the Honeydew and Petrolia area have been affected by at least fourteen intensity ≥ VI events and five

intensity VII's in the past forty years and chimneys have been reported damaged in the Petrolia area sixteen times since the late 1800's (Dengler and others this volume). Perhaps as a consequence, many residents have now replaced masonry chimneys with metal stovepipe which is much better able to withstand ground shaking.

Slumping of the roadbed resulted in tensional cracks which cut the Mattole River road in several places along a 3 mile stretch just west of Honeydew. Similar failures occurred along Wilder Ridge road for two miles southeast of Honeydew, and the settling caused 7-8 centimeter high escarpments to form across the approaches to both Bear Trap and Honeydew Creek bridges. A landslide completely covered Wilder Ridge road with over 600 cubic yards of debris on the north side of Honeydew Creek Bridge, halting through traffic the day of the quake. Numerous tensional cracks and slumping features were obvious as one continued south along Wilder Ridge road for the next 6 km.

Oriented Surface Cracks

A linear zone of surface cracks were observed along Wilder Ridge road about six kilometers south of Honeydew (figure 2,3). Individual cracks typically ranged between ten and twenty meters in length at any one locality and were noticed both along the ridge and in several localities on the ridge flanks. Cracks in this zone generally exhibited a northwest trend with both left and right stepping patterns. The cracks along the ridge showed one to five centimeters of extension, and had in some cases a small left lateral component of less than a centimeter. Along Wilder Ridge Road, the cracks showed increased extension and grew in length at several localities in the days following the earthquake.

The cracks followed a northwest trend along Wilder ridge and crossed the switchbacks descending from the ridge. Further to the northwest, they crossed Honeydew Creek where they were associated with displaced boulders. After Honeydew Creek, the cracks crossed Smith Etter Road on Bear Trap Ridge, disrupted Bear Trap Creek, cut across the Mattole River and Barrel roads, and were last observed cutting a young fluvial terrace in the Upper North Fork of the Mattole River. The cracks were often obscured by numerous large landslides, but could always be picked up again along the same northwest trend on the other side of the landslide.

Displaced Boulders

The clearest indication of strong motion was disrupted stream bed cobbles associated with the cracks which crossed Honeydew Creek. Numerous cobbles and boulders up to a meter in diameter were thrown out of their positions in a zone within 15 to 35 meters of the cracks as they crossed the stream channel. These cobbles had been imbedded several centimeters into the ground and primarily showed westward displacements (figure 4). Larger boulders were more likely to be dislodged than smaller ones, presumably because their greater inertia could more easily overcome the cohesive hold of the sediment socket as the ground moved. Several boulders had been completely flipped over, with many moving as much as 25 cm from their initial location. Logs in this same zone also showed signs of displacement and rotation to the west. Disrupted boulders were also found associated with the tensional cracks in Bear Trap Creek, the next drainage to the northwest. The most impressive feature of the displaced boulders in the stream channels was the narrowness of the zone in which they occurred, suggesting strong ground motions had been strongly focused.

Water Flow Changes

Almost all of the residents in the epicentral area noted an increase in flow in the Mattole River and a number of other streams in the area in the days following the earthquake. It was all the more striking coming during the driest time of the year and after six years of drought conditions. The flow for the Mattole River increased steadily from 28 cubic feet per second prior to the earthquake to 82 cubic feet a second in the six days following the earthquake (figure 5). The only precipitation during this period was a small storm on the 26th of August which added a short duration peak to the hydrograph. The earthquake-induced flow, after reaching a peak, slowly decayed to pre-earthquake levels in about 60 days.

Many residents also reported changes in their well levels and springs. Most reported increased flows after the earthquake; the community of Briceland whose water system was dry prior to the quake, enjoyed a copious supply for several weeks after the temblor. A few residents reported decreased flows, and we heard one instance of a spring changing its location entirely. Another landowner reported that his reliable, cold spring over 500 feet in elevation above the Mattole River became "river water warm one half hour prior to the quake".

Liquifaction

Liquifaction was observed in the Mattole River and Honeydew Creek channels, where startled residents watched the water become turbid moments after the shaking subsided. This muddying of the water was caused by liquifaction of the riverbed sediments that resulted in the venting of water and fine sediments all along the river bottom, and not initially from landslides that fell into the creek or stream from the surrounding hillslopes (although these sources provided a subsequent muddying of the flow). Tensional cracks also formed along the dry sections of the river channel deposits for hundreds of feet, and along these cracks turbid water and sand was ejected, sometimes concentrated in a single vent. A typical vent exhibited a central area of large cobbles surrounded by a perimeter of fine sand, with a brown stain of even finer material which had settled on the periphery (figure 6).

RELATION OF FAULTING AND SURFACE PHENOMENA

The most striking feature of the Honeydew earthquake was the concentration of damage, landslides, gravity slumping, rockfalls, and sand blows in a narrow zone 10 km east of the epicenter. Within this zone, tensional cracks formed along a narrow northwest trend, and were followed for approximately 6 km. The first motions recorded by seismographs suggest that slip occurred at depth along a northwest trending reverse fault, having either a northeast or southwest dip of 45 degrees (Oppenheimer, 1991). Since the area is known to have southwest dipping reverse faults (McLaughlin and others, 1982), the southwest dipping solution seems the more plausible.

The pattern of strong ground motion and surface effects can be explained by two different arguments, both calling for reverse slip on a buried fault which did not reach the surface. First, the concentration of effects near Honeydew may be due to the focusing of strong motions in the up dip region 10 km east of the epicenter. This is similar to the Whittier Narrows earthquake (October 2, 1987 M=5.9), which produced an isoseismal pattern resembling that of the Honeydew earthquake (McPherson and Dengler, 1992; Hauksson and others, 1988). The focused shaking could have caused the tensional cracks along Wilder Ridge as the ridge spread laterally in response to the strong ground motion.

Griscom, A., 1973, Tectonics at the junction of San Andreas fault and the Mendocino fracture zone from gravity and magnetic data, in Kovach, R. L. and A. Nur, eds., Proceedings of the conference on tectonic problems of the San Andreas fault system, Stanford University Publications in the Geological Sciences, vol. 13, p 383-390.

Hart, E.W., Byrant, W.A., Wills,C.J. and Treiman,J.A., 1990, The search for fault rupture and significance of ridgetop fissures, Santa Cruz Mountains, California, in The Loma Prieta (Santa Cruz Mountains), California earthquake of 17 October, 1989, S.R. McNutt and R.H. Syndor, eds California Division of Mines and Geology Special Publication 104, p 83-94.

Hauksson, E., Jones, L. M., Davis, T. L., Hutton, L. K., Brady, A. B., Reasenberg, p. R., Michael, A. J., Yerkes, R. F., Williams, P., Reagor, G., Stover, C.W., Bent, A. L., Shakal, A. K., Etheredge, E., Porcella, R. L., Bufe, C. G., Johnston, M. J. S., and Cranswick, E., 1988, The 1987 Whittier Narrows Earthquake in the Los Angeles Metropolitan area, California, Science, vol.239, p. 1409-1412.

Kelsey, H. M.and Carver, G. A., 1988, Late Neogene and Quaternary tectonics associated with the northward growth of the San Andreas fault, northern California, Journal of Geophysical Research, vol. 93, p. 4797-4819.

King, G. C. P.and Vita-Finzi, C., 1981, Active folding in the Algerian earthquake of 10 October 1980, Nature, vol. 292, pp22-26.

Lajoie, K. R., Sarna-Wojcicki, A.M., and Ota, Y., 1982, Emergent Holocene marine terraces at Ventura and Cape Mendocino, California -- indicators of high tectonic uplift rate, (abstract) Geological Society of America, Cordilleran Section, Abstracts with Programs, vol. 14, p. 178.

Lawson, A. C., 1908, The California Earthquake of April 18, 1906, Carnegie Institute, Washington D. C.

Merrits, D. and Bull, W. B., 1989, Interpreting Quaternary uplift rates at the Mendocino Triple junction northern California, from uplifted marine terraces, Geology, v.17, p. 1020-24.

Merrits, D. and Vincent, K. R., 1989, Geomorphic response of coastal streams to low, intermediate, and high rates of uplift, Mendocino triple junction region, northern California, Geological Society of Amerca Bulletin, vol. 101, p. 1373-1388.

McCulloch, D. S., 1989, Evolution of the offshore central California Margin, in The Geology of North America, Vol. N, The eastern Pacific Ocean and Hawaii, The Geological Society of America, p. 439-469.

McLaughlin, R. J., King, S., Poore, R., McDougall,K., and Buetner,E., 1982, Post-middle Miocene accretion of Franciscan rocks, northwestern California, Geological Society of Amerca Bulletin, vol. 93, p. 595-605.

McLaughlin, R., LaJoie, K., Sorg, D., Morrison,S., and Wolfe, J., 1983, Tectonic uplift of a middle Wisconsin marine platform near the Mendocino triple junction, CA, Geology, vol. 11, p. 35-39.

McLaughlin, R. J., Sliter,W.V., Clarke Jr.,S. H., McCulloch, D. S., Frederiksen,N.O., and Ingebretson, D. C., 1988, Implications of onshore and offshore structure for location and Cenezoic evolution of the Mendocino triple junction, (abstract) Geological Society of America Abstracts with Program, vol. 20, p A382.

McLaughlin, R. J., Sliter, W. V., Frederiksen, N. O., Harbet, W. P., and McCulloch, D. S., in press, Plate motion recorded by tectonostratigraphic terranes of the Franciscan Complex in the vicinity of the Mendocino triple junction, USGS Bulletin.

McPherson, R.C., 1989, Seismicity and Focal Mechanisms near Cape Mendocino, Northern California: 1974-1984, unpublished Master Thesis, Humboldt State University, Arcata, Ca. 95521, 75pp.

McPherson, R. C. and L. A. Dengler, 1992, The August 17, 1991 Honeydew earthquake, California Geology, vol. 44, April 1992.

McPherson, R. C., L. A. Dengler, and D. Oppenheimer, 1991, Evidence of compressional tectonics in the King Range, California: the 1991 Honeydew earthquake, (abstract) EOS, Transactions of the American Geophysical Union, vol. 72, p. 315.

Oppenheimer, D. H., The 1991 M6.0 Honeydew, California earthquake, (abstract) EOS, Transactions of the American Geophysical Union, vol. 72, p. 311.

Ponti, Daniel J., Wells, Ray E., 1991, Off-Fault Ground Ruptures in the Santa Cruz Mountains, California: Ridge-Top Spreading vs. Tectonic Extension During the Loma Prieta Earthquake, Bulletin of the Seismological Society of America, Bulletin of the Seismological Society of America, vol. 81, p 1480-1510.

Figure 4. Displaced stream cobble in Honeydew Creek. This cobble has been displaced to the west. Dashed line outlines original position of cobble.

Figure 3. Oriented northwest tensional cracks crossing the Beaver Slide Cutoff about 4 km south of Honeydew.

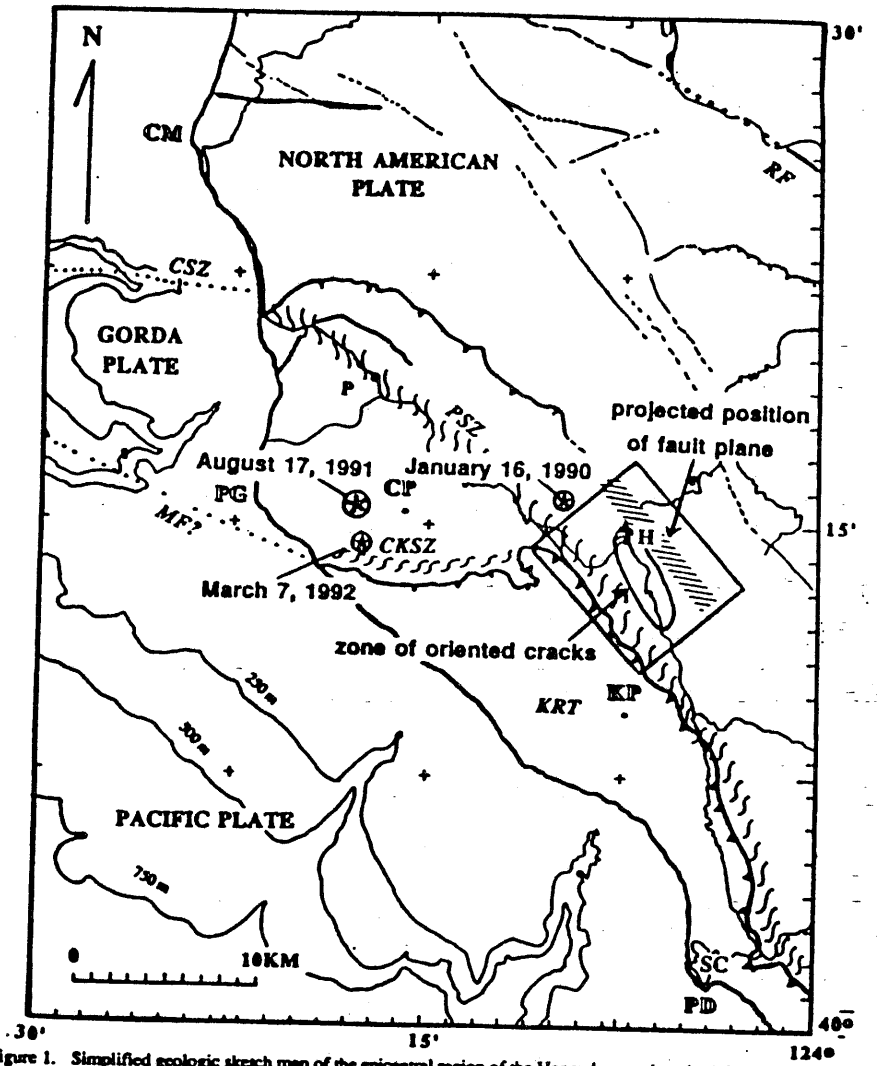

Figure 1. Simplified geologic sketch map of the epicentral region of the Honeydew earthquake (after McLaughlin and others,in press; Clarke, 1992). Abbreviations are as follows: Towns (bold) - P: Petrolia, H: Honeydew, SC: Shelter Cove. Geologic features (in italics): KRT: King Range Terrane, PSZ: Petrolia shear zone, CKSZ: Cooskie shear zone, RF: Russ Fault, MF: Mendocino fault, CSZ: Cascadia subduction zone boundary. Geographic features(outlined): CM: Cape Mendocino, PG: Punta Gorda, PD: Point Delgada, CP: Cooskie Peak, KP: King Peak. The epicenters of the January 1990, August 17, 1991, and March 7, 1992 earthquakes are shown by the stars. Also shown is the region of oriented surface cracks and the projected surface position of the fault plane. The rectangular region is enlarged in figure 2.

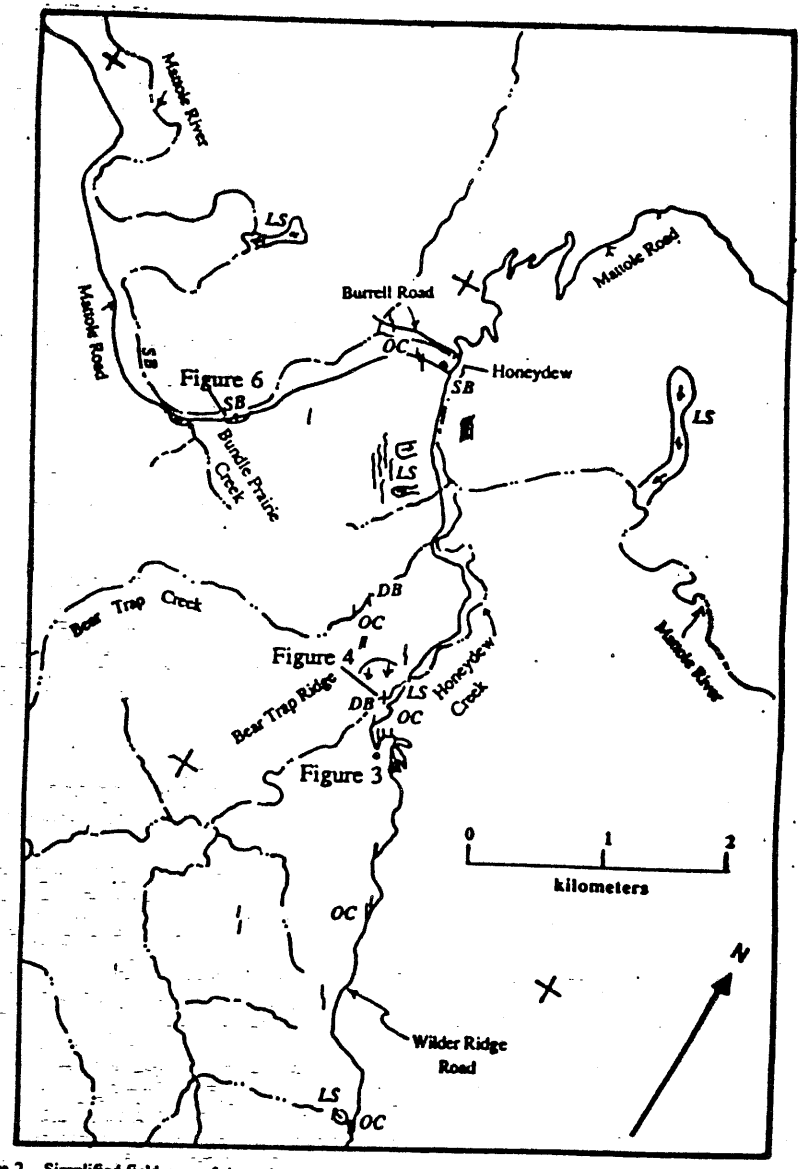

Figure 2. Simplified field map of the epicentral region showing locations of roads and geographic features and mapped surface effects of the Honeydew earthquake. *LS*: reactivated landslide, *DB*: displaced boulders, *SB*: sand blows, *OC*: oriented cracks (shown by small lines). Locations of Figures 3, 4 and 6 are also shown.

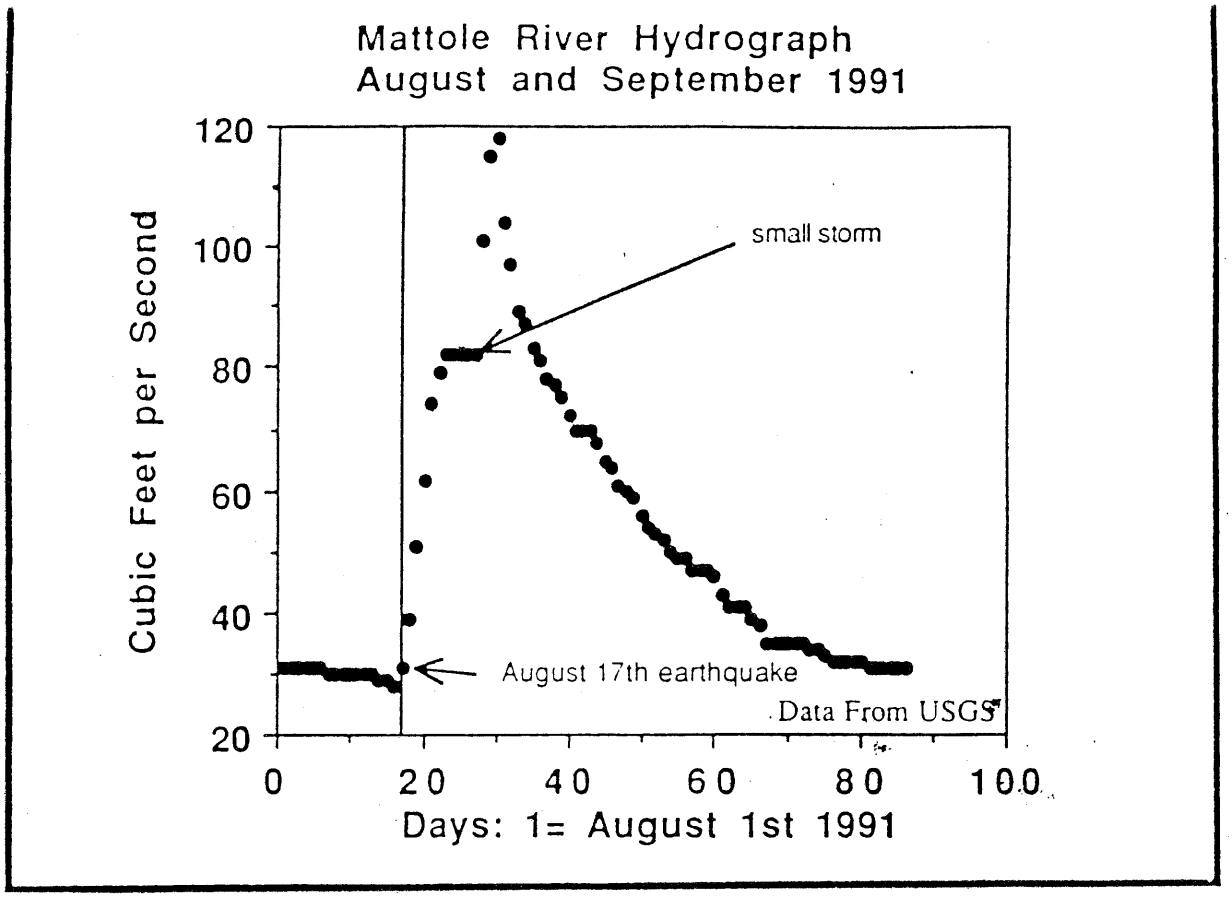

Figure 5. Mattole River hydrograph for August - October 1991. Gauging station is located near the mouth of the Mattole River to the southwest of Petrolia (data from the USGS).

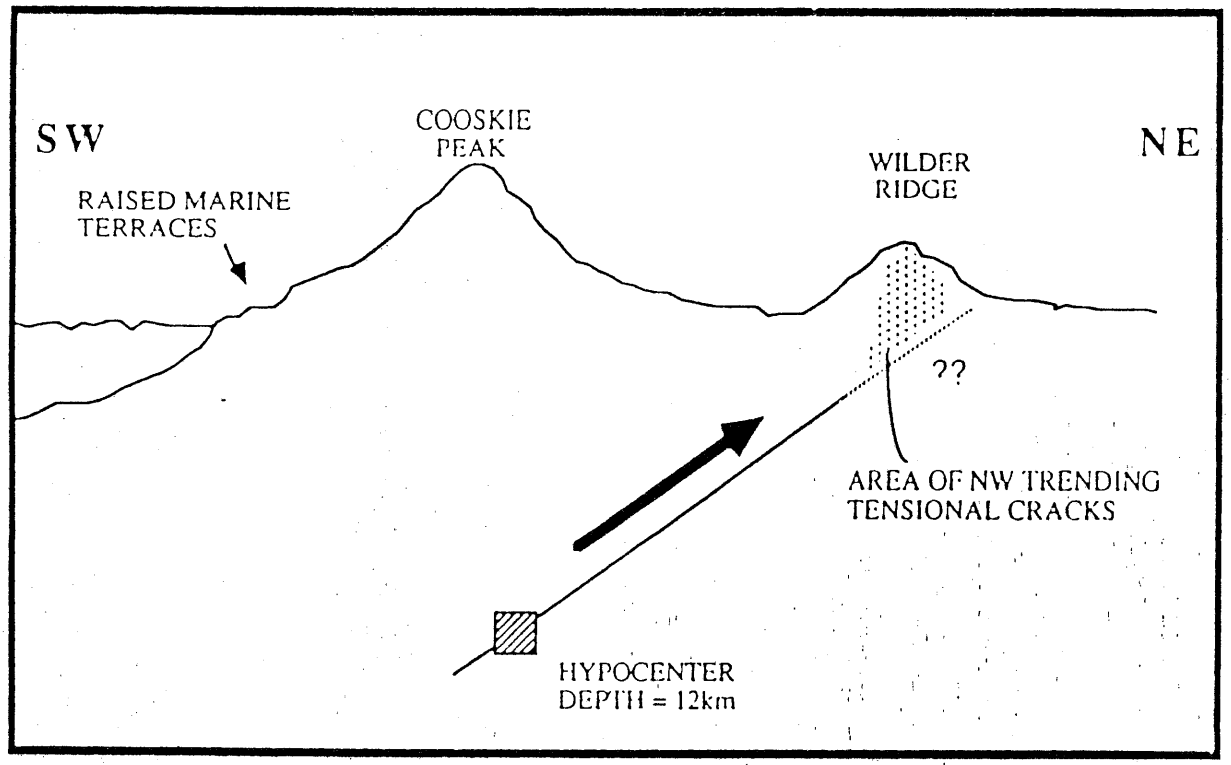

Figure 7. Simplified model of fault motion during the Honeydew earthquake. The square box shows the position of the hypocenter (about 12 km under Cooskie Peak). First motion studies (Oppenheimer, 1991) and surface features suggest that the hanging wall of the fault moved up and to the east during the earthquake. The fault rupture stopped before reaching the surface and the mapped zone of oriented cracks near Honeydew may represent nose failure in the hanging wall.

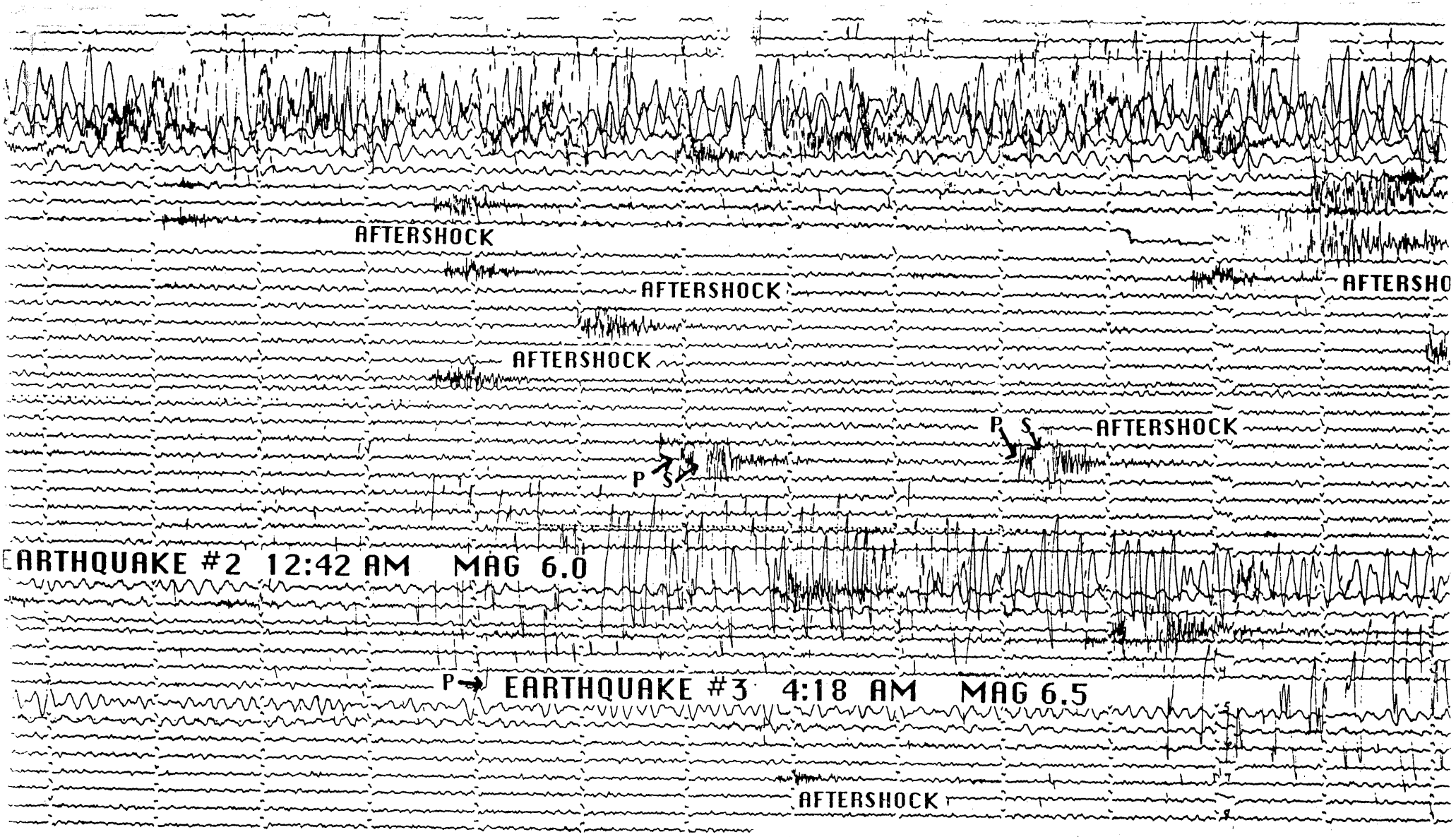

MENDOCINO TRIPLE JUNCTION

AND THE

CASCADIA SUBDUCTION ZONE